Durham E-Theses

Acoustic observations in seabed materials

Alasdair G. McKay

How to cite:

McKay, Alasdair G. (1983) Acoustic observations in seabed materials. Doctoral thesis, Durham University.

Use policy

Acoustic Observations

in

Seabed Materials.

Alasdair G. McKay

Volume 2 : seismogramme figures and included reprints of papers

Durham

December 1983

13. AUG. 1984

VOLUME 2

a) Figures for seismogramme no. 1289.

(fig. 9.24 - fig. 9.44)

b) Figures for seismogramme no. 1281.

(fig. 9.45 - fig. 9.73)

c) Figures for seismogramme no. 496.

(fig. 9.76 - fig. 9.123)

d) More figures for nos. 1289 and 1281.

(fig.9.124 - fig. 9.131)

INCLUDED IN POCKET

1. OVERLAYS

Overlay for field seismogramme no. 1289.

Overlay for field seismogramme no. 1281.

Overlay for field seismogramme no. 496.

2. PUBLISHED PAPERS AND OTHER REPORTS.

McKay and Peacock (1970)

McKay (1974)

McKay (1980a)

McKay (1980b)

McKay and McKay (1982)

McKay (1983)

Howells and McKay (1977)

VOLUME 2

a) Figures for seismogramme no. 1289.

(fig. 9.24 - fig. 9.44)

b) Figures for seismogramme no. 1281.

(fig. 9.45 - fig. 9.73)

c) Figures for seismogramme no. 469.

(fig. 9.76 - fig. 9.123)

d) More figures for nos. 1289 and 1281.

(fig.9.124 - fig. 9.131)

INCLUDED IN POCKET

1. OVERLAYS

Overlay for field seismogramme no. 1289.

Overlay for field seismogramme no. 1281.

Overlay for field seismogramme no. 469.

2. PUBLISHED PAPERS AND OTHER REPORTS.

McKay and Peacock (1970)

McKay (1974)

McKay (1980a)

McKay (1980b)

McKay and McKay (1982)

McKay (1983)

Howells and McKay (1977)

Synthetic seismogramme models

for No. 1289.

(figs. 9.24 to 9.44)

THICKNESS (M.)	P-VELOCITY (M/S.)	S-VELOCITY (M/S.)	DENSITY (G/ML)	1/Q P	1/Q S
74.4	1.460	0.000	1.03	0.00000	0.00000
6.1	1.480	0.010	1.65	0.01000	0.04000
3.4	1.934	0.532	2.00	0.00100	0.03000
3.4	1.953	0.537	2.00	0.00100	0.03000
3.4	1.972	0.542	2.00	0.00100	0.03000
3.5	1.991	0.547	2.00	0.00100	0.03000
3.5	2.009	0.553	2.00	0.00100	0.03000
3.5	2.028	0.559	2.00	0.00100	0.03000
3.6	2.047	0.563	2.00	0.00100	0.03000
3.6	2.066	0.568	2.00	0.00100	0.03000
	4.700	2.550	1.98	0.01000	0.06000

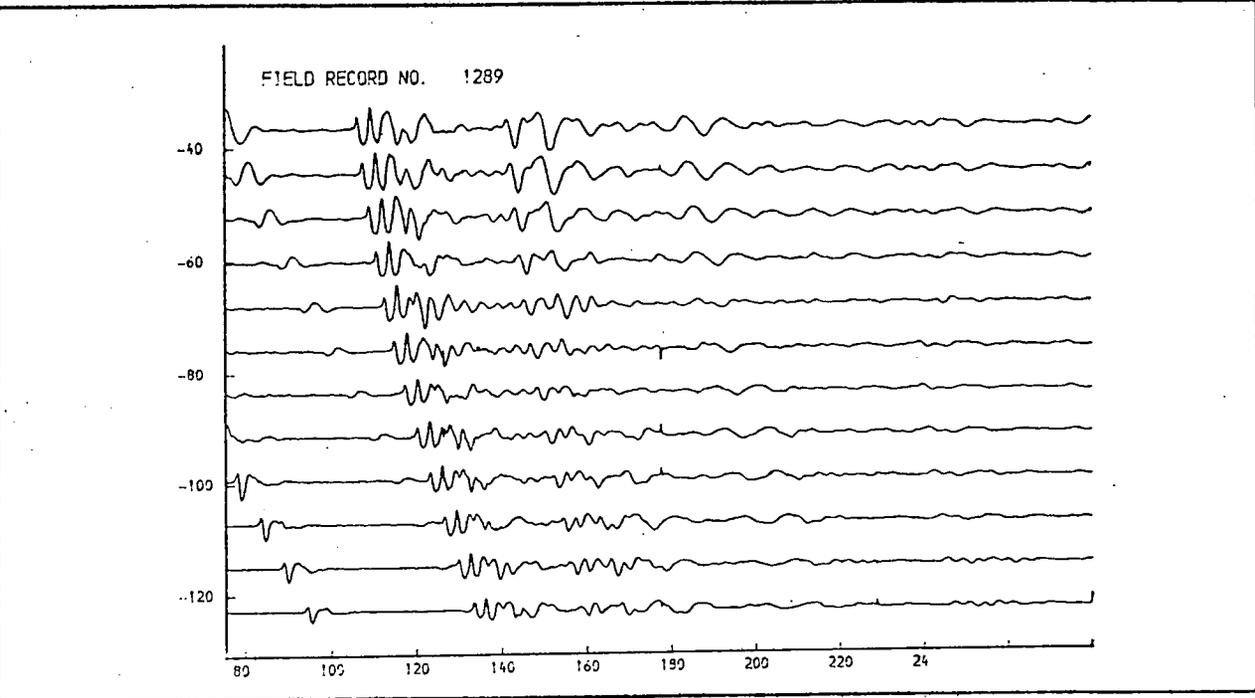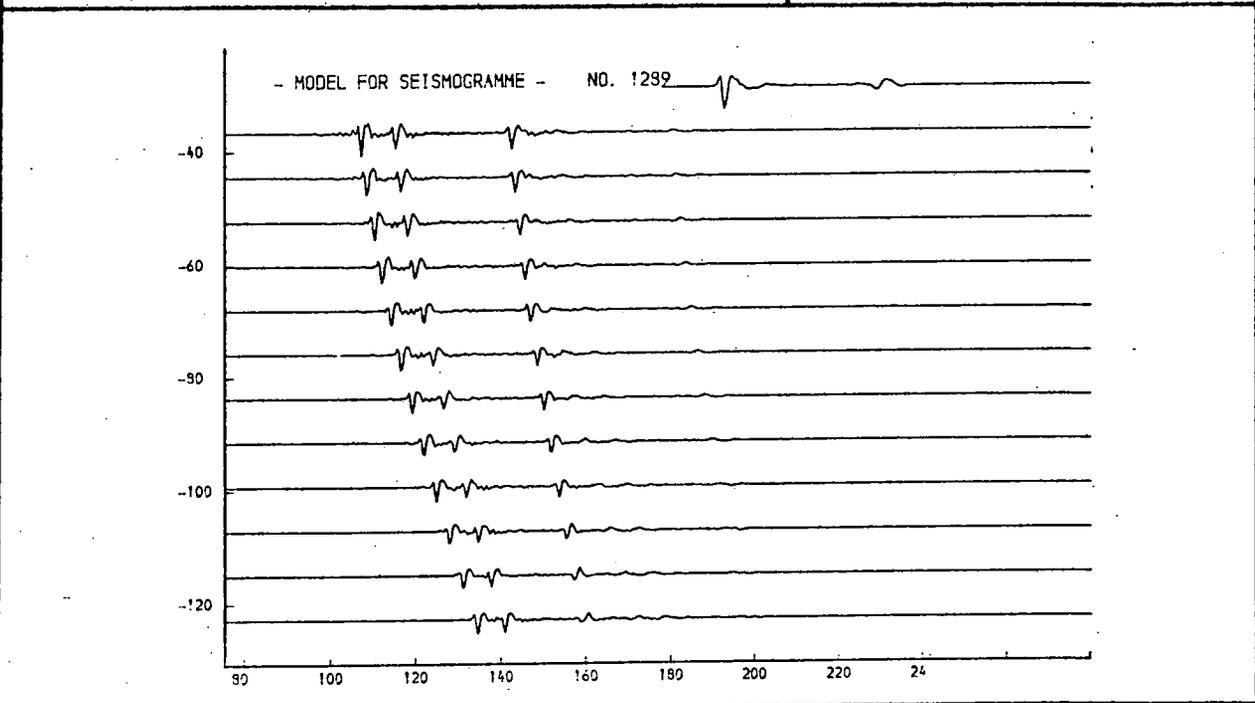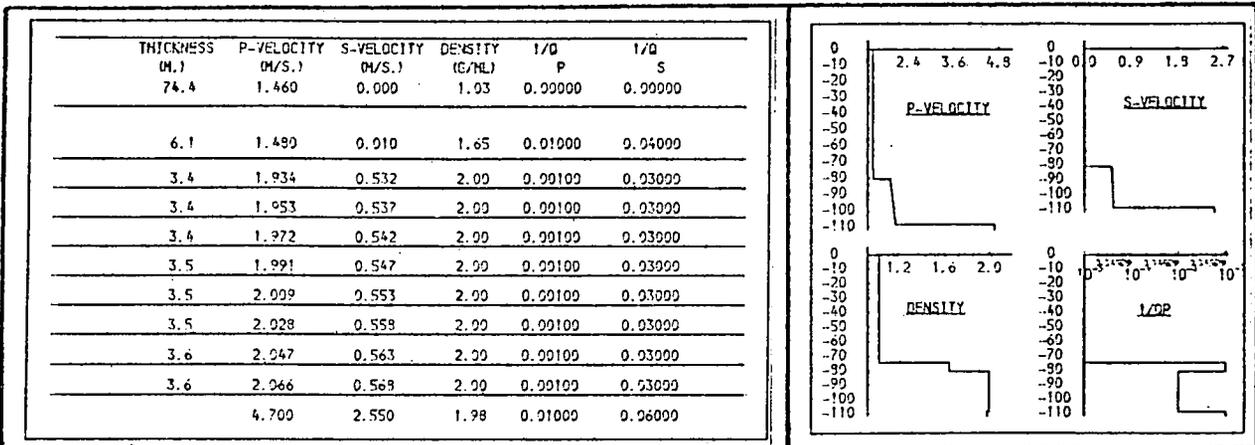- MODEL FOR SEISMOGRAMME - NO. 1289

FIELD RECORD NO. 1289

Fig. 9.24. Model for No. 1289.

Suggested model for seismogramme no. 1289, constructed in a wide frequency band (50 to 1000 Hz.). The possible value ranges for the parameters are discussed in the text and illustrated by the models shown in figs. 9.25 to 9.44 (see volume 2).

THICKNESS (M.)	P-VELOCITY (M/S.)	S-VELOCITY (M/S.)	DENSITY (G/ML)	1/Q P	1/Q S
74.4	1.460	0.000	1.03	0.00000	0.00000
5.7	1.400	0.010	1.65	0.02000	0.04000
3.9	2.084	0.533	2.00	0.00050	0.00100
3.9	2.103	0.538	2.00	0.00050	0.00100
3.9	2.122	0.543	2.00	0.00050	0.00100
3.9	2.141	0.549	2.00	0.00050	0.00100
3.9	2.159	0.552	2.00	0.00050	0.00100
3.9	2.178	0.557	2.00	0.00050	0.00100
4.0	2.197	0.562	2.00	0.00050	0.00100
4.0	2.216	0.567	2.00	0.00050	0.00100
	4.700	2.550	1.98	0.10000	0.20000

NO. 1289.   P. LAYER 1   P = 1.40
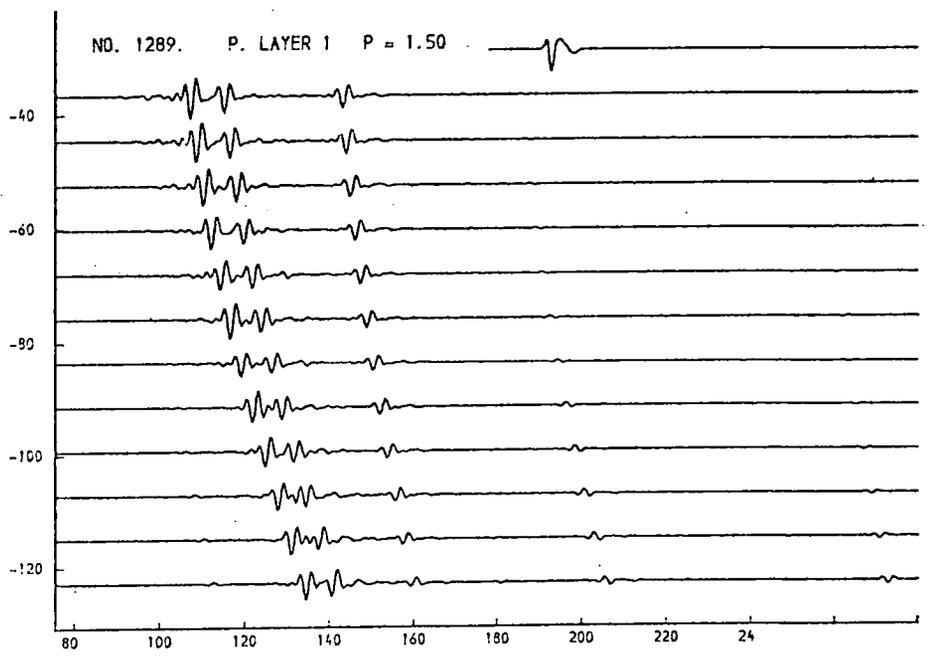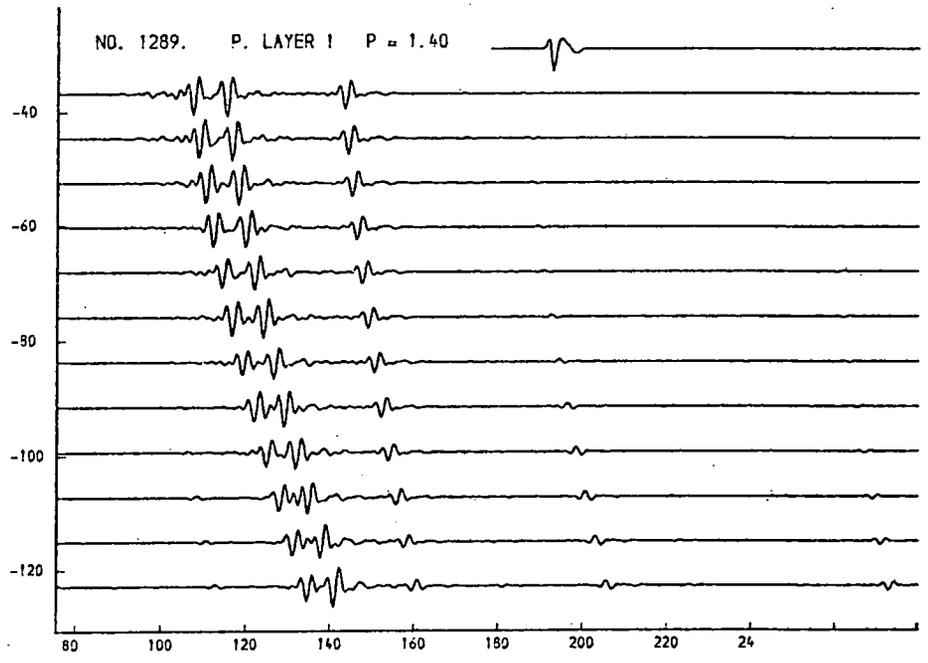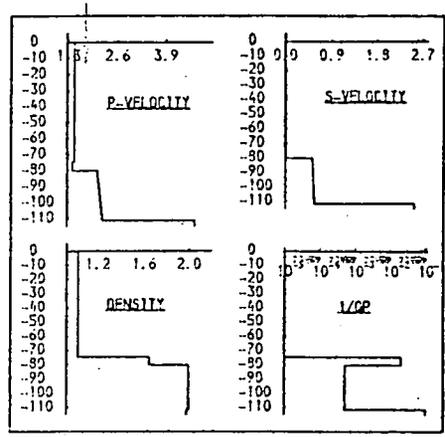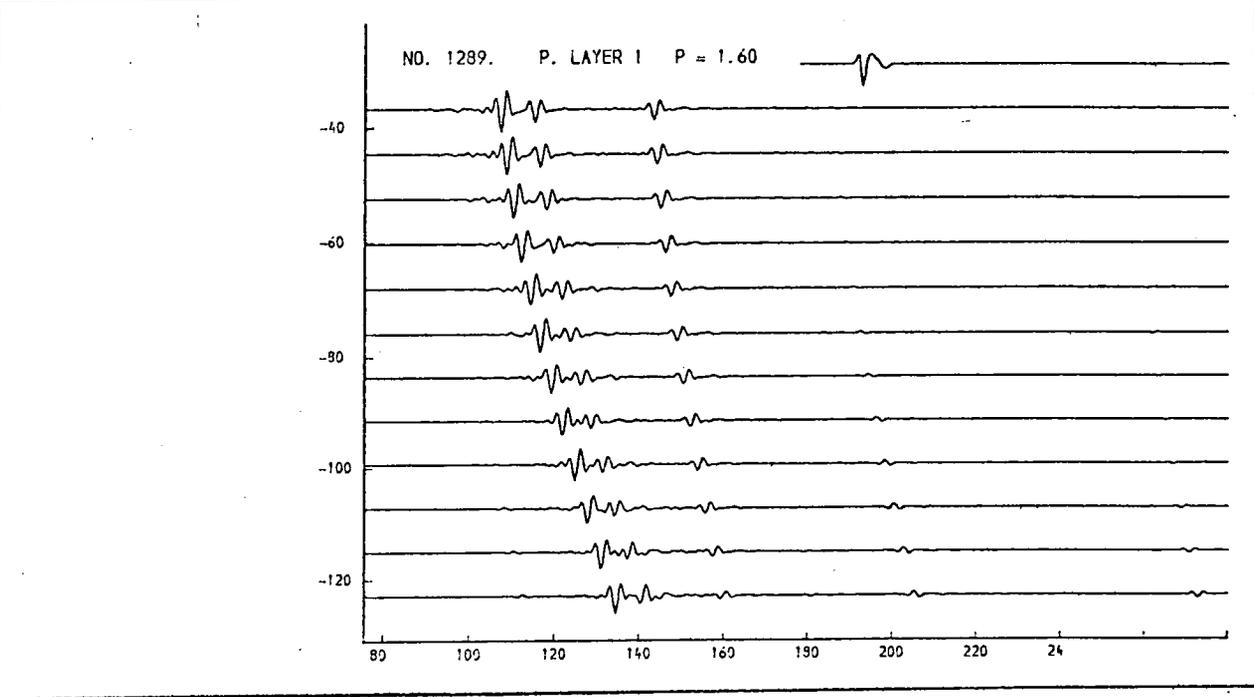
NO. 1289.   P. LAYER 1   P = 1.50

Fig. 9.25a. P-velocity, layer 1.

Layer 1 is barely resolved, and no exact fit for p-velocity is possible on the basis of fitting arrival times.

THICKNESS (M.)	P-VELOCITY (M/S.)	S-VELOCITY (M/S.)	DENSITY (G/ML)	1/Q P	1/Q S
74.4	1.460	0.000	1.03	0.00000	0.00000
6.3	1.550	0.010	1.65	0.02000	0.04000
3.9	2.084	0.533	2.00	0.00050	0.00100
3.9	2.103	0.538	2.00	0.00050	0.00100
3.9	2.122	0.543	2.00	0.00050	0.00100
3.9	2.141	0.548	2.00	0.00050	0.00100
3.9	2.159	0.552	2.00	0.00050	0.00100
3.9	2.178	0.557	2.00	0.00050	0.00100
4.0	2.197	0.562	2.00	0.00050	0.00100
4.0	2.216	0.567	2.00	0.00050	0.00100
	4.700	2.550	1.93	0.10000	0.20000

NO. 1289.   P. LAYER 1   P = 1.55
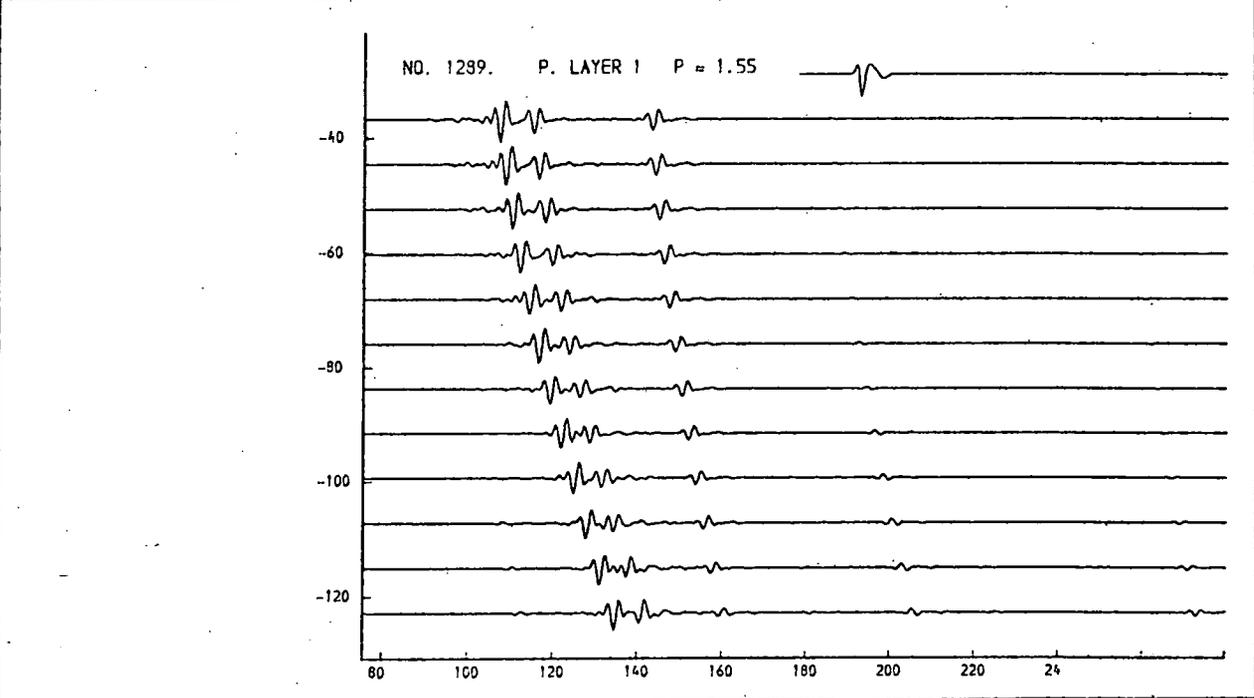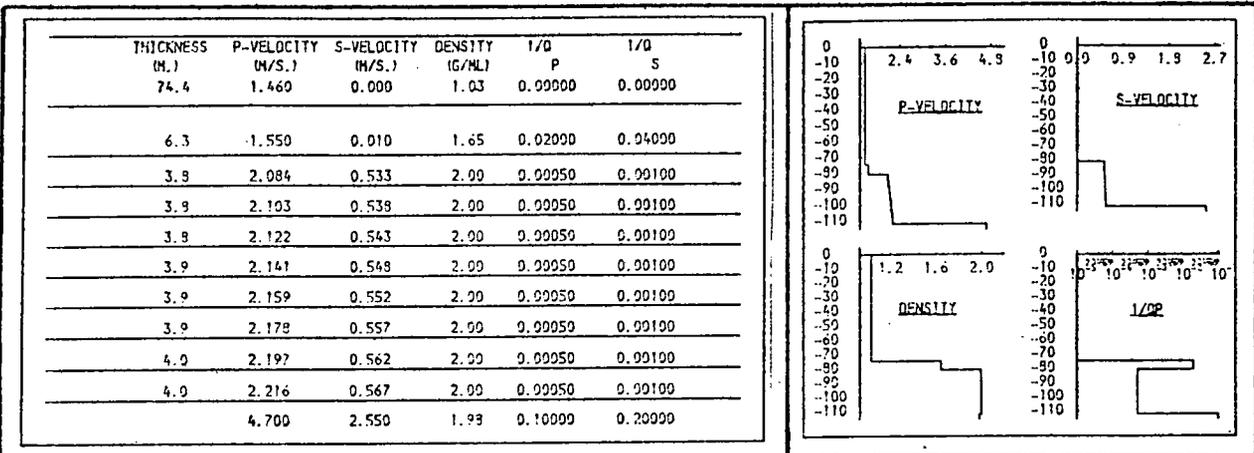
NO. 1289.   P. LAYER 1   P = 1.60

Fig. 9.25b.   P-velocity, layer 1.

Layer 1 is barely resolved, and no exact fit for p-velocity is possible on the basis of fitting arrival times.

THICKNESS (M.)	P-VELOCITY (M/S.)	S-VELOCITY (M/S.)	DENSITY (G/ML)	1/Q P	1/Q S
74.4	1.460	0.000	1.03	0.00000	0.00000
6.0	1.480	0.001	1.65	0.02000	0.04000
3.8	2.084	0.533	2.00	0.00050	0.00100
3.8	2.103	0.539	2.00	0.00050	0.00100
3.8	2.122	0.543	2.00	0.00050	0.00100
3.9	2.141	0.545	2.00	0.00050	0.00100
3.9	2.159	0.552	2.00	0.00050	0.00100
3.9	2.178	0.557	2.00	0.00050	0.00100
4.0	2.197	0.562	2.00	0.00050	0.00100
4.0	2.216	0.567	2.00	0.00050	0.00100
	4.700	2.559	1.95	0.10000	0.20000

NO. 1289.   S. LAYER 1   S = 0.001
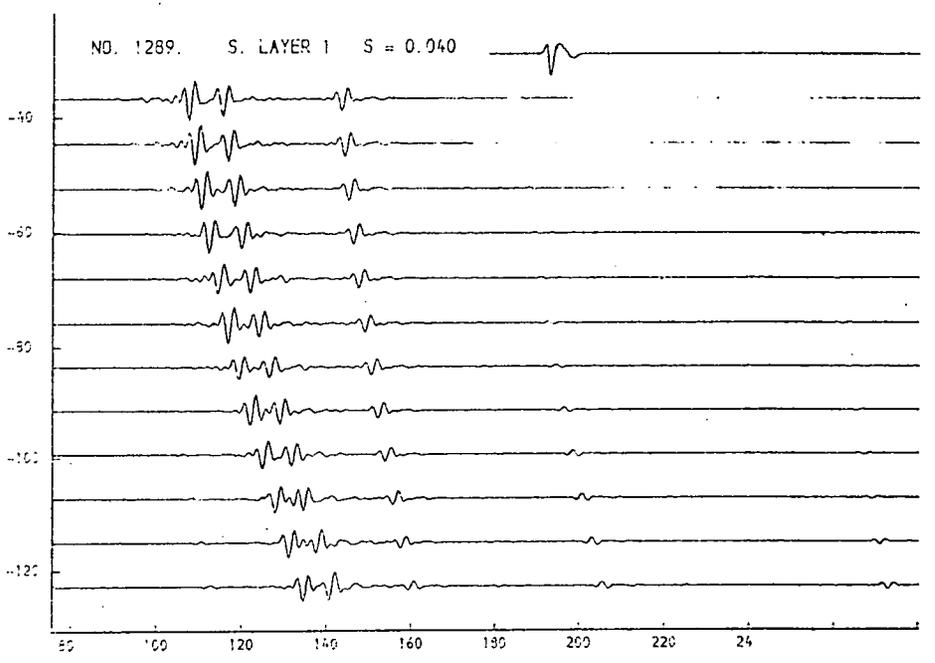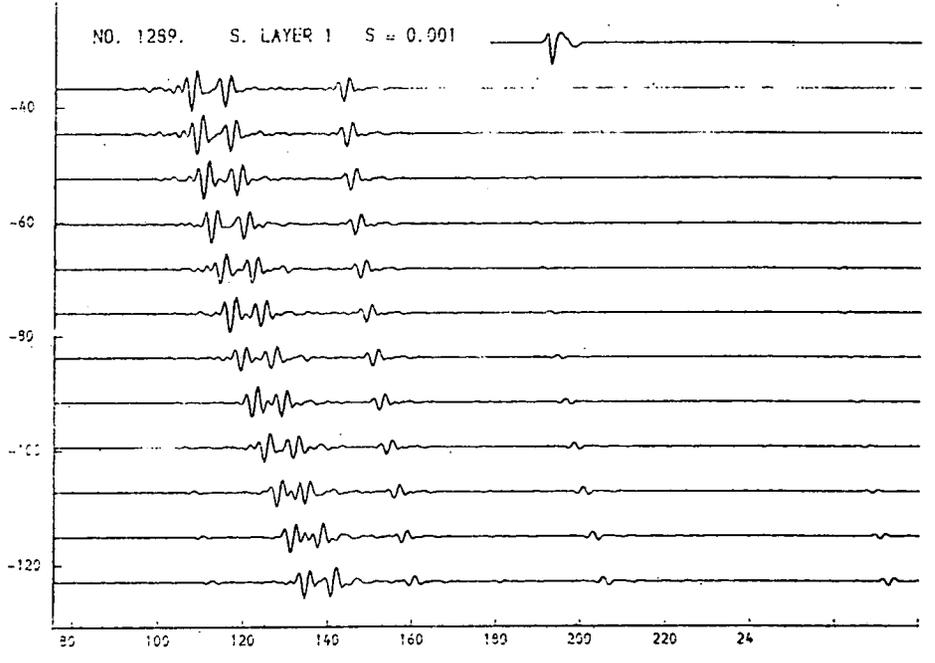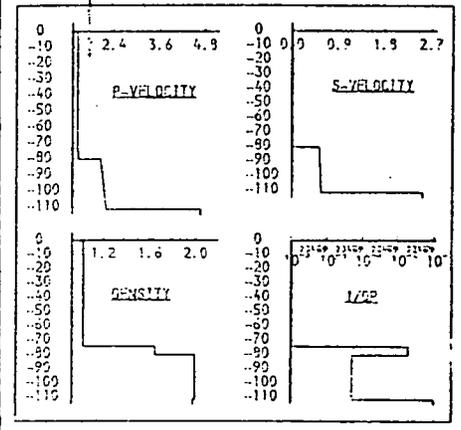
NO. 1289.   S. LAYER 1   S = 0.040

Fig. 9.26a. S-velocity, layer 1.

The model appears insensitive to reasonable changes in the s-velocity in layer 1 between 1 and 200m./sec.

THICKNESS (M.)	P-VELOCITY (M/S.)	S-VELOCITY (M/S.)	DENSITY (G/ML)	1/Q P	1/Q S
74.4	1.460	0.000	1.03	0.00000	0.00000
6.0	1.480	0.200	1.65	0.02000	0.04000
3.9	2.084	0.533	2.00	0.00050	0.00100
3.9	2.103	0.538	2.00	0.00050	0.00100
3.9	2.122	0.543	2.00	0.00050	0.00100
3.9	2.141	0.548	2.00	0.00050	0.00100
3.9	2.159	0.552	2.00	0.00050	0.00100
3.9	2.178	0.557	2.00	0.00050	0.00100
4.0	2.197	0.562	2.00	0.00050	0.00100
4.0	2.216	0.567	2.00	0.00050	0.00100
	4.700	2.550	1.99	0.10000	0.20000

NO. 1289.   S. LAYER 1   S = 0.100
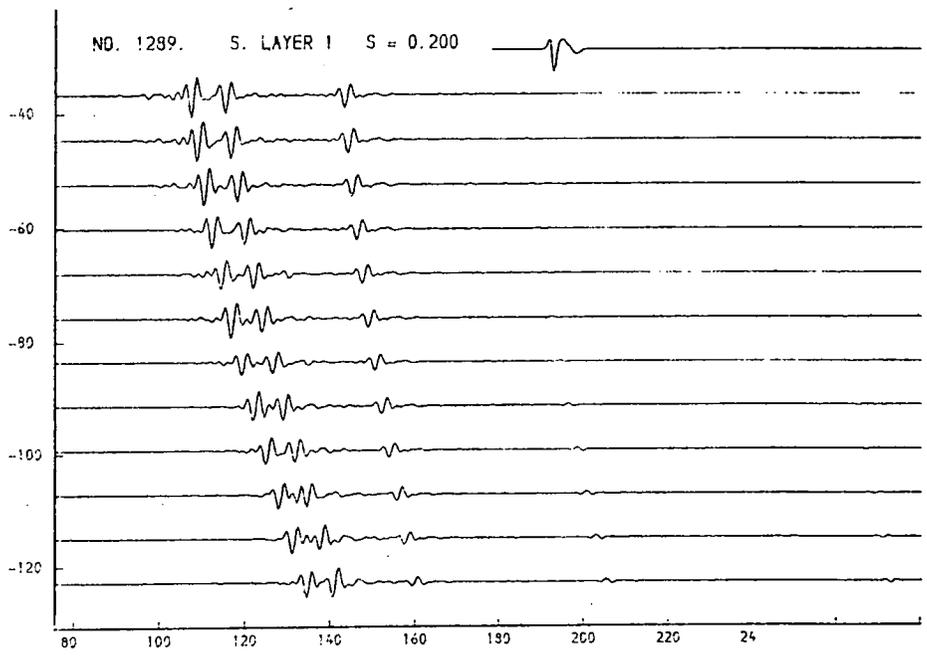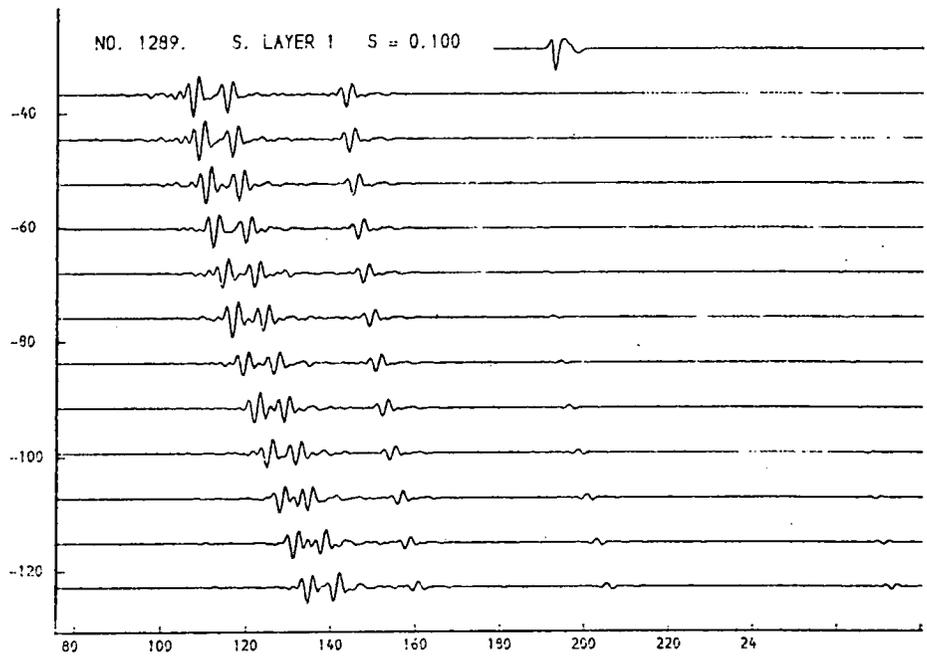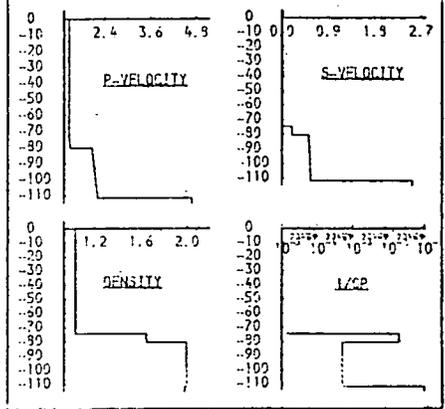
NO. 1289.   S. LAYER 1   S = 0.200

Fig. 9.26b.   S-velocity, layer 1.

The model appears insensitive to reasonable changes in the s-velocity in layer 1 between 1 and 200m./sec.

THICKNESS (M.)	P-VELOCITY (M/S.)	S-VELOCITY (M/S.)	DENSITY (G/ML)	1/Q P	1/Q S
74.4	1.460	0.000	1.03	0.00000	0.00000
6.0	1.480	0.010	1.55	0.02000	0.04000
3.9	2.084	0.533	2.00	0.00050	0.00100
3.9	2.103	0.538	2.00	0.00050	0.00100
3.9	2.122	0.543	2.00	0.00050	0.00100
3.9	2.141	0.548	2.00	0.00050	0.00100
3.9	2.159	0.552	2.00	0.00050	0.00100
3.9	2.178	0.557	2.00	0.00050	0.00100
4.0	2.197	0.562	2.00	0.00050	0.00100
4.0	2.216	0.567	2.00	0.00050	0.00100
	4.700	2.550	1.99	0.10000	0.20000

NO. 1289. DENSITY LAYER 1 RH = 1.55
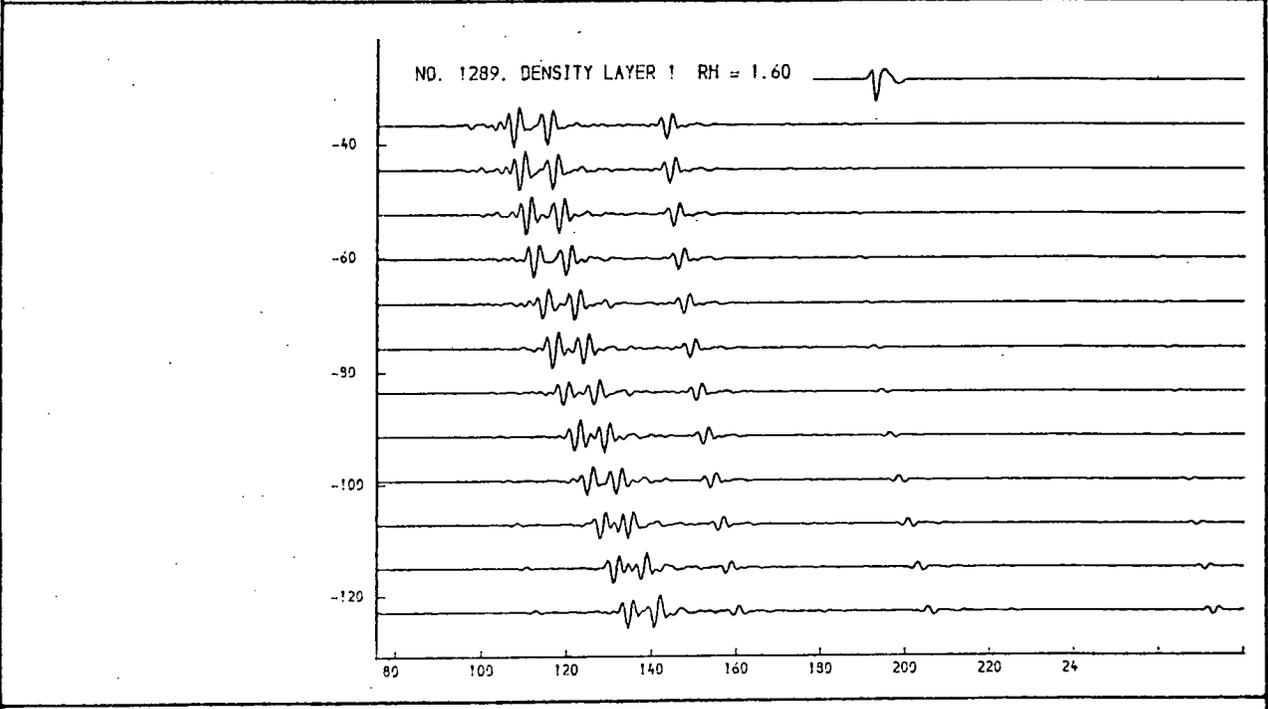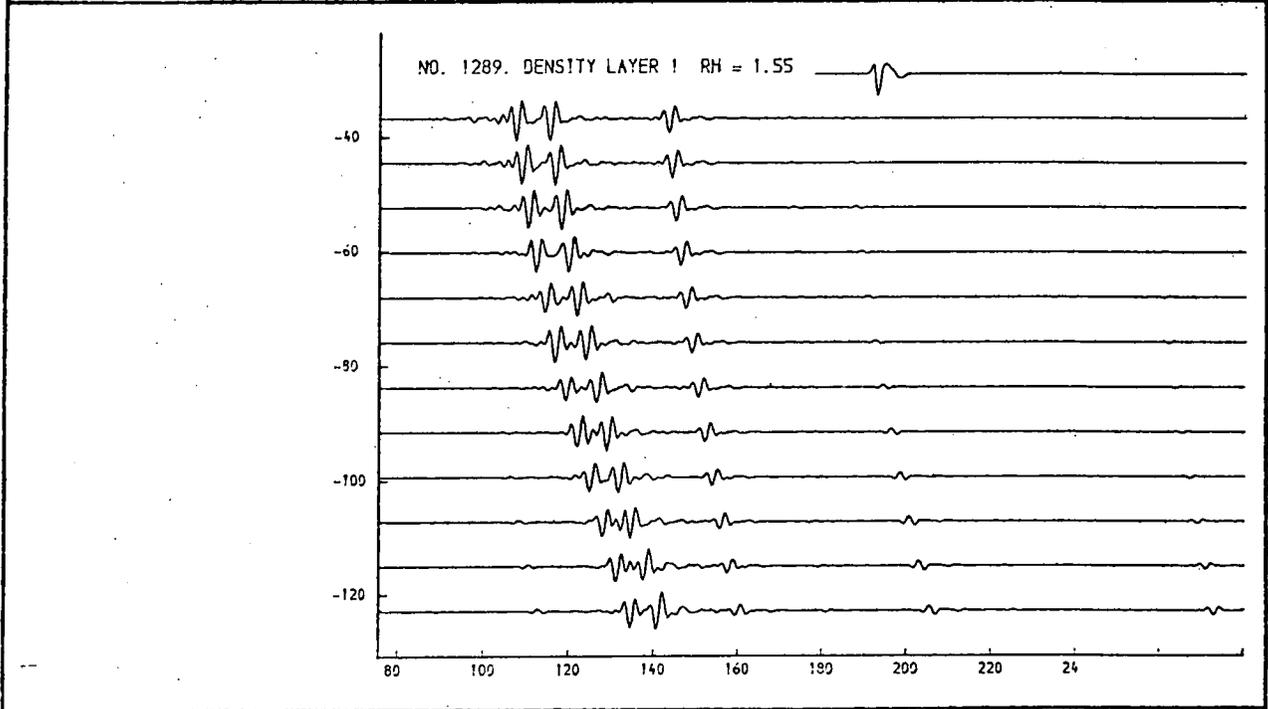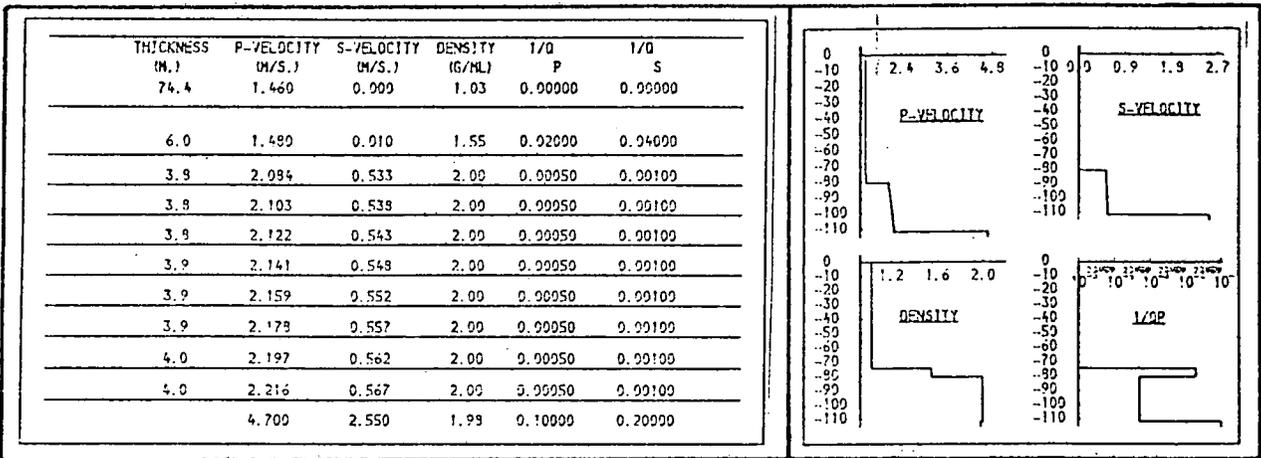
NO. 1289. DENSITY LAYER 1 RH = 1.60

Fig. 9.27a. Density, layer 1.

Density affects the overall amplitude of reflectors, but has little influence on its relative variation with offset distance.

THICKNESS (M.)	P-VELOCITY (M/S.)	S-VELOCITY (M/S.)	DENSITY (G/ML)	1/Q P	1/Q S
74.4	1.460	0.000	1.03	0.00000	0.00000
6.0	1.480	0.010	1.70	0.02000	0.04000
3.9	2.084	0.533	2.00	0.00050	0.00100
3.8	2.103	0.538	2.00	0.00050	0.00100
3.9	2.122	0.543	2.00	0.00050	0.00100
3.9	2.141	0.548	2.00	0.00050	0.00100
3.9	2.159	0.552	2.00	0.00050	0.00100
3.9	2.179	0.557	2.00	0.00050	0.00100
4.0	2.197	0.562	2.00	0.00050	0.00100
4.0	2.216	0.567	2.00	0.00050	0.00100
	4.700	2.550	1.99	0.10000	0.20000

NO. 1289. DENSITY LAYER 1   RH = 1.70
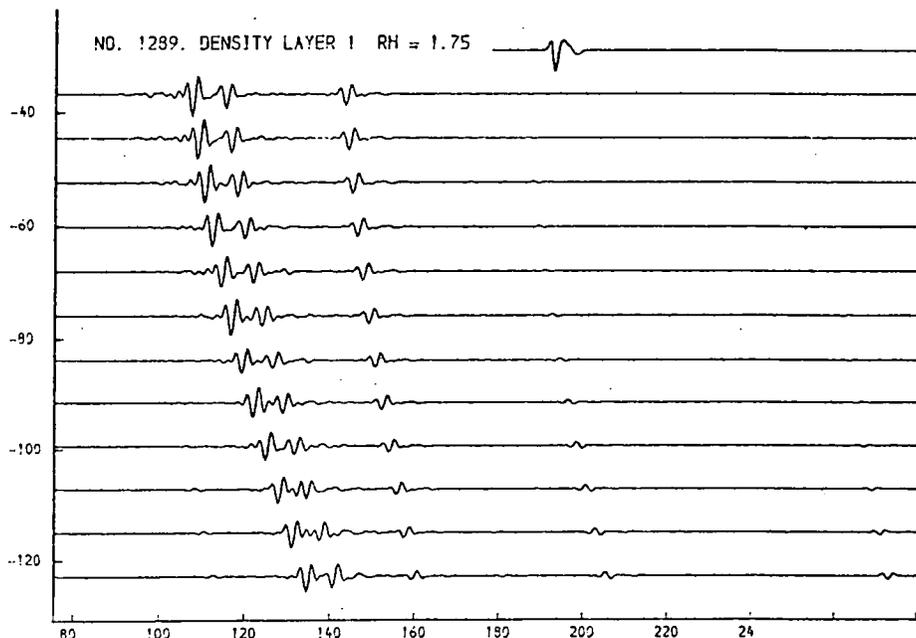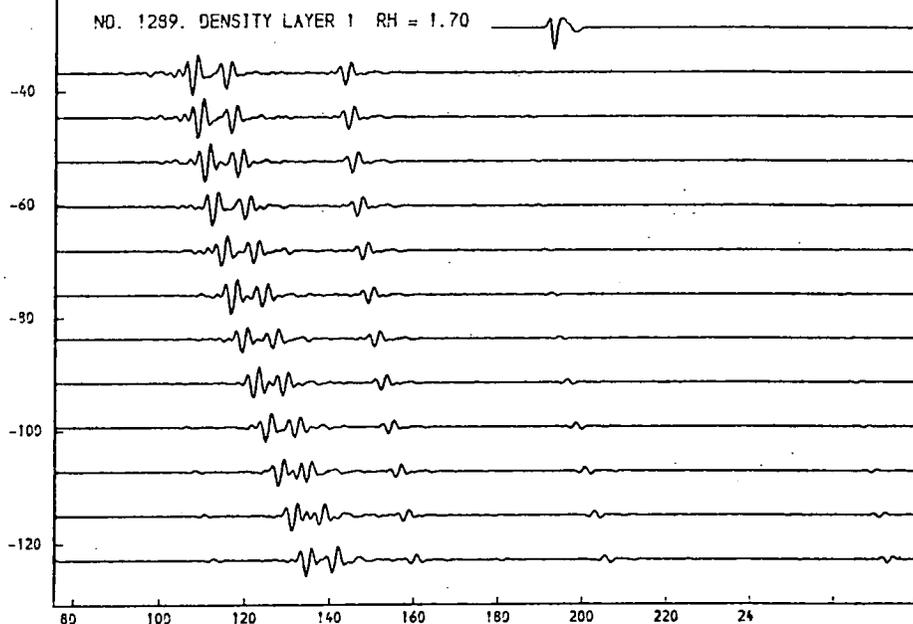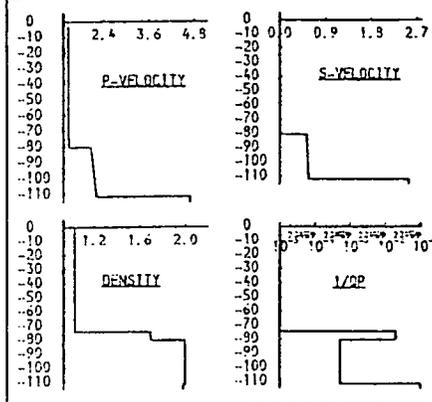
NO. 1289. DENSITY LAYER 1   RH = 1.75

Fig. 9.27b.   Density, layer 1.

Density affects the overall amplitude of reflectors, but has little influence on its relative variation with offset distance.

THICKNESS (M.)	P-VELOCITY (M/S.)	S-VELOCITY (M/S.)	DENSITY (G/ML)	1/Q P	1/Q S
74.4	1.460	0.000	1.03	0.00000	0.00000
6.1	1.480	0.010	1.65	0.00100	0.04000
3.7	1.934	0.532	2.00	0.00100	0.03000
3.9	1.953	0.537	2.00	0.00100	0.03000
3.9	1.972	0.542	2.00	0.00100	0.03000
3.8	1.991	0.547	2.00	0.00100	0.03000
3.9	2.009	0.553	2.00	0.00100	0.03000
3.9	2.028	0.559	2.00	0.00100	0.03000
3.9	2.047	0.563	2.00	0.00100	0.03000
4.0	2.066	0.569	2.00	0.00100	0.03000
	4.700	2.550	1.99	0.03000	0.06000

-ATTEN LAYER 1-   1/QP = 0.001 NO. 1289
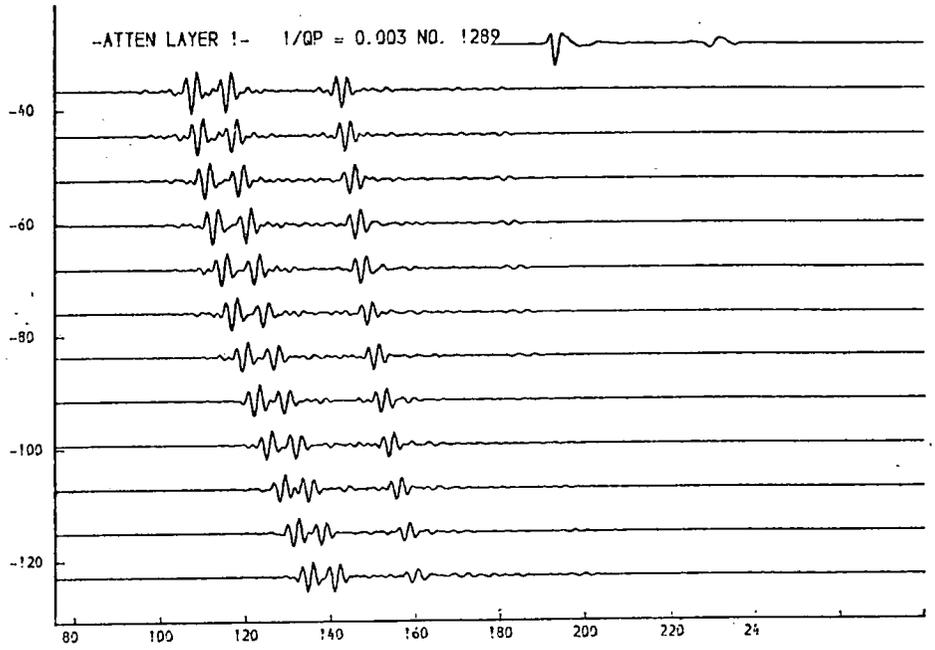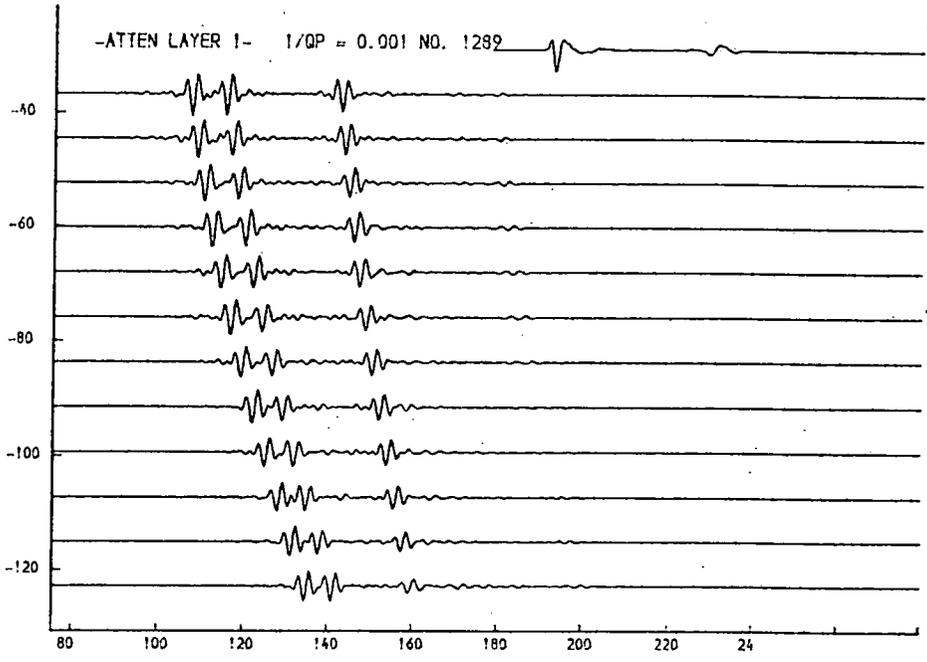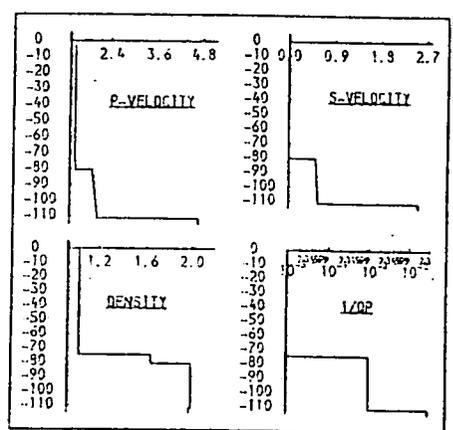
-ATTEN LAYER 1-   1/QP = 0.003 NO. 1289

Fig. 9.28a. 1/Qp, layer 1.

The effect of attenuation on reflectors r1 and r2.

THICKNESS (M.)	P-VELOCITY (M/S.)	S-VELOCITY (M/S.)	DENSITY (G/ML)	1/Q P	1/Q S
74.4	1.460	0.000	1.03	0.00000	0.00000
6.1	1.480	0.010	1.65	0.01000	0.04000
3.7	1.934	0.532	2.00	0.00100	0.03000
3.8	1.953	0.537	2.00	0.00100	0.03000
3.9	1.972	0.542	2.00	0.00100	0.03000
3.9	1.991	0.547	2.00	0.00100	0.03000
3.9	2.009	0.553	2.00	0.00100	0.03000
3.9	2.028	0.559	2.00	0.00100	0.03000
3.9	2.047	0.563	2.00	0.00100	0.03000
4.0	2.066	0.569	2.00	0.00100	0.03000
	4.700	2.550	1.95	0.03000	0.06000

-ATTEN LAYER 1-   1/QP = 0.01   NO. 1289
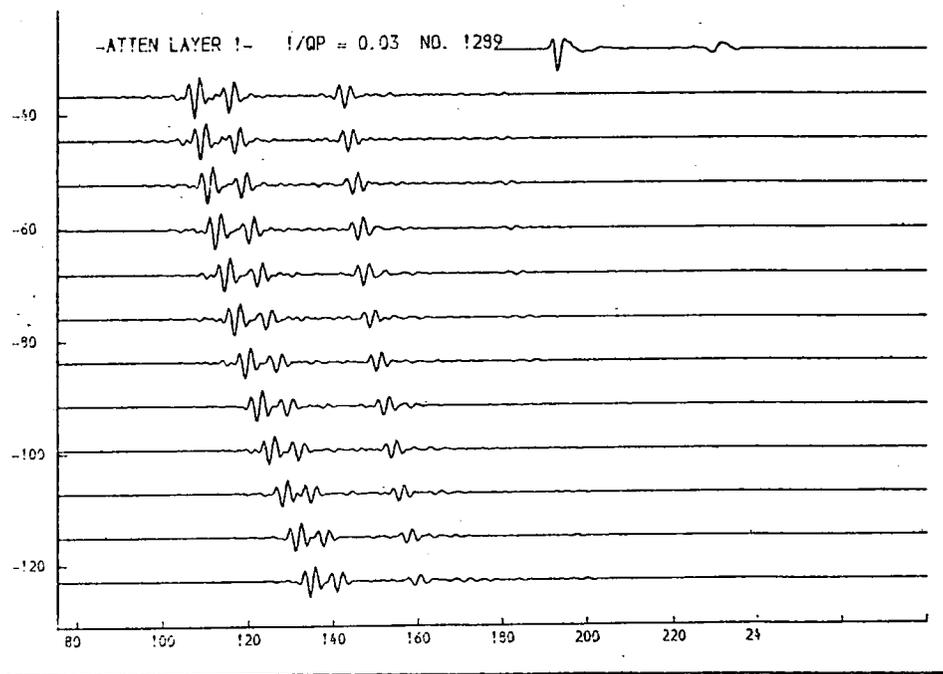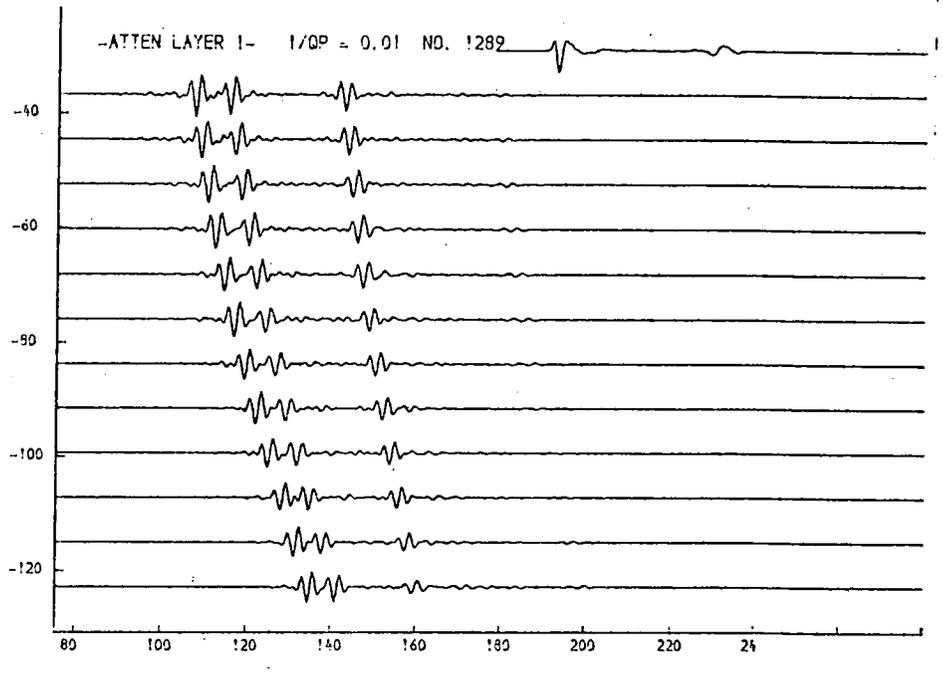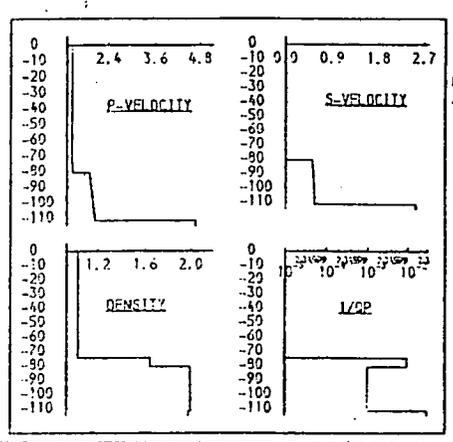
-ATTEN LAYER 1-   1/QP = 0.03   NO. 1299

Fig. 9.28b. 1/Qp, layer 1.

The effect of attenuation on reflectors r1 and r2.

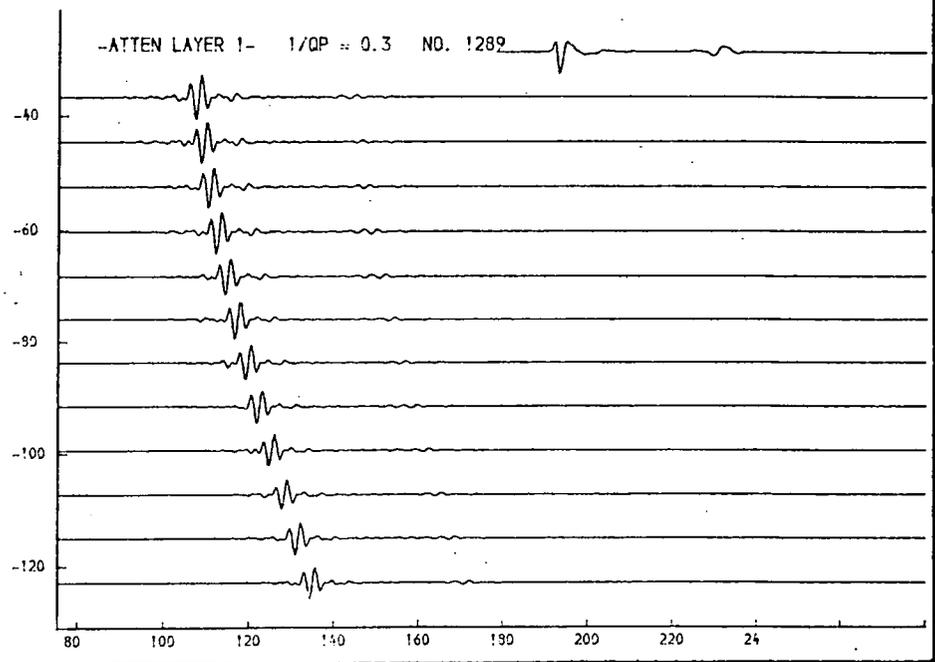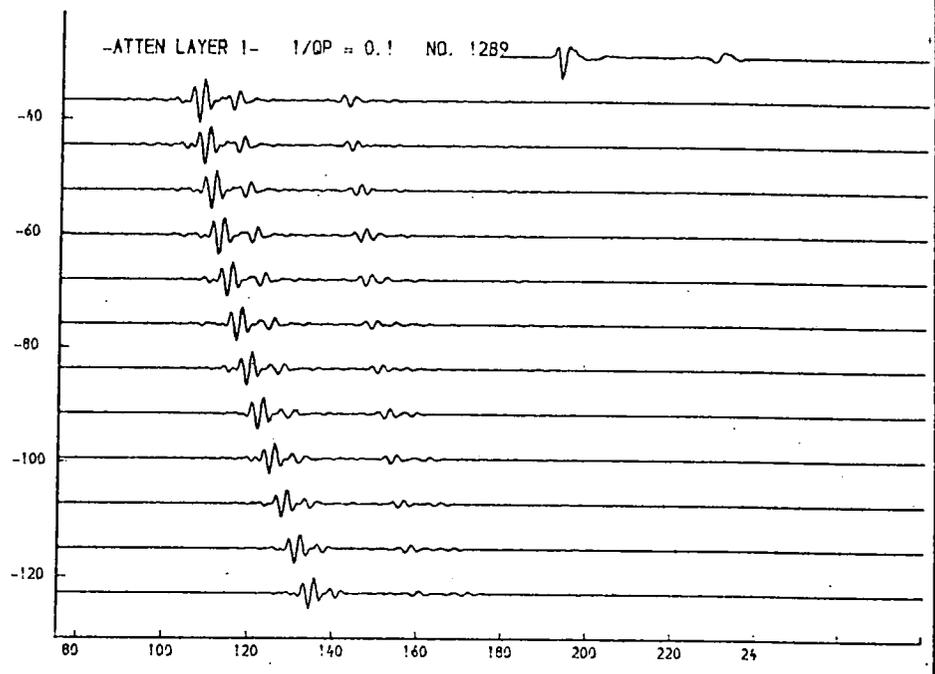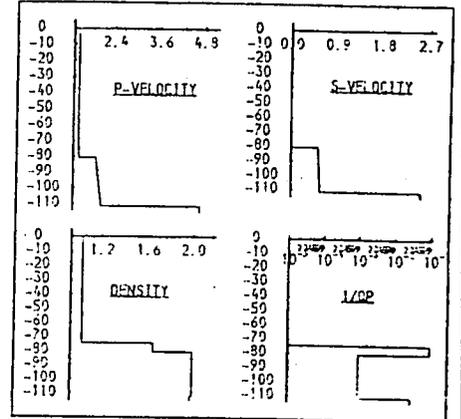| THICKNESS (M.)	P-VELOCITY (M/S.)	S-VELOCITY (M/S.)	DENSITY (G/ML)	1/Q P	1/Q S
74.4	1.460	0.000	1.03	0.00000	0.00000
6.1	1.480	0.010	1.65	0.10000	0.04000
3.7	1.934	0.532	2.00	0.00100	0.03000
3.8	1.953	0.537	2.00	0.00100	0.03000
3.8	1.972	0.542	2.00	0.00100	0.03000
3.9	1.991	0.547	2.00	0.00100	0.03000
3.9	2.009	0.553	2.00	0.00100	0.03000
3.9	2.028	0.558	2.00	0.00100	0.03000
3.9	2.047	0.563	2.00	0.00100	0.03000
4.0	2.066	0.568	2.00	0.00100	0.03000
	4.700	2.550	1.99	0.03000	0.06000

Fig. 9.28c. 1/Qp, layer 1.

The effect of attenuation on reflectors r1 and r2.

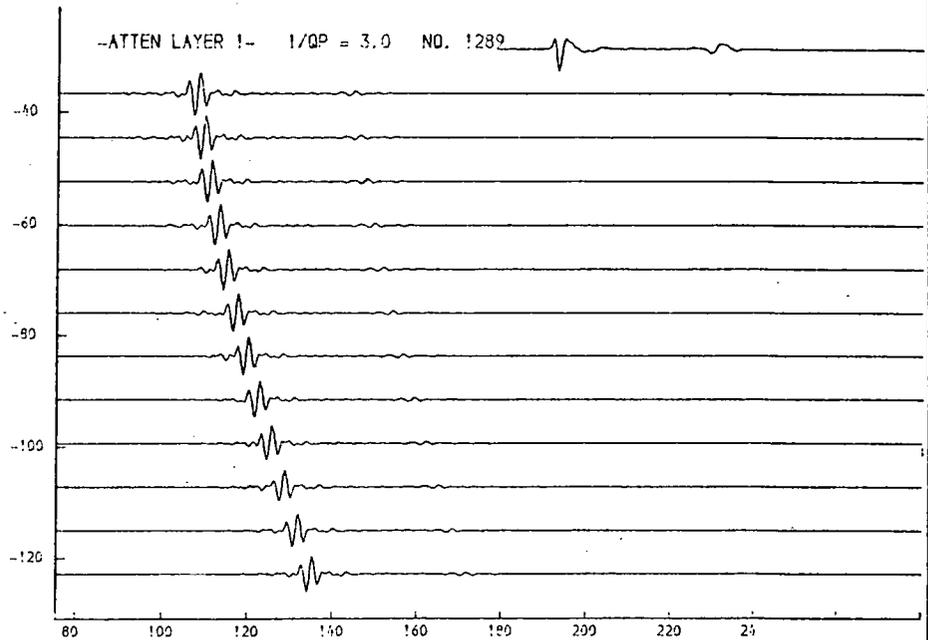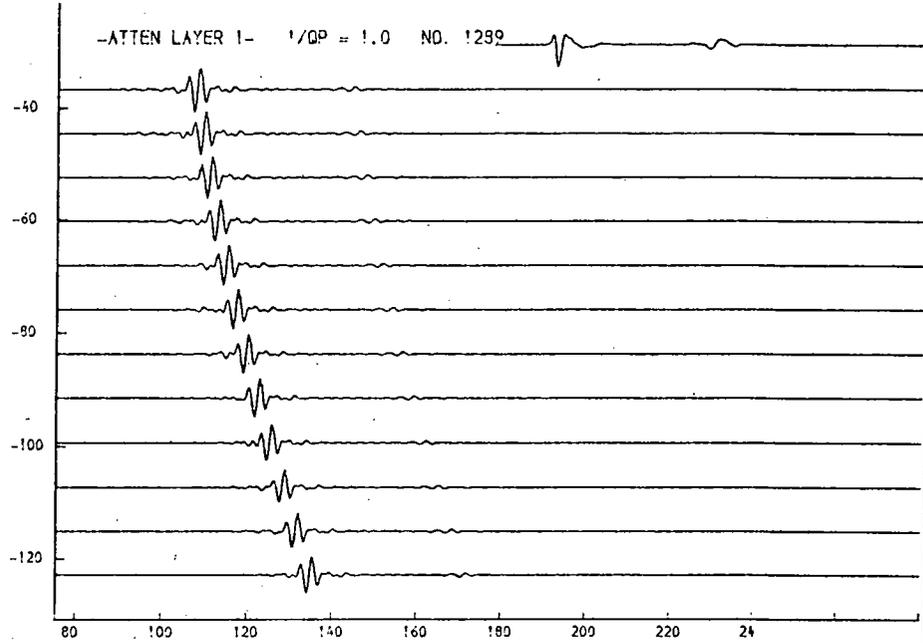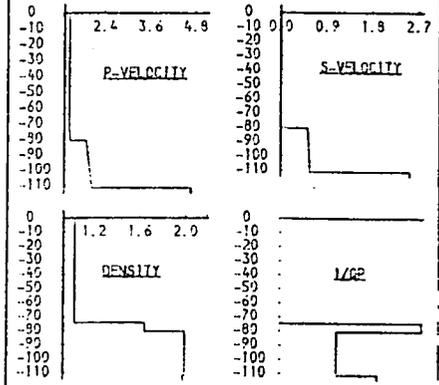| THICKNESS (M.)	P-VELOCITY (M/S.)	S-VELOCITY (M/S.)	DENSITY (G/ML)	1/Q P	1/Q S
74.4	1.460	0.000	1.03	0.00000	0.00000
6.1	1.480	0.010	1.65	1.00000	0.04000
3.7	1.934	0.532	2.00	0.00100	0.03000
3.9	1.953	0.537	2.00	0.00100	0.03000
3.9	1.972	0.542	2.00	0.00100	0.03000
3.9	1.991	0.547	2.00	0.00100	0.03000
3.9	2.009	0.553	2.00	0.00100	0.03000
3.9	2.028	0.559	2.00	0.00100	0.03000
3.9	2.047	0.563	2.00	0.00100	0.03000
4.0	2.066	0.569	2.00	0.00100	0.03000
	4.700	2.550	1.98	0.03000	0.06000

Fig. 9.28d. 1/Qp, layer 1.

The effect of attenuation on reflectors r1 and r2.

THICKNESS (M.)	P-VELOCITY (M/S.)	S-VELOCITY (M/S.)	DENSITY (G/ML)	1/Q P	1/Q S
74.4	1.460	0.000	1.03	0.00000	0.00000
6.1	1.480	0.010	1.65	0.02000	0.00100
3.7	1.934	0.532	2.00	0.00100	0.03000
3.8	1.953	0.537	2.00	0.00100	0.03000
3.8	1.972	0.542	2.00	0.00100	0.03000
3.8	1.991	0.547	2.00	0.00100	0.03000
3.9	2.009	0.553	2.00	0.00100	0.03000
3.9	2.028	0.559	2.00	0.00100	0.03000
3.9	2.047	0.563	2.00	0.00100	0.03000
4.0	2.066	0.569	2.00	0.00100	0.03000
	4.700	2.550	1.99	0.03000	0.06000

- S-ATTEN LAYER 1 1/QS = 0.001 NO. 1289

- S-ATTEN LAYER 1 1/QS = 0.01 NO. 1289

Fig. 9.29a 1/Qs, layer 1.

THICKNESS (M.)	P-VELOCITY (M/S.)	S-VELOCITY (M/S.)	DENSITY (G/ML)	1/Q P	1/Q S
74.4	1.460	0.000	1.03	0.00000	0.00000
6.1	1.480	0.910	1.65	0.02000	0.10000
3.7	1.934	0.532	2.00	0.00100	0.03000
3.9	1.953	0.537	2.00	0.00100	0.03000
3.9	1.972	0.542	2.00	0.00100	0.03000
3.9	1.991	0.547	2.00	0.00100	0.03000
3.9	2.009	0.553	2.00	0.00100	0.03000
3.9	2.028	0.558	2.00	0.00100	0.03000
3.9	2.047	0.563	2.00	0.00100	0.03000
4.0	2.066	0.569	2.00	0.00100	0.03000
	4.700	2.550	1.99	0.03000	0.06000

Fig. 9.29b 1/Qs, layer 1.

THICKNESS (M.)	P-VELOCITY (M/S.)	S-VELOCITY (M/S.)	DENSITY (G/ML)	1/Q P	1/Q S
74.4	1.460	0.000	1.03	0.00000	0.00000
6.1	1.480	0.010	1.65	0.00100	0.04000
3.7	1.984	0.532	2.00	0.00100	0.03000
3.8	2.003	0.537	2.00	0.00100	0.03000
3.8	2.022	0.542	2.00	0.00100	0.03000
3.9	2.041	0.547	2.00	0.00100	0.03000
3.9	2.059	0.553	2.00	0.00100	0.03000
3.9	2.078	0.559	2.00	0.00100	0.03000
3.9	2.097	0.563	2.00	0.00100	0.03000
4.0	2.116	0.569	2.00	0.00100	0.03000
	4.700	2.550	1.98	0.03000	0.06000

- P - LAYER 2   P = 2.05   NO. 1289

- P - LAYER 2   P = 2.10   NO. 1289

Fig. 9.30a. P-velocity, layer 2.

The reflector r2 is well-resolved and a value for p-velocity is found by fitting arrival times.

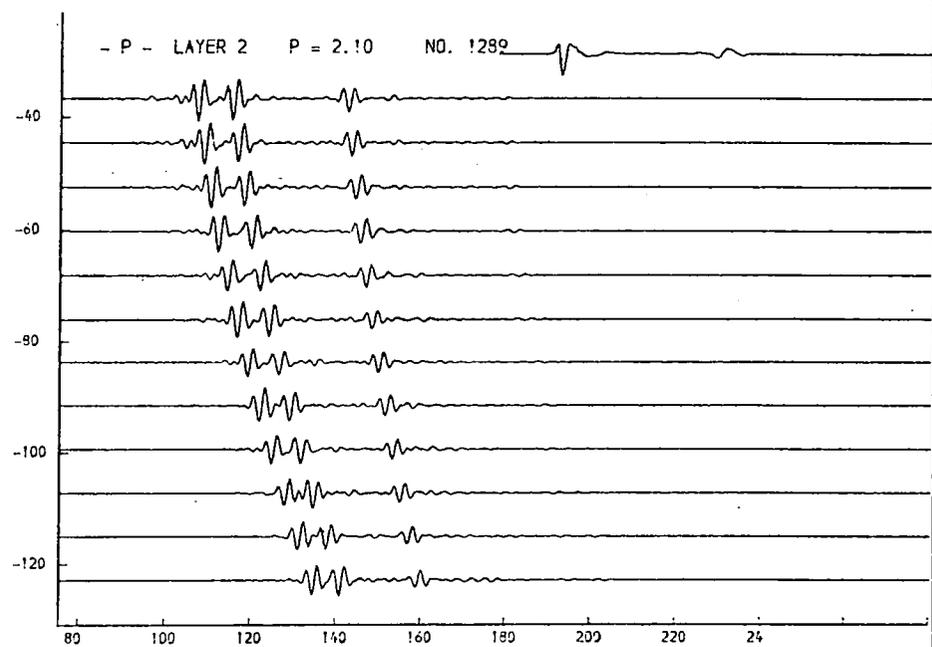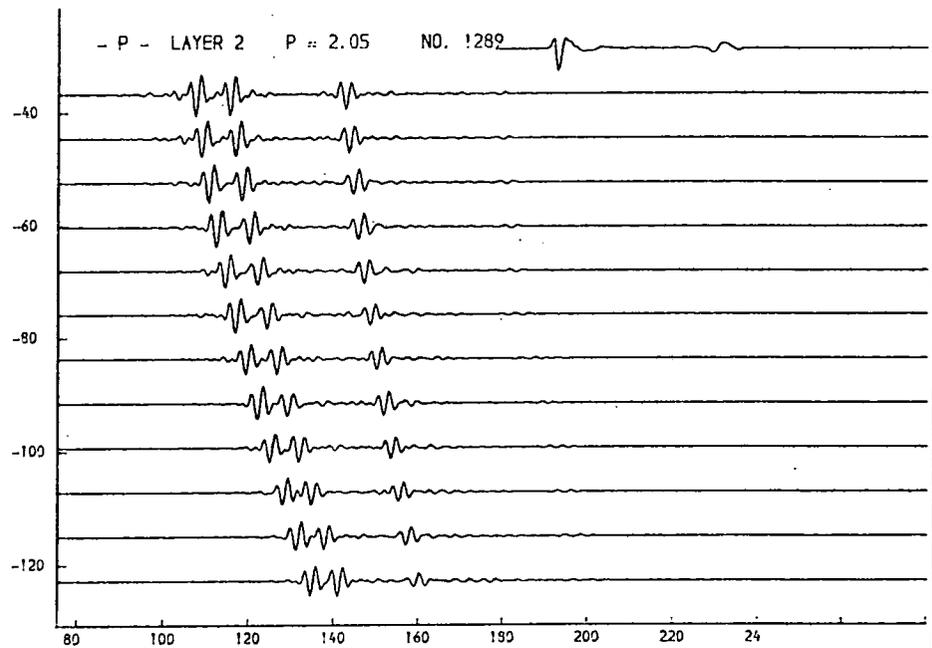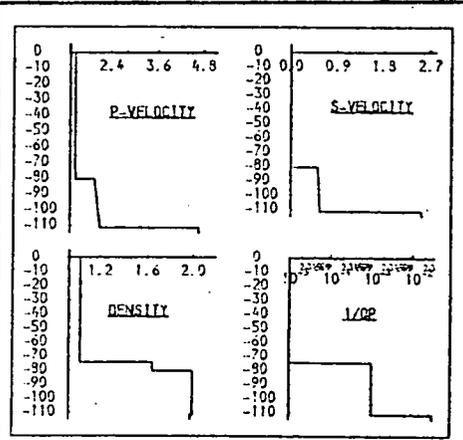| THICKNESS (M.)	P-VELOCITY (M/S.)	S-VELOCITY (M/S.)	DENSITY (G/ML)	1/Q P	1/Q S
74.4	1.460	0.000	1.03	0.00000	0.00000
6.1	1.490	0.010	1.65	0.00100	0.04000
3.7	1.934	0.531	2.00	0.00100	0.03000
3.3	1.953	0.536	2.00	0.00100	0.03000
3.8	1.972	0.542	2.00	0.00100	0.03000
3.8	1.991	0.547	2.00	0.00100	0.03000
3.9	1.909	0.553	2.00	0.00100	0.03000
3.9	1.923	0.558	2.00	0.00100	0.03000
3.9	1.947	0.564	2.00	0.00100	0.03000
4.9	1.966	0.569	2.00	0.00100	0.03000
	4.700	2.550	1.93	0.03000	0.06000
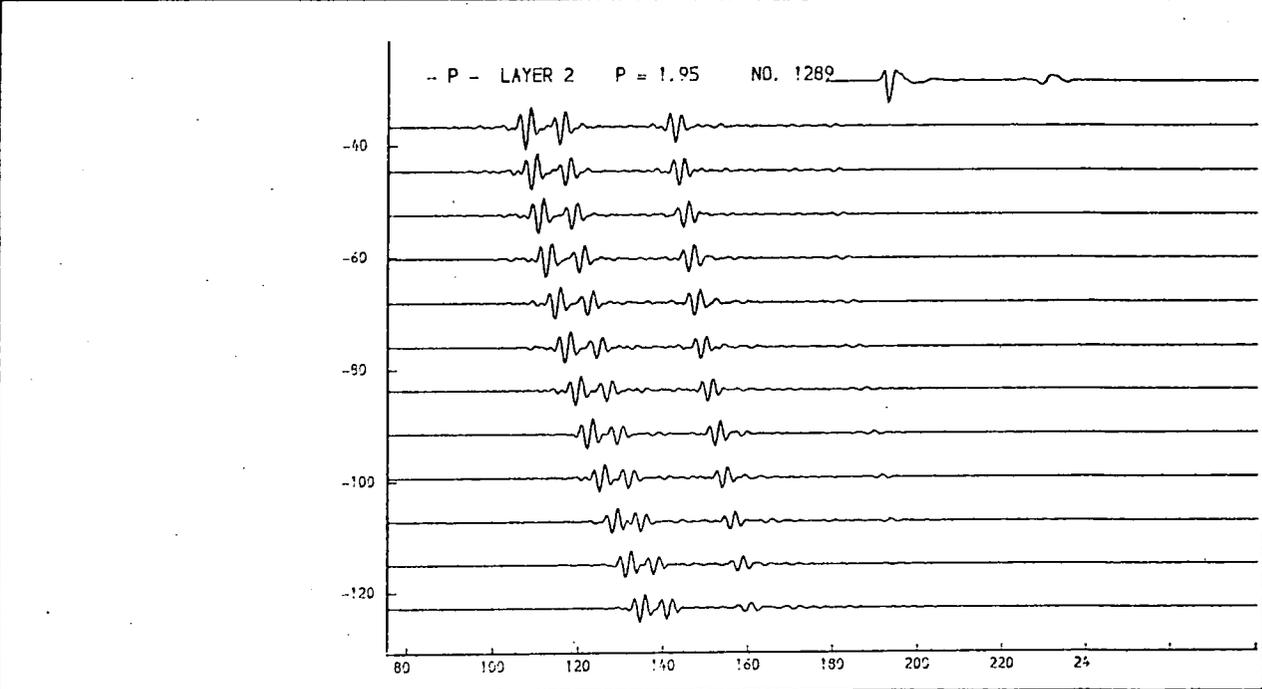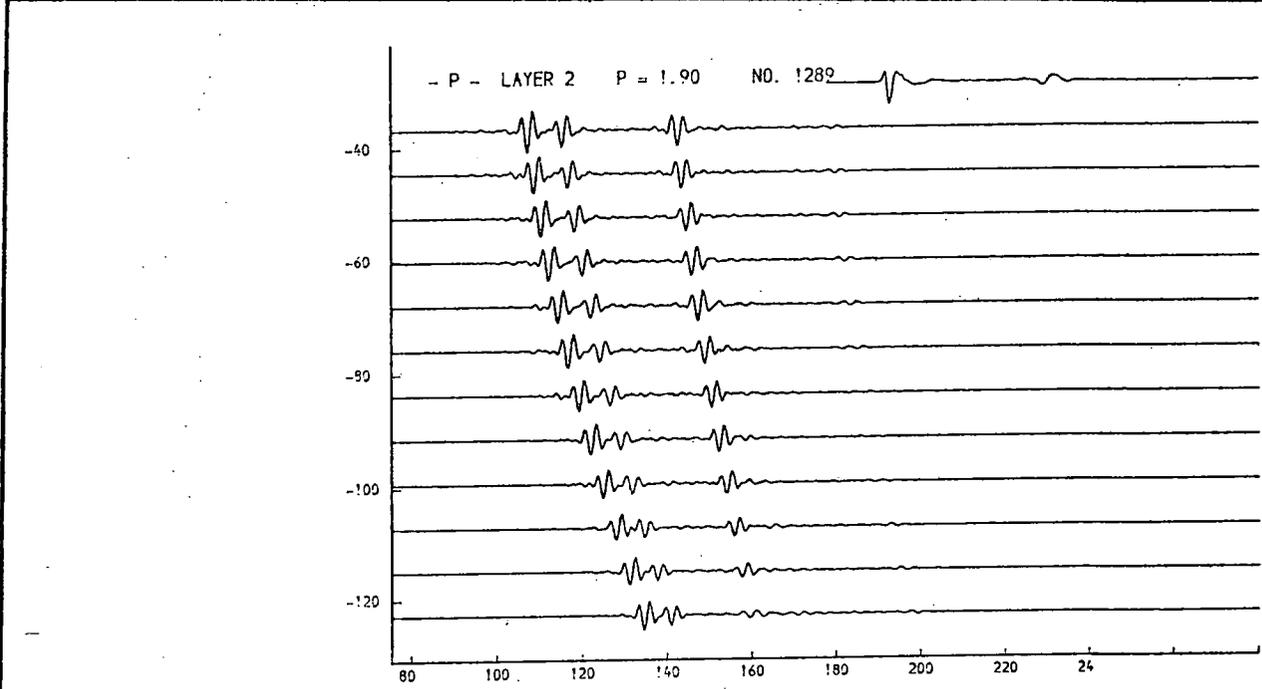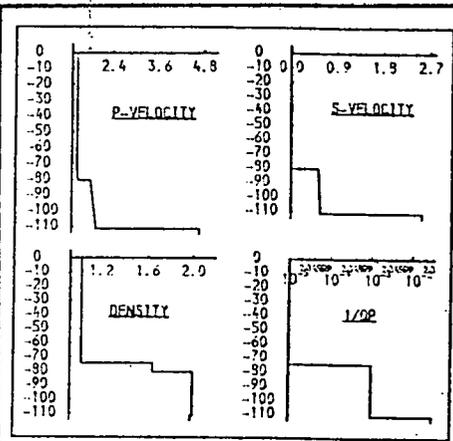
Fig. 9.30b. P-velocity, layer 2.

The reflector r2 is well-resolved and a value for p-velocity is found by fitting arrival times.

THICKNESS (M.)	P-VELOCITY (M/S.)	S-VELOCITY (M/S.)	DENSITY (G/ML)	1/Q P	1/Q S
74.4	1.460	0.000	1.03	0.00000	0.00000
6.1	1.480	0.010	1.65	0.02000	0.04000
3.7	1.934	0.097	2.00	0.00100	0.00050
3.9	1.953	0.098	2.00	0.00100	0.00050
3.9	1.972	0.099	2.00	0.00100	0.00050
3.9	1.991	0.100	2.00	0.00100	0.00050
3.9	2.009	0.100	2.00	0.00100	0.00050
3.9	2.028	0.101	2.00	0.00100	0.00050
3.9	2.047	0.102	2.00	0.00100	0.00050
4.0	2.066	0.103	2.00	0.00100	0.00050
	4.700	2.550	1.98	0.03000	0.06000

Fig. 9.31a. S-velocity, layer 2.

Changing this s-velocity causes the migration of a later arrival "i" across the model. This arrival is identified as a p-s conversion. (1/Qs, layer 2 is kept low in fig. 9.31 so that this phenomenon may be seen.)

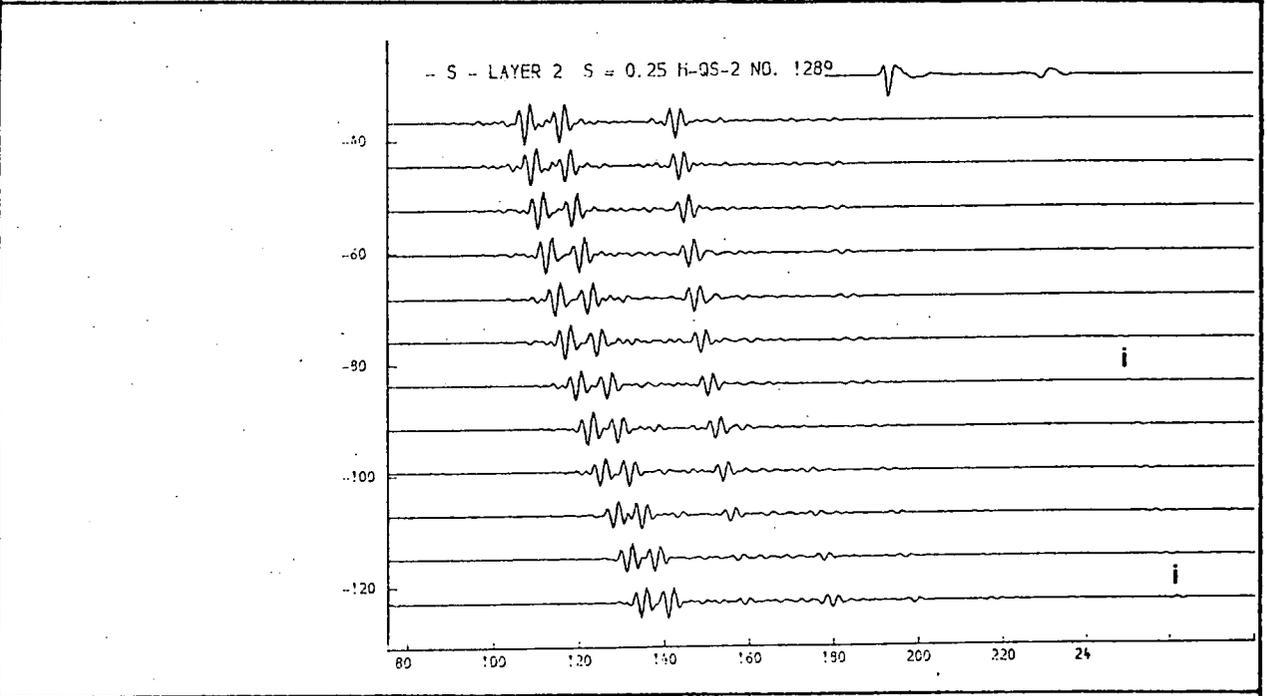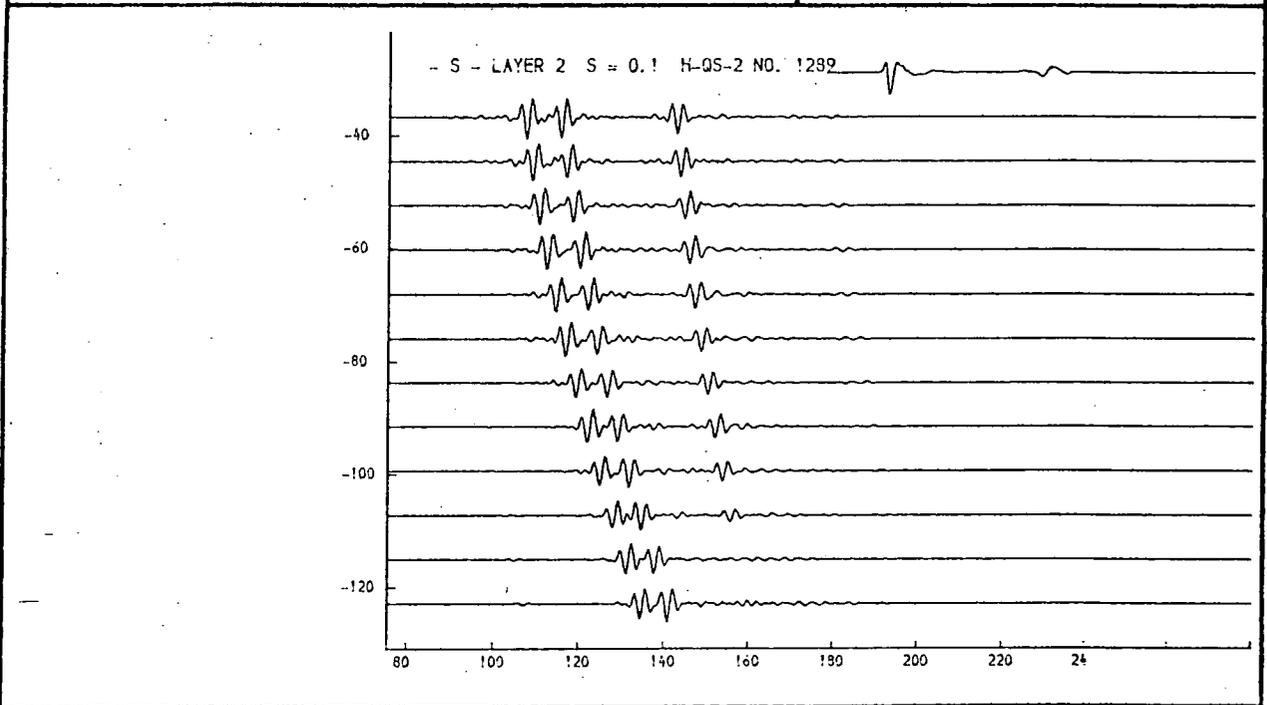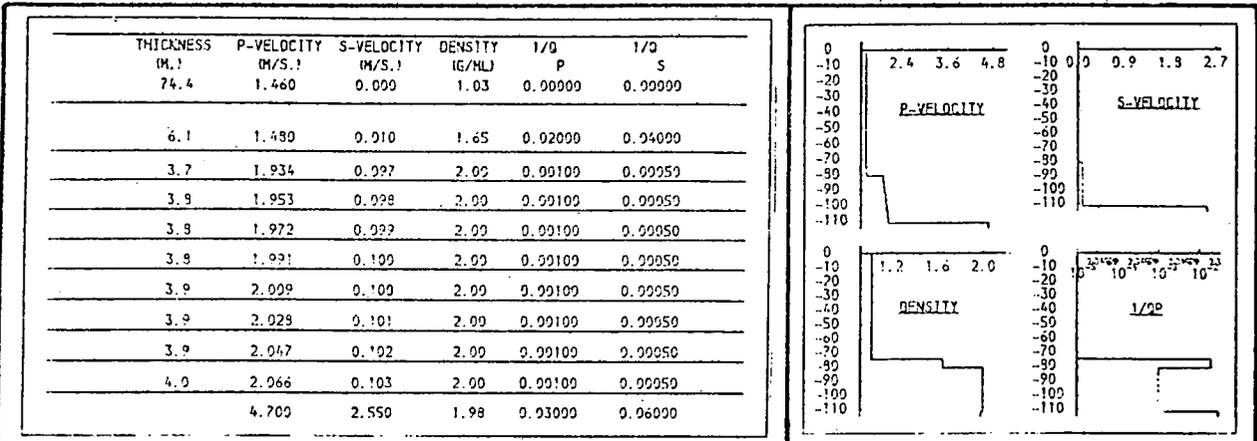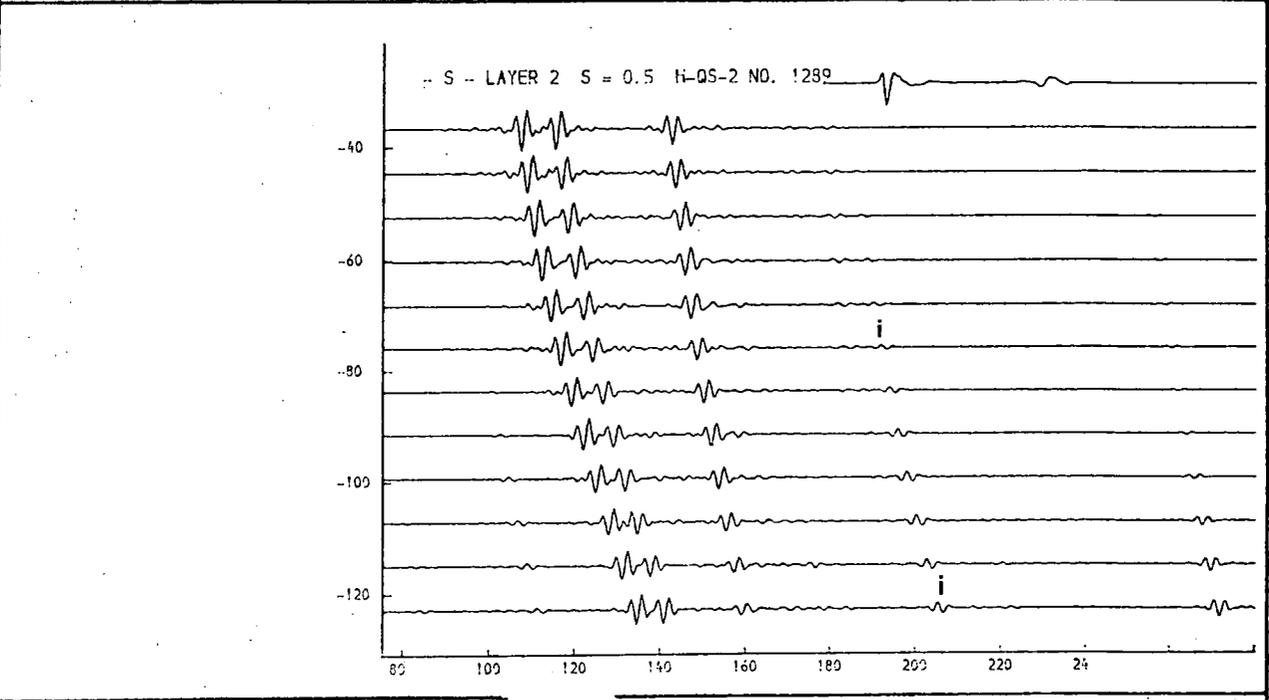| THICKNESS (M.)	P-VELOCITY (M/S.)	S-VELOCITY (M/S.)	DENSITY (G/ML)	1/Q P	1/Q S
74.4	1.460	0.000	1.03	0.00000	0.00000
6.1	1.480	0.010	1.65	0.02000	0.04000
3.7	1.934	0.387	2.00	0.00100	0.00050
3.8	1.953	0.391	2.00	0.00100	0.00050
3.9	1.972	0.394	2.00	0.00100	0.00050
3.9	1.991	0.398	2.00	0.00100	0.00050
3.9	2.009	0.402	2.00	0.00100	0.00050
3.9	2.028	0.406	2.00	0.00100	0.00050
3.9	2.047	0.409	2.00	0.00100	0.00050
4.0	2.066	0.413	2.00	0.00100	0.00050
	4.700	2.550	1.98	0.03000	0.06000

Fig. 9.31b. S-velocity, layer 2.

Changing this s-velocity causes the migration of a later
arrival "i" across the model. This arrival is identified
as a p-s conversion. (1/Qs, layer 2 is kept low in fig.
9.31 so that this phenomenon may be seen.)

THICKNESS (M.)	P-VELOCITY (M/S.)	S-VELOCITY (M/S.)	DENSITY (G/ML)	1/Q P	1/Q S
74.4	1.460	0.000	1.03	0.00000	0.00000
6.1	1.490	0.010	1.65	0.02000	0.04000
3.6	1.934	0.677	2.00	0.00200	0.00400
3.6	1.953	0.684	2.00	0.00200	0.00400
3.7	1.972	0.690	2.00	0.00200	0.00400
3.7	1.991	0.697	2.00	0.00200	0.00400
3.7	2.009	0.703	2.00	0.00200	0.00400
3.8	2.029	0.710	2.00	0.00200	0.00400
3.8	2.047	0.716	2.00	0.00200	0.00400
3.8	2.066	0.723	2.00	0.00200	0.00400
	4.700	2.550	1.98	0.01000	0.02000

Fig. 9.31c. S-velocity, layer 2.

Changing this s-velocity causes the migration of a later arrival "i" across the model. This arrival is identified as a p-s conversion. (1/Qs, layer 2 is kept low in fig. 9.31 so that this phenomenon may be seen.)
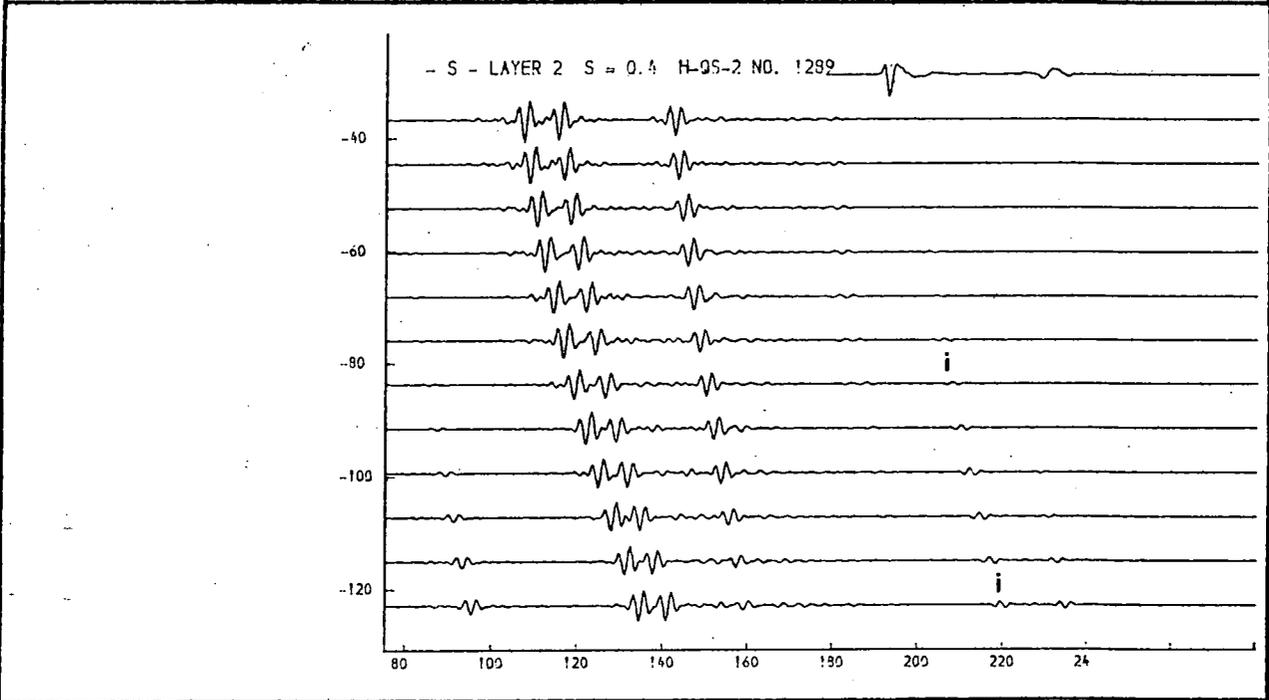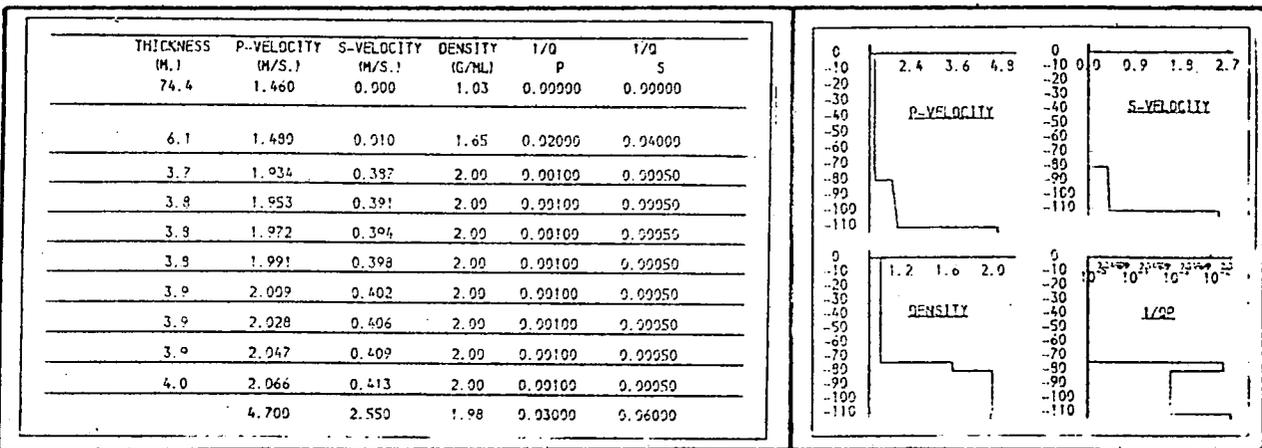
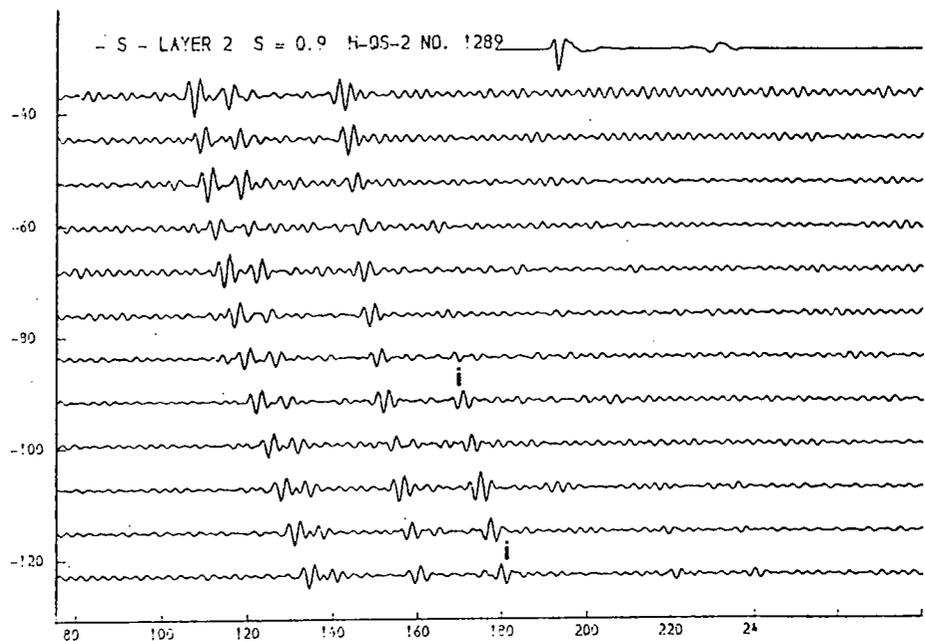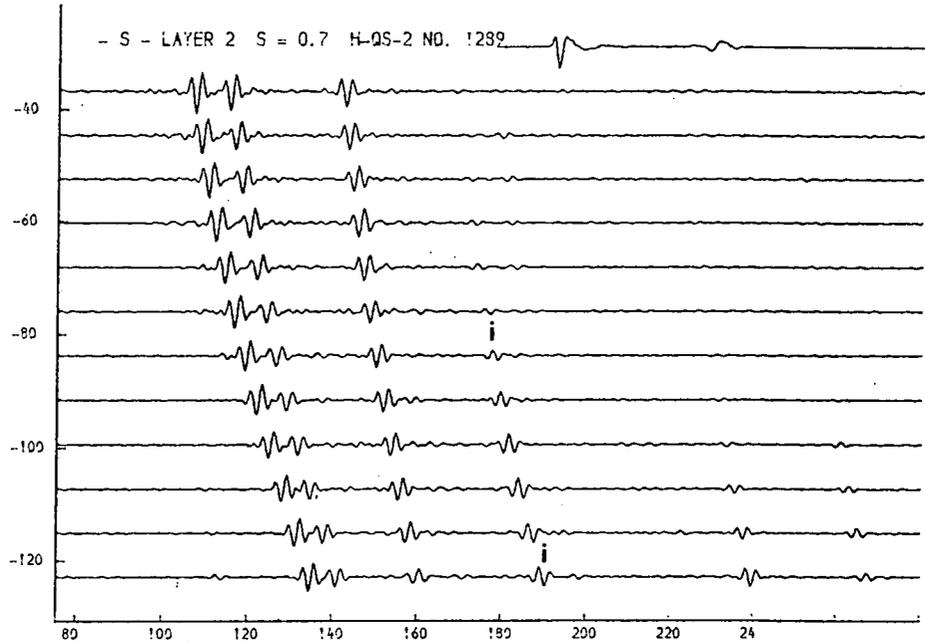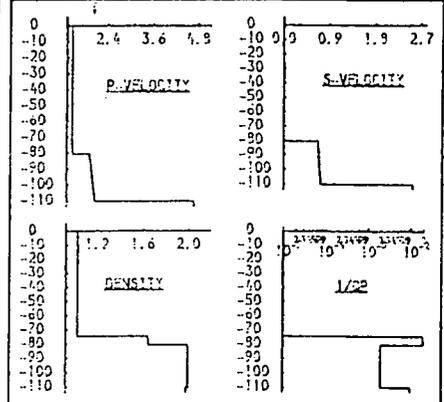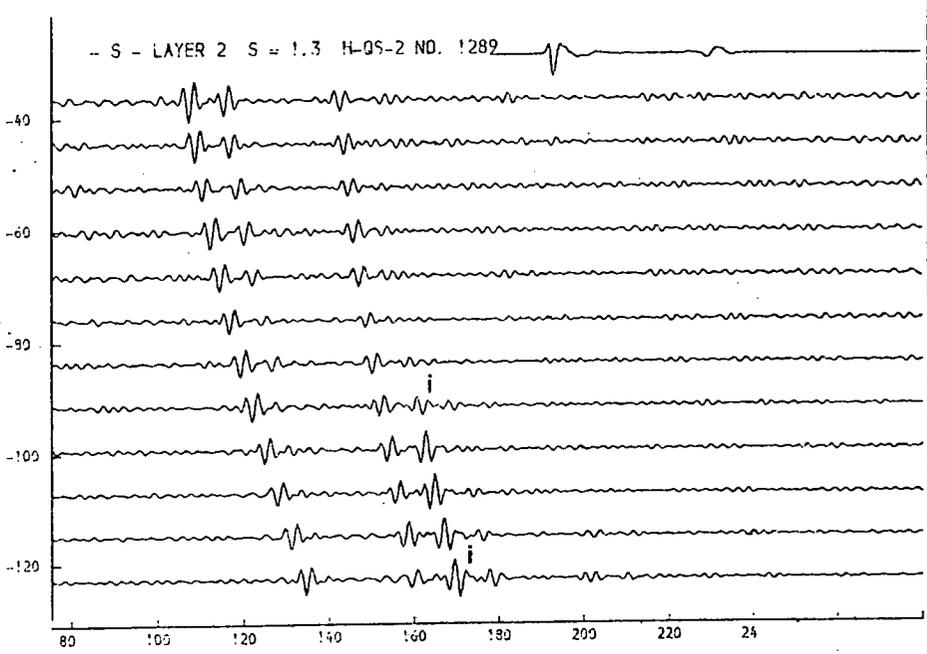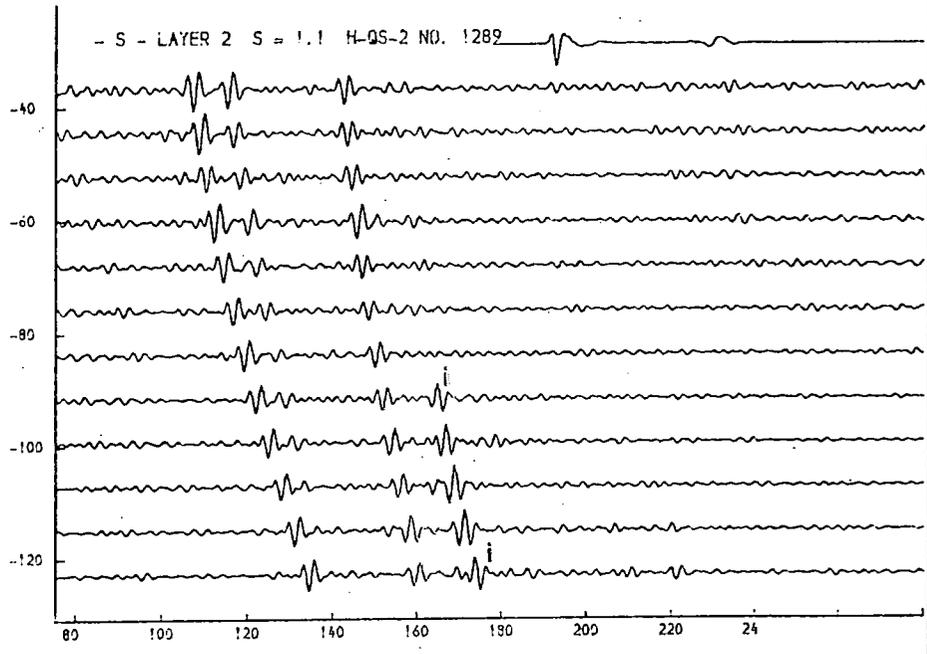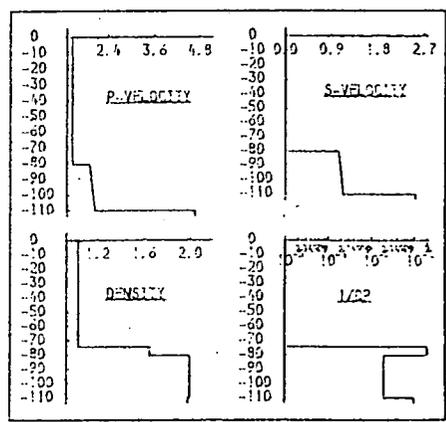| THICKNESS (M.)	P-VELOCITY (M/S.)	S-VELOCITY (M/S.)	DENSITY (G/ML)	1/Q P	1/Q S
74.4	1.460	0.000	1.03	0.00000	0.00000
6.1	1.480	0.010	1.65	0.02000	0.04000
3.6	1.934	1.064	2.00	0.00200	0.00400
3.6	1.953	1.074	2.00	0.00200	0.00400
3.7	1.972	1.085	2.00	0.00200	0.00400
3.7	1.991	1.095	2.00	0.00200	0.00400
3.7	2.009	1.105	2.00	0.00200	0.00400
3.8	2.028	1.115	2.00	0.00200	0.00400
3.8	2.047	1.126	2.00	0.00200	0.00400
3.9	2.066	1.136	2.00	0.00200	0.00400
	4.700	2.550	1.99	0.01000	0.02000

Fig. 9.31d. S-velocity, layer 2.

Changing this s-velocity causes the migration of a later arrival "i" across the model. This arrival is identified as a p-s conversion. (1/Qs, layer 2 is kept low in fig. 9.31 so that this phenomenon may be seen.)

THICKNESS (M.)	P-VELOCITY (M/S.)	S-VELOCITY (M/S.)	DENSITY (G/ML)	1/Q P	1/Q S
74.4	1.460	0.000	1.03	0.00000	0.00000
6.1	1.490	0.010	1.65	0.01000	0.04000
3.4	1.934	0.532	1.90	0.00100	0.03000
3.4	1.953	0.537	1.90	0.00100	0.03000
3.4	1.972	0.542	1.90	0.00100	0.03000
3.5	1.991	0.547	1.90	0.00100	0.03000
3.5	2.009	0.553	1.90	0.00100	0.03000
3.5	2.028	0.559	1.90	0.00100	0.03000
3.6	2.047	0.563	1.90	0.00100	0.03000
3.6	2.066	0.569	1.90	0.00100	0.03000
	4.700	2.550	1.98	0.01000	0.06000

−DENSITY LAYER 2−   RHO = 1.90 NO. 1289

−DENSITY LAYER 2−   RHO = 1.95 NO. 1289

Fig. 9.32a. Density, layer 2.

Variation of density affects the overall amplitude of reflectors r1 and r2 but has little influence on variation with offset distance.

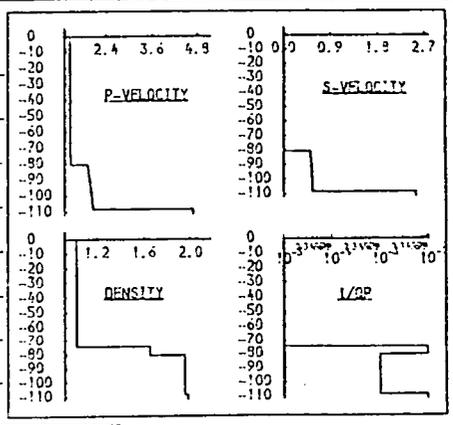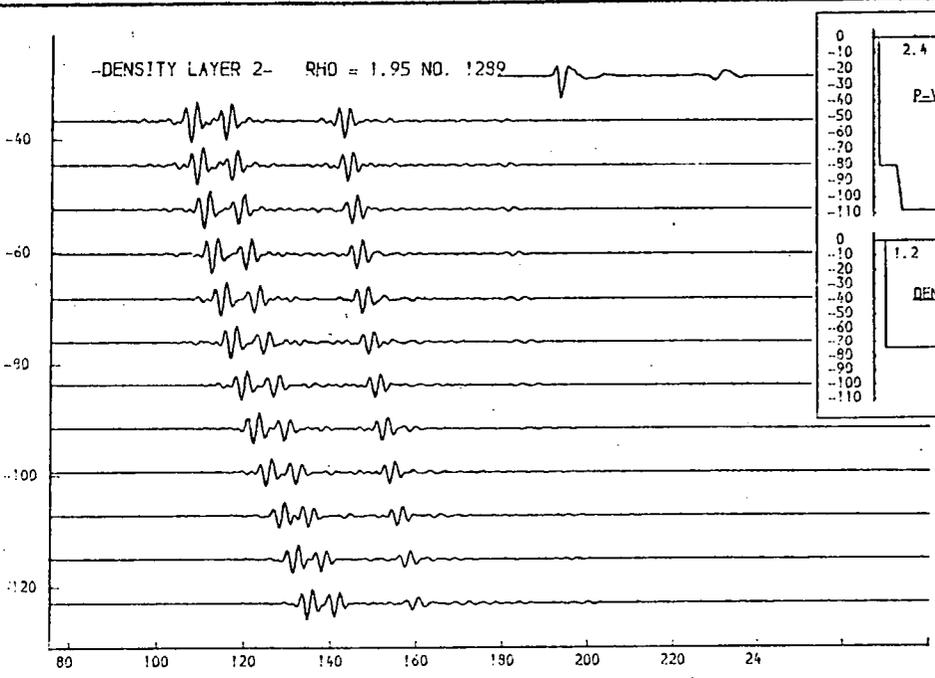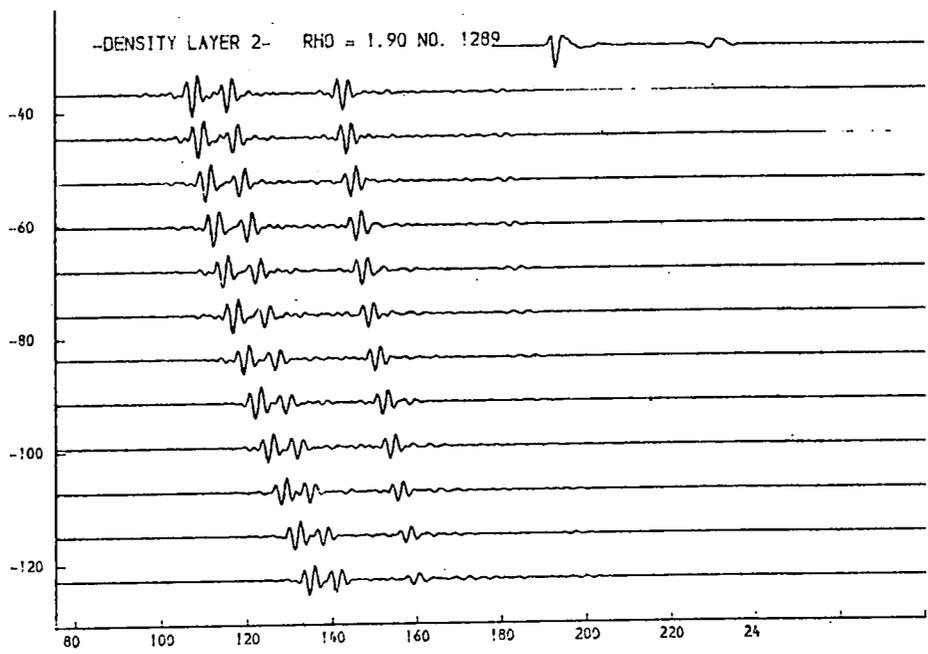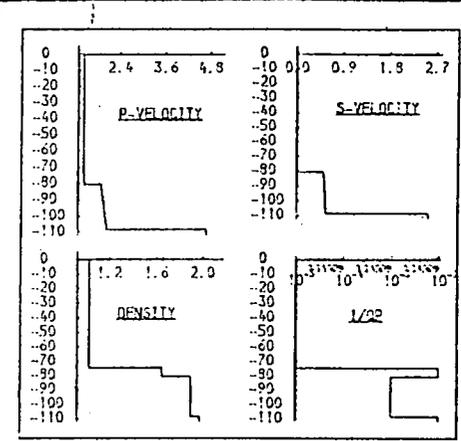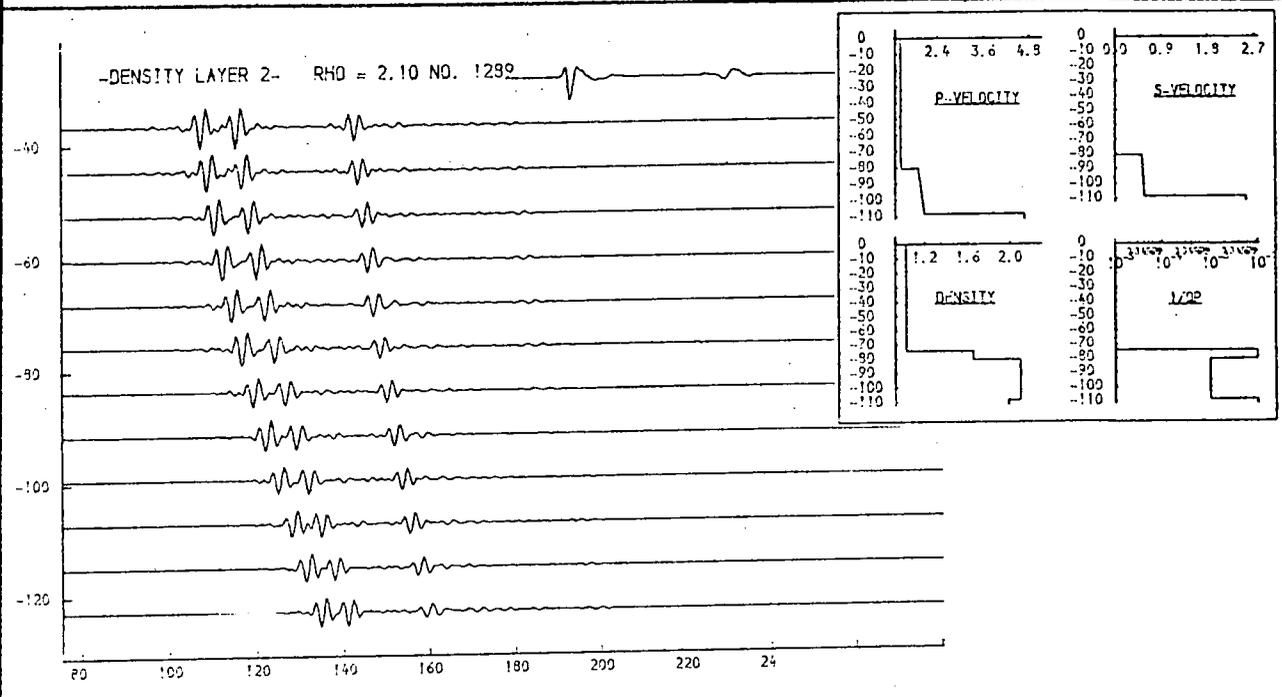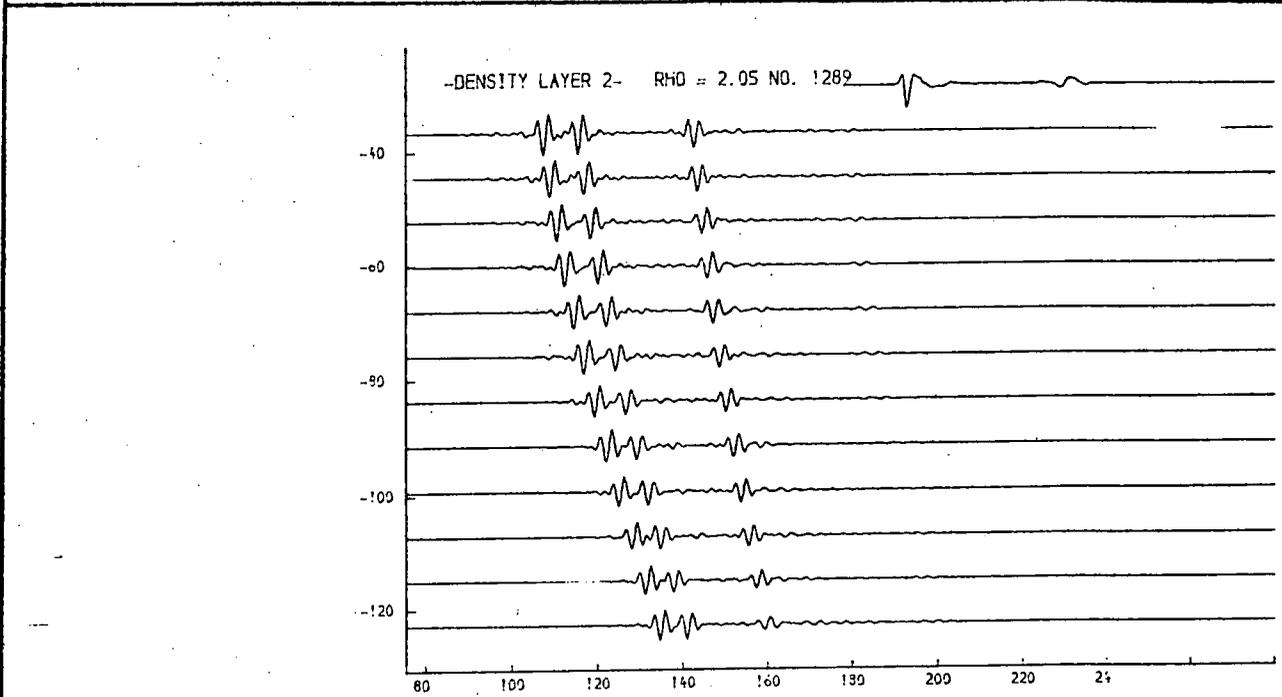| THICKNESS (M.)	P-VELOCITY (M/S.)	S-VELOCITY (M/S.)	DENSITY (G/ML)	1/Q P	1/Q S
74.4	1.460	0.000	1.03	0.00000	0.00000
6.1	1.490	0.010	1.65	0.01000	0.04000
3.4	1.931	0.532	2.05	0.00100	0.03000
3.4	1.953	0.537	2.05	0.00100	0.03000
3.4	1.972	0.542	2.05	0.00100	0.03000
3.5	1.991	0.547	2.05	0.00100	0.03000
3.5	2.009	0.553	2.05	0.00100	0.03000
3.5	2.028	0.559	2.05	0.00100	0.03000
3.6	2.047	0.563	2.05	0.00100	0.03000
3.6	2.066	0.568	2.05	0.00100	0.03000
	4.700	2.550	1.99	0.01000	0.06000

Fig. 9.32b. Density, layer 2.

Variation of density affects the overall amplitude of reflectors r1 and r2 but has little influence on variation with offset distance.

THICKNESS (M.)	P-VELOCITY (M/S.)	S-VELOCITY (M/S.)	DENSITY (G/ML)	1/Q P	1/Q S
74.4	1.460	0.000	1.03	0.00000	0.00000
6.1	1.480	0.010	1.65	0.02000	0.04000
3.7	1.934	0.532	2.00	0.00030	0.03000
3.8	1.953	0.537	2.00	0.00030	0.03000
3.9	1.972	0.542	2.00	0.00030	0.03000
3.9	1.991	0.547	2.00	0.00030	0.03000
3.9	2.009	0.553	2.00	0.00030	0.03000
3.9	2.028	0.558	2.00	0.00030	0.03000
3.9	2.047	0.563	2.00	0.00030	0.03000
4.0	2.066	0.569	2.00	0.00030	0.03000
	4.700	2.550	1.98	0.03000	0.06000

Fig. 9.33a. 1/Qp, layer 2.

Variation of 1/Qp suggests an upper limit for this parameter, above which the amplitude of the reflector r2 is seen to decrease.

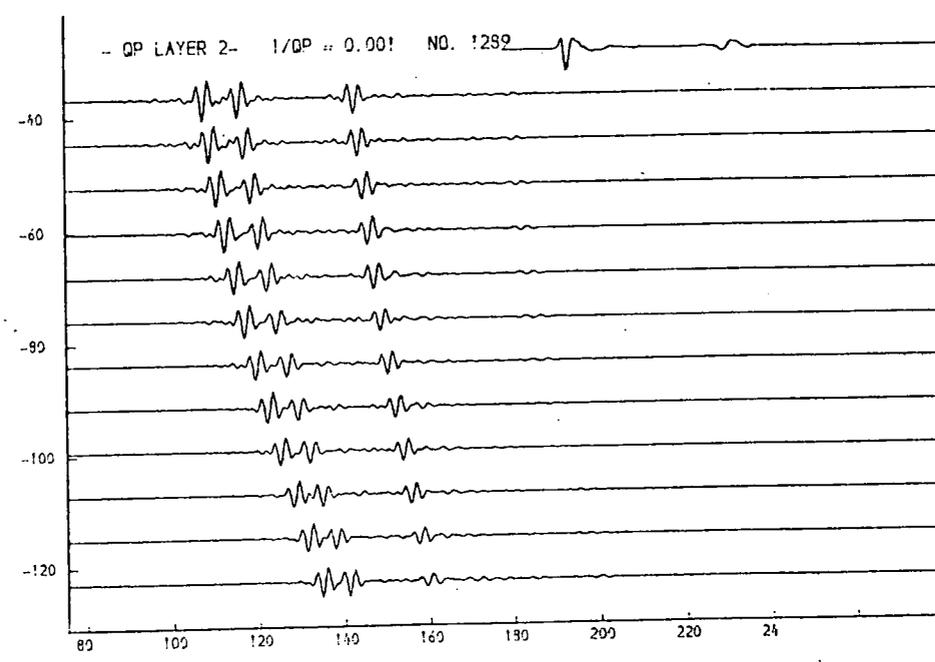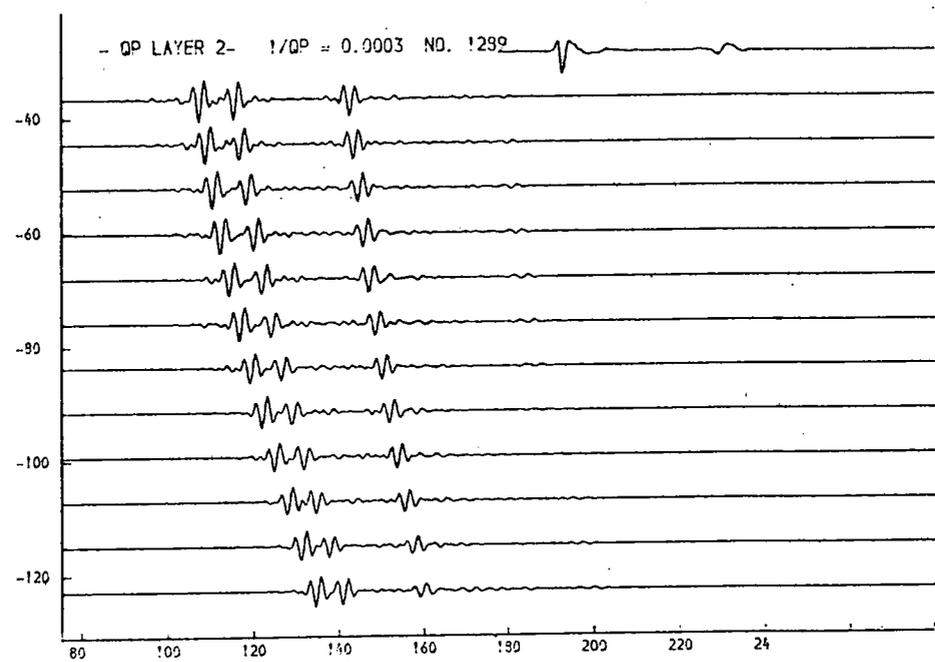| THICKNESS (M.)	P-VELOCITY (M/S.)	S-VELOCITY (M/S.)	DENSITY (G/ML)	1/Q P	1/Q S
74.4	1.460	0.000	1.03	0.00000	0.00000
6.1	1.490	0.010	1.65	0.02000	0.04000
3.7	1.934	0.532	2.00	0.00300	0.03000
3.8	1.953	0.537	2.00	0.00300	0.03000
3.9	1.972	0.542	2.00	0.00300	0.03000
3.9	1.991	0.547	2.00	0.00300	0.03000
3.9	2.009	0.553	2.00	0.00300	0.03000
3.9	2.028	0.558	2.00	0.00300	0.03000
3.9	2.047	0.563	2.00	0.00300	0.03000
4.0	2.066	0.569	2.00	0.00300	0.03000
	4.700	2.550	1.98	0.03000	0.06000

Fig. 9.33b. 1/Qp, layer 2.

Variation of 1/Qp suggests an upper limit for this parameter, above which the amplitude of the reflector r2 is seen to decrease.

THICKNESS (M.)	P-VELOCITY (M/S.)	S-VELOCITY (M/S.)	DENSITY (C/ML)	1/Q P	1/Q S
74.4	1.460	0.000	1.03	0.00000	0.00000
6.1	1.490	0.010	1.65	0.02000	0.04000
3.7	1.934	0.532	2.00	0.00200	0.03000
3.9	1.953	0.537	2.00	0.00200	0.03000
3.9	1.972	0.542	2.00	0.00200	0.03000
3.9	1.991	0.547	2.00	0.00200	0.03000
3.9	2.009	0.553	2.00	0.00200	0.03000
3.9	2.028	0.559	2.00	0.00200	0.03000
3.9	2.047	0.563	2.00	0.00200	0.03000
4.0	2.066	0.568	2.00	0.00200	0.03000
	4.700	2.550	1.98	0.03000	0.06000

P-VELOCITY   S-VELOCITY   DENSITY   1/QP

– QP LAYER 2 –   1/QP = 0.002   NO. 1289

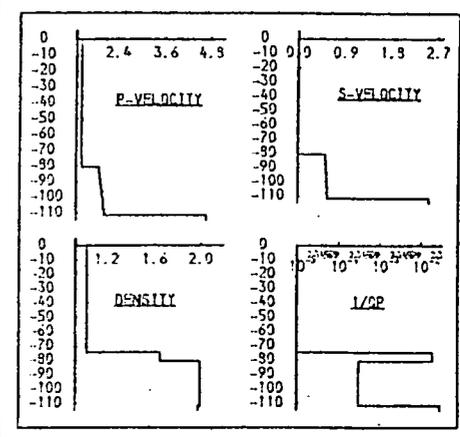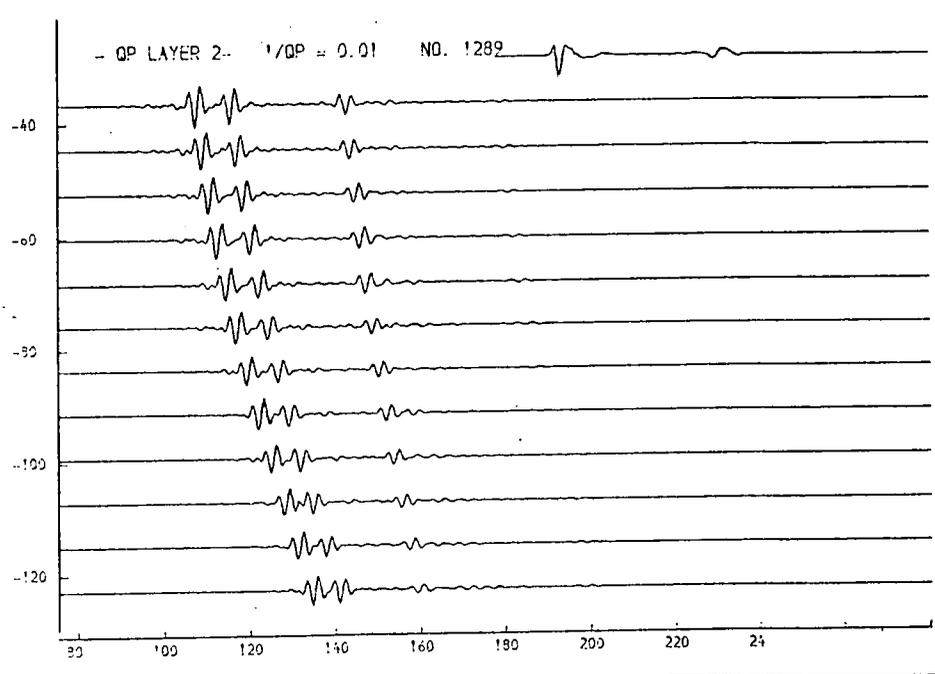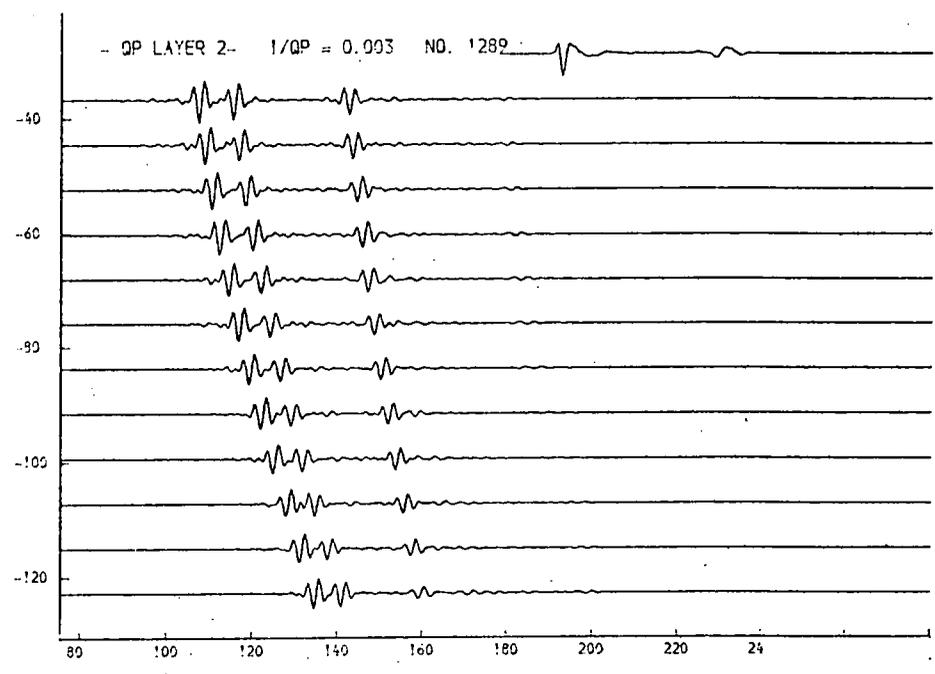– QP LAYER 2 –   1/QP = 0.007   NO. 1289

Fig. 9.33c. 1/Qp, layer 2.

Variation of 1/Qp suggests an upper limit for this parameter, above which the amplitude of the reflector r2 is seen to decrease.

THICKNESS (M.)	P-VELOCITY (M/S.)	S-VELOCITY (M/S.)	DENSITY (G/ML)	1/Q P	1/Q S
74.4	1.460	0.000	1.03	0.00000	0.00000
6.1	1.480	0.010	1.65	0.02000	0.04000
3.7	1.934	0.532	2.00	0.03000	0.03000
3.9	1.953	0.537	2.00	0.03000	0.03000
3.9	1.972	0.542	2.00	0.03000	0.03000
3.9	1.991	0.547	2.00	0.03000	0.03000
3.9	2.009	0.553	2.00	0.03000	0.03000
3.9	2.028	0.558	2.00	0.03000	0.03000
3.9	2.047	0.563	2.00	0.03000	0.03000
4.0	2.066	0.568	2.00	0.03000	0.03000
	4.700	2.550	1.98	0.03000	0.06000

— QP LAYER 2— 1/QP = 0.03   NO. 1289
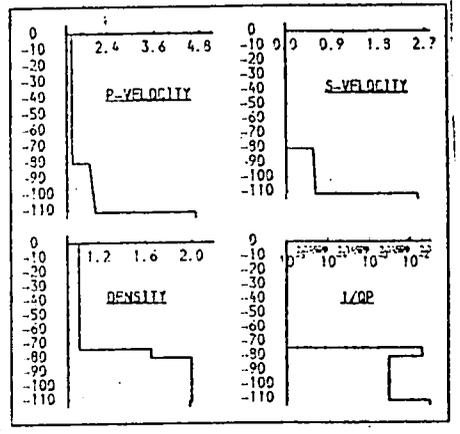

— QP LAYER 2— 1/QP = 0.1   NO. 1292
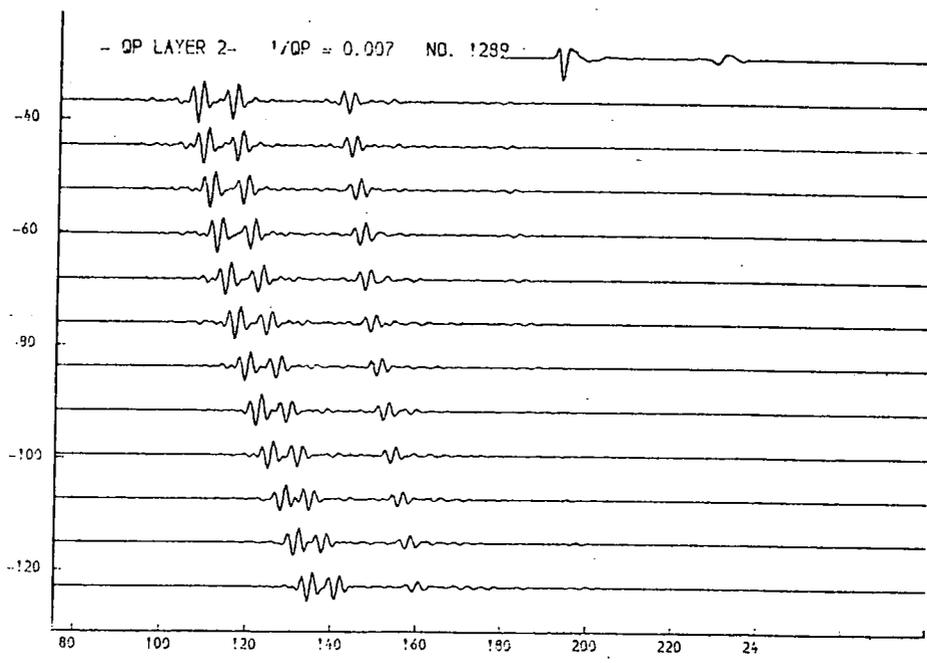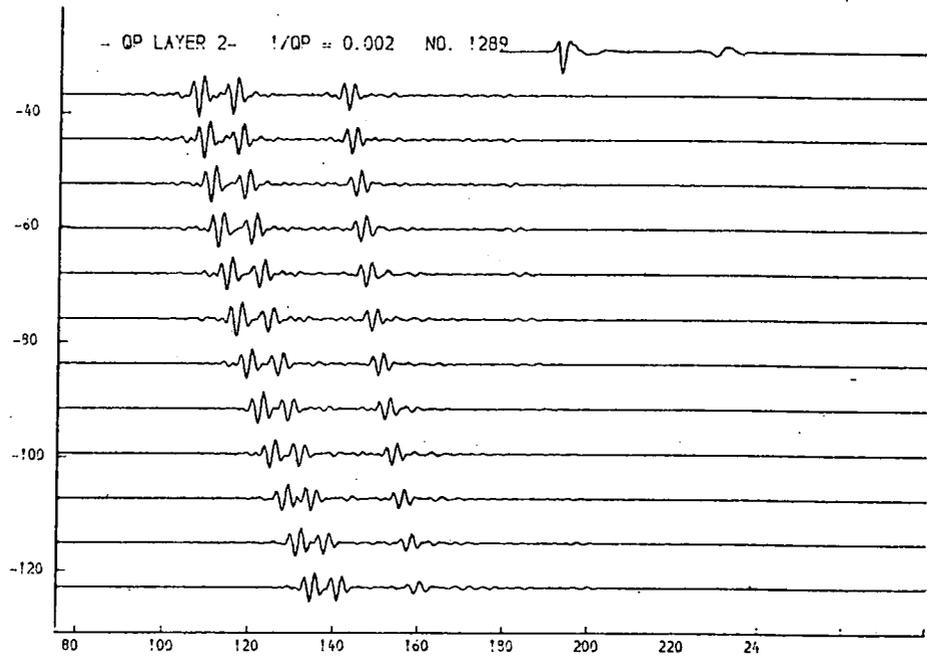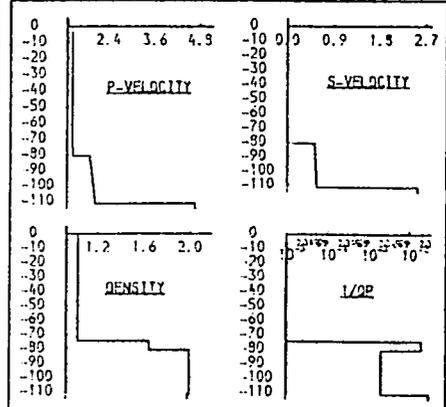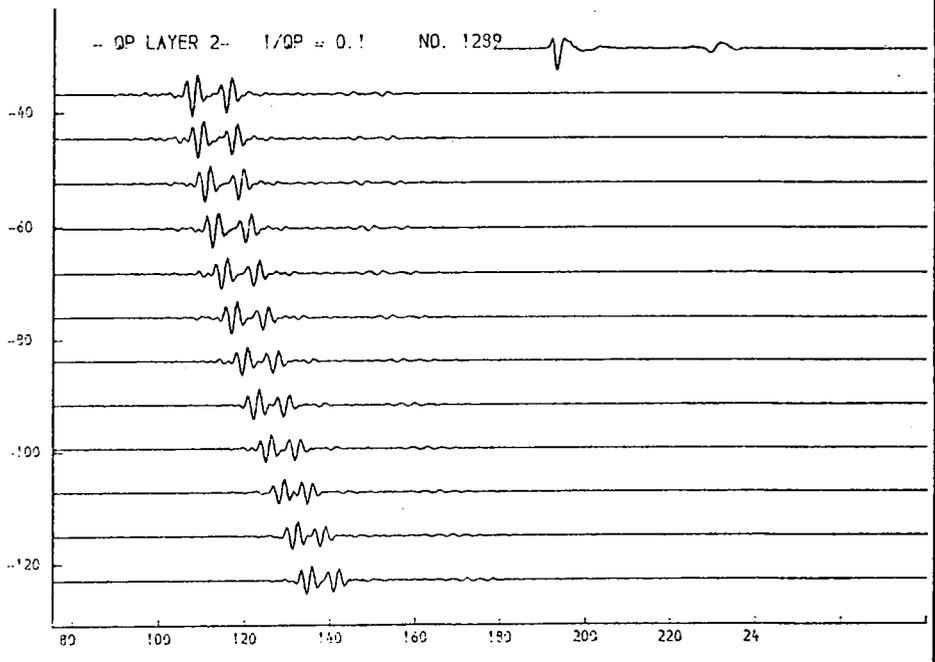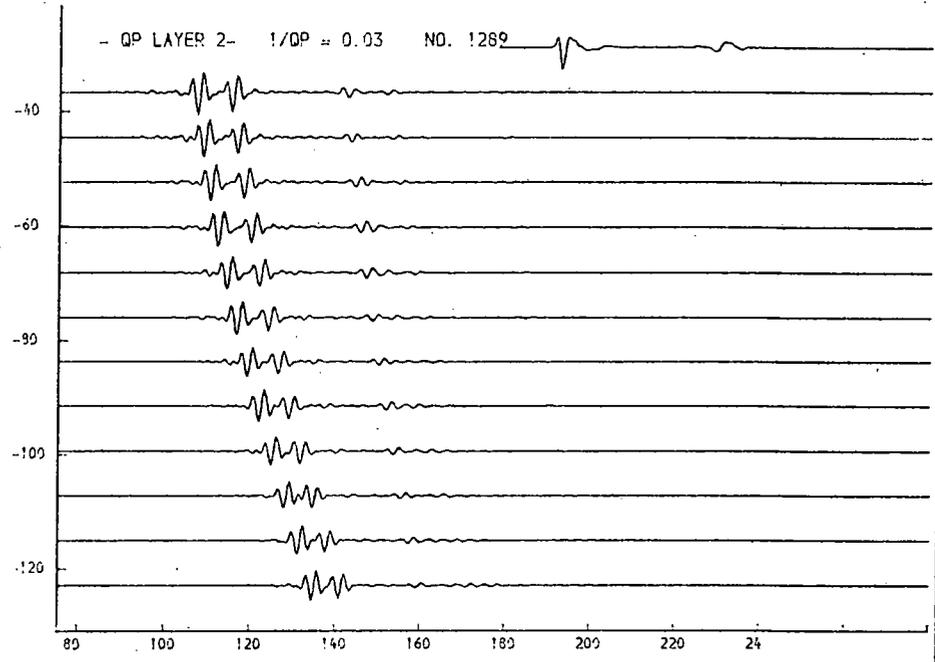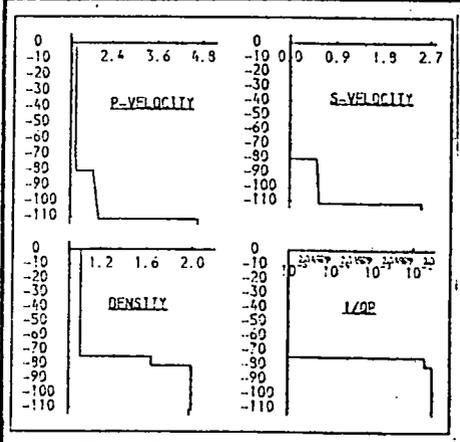
Fig. 9.33d. 1/Qp, layer 2.

Variation of 1/Qp suggests an upper limit for this parameter, above which the amplitude of the reflector r2 is seen to decrease.

THICKNESS (M.)	P-VELOCITY (M/S.)	S-VELOCITY (M/S.)	DENSITY (G/ML)	1/Q P	1/Q S
74.4	1.460	0.000	1.03	0.00000	0.00000
6.1	1.480	0.010	1.65	0.02000	0.04000
2.9	1.563	0.430	2.00	0.00200	0.03000
3.1	1.698	0.464	2.00	0.00200	0.03000
3.3	1.813	0.498	2.00	0.00200	0.03000
3.6	1.938	0.533	2.00	0.00200	0.03000
3.8	2.063	0.567	2.00	0.00200	0.03000
4.0	2.188	0.602	2.00	0.00200	0.03000
4.3	2.313	0.636	2.00	0.00200	0.03000
4.5	2.438	0.670	2.00	0.00200	0.03000
	4.700	2.650	1.98	0.03000	0.06000

Fig. 9.34a. 1/Qp, layer 2 (linear p-velocity gradient).

The presence of a greater change in p-velocity above the reflector r2 does not significantly affect possible values for 1/Qp. The fit with reflectors r1 and r2 is degraded.

THICKNESS (M.)	P-VELOCITY (M/S.)	S-VELOCITY (M/S.)	DENSITY (G/ML)	1/Q P	1/Q S
74.4	1.460	0.000	1.03	0.00000	0.00000
6.1	1.480	0.010	1.65	0.02000	0.04000
2.9	1.563	0.430	2.00	0.02000	0.03000
3.1	1.699	0.464	2.00	0.02000	0.03000
3.3	1.913	0.498	2.00	0.02000	0.03000
3.6	1.939	0.533	2.00	0.02000	0.03000
3.8	2.063	0.567	2.00	0.02000	0.03000
4.0	2.199	0.602	2.00	0.02000	0.03000
4.3	2.313	0.636	2.00	0.02000	0.03000
4.5	2.439	0.670	2.00	0.02000	0.03000
	4.700	2.650	1.98	0.03000	0.06000

--QP- LAYER 2   1/QP = 0.02   NO. 1289
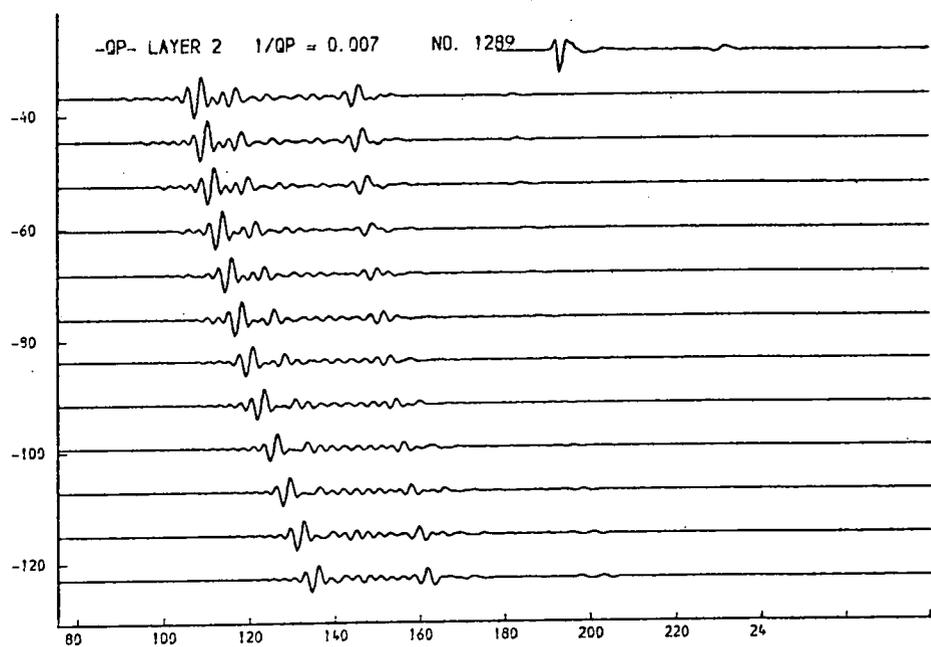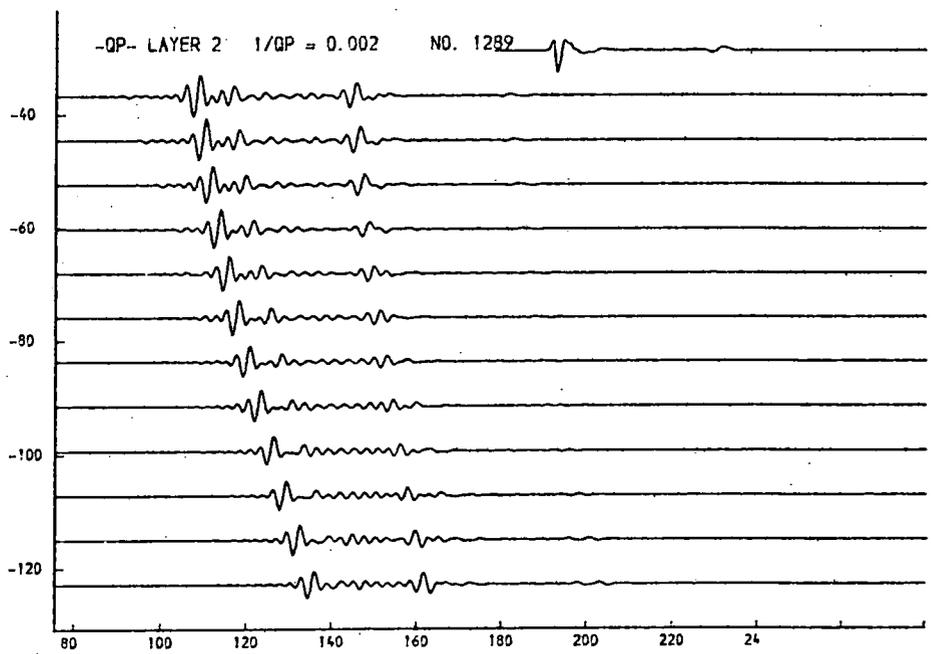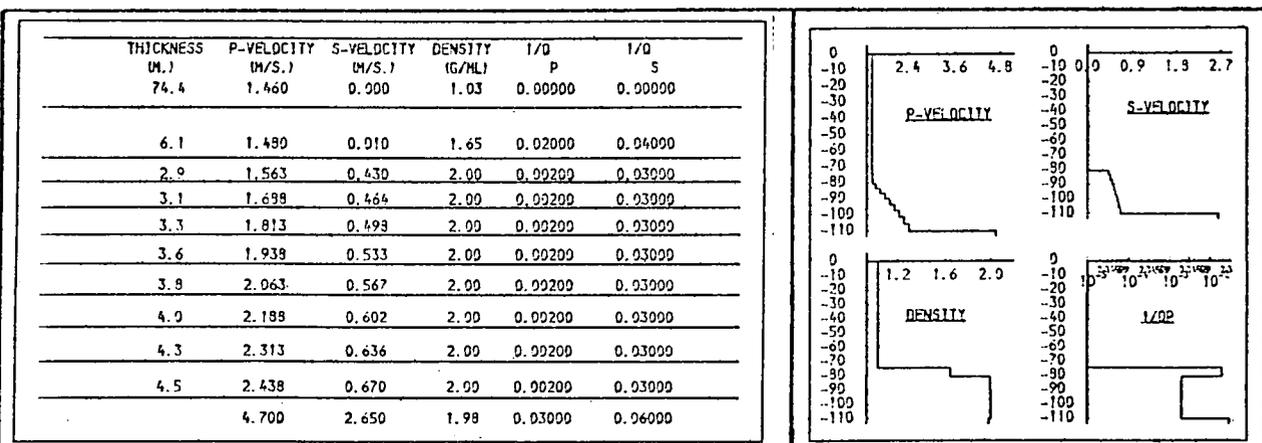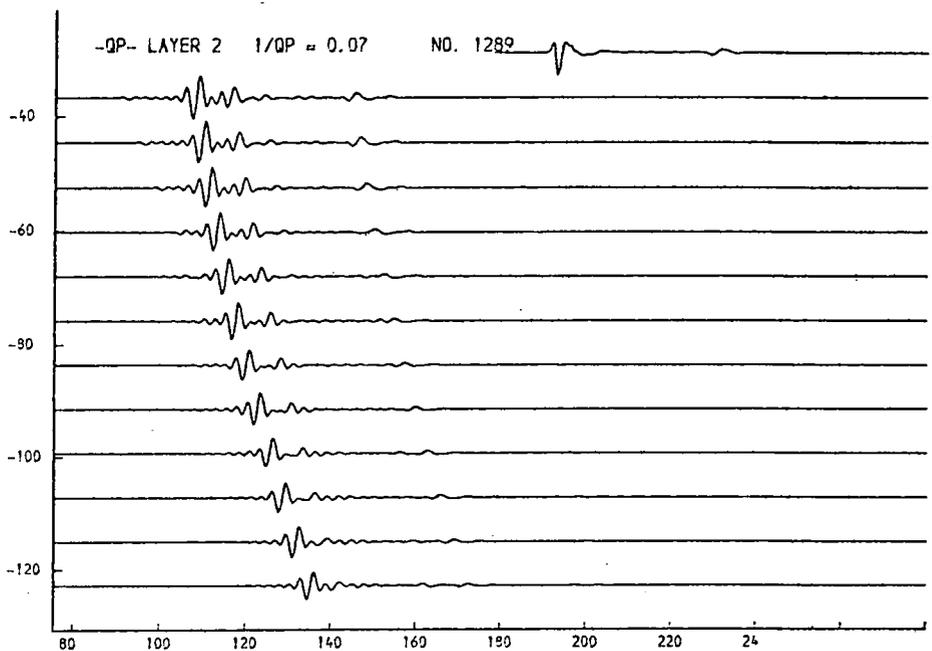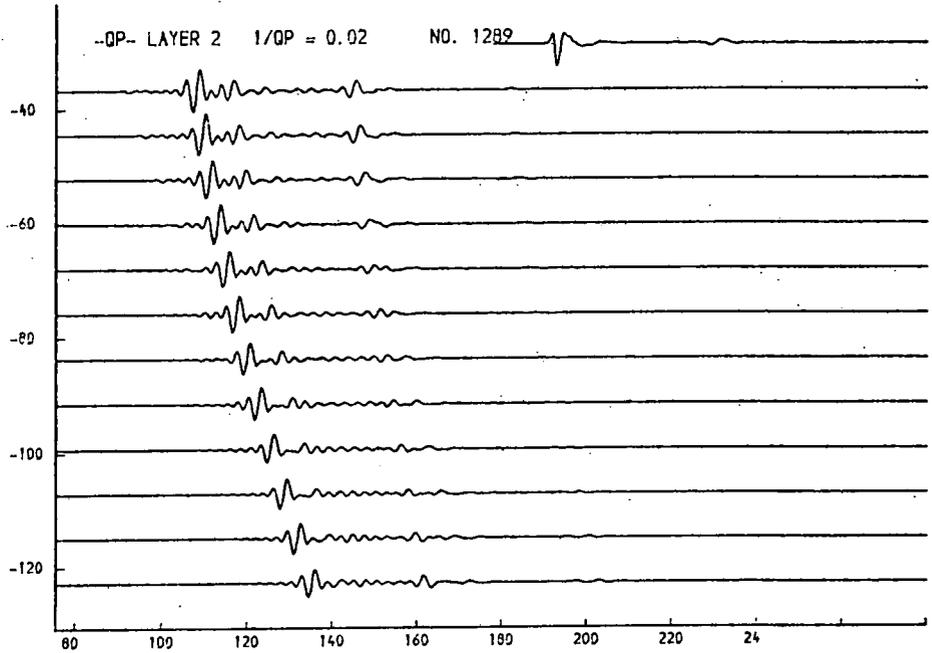

--QP- LAYER 2   1/QP = 0.07   NO. 1289
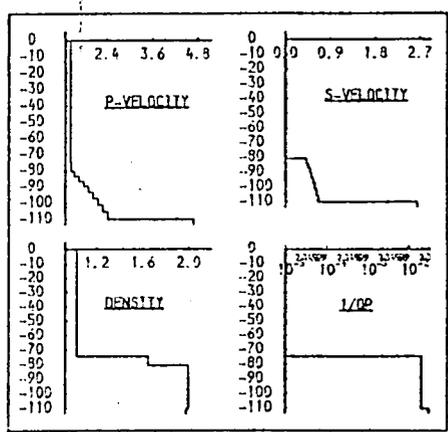
Fig. 9.34b. 1/Qp, layer 2 (linear p-velocity gradient).

The presence of a greater change in p-velocity above the reflector r2 does not significantly affect possible values for 1/Qp. The fit with reflectors r1 and r2 is degraded.

THICKNESS (M.)	P-VELOCITY (M/S.)	S-VELOCITY (M/S.)	DENSITY (G/ML)	1/Q P	1/Q S		THICKNESS (M.)	P-VELOCITY (M/S.)	S-VELOCITY (M/S.)	DENSITY (G/ML)	1/Q P	1/Q S
74.4	1.460	0.000	1.03	0.00000	0.00000		74.4	1.460	0.000	1.03	0.00000	0.00000
6.1	1.490	0.010	1.65	0.02000	0.04000		6.1	1.490	0.010	1.65	0.02000	0.04000
14.9	1.925	0.529	2.00	0.01000	0.03000		14.9	1.925	0.529	2.00	0.03000	0.03000
7.6	1.975	0.543	2.00	0.01000	0.03000		7.6	1.975	0.543	2.00	0.03000	0.03000
4.0	2.065	0.569	2.00	0.01000	0.03000		4.0	2.065	0.569	2.00	0.03000	0.03000
2.1	2.195	0.601	2.00	0.01000	0.03000		2.1	2.195	0.601	2.00	0.03000	0.03000
2.3	2.335	0.656	2.00	0.01000	0.03000		2.3	2.335	0.656	2.00	0.03000	0.03000
	4.700	2.550	1.98	0.05000	0.10000			4.700	2.550	1.98	0.05000	0.10000

Fig. 9.35b. 1/Qp, layer 2 (curved p-velocity gradient).

This type of gradient helps restore the fit with r1, but still does not significantly affect possible values for 1/Qp. The fit with reflector r2 remains poor.

THICKNESS (M.)	P-VELOCITY (M/S.)	S-VELOCITY (M/S.)	DENSITY (G/ML)	1/Q P	1/Q S
74.4	1.460	0.000	1.03	0.00000	0.00000
6.1	1.480	0.010	1.65	0.02000	0.04000
14.9	1.925	0.529	2.00	0.00100	0.03000
7.6	1.975	0.543	2.00	0.00100	0.03000
4.0	2.065	0.569	2.00	0.00100	0.03000
2.1	2.155	0.601	2.00	0.00100	0.03000
2.3	2.395	0.656	2.00	0.00100	0.03000
	4.700	2.550	1.98	0.05000	0.10000

- GRADT. L2 - 1/QP = 0.001   NO. 1289
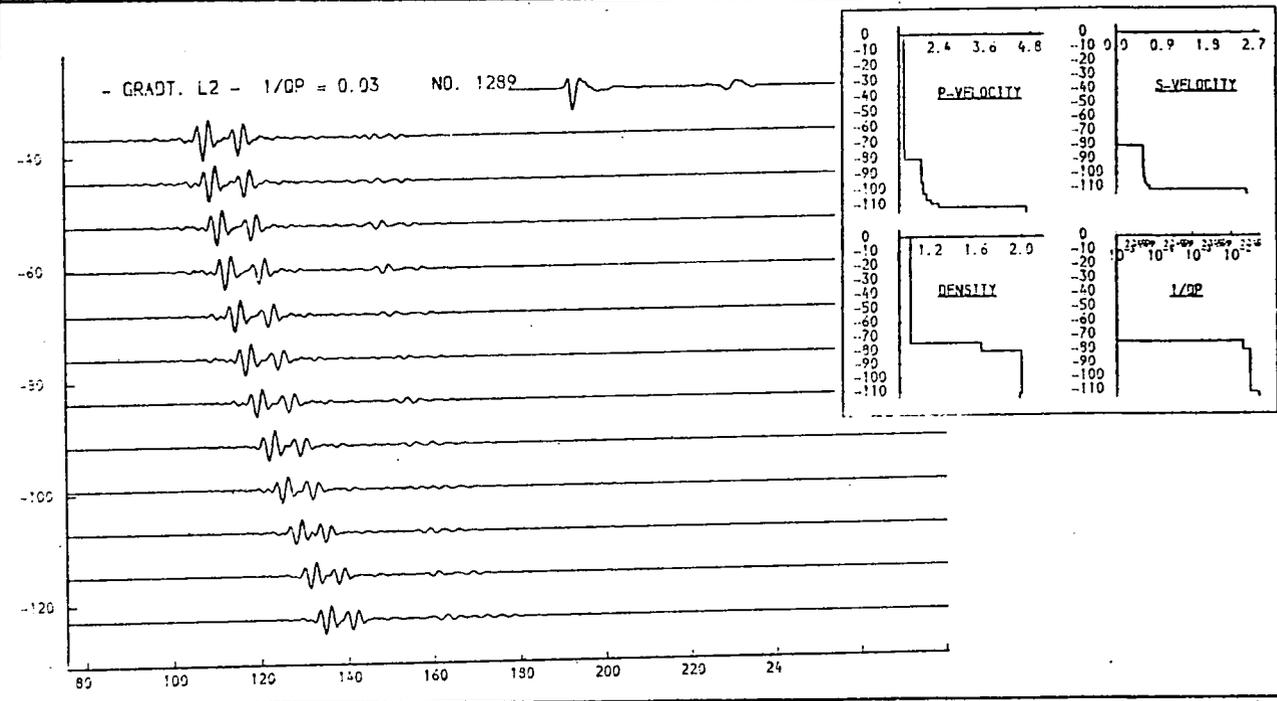
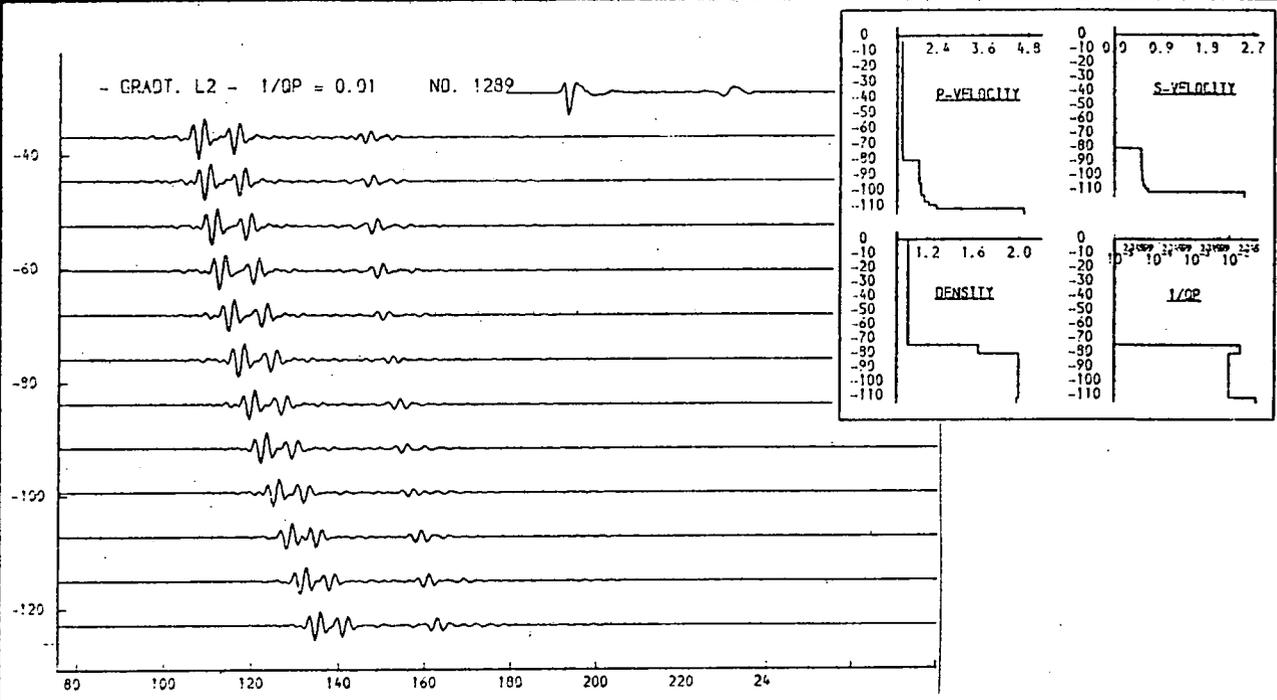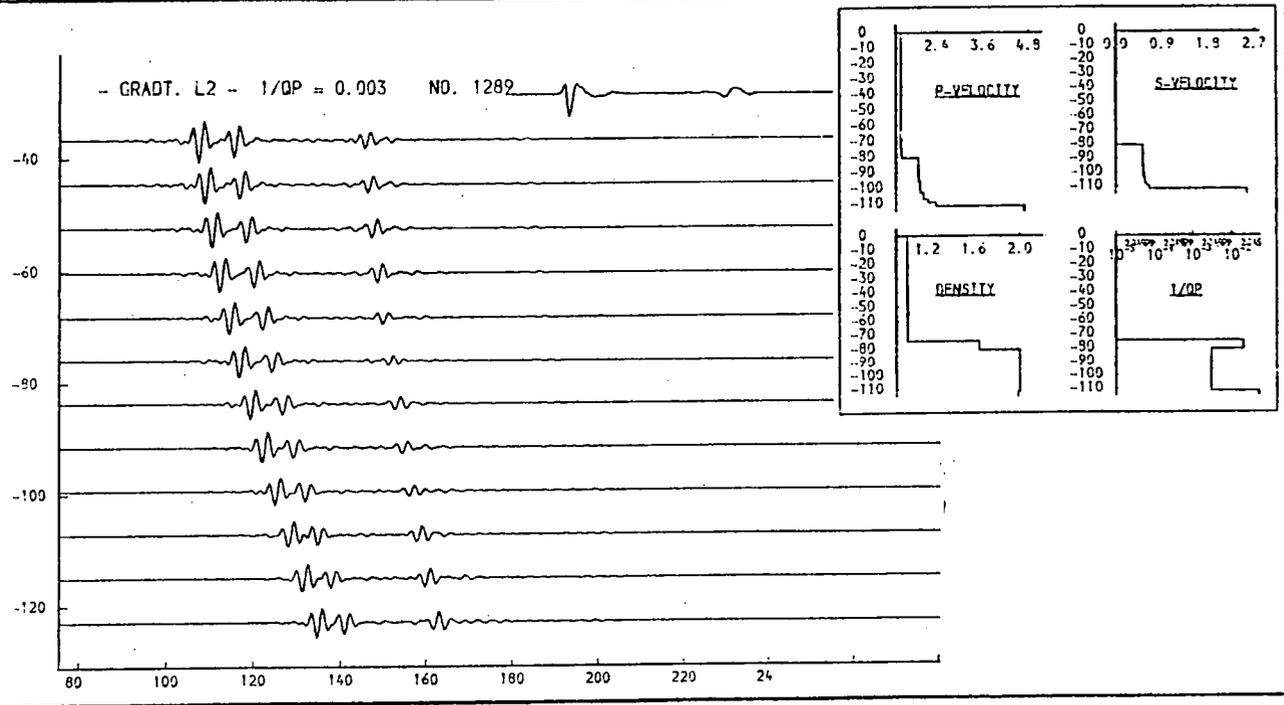- GRADT. L2 - 1/QP = 0.003   NO. 1289
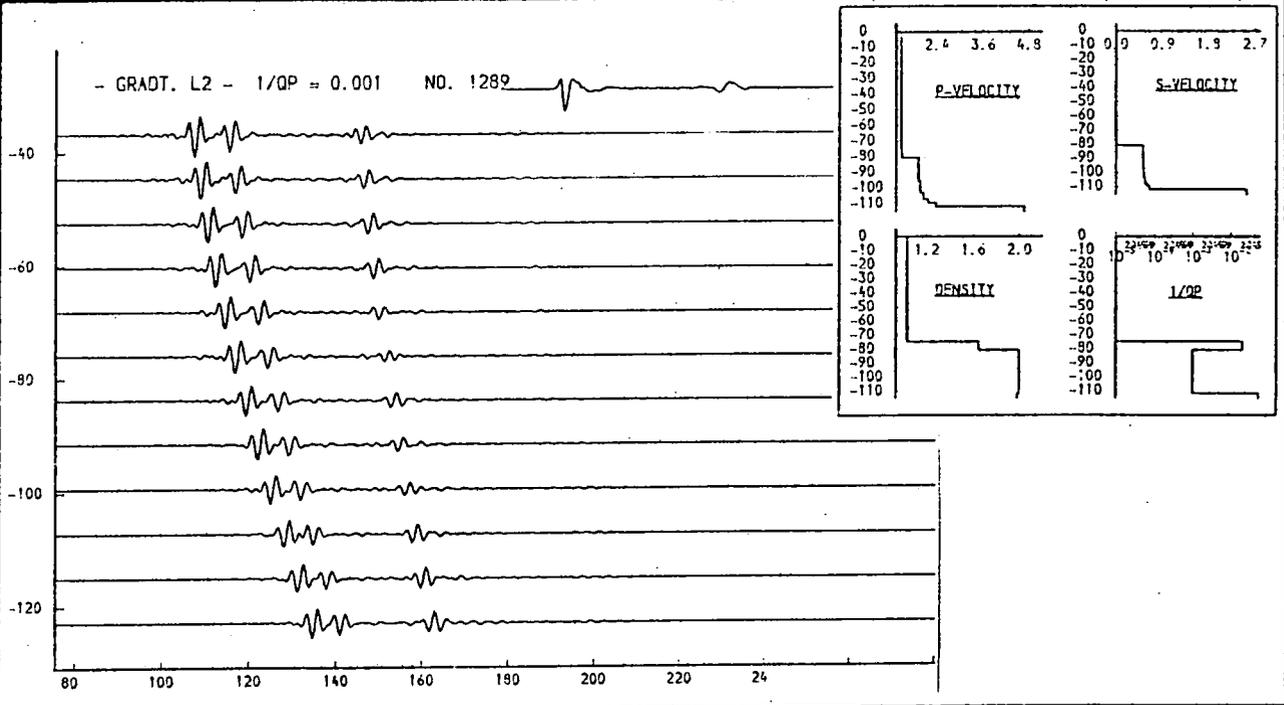
Fig. 9.35a. 1/Qp, layer 2 (curved p-velocity gradient).

This type of gradient helps restore the fit with r1, but still does not significantly affect possible values for 1/Qp. The fit with reflector r2 remains poor.

THICKNESS (M.)	P-VELOCITY (M/S.)	S-VELOCITY (M/S.)	DENSITY (G/ML)	1/Q P	1/Q S
74.4	1.460	0.900	1.03	0.00000	0.00000
6.1	1.480	0.010	1.65	0.02000	0.04000
3.6	1.934	0.532	2.00	0.00200	0.00400
3.6	1.953	0.537	2.00	0.00200	0.00400
3.6	1.972	0.542	2.00	0.00200	0.00400
3.7	1.991	0.547	2.00	0.00200	0.00400
3.7	2.009	0.553	2.00	0.00200	0.00400
3.7	2.028	0.558	2.00	0.00200	0.00400
3.8	2.047	0.563	2.00	0.00200	0.00400
3.9	2.066	0.568	2.00	0.00200	0.00400
	4.700	2.650	1.98	0.03000	0.06000

Fig. 9.36a. 1/Qs, layer 2.

Variations of this parameter can control the p-s converted arrival shown in figs. 9.31a-d.

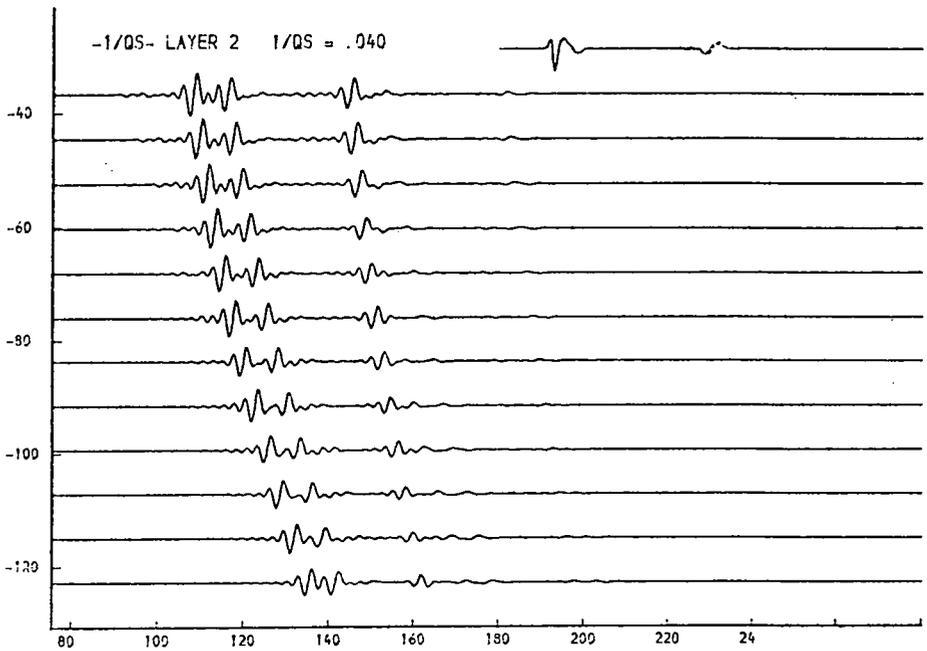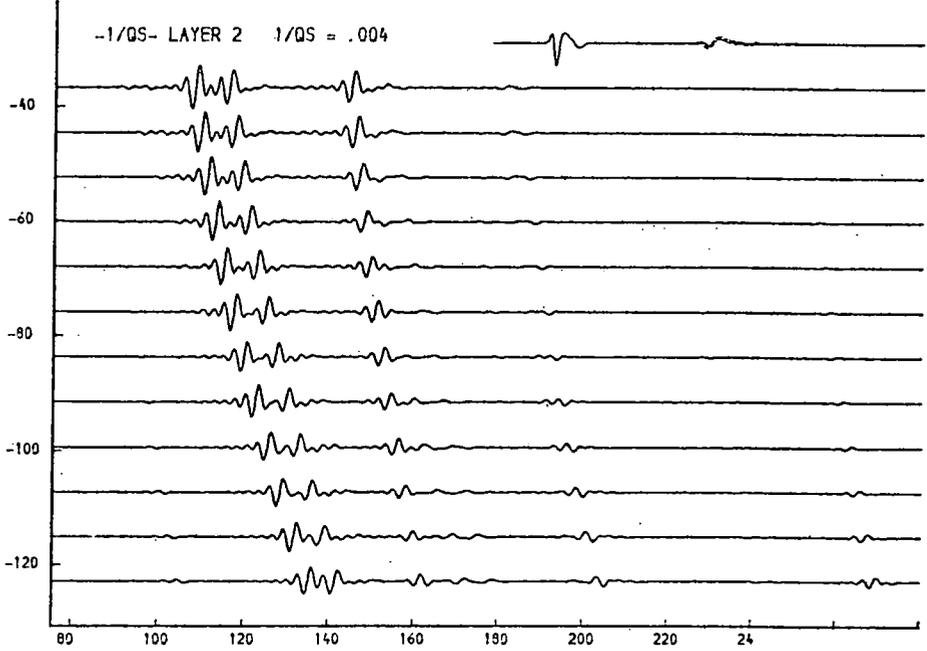| THICKNESS (M.)	P-VELOCITY (M/S.)	S-VELOCITY (M/S.)	DENSITY (G/ML)	1/Q P	1/Q S
74.4	1.460	0.000	1.03	0.00000	0.00000
6.1	1.480	0.010	1.65	0.02000	0.04000
3.6	1.934	0.532	2.00	0.00200	0.40000
3.6	1.953	0.537	2.00	0.00200	0.40000
3.6	1.972	0.542	2.00	0.00200	0.40000
3.7	1.991	0.547	2.00	0.00200	0.40000
3.7	2.009	0.553	2.00	0.00200	0.40000
3.7	2.028	0.558	2.00	0.00200	0.40000
3.8	2.047	0.563	2.00	0.00200	0.40000
3.8	2.066	0.568	2.00	0.00200	0.40000
	4.700	2.650	1.98	0.03000	0.06000

Fig. 9.36b. 1/Qs, layer 2.

Variations of this parameter can control the p-s converted arrival shown in figs. 9.31a-d.

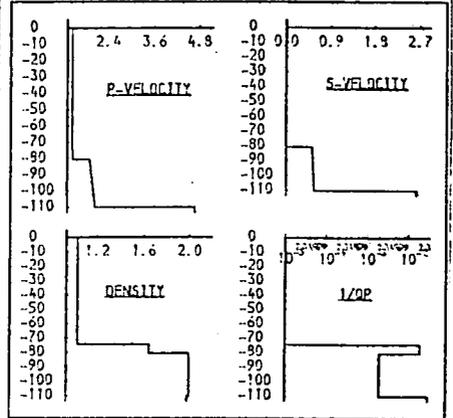| THICKNESS (M.)	P-VELOCITY (M/S.)	S-VELOCITY (M/S.)	DENSITY (G/ML)	1/Q P	1/Q S
74.4	1.460	0.000	1.03	0.00000	0.00000
6.1	1.480	0.010	1.65	0.02000	0.04000
3.5	1.869	0.511	2.00	0.00300	0.00500
3.5	1.906	0.524	2.00	0.00300	0.00500
3.6	1.944	0.535	2.00	0.00300	0.00500
3.7	1.991	0.545	2.00	0.00300	0.00500
3.7	2.019	0.555	2.00	0.00300	0.00500
3.9	2.056	0.565	2.00	0.00300	0.00500
3.9	2.094	0.576	2.00	0.00300	0.00500
4.0	2.131	0.586	2.00	0.00300	0.00500
	4.700	2.550	1.98	0.03000	0.06000

Fig. 9.37a. 1/Qs, layer 2.

Variations of this parameter can control the p-s converted arrival shown in figs. 9.31a-d.

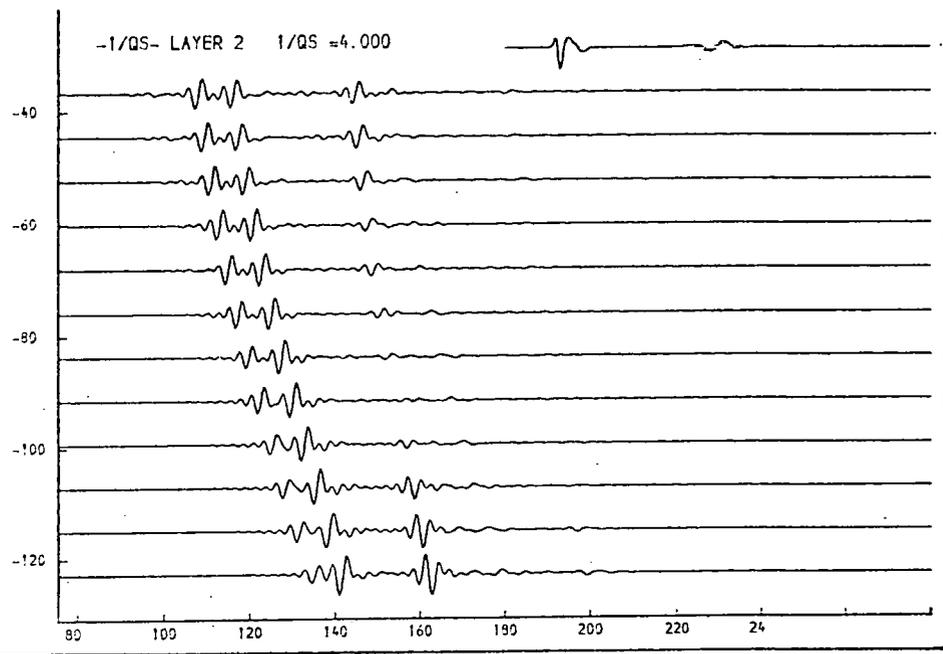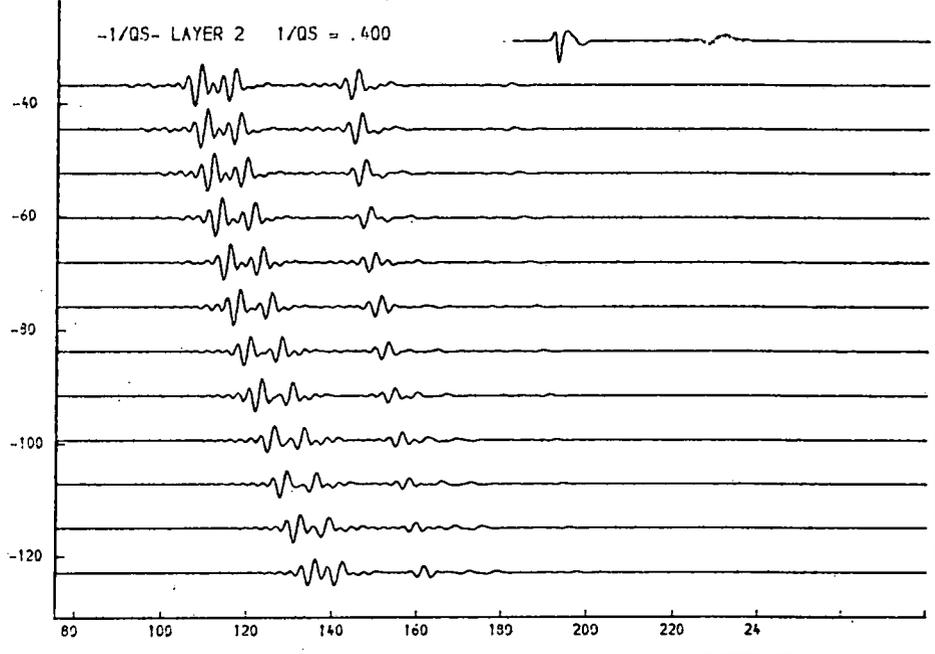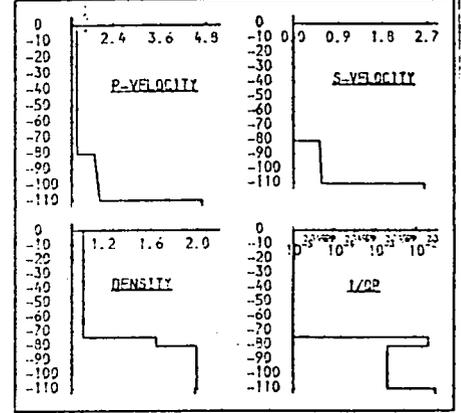| THICKNESS (M.)	P-VELOCITY (M/S.)	S-VELOCITY (M/S.)	DENSITY (G/ML)	1/Q P	1/Q S
74.4	1.460	0.000	1.03	0.00000	0.00000
6.1	1.480	0.010	1.65	0.02000	0.04000
3.5	1.869	0.514	2.00	0.00300	0.02000
3.5	1.906	0.524	2.00	0.00300	0.02000
3.6	1.944	0.535	2.00	0.00300	0.02000
3.7	1.981	0.545	2.00	0.00300	0.02000
3.7	2.019	0.555	2.00	0.00300	0.02000
3.8	2.056	0.565	2.00	0.00300	0.02000
3.9	2.094	0.576	2.00	0.00300	0.02000
4.0	2.131	0.586	2.00	0.00300	0.02000
	4.700	2.550	1.38	0.03000	0.06000

Fig. 9.37b. 1/Qs, layer 2.

Variations of this parameter can control the p-s converted arrival shown in figs. 9.31a-d.

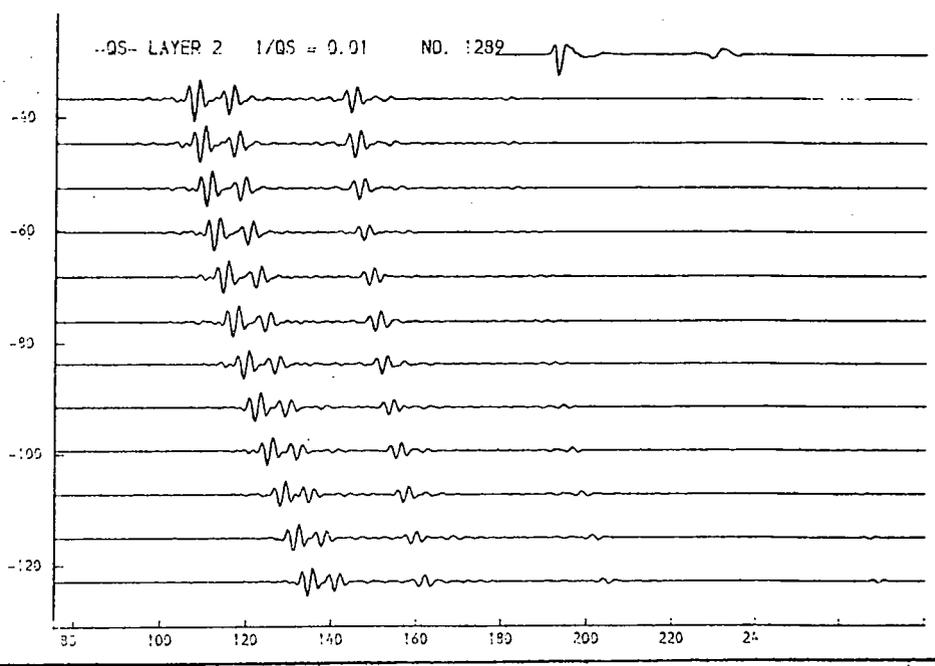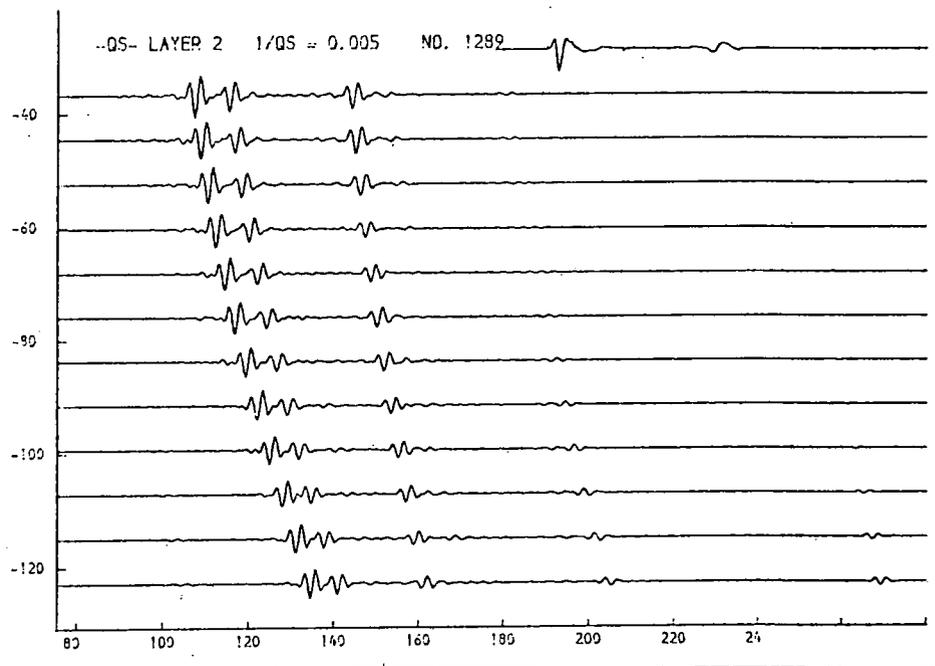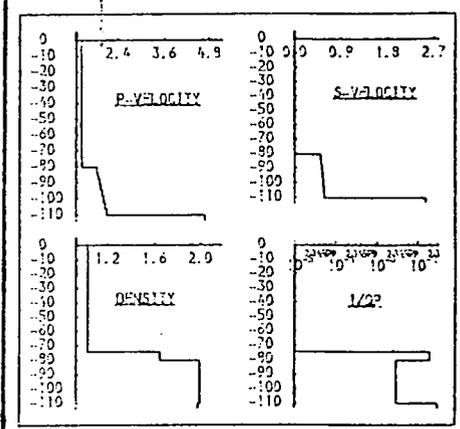| THICKNESS (M.)	P-VELOCITY (M/S.)	S-VELOCITY (M/S.)	DENSITY (G/ML)	1/Q P	1/Q S
74.4	1.460	0.000	1.03	0.00000	0.00000
6.1	1.480	0.010	1.65	0.02000	0.04000
3.7	1.934	0.870	2.00	0.00100	0.01000
3.8	1.953	0.879	2.00	0.00100	0.01000
3.8	1.972	0.937	2.00	0.00100	0.01000
3.8	1.991	0.896	2.00	0.00100	0.01000
3.9	2.009	0.904	2.00	0.00100	0.01000
3.9	2.028	0.913	2.00	0.00100	0.01000
3.9	2.047	0.921	2.00	0.00100	0.01000
4.0	2.066	0.930	2.00	0.00100	0.01000
	4.700	2.550	1.98	0.03000	0.06000
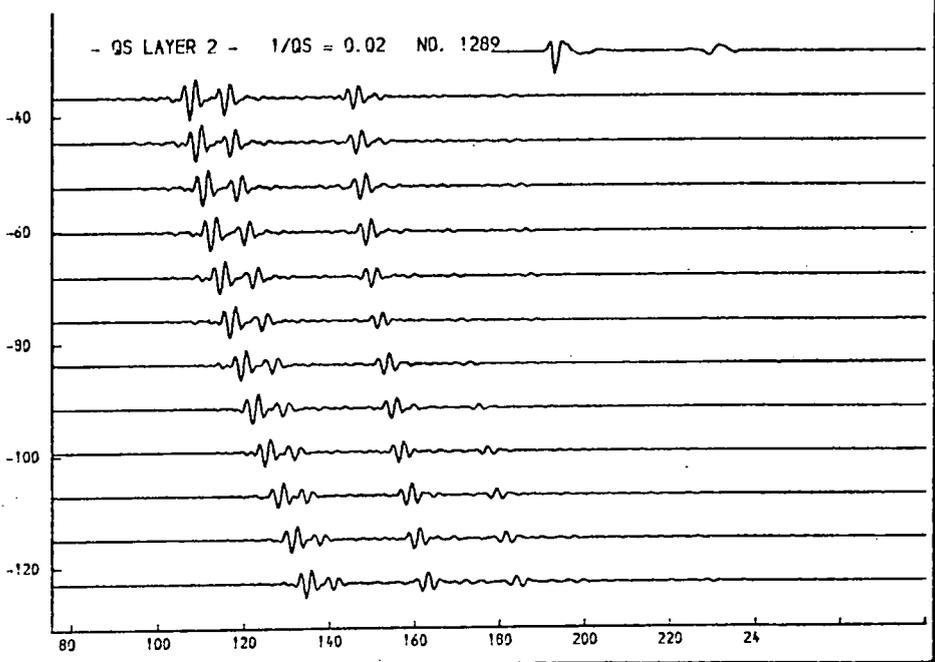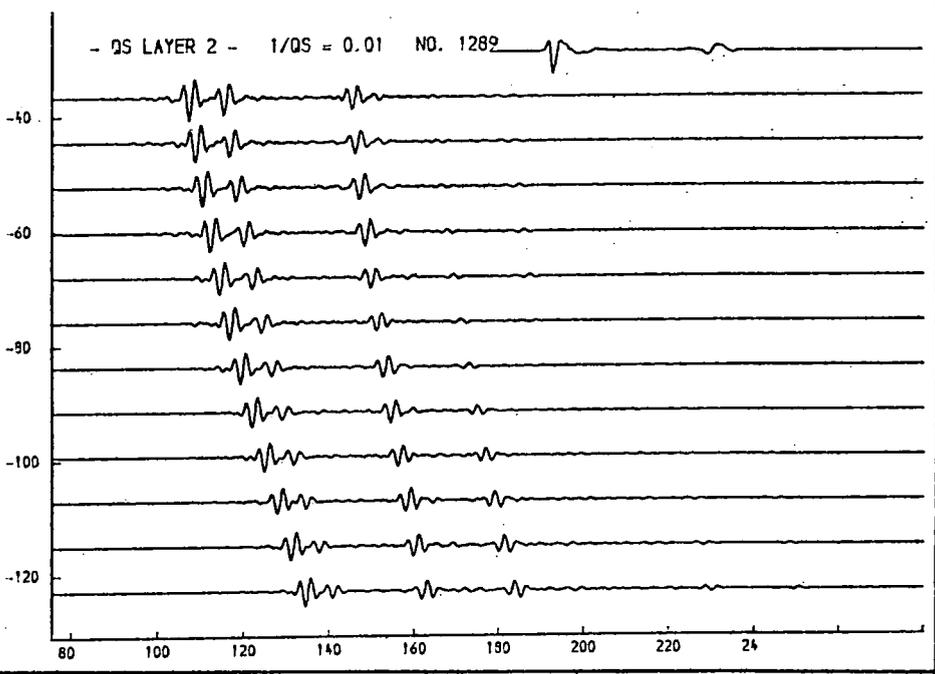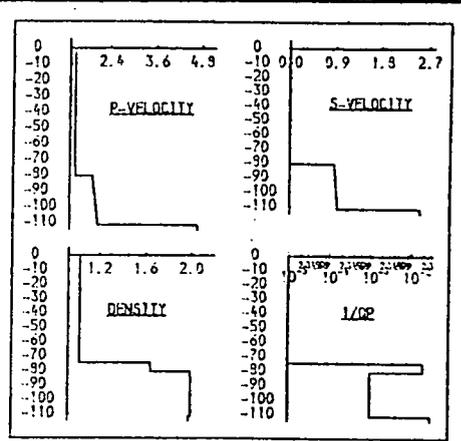
Fig. 9.37c. 1/Qs, layer 2.

Variations of this parameter can control the p-s converted arrival shown in figs. 9.31a-d.

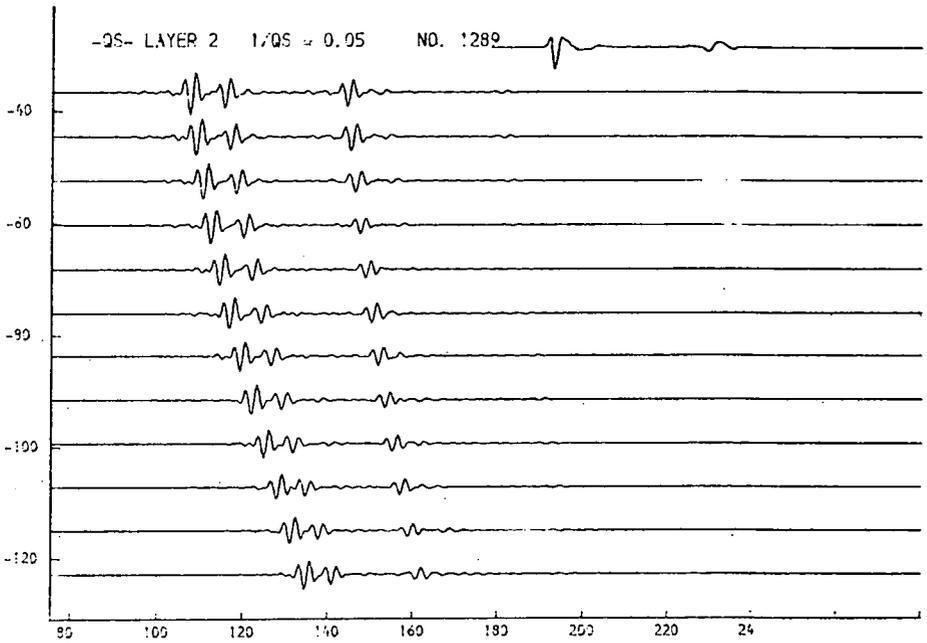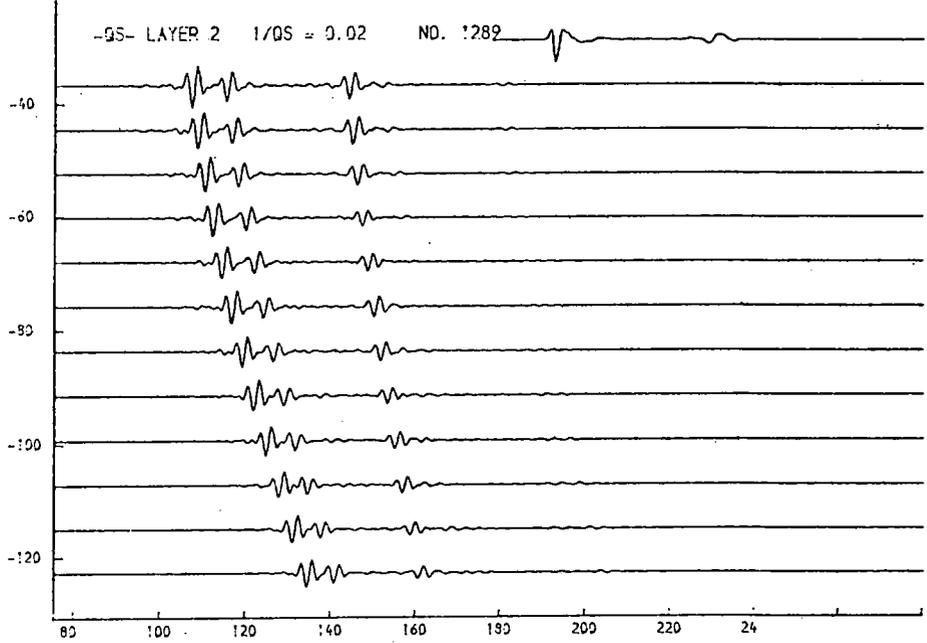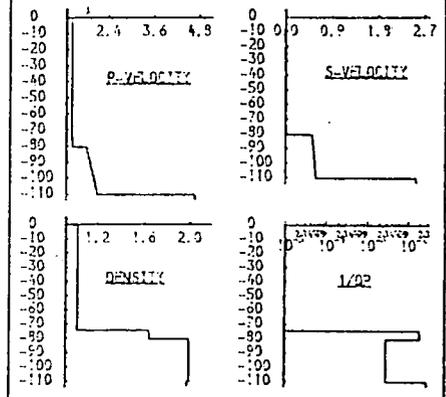| THICKNESS (M.)	P-VELOCITY (M/S.)	S-VELOCITY (M/S.)	DENSITY (G/ML)	1/Q P	1/Q S
74.4	1.460	0.000	1.03	0.00000	0.00000
6.1	1.490	0.010	1.65	0.02000	0.04000
3.7	1.934	0.870	2.00	0.00100	0.05000
3.9	1.953	0.879	2.00	0.00100	0.05000
3.9	1.972	0.887	2.00	0.00100	0.05000
3.9	1.991	0.896	2.00	0.00100	0.05000
3.9	2.009	0.904	2.00	0.00100	0.05000
3.9	2.028	0.913	2.00	0.00100	0.05000
3.9	2.047	0.921	2.00	0.00100	0.05000
4.0	2.066	0.930	2.00	0.00100	0.05000
	4.700	2.550	1.98	0.03000	0.06000

Fig. 9.37d. 1/Qs, layer 2.

Variations of this parameter can control the p-s converted arrival shown in figs. 9.31a-d.

THICKNESS (M.)	P-VELOCITY (M/S.)	S-VELOCITY (M/S.)	DENSITY (G/ML)	1/Q P	1/Q S
74.4	1.460	0.000	1.03	0.00000	0.00000
6.1	1.480	0.010	1.65	0.02000	0.20000
3.6	1.934	0.532	2.00	0.00200	0.20000
3.6	1.953	0.537	2.00	0.00200	0.20000
3.6	1.972	0.542	2.00	0.00200	0.20000
3.7	1.991	0.547	2.00	0.00200	0.20000
3.7	2.009	0.553	2.00	0.00200	0.20000
3.7	2.028	0.559	2.00	0.00200	0.20000
3.9	2.047	0.563	2.00	0.00200	0.20000
3.9	2.066	0.569	2.00	0.00200	0.20000
	4.700	2.650	1.98	0.03000	0.30000

Fig. 9.38a. P-velocity, layer 3.

The main influence of this parameter is on the overall amplitude of the reflexion r2. Note frequency range in this figure is 100-450Hz.

THICKNESS (M.)	P-VELOCITY (M/S.)	S-VELOCITY (M/S.)	DENSITY (G/ML)	1/Q P	1/Q S
74.4	1.460	0.000	1.03	0.00000	0.00000
6.1	1.480	0.010	1.65	0.02000	0.20000
3.6	1.934	0.532	2.00	0.00200	0.20000
3.6	1.953	0.537	2.00	0.00200	0.20000
3.6	1.972	0.542	2.00	0.00200	0.20000
3.7	1.991	0.547	2.00	0.00200	0.20000
3.7	2.009	0.553	2.00	0.00200	0.20000
3.7	2.028	0.558	2.00	0.00200	0.20000
3.9	2.047	0.563	2.00	0.00200	0.20000
3.9	2.066	0.569	2.00	0.00200	0.20000
	5.300	2.650	1.99	0.03000	0.30000

Fig. 9.38b. P-velocity, layer 3.

The main influence of this parameter is on the overall amplitude of the reflexion r2. Note frequency range in this figure is 100-450Hz.

THICKNESS (M.)	P-VELOCITY (M/S.)	S-VELOCITY (M/S.)	DENSITY (G/ML)	1/Q P	1/Q S
74.4	1.460	0.000	1.03	0.00000	0.00000
6.1	1.480	0.010	1.65	0.02000	0.20000
3.6	1.934	0.532	2.00	0.00200	0.20000
3.6	1.953	0.537	2.00	0.00200	0.20000
3.6	1.972	0.542	2.00	0.00200	0.20000
3.7	1.991	0.547	2.00	0.00200	0.20000
3.7	2.009	0.553	2.00	0.00200	0.20000
3.7	2.029	0.558	2.00	0.00200	0.20000
3.9	2.047	0.563	2.00	0.00200	0.20000
3.9	2.066	0.569	2.00	0.00200	0.20000
	4.500	2.650	1.98	0.03000	0.30000

Fig. 9.38c. P-velocity, layer 3.

The main influence of this parameter is on the overall amplitude of the reflexion r2. Note frequency range in this figure is 100-450Hz.

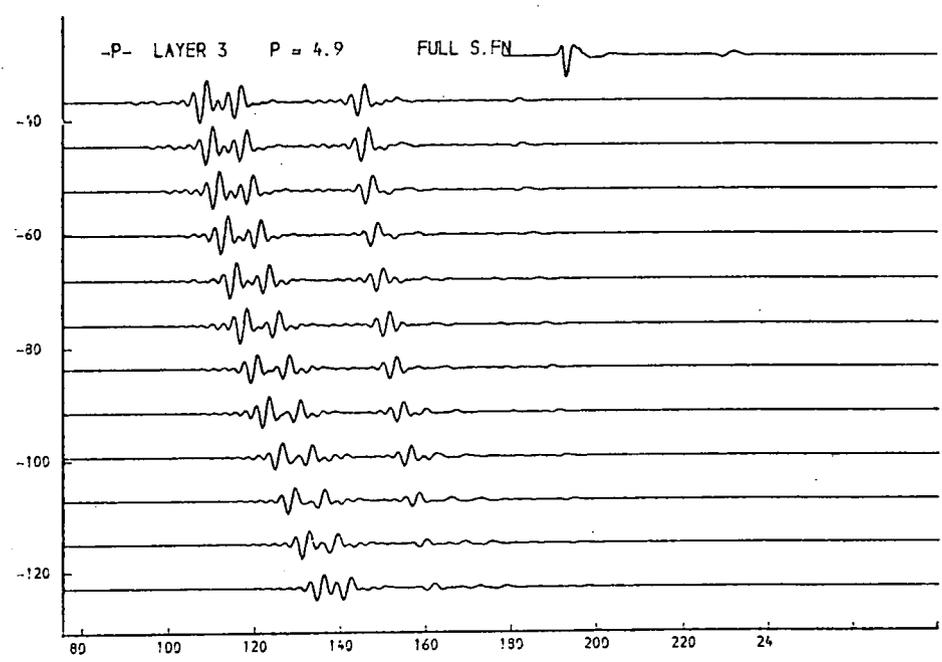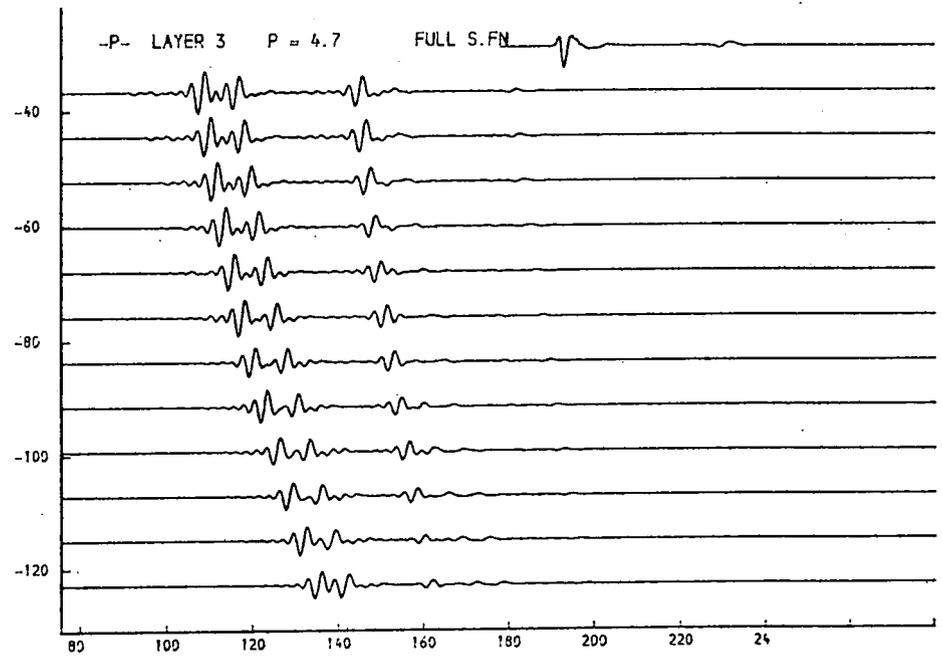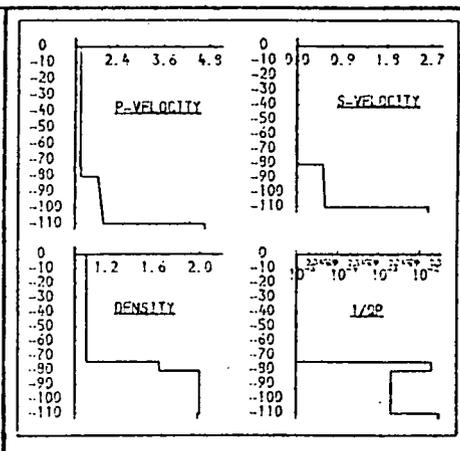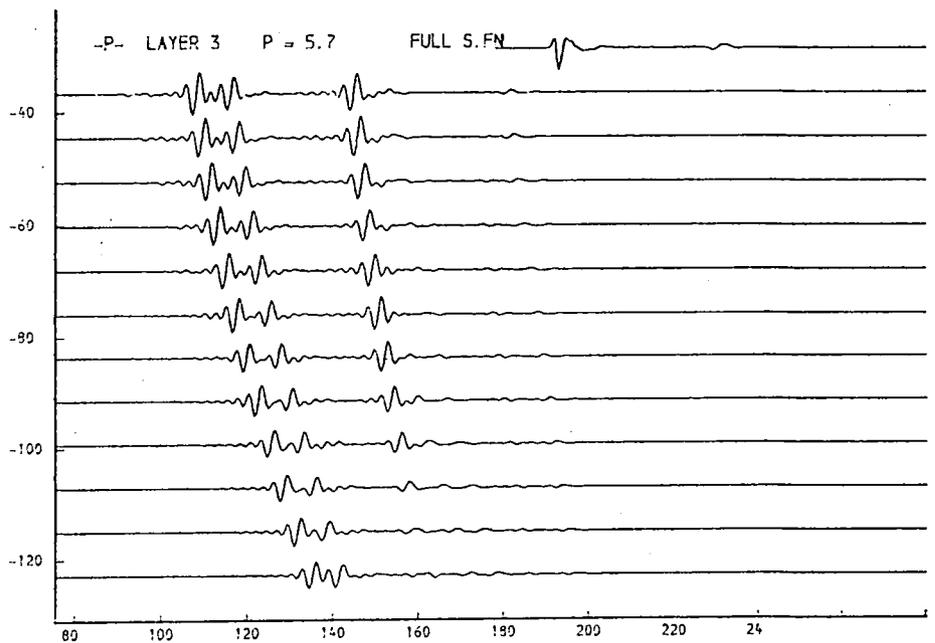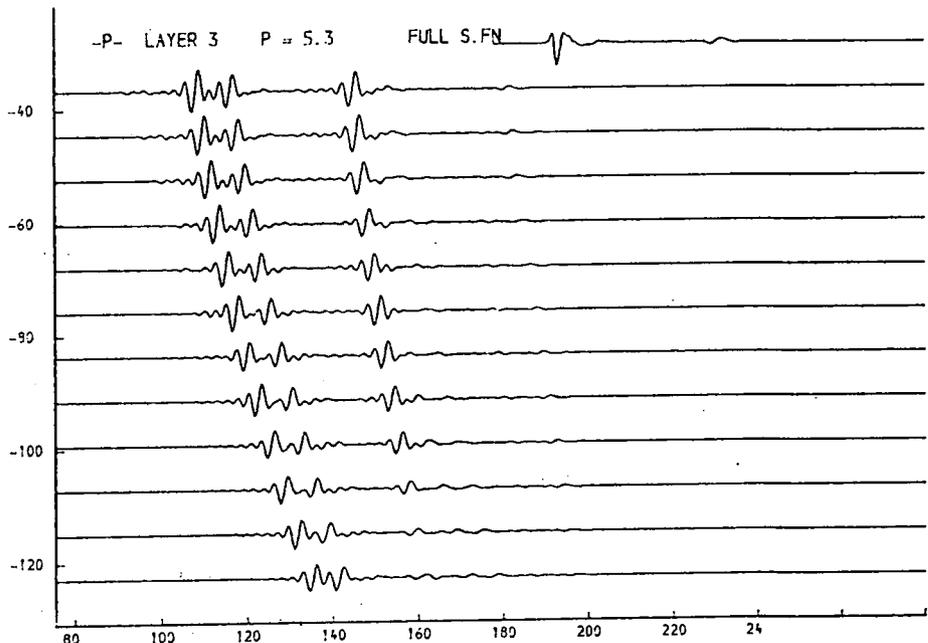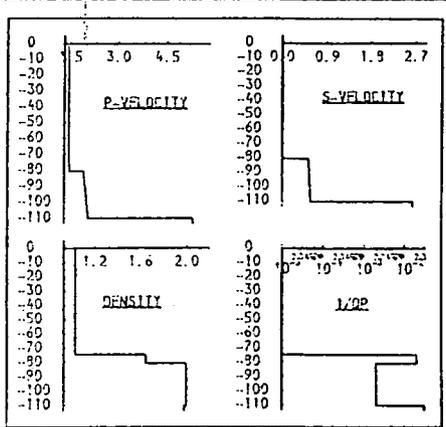| THICKNESS (M.)	P-VELOCITY (M/S.)	S-VELOCITY (M/S.)	DENSITY (C/ML)	1/Q P	1/Q S
74.4	1.460	0.000	1.03	0.00000	0.00000
6.1	1.480	0.010	1.65	0.02000	0.20000
3.6	1.934	0.532	2.00	0.00200	0.20000
3.6	1.953	0.537	2.00	0.00200	0.20000
3.6	1.972	0.542	2.00	0.00200	0.20000
3.7	1.991	0.547	2.00	0.00200	0.20000
3.7	2.009	0.553	2.00	0.00200	0.20000
3.7	2.029	0.558	2.00	0.00200	0.20000
3.8	2.047	0.563	2.00	0.00200	0.20000
3.9	2.066	0.569	2.00	0.00200	0.20000
	4.100	2.650	1.93	0.03000	0.30000

Fig. 9.38d. P-velocity, layer 3.

The main influence of this parameter is on the overall amplitude of the reflexion r2. Note frequency range in this figure is 100-450Hz.

THICKNESS (M.)	P-VELOCITY (M/S.)	S-VELOCITY (M/S.)	DENSITY (G/ML)	1/Q P	1/Q S
74.4	1.460	0.000	1.03	0.00000	0.00000
6.1	1.480	0.010	1.65	0.02000	0.20000
3.6	1.934	0.532	2.00	0.00200	0.20000
3.6	1.953	0.537	2.00	0.00200	0.20000
3.6	1.972	0.542	2.00	0.00200	0.20000
3.7	1.991	0.547	2.00	0.00200	0.20000
3.7	2.009	0.553	2.00	0.00200	0.20000
3.7	2.029	0.558	2.00	0.00200	0.20000
3.8	2.047	0.563	2.00	0.00200	0.20000
3.8	2.066	0.568	2.00	0.00200	0.20000
	4.700	2.200	1.99	0.03000	0.30000

Fig. 9.39a. S-velocity, layer 3.

Variation of s-velocity influences the change with offset of the amplitude of r2. Note frequency range in this figure is 100-450Hz.

THICKNESS (M.)	P-VELOCITY (M/S.)	S-VELOCITY (M/S.)	DENSITY (G/ML)	1/Q P	1/Q S
74.4	1.460	0.000	1.03	0.00000	0.00000
6.1	1.490	0.010	1.65	0.02000	0.04000
3.6	1.934	0.532	2.00	0.00200	0.40000
3.6	1.953	0.537	2.00	0.00200	0.40000
3.6	1.972	0.542	2.00	0.00200	0.40000
3.7	1.991	0.547	2.00	0.00200	0.40000
3.7	2.009	0.553	2.00	0.00200	0.40000
3.7	2.028	0.559	2.00	0.00200	0.40000
3.3	2.047	0.563	2.00	0.00200	0.40000
3.6	2.066	0.568	2.00	0.00200	0.40000
	4.700	2.250	1.98	0.03000	0.06000

Fig. 9.39b. S-velocity, layer 3.

Variation of s-velocity influences the change with offset
of the amplitude of r2.   Note frequency range in this
figure is 100-450Hz.

THICKNESS (M.)	P-VELOCITY (M/S.)	S-VELOCITY (M/S.)	DENSITY (G/ML)	1/Q P	1/Q S
74.4	1.460	0.000	1.03	0.00000	0.00000
6.1	1.490	0.010	1.65	0.02000	0.04000
3.6	1.934	0.532	2.00	0.00200	0.40000
3.6	1.953	0.537	2.00	0.00200	0.40000
3.6	1.972	0.542	2.00	0.00200	0.40000
3.7	1.991	0.547	2.00	0.00200	0.40000
3.7	2.009	0.553	2.00	0.00200	0.40000
3.7	2.029	0.559	2.00	0.00200	0.40000
3.9	2.047	0.563	2.00	0.00200	0.40000
3.8	2.066	0.568	2.00	0.00200	0.40000
	4.700	2.950	1.98	0.03000	0.06000

-S- LAYER 3   S = 2.80

-S- LAYER 3   S = 2.95
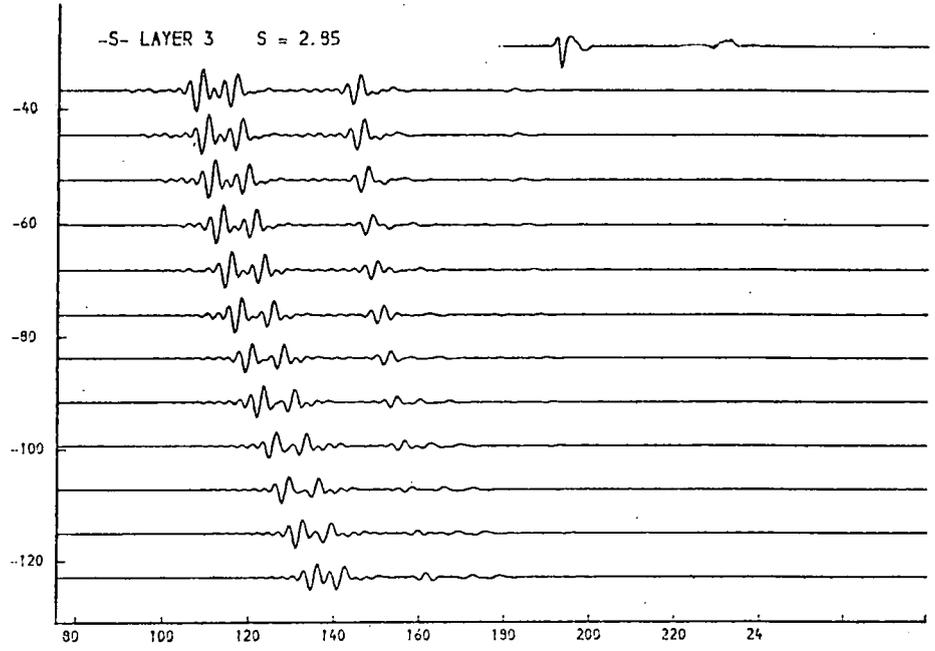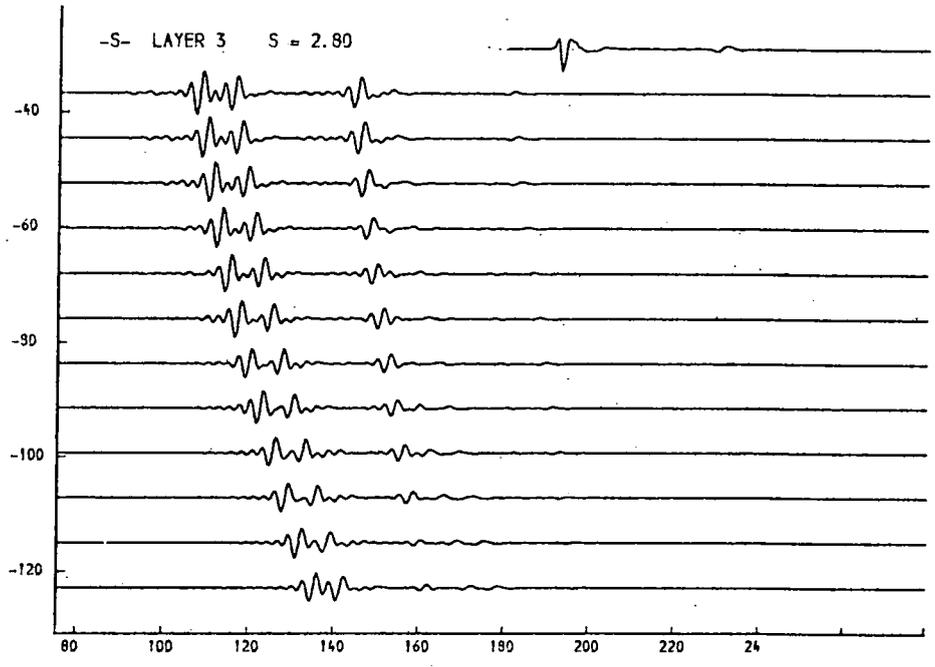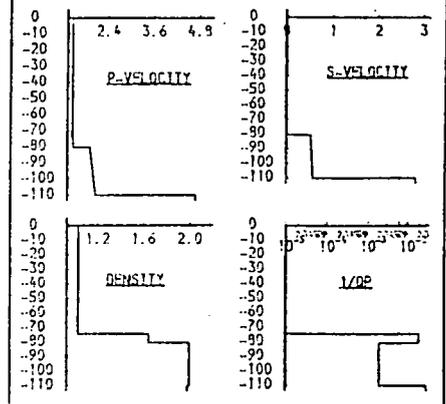
Fig. 9.39c. S-velocity, layer 3.

Variation of s-velocity influences the change with offset of the amplitude of r2. Note frequency range in this figure is 100-450Hz.

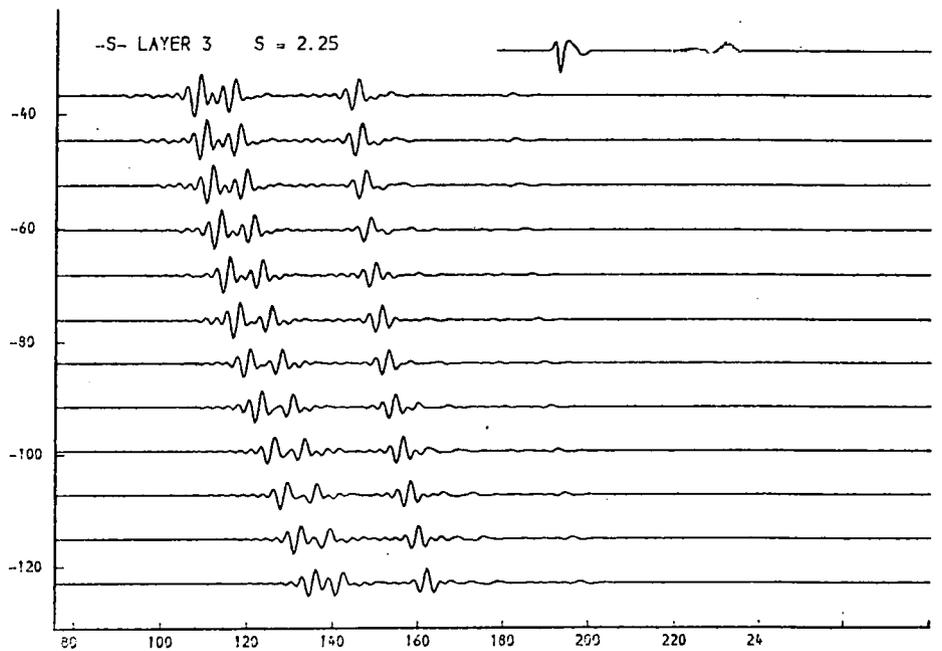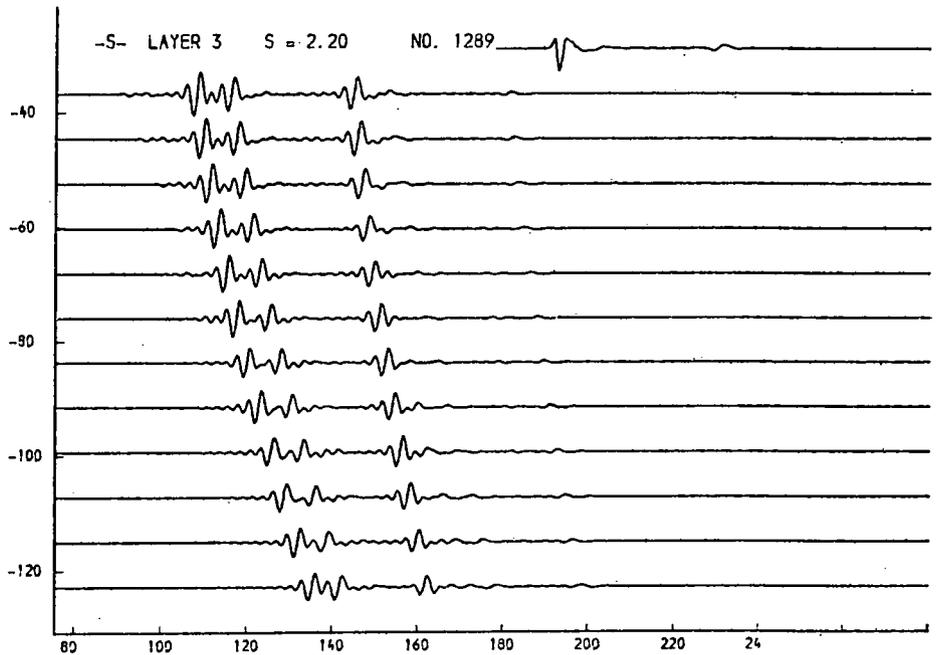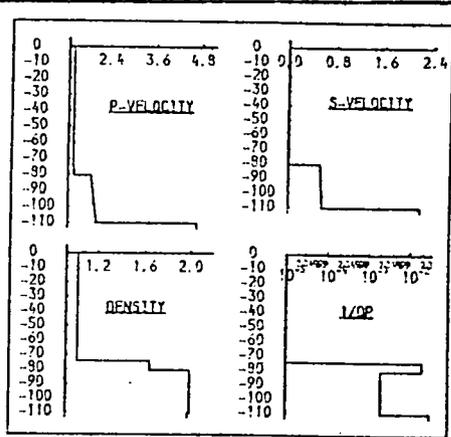| THICKNESS (M.)	P-VELOCITY (M/S.)	S-VELOCITY (M/S.)	DENSITY (G/ML)	1/Q P	1/Q S
74.4	1.460	0.000	1.03	0.00000	0.00000
6.1	1.480	0.010	1.65	0.02000	0.20000
3.6	1.934	0.532	2.00	0.00200	0.20000
3.6	1.953	0.537	2.00	0.00200	0.20000
3.6	1.972	0.542	2.00	0.00200	0.20000
3.7	1.991	0.547	2.00	0.00200	0.20000
3.7	2.009	0.553	2.00	0.00200	0.20000
3.7	2.029	0.559	2.00	0.00200	0.20000
3.8	2.047	0.563	2.00	0.00200	0.20000
3.8	2.066	0.569	2.00	0.00200	0.20000
	4.700	2.800	1.98	0.03000	0.30000

Fig. 9.39d. S-velocity, layer 3.

Variation of s-velocity influences the change with offset of the amplitude of r2. Note frequency range in this figure is 100-450Hz.

THICKNESS (M.)	P-VELOCITY (M/S.)	S-VELOCITY (M/S.)	DENSITY (G/ML)	1/Q P	1/Q S
74.4	1.460	0.000	1.03	0.00000	0.00000
6.1	1.480	0.010	1.65	0.02000	0.04000
3.7	1.934	0.532	2.00	0.00100	0.03000
3.8	1.953	0.537	2.00	0.00100	0.03000
3.9	1.972	0.542	2.00	0.00100	0.03000
3.9	1.991	0.547	2.00	0.00100	0.03000
3.9	2.009	0.553	2.00	0.00100	0.03000
3.9	2.028	0.559	2.00	0.00100	0.03000
3.9	2.047	0.563	2.00	0.00100	0.03000
4.0	2.066	0.569	2.00	0.00100	0.03000
	4.700	2.550	1.90	0.03000	0.06000
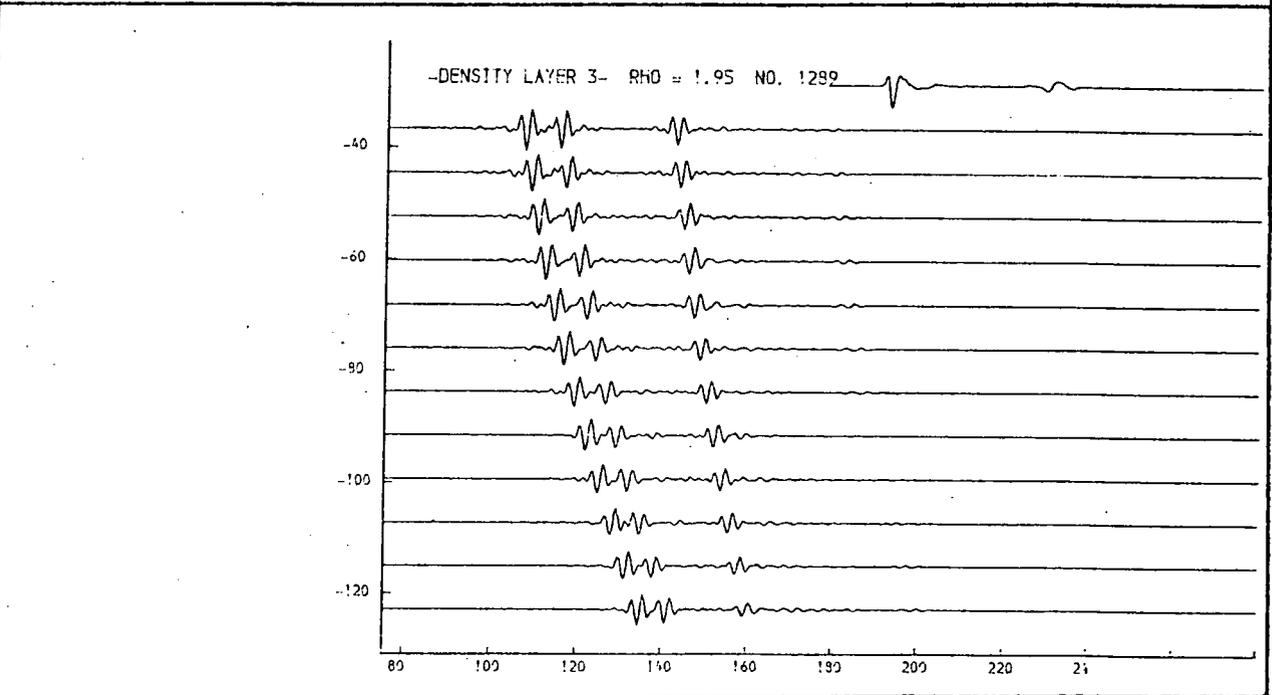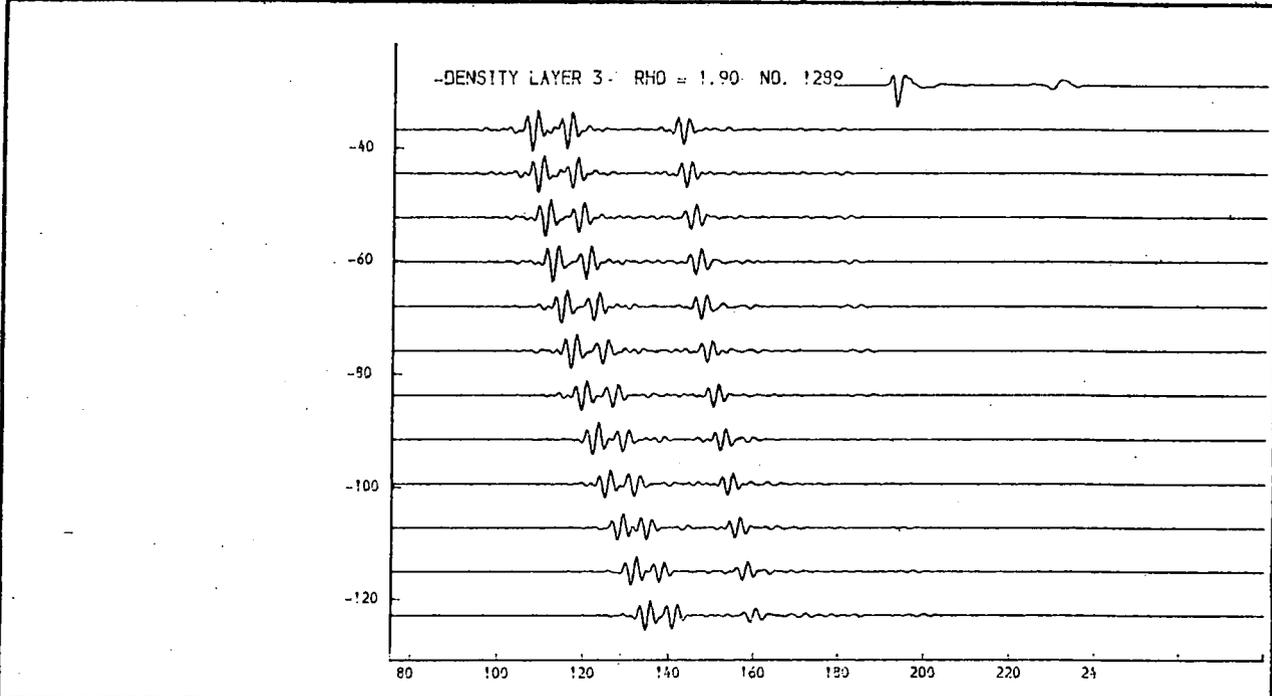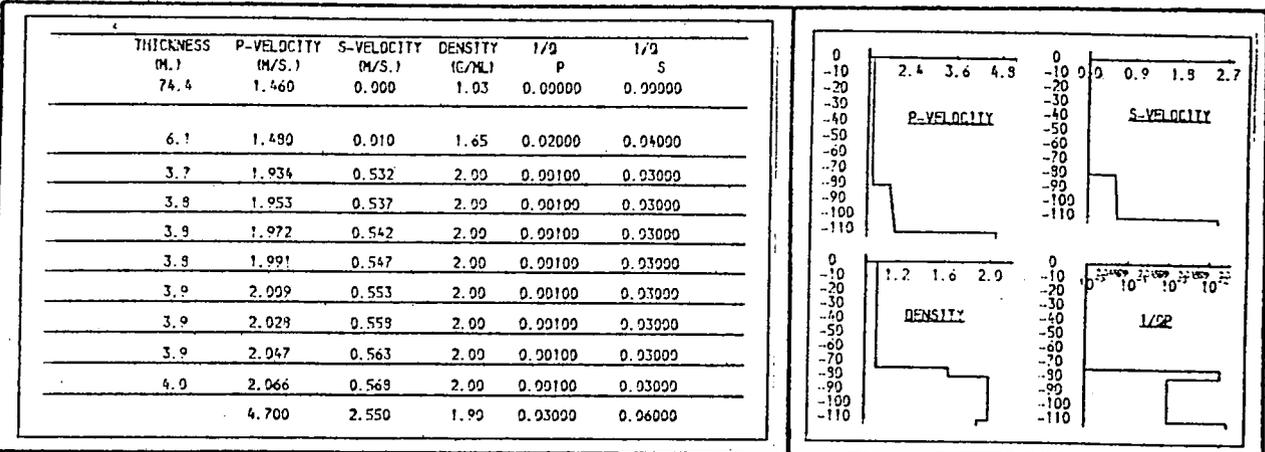
Fig. 9.40a.   Density, layer 3.

As with layers 1 and 2, density is seen to affect the overall amplitude of a reflector (here, r2), but has little influence on its relative variation with offset distance.

THICKNESS (M.)	P-VELOCITY (M/S.)	S-VELOCITY (M/S.)	DENSITY (G/ML)	1/Q P	1/Q S
74.4	1.460	0.000	1.03	0.00000	0.00000
6.1	1.490	0.010	1.65	0.02000	0.04000
3.7	1.934	0.532	2.00	0.00100	0.03000
3.8	1.953	0.537	2.00	0.00100	0.03000
3.8	1.972	0.542	2.00	0.00100	0.03000
3.8	1.991	0.547	2.00	0.00100	0.03000
3.9	2.009	0.553	2.00	0.00100	0.03000
3.9	2.029	0.558	2.00	0.00100	0.03000
3.9	2.047	0.563	2.00	0.00100	0.03000
4.0	2.066	0.568	2.00	0.00100	0.03000
	4.700	2.550	2.05	0.03000	0.06000

--DENSITY LAYER 3. RHO = 2.05 NO. 1289

--DENSITY LAYER 3. RHO = 2.10 NO. 1289

Fig. 9.40b. Density, layer 3.

As with layers 1 and 2, density is seen to affect the overall amplitude of a reflector (here, r2), but has little influence on its relative variation with offset distance.

THICKNESS (M.)	P-VELOCITY (M/S.)	S-VELOCITY (M/S.)	DENSITY (G/ML)	1/Q P	1/Q S
74.4	1.460	0.000	1.03	0.00000	0.00000
6.1	1.480	0.010	1.65	0.02000	0.04000
3.7	1.934	0.532	2.00	0.00100	0.03000
3.8	1.953	0.537	2.00	0.00100	0.03000
3.8	1.972	0.542	2.00	0.00100	0.03000
3.8	1.991	0.547	2.00	0.00100	0.03000
3.9	2.009	0.553	2.00	0.00100	0.03000
3.9	2.028	0.558	2.00	0.00100	0.03000
3.9	2.047	0.563	2.00	0.00100	0.03000
4.0	2.066	0.568	2.00	0.00100	0.03000
	4.700	2.550	1.99	0.00100	0.06000

Fig. 9.41a. 1/Qp, layer 3.

Higher values for this parameter influence reflector r2 at the higher offset distances.

THICKNESS (M.)	P-VELOCITY (M/S.)	S-VELOCITY (M/S.)	DENSITY (G/ML)	1/Q P	1/Q S
74.4	1.460	0.000	1.03	0.00000	0.00000
6.1	1.430	0.010	1.65	0.02000	0.04000
3.7	1.934	0.532	2.00	0.00100	0.03000
3.9	1.953	0.537	2.00	0.00100	0.03000
3.9	1.972	0.542	2.00	0.00100	0.03000
3.9	1.991	0.547	2.00	0.00100	0.03000
3.9	2.009	0.553	2.00	0.00100	0.03000
3.9	2.028	0.558	2.00	0.00100	0.03000
3.9	2.047	0.563	2.00	0.00100	0.03000
4.0	2.066	0.568	2.00	0.00100	0.03000
	4.700	2.550	1.99	0.01000	0.06000

-- QP LAYER 3 -- 1/QP = 0.01 NO. 1289

-- QP LAYER 3 -- 1/QP = 0.02 NO. 1289

Fig. 9.41b. 1/Qp, layer 3.

Higher values for this parameter influence reflector r2 at the higher offset distances.

THICKNESS (M.)	P-VELOCITY (M/S.)	S-VELOCITY (M/S.)	DENSITY (G/ML)	1/Q P	1/Q S
74.4	1.460	0.000	1.03	0.00000	0.00000
6.1	1.480	0.010	1.65	0.02000	0.04000
3.7	1.934	0.532	2.00	0.00100	0.03000
3.8	1.953	0.537	2.00	0.00100	0.03000
3.8	1.972	0.542	2.00	0.00100	0.03000
3.9	1.991	0.547	2.00	0.00100	0.03000
3.9	2.009	0.553	2.00	0.00100	0.03000
3.9	2.028	0.558	2.00	0.00100	0.03000
3.9	2.047	0.563	2.00	0.00100	0.03000
4.0	2.066	0.568	2.00	0.00100	0.03000
	4.700	2.550	1.98	0.03000	0.06000

Fig. 9.41c. 1/Qp, layer 3.

Higher values for this parameter influence reflector r2 at the higher offset distances.

THICKNESS (M.)	P-VELOCITY (M/S.)	S-VELOCITY (M/S.)	DENSITY (G/ML)	1/Q P	1/Q S
74.4	1.460	0.000	1.03	0.00000	0.00000
6.1	1.490	0.010	1.65	0.02000	0.04000
3.7	1.934	0.532	2.00	0.00100	0.03000
3.9	1.953	0.537	2.00	0.00100	0.03000
3.9	1.972	0.542	2.00	0.00100	0.03000
3.9	1.991	0.547	2.00	0.00100	0.03000
3.9	2.009	0.553	2.00	0.00100	0.03000
3.9	2.028	0.558	2.00	0.00100	0.03000
3.9	2.047	0.563	2.00	0.00100	0.03000
4.0	2.066	0.568	2.00	0.00100	0.03000
	4.700	2.550	1.99	0.10000	0.06000

— QP LAYER 3 —   1/QP = 0.1   NO. 1289
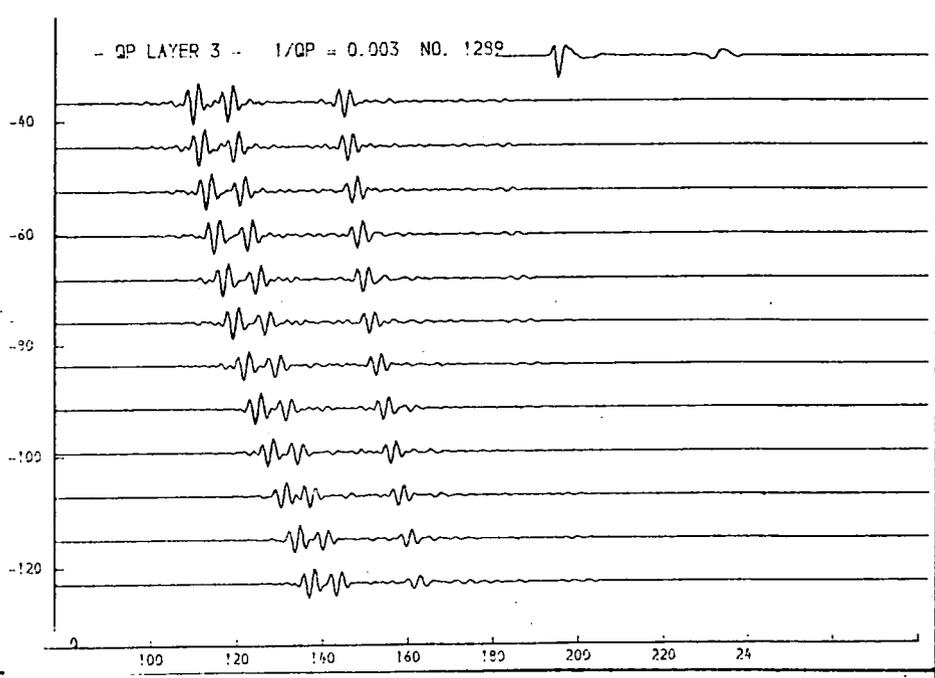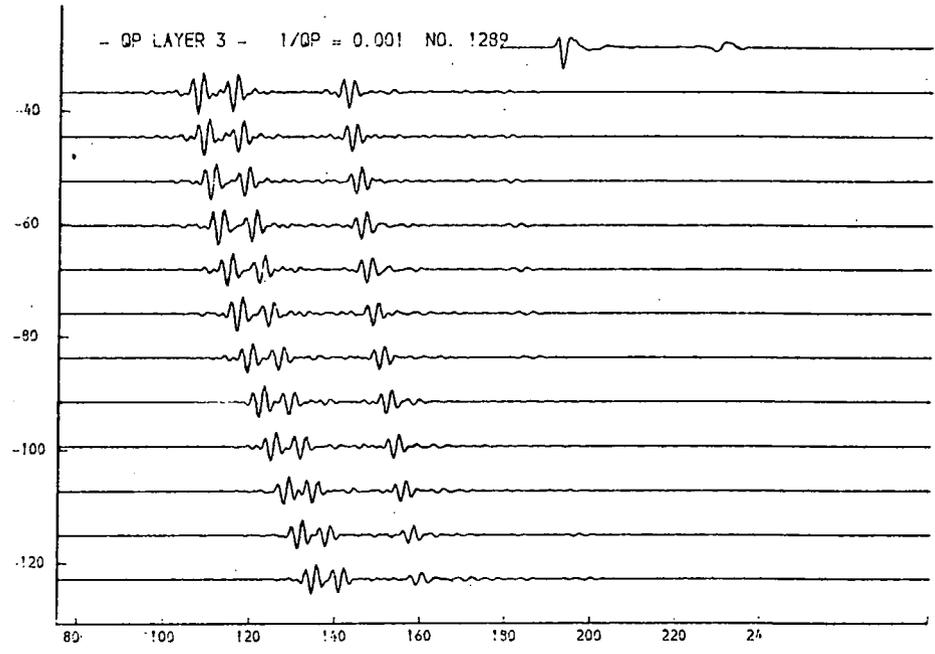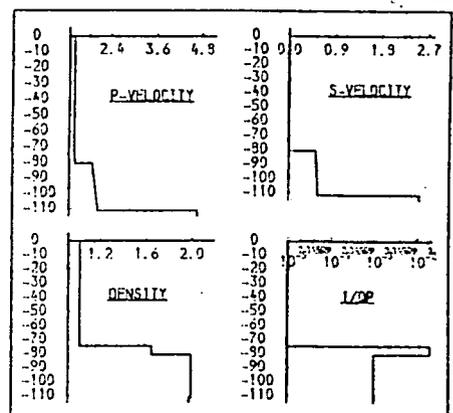
— QP LAYER 3 —   1/QP = 0.3   NO. 1289

Fig. 9.41d. 1/Qp, layer 3.

Higher values for this parameter influence reflector r2 at the higher offset distances.

THICKNESS (M.)	P-VELOCITY (M/S.)	S-VELOCITY (M/S.)	DENSITY (G/ML)	1/Q P	1/Q S
74.4	1.460	0.000	1.03	0.00000	0.00000
6.1	1.480	0.010	1.65	0.02000	0.04000
3.7	1.934	0.870	2.00	0.00100	0.03000
3.9	1.953	0.879	2.00	0.00100	0.03000
3.8	1.972	0.887	2.00	0.00100	0.03000
3.9	1.991	0.896	2.00	0.00100	0.03000
3.9	2.009	0.904	2.00	0.00100	0.03000
3.9	2.028	0.913	2.00	0.00100	0.03000
3.9	2.047	0.921	2.00	0.00100	0.03000
4.0	2.066	0.930	2.00	0.00100	0.03000
	4.700	2.550	1.99	0.00100	0.06000

Fig. 9.42a. 1/Qp, layer 3.

When the s-velocity in layer 2 takes a high value (0.9km/sec), 1/Qp is required to be higher to control the rise of reflector r2 at the higher offset distances.

THICKNESS (M.)	P-VELOCITY (M/S.)	S-VELOCITY (M/S.)	DENSITY (G/ML)	1/Q P	1/Q S
74.4	1.460	0.000	1.03	0.00000	0.00000
6.1	1.480	0.010	1.65	0.02000	0.04000
3.7	1.934	0.870	2.00	0.00100	0.03000
3.3	1.953	0.879	2.00	0.00100	0.03000
3.9	1.972	0.887	2.00	0.00100	0.03000
3.9	1.991	0.896	2.00	0.00100	0.03000
3.9	2.009	0.904	2.00	0.00100	0.03000
3.9	2.028	0.913	2.00	0.00100	0.03000
3.9	2.047	0.921	2.00	0.00100	0.03000
4.0	2.066	0.930	2.00	0.00100	0.03000
	4.700	2.550	1.98	0.01000	0.06000

P-VELOCITY   2.4 3.6 4.8

S-VELOCITY   0.9 1.9 2.7

DENSITY   1.2 1.6 2.0

1/QP

--QP LAYER 3-- S=.9 1/QP = 0.01 NO. 1289

-QP LAYER 3-- S=.9 1/QP = 0.02 NO. 1289

Fig. 9.42b. 1/Qp, layer 3.

When the s-velocity in layer 2 takes a high value (0.9km/sec), 1/Qp is required to be higher to control the rise of reflector r2 at the higher offset distances.

THICKNESS (M.)	P-VELOCITY (M/S.)	S-VELOCITY (M/S.)	DENSITY (G/ML)	1/Q P	1/Q S
74.4	1.460	0.000	1.03	0.00000	0.00000
6.1	1.480	0.010	1.65	0.02000	0.04000
3.7	1.934	0.870	2.00	0.00100	0.03000
3.8	1.953	0.879	2.00	0.00100	0.03000
3.8	1.972	0.887	2.00	0.00100	0.03000
3.8	1.991	0.896	2.00	0.00100	0.03000
3.9	2.009	0.904	2.00	0.00100	0.03000
3.9	2.028	0.913	2.00	0.00100	0.03000
3.9	2.047	0.921	2.00	0.00100	0.03000
4.0	2.066	0.930	2.00	0.00100	0.03000
	4.700	2.550	1.98	0.10000	0.06000
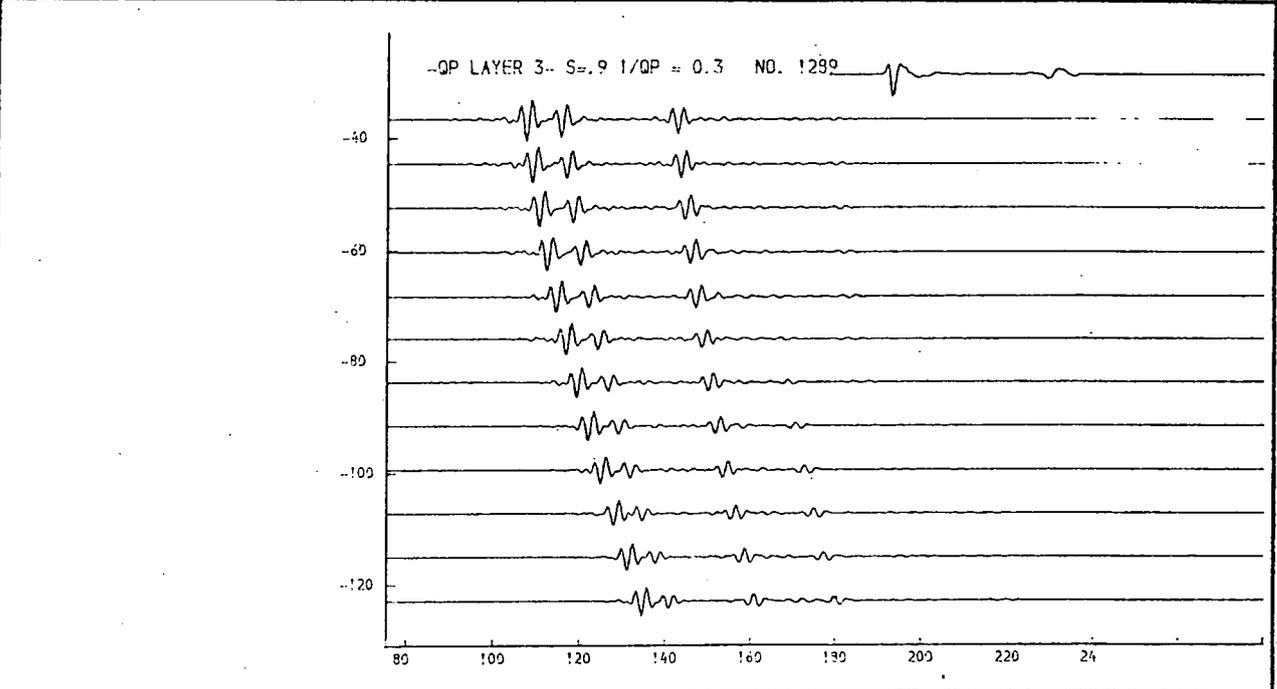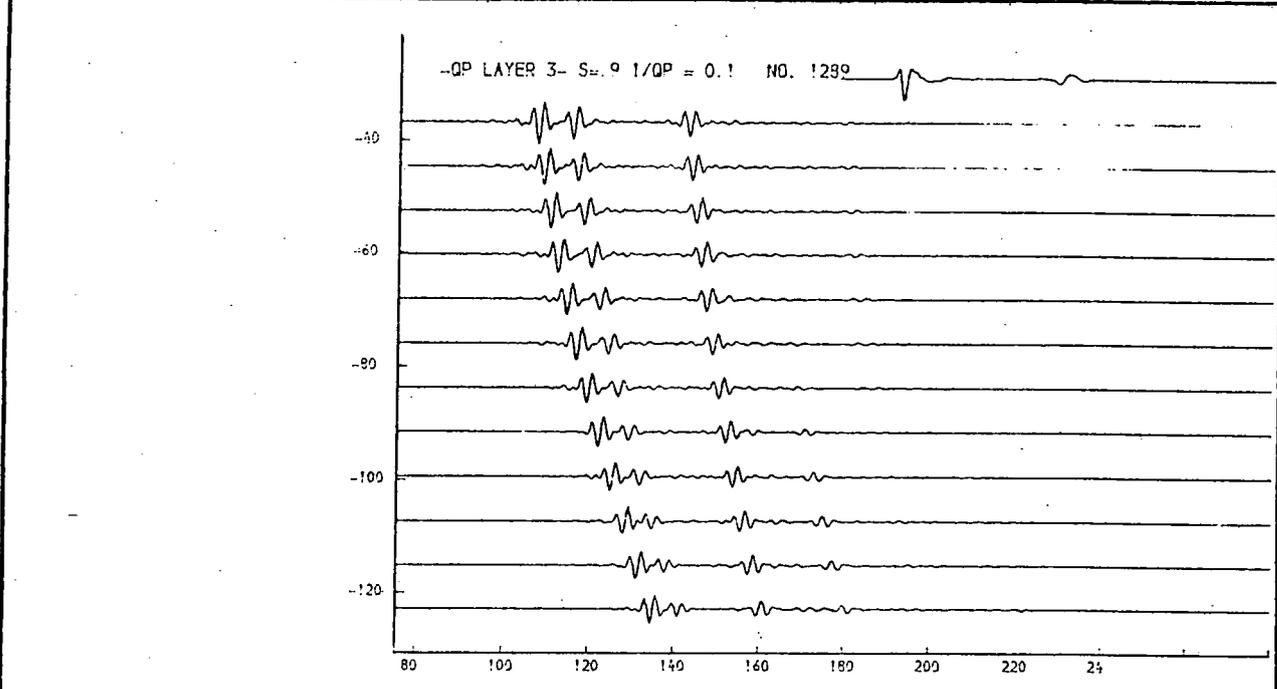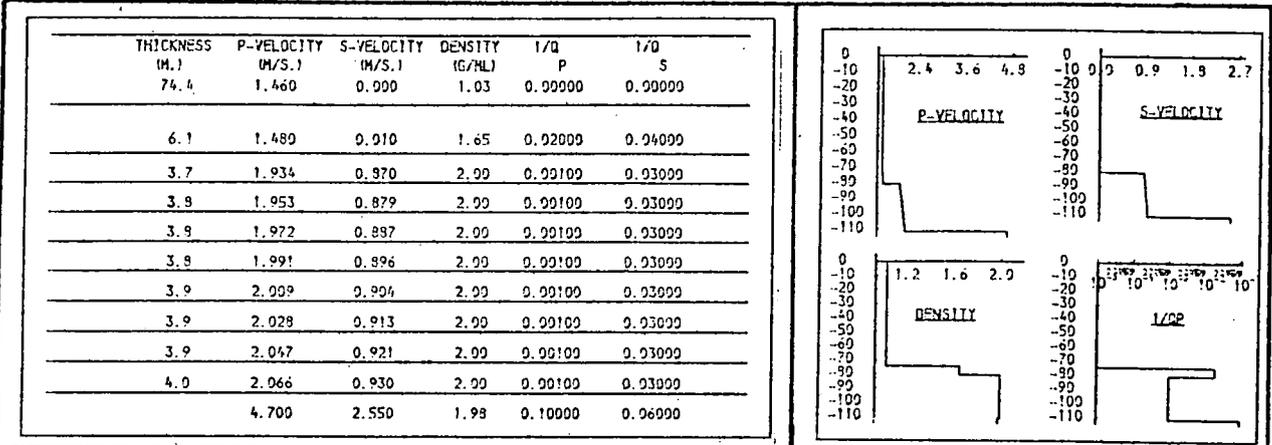
Fig. 9.42c. 1/Qp, layer 3.

When the s-velocity in layer 2 takes a high value (0.9km/sec), 1/Qp is required to be higher to control the rise of reflector r2 at the higher offset distances.

THICKNESS (M.)	P-VELOCITY (M/S.)	S-VELOCITY (M/S.)	DENSITY (G/ML)	1/Q P	1/Q S
74.4	1.460	0.000	1.03	0.00000	0.00000
6.1	1.480	0.010	1.65	0.02000	0.04000
3.7	1.934	0.870	2.00	0.00100	0.03000
3.8	1.953	0.879	2.00	0.00100	0.03000
3.8	1.972	0.887	2.00	0.00100	0.03000
3.9	1.991	0.896	2.00	0.00100	0.03000
3.9	2.009	0.904	2.00	0.00100	0.03000
3.9	2.028	0.913	2.00	0.00100	0.03000
3.9	2.047	0.921	2.00	0.00100	0.03000
4.0	2.066	0.930	2.00	0.00100	0.03000
	4.700	2.550	1.99	1.00000	0.06000

-QP LAYER 3- S=.9 1/QP = 1.0   NO. 1289

-QP LAYER 3- S=.9 1/QP = 3.0   NO. 1289

Fig. 9.42d. 1/Qp, layer 3.

When the s-velocity in layer 2 takes a high value (0.9km/sec), 1/Qp is required to be higher to control the rise of reflector r2 at the higher offset distances.

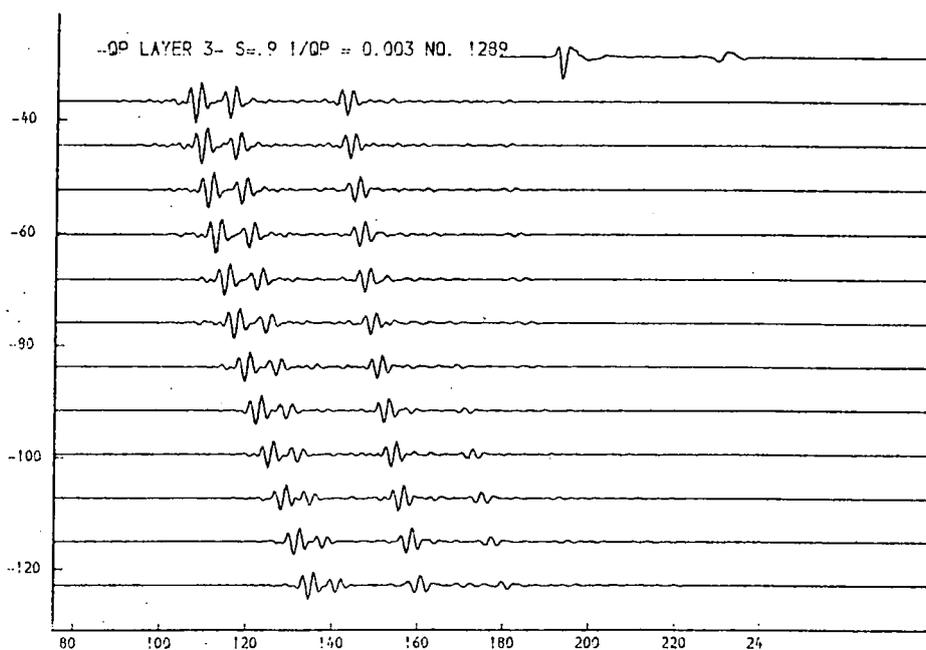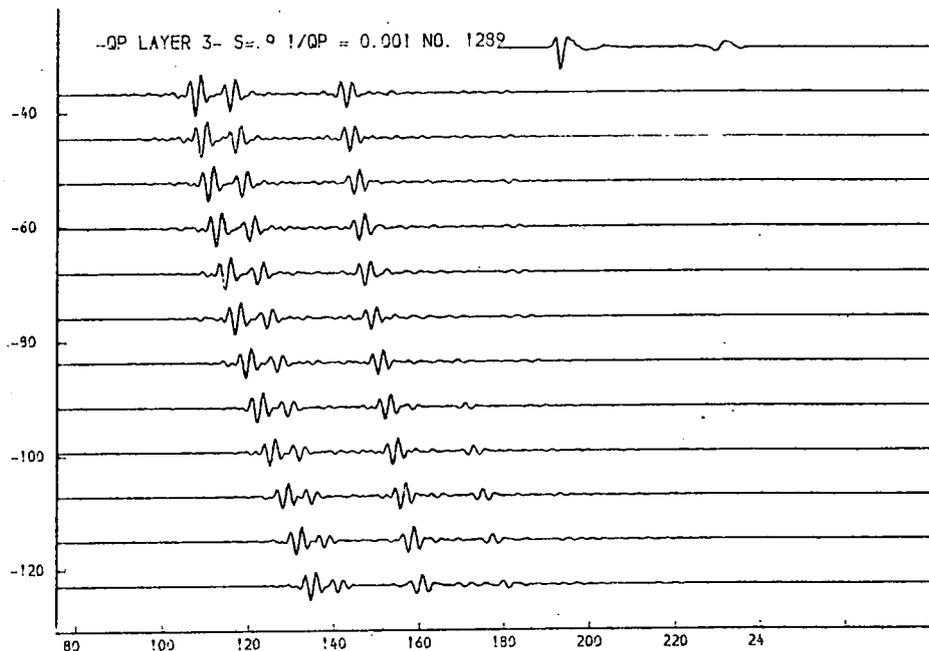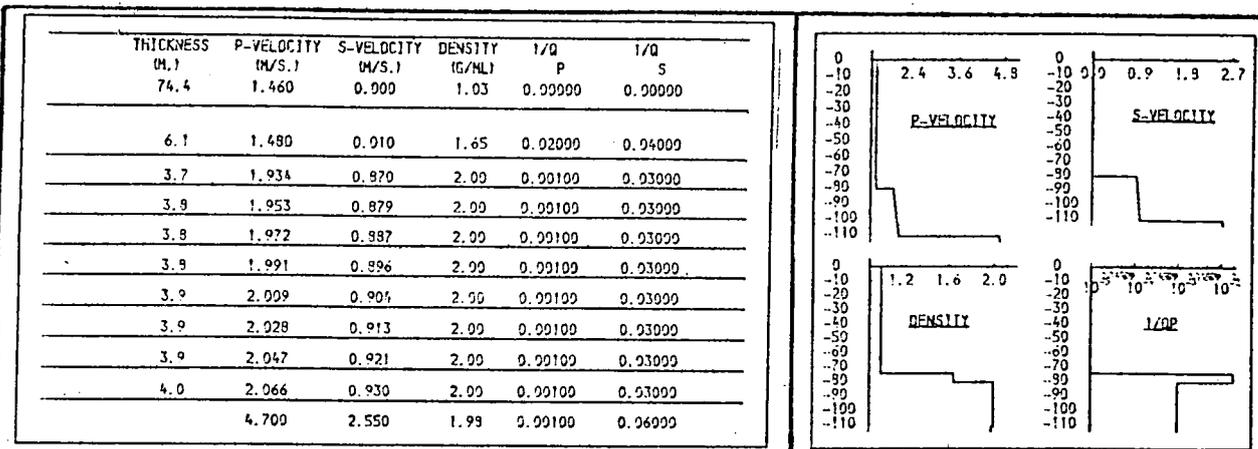| THICKNESS (M.)	P-VELOCITY (M/S.)	S-VELOCITY (M/S.)	DENSITY (G/ML)	1/Q P	1/Q S
74.4	1.460	0.000	1.03	0.00000	0.00000
6.1	1.480	0.010	1.65	0.02000	0.04000
3.5	1.913	0.526	2.00	0.00300	0.03000
3.6	1.939	0.533	2.00	0.00300	0.03000
3.6	1.962	0.540	2.00	0.00300	0.03000
3.7	1.988	0.547	2.00	0.00300	0.03000
3.7	2.012	0.553	2.00	0.00300	0.03000
3.9	2.039	0.560	2.00	0.00300	0.03000
3.9	2.063	0.567	2.00	0.00300	0.03000
3.9	2.097	0.574	2.00	0.00300	0.03000
	4.700	2.550	1.98	0.03000	0.00030

Fig. 9.43a. 1/Qs, layer 3.

This   parameter   does   not   greatly   influence   the seismogramme.

THICKNESS (M.)	P-VELOCITY (M/S.)	S-VELOCITY (M/S.)	DENSITY (G/ML)	1/Q P	1/Q S
74.4	1.460	0.000	1.03	0.00000	0.00000
6.1	1.480	0.010	1.65	0.02000	0.04000
3.5	1.913	0.526	2.00	0.00300	0.03000
3.6	1.939	0.533	2.00	0.00300	0.03000
3.6	1.962	0.540	2.00	0.00300	0.03000
3.7	1.988	0.547	2.00	0.00300	0.03000
3.7	2.012	0.553	2.00	0.00300	0.03000
3.8	2.039	0.560	2.00	0.00300	0.03000
3.9	2.063	0.567	2.00	0.00300	0.03000
3.9	2.087	0.574	2.00	0.00300	0.03000
	4.700	2.550	1.98	0.03000	0.00300

Fig. 9.43b. 1/Qs, layer 3.

This parameter does not greatly influence the seismogramme.

THICKNESS (M.)	P-VELOCITY (M/S.)	S-VELOCITY (M/S.)	DENSITY (G/ML)	1/Q P	1/Q S
74.4	1.460	0.000	1.03	0.00000	0.00000
6.1	1.490	0.010	1.65	0.02000	0.04000
3.5	1.913	0.526	2.00	0.00300	0.03000
3.6	1.938	0.533	2.00	0.00300	0.03000
3.6	1.962	0.540	2.00	0.00300	0.03000
3.7	1.998	0.547	2.00	0.00300	0.03000
3.7	2.012	0.553	2.00	0.00300	0.03000
3.8	2.038	0.560	2.00	0.00300	0.03000
3.8	2.063	0.567	2.00	0.00300	0.03000
3.9	2.087	0.574	2.00	0.00300	0.03000
	4.700	2.550	1.98	0.03000	0.03000
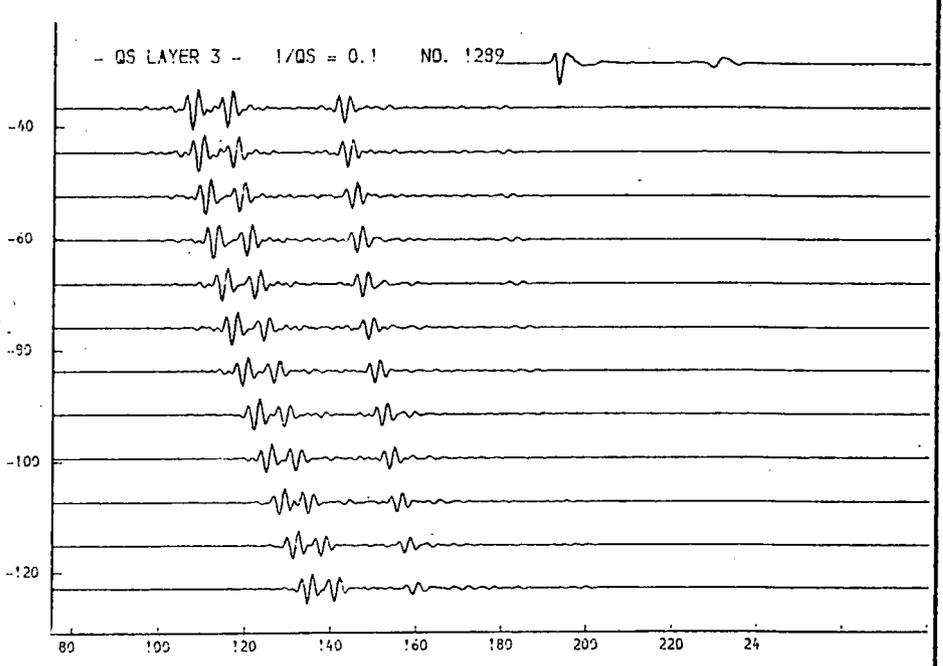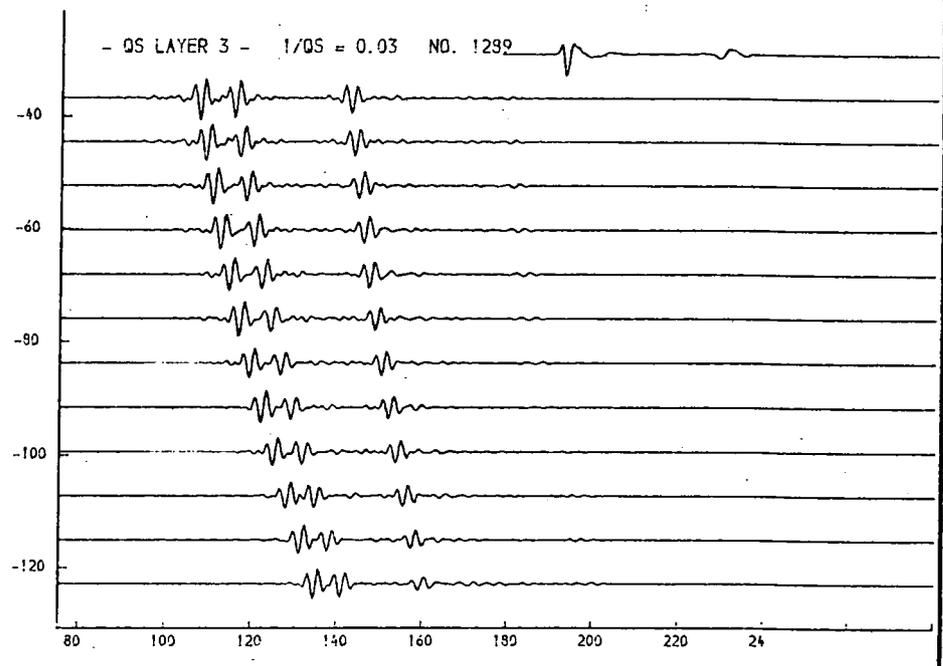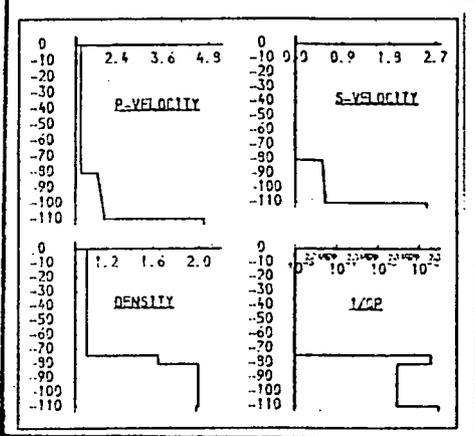
Fig. 9.43c. 1/Qs, layer 3.

This parameter does not greatly influence the seismogramme.

THICKNESS (M.)	P-VELOCITY (M/S.)	S-VELOCITY (M/S.)	DENSITY (G/ML)	1/Q P	1/Q S
74.4	1.460	0.000	1.03	0.00000	0.00000
6.1	1.480	0.010	1.65	0.02000	0.04000
3.5	1.913	0.526	2.00	0.00300	0.03000
3.6	1.938	0.533	2.00	0.00300	0.03000
3.6	1.962	0.540	2.00	0.00300	0.03000
3.7	1.988	0.547	2.00	0.00300	0.03000
3.7	2.012	0.553	2.00	0.00300	0.03000
3.8	2.038	0.560	2.00	0.00300	0.03000
3.9	2.063	0.567	2.00	0.00300	0.03000
3.9	2.087	0.574	2.00	0.00300	0.03000
	4.700	2.550	1.98	0.03000	0.30000

Fig. 9.43d. 1/Qs, layer 3.

This parameter does not greatly influence the seismogramme. The odd appearance of r2 for 1/Qs=1.0 is attributed to the breaking down of the theoretical basis of the model for high attenuation.

THICKNESS (M.)	P-VELOCITY (M/S.)	S-VELOCITY (M/S.)	DENSITY (G/ML)	1/Q P	1/Q S
74.4	1.460	0.000	1.03	0.00000	0.00000
6.1	1.480	0.010	1.65	0.02000	0.04000
3.8	1.956	0.539	2.00	0.00100	0.03000
3.8	1.969	0.541	2.00	0.00100	0.03000
3.8	1.981	0.545	2.00	0.00100	0.03000
3.8	1.994	0.549	2.00	0.00100	0.03000
3.9	2.006	0.552	2.00	0.00100	0.03000
3.9	2.019	0.555	2.00	0.00100	0.03000
3.9	2.031	0.559	2.00	0.00100	0.03000
3.9	2.044	0.562	2.00	0.00100	0.03000
	4.700	2.550	1.98	0.03000	0.06000

THICKNESS (M.)	P-VELOCITY (M/S.)	S-VELOCITY (M/S.)	DENSITY (G/ML)	1/Q P	1/Q S
74.4	1.460	0.000	1.03	0.00000	0.00000
6.1	1.480	0.010	1.65	0.02000	0.04000
3.7	1.913	0.526	2.00	0.00100	0.03000
3.7	1.938	0.533	2.00	0.00100	0.03000
3.8	1.962	0.540	2.00	0.00100	0.03000
3.8	1.988	0.547	2.00	0.00100	0.03000
3.9	2.012	0.553	2.00	0.00100	0.03000
3.9	2.038	0.560	2.00	0.00100	0.03000
4.0	2.063	0.567	2.00	0.00100	0.03000
4.0	2.092	0.574	2.00	0.00100	0.03000
	4.700	2.550	1.98	0.03000	0.06000

Fig. 9.44a. Velocity gradients, layer 2.

A gradient of wide range (c.f. fig. 9.22) has a significant effect on the amplitude for large offset distance. Gradients covering a narrower range of velocity have a similar but smaller effect.

THICKNESS (M.)	P-VELOCITY (M/S.)	S-VELOCITY (M/S.)	DENSITY (G/ML)	1/Q P	1/Q S	THICKNESS (M.)	P-VELOCITY (M/S.)	S-VELOCITY (M/S.)	DENSITY (G/ML)	1/Q P	1/Q S
74.4	1.460	0.000	1.03	0.00000	0.00000	74.4	1.460	0.000	1.03	0.00000	0.00000
6.1	1.480	0.010	1.65	0.02000	0.04000	6.1	1.480	0.010	1.65	0.02000	0.04000
3.5	1.925	0.502	2.00	0.00100	0.03000	3.3	1.738	0.478	2.00	0.00100	0.03000
3.6	1.975	0.516	2.00	0.00100	0.03000	3.5	1.913	0.498	2.00	0.00100	0.03000
3.7	1.925	0.529	2.00	0.00100	0.03000	3.6	1.987	0.519	2.00	0.00100	0.03000
3.8	1.975	0.543	2.00	0.00100	0.03000	3.8	1.962	0.540	2.00	0.00100	0.03000
3.9	2.025	0.557	2.00	0.00100	0.03000	3.0	2.039	0.560	2.00	0.00100	0.03000
4.0	2.075	0.571	2.00	0.00100	0.03000	4.1	2.113	0.581	2.00	0.00100	0.03000
4.1	2.125	0.584	2.00	0.00100	0.03000	4.2	2.198	0.602	2.00	0.00100	0.03000
4.2	2.175	0.598	2.00	0.00100	0.03000	4.4	2.262	0.622	2.00	0.00100	0.03000
	4.700	2.550	1.99	0.03000	0.06000		4.700	2.550	1.99	0.03000	0.06000
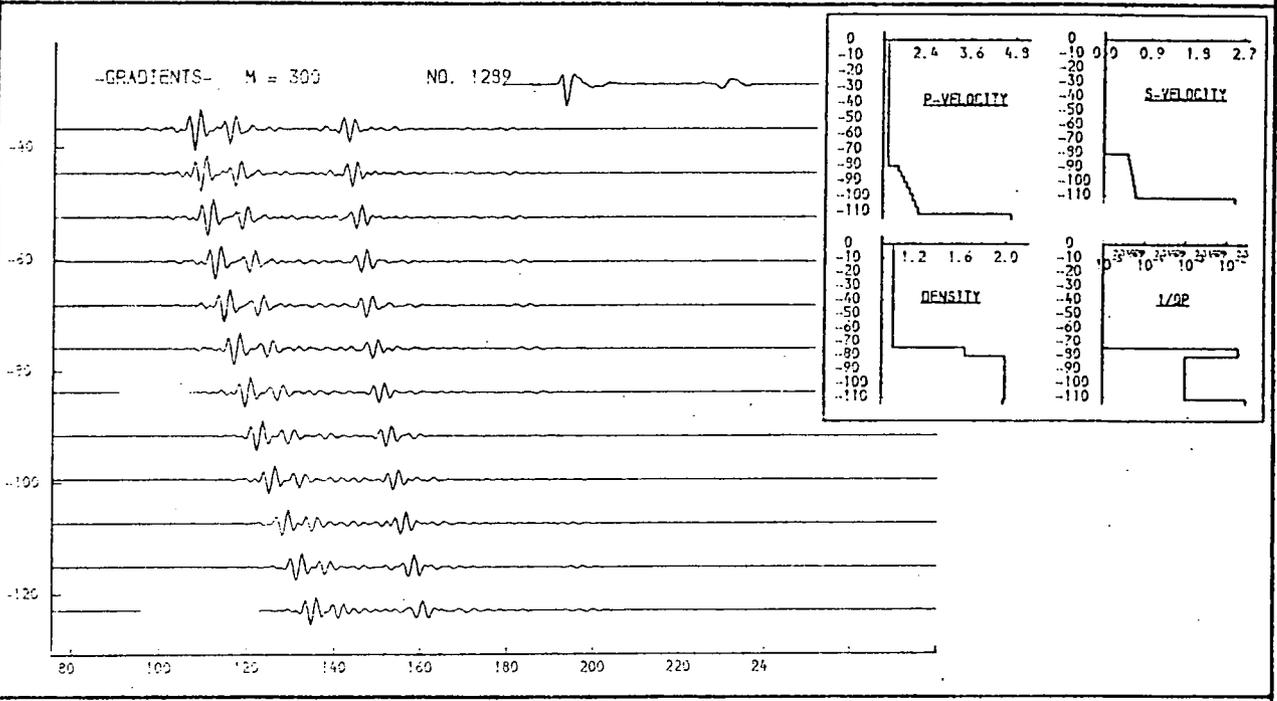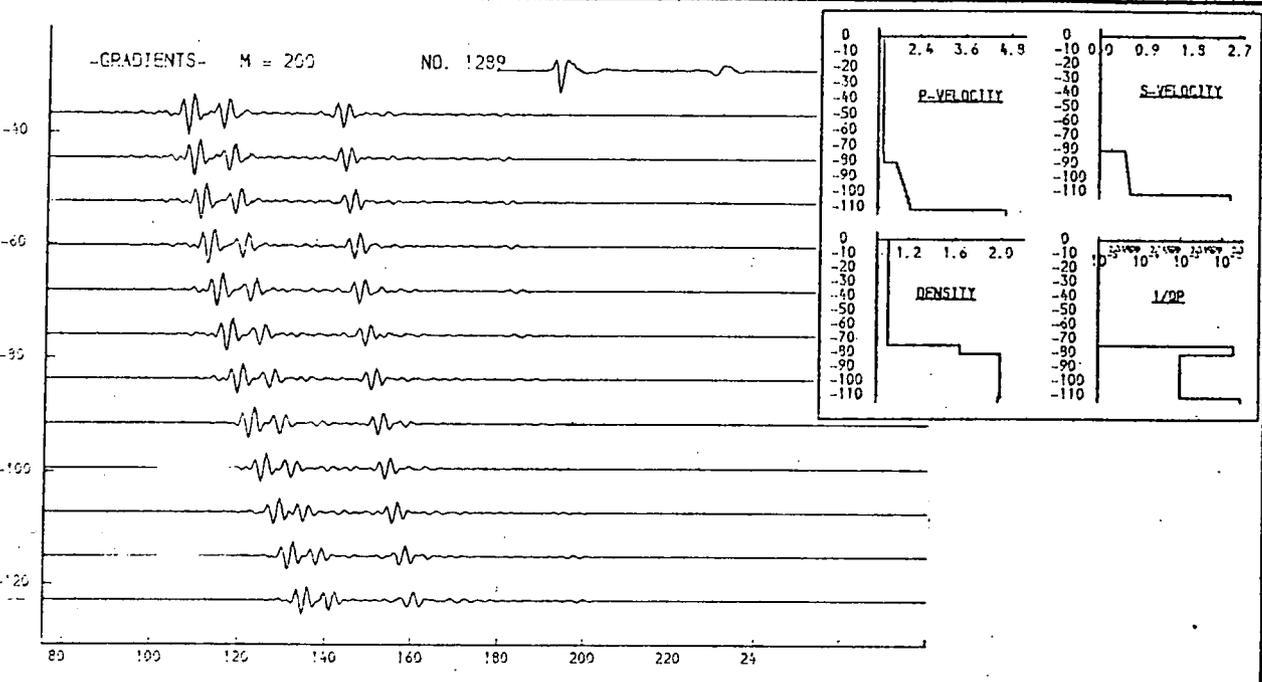
Fig. 9.44b. Velocity gradients, layer 2.

A gradient of wide range (c.f. fig. 9.22) has a significant effect on the amplitude for large offset distance. Gradients covering a narrower range of velocity have a similar but smaller effect.

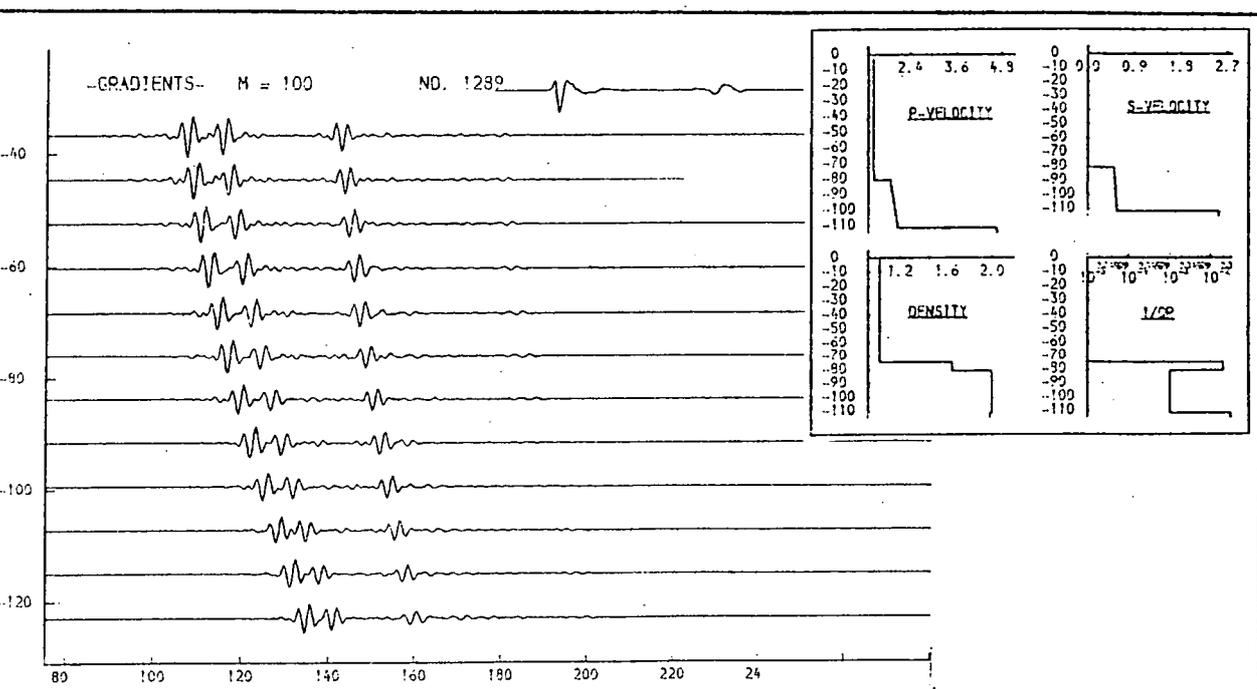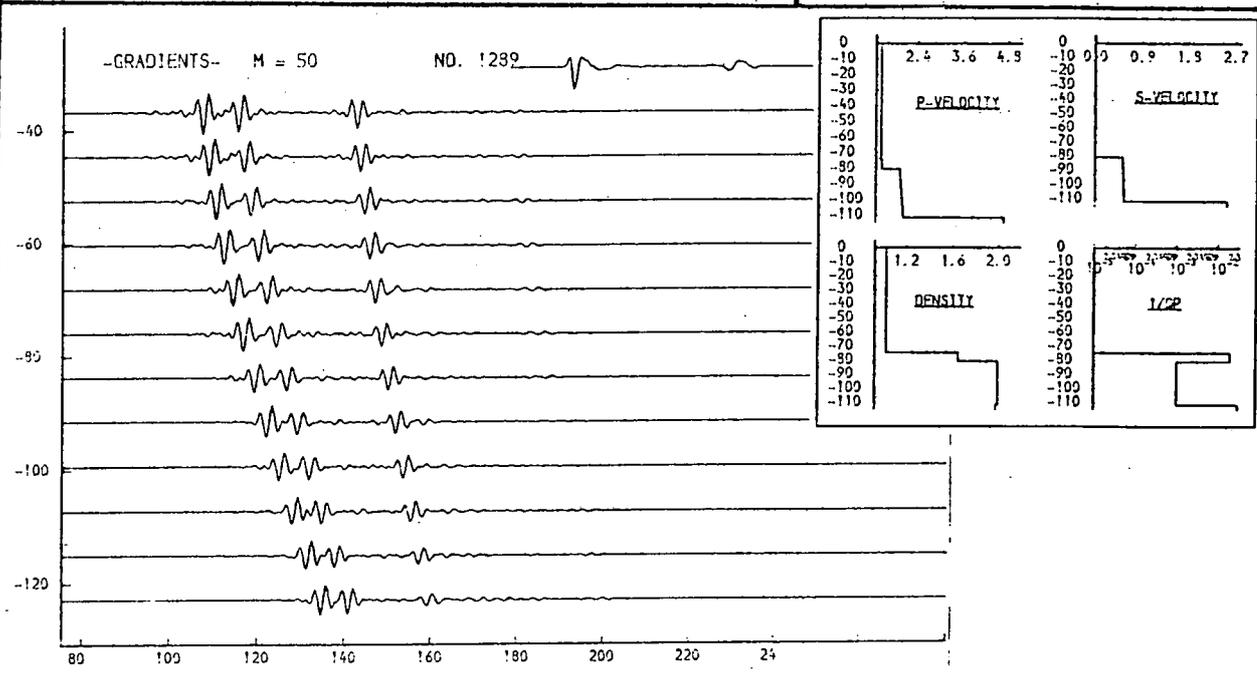| THICKNESS (M.)	P-VELOCITY (M/S.)	S-VELOCITY (M/S.)	DENSITY (G/ML)	1/Q P	1/Q S		THICKNESS (M.)	P-VELOCITY (M/S.)	S-VELOCITY (M/S.)	DENSITY (G/ML)	1/Q P	1/Q S
74.4	1.460	0.000	1.03	0.00000	0.00000		74.4	1.460	0.000	1.03	0.00000	0.00000
6.1	1.480	0.010	1.65	0.02000	0.04000		6.1	1.480	0.010	1.65	0.02000	0.04000
3.7	1.934	0.510	2.00	0.00100	0.00100		3.7	1.934	0.445	2.00	0.00100	0.00100
3.9	1.953	0.520	2.00	0.00100	0.00100		3.9	1.953	0.475	2.00	0.00100	0.00100
3.9	1.972	0.530	2.00	0.00100	0.00100		3.9	1.972	0.505	2.00	0.00100	0.00100
3.9	1.991	0.540	2.00	0.00100	0.00100		3.9	1.991	0.535	2.00	0.00100	0.00100
3.9	2.009	0.550	2.00	0.00100	0.00100		3.9	2.009	0.565	2.00	0.00100	0.00100
3.9	2.028	0.560	2.00	0.00100	0.00100		3.9	2.028	0.595	2.00	0.00100	0.00100
3.9	2.047	0.570	2.00	0.00100	0.00100		3.9	2.047	0.625	2.00	0.00100	0.00100
4.0	2.066	0.580	2.00	0.00100	0.00100		4.0	2.066	0.655	2.00	0.00100	0.00100
	4.700	2.550	1.98	0.03000	0.06000			4.700	2.550	1.98	0.03000	0.06000

-GRADT. IN S (LAYER 2) - LOW   NO. 1289

P-VELOCITY   S-VELOCITY   DENSITY   1/QP

-GRADT. IN S (LAYER 2) - MID   NO. 1289

P-VELOCITY   S-VELOCITY   DENSITY   1/QP

Fig. 9.44c. Layer 2, s-velocity gradient.

The introduction of small gradients in the s-velocity in layer 2 does not greatly influence the seismogramme model, and when the value of 1/Qs (layer 2) is low, an arrival attributed to p-s conversion in layer 2 can be seen as a late arrival.

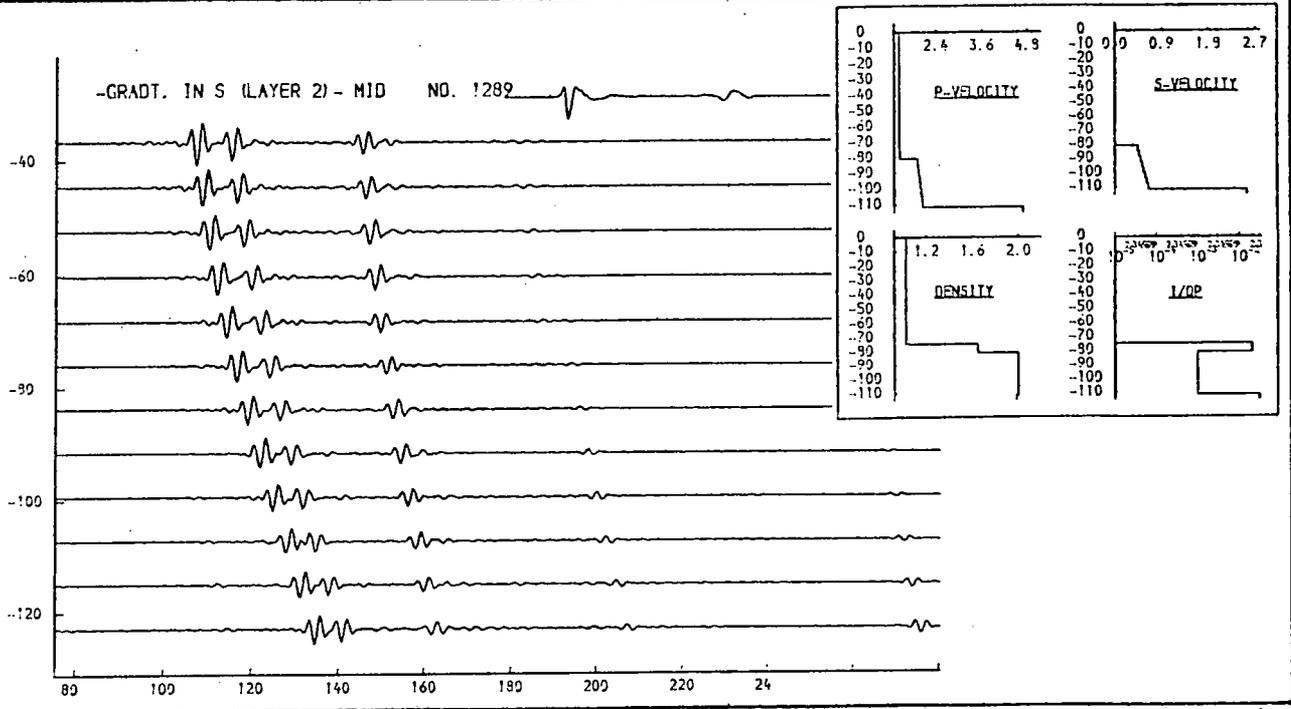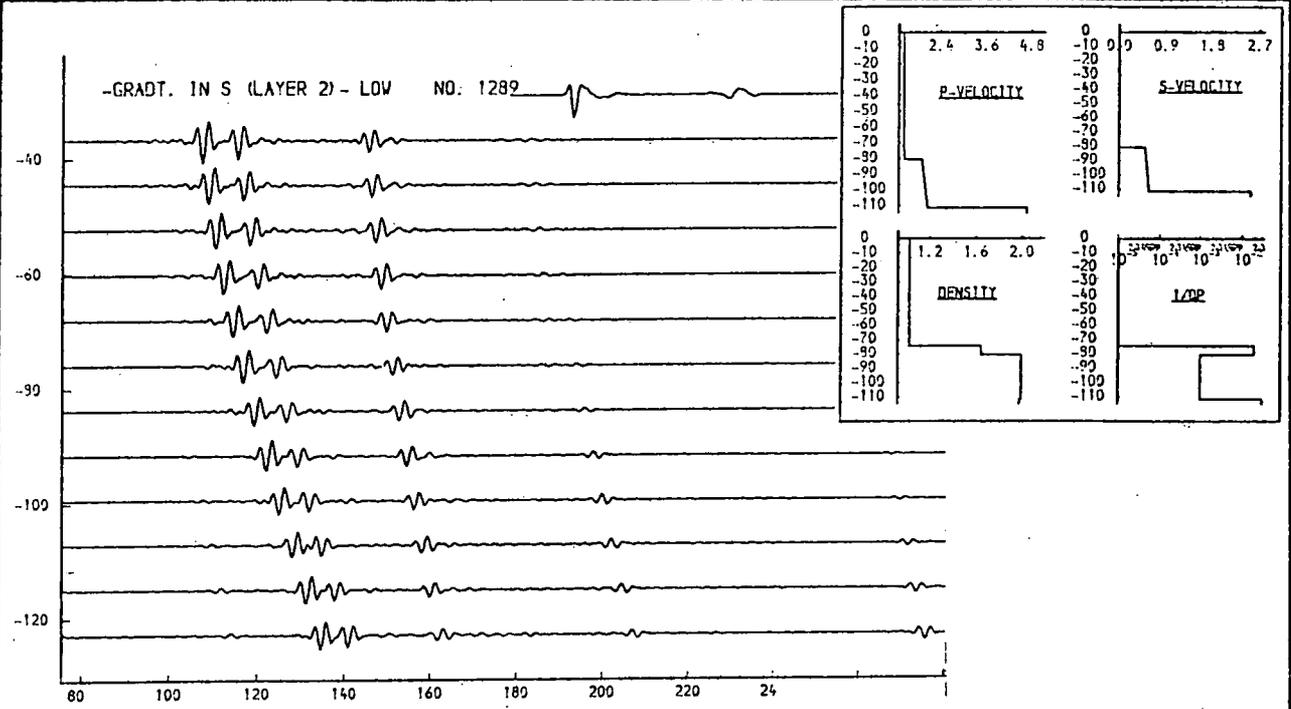| THICKNESS (M.)	P-VELOCITY (M/S.)	S-VELOCITY (M/S.)	DENSITY (G/ML)	1/Q P	1/Q S
74.4	1.460	0.000	1.03	0.00000	0.00000
6.1	1.480	0.010	1.65	0.02000	0.04000
3.7	1.934	0.360	2.00	0.00100	0.00100
3.9	1.953	0.400	2.00	0.00100	0.00100
3.9	1.972	0.460	2.00	0.00100	0.00100
3.9	1.991	0.520	2.00	0.00100	0.00100
3.9	2.009	0.580	2.00	0.00100	0.00100
3.9	2.028	0.640	2.00	0.00100	0.00100
3.9	2.047	0.700	2.00	0.00100	0.00100
4.0	2.066	0.760	2.00	0.00100	0.00100
	4.700	2.550	1.98	0.03000	0.06000

| THICKNESS (M.)	P-VELOCITY (M/S.)	S-VELOCITY (M/S.)	DENSITY (G/ML)	1/Q P	1/Q S
74.4	1.460	0.000	1.03	0.00000	0.00000
6.1	1.480	0.010	1.65	0.02000	0.04000
3.7	1.934	0.150	2.00	0.00100	0.00100
3.9	1.953	0.250	2.00	0.00100	0.00100
3.9	1.972	0.350	2.00	0.00100	0.00100
3.9	1.991	0.450	2.00	0.00100	0.00100
3.9	2.009	0.550	2.00	0.00100	0.00100
3.9	2.028	0.650	2.00	0.00100	0.00100
3.9	2.047	0.750	2.00	0.00100	0.00100
4.0	2.966	0.950	2.00	0.00100	0.00100
	4.700	2.550	1.98	0.03000	0.06000
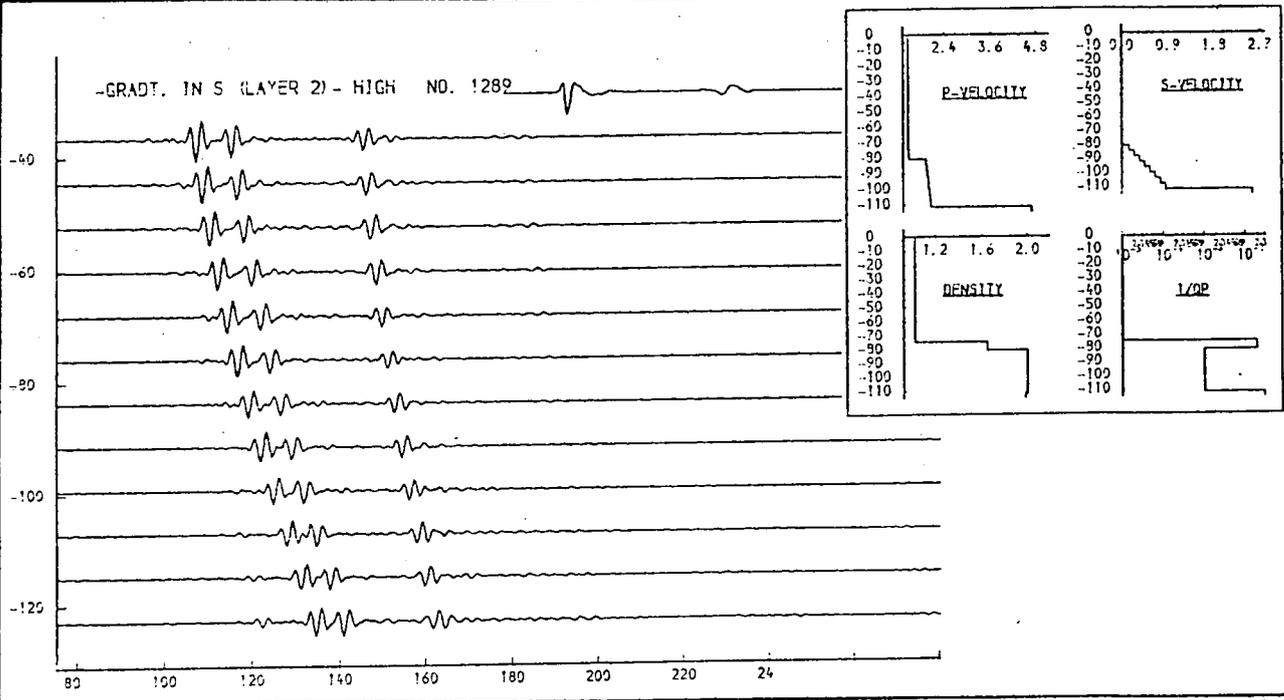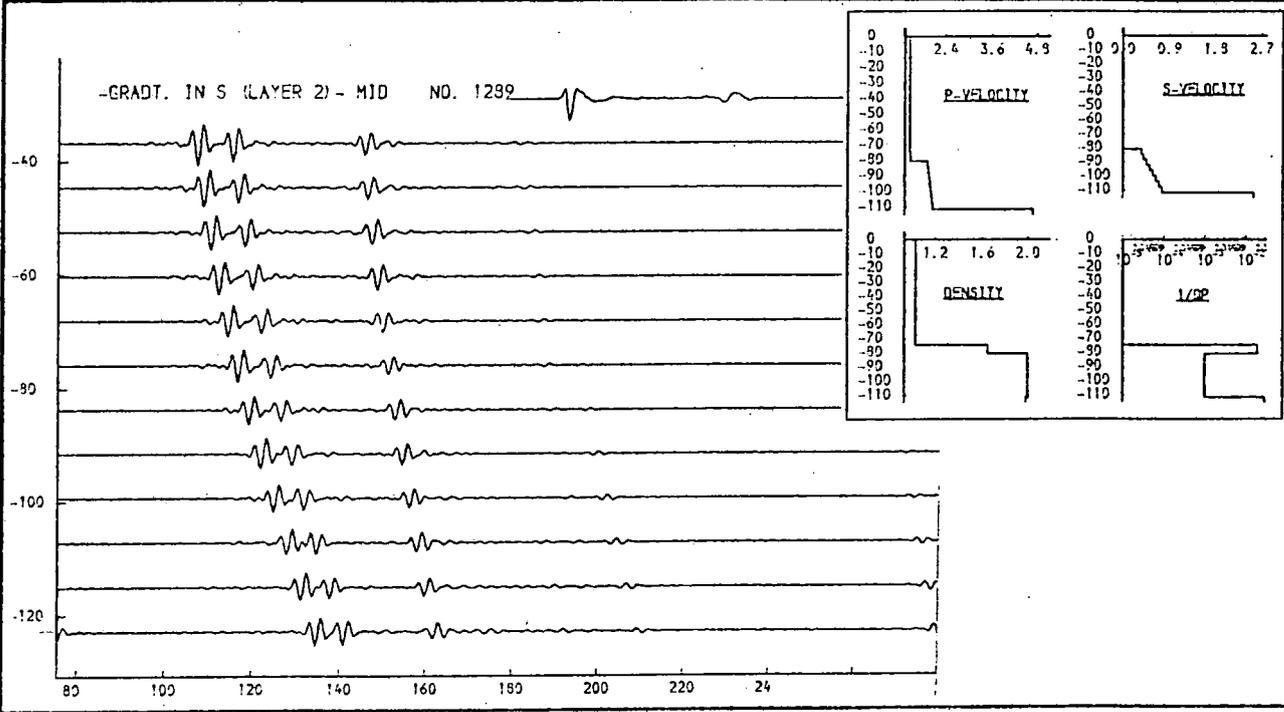
Fig. 9.44d. Layer 2, s-velocity gradient.

When a more pronounced gradient in the s-velocity of layer 2 is introduced, the p-s converted arrival is suppressed (c.f. figs. 9.44c, 9.31b-d), but r2 becomes too large at high offset.

Synthetic seismogramme models

for No. 1281

(figs. 9.45 to 9.73)

THICKNESS (M.)	P-VELOCITY (M/S.)	S-VELOCITY (M/S.)	DENSITY (G/ML)	1/Q P	1/Q S
63.0	1.460	0.000	1.03	0.00001	0.00001
0.2	1.460	0.010	1.65	0.02000	0.04000
4.9	1.934	0.532	2.00	0.00200	0.02000
4.9	1.953	0.537	2.00	0.00200	0.02000
4.9	1.972	0.542	2.00	0.00200	0.02000
5.0	1.991	0.547	2.00	0.00200	0.02000
5.0	2.009	0.553	2.00	0.00200	0.02000
5.1	2.028	0.558	2.00	0.00200	0.02000
5.1	2.047	0.563	2.00	0.00200	0.02000
5.2	2.066	0.568	2.00	0.00200	0.02000
	4.700	2.900	1.99	0.02000	0.04000

— MODEL FOR SEISMOGRAMME NO. 1281 —
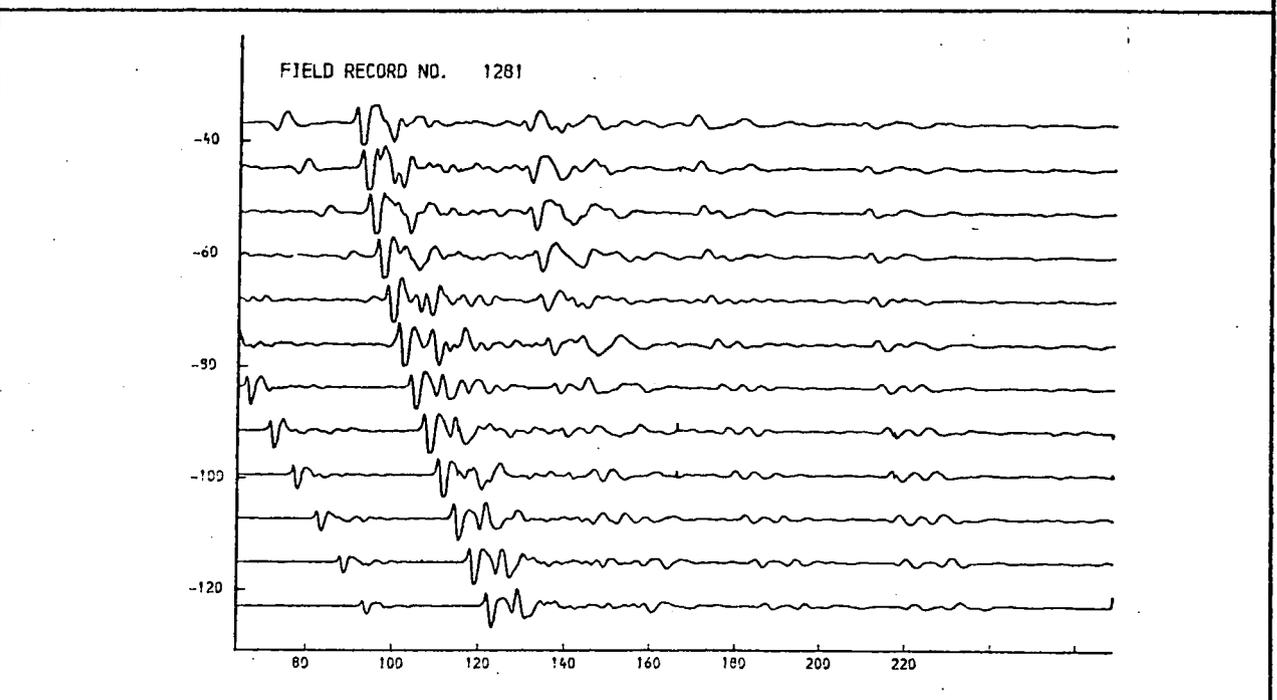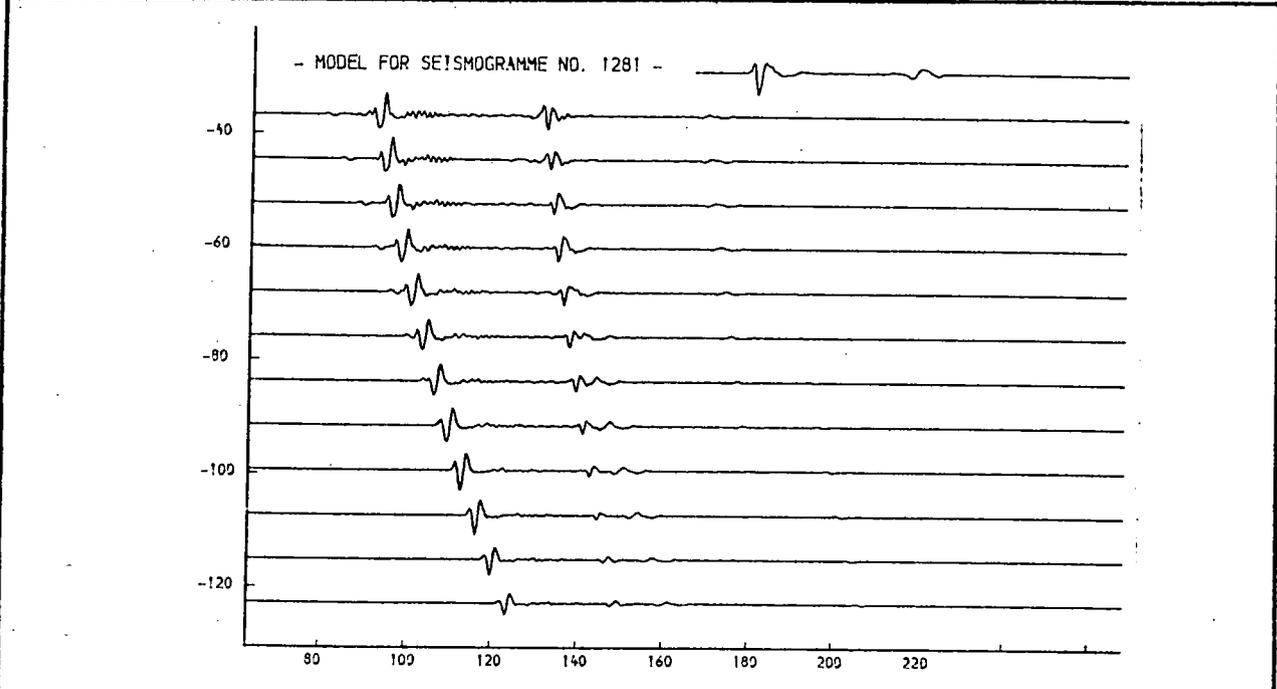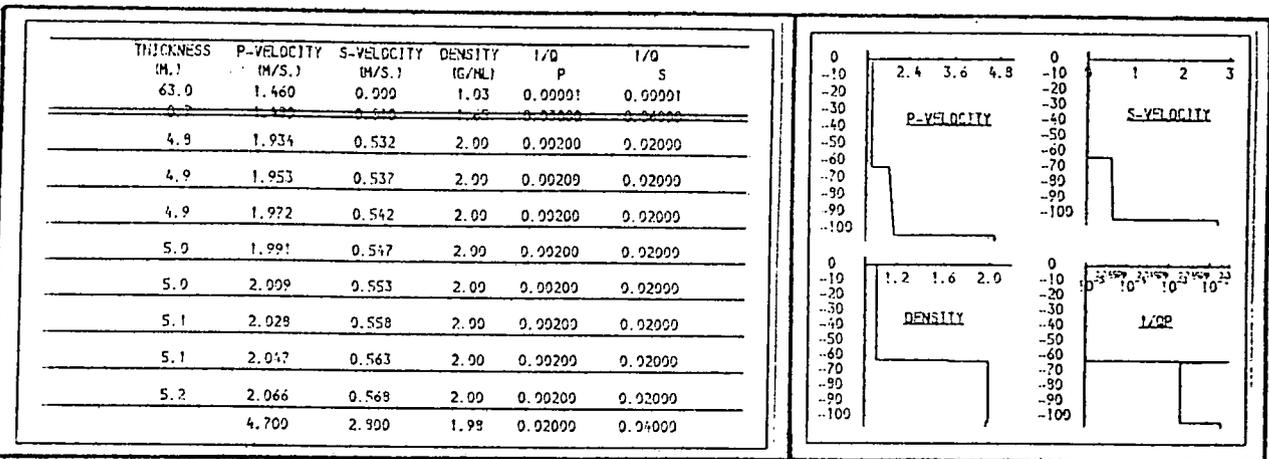

FIELD RECORD NO. 1281

Fig. 9.45. Model for No. 1281.

Suggested model for seismogramme no. 1281, constructed in a wide frequency band (50 to 1000 Hz.). The possible value ranges for the parameters are discussed in the text and illustrated by the models shown in figs. 9.46 to 9.62 (see volume 2).

THICKNESS (M.)	P-VELOCITY (M/S.)	S-VELOCITY (M/S.)	DENSITY (G/ML)	1/Q P	1/Q S
63.0	1.460	0.0	1.03	0.00001	0.00001
0.0	1.480	0.510	1.65	0.02000	0.04000
4.8	1.913	0.526	2.00	0.00200	0.02000
4.8	1.939	0.533	2.00	0.00200	0.02000
4.9	1.962	0.540	2.00	0.00200	0.02000
5.0	1.988	0.547	2.00	0.00200	0.02000
5.0	2.012	0.553	2.00	0.00200	0.02000
5.1	2.039	0.560	2.00	0.00200	0.02000
5.2	2.063	0.567	2.00	0.00200	0.02000
5.2	2.087	0.574	2.00	0.00200	0.02000
	4.200	3.000	1.98	0.01000	0.02000

Fig. 9.46a. Thickness of top layer.

This layer is unresolved. Its thickness influences the amplitude of the arrival "r2".

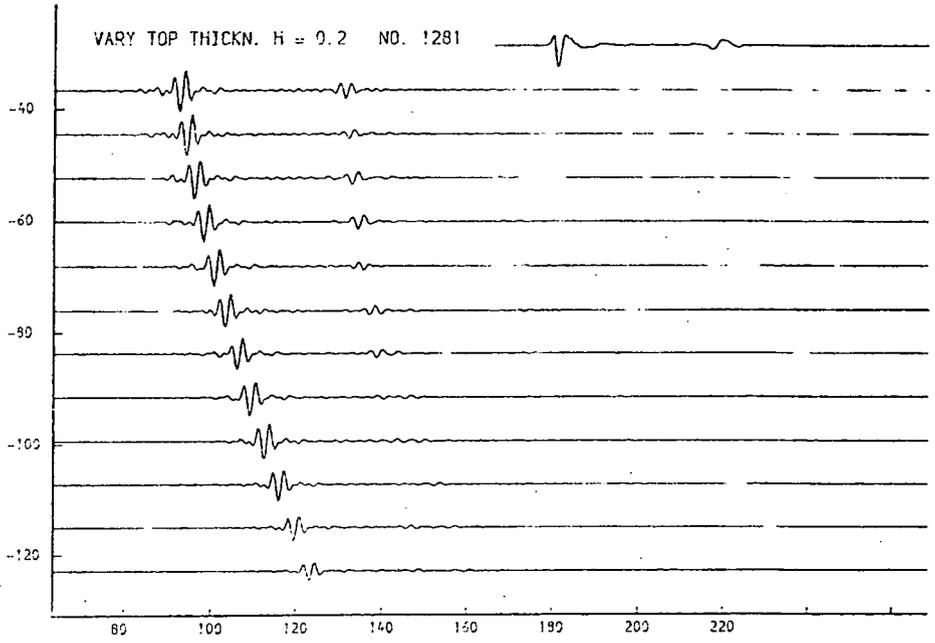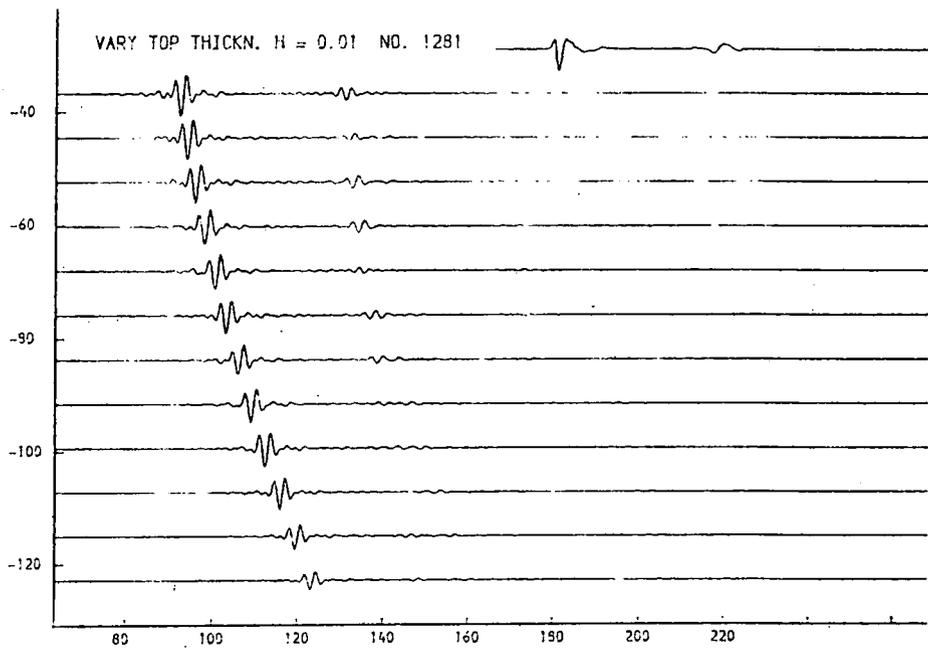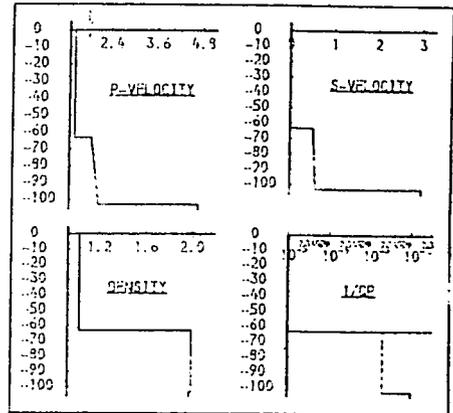| THICKNESS (M.)	P-VELOCITY (M/S.)	S-VELOCITY (M/S.)	DENSITY (G/ML)	1/Q P	1/Q S
63.9	1.460	0.000	1.03	0.00001	0.00001
0.3	1.480	0.210	1.65	0.03000	0.04000
4.8	1.913	0.200	2.00	0.00200	0.01000
4.8	1.938	0.300	2.00	0.00200	0.01000
4.9	1.962	0.400	2.00	0.00200	0.01000
5.0	1.998	0.500	2.00	0.00200	0.01000
5.0	2.012	0.600	2.00	0.00200	0.01000
5.1	2.039	0.700	2.00	0.00200	0.01000
5.2	2.063	0.800	2.00	0.00200	0.01000
5.2	2.087	0.900	2.00	0.00200	0.01000
	4.700	2.800	1.99	0.10000	0.20000

Fig. 9.46b. Thickness of top layer.

This layer is unresolved. Its thickness influences the amplitude of the arrival "r2".

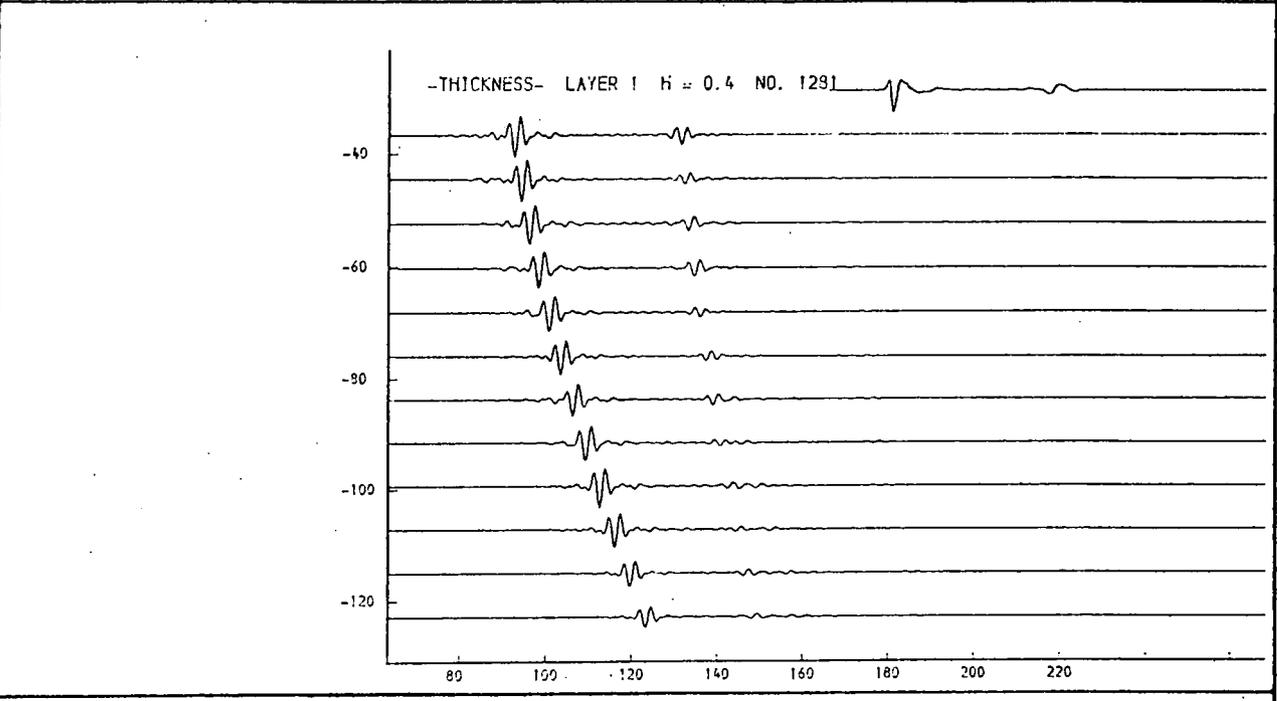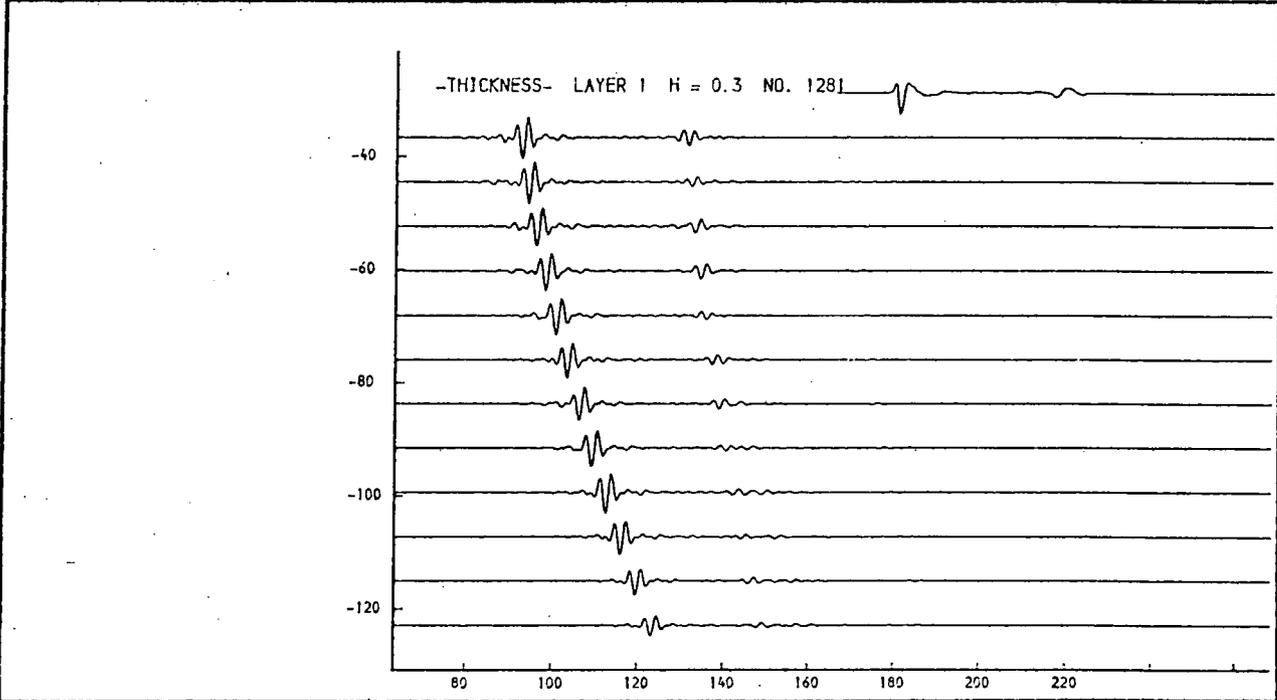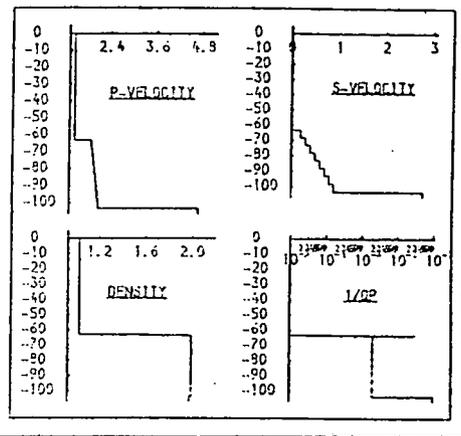| THICKNESS (M.)	P-VELOCITY (M/S.)	S-VELOCITY (M/S.)	DENSITY (G/ML)	1/Q P	1/Q S
63.0	1.460	0.000	1.03	0.00001	0.00001
0.5	1.480	0.010	1.65	0.01000	0.04000
4.9	1.913	0.200	2.00	0.00200	0.01000
4.9	1.938	0.300	2.00	0.00200	0.01000
4.9	1.962	0.400	2.00	0.00200	0.01000
5.0	1.988	0.500	2.00	0.00200	0.01000
5.0	2.012	0.600	2.00	0.00200	0.01000
5.1	2.038	0.700	2.00	0.00200	0.01000
5.2	2.063	0.800	2.00	0.00200	0.01000
5.2	2.087	0.900	2.00	0.00200	0.01000
	4.700	2.900	1.98	0.10000	0.20000

Fig. 9.46c. Thickness of top layer.

This layer is unresolved. Its thickness influences the amplitude of the arrival "r2".

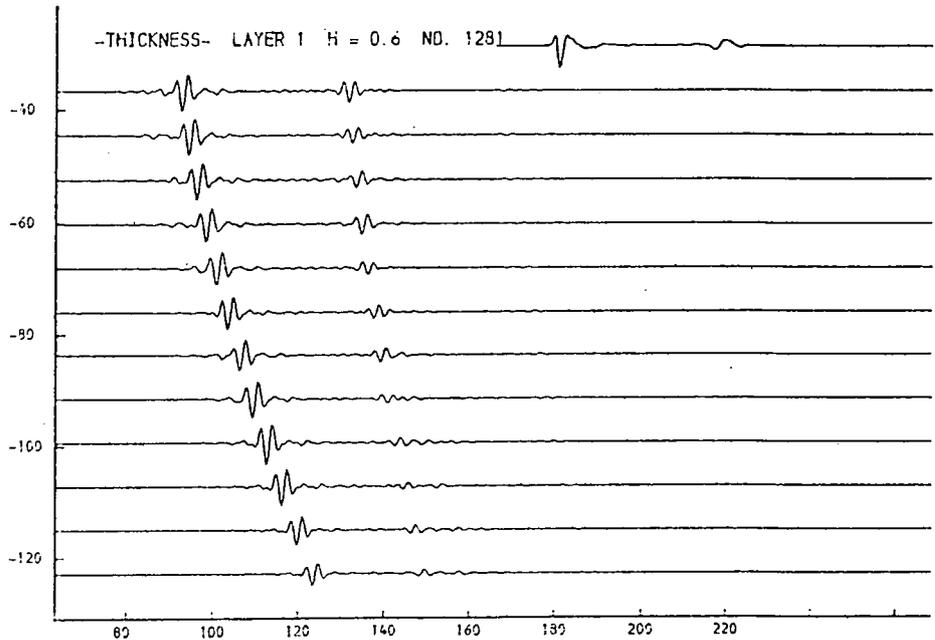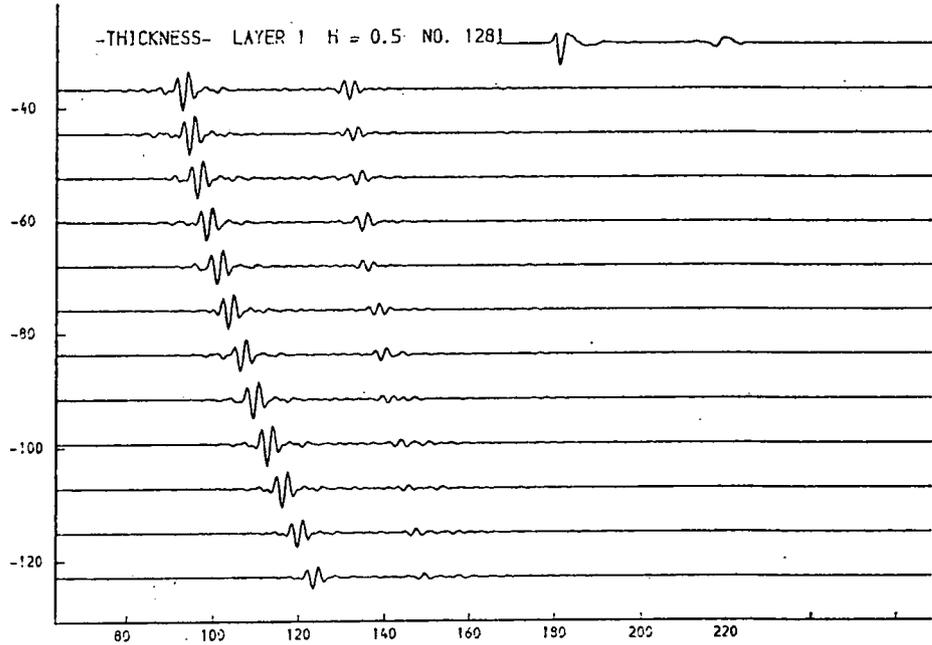| THICKNESS (M.)	P-VELOCITY (M/S.)	S-VELOCITY (M/S.)	DENSITY (G/ML)	1/Q P	1/Q S
63.0	1.460	0.000	1.03	0.00001	0.00001
5.2	1.489	0.100	2.00	0.00200	0.01000
4.9	1.913	0.200	2.00	0.00200	0.01000
4.8	1.938	0.300	2.00	0.00200	0.01000
4.9	1.962	0.400	2.00	0.00200	0.01000
5.0	1.989	0.500	2.00	0.00200	0.01000
5.0	2.012	0.600	2.00	0.00200	0.01000
5.1	2.038	0.700	2.00	0.00200	0.01000
5.2	2.063	0.800	2.00	0.00200	0.01000
5.2	2.087	0.900	2.00	0.00200	0.01000
	4.700	2.800	1.98	0.10000	0.20000

Fig. 9.46d.   Thickness of top layer.

This layer is unresolved. Its thickness influences the amplitude of the arrival "r2".

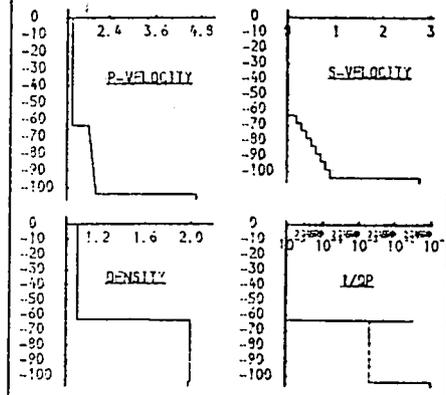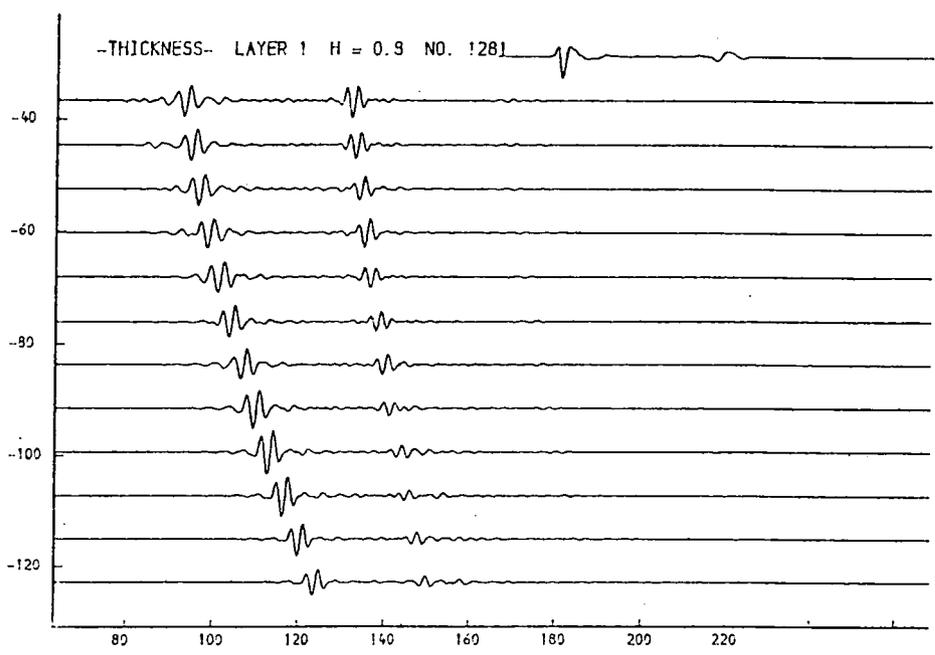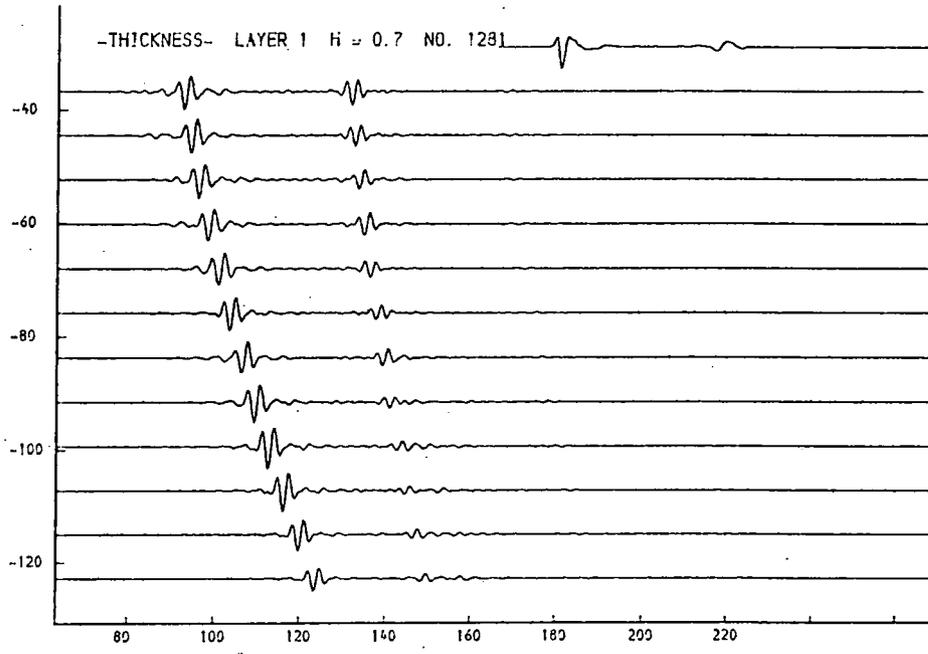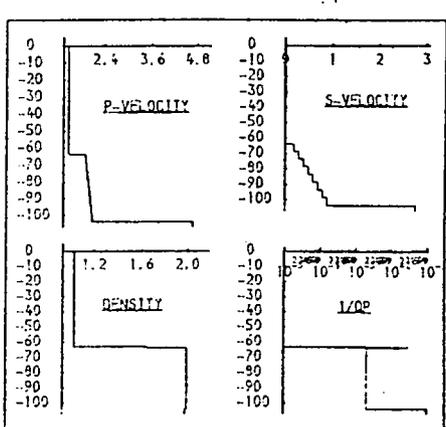| THICKNESS (M.)	P-VELOCITY (M/S.)	S-VELOCITY (M/S.)	DENSITY (G/ML)	1/Q P	1/Q S
63.0	1.460	0.000	1.03	0.00001	0.00001
		0.310	1.63	0.00000	0.00000
4.9	1.913	0.200	2.00	0.00200	0.01000
4.8	1.938	0.300	2.00	0.00200	0.01000
4.9	1.962	0.400	2.00	0.00200	0.01000
5.0	1.989	0.500	2.00	0.00200	0.01000
5.0	2.012	0.600	2.00	0.00200	0.01000
5.1	2.038	0.700	2.00	0.00200	0.01000
5.2	2.063	0.800	2.00	0.00200	0.01000
5.2	2.087	0.900	2.00	0.00200	0.01000
	4.700	2.900	1.98	0.10000	0.20000

Fig. 9.46e. Thickness of top layer.

This layer is unresolved. Its thickness influences the amplitude of the arrival "r2".

THICKNESS (M.)	P-VELOCITY (M/S.)	S-VELOCITY (M/S.)	DENSITY (G/ML)	1/Q P	1/Q S
63.0	1.460	0.000	1.03	0.00001	0.00001
	1.930	0.519	1.65	0.00200	0.02000
4.9	1.934	0.532	2.00	0.00200	0.02000
4.9	1.953	0.537	2.00	0.00200	0.02000
4.9	1.972	0.542	2.00	0.00200	0.02000
5.0	1.991	0.547	2.00	0.00200	0.02000
5.0	2.009	0.553	2.00	0.00200	0.02000
5.1	2.028	0.558	2.00	0.00200	0.02000
5.1	2.047	0.563	2.00	0.00200	0.02000
5.2	2.066	0.569	2.00	0.00200	0.02000
	4.700	2.900	1.98	0.02000	0.04000

Fig. 9.47. Layer 1, p-velocity.

Very low velocities, such as might be found in a highly gasified sediment produce too great a reduction in the amplitude of r2.

THICKNESS (M.)	P-VELOCITY (M/S.)	S-VELOCITY (M/S.)	DENSITY (G/ML)	1/Q P	1/Q S
63.0	1.460	0.000	1.03	0.00001	0.00001
	1.439	0.613	1.93	0.07000	0.24000
4.9	1.913	0.200	2.00	0.00200	0.01000
4.9	1.939	0.300	2.00	0.00200	0.01000
4.9	1.962	0.400	2.00	0.00200	0.01000
5.0	1.988	0.500	2.00	0.00200	0.01000
5.0	2.012	0.600	2.00	0.00200	0.01000
5.1	2.039	0.700	2.00	0.00200	0.01000
5.2	2.063	0.800	2.00	0.00200	0.01000
5.2	2.087	0.900	2.00	0.00200	0.01000
	4.700	2.900	1.98	0.10000	0.20000

Fig. 9.48a.   P-velocity, layer 1.

This parameter influences the amplitude of the deeper reflector r2.

THICKNESS (M.)	P-VELOCITY (M/S.)	S-VELOCITY (M/S.)	DENSITY (G/ML)	1/Q P	1/Q S
63.0	1.460	0.000	1.03	0.00001	0.00001
	1.5	0.010		0.07000	0.0000
4.8	1.913	0.200	2.00	0.00200	0.01000
4.9	1.938	0.300	2.00	0.00200	0.01000
4.9	1.962	0.400	2.00	0.00200	0.01000
5.0	1.989	0.500	2.00	0.00200	0.01000
5.0	2.012	0.600	2.00	0.00200	0.01000
5.1	2.038	0.700	2.00	0.00200	0.01000
5.2	2.063	0.800	2.00	0.00200	0.01000
5.2	2.087	0.900	2.00	0.00200	0.01000
	4.700	2.800	1.98	0.10000	0.20000

-P- LAYER 1   P = 1.50   NO. 1281

-P- LAYER 1   P = 1.60   NO. 1281

Fig. 9.48b. P-velocity, layer 1.

This parameter influences the amplitude of the deeper reflector r2.

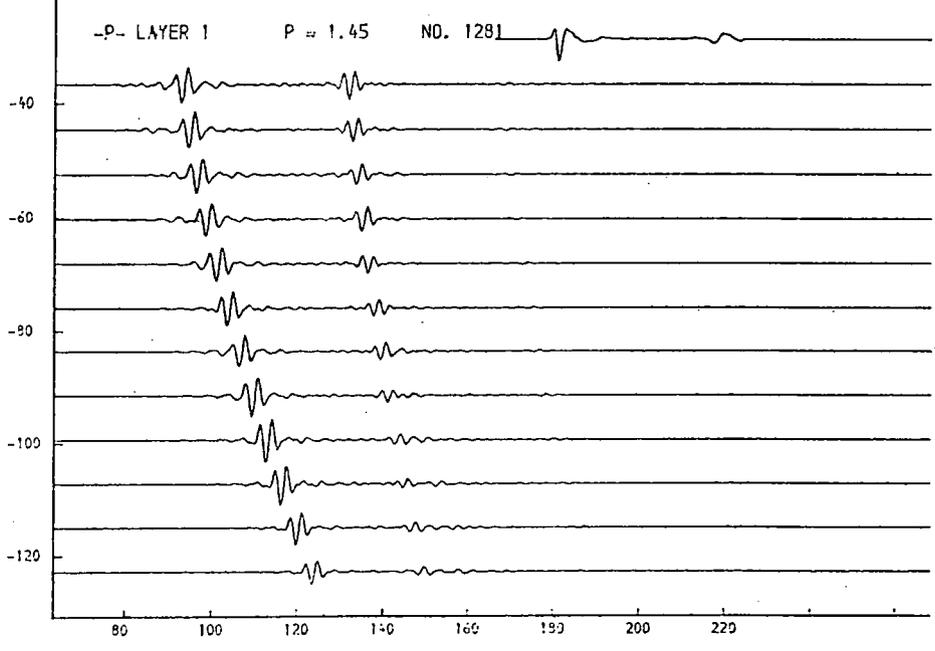| THICKNESS (M.)	P-VELOCITY (M/S.)	S-VELOCITY (M/S.)	DENSITY (G/ML)	1/Q P	1/Q S
63.0	1.460	0.000	1.03	0.00001	0.00001
	1.460	0.001	1.03	0.02000	0.04000
4.9	1.934	0.532	2.00	0.00200	0.02000
4.9	1.953	0.537	2.00	0.00200	0.02000
4.9	1.972	0.542	2.00	0.00200	0.02000
5.0	1.991	0.547	2.00	0.00200	0.02000
5.0	2.009	0.553	2.00	0.00200	0.02000
5.1	2.028	0.558	2.00	0.00200	0.02000
5.1	2.047	0.563	2.00	0.00200	0.02000
5.2	2.066	0.568	2.00	0.00200	0.02000
	4.700	2.300	1.98	0.02000	0.04000

Fig. 9.49a.   S-velocity, layer 1.

THICKNESS (M.)	P-VELOCITY (M/S.)	S-VELOCITY (M/S.)	DENSITY (G/ML)	1/Q P	1/Q S
63.0	1.460	0.000	1.03	0.00001	0.00001
4.8	1.934	0.532	2.00	0.00200	0.02000
4.9	1.953	0.537	2.00	0.00200	0.02000
4.9	1.972	0.542	2.00	0.00200	0.02000
5.0	1.991	0.547	2.00	0.00200	0.02000
5.0	2.009	0.553	2.00	0.00200	0.02000
5.1	2.028	0.558	2.00	0.00200	0.02000
5.1	2.047	0.563	2.00	0.00200	0.02000
5.2	2.066	0.568	2.00	0.00200	0.02000
	4.700	2.900	1.98	0.02000	0.04000

Fig. 9.49b. S-velocity, layer 1.

THICKNESS (M.)	P-VELOCITY (M/S.)	S-VELOCITY (M/S.)	DENSITY (G/ML)	1/Q P	1/Q S
63.0	1.460	0.000	1.03	0.00001	0.00001
0.7	1.433	0.010	1.15	0.03000	0.04000
4.8	1.934	0.532	2.00	0.00200	0.02000
4.9	1.953	0.537	2.00	0.00200	0.02000
4.9	1.972	0.542	2.00	0.00200	0.02000
5.0	1.991	0.547	2.00	0.00200	0.02000
5.0	2.009	0.553	2.00	0.00200	0.02000
5.1	2.029	0.558	2.00	0.00200	0.02000
5.1	2.047	0.563	2.00	0.00200	0.02000
5.2	2.066	0.568	2.00	0.00200	0.02000
	4.700	2.900	1.98	0.02000	0.04000

P-VELOCITY   2.4 3.6 4.8

S-VELOCITY   1 2 3

DENSITY   1.2 1.6 2.0

1/QP

-DENSITY- LAYER 1   RHO = 1.45   NO. 1281

-DENSITY- LAYER 1   RHO = 1.55   NO. 1281

Fig. 9.50a.   Density, layer 1.

This parameter has little influence on the model.

THICKNESS (M.)	P-VELOCITY (M/S.)	S-VELOCITY (M/S.)	DENSITY (G/ML)	1/Q P	1/Q S
63.0	1.460	0.000	1.03	0.00001	0.00001
0.2	1.430	0.010	1.25	0.03000	0.06000
4.8	1.934	0.532	2.00	0.00200	0.02000
4.9	1.953	0.537	2.00	0.00200	0.02000
4.9	1.972	0.542	2.00	0.00200	0.02000
5.0	1.991	0.547	2.00	0.00200	0.02000
5.0	2.009	0.553	2.00	0.00200	0.02000
5.1	2.028	0.558	2.00	0.00200	0.02000
5.1	2.047	0.563	2.00	0.00200	0.02000
5.2	2.066	0.568	2.00	0.00200	0.02000
	4.700	2.800	1.98	0.02000	0.04000

-DENSITY- LAYER 1   RHO = 1.75   NO. 1281

-DENSITY- LAYER 1   RHO = 1.85   NO. 1281

Fig. 9.50b.   Density, layer 1.

This parameter has little influence on the model.

THICKNESS (M.)	P-VELOCITY (M/S.)	S-VELOCITY (M/S.)	DENSITY (G/ML)	1/Q P	1/Q S
63.0	1.460	0.000	1.03	0.00001	0.00001
0.2	1.490	0.010	1.05	0.70000	0.04000
4.8	1.934	0.532	2.00	0.00200	0.02000
4.9	1.953	0.537	2.00	0.00200	0.02000
4.9	1.972	0.542	2.00	0.00200	0.02000
5.0	1.991	0.547	2.00	0.00200	0.02000
5.0	2.009	0.553	2.00	0.00200	0.02000
5.1	2.028	0.559	2.00	0.00200	0.02000
5.1	2.047	0.563	2.00	0.00200	0.02000
5.2	2.066	0.569	2.00	0.00200	0.02000
	4.700	2.800	1.98	0.02000	0.04000

Fig. 9.51a. 1/Qp, layer 1.

Very high values influence the amplitude of r2.

THICKNESS (M.)	P-VELOCITY (M/S.)	S-VELOCITY (M/S.)	DENSITY (G/ML)	1/Q P	1/Q S
63.0	1.460	0.000	1.03	0.00001	0.00001
0.7	1.480	0.010	1.65	0.00200	0.04000
4.9	1.934	0.532	2.00	0.00200	0.02000
4.9	1.953	0.537	2.00	0.00200	0.02000
4.9	1.972	0.542	2.00	0.00200	0.02000
5.0	1.991	0.547	2.00	0.00200	0.02000
5.0	2.009	0.553	2.00	0.00200	0.02000
5.1	2.028	0.558	2.00	0.00200	0.02000
5.1	2.047	0.563	2.00	0.00200	0.02000
5.2	2.066	0.569	2.00	0.00200	0.02000
	4.700	2.900	1.98	0.02000	0.04000

P-VELOCITY
S-VELOCITY
DENSITY
1/QP

−QP− LAYER 1   1/QP = 0.003   NO. 1281

−QP− LAYER 1   1/QP = 0.03   NO. 1281

Fig. 9.51b. 1/Qp, layer 1.

The model is insensitive to more reasonable values over a wide range.

THICKNESS (M.)	P-VELOCITY (M/S.)	S-VELOCITY (M/S.)	DENSITY (G/ML)	1/Q P	1/Q S
63.0	1.460	0.000	1.03	0.00001	0.00001
	1.450	0.510	1.85	0.00200	0.02000
4.9	1.934	0.532	2.00	0.00200	0.02000
4.9	1.953	0.537	2.00	0.00200	0.02000
4.9	1.972	0.542	2.00	0.00200	0.02000
5.0	1.991	0.547	2.00	0.00200	0.02000
5.0	2.009	0.553	2.00	0.00200	0.02000
5.1	2.028	0.558	2.00	0.00200	0.02000
5.1	2.047	0.563	2.00	0.00200	0.02000
5.2	2.066	0.568	2.00	0.00200	0.02000
	4.700	2.900	1.98	0.02000	0.04000

Fig. 9.52a. Layer 1, 1/Qs.

The model appears to be independent of this parameter.

THICKNESS (M.)	P-VELOCITY (M/S.)	S-VELOCITY (M/S.)	DENSITY (G/ML)	1/Q P	1/Q S
63.0	1.460	0.000	1.03	0.00001	0.00001
	1.430	0.010	1.45	0.00200	0.00002
4.8	1.934	0.532	2.00	0.00200	0.02000
4.9	1.953	0.537	2.00	0.00200	0.02000
4.9	1.972	0.542	2.00	0.00200	0.02000
5.0	1.991	0.547	2.00	0.00200	0.02000
5.0	2.009	0.553	2.00	0.00200	0.02000
5.1	2.028	0.558	2.00	0.00200	0.02000
5.1	2.047	0.563	2.00	0.00200	0.02000
5.2	2.066	0.569	2.00	0.00200	0.02000
	4.700	2.900	1.98	0.02000	0.04000

Fig. 9.52b. Layer 1, 1/Qs.

The model appears to be independent of this parameter.

THICKNESS (M.)	P-VELOCITY (M/S.)	S-VELOCITY (M/S.)	DENSITY (G/ML)	1/Q P	1/Q S
63.0	1.460	0.000	1.03	0.00001	0.00001
0.3	1.490	0.313	1.65	0.02000	0.04000
4.8	1.934	0.531	2.00	0.00200	0.02000
4.9	1.953	0.536	2.00	0.00200	0.02000
4.9	1.972	0.542	2.00	0.00200	0.02000
5.0	1.991	0.547	2.00	0.00200	0.02000
5.0	1.909	0.553	2.00	0.00200	0.02000
5.1	1.928	0.558	2.00	0.00200	0.02000
5.1	1.947	0.564	2.00	0.00200	0.02000
5.2	1.966	0.569	2.00	0.00200	0.02000
	4.700	2.800	1.99	0.02000	0.04000
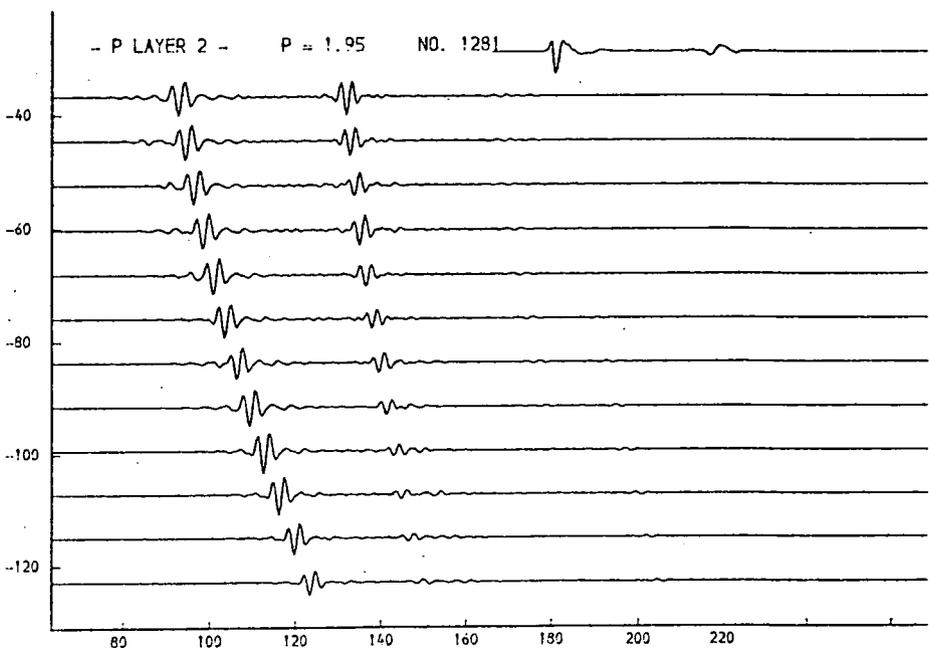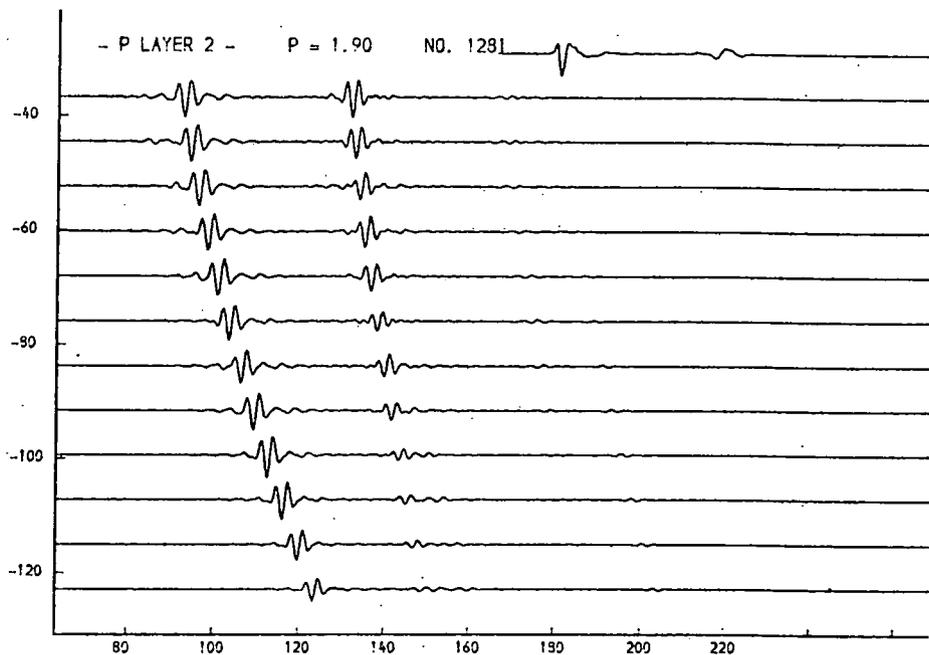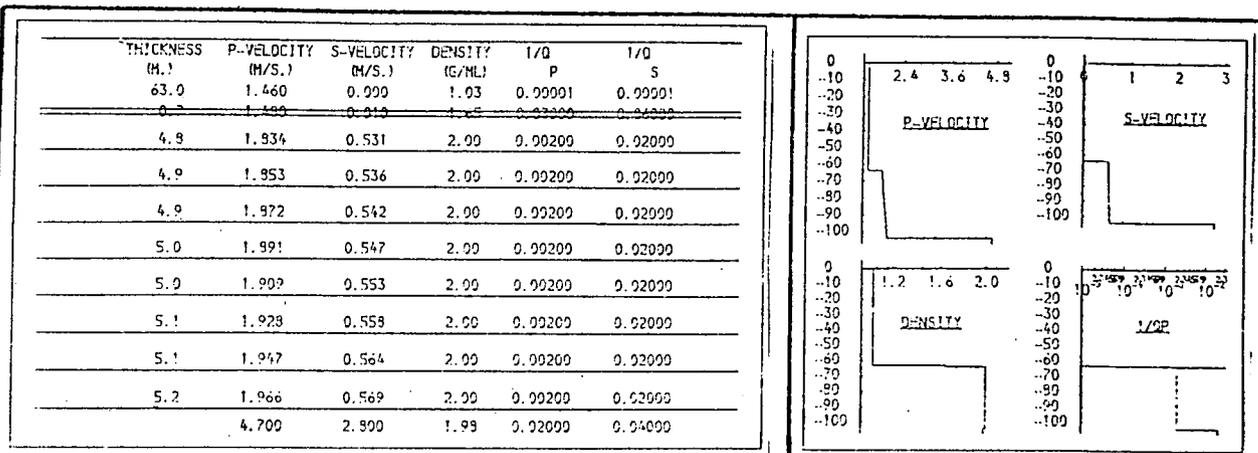
Fig. 9.53a. Layer 2, p-velocity.

The fitting of arrivals on the basis of travel times shows that the p-velocity in this layer is about 2.00+0.05km/sec. This value is confirmed by the amplitude variation which can be seen in the models shown here.

THICKNESS (M.)	P-VELOCITY (M/S.)	S-VELOCITY (M/S.)	DENSITY (G/ML)	1/Q P	1/Q S
63.0	1.460	0.000	1.03	0.00001	0.00001
0.3	1.460	0.040	1.25	0.03000	0.04000
4.8	1.984	0.532	2.00	0.00200	0.02000
4.9	2.003	0.537	2.00	0.00200	0.02000
4.9	2.022	0.542	2.00	0.00200	0.02000
5.0	2.041	0.547	2.00	0.00200	0.02000
5.0	2.059	0.553	2.00	0.00200	0.02000
5.1	2.079	0.558	2.00	0.00200	0.02000
5.1	2.097	0.563	2.00	0.00200	0.02000
5.2	2.116	0.568	2.00	0.00200	0.02000
	4.700	2.900	1.98	0.02000	0.04000
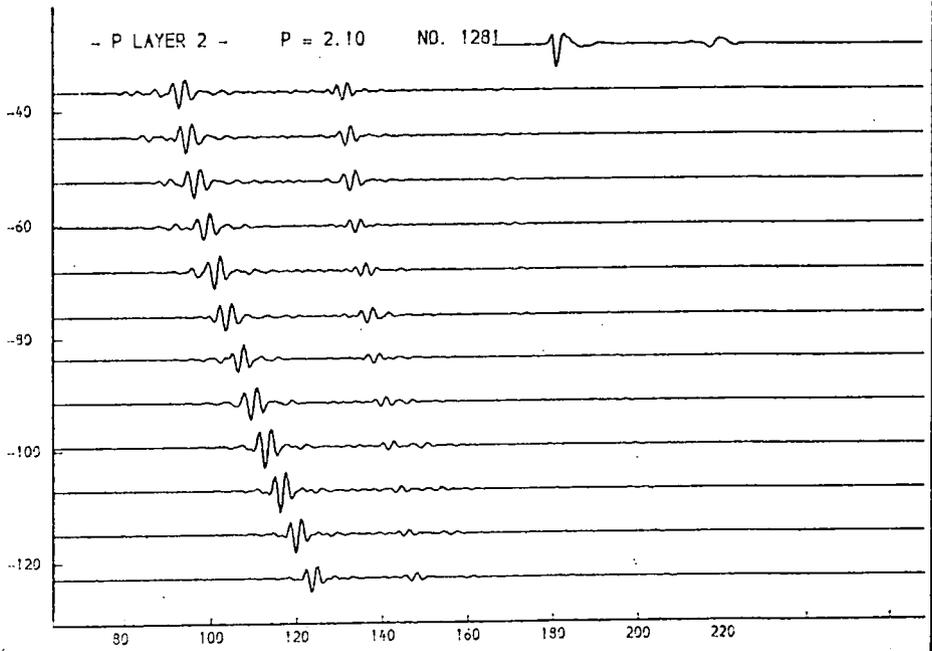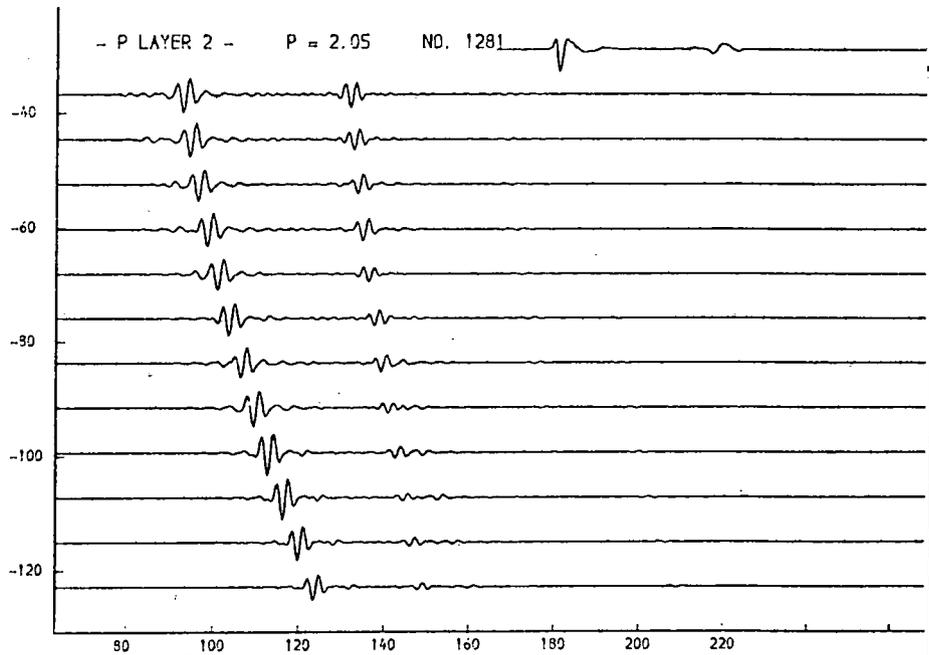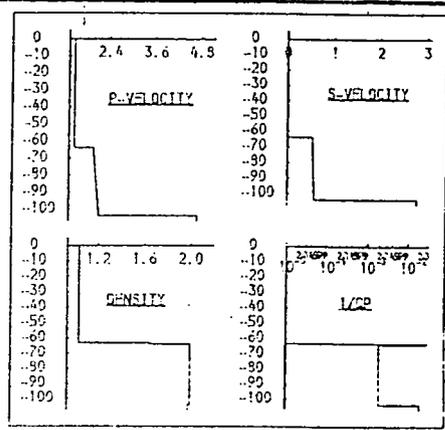
Fig. 9.53b. Layer 2, p-velocity.

The fitting of arrivals on the basis of travel times shows that the p-velocity in this layer is about 2.00+0.05km/sec. This value is confirmed by the amplitude variation which can be seen in the models shown here.

THICKNESS (M.)	P-VELOCITY (M/S.)	S-VELOCITY (M/S.)	DENSITY (G/ML)	1/Q P	1/Q S
63.0	1.460	0.000	1.03	0.00001	0.00001
0.2	1.460	0.310	1.65	0.02000	0.04000
4.8	1.934	0.290	2.00	0.00200	0.02000
4.9	1.953	0.293	2.00	0.00200	0.02000
4.9	1.972	0.296	2.00	0.00200	0.02000
5.0	1.991	0.299	2.00	0.00200	0.02000
5.0	2.009	0.301	2.00	0.00200	0.02000
5.1	2.028	0.304	2.00	0.00200	0.02000
5.1	2.047	0.307	2.00	0.00200	0.02000
5.2	2.066	0.310	2.00	0.00200	0.02000
	4.700	2.800	1.93	0.02000	0.04000

Fig. 9.54a. Layer 2, s-velocity.

As with seismogramme No. 1289 (see fig. 9.31), the changing of this parameter causes the migration across the model of a later arrival identified as a p-s conversion. The amplitude of this arrival is controlled by the value of 1/Qs (layer 2), but for the higher values of s-velocity shown, it still breaks through.

THICKNESS (M.)	P-VELOCITY (M/S.)	S-VELOCITY (M/S.)	DENSITY (G/ML)	1/Q P	1/Q S
63.0	1.460	0.000	1.03	0.00001	0.00001
0.3	1.489	0.013	1.65	0.03000	0.04000
4.8	1.934	0.484	2.00	0.00200	0.02000
4.9	1.953	0.488	2.00	0.00200	0.02000
4.9	1.972	0.493	2.00	0.00200	0.02000
5.0	1.991	0.498	2.00	0.00200	0.02000
5.0	2.009	0.502	2.00	0.00200	0.02000
5.1	2.028	0.507	2.00	0.00200	0.02000
5.1	2.047	0.512	2.00	0.00200	0.02000
5.2	2.066	0.516	2.00	0.00200	0.02000
	4.700	2.900	1.98	0.02000	0.04000
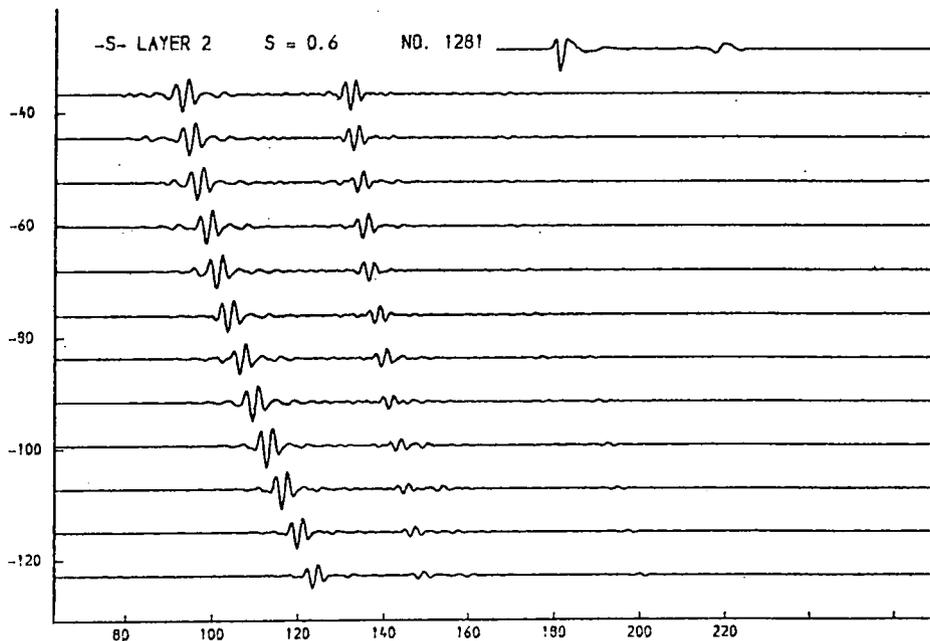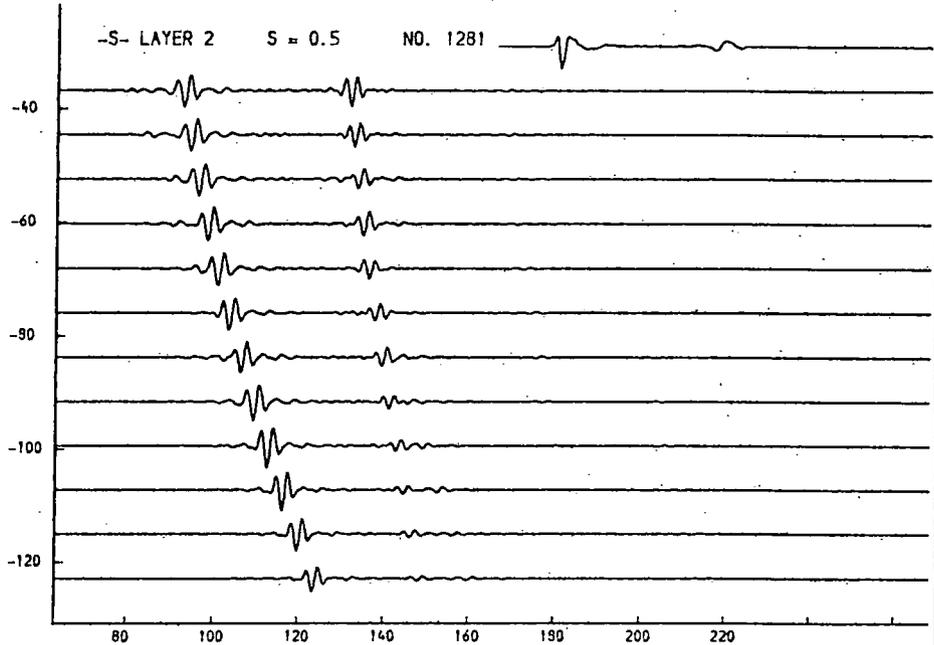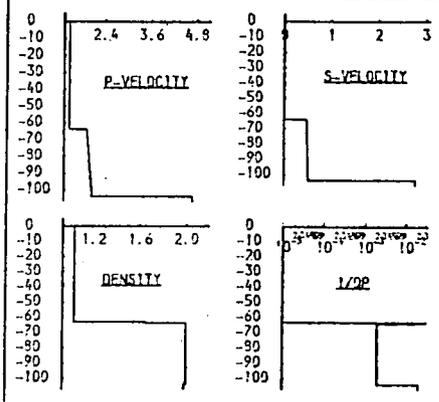
Fig. 9.54b. Layer 2, s-velocity.

As with seismogramme No. 1281 (see fig. 9.31), the changing of this parameter causes the migration across the model of a later arrival identified as a p-s conversion. The amplitude of this arrival is controlled by the value of 1/Qs (layer 2), but for the higher values of s-velocity shown, it still breaks through.

THICKNESS (M.)	P-VELOCITY (M/S.)	S-VELOCITY (M/S.)	DENSITY (G/ML)	1/Q P	1/Q S
63.0	1.460	0.000	1.03	0.00001	0.00001
4.9	1.934	0.677	2.00	0.00200	0.02000
4.9	1.953	0.694	2.00	0.00200	0.02000
4.9	1.972	0.690	2.00	0.00200	0.02000
5.0	1.991	0.697	2.00	0.00200	0.02000
5.0	2.009	0.703	2.00	0.00200	0.02000
5.1	2.029	0.710	2.00	0.00200	0.02000
5.1	2.047	0.716	2.00	0.00001	0.02000
5.2	2.066	0.723	2.00	0.00200	0.02000
	4.700	2.900	1.99	0.02000	0.04000

-S- LAYER 2   S = 0.7   NO. 1281

-S- LAYER 2   S = 0.9   NO. 1281

Fig. 9.54c.   Layer 2, s-velocity.

As with seismogramme No. 1289 (see fig. 9.31), the changing of this parameter causes the migration across the model of a later arrival identified as a p-s conversion. The amplitude of this arrival is controlled by the value of 1/Qs (layer 2), but for the higher values of s-velocity shown, it still breaks through.

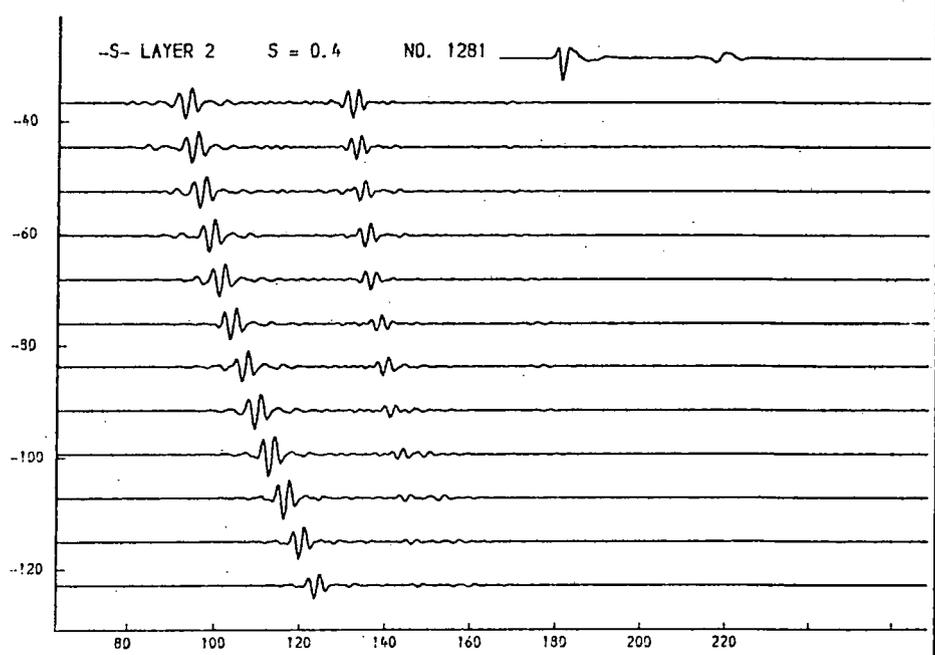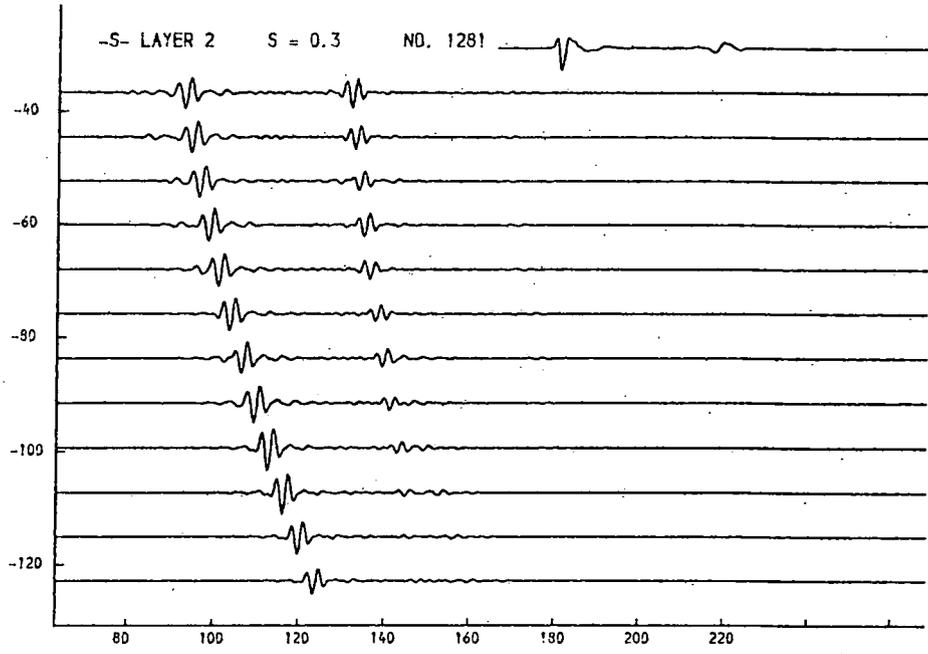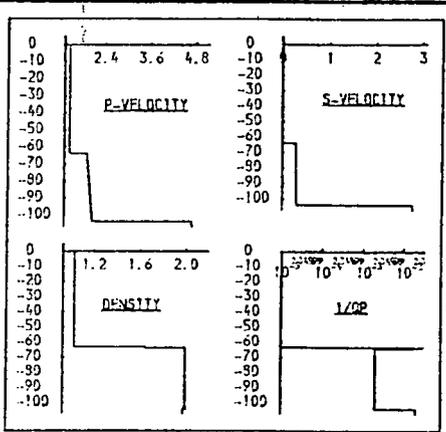| THICKNESS (M.)	P-VELOCITY (M/S.)	S-VELOCITY (M/S.)	DENSITY (G/ML)	1/Q P	1/Q S
63.0	1.460	0.000	1.03	0.00001	0.00001
0.2	1.460	0.010	1.03	0.02000	0.04000
4.8	1.934	0.967	2.00	0.00200	0.02000
4.9	1.953	0.977	2.00	0.00200	0.02000
4.9	1.972	0.986	2.00	0.00200	0.02000
5.0	1.991	0.995	2.00	0.00200	0.02000
5.0	2.009	1.005	2.00	0.00200	0.02000
5.1	2.028	1.014	2.00	0.00200	0.02000
5.1	2.047	1.023	2.00	0.00200	0.02000
5.2	2.066	1.033	2.00	0.00200	0.02000
	4.700	2.800	1.98	0.02000	0.04000

Fig. 9.54d. Layer 2, s-velocity.

As with seismogramme No. 1289 (see fig. 9.31), the changing of this parameter causes the migration across the model of a later arrival identified as a p-s conversion. The amplitude of this arrival is controlled by the value of 1/Qs (layer 2), but for the higher values of s-velocity shown, it still breaks through.

THICKNESS (M.)	P-VELOCITY (M/S.)	S-VELOCITY (M/S.)	DENSITY (G/ML)	1/Q P	1/Q S
63.0	1.460	0.000	1.03	0.00001	0.00001
0.3	1.480	0.010	1.45	0.02000	0.04000
4.9	1.934	0.532	1.80	0.00200	0.02000
4.9	1.953	0.537	1.80	0.00200	0.02000
4.9	1.972	0.542	1.80	0.00200	0.02000
5.0	1.991	0.547	1.80	0.00200	0.02000
5.0	2.009	0.553	1.80	0.00200	0.02000
5.1	2.023	0.559	1.80	0.00200	0.02000
5.1	2.047	0.563	1.80	0.00200	0.02000
5.2	2.066	0.569	1.80	0.00200	0.02000
	4.700	2.800	1.98	0.02000	0.04000

-DENSITY- LAYER 2 RHO = 1.90 NO. 1281

-DENSITY- LAYER 2 RHO = 1.90 NO. 1281
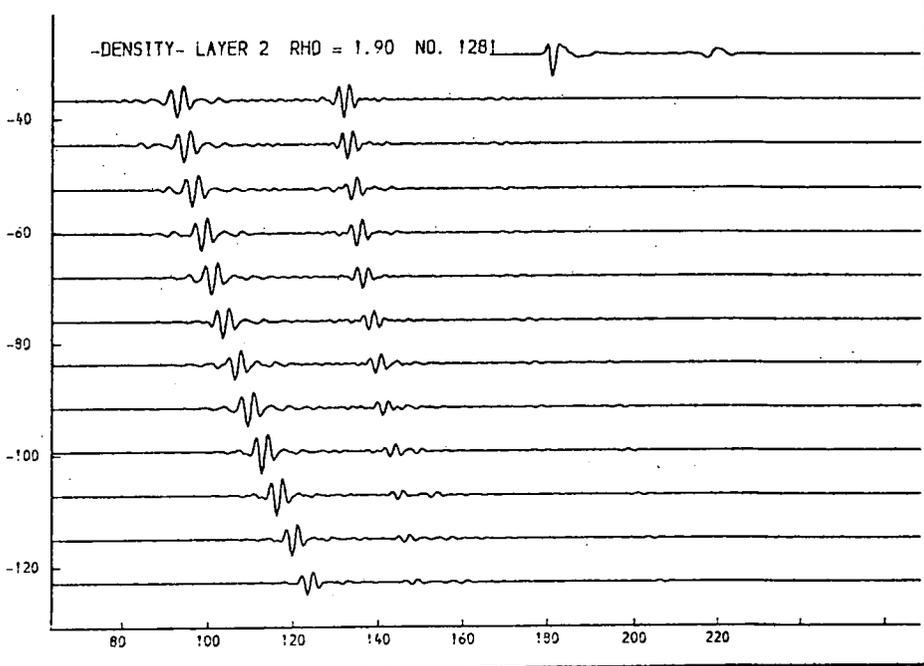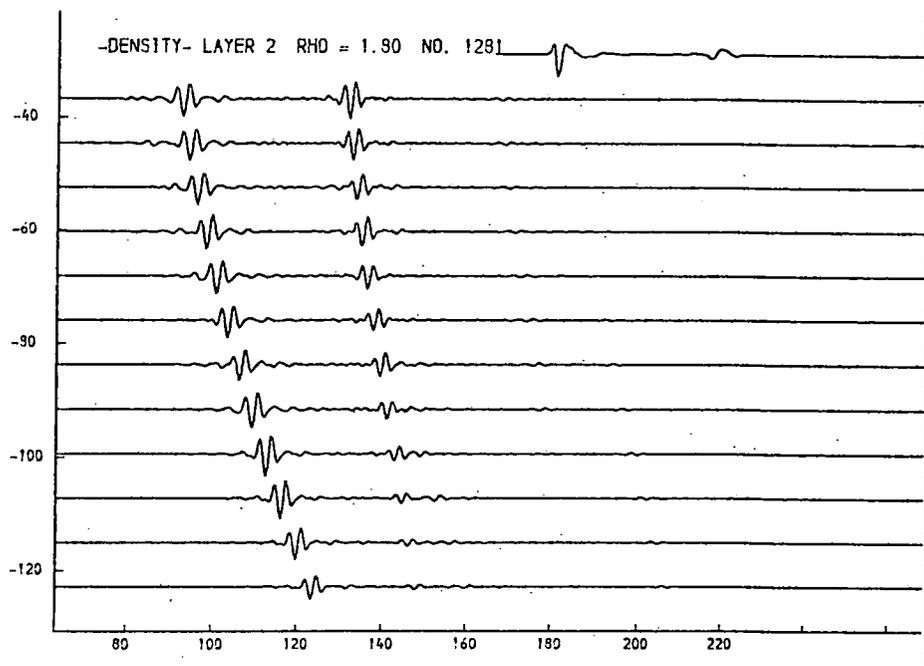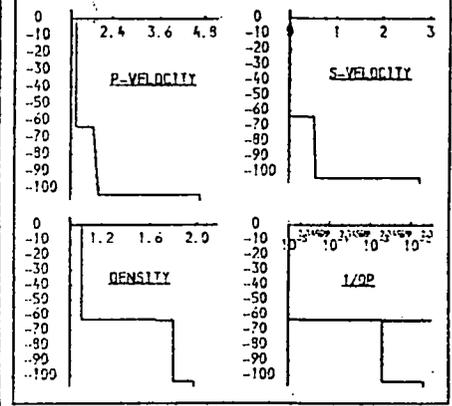
Fig. 9.55a.   Layer 2, density.

This parameter influences the amplitude of r2 at the lower offset distances.

THICKNESS (M.)	P-VELOCITY (M/S.)	S-VELOCITY (M/S.)	DENSITY (G/ML)	1/Q P	1/Q S
63.0	1.460	0.000	1.03	0.00001	0.00001
0.2	1.400	0.210	1.65	0.02000	0.04000
4.8	1.934	0.532	2.10	0.00200	0.02000
4.9	1.953	0.537	2.10	0.00200	0.02000
4.9	1.972	0.542	2.10	0.00200	0.02000
5.0	1.991	0.547	2.10	0.00200	0.02000
5.0	2.009	0.553	2.10	0.00200	0.02000
5.1	2.028	0.558	2.10	0.00200	0.02000
5.1	2.047	0.563	2.10	0.00200	0.02000
5.2	2.066	0.568	2.10	0.00200	0.02000
	4.700	2.800	1.98	0.02000	0.04000

-DENSITY- LAYER 2   RHO = 2.10   NO. 1281

-DENSITY- LAYER 2   RHO = 2.20   NO. 1281
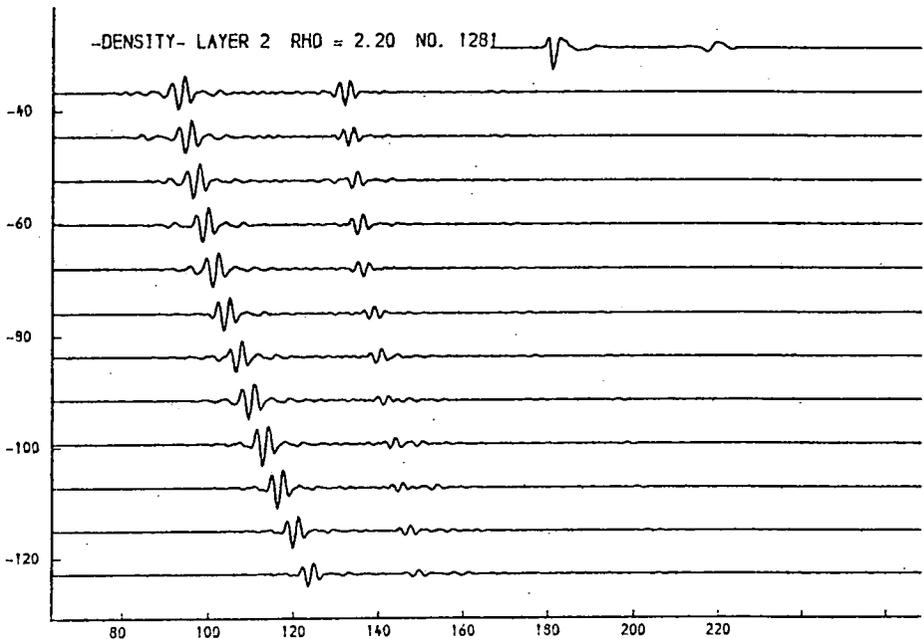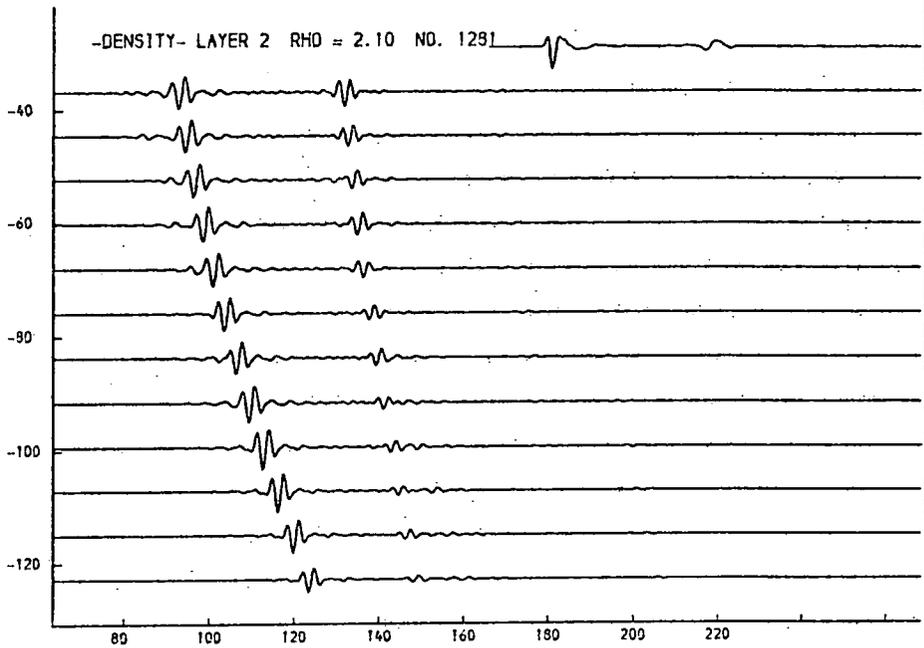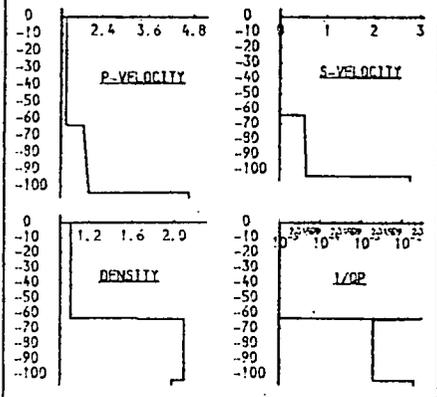
Fig. 9.55b. Layer 2, density.

This parameter influences the amplitude of r2 at the lower offset distances.

THICKNESS (M.)	P-VELOCITY (M/S.)	S-VELOCITY (M/S.)	DENSITY (G/ML)	1/Q P	1/Q S
63.0	1.460	0.000	1.03	0.00001	0.00001
0.7	1.190	0.210	1.03	0.03010	0.04000
4.8	1.934	0.532	2.00	0.00050	0.02000
4.9	1.953	0.537	2.00	0.00050	0.02000
4.9	1.972	0.542	2.00	0.00050	0.02000
5.0	1.991	0.547	2.00	0.00050	0.02000
5.0	2.009	0.553	2.00	0.00050	0.02000
5.1	2.028	0.558	2.00	0.00050	0.02000
5.1	2.047	0.563	2.00	0.00050	0.02000
5.2	2.066	0.568	2.00	0.00050	0.02000
	4.700	2.800	1.98	0.02000	0.04000

-QP- LAYER 2 1/QP = 0.0005   NO. 1281

-QP- LAYER 2 1/QP = 0.001   NO. 1281

Fig. 9.56a. Layer 2, 1/Qp.

Higher values for this parameter reduce the amplitude of r2 in an unacceptable way.

THICKNESS (M.)	P-VELOCITY (M/S.)	S-VELOCITY (M/S.)	DENSITY (G/ML)	1/Q P	1/Q S
63.0	1.460	0.000	1.03	0.00001	0.00001
0.2	1.430	0.010	1.65	0.02000	0.04000
4.8	1.934	0.532	2.00	0.00200	0.02000
4.9	1.953	0.537	2.00	0.00200	0.02000
4.9	1.972	0.542	2.00	0.00200	0.02000
5.0	1.991	0.547	2.00	0.00200	0.02000
5.0	2.009	0.553	2.00	0.00200	0.02000
5.1	2.028	0.558	2.00	0.00200	0.02000
5.1	2.047	0.563	2.00	0.00200	0.02000
5.2	2.066	0.568	2.00	0.00200	0.02000
	4.700	2.800	1.93	0.02000	0.04000

Fig. 9.56b. Layer 2, 1/Qp.

Higher values for this parameter reduce the amplitude of r2 in an unacceptable way.

THICKNESS (M.)	P-VELOCITY (M/S.)	S-VELOCITY (M/S.)	DENSITY (G/ML)	1/Q P	1/Q S
63.0	1.460	0.000	1.03	0.00001	0.00001
0.7	1.482	0.010	1.65	0.03000	0.06000
4.9	1.934	0.532	2.00	0.00400	0.02000
4.9	1.953	0.537	2.00	0.00400	0.02000
4.9	1.972	0.542	2.00	0.00400	0.02000
5.0	1.991	0.547	2.00	0.00400	0.02000
5.0	2.009	0.553	2.00	0.00400	0.02000
5.1	2.028	0.558	2.00	0.00400	0.02000
5.1	2.047	0.563	2.00	0.00400	0.02000
5.2	2.066	0.569	2.00	0.00400	0.02000
	4.700	2.900	1.98	0.02000	0.04000
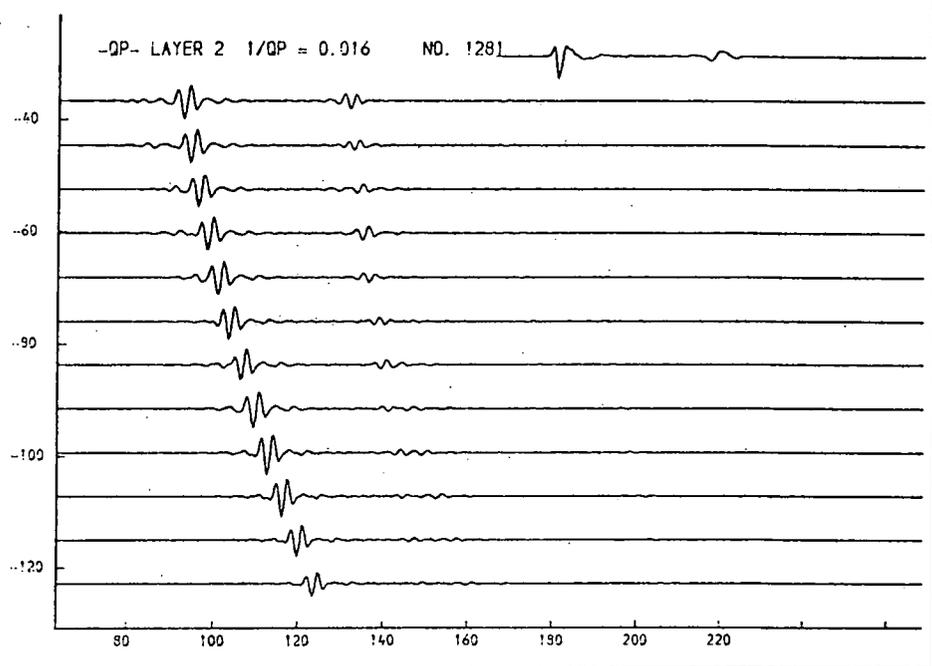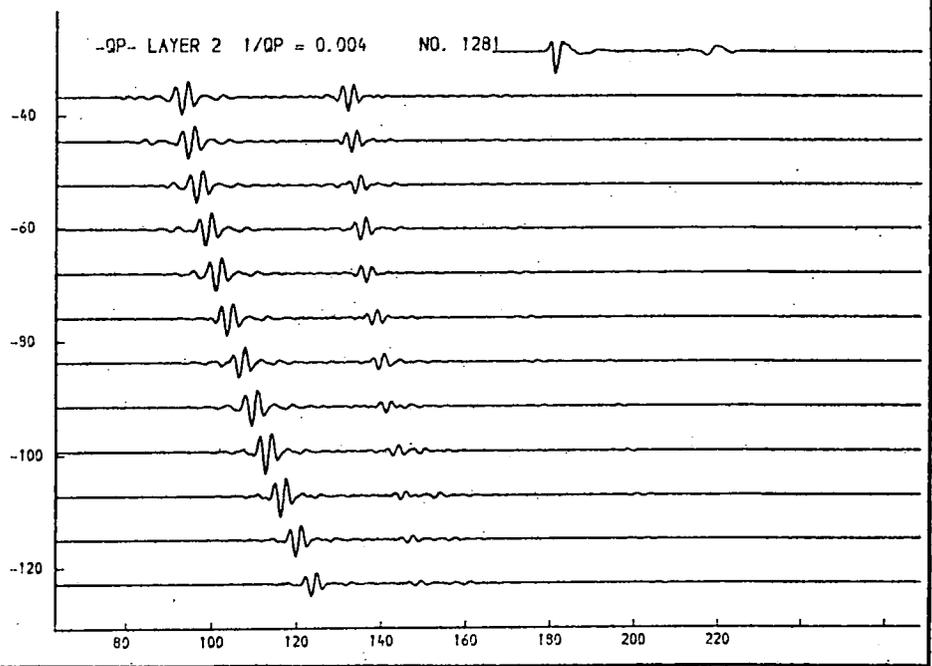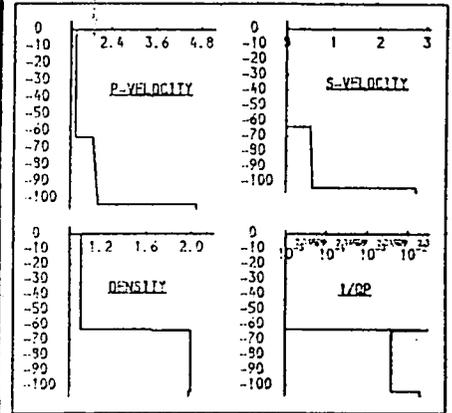
Fig. 9.56c. Layer 2, 1/Qp.

Higher values for this parameter reduce the amplitude of r2 in an unacceptable way.

THICKNESS (M.)	P-VELOCITY (M/S.)	S-VELOCITY (M/S.)	DENSITY (G/ML)	1/Q P	1/Q S
63.0	1.460	0.000	1.03	0.00001	0.00001
0.0	1.490	0.010	1.05	0.00100	0.04000
4.9	1.934	0.532	2.00	0.00200	0.00050
4.9	1.953	0.537	2.00	0.00200	0.00050
4.9	1.972	0.542	2.00	0.00200	0.00050
5.0	1.991	0.547	2.00	0.00200	0.00050
5.0	2.009	0.553	2.00	0.00200	0.00050
5.1	2.028	0.558	2.00	0.00200	0.00050
5.1	2.047	0.563	2.00	0.00200	0.00050
5.2	2.066	0.569	2.00	0.00200	0.00050
	4.700	2.900	1.93	0.02000	0.04000

Fig. 9.57a. Layer 2, 1/Qs.

This parameter controls the amplitude of the p-s conversion (see figs. 9.36, 9.37)

THICKNESS (M.)	P-VELOCITY (M/S.)	S-VELOCITY (M/S.)	DENSITY (G/ML)	1/Q P	1/Q S
63.0	1.460	0.000	1.03	0.00001	0.00001
0.2	1.460	0.000	1.03	0.00200	0.00500
4.9	1.934	0.532	2.00	0.00200	0.00500
4.9	1.953	0.537	2.00	0.00200	0.00500
4.9	1.972	0.542	2.00	0.00200	0.00500
5.0	1.991	0.547	2.00	0.00200	0.00500
5.0	2.009	0.553	2.00	0.00200	0.00500
5.1	2.029	0.558	2.00	0.00200	0.00500
5.1	2.047	0.563	2.00	0.00200	0.00500
5.2	2.066	0.569	2.00	0.00200	0.00500
	4.700	2.900	1.98	0.02000	0.04000

P-VELOCITY

S-VELOCITY

DENSITY

1/QP

-QS- LAYER 2   1/QS = 0.005   NO.1281

-QS- LAYER 2   1/QS = 0.01   NO.1281
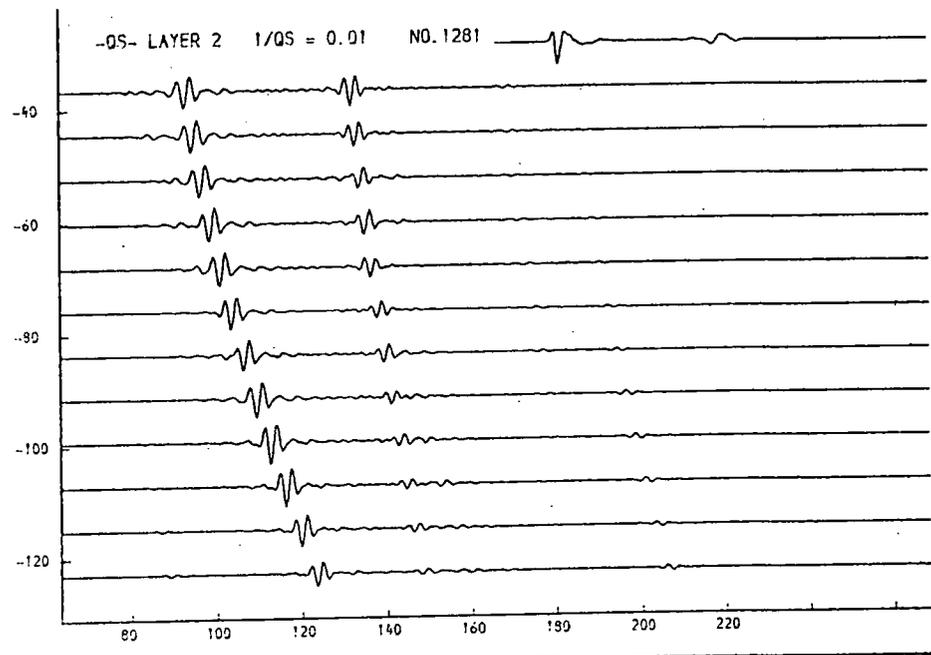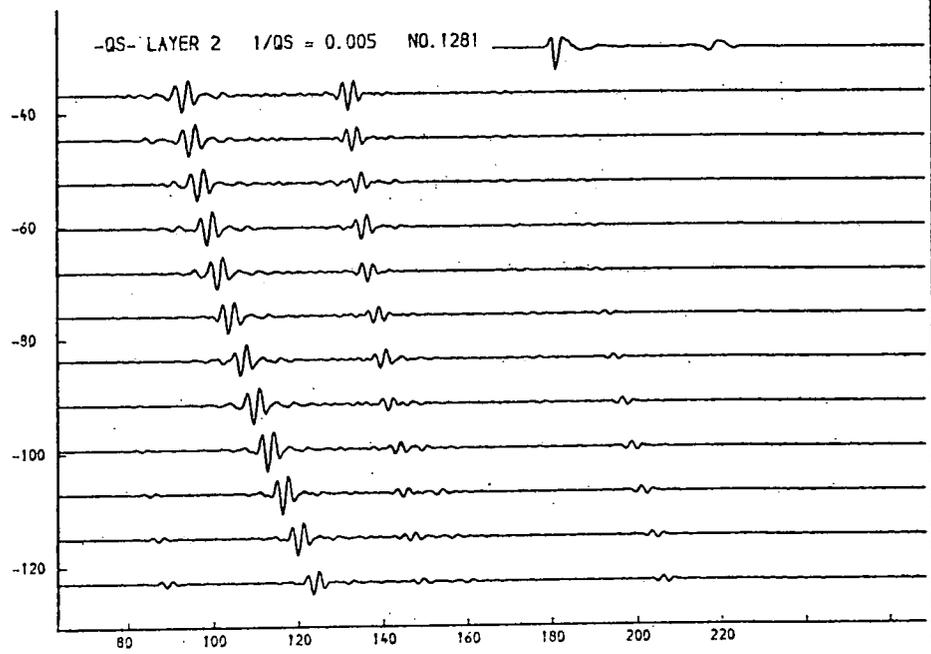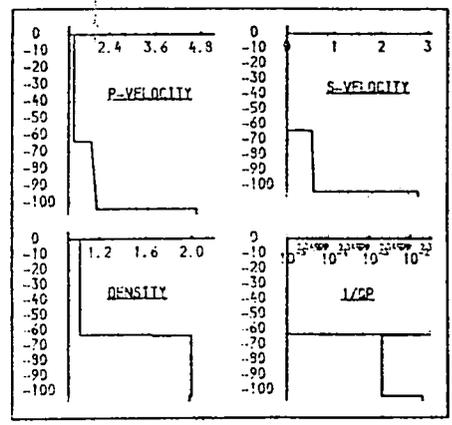
Fig. 9.57b. Layer 2, 1/Qs.

This parameter controls the amplitude of the p-s conversion (see figs. 9.36, 9.37)

THICKNESS (M.)	P-VELOCITY (M/S.)	S-VELOCITY (M/S.)	DENSITY (G/ML)	1/Q P	1/Q S
63.0	1.460	0.000	1.03	0.00001	0.00001
		0.510	1.45	0.03000	0.04000
4.8	1.934	0.532	2.00	0.00200	0.02000
4.9	1.953	0.537	2.00	0.00200	0.02000
4.9	1.972	0.542	2.00	0.00200	0.02000
5.0	1.991	0.547	2.00	0.00200	0.02000
5.0	2.009	0.553	2.00	0.00200	0.02000
5.1	2.028	0.558	2.00	0.00200	0.02000
5.1	2.047	0.563	2.00	0.00200	0.02000
5.2	2.066	0.568	2.00	0.00200	0.02000
	4.700	2.800	1.98	0.02000	0.04000

-QS- LAYER 2   1/QS = 0.02   NO. 1281

-QS- LAYER 2   1/QS = 0.03   NO. 1281

Fig. 9.57c.   Layer 2, 1/Qs.

This parameter controls the amplitude of the p-s conversion (see figs. 9.36, 9.37)

THICKNESS (M.)	P-VELOCITY (M/S.)	S-VELOCITY (M/S.)	DENSITY (G/ML)	1/Q P	1/Q S
63.0	1.460	0.000	1.93	0.00001	0.00001
0.0	1.932	0.010	1.95	0.02000	0.04000
4.9	1.934	0.532	2.00	0.00200	0.04000
4.9	1.953	0.537	2.00	0.00200	0.04000
4.9	1.972	0.542	2.00	0.00200	0.04000
5.0	1.991	0.547	2.00	0.00200	0.04000
5.0	2.009	0.553	2.00	0.00200	0.04000
5.1	2.029	0.559	2.00	0.00200	0.04000
5.1	2.047	0.563	2.00	0.00200	0.04000
5.2	2.066	0.568	2.00	0.00200	0.04000
	4.700	2.900	1.93	0.02000	0.04000

-QS- LAYER 2   1/QS = 0.04   NO.1281

-QS- LAYER 2   1/QS = 0.08   NO.1281
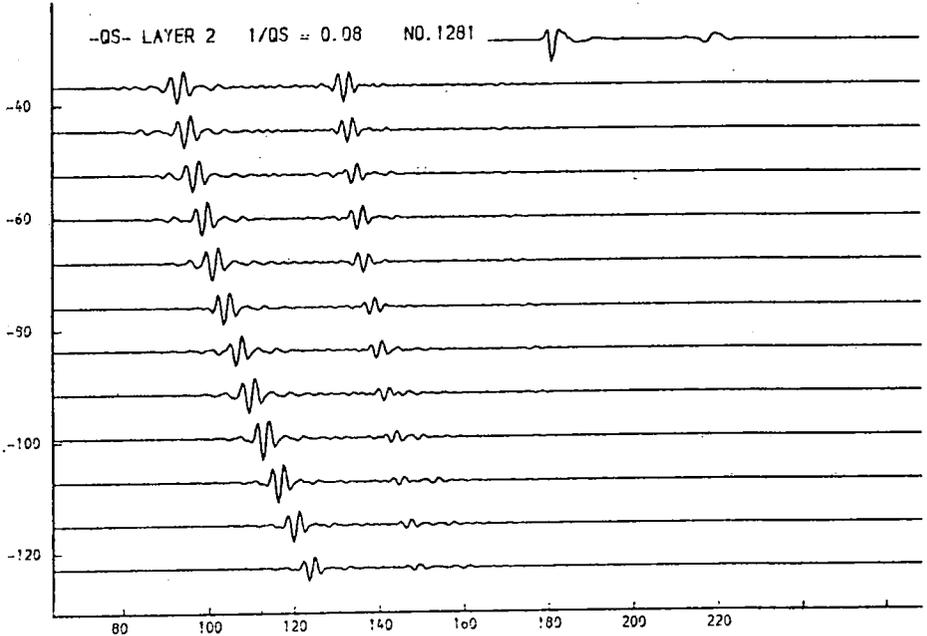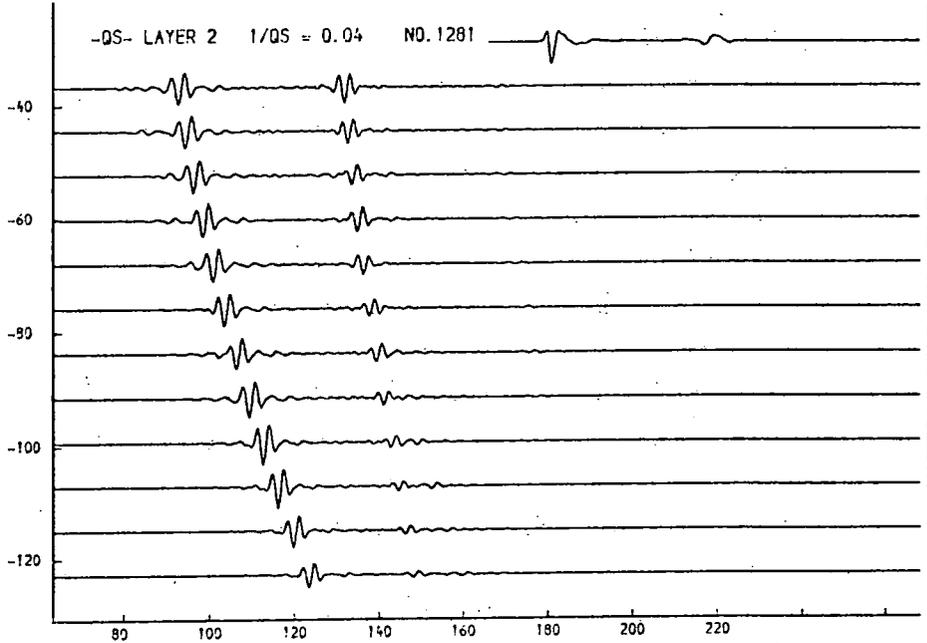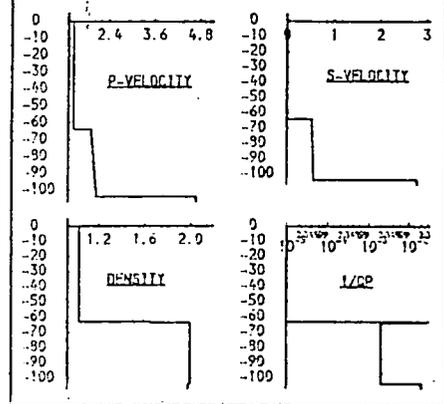
Fig. 9.57d. Layer 2, 1/Qs.

This parameter controls the amplitude of the p-s conversion (see figs. 9.36,9.37)

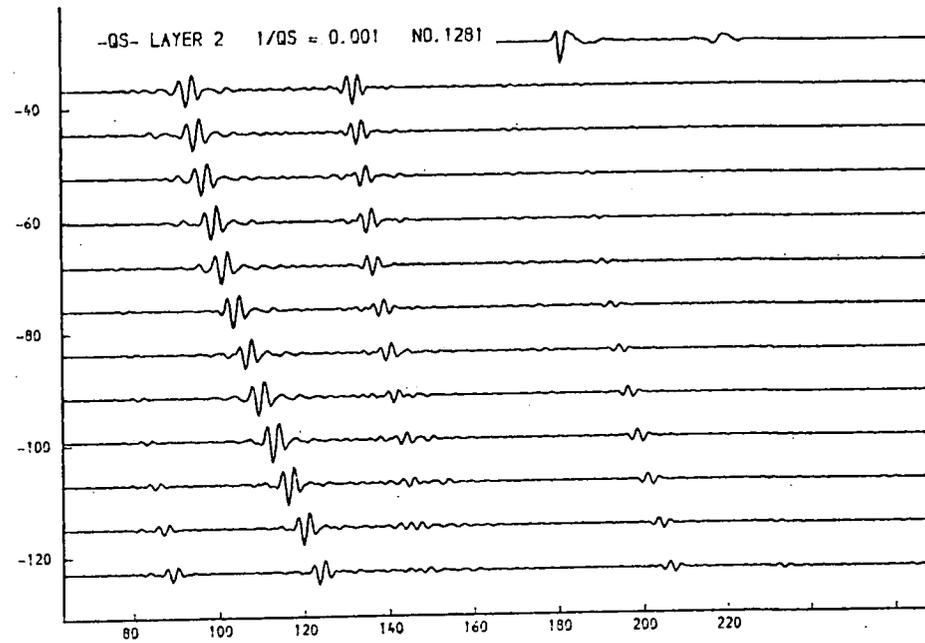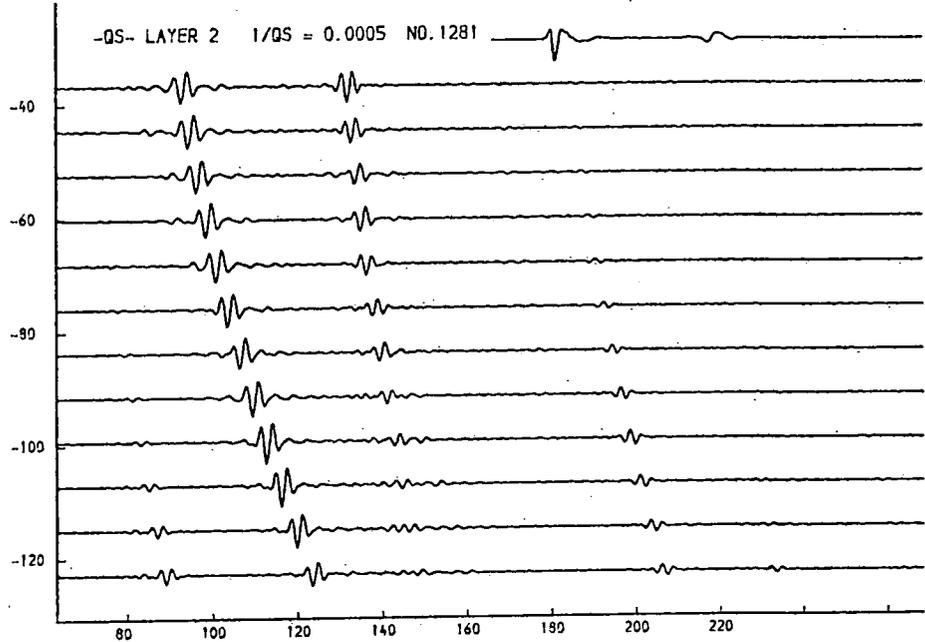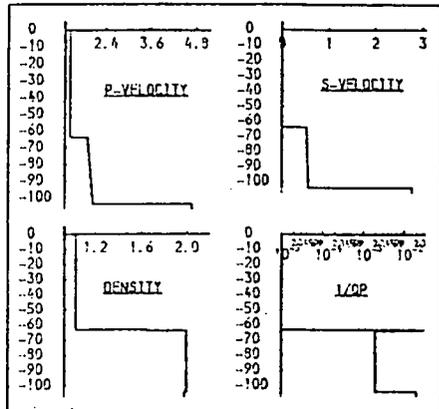| THICKNESS (M.)	P-VELOCITY (M/S.)	S-VELOCITY (M/S.)	DENSITY (G/ML)	1/Q P	1/Q S
63.0	1.460	0.000	1.03	0.00001	0.00001
~~0.2~~	~~1.400~~	~~0.010~~	~~1.05~~	~~0.02000~~	~~0.04000~~
4.8	1.934	0.532	2.00	0.00200	0.16000
4.9	1.953	0.537	2.00	0.00200	0.16000
4.9	1.972	0.542	2.00	0.00200	0.16000
5.0	1.991	0.547	2.00	0.00200	0.16000
5.0	2.009	0.553	2.00	0.00200	0.16000
5.1	2.028	0.559	2.00	0.00200	0.16000
5.1	2.047	0.563	2.00	0.00200	0.16000
5.2	2.066	0.569	2.00	0.00200	0.16000
	4.700	2.900	1.98	0.02000	0.04000
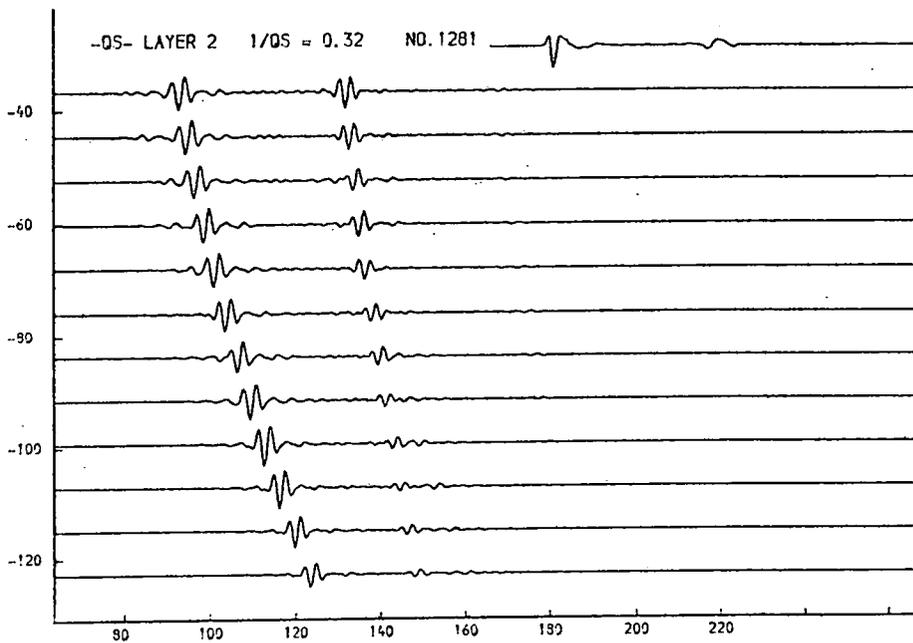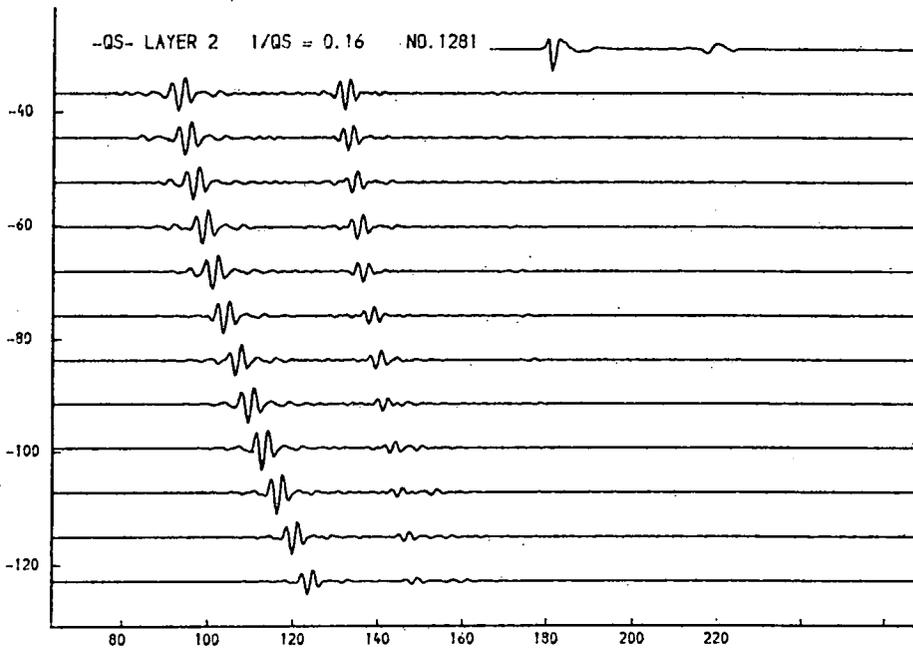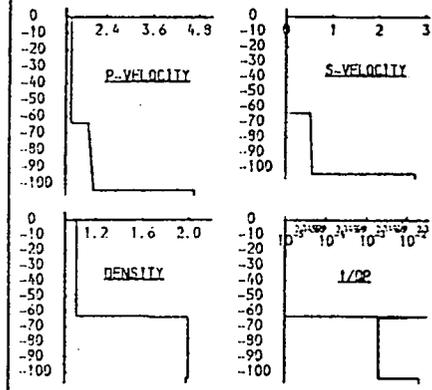
Fig. 9.57e. Layer 2, 1/Qs.

This parameter controls the amplitude of the p-s conversion (see figs. 9.36, 9.37)

Fig. 9.58a. Layer 3, p-velocity.

This parameter controls the amplitude of r2. Quite a wide
range appears possible.

THICKNESS (M.)	P-VELOCITY (M/S.)	S-VELOCITY (M/S.)	DENSITY (G/ML)	1/Q P	1/Q S
63.0	1.460	0.000	1.03	0.00001	0.00001
0.2	1.460	0.010	1.05	0.02000	0.04000
4.8	1.934	0.532	2.00	0.00200	0.02000
4.9	1.953	0.537	2.00	0.00200	0.02000
4.9	1.972	0.542	2.00	0.00200	0.02000
5.0	1.991	0.547	2.00	0.00200	0.02000
5.0	2.009	0.553	2.00	0.00200	0.02000
5.1	2.028	0.559	2.00	0.00200	0.02000
5.1	2.047	0.563	2.00	0.00200	0.02000
5.2	2.066	0.569	2.00	0.00200	0.02000
	4.300	2.900	1.98	0.02000	0.04000

-P- LAYER 3   P = 4.3   NO. 1281

-P- LAYER 3   P = 4.5   NO. 1281
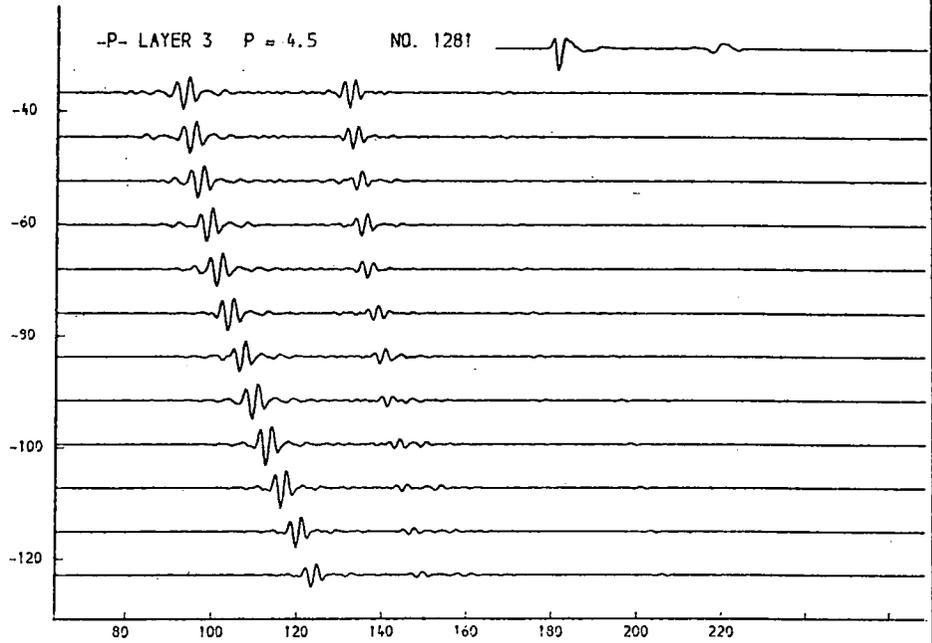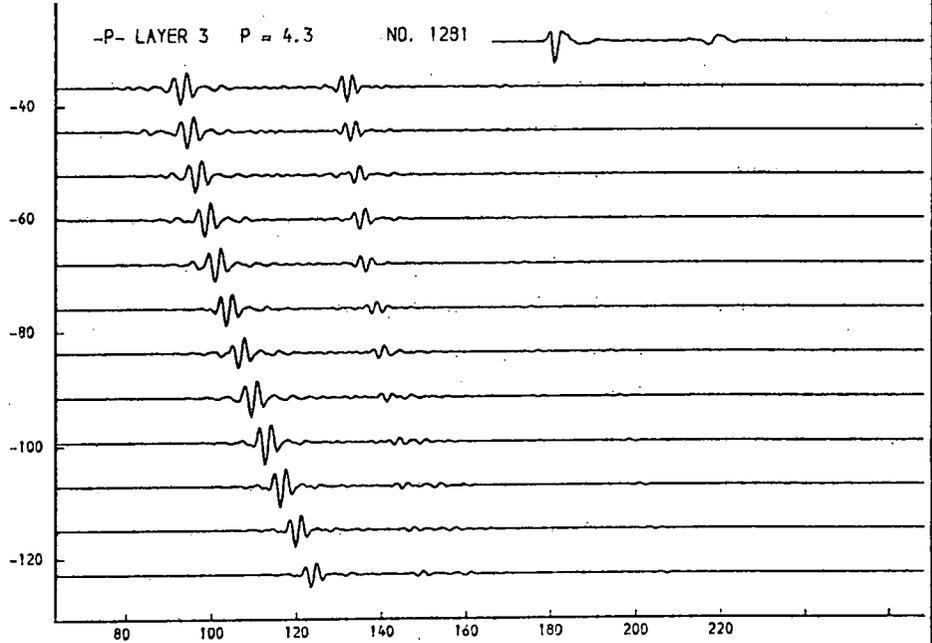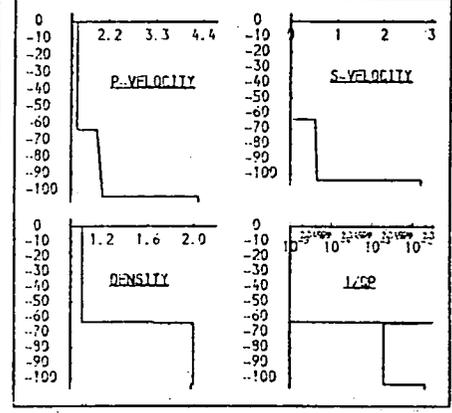
Fig. 9.58b. Layer 3, p-velocity.

This parameter controls the amplitude of r2. Quite a wide range appears possible.

THICKNESS (M.)	P-VELOCITY (M/S.)	S-VELOCITY (M/S.)	DENSITY (G/ML)	1/Q P	1/Q S
63.0	1.460	0.000	1.03	0.00001	0.00001
	1.460	0.000	1.05	0.00000	0.00000
4.8	1.934	0.532	2.00	0.00200	0.02000
4.9	1.953	0.537	2.00	0.00200	0.02000
4.9	1.972	0.542	2.00	0.00200	0.02000
5.0	1.991	0.547	2.00	0.00200	0.02000
5.0	2.009	0.553	2.00	0.00200	0.02000
5.1	2.028	0.559	2.00	0.00200	0.02000
5.1	2.047	0.563	2.00	0.00200	0.02000
5.2	2.066	0.569	2.00	0.00200	0.02000
	4.900	2.900	1.99	0.02000	0.04000

−P− LAYER 3   P = 4.9   NO. 1281

−P− LAYER 3   P = 5.1   NO. 1281
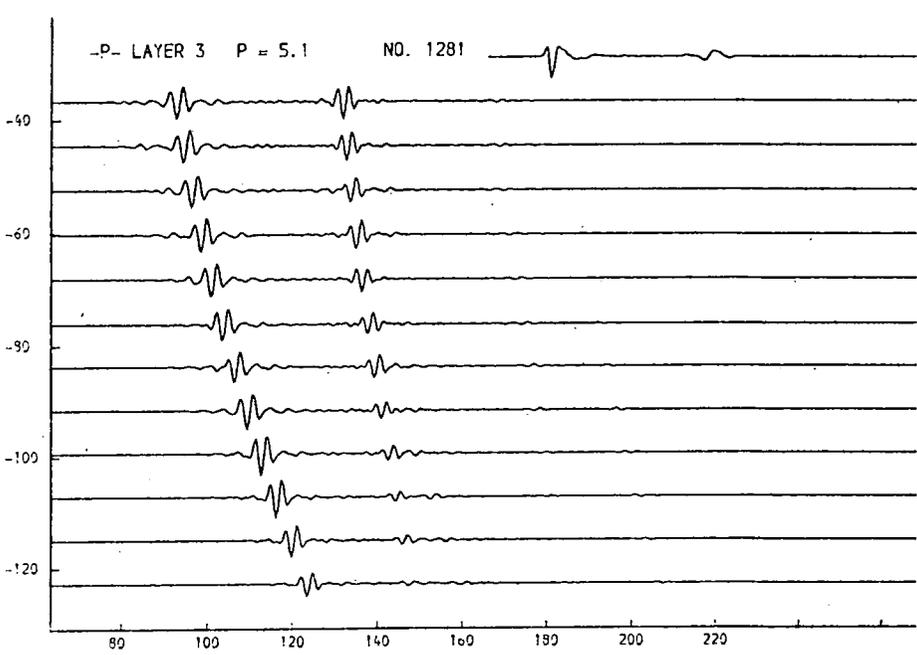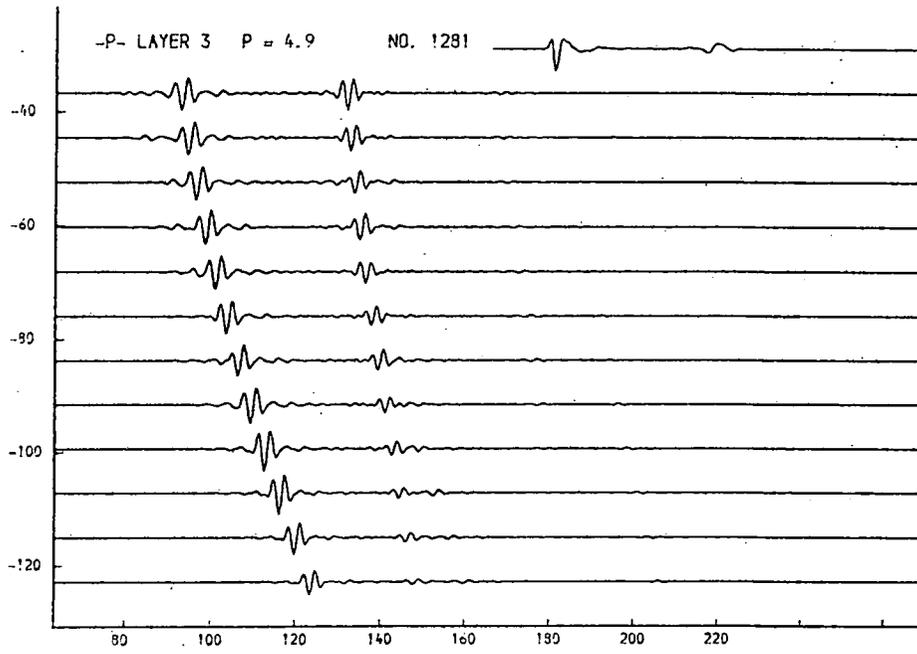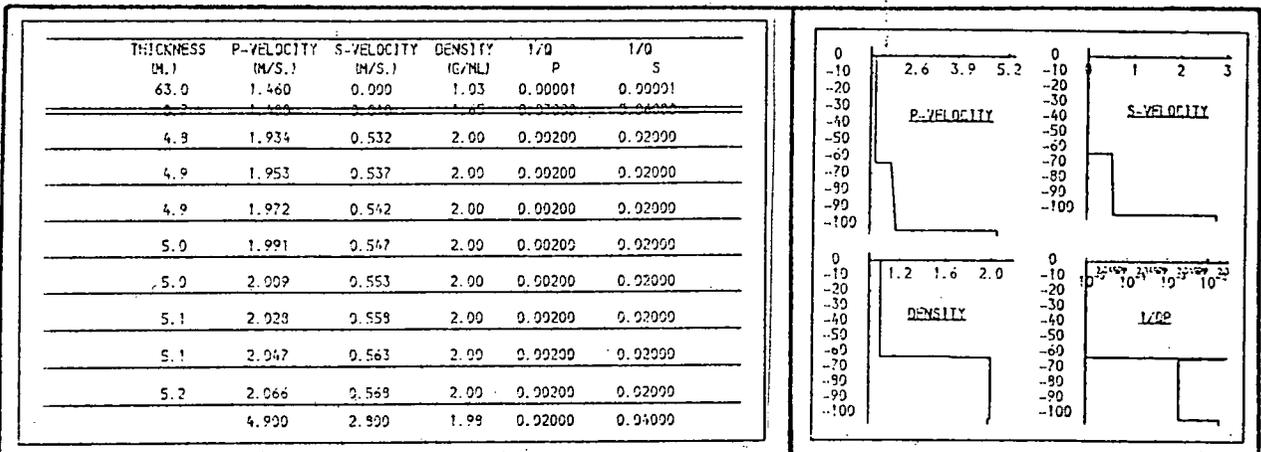
Fig. 9.58c.   Layer 3, p-velocity.

This parameter controls the amplitude of r2.   Quite a wide
range appears possible.

THICKNESS (M.)	P-VELOCITY (M/S.)	S-VELOCITY (M/S.)	DENSITY (G/ML)	1/Q P	1/Q S
63.0	1.460	0.000	1.03	0.00001	0.00001
	1.490	0.010	1.65	0.03000	0.06000
4.9	1.934	0.532	2.00	0.00200	0.02000
4.9	1.953	0.537	2.00	0.00200	0.02000
4.9	1.972	0.542	2.00	0.00200	0.02000
5.0	1.991	0.547	2.00	0.00200	0.02000
5.0	2.009	0.553	2.00	0.00200	0.02000
5.1	2.028	0.559	2.00	0.00200	0.02000
5.1	2.047	0.563	2.00	0.00200	0.02000
5.2	2.066	0.568	2.00	0.00200	0.02000
	5.300	2.800	1.98	0.02000	0.04000

Fig. 9.58d. Layer 3, p-velocity.

This parameter controls the amplitude of r2. Quite a wide range appears possible.

THICKNESS (M.)	P-VELOCITY (M/S.)	S-VELOCITY (M/S.)	DENSITY (G/ML)	1/Q P	1/Q S
63.0	1.460	0.000	1.03	0.00001	0.00001
		0.010			0.04000
4.8	1.934	0.532	2.00	0.00200	0.01000
4.9	1.953	0.537	2.00	0.00200	0.01000
4.9	1.972	0.542	2.00	0.00200	0.01000
5.0	1.991	0.547	2.00	0.00200	0.01000
5.0	2.009	0.553	2.00	0.00200	0.01000
5.1	2.029	0.558	2.00	0.00200	0.01000
5.1	2.047	0.563	2.00	0.00200	0.01000
5.2	2.066	0.569	2.00	0.00200	0.01000
	4.700	2.100	1.98	0.02000	0.04000

Fig. 9.59a. Layer 3, s-velocity.

Higher values for this parameter give too rapid fall-off in the amplitude of r2 with increasing offset. Lower values lead to an unacceptably high amplitude for r2 at large offset.

THICKNESS (M.)	P-VELOCITY (M/S.)	S-VELOCITY (M/S.)	DENSITY (G/ML)	1/Q P	1/Q S
63.0	1.460	0.000	1.03	0.00001	0.00001
4.8	1.934	0.532	2.00	0.00200	0.01000
4.9	1.953	0.537	2.00	0.00200	0.01000
4.9	1.972	0.542	2.00	0.00200	0.01000
5.0	1.991	0.547	2.00	0.00200	0.01000
5.0	2.009	0.553	2.00	0.00200	0.01000
5.1	2.028	0.559	2.00	0.00200	0.01000
5.1	2.047	0.563	2.00	0.00200	0.01000
5.2	2.066	0.568	2.00	0.00200	0.01000
	4.700	2.500	1.99	0.02000	0.04000

-S- LAYER 3   S = 2.5   NO. 1281

-S- LAYER 3   S = 2.3   NO. 1281

Fig. 9.59b.   Layer 3, s-velocity.

Higher values for this parameter give too rapid fall-off in the amplitude of r2 with increasing offset. Lower values lead to an unacceptably high amplitude for r2 at large offset.

THICKNESS (M.)	P-VELOCITY (M/S.)	S-VELOCITY (M/S.)	DENSITY (G/ML)	1/Q P	1/Q S
63.0	1.460	0.000	1.03	0.00001	0.00001
4.9	1.490	0.018	1.95	0.03000	0.04000
4.9	1.934	0.532	2.00	0.00200	0.01000
4.9	1.953	0.537	2.00	0.00200	0.01000
4.9	1.972	0.542	2.00	0.00200	0.01000
5.0	1.991	0.547	2.00	0.00200	0.01000
5.0	2.009	0.553	2.00	0.00200	0.01000
5.1	2.028	0.559	2.00	0.00200	0.01000
5.1	2.047	0.563	2.00	0.00200	0.01000
5.2	2.066	0.568	2.00	0.00200	0.01000
	4.700	2.900	1.98	0.02000	0.04000

Fig. 9.59c. Layer 3, s-velocity.

Higher values for this parameter give too rapid fall-off in the amplitude of r2 with increasing offset. Lower values lead to an unacceptably high amplitude for r2 at large offset.

THICKNESS (M.)	P-VELOCITY (M/S.)	S-VELOCITY (M/S.)	DENSITY (G/ML)	1/Q P	1/Q S
63.0	1.460	0.000	1.03	0.00001	0.00001
4.9	1.934	0.532	2.00	0.00200	0.01000
4.9	1.953	0.537	2.00	0.00200	0.01000
4.9	1.972	0.542	2.00	0.00200	0.01000
5.0	1.991	0.547	2.00	0.00200	0.01000
5.0	2.009	0.553	2.00	0.00200	0.01000
5.1	2.028	0.558	2.00	0.00200	0.01000
5.1	2.047	0.563	2.00	0.00200	0.01000
5.2	2.066	0.568	2.00	0.00200	0.01000
	4.700	3.300	1.98	0.02000	0.04000
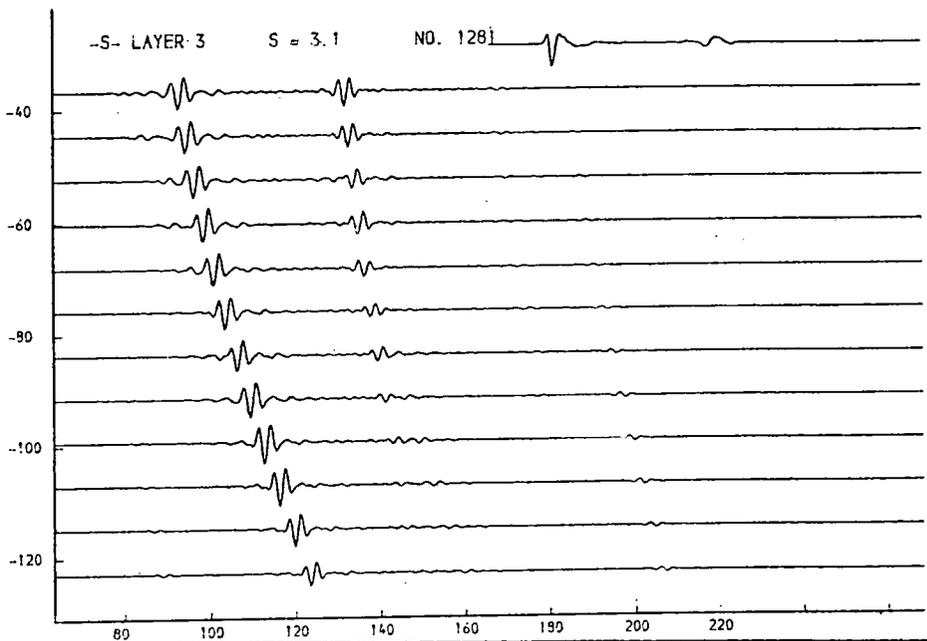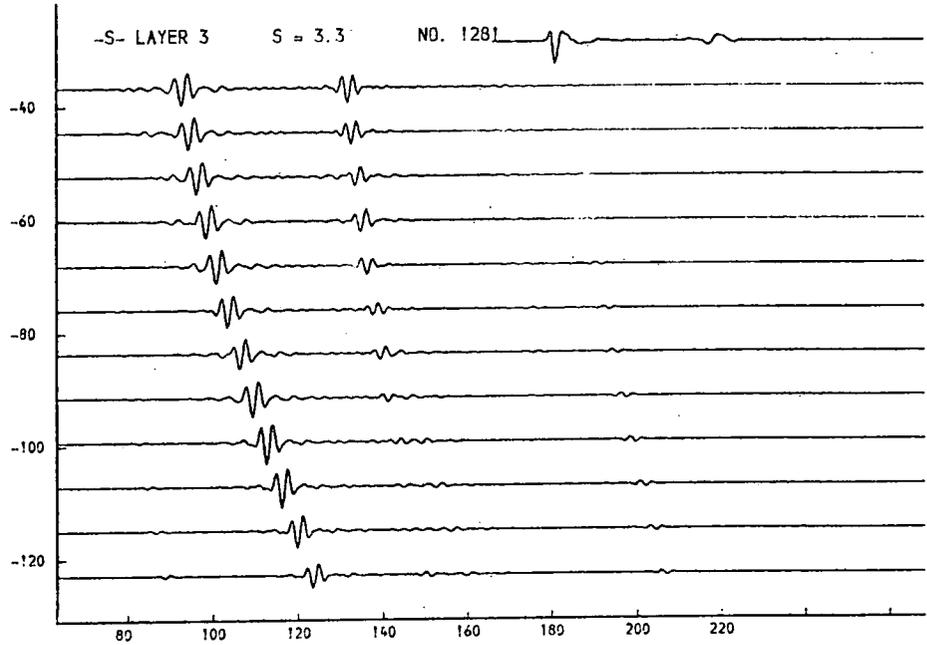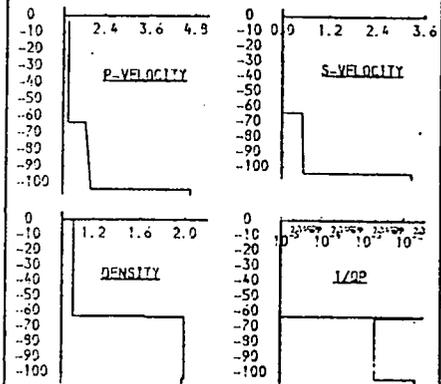
Fig. 9.59d. Layer 3, s-velocity.

Higher values for this parameter give too rapid fall-off in the amplitude of r2 with increasing offset. Lower values lead to an unacceptably high amplitude for r2 at large offset.

THICKNESS (M.)	P-VELOCITY (M/S.)	S-VELOCITY (M/S.)	DENSITY (G/ML)	1/Q P	1/Q S
63.0	1.460	0.000	1.03	0.00001	0.00001
	1.460	0.000	1.03	0.01000	0.00001
4.9	1.913	0.526	2.00	0.00200	0.01000
4.9	1.938	0.533	2.00	0.00200	0.01000
4.9	1.962	0.540	2.00	0.00200	0.01000
5.0	1.999	0.547	2.00	0.00200	0.01000
5.0	2.012	0.553	2.00	0.00200	0.01000
5.1	2.038	0.560	2.00	0.00200	0.01000
5.2	2.063	0.567	2.00	0.00200	0.01000
5.2	2.087	0.574	2.00	0.00200	0.01000
	4.700	2.900	1.90	0.10000	0.20000

-DENSITY- LAYER 3 RHO = 1.90 NO. 1281

-DENSITY- LAYER 3 RHO = 1.90 NO. 1281
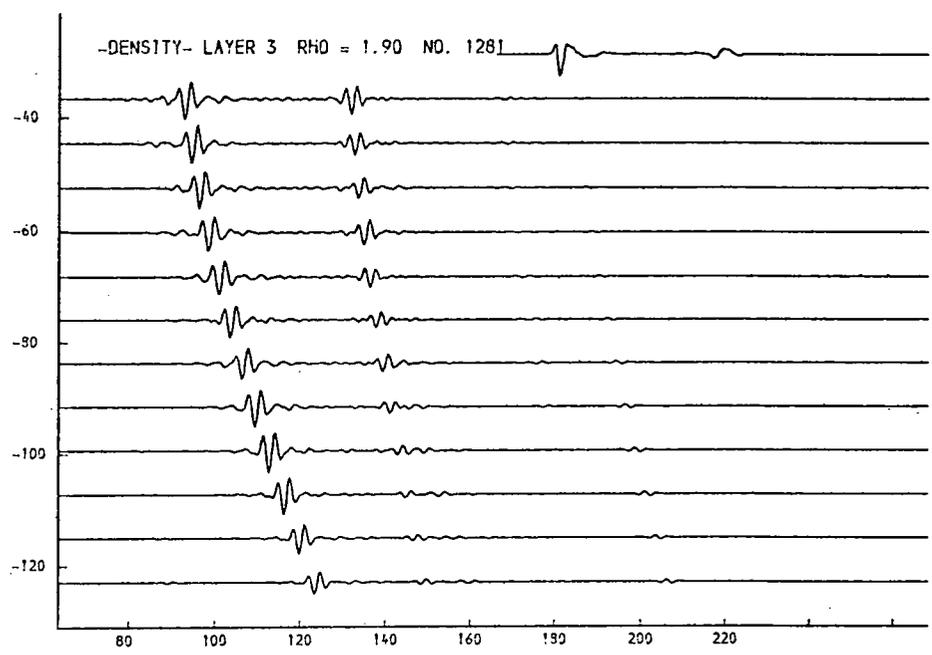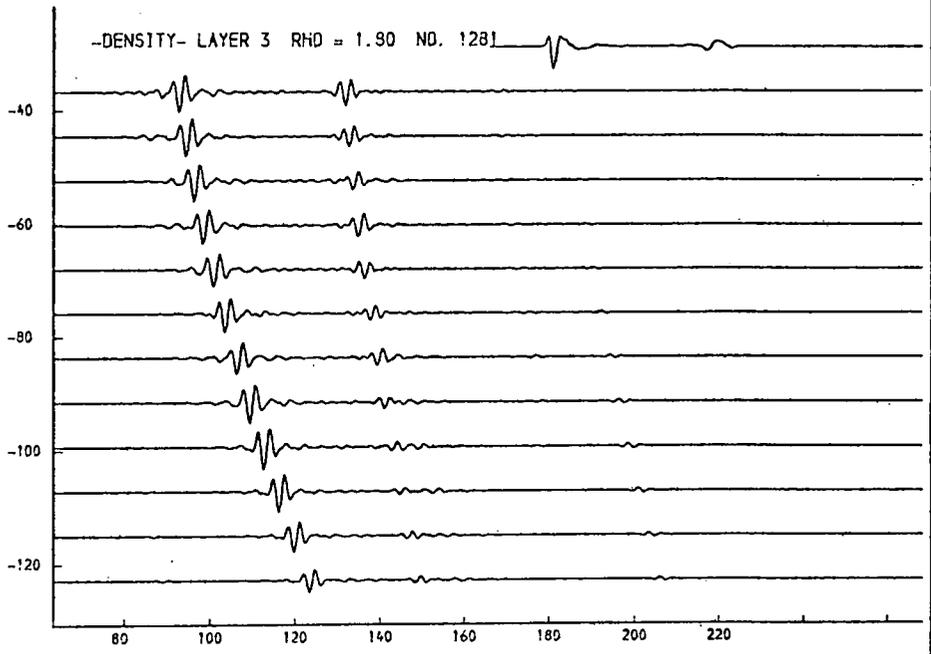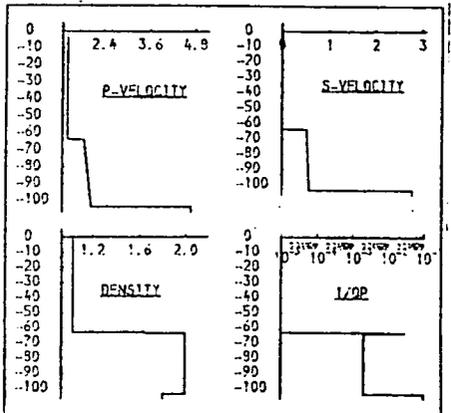
Fig. 9.60a. Layer 3, density.

Variations in density show up as variations in the amplitude of r2.

THICKNESS (M.)	P-VELOCITY (M/S.)	S-VELOCITY (M/S.)	DENSITY (G/ML)	1/Q P	1/Q S
63.0	1.460	0.000	1.03	0.00001	0.00001
			1.65	0.02000	0.04000
4.8	1.913	0.526	2.00	0.00200	0.01000
4.8	1.938	0.533	2.00	0.00200	0.01000
4.9	1.962	0.540	2.00	0.00200	0.01000
5.0	1.988	0.547	2.00	0.00200	0.01000
5.0	2.012	0.553	2.00	0.00200	0.01000
5.1	2.033	0.560	2.00	0.00200	0.01000
5.2	2.063	0.567	2.00	0.00200	0.01000
5.2	2.087	0.574	2.00	0.00200	0.01000
	4.700	2.900	2.10	0.10000	0.20000
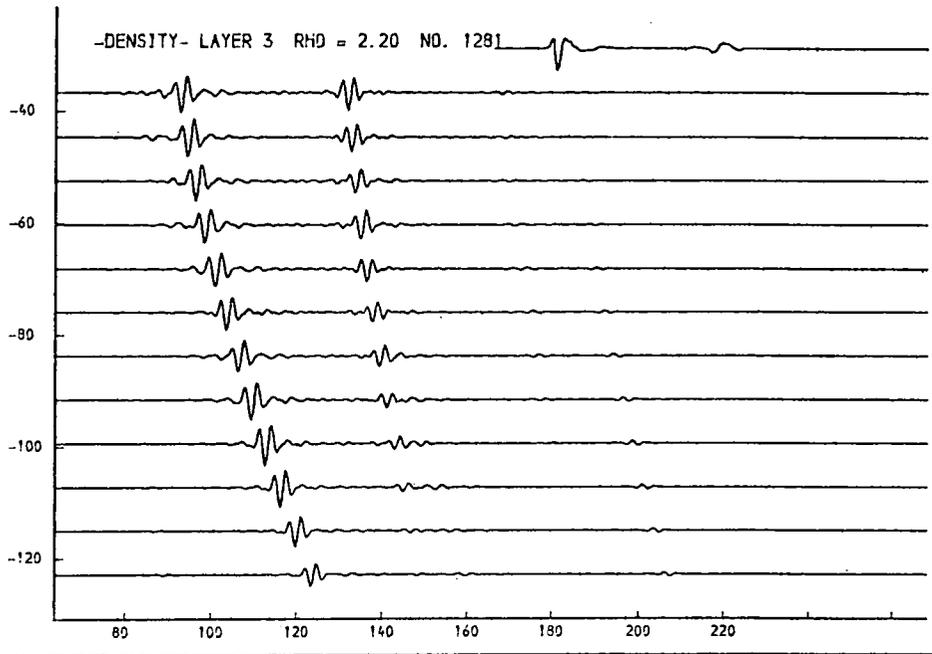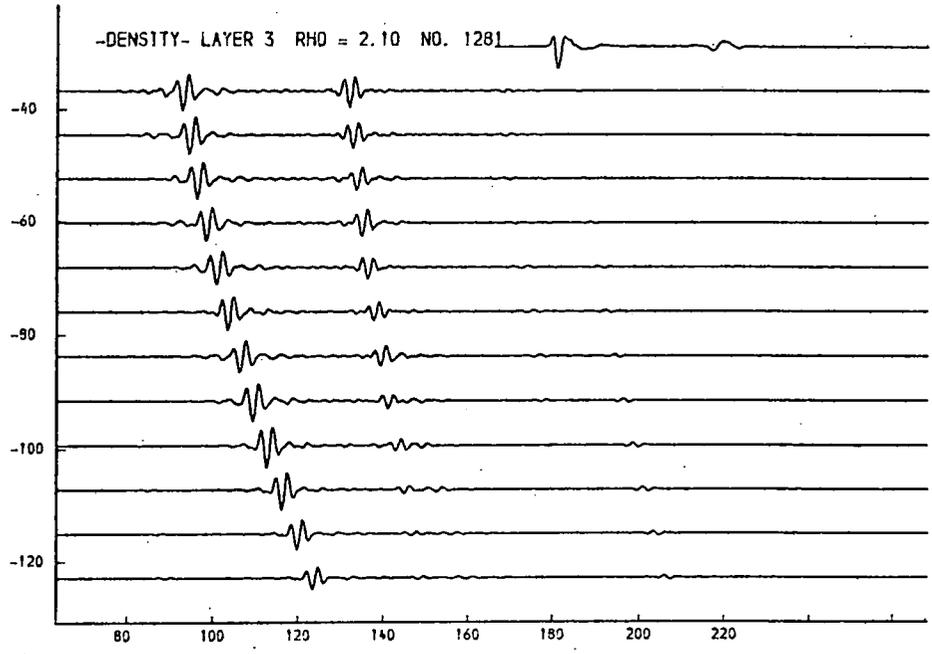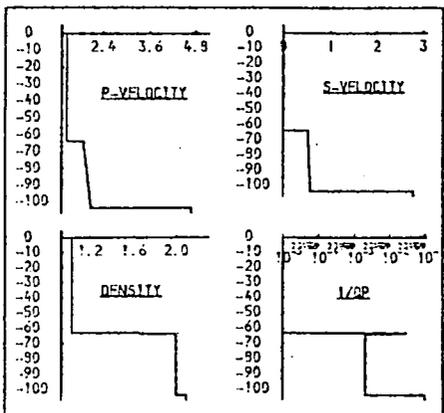
Fig. 9.60b. Layer 3, density.

Variations in density show up as variations in the amplitude of r2.

THICKNESS (M.)	P-VELOCITY (M/S.)	S-VELOCITY (M/S.)	DENSITY (G/ML)	1/Q P	1/Q S
63.0	1.460	0.000	1.03	0.00001	0.00001
0.3	1.400	0.010	1.05	0.02000	0.04000
4.8	1.934	0.532	2.00	0.00200	0.02000
4.9	1.953	0.537	2.00	0.00200	0.02000
4.9	1.972	0.542	2.00	0.00200	0.02000
5.0	1.991	0.547	2.00	0.00200	0.02000
5.0	2.009	0.553	2.00	0.00200	0.02000
5.1	2.028	0.558	2.00	0.00200	0.02000
5.1	2.047	0.563	2.00	0.00200	0.02000
5.2	2.066	0.569	2.00	0.00200	0.02000
	4.700	2.900	1.98	0.00100	0.04000

Fig. 9.61a.   Layer 3, 1/Qp.

Lower values of attenuation appear possible; very high values produce too rapid a fall-off in r2 with increasing offset.

THICKNESS (M.)	P-VELOCITY (M/S.)	S-VELOCITY (M/S.)	DENSITY (G/ML)	1/Q P	1/Q S
63.0	1.460	0.000	1.03	0.00001	0.00001
0.2	1.460		1.05	0.02000	0.04000
4.9	1.934	0.532	2.00	0.00200	0.02000
4.9	1.953	0.537	2.00	0.00200	0.02000
4.9	1.972	0.542	2.00	0.00200	0.02000
5.0	1.991	0.547	2.00	0.00200	0.02000
5.0	2.009	0.553	2.00	0.00200	0.02000
5.1	2.029	0.558	2.00	0.00200	0.02000
5.1	2.047	0.563	2.00	0.00200	0.02000
5.2	2.066	0.569	2.00	0.00200	0.02000
	4.700	2.900	1.98	0.01000	0.04000

Fig. 9.61b.   Layer 3, 1/Qp.

Lower values of attenuation appear possible; very high values produce too rapid a fall-off in r2 with increasing offset.

THICKNESS (M.)	P-VELOCITY (M/S.)	S-VELOCITY (M/S.)	DENSITY (G/ML)	1/Q P	1/Q S
63.0	1.460	0.000	1.03	0.00001	0.00001
			1.65		
4.9	1.934	0.532	2.00	0.00200	0.02000
4.9	1.953	0.537	2.00	0.00200	0.02000
4.9	1.972	0.542	2.00	0.00200	0.02000
5.0	1.991	0.547	2.00	0.00200	0.02000
5.0	2.009	0.553	2.00	0.00200	0.02000
5.1	2.029	0.558	2.00	0.00200	0.02000
5.1	2.047	0.563	2.00	0.00200	0.02000
5.2	2.066	0.569	2.00	0.00200	0.02000
	4.700	2.800	1.99	0.10000	0.04000

Fig. 9.61c.   Layer 3, 1/Qp.

Lower values of attenuation appear possible; very high values produce too rapid a fall-off in r2 with increasing offset.

THICKNESS (M.)	P-VELOCITY (M/S.)	S-VELOCITY (M/S.)	DENSITY (G/ML)	1/Q P	1/Q S
63.0	1.460	0.000	1.03	0.00001	0.00001
4.9	1.934	0.532	2.00	0.00200	0.02000
4.9	1.953	0.537	2.00	0.00200	0.02000
4.9	1.972	0.542	2.00	0.00200	0.02000
5.0	1.991	0.547	2.00	0.00200	0.02000
5.0	2.009	0.553	2.00	0.00200	0.02000
5.1	2.029	0.559	2.00	0.00200	0.02000
5.1	2.047	0.563	2.00	0.00200	0.02000
5.2	2.066	0.569	2.00	0.00200	0.02000
	4.700	2.900	1.98	1.00000	0.04000

Fig. 9.61d.   Layer 3, 1/Qp.

Lower values of attenuation appear possible; very high values produce too rapid a fall-off in r2 with increasing offset.

THICKNESS (M.)	P-VELOCITY (M/S.)	S-VELOCITY (M/S.)	DENSITY (G/ML)	1/Q P	1/Q S
63.0	1.460	0.000	1.03	0.00001	0.00001
	1.460	0.510	1.05	0.02000	0.04000
4.9	1.934	0.532	2.00	0.00200	0.02000
4.9	1.953	0.537	2.00	0.00200	0.02000
4.9	1.972	0.542	2.00	0.00200	0.02000
5.0	1.991	0.547	2.00	0.00200	0.02000
5.0	2.009	0.553	2.00	0.00200	0.02000
5.1	2.028	0.559	2.00	0.00200	0.02000
5.1	2.047	0.563	2.00	0.00200	0.02000
5.2	2.066	0.568	2.00	0.00200	0.02000
	4.700	2.900	1.98	0.02000	0.00300

Fig. 9.62a.   Layer 3, 1/Qs.

The model appears independent of this parameter.   Effects
produced for very high values are considered spurious.

THICKNESS (M.)	P-VELOCITY (M/S.)	S-VELOCITY (M/S.)	DENSITY (G/ML)	1/Q P	1/Q S
63.0	1.460	0.000	1.03	0.00001	0.00001
4.8	1.934	0.532	2.00	0.00200	0.02000
4.9	1.953	0.537	2.00	0.00200	0.02000
4.9	1.972	0.542	2.00	0.00200	0.02000
5.0	1.991	0.547	2.00	0.00200	0.02000
5.0	2.009	0.553	2.00	0.00200	0.02000
5.1	2.028	0.558	2.00	0.00200	0.02000
5.1	2.047	0.563	2.00	0.00200	0.02000
5.2	2.066	0.569	2.00	0.00200	0.02000
	4.700	2.900	1.98	0.02000	0.30000

Fig. 9.62b.   Layer 3, 1/Qs.

The model appears independent of this parameter.   Effects produced for very high values are considered spurious.

THICKNESS (M.)	P-VELOCITY (M/S.)	S-VELOCITY (M/S.)	DENSITY (G/ML)	1/Q P	1/Q S	THICKNESS (M.)	P-VELOCITY (M/S.)	S-VELOCITY (M/S.)	DENSITY (G/ML)	1/Q P	1/Q S
63.0	1.460	0.000	1.03	0.00001	0.00001	63.0	1.460	0.000	1.03	0.00001	0.00001
4.9	1.956	0.539	2.00	0.00200	0.02000	4.7	1.969	0.514	2.00	0.00200	0.02000
4.9	1.969	0.541	2.00	0.00200	0.02000	4.8	1.906	0.524	2.00	0.00200	0.02000
5.0	1.981	0.545	2.00	0.00200	0.02000	4.9	1.944	0.535	2.00	0.00200	0.02000
5.0	1.994	0.548	2.00	0.00200	0.02000	5.0	1.991	0.545	2.00	0.00200	0.02000
5.0	2.006	0.552	2.00	0.00200	0.02000	5.0	2.019	0.555	2.00	0.00200	0.02000
5.0	2.019	0.555	2.00	0.00200	0.02000	5.1	2.056	0.565	2.00	0.00200	0.02000
5.1	2.031	0.559	2.00	0.00200	0.02000	5.2	2.094	0.576	2.00	0.00200	0.02000
5.1	2.044	0.562	2.00	0.00200	0.02000	5.3	2.131	0.586	2.00	0.00200	0.02000
	4.700	2.900	1.98	0.02000	0.04000		4.700	2.900	1.98	0.02000	0.04000
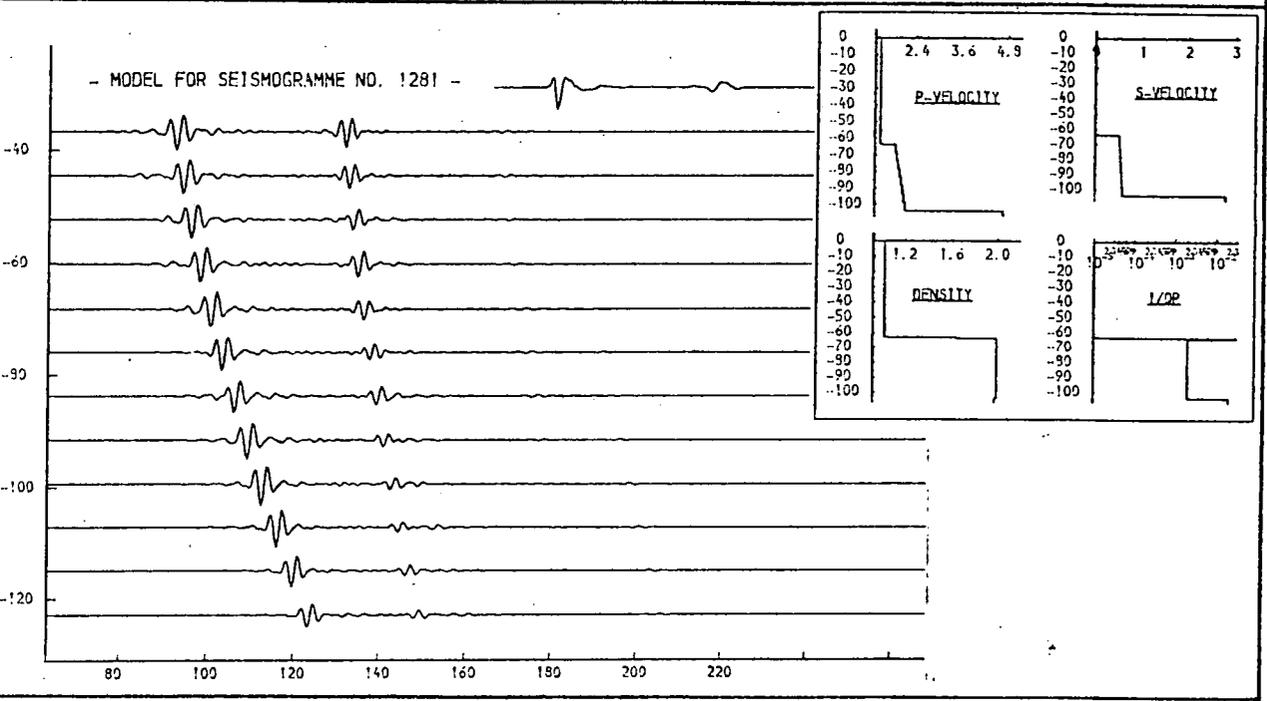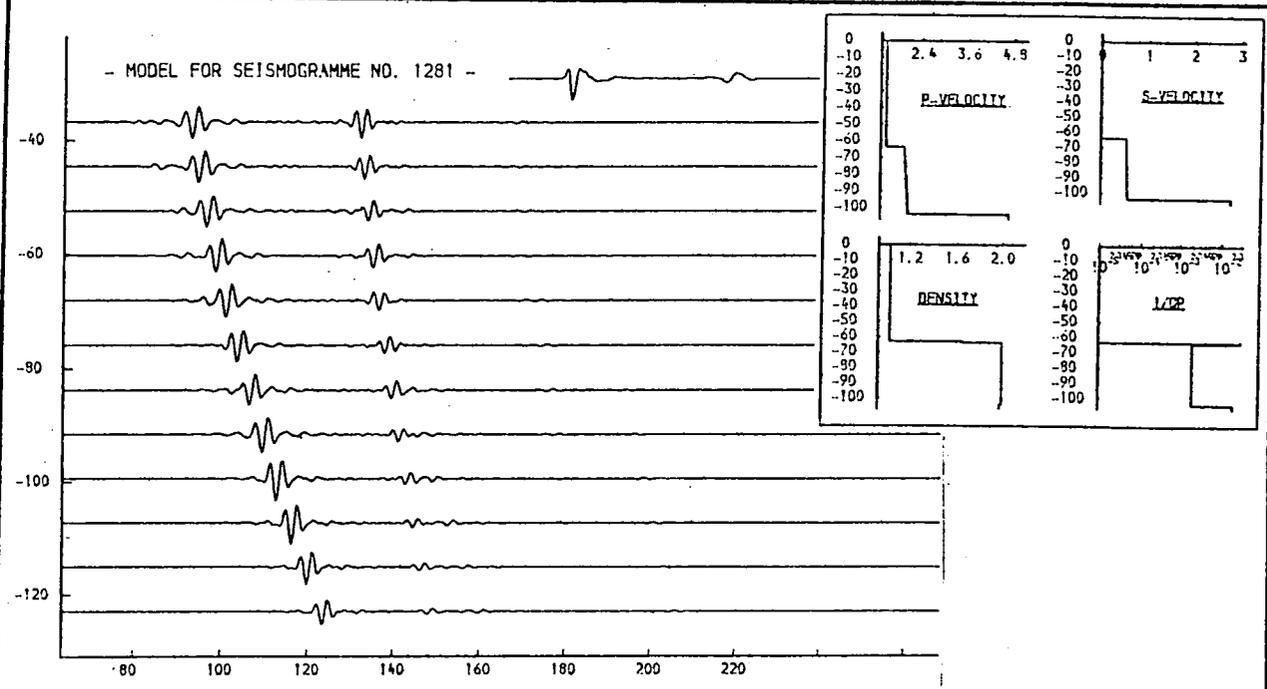
Fig. 9.63a. Variation of velocity gradient.

The effect of increasing the velocity gradient is seen in the amplitude of r2 at higher offset distance. This amplitude begins to rise for a gradient of ca. 7m/sec/m. (lower figure), when compared with that for a lower gradient of 2m/sec/m. (upper figure).

THICKNESS (M.)	P-VELOCITY (M/S.)	S-VELOCITY (M/S.)	DENSITY (G/ML)	1/Q P	1/Q S
63.0	1.460	0.000	1.03	0.00001	0.00001
	1.420	0.510	1.03	0.00200	0.04000
4.8	1.913	0.526	2.00	0.00200	0.02000
4.8	1.938	0.533	2.00	0.00200	0.02000
4.9	1.962	0.540	2.00	0.00200	0.02000
5.0	1.988	0.547	2.00	0.00200	0.02000
5.0	2.012	0.553	2.00	0.00200	0.02000
5.1	2.039	0.560	2.00	0.00200	0.02000
5.2	2.063	0.567	2.00	0.00200	0.02000
5.2	2.087	0.574	2.00	0.00200	0.02000
	4.700	2.800	1.98	0.02000	0.04000

THICKNESS (M.)	P-VELOCITY (M/S.)	S-VELOCITY (M/S.)	DENSITY (G/ML)	1/Q P	1/Q S
63.0	1.460	0.000	1.03	0.00001	0.00001
	1.420	0.510	1.05	0.00200	0.04000
4.9	1.934	0.532	2.00	0.00200	0.02000
4.9	1.953	0.537	2.00	0.00200	0.02000
4.9	1.972	0.542	2.00	0.00200	0.02000
5.0	1.991	0.547	2.00	0.00200	0.02000
5.0	2.009	0.553	2.00	0.00200	0.02000
5.1	2.028	0.558	2.00	0.00200	0.02000
5.1	2.047	0.563	2.00	0.00200	0.02000
5.2	2.066	0.568	2.00	0.00200	0.02000
	4.700	2.800	1.98	0.02000	0.04000

Fig. 9.63b. Variation of velocity gradient.

Lower values for the velocity gradient of 4m/sec/m. (above) and 3m/sec/m. (below) do not show obvious amplitude increase at high offset.

THICKNESS (M.)	P-VELOCITY (M/S.)	S-VELOCITY (M/S.)	DENSITY (G/ML)	1/Q P	1/Q S
63.0	1.460	0.000	1.03	0.00001	0.00001
0.5	1.420	0.010	1.20	0.33500	0.34000
4.9	1.956	0.538	2.00	0.00200	0.02000
4.9	1.969	0.541	2.00	0.00200	0.02000
5.0	1.981	0.545	2.00	0.00200	0.02000
5.0	1.994	0.548	2.00	0.00200	0.02000
5.0	2.006	0.552	2.00	0.00200	0.02000
5.0	2.019	0.555	2.00	0.00200	0.02000
5.1	2.031	0.552	2.00	0.00200	0.02000
5.1	2.044	0.562	2.00	0.00200	0.02000
	4.700	2.900	1.98	0.10000	0.20000

Fig. 9.64a. Variation of velocity gradient.

When the value of 1/Qp is high (0.1 in the above models the effect of increasing velocity gradient is less evident in the amplitude of the event r2 at high offset (c.f. fig. 9.63a). Upper model has gradient of 2m/sec/m.; lower one, 4m/sec/m.

THICKNESS (M.)	P-VELOCITY (M/S.)	S-VELOCITY (M/S.)	DENSITY (G/ML)	1/Q P	1/Q S
63.0	1.460	0.000	1.03	0.00001	0.00001
		0.010	1.65	0.03000	0.06000
4.6	1.825	0.502	2.00	0.00200	0.02000
4.7	1.875	0.516	2.00	0.00200	0.02000
4.8	1.925	0.529	2.00	0.00200	0.02000
4.9	1.975	0.543	2.00	0.00200	0.02000
5.1	2.025	0.557	2.00	0.00200	0.02000
5.2	2.075	0.571	2.00	0.00200	0.02000
5.3	2.125	0.594	2.00	0.00200	0.02000
5.4	2.175	0.598	2.00	0.00200	0.02000
	4.700	2.800	1.98	0.10000	0.20000

Fig. 9.64b. Variation of velocity gradient.

Even for a gradient of 8m/sec/m. (upper model) no amplitude rise occurs at high offset when 1/Qp=0.1. Only when the gradient takes a value approaching 20m/sec/m. (lower model) does this amplitude rise start to occur.

THICKNESS (M.)	P-VELOCITY (M/S.)	S-VELOCITY (M/S.)	DENSITY (G/ML)	1/Q P	1/Q S
63.0	1.460	0.000	1.03	0.00001	0.00001
0.5	1.480	0.310	1.65	0.03000	0.04000
4.3	1.739	0.550	2.00	0.00200	0.02000
4.5	1.913	0.550	2.00	0.00200	0.02000
4.7	1.937	0.550	2.00	0.00200	0.02000
4.9	1.962	0.550	2.00	0.00200	0.02000
5.1	2.039	0.550	2.00	0.00200	0.02000
5.3	2.113	0.550	2.00	0.00200	0.02000
5.5	2.188	0.550	2.00	0.00200	0.02000
5.7	2.262	0.550	2.00	0.00200	0.02000
	4.700	2.800	1.99	0.10000	0.20000

VARY -S- GRADT.   NONE   NO. 1281

VARY -S- GRADT.   SMALL   NO. 1281
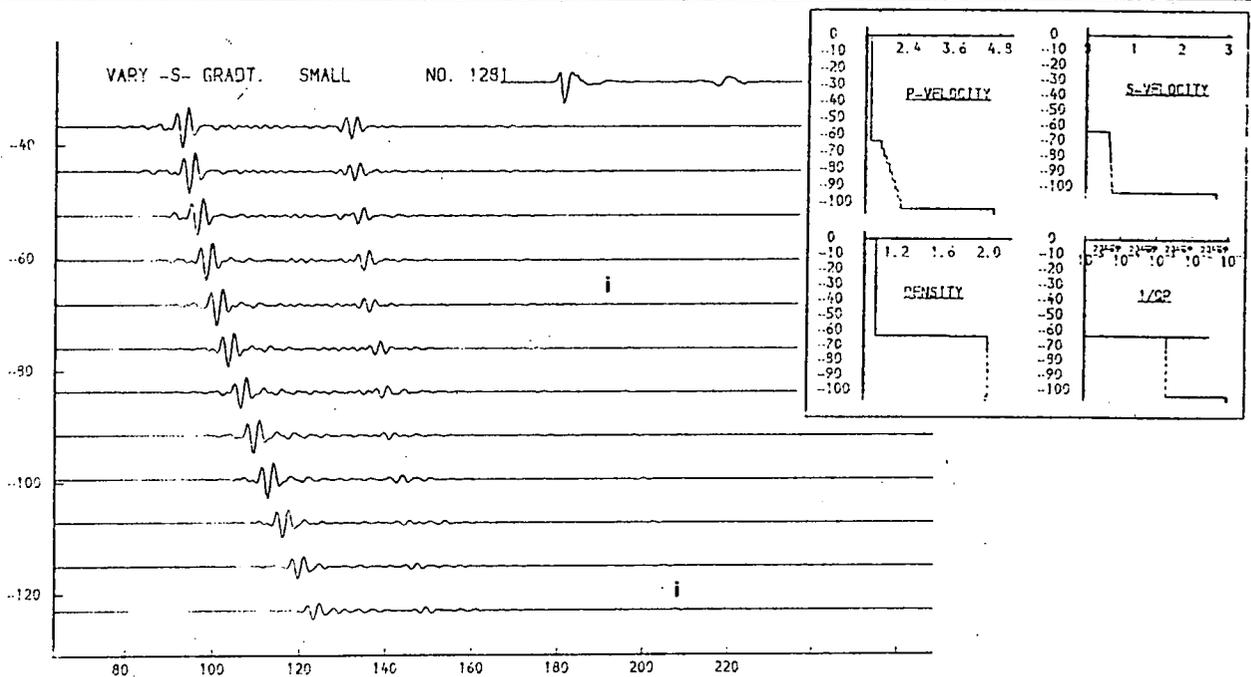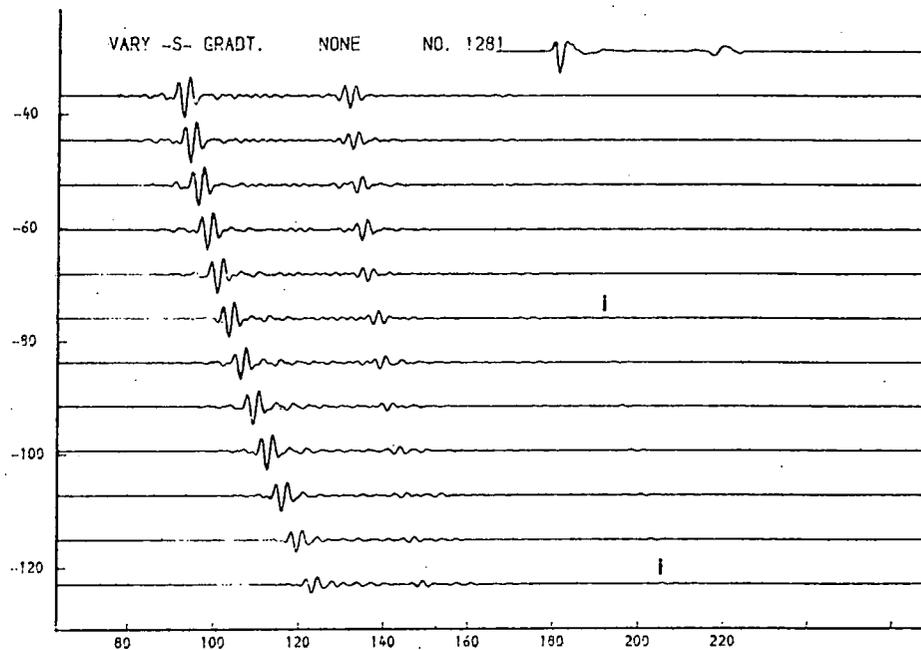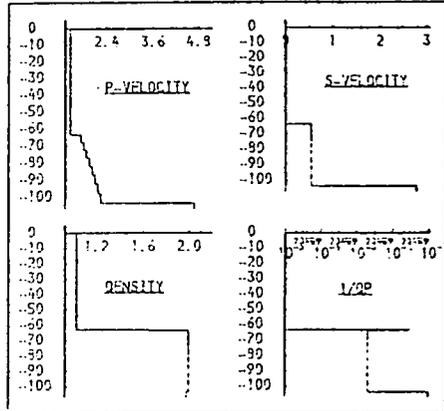
Fig. 9.65a. Variation of s-velocity gradient.

This figure and the one following, show that increasing s-velocity gradient in layer 2 suppresses further the residual p-s conversion ("i" above) which is already controlled by the value of 1/Qs. (Compare with figs. 9.31b, 9.37a,b and 9.44c,d).

THICKNESS (M.)	P-VELOCITY (M/S.)	S-VELOCITY (M/S.)	DENSITY (G/ML)	1/Q P	1/Q S
63.0	1.460	0.000	1.03	0.00001	0.00001
3.5	1.430	0.410	1.05	0.00000	0.00000
4.3	1.739	0.400	2.00	0.00200	0.02000
4.5	1.513	0.440	2.00	0.00200	0.02000
4.7	1.997	0.480	2.00	0.00200	0.02000
4.9	1.962	0.520	2.00	0.00200	0.02000
5.1	2.039	0.560	2.00	0.00200	0.02000
5.3	2.113	0.600	2.00	0.00200	0.02000
5.5	2.198	0.640	2.00	0.00200	0.02000
5.7	2.262	0.680	2.00	0.00200	0.02000
	4.700	2.800	1.98	0.10000	0.20000

VARY -S- GRADT.   MID   NO. 1281

VARY -S- GRADT.   STRONG   NO. 1281
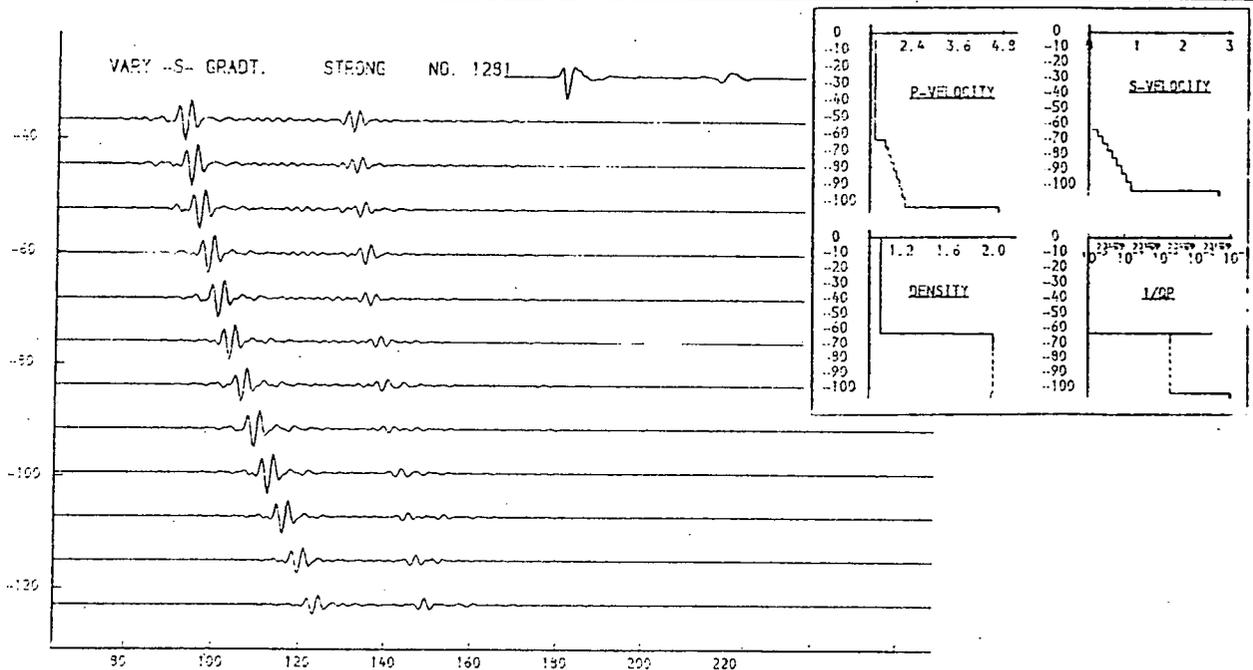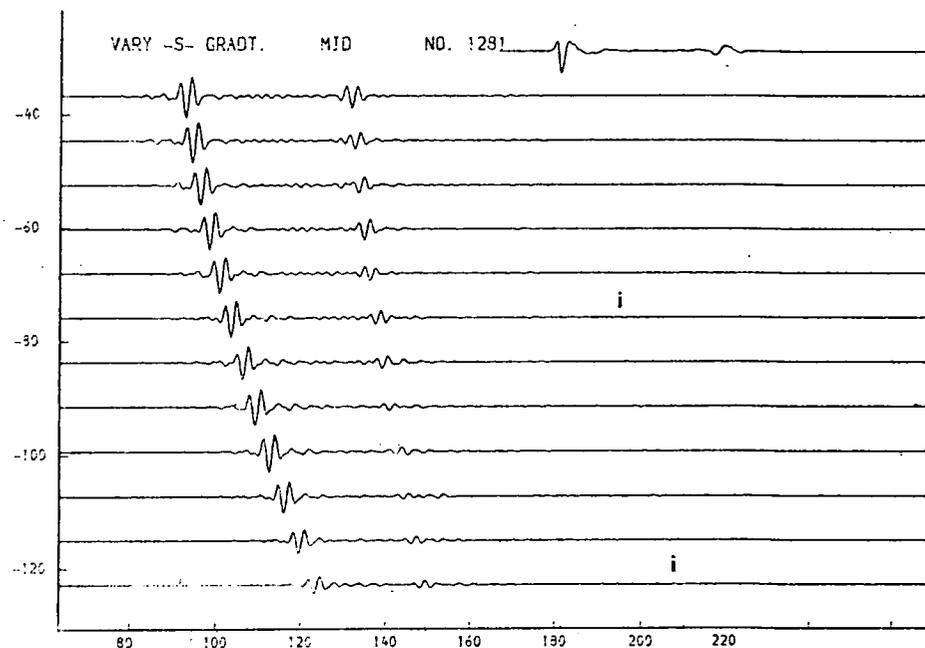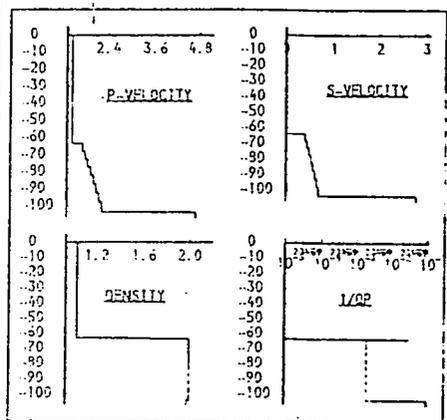
Fig. 9.65b. Variation of s-velocity gradient.

When the value of the s-velocity gradient rises to over 20m/sec/m. (lower model) the converted arrival "i" is suppressed, but the amplitude of r2 at high offset begins to rise.

THICKNESS (H.)	P-VELOCITY (M/S.)	S-VELOCITY (M/S.)	DENSITY (G/ML)	1/Q P	1/Q S
63.0	1.460	0.000	1.03	0.00001	0.00001
0.2	1.490	0.010	1.49	0.03000	0.06000
4.6	1.925	0.550	2.00	0.00200	0.02000
4.7	1.975	0.550	2.00	0.00200	0.02000
4.8	1.925	0.550	2.00	0.00200	0.02000
4.9	1.975	0.550	2.00	0.00200	0.02000
5.1	2.025	0.550	2.00	0.00200	0.02000
5.2	2.075	0.550	2.00	0.00200	0.02000
5.3	2.125	0.550	2.00	0.00200	0.02000
5.4	2.175	0.550	2.00	0.00200	0.02000
	4.700	2.800	1.98	0.01000	0.02000

-S- GRADT. LAYER 2   NONE   NO. 1281

-S- GRADT. LAYER 2   WEAK   NO. 1281

Fig. 9.66a.   Variation of s-velocity gradient.

If the same variations in s-velocity gradient are made (see figs. 65a,b) when the attenuation in layer 3 is lower (1/Qp=0.01, 1/Qs=0.02) then the influence on the amplitude of r2 at high gradient is more pronounced.

THICKNESS (M.)	P-VELOCITY (M/S.)	S-VELOCITY (M/S.)	DENSITY (G/ML)	1/Q P	1/Q S
63.0	1.460	0.000	1.03	0.00001	0.00001
	1.???	0.410	1.65	0.0?000	0.0?000
4.6	1.925	0.400	2.00	0.00200	0.02000
4.7	1.925	0.450	2.00	0.00200	0.02000
4.8	1.925	0.500	2.00	0.00200	0.02000
4.9	1.975	0.550	2.00	0.00200	0.02000
5.1	2.025	0.600	2.00	0.00200	0.02000
5.2	2.075	0.650	2.00	0.00200	0.02000
5.3	2.125	0.700	2.00	0.00200	0.02000
5.4	2.175	0.750	2.00	0.00200	0.02000
	4.700	2.900	1.98	0.01000	0.02000

-S- GRADT. LAYER 2   MID   NO. 1281

-S- GRADT. LAYER 2   STRONG   NO. 1281

P-VELOCITY   S-VELOCITY   DENSITY   1/QP
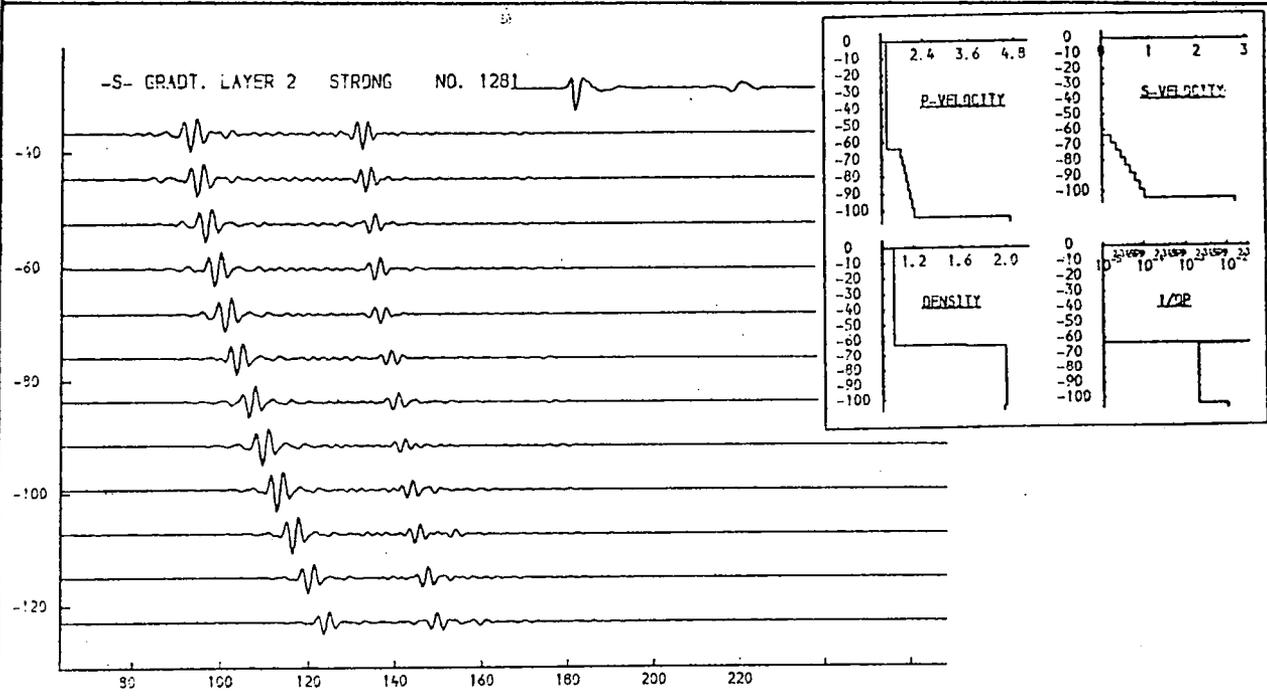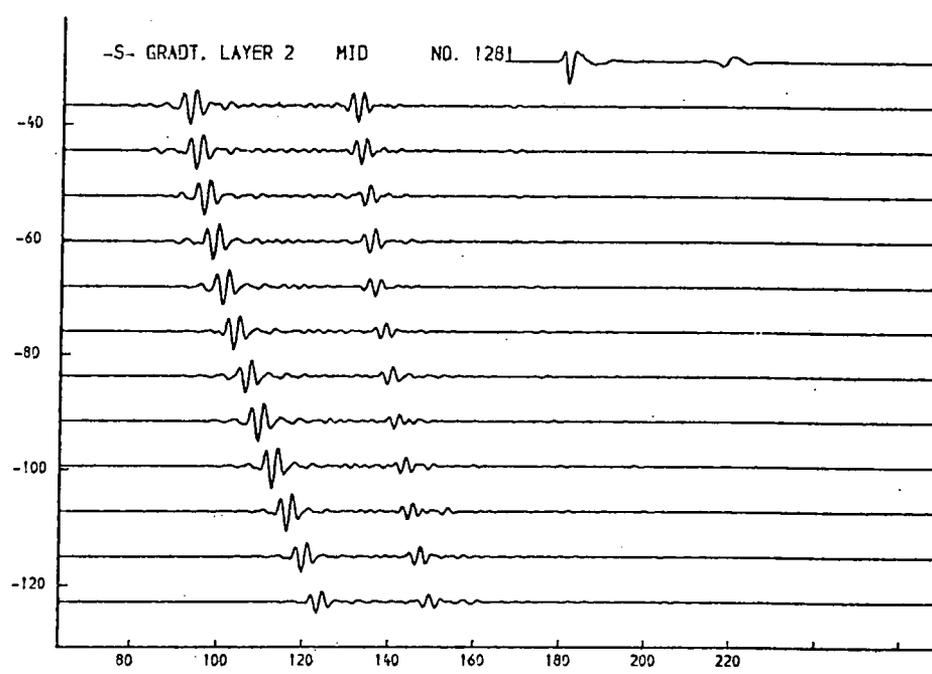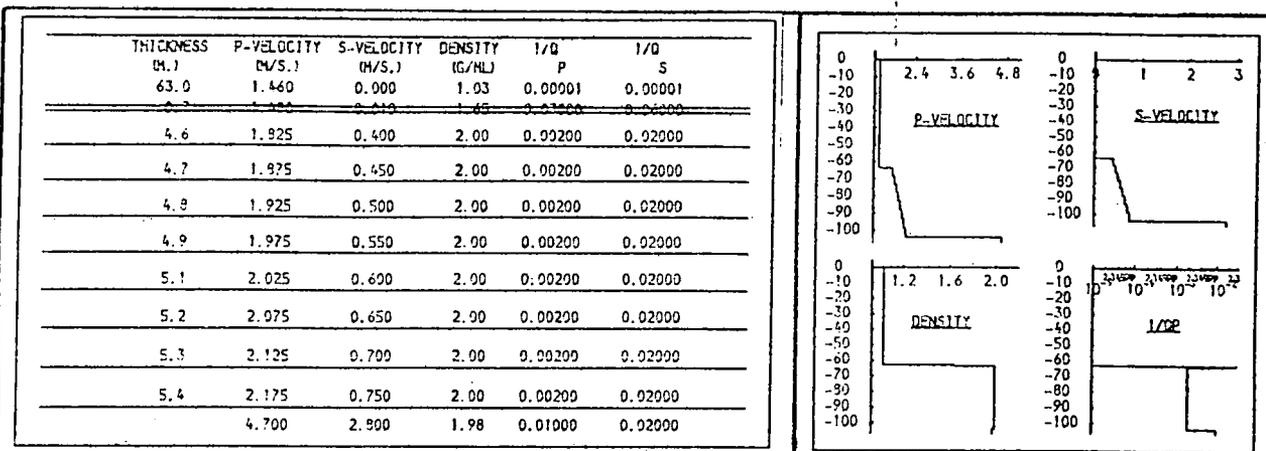
Fig. 9.66b. Variation of s-velocity gradient.

If the same variations in s-velocity gradient are made
(see figs. 65a,b) when the attenuation in layer 3 is lower
(1/Qp=0.01, 1/Qs=0.02) then the influence on the amplitude
of r2 at high gradient is more pronounced.

THICKNESS (M.)	P-VELOCITY (M/S.)	S-VELOCITY (M/S.)	DENSITY (G/ML)	1/Q P	1/Q S
63.0	1.460	0.000	1.03	0.00001	0.00001
0.5	1.400	0.010	1.05	0.03000	0.06000
3.9	1.563	0.234	2.00	0.00200	0.02000
4.2	1.688	0.253	2.00	0.00200	0.02000
4.5	1.813	0.272	2.00	0.00200	0.02000
4.9	1.938	0.291	2.00	0.00200	0.02000
5.2	2.063	0.309	2.00	0.00200	0.02000
5.5	2.188	0.328	2.00	0.00200	0.02000
5.8	2.313	0.347	2.00	0.00200	0.02000
6.1	2.438	0.366	2.00	0.00200	0.02000
	4.700	2.900	1.98	0.10000	0.20000

Fig. 9.67a. Layer 2, s-velocity.

The presence of the p-velocity gradient has no pronounced influence for low values of this s-velocity (c.f. fig. 9.54a).

THICKNESS (M.)	P-VELOCITY (M/S.)	S-VELOCITY (M/S.)	DENSITY (G/ML)	1/Q P	1/Q S
63.0	1.460	0.000	1.03	0.00001	0.00001
0.5	1.490	0.010	1.05	0.53000	0.06000
3.9	1.563	0.391	2.00	0.00200	0.02000
4.2	1.688	0.422	2.00	0.00200	0.02000
4.5	1.813	0.453	2.00	0.00200	0.02000
4.9	1.938	0.484	2.00	0.00200	0.02000
5.2	2.063	0.516	2.00	0.00200	0.02000
5.5	2.198	0.547	2.00	0.00200	0.02000
5.8	2.313	0.578	2.00	0.00200	0.02000
6.1	2.438	0.609	2.00	0.00200	0.02000
	4.700	2.800	1.98	0.10000	0.30000
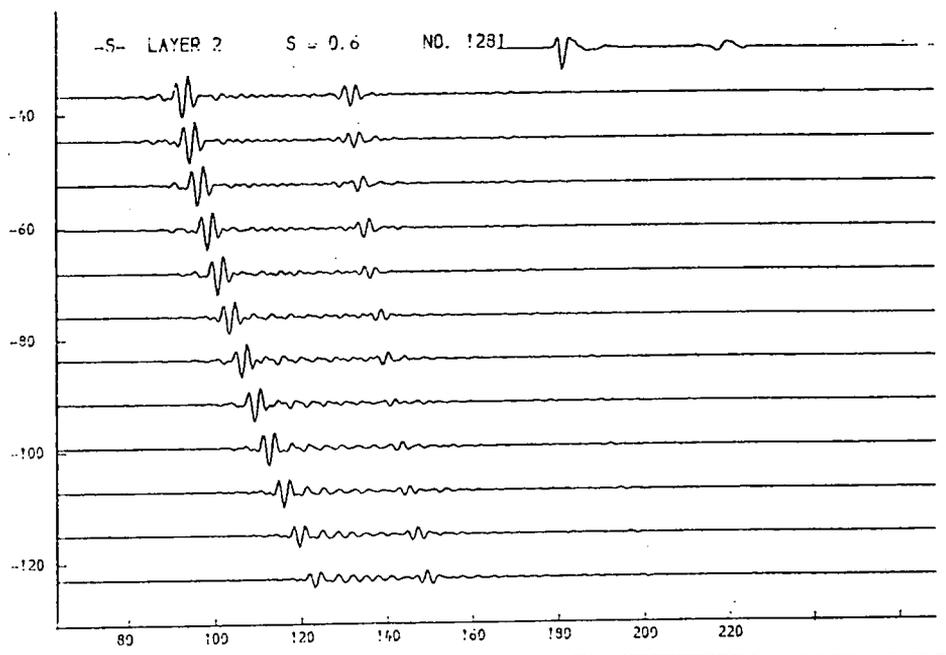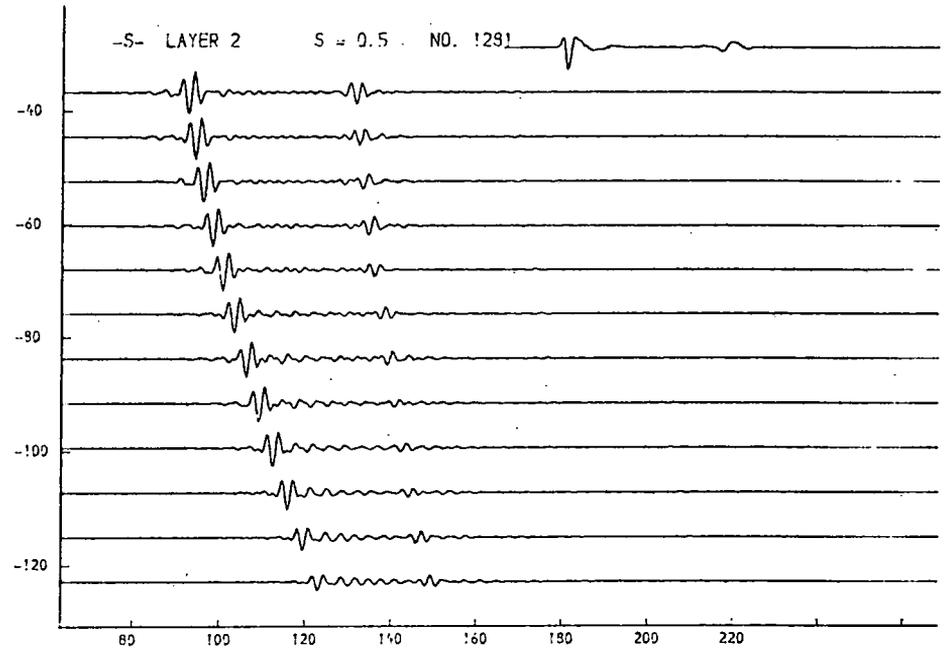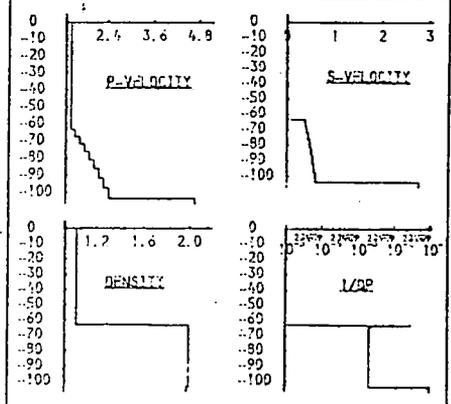
Fig. 9.67b.   Layer 2, s-velocity.

At   intermediate values of this parameter, the presence of
the p-velocity gradient produces a rise in   the   amplitude
of r2 at high offset (c.f. figs. 9.54b,c).

THICKNESS (M.)	P-VELOCITY (M/S.)	S-VELOCITY (M/S.)	DENSITY (G/ML)	1/Q P	1/Q S
63.0	1.460	0.000	1.03	0.00001	0.00001
0.5	1.499	0.210	1.95	0.03000	0.04000
3.9	1.563	0.547	2.00	0.00200	0.02000
4.2	1.688	0.591	2.00	0.00200	0.02000
4.5	1.913	0.634	2.00	0.00200	0.02000
4.8	1.938	0.678	2.00	0.00200	0.02000
5.2	2.063	0.722	2.00	0.00200	0.02000
5.5	2.199	0.766	2.00	0.00200	0.02000
5.8	2.313	0.809	2.00	0.00200	0.02000
6.1	2.439	0.853	2.00	0.00200	0.02000
	4.700	2.900	1.99	0.10000	0.20000

-S- LAYER 2   S = 0.7   NO. 1281

-S- LAYER 2   S = 0.9   NO. 1281
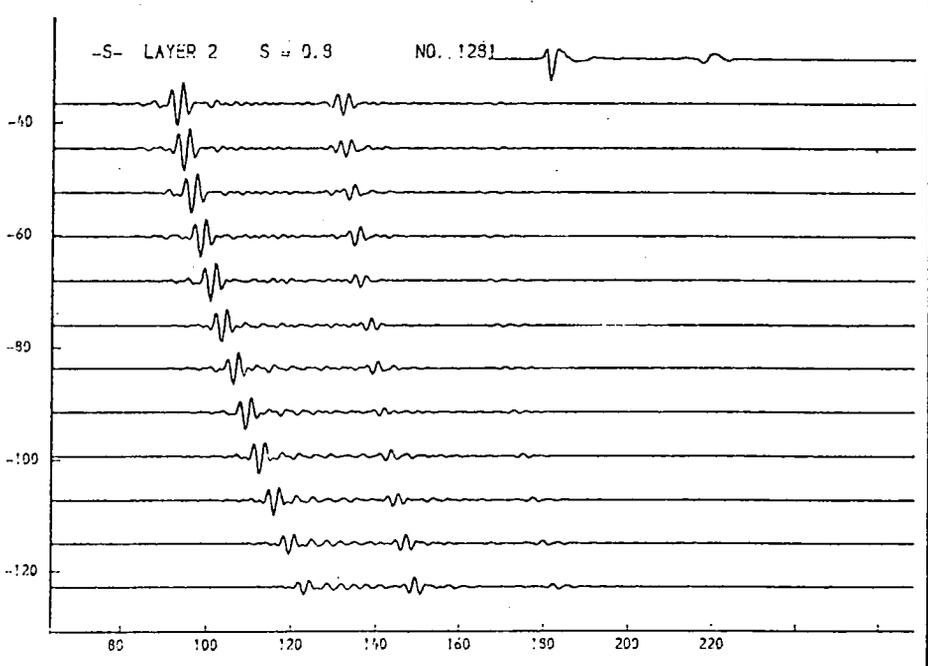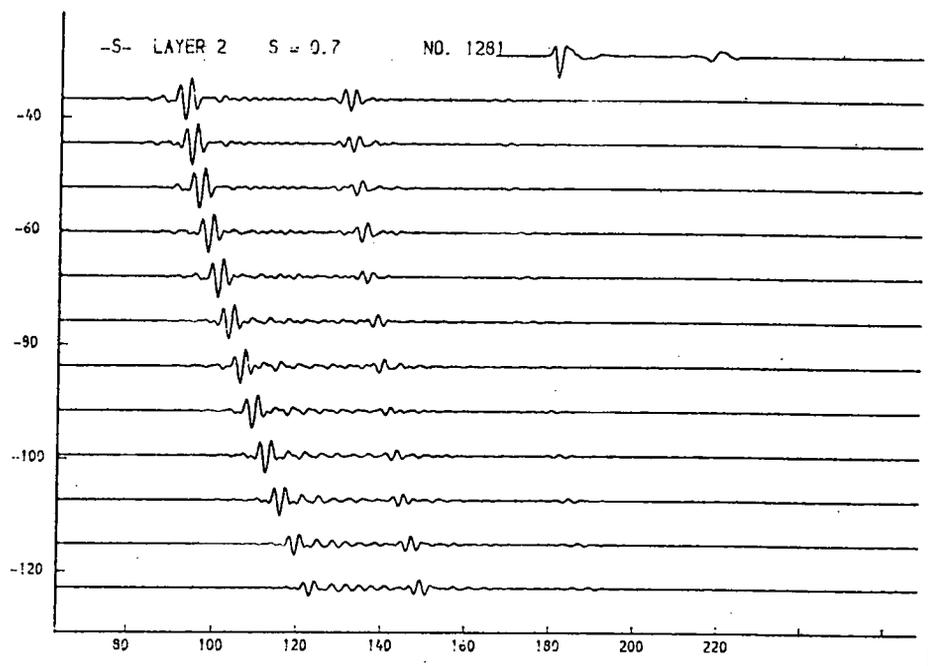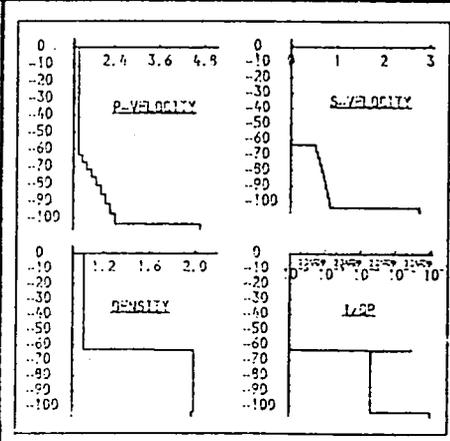
Fig. 9.67c. Layer 2, s-velocity.

At intermediate values of this parameter, the presence of
the p-velocity gradient produces a rise in the amplitude
of r2 at high offset (c.f. figs. 9.54b,c).

THICKNESS (M.)	P-VELOCITY (M/S.)	S-VELOCITY (M/S.)	DENSITY (G/ML)	1/Q P	1/Q S
63.0	1.460	0.000	1.03	0.00001	0.00001
0.5	1.460	0.310	1.05	0.07000	0.06000
3.9	1.563	0.791	2.00	0.00200	0.02000
4.2	1.658	0.944	2.00	0.00200	0.02000
4.5	1.813	0.906	2.00	0.00200	0.02000
4.9	1.938	0.969	2.00	0.00200	0.02000
5.2	2.063	1.031	2.00	0.00200	0.02000
5.5	2.198	1.094	2.00	0.00200	0.02000
5.9	2.313	1.156	2.00	0.00200	0.02000
6.1	2.439	1.219	2.00	0.00200	0.02000
	4.700	2.900	1.99	0.10000	0.20000
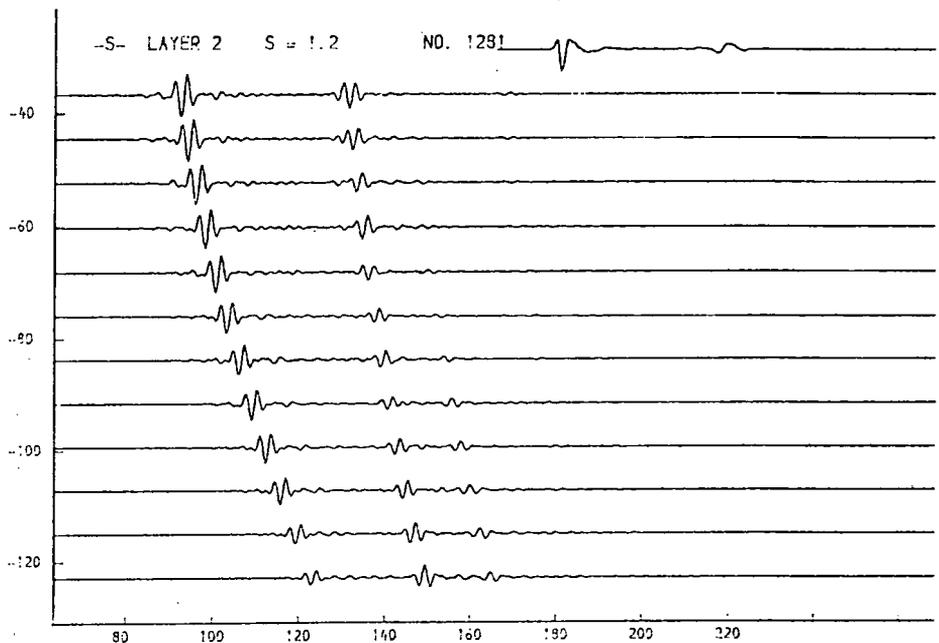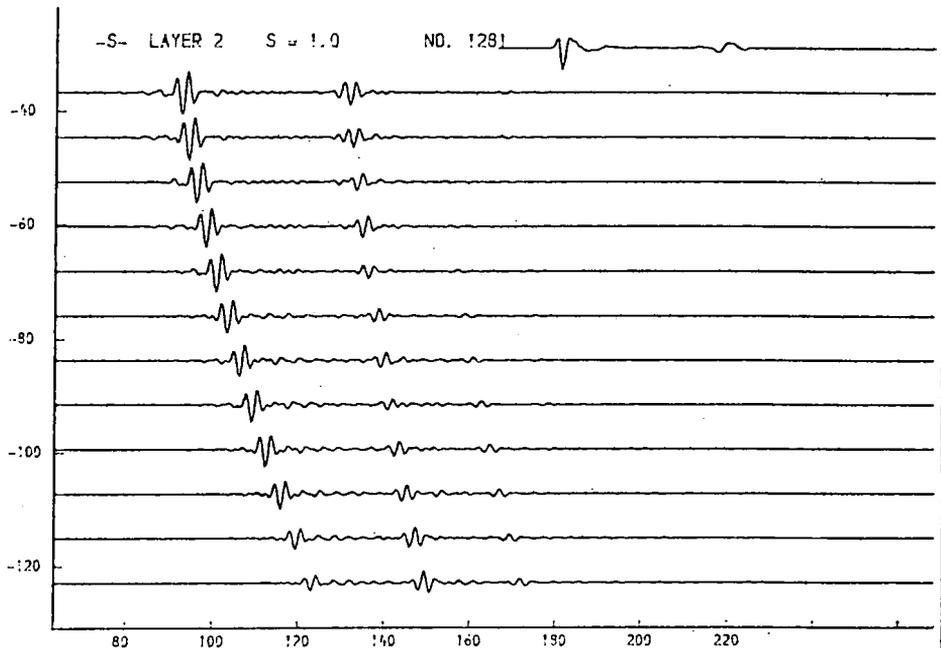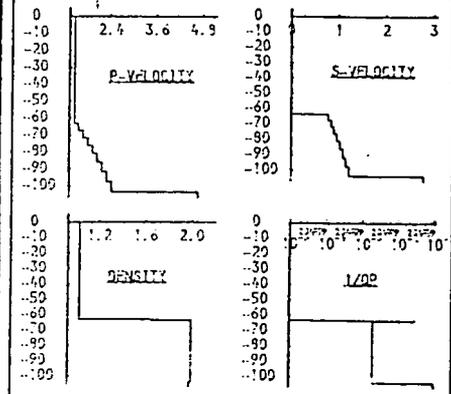
Fig. 9.67d. Layer 2, s-velocity.

For high values of this parameter, the influence of the p-velocity gradient is diminished (c.f. fig. 9.54d).

THICKNESS (M.)	P-VELOCITY (M/S.)	S-VELOCITY (M/S.)	DENSITY (G/ML)	1/Q P	1/Q S
63.0	1.460	0.000	1.03	0.00001	0.00001
0.5	1.460	0.010	1.05	0.03000	0.06000
4.1	1.650	0.454	2.00	0.00100	0.02000
4.4	1.750	0.481	2.00	0.00100	0.02000
4.6	1.950	0.509	2.00	0.00100	0.02000
4.9	1.950	0.536	2.00	0.00100	0.02000
5.1	2.050	0.564	2.00	0.00100	0.02000
5.4	2.150	0.591	2.00	0.00100	0.02000
5.6	2.250	0.619	2.00	0.00100	0.02000
5.9	2.350	0.646	2.00	0.00100	0.02000
	4.700	2.900	1.98	0.10000	0.20000
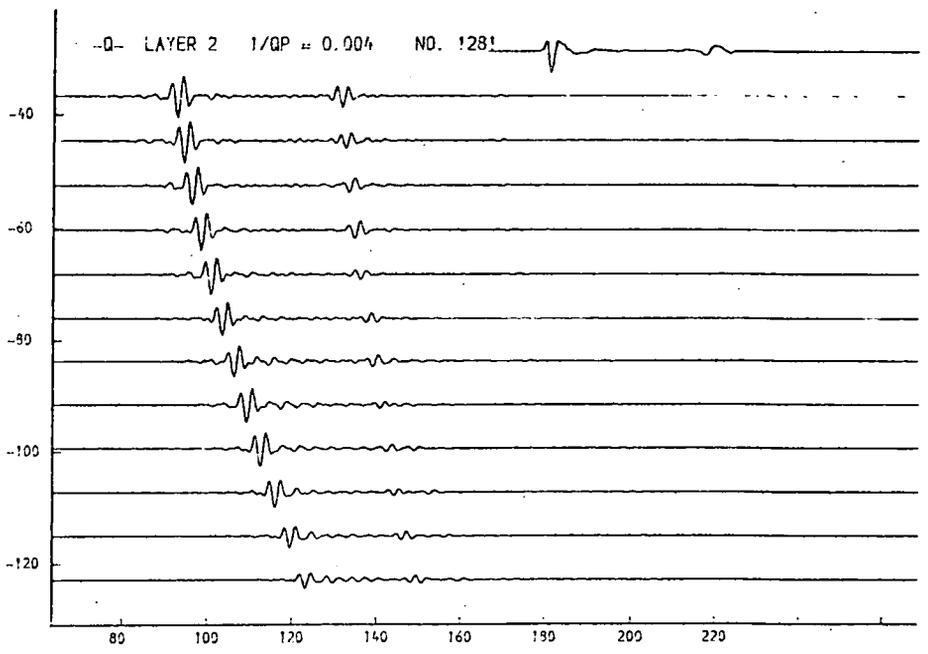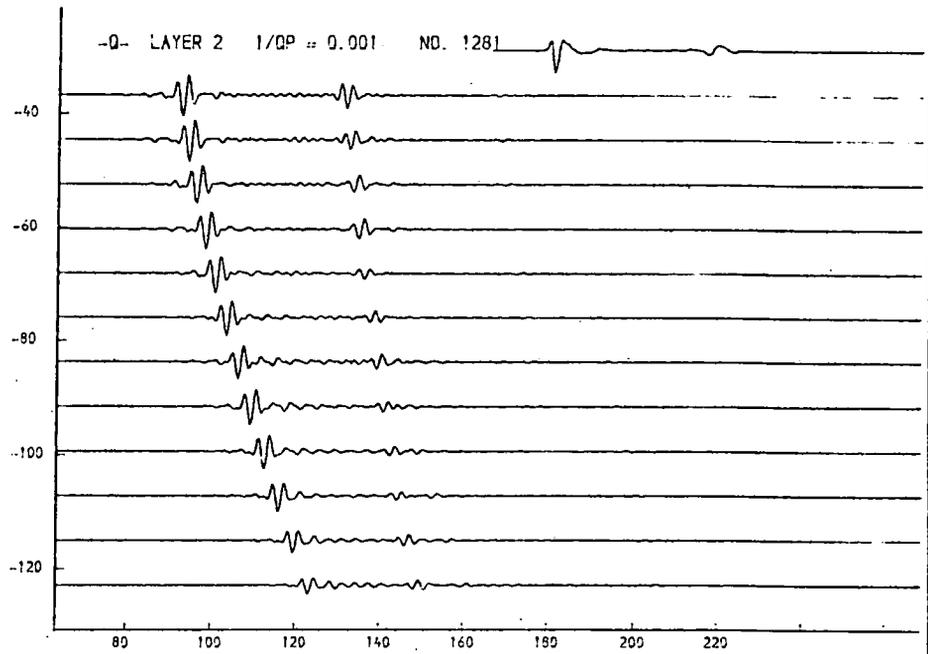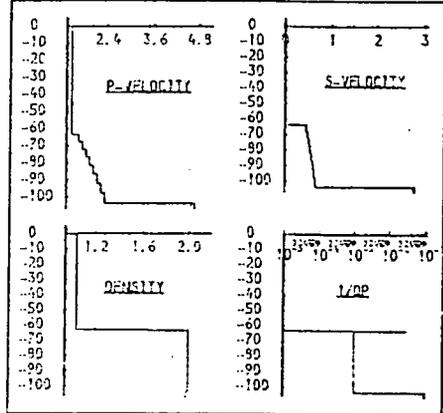
Fig. 9.68a.   Layer 2, p-attenuation.

This parameter appears to exert its influence in much the same way whether or not the high p-velocity gradient is present (c.f. fig. 9.56a,b,c).

THICKNESS (M.)	P-VELOCITY (M/S.)	S-VELOCITY (M/S.)	DENSITY (G/ML)	1/Q P	1/Q S
63.0	1.460	0.000	1.03	0.00001	0.00001
0.5	1.460	0.010	1.05	0.03000	0.06000
4.1	1.650	0.454	2.00	0.00800	0.02000
4.4	1.750	0.481	2.00	0.00800	0.02000
4.6	1.850	0.509	2.00	0.00800	0.02000
4.9	1.950	0.536	2.00	0.00800	0.02000
5.1	2.050	0.564	2.00	0.00800	0.02000
5.4	2.150	0.591	2.00	0.00800	0.02000
5.6	2.250	0.619	2.00	0.00800	0.02000
5.9	2.350	0.646	2.00	0.00800	0.02000
	4.700	2.500	1.98	0.10000	0.20000

Fig. 9.68b. Layer 2, p-attenuation.

This parameter appears to exert its influence in much the same way whether or not the high p-velocity gradient is present (c.f. fig. 9.56a,b,c).

THICKNESS (M.)	P-VELOCITY (M/S.)	S-VELOCITY (M/S.)	DENSITY (G/ML)	1/Q P	1/Q S
63.0	1.460	0.000	1.03	0.00001	0.00001
0.5	1.490	0.010	1.65	0.03000	0.06000
4.1	1.650	0.454	2.00	0.00200	0.00050
4.4	1.750	0.491	2.00	0.00200	0.00050
4.6	1.950	0.509	2.00	0.00200	0.00050
4.9	1.950	0.536	2.00	0.00200	0.00050
5.1	2.050	0.564	2.00	0.00200	0.00050
5.4	2.150	0.591	2.00	0.00200	0.00050
5.6	2.250	0.619	2.00	0.00200	0.00050
5.9	2.350	0.646	2.00	0.00200	0.00050
	4.700	2.900	1.99	0.10000	0.20000
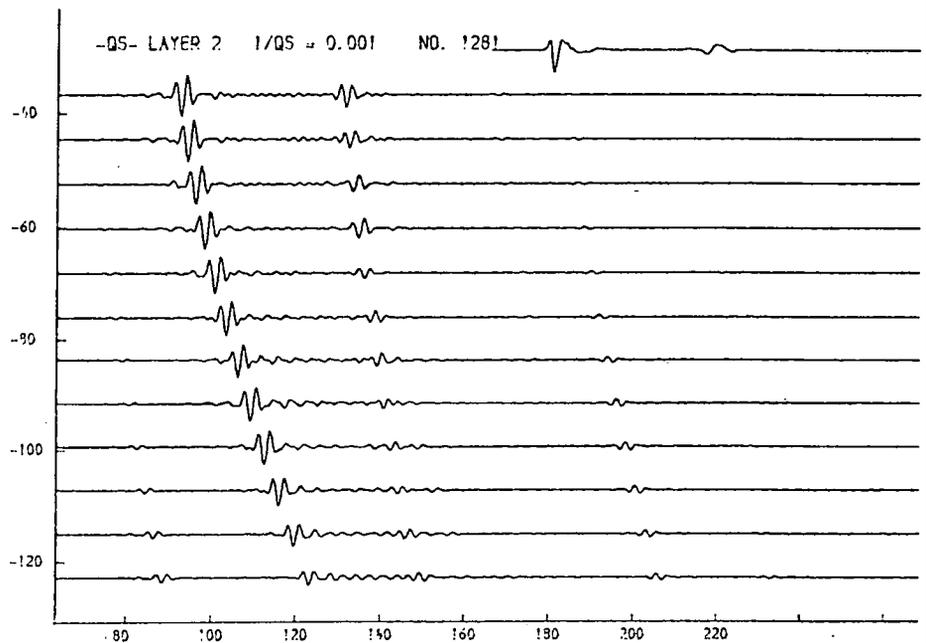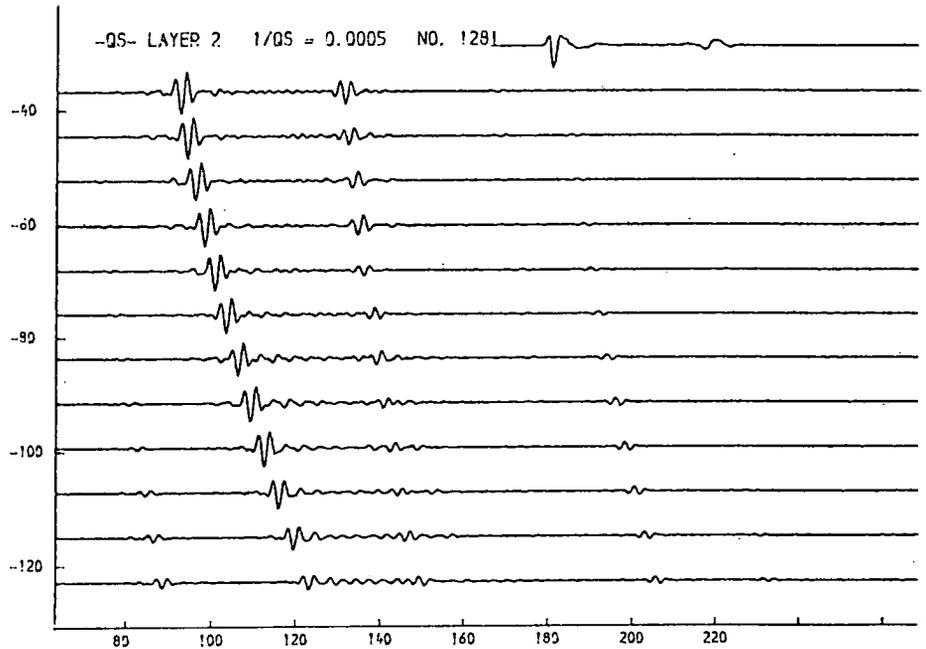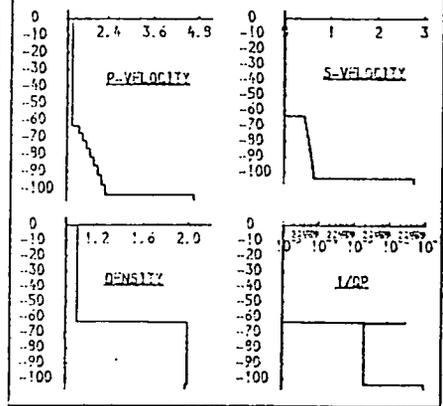
Fig. 9.69a.   Layer 2, s-attenuation.

The velocity gradient does not greatly influence the effect of this parameter (c.f. figs. 9.57a-e).

THICKNESS (M.)	P-VELOCITY (M/S.)	S-VELOCITY (M/S.)	DENSITY (G/ML)	1/Q P	1/Q S
63.0	1.460	0.000	1.03	0.00001	0.00001
0.5	1.490	0.010	1.65	0.03000	0.06950
4.1	1.650	0.454	2.00	0.00200	0.00500
4.4	1.750	0.481	2.00	0.00200	0.00500
4.6	1.850	0.509	2.00	0.00200	0.00500
4.9	1.950	0.536	2.00	0.00200	0.00500
5.1	2.050	0.564	2.00	0.00200	0.00500
5.4	2.150	0.591	2.00	0.00200	0.00500
5.6	2.250	0.619	2.00	0.00200	0.00500
5.9	2.350	0.646	2.00	0.00200	0.00500
	4.700	2.900	1.99	0.10000	0.20000
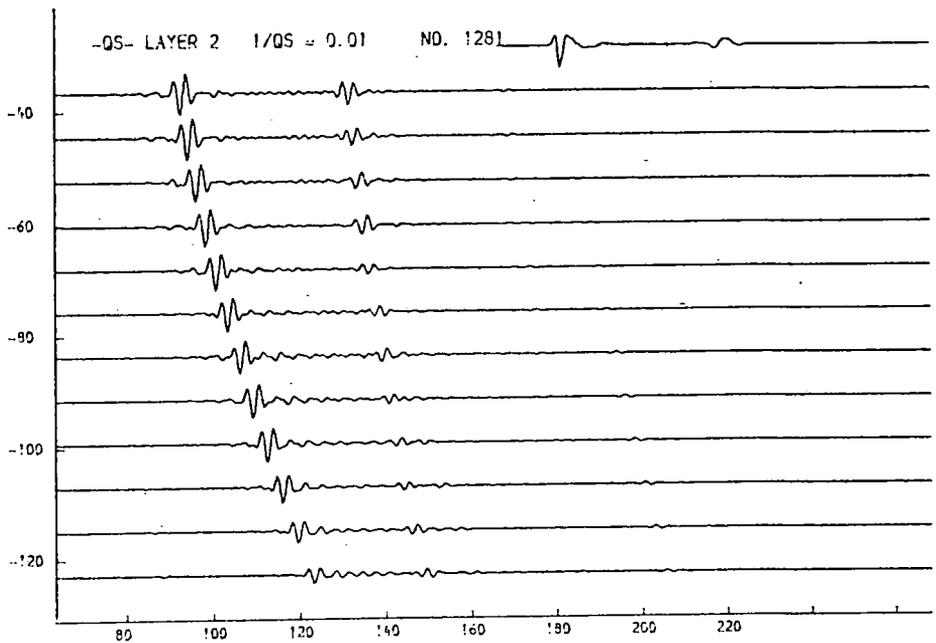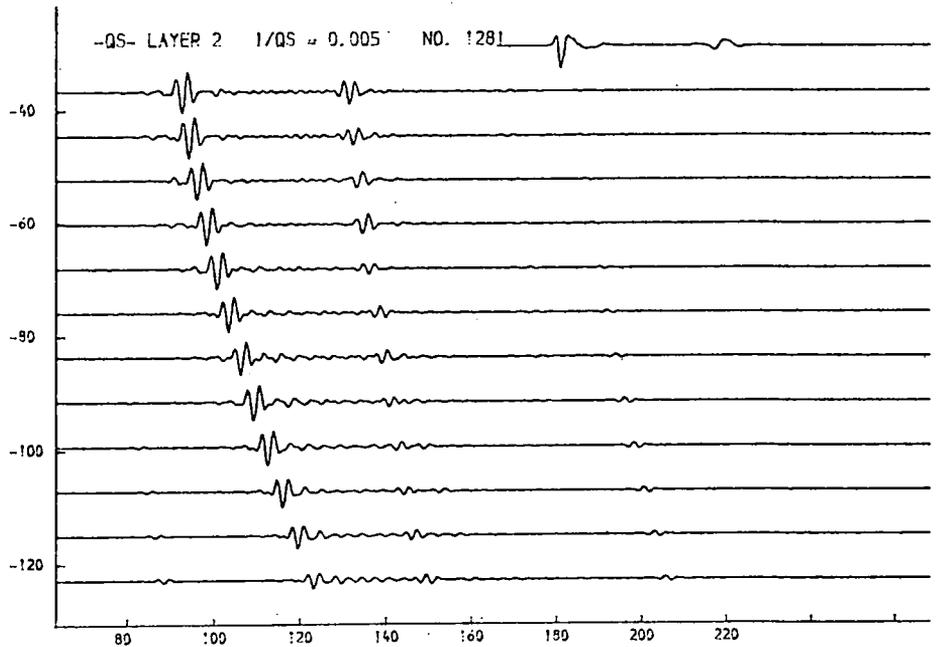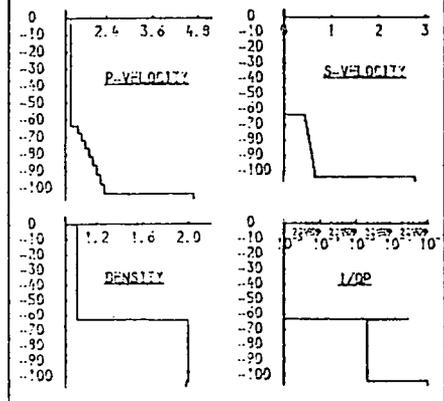
Fig. 9.69b. Layer 2, s-attenuation.

The velocity gradient does not greatly influence the effect of this parameter (c.f. figs. 9.57a-e).

THICKNESS (M.)	P-VELOCITY (M/S.)	S-VELOCITY (M/S.)	DENSITY (G/ML)	1/Q P	1/Q S
63.0	1.460	0.000	1.03	0.00001	0.00001
0.5	1.460	0.313	1.05	0.03000	0.04000
4.1	1.650	0.454	2.00	0.00200	0.04000
4.4	1.750	0.481	2.00	0.00200	0.04000
4.6	1.850	0.509	2.00	0.00200	0.04000
4.9	1.950	0.536	2.00	0.00200	0.04000
5.1	2.050	0.564	2.00	0.00200	0.04000
5.4	2.150	0.591	2.00	0.00200	0.04000
5.6	2.250	0.619	2.00	0.00200	0.04000
5.9	2.350	0.646	2.00	0.00200	0.04000
	4.700	2.800	1.98	0.10000	0.20000
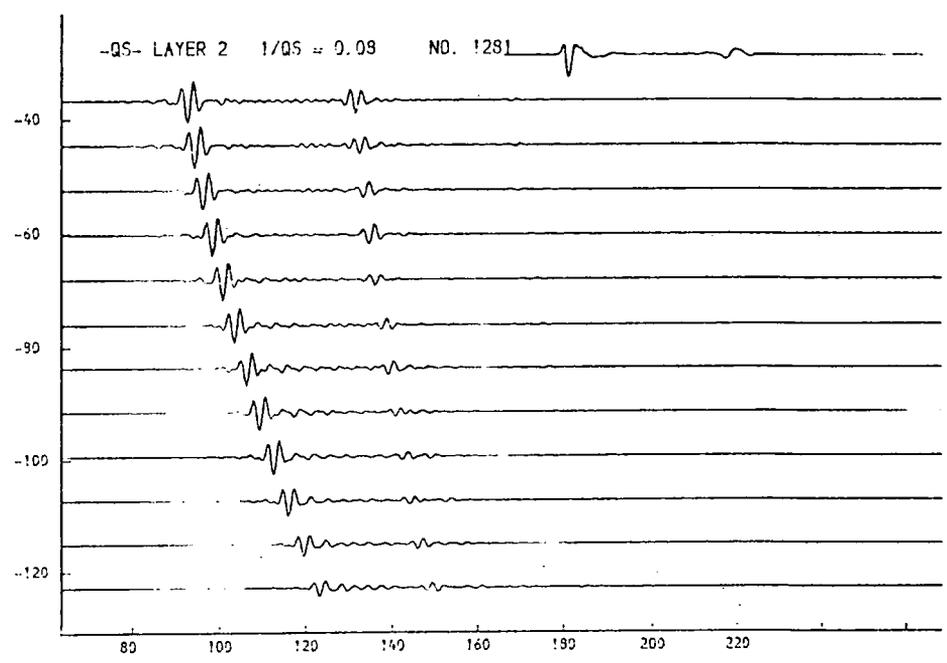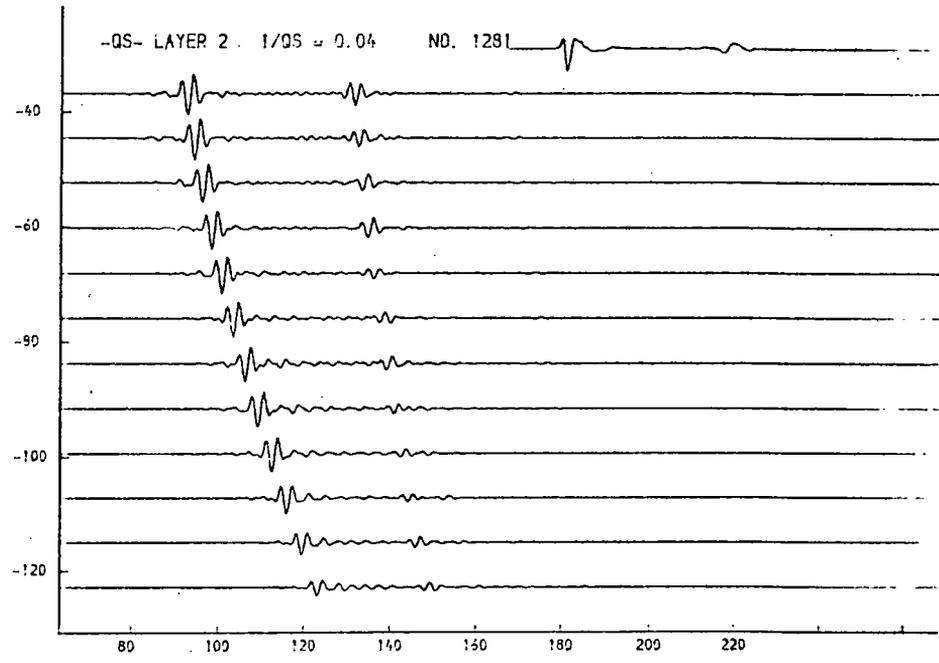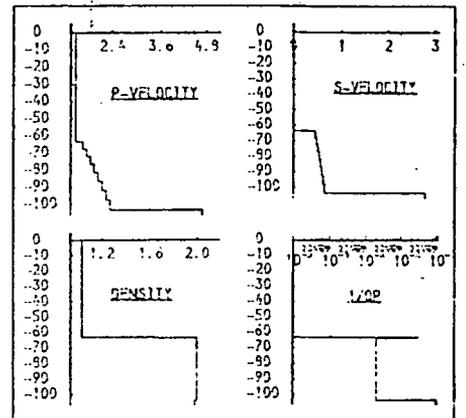
Fig. 9.69c. Layer 2, s-attenuation.

The velocity gradient does not greatly influence the effect of this parameter (c.f. figs. 9.57a-e).

THICKNESS (M.)	P-VELOCITY (M/S.)	S-VELOCITY (M/S.)	DENSITY (G/ML)	1/Q P	1/Q S
63.0	1.460	0.000	1.03	0.00001	0.00001
6.5	1.490	0.449	1.65	0.03000	0.36000
4.1	1.650	0.454	2.00	0.00200	0.16000
4.4	1.750	0.481	2.00	0.00200	0.16000
4.6	1.850	0.509	2.00	0.00200	0.16000
4.9	1.950	0.536	2.00	0.00200	0.16000
5.1	2.050	0.564	2.00	0.00200	0.16000
5.4	2.150	0.591	2.00	0.00200	0.16000
5.6	2.250	0.619	2.00	0.00200	0.16000
5.9	2.350	0.646	2.00	0.00200	0.16000
	4.700	2.900	1.98	0.10000	0.20000

-QS- LAYER 2   1/QS = 0.16   NO. 1281

-QS- LAYER 2   1/QS = 0.32   NO. 1281
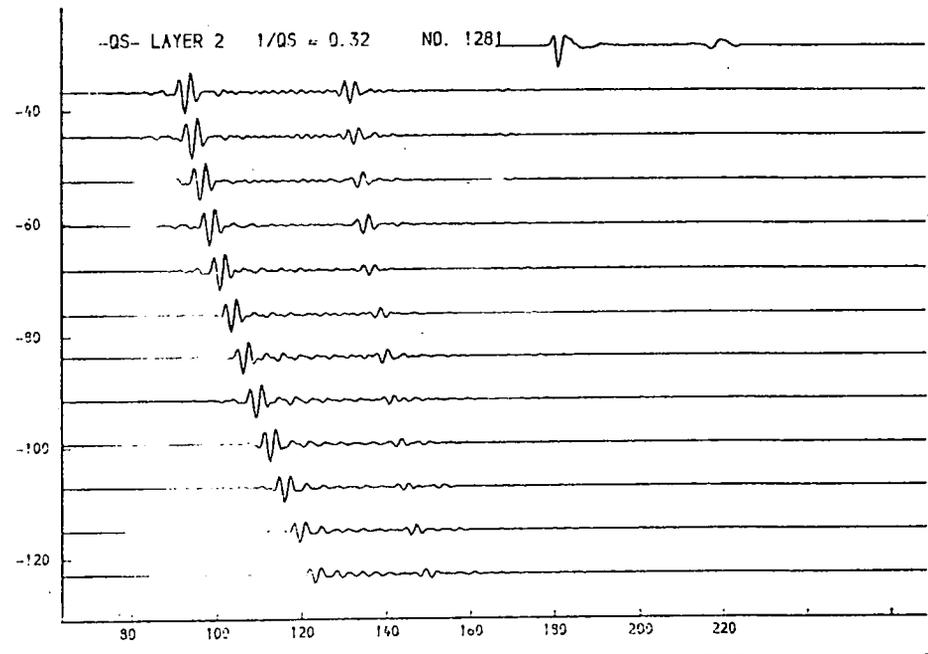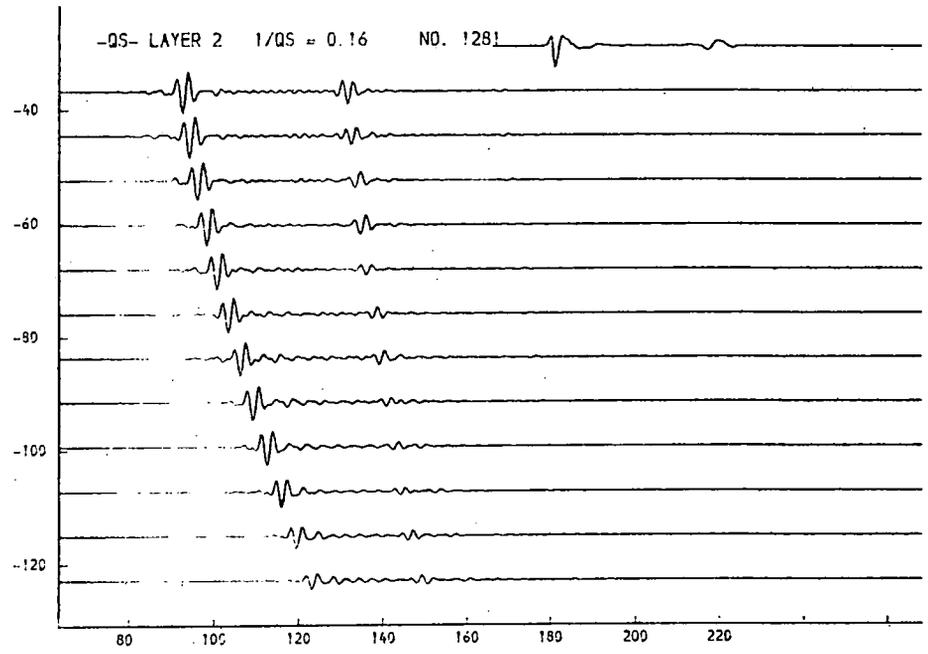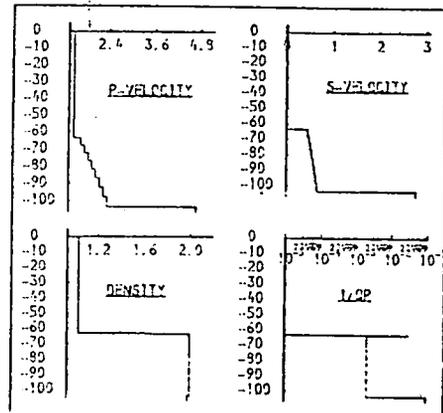
Fig. 9.69d. Layer 2, s-attenuation.

The velocity gradient does not greatly influence the effect of this parameter (c.f. figs. 9.57a-e).

THICKNESS (M.)	P-VELOCITY (M/S.)	S-VELOCITY (M/S.)	DENSITY (G/HL)	1/Q P	1/Q S
63.0	1.460	0.0	1.03	0.00001	0.00001
0.5	1.490	0.010	1.65	0.07000	0.04000
4.1	1.650	0.454	2.00	0.00200	0.02000
4.4	1.750	0.481	2.00	0.00200	0.02000
4.6	1.850	0.509	2.00	0.00200	0.02000
4.9	1.950	0.536	2.00	0.00200	0.02000
5.1	2.050	0.564	2.00	0.00200	0.02000
5.4	2.150	0.591	2.00	0.00200	0.02000
5.6	2.250	0.619	2.00	0.00200	0.02000
5.9	2.350	0.646	2.00	0.00200	0.02000
	3.900	2.300	1.79	0.10000	0.20000

Fig. 9.70a. Layer 3, p-velocity.

This parameter is not greatly influenced by the presence of the velocity gradient in layer 2.

THICKNESS (M.)	P-VELOCITY (M/S.)	S-VELOCITY (M/S.)	DENSITY (G/ML)	1/Q P	1/Q S
63.0	1.460	0.0	1.03	0.00001	0.00001
0.5	1.400	0.510	1.65	0.02000	0.04000
4.1	1.650	0.454	2.00	0.00200	0.02000
4.4	1.750	0.481	2.00	0.00200	0.02000
4.6	1.850	0.509	2.00	0.00200	0.02000
4.9	1.950	0.536	2.00	0.00200	0.02000
5.1	2.050	0.564	2.00	0.00200	0.02000
5.4	2.150	0.591	2.00	0.00200	0.02000
5.6	2.250	0.619	2.00	0.00200	0.02000
5.9	2.350	0.646	2.00	0.00200	0.02000
	4.700	2.800	1.98	0.10000	0.20000

Fig. 9.70b. Layer 3, p-velocity.

This parameter is not greatly influenced by the presence
of the velocity gradient in layer 2.

THICKNESS (M.)	P-VELOCITY (M/S.)	S-VELOCITY (M/S.)	DENSITY (G/ML)	1/Q P	1/Q S
63.0	1.460	0.0	1.93	0.00001	0.00001
0.5	1.480	0.910	1.65	0.01000	0.04000
4.1	1.650	0.454	2.00	0.00200	0.02000
4.4	1.750	0.481	2.00	0.00200	0.02000
4.6	1.850	0.509	2.00	0.00200	0.02000
4.9	1.950	0.536	2.00	0.00200	0.02000
5.1	2.050	0.564	2.00	0.00200	0.02000
5.4	2.150	0.591	2.00	0.00200	0.02000
5.6	2.250	0.619	2.00	0.00200	0.02000
5.9	2.350	0.646	2.00	0.00200	0.02000
	4.900	2.900	1.98	0.10000	0.20000

Fig. 9.70c. Layer 3, p-velocity.

This parameter is not greatly influenced by the presence of the velocity gradient in layer 2.

THICKNESS (M.)	P-VELOCITY (M/S.)	S-VELOCITY (M/S.)	DENSITY (G/ML)	1/Q P	1/Q S
63.0	1.460	0.0	1.03	0.00001	0.00001
0.5	1.400	0.010	1.65	0.07000	0.04000
4.1	1.650	0.454	2.00	0.00200	0.02000
4.4	1.750	0.481	2.00	0.00200	0.02000
4.6	1.950	0.509	2.00	0.00200	0.02000
4.9	1.950	0.536	2.00	0.00200	0.02000
5.1	2.050	0.564	2.00	0.00200	0.02000
5.4	2.150	0.591	2.00	0.00200	0.02000
5.6	2.250	0.619	2.00	0.00200	0.02000
5.9	2.350	0.646	2.00	0.00200	0.02000
	5.300	2.900	1.98	0.10000	0.20000

-P- LAYER 3   P=5.3   NO. 1281

-P- LAYER 3   P=5.5   NO. 1281

Fig. 9.70d. Layer 3, p-velocity.

This parameter is not greatly influenced by the presence
of the velocity gradient in layer 2.

THICKNESS (M.)	P-VELOCITY (M/S.)	S-VELOCITY (M/S.)	DENSITY (G/HL)	1/Q P	1/Q S
63.0	1.460	0.0	1.03	0.00001	0.00001
6.5	1.500	0.010	1.65	0.02000	0.04000
4.1	1.650	0.454	2.00	0.00200	0.02000
4.4	1.750	0.481	2.00	0.00200	0.02000
4.6	1.850	0.509	2.00	0.00200	0.02000
4.9	1.950	0.536	2.00	0.00200	0.02000
5.1	2.050	0.564	2.00	0.00200	0.02000
5.4	2.150	0.591	2.00	0.00200	0.02000
5.6	2.250	0.619	2.00	0.00200	0.02000
5.9	2.350	0.646	2.00	0.00200	0.02000
	4.700	1.900	1.99	0.10000	0.20000
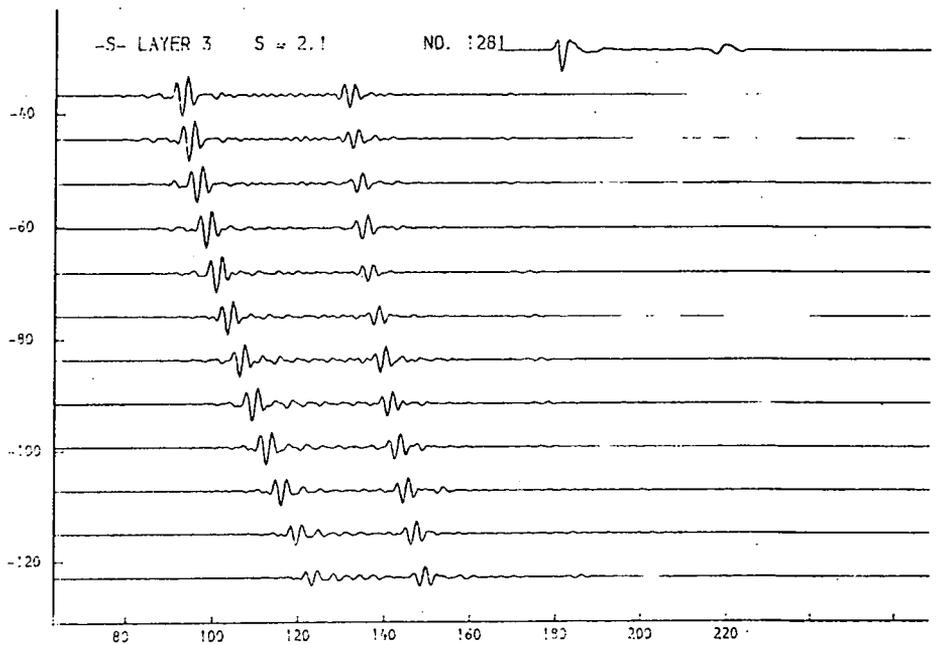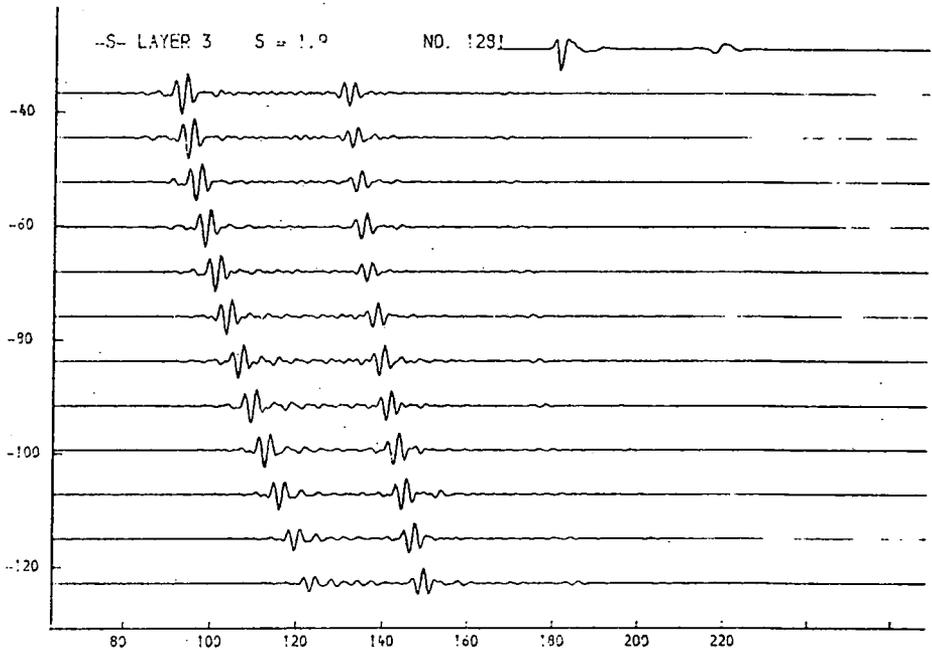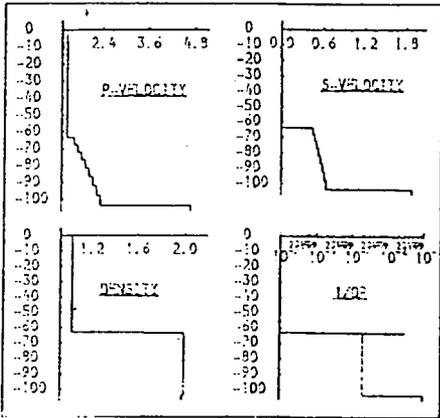
Fig. 9.71a. Layer 3, s-velocity.

At lower values of this parameter, the influence of the p-velocity gradient is not very evident (c.f. figs. 9.59a,b).

THICKNESS (M.)	P-VELOCITY (M/S.)	S-VELOCITY (M/S.)	DENSITY (G/ML)	1/Q P	1/Q S
63.0	1.460	0.0	1.03	0.00001	0.00001
0.5	1.400	0.010	1.65	0.07000	0.06000
4.1	1.650	0.454	2.00	0.00200	0.02000
4.4	1.750	0.481	2.00	0.00200	0.02000
4.6	1.850	0.509	2.00	0.00200	0.02000
4.9	1.950	0.536	2.00	0.00200	0.02000
5.1	2.050	0.564	2.00	0.00200	0.02000
5.4	2.150	0.591	2.00	0.00200	0.02000
5.6	2.250	0.619	2.00	0.00200	0.02000
5.9	2.350	0.646	2.00	0.00200	0.02000
	4.700	2.300	1.98	0.10000	0.20000

Fig. 9.71b. Layer 3, s-velocity.

At lower values of this parameter, the influence of the p-velocity gradient is not very evident (c.f. figs. 9.59a,b).

THICKNESS (M.)	P-VELOCITY (M/S.)	S-VELOCITY (M/S.)	DENSITY (G/ML)	1/Q P	1/Q S
63.0	1.460	0.0	1.03	0.00001	0.00001
0.5	1.490	0.010	1.05	0.97000	0.36000
4.1	1.650	0.454	2.00	0.00200	0.02000
4.4	1.750	0.481	2.00	0.00200	0.02000
4.6	1.850	0.509	2.00	0.00200	0.02000
4.9	1.950	0.536	2.00	0.00200	0.02000
5.1	2.050	0.564	2.00	0.00200	0.02000
5.4	2.150	0.591	2.00	0.00200	0.02000
5.6	2.250	0.619	2.00	0.00200	0.02000
5.9	2.350	0.646	2.00	0.00200	0.02000
	4.700	2.700	1.98	0.10000	0.20000
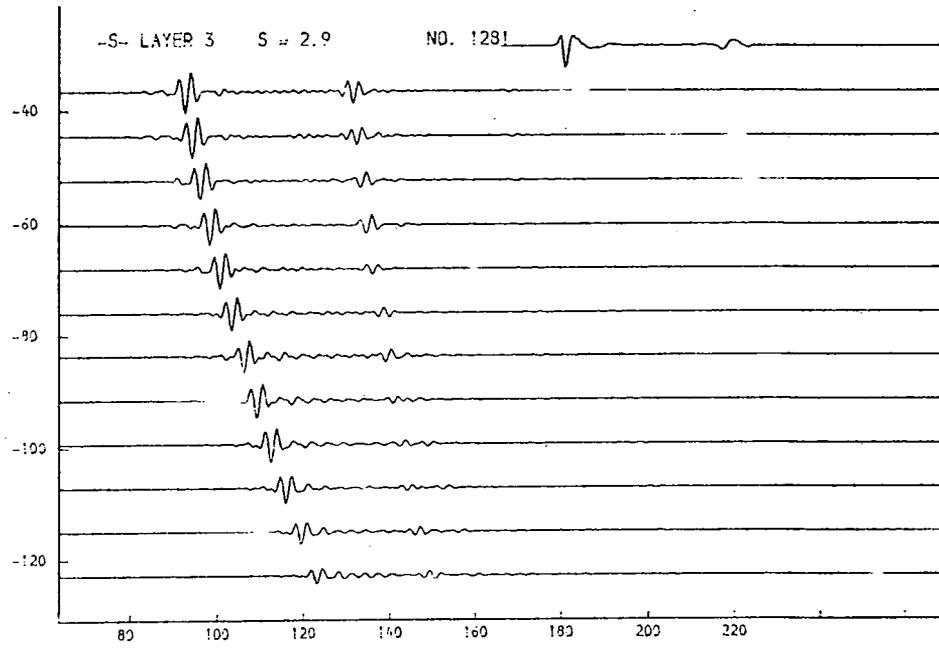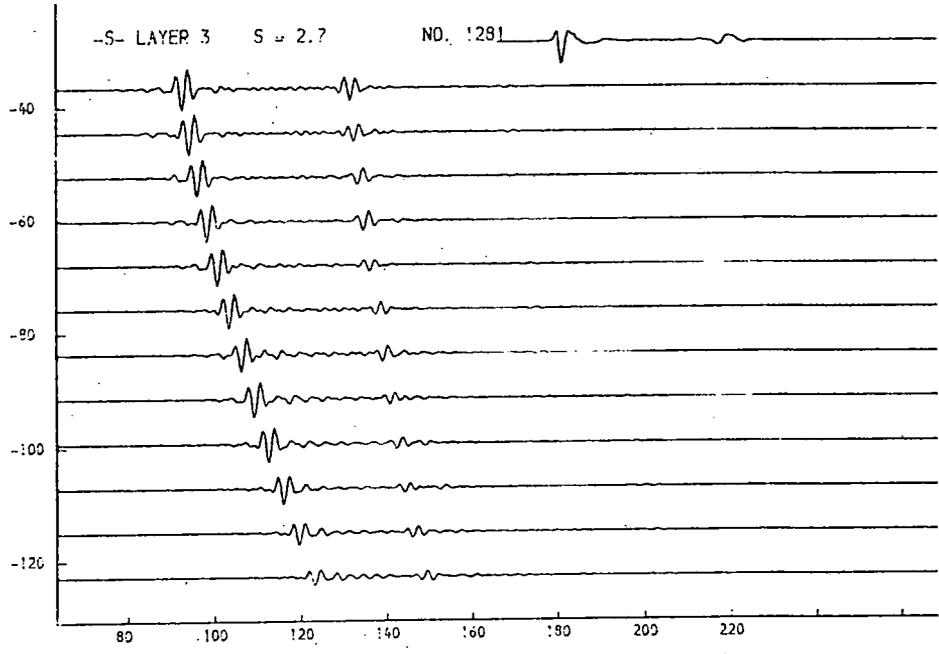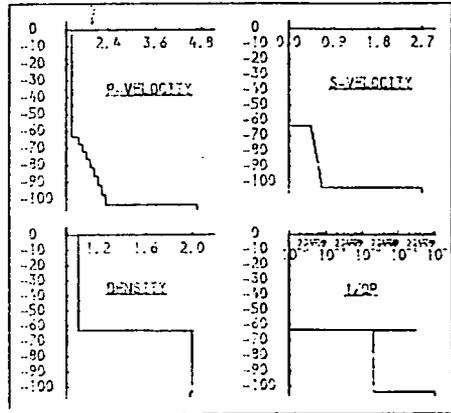
Fig. 9.71c. Layer 3, s-velocity.

At the higher values for this parameter, the amplitude of
r2 at high offset is greater when the high p-velocity
gradient is present (c.f. figs. 9.59c,d).

THICKNESS (M.)	P-VELOCITY (M/S.)	S-VELOCITY (M/S.)	DENSITY (G/ML)	1/Q P	1/Q S
63.0	1.460	0.0	1.03	0.00001	0.00001
0.5	1.490	0.010	1.05	0.03000	0.06000
4.1	1.650	0.454	2.00	0.00200	0.02000
4.4	1.750	0.481	2.00	0.00200	0.02000
4.6	1.850	0.509	2.00	0.00200	0.02000
4.9	1.950	0.536	2.00	0.00200	0.02000
5.1	2.050	0.564	2.00	0.00200	0.02000
5.4	2.150	0.591	2.00	0.00200	0.02000
5.6	2.250	0.619	2.00	0.00200	0.02000
5.9	2.350	0.646	2.00	0.00200	0.02000
	4.700	3.100	1.98	0.10000	0.20000
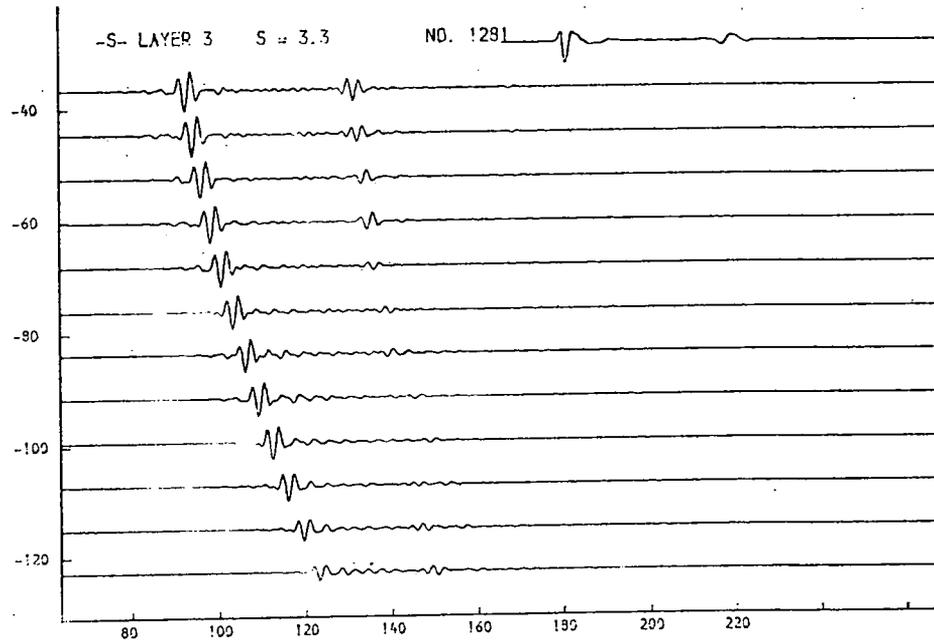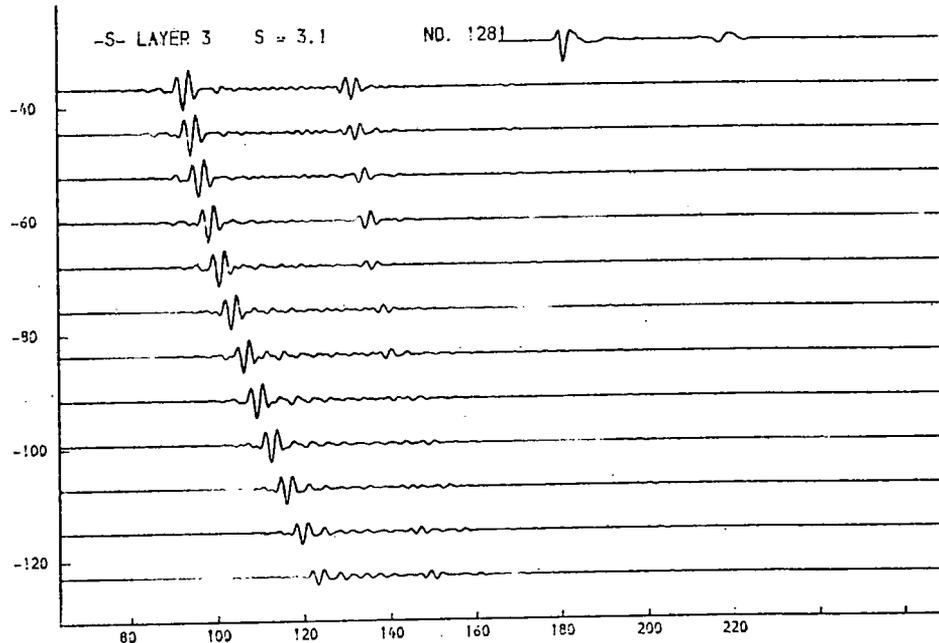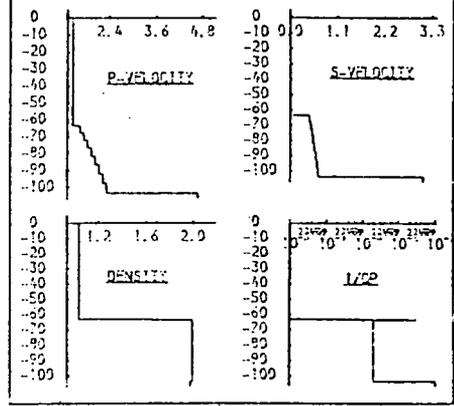
Fig. 9.71d.   Layer 3, s-velocity.

At the higher values for this parameter, the amplitude of r2 at high offset is greater when the high p-velocity gradient is present (c.f. figs. 9.59c,d).

THICKNESS (M.)	P-VELOCITY (M/S.)	S-VELOCITY (M/S.)	DENSITY (G/ML)	1/Q P	1/Q S
63.0	1.460	0.0	1.03	0.00001	0.00001
6.5	1.500	0.010	1.65	0.02000	0.04000
4.1	1.650	0.454	2.00	0.00200	0.02000
4.4	1.750	0.481	2.00	0.00200	0.02000
4.6	1.850	0.509	2.00	0.00200	0.02000
4.9	1.950	0.536	2.00	0.00200	0.02000
5.1	2.050	0.564	2.00	0.00200	0.02000
5.4	2.150	0.591	2.00	0.00200	0.02000
5.6	2.250	0.619	2.00	0.00200	0.02000
5.9	2.350	0.646	2.00	0.00200	0.02000
	2.900	1.98	0.00100	0.20000	

Fig. 9.72a.   Layer 3, p-attenuation.

Over a wide range of values for this parameter, the amplitude of r2 at high offset is seen to be greater in the presence of the p-velocity gradient (c.f. figs. 9.61a,b,c,d).

THICKNESS (M.)	P-VELOCITY (M/S.)	S-VELOCITY (M/S.)	DENSITY (G/ML)	1/Q P	1/Q S
63.0	1.460	0.0	1.03	0.00001	0.00001
0.5	1.490	0.010	1.65	0.03000	0.06000
4.1	1.650	0.454	2.00	0.00200	0.02000
4.4	1.750	0.481	2.00	0.00200	0.02000
4.6	1.950	0.509	2.00	0.00200	0.02000
4.9	1.950	0.536	2.00	0.00200	0.02000
5.1	2.050	0.564	2.00	0.00200	0.02000
5.4	2.150	0.591	2.00	0.00200	0.02000
5.6	2.250	0.619	2.00	0.00200	0.02000
5.9	2.350	0.646	2.00	0.00200	0.02000
	4.700	2.800	1.99	0.01000	0.20000
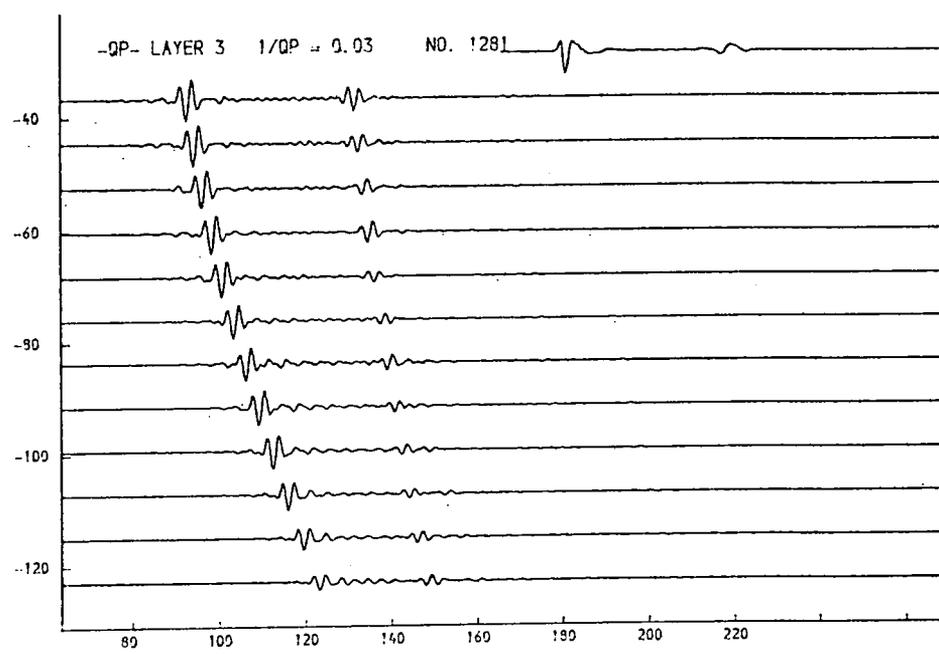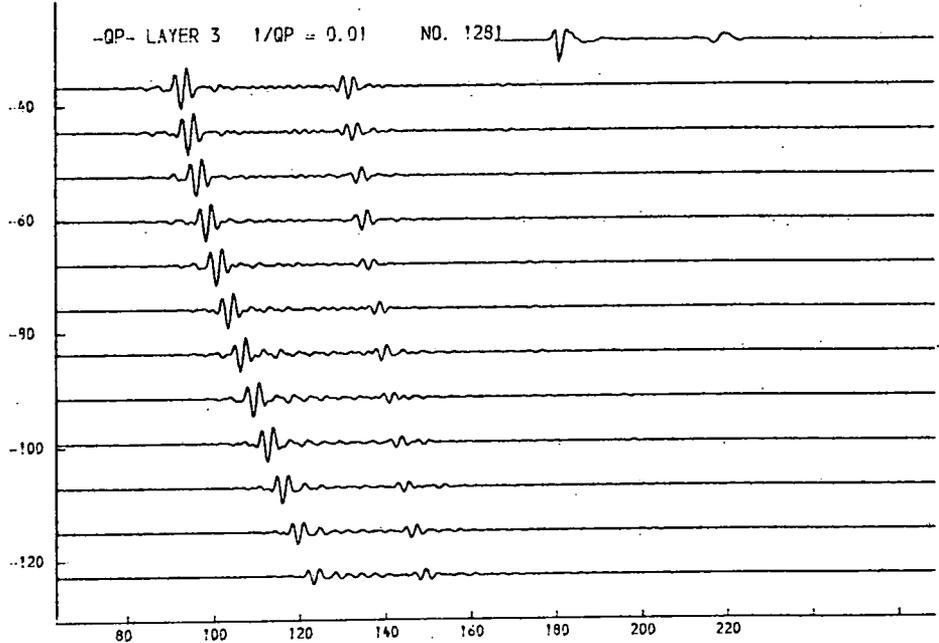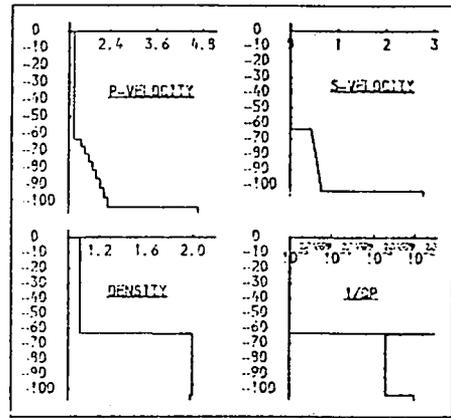
Fig. 9.72b. Layer 3, p-attenuation.

Over a wide range of values for this parameter, the amplitude of r2 at high offset is seen to be greater in the presence of the p-velocity gradient (c.f. figs. 9.61a,b,c,d).

THICKNESS (M.)	P-VELOCITY (M/S.)	S-VELOCITY (M/S.)	DENSITY (G/ML)	1/Q P	1/Q S
63.0	1.460	0.0	1.93	0.00001	0.00001
0.5	1.600	0.010	1.65	0.03000	0.04000
4.1	1.650	0.454	2.00	0.00200	0.02000
4.4	1.750	0.481	2.00	0.00200	0.02000
4.6	1.850	0.509	2.00	0.00200	0.02000
4.9	1.950	0.536	2.00	0.00200	0.02000
5.1	2.050	0.564	2.00	0.00200	0.02000
5.4	2.150	0.591	2.00	0.00200	0.02000
5.6	2.250	0.619	2.00	0.00200	0.02000
5.9	2.350	0.646	2.00	0.00200	0.02000
	4.700	2.900	1.98	0.30000	0.20000
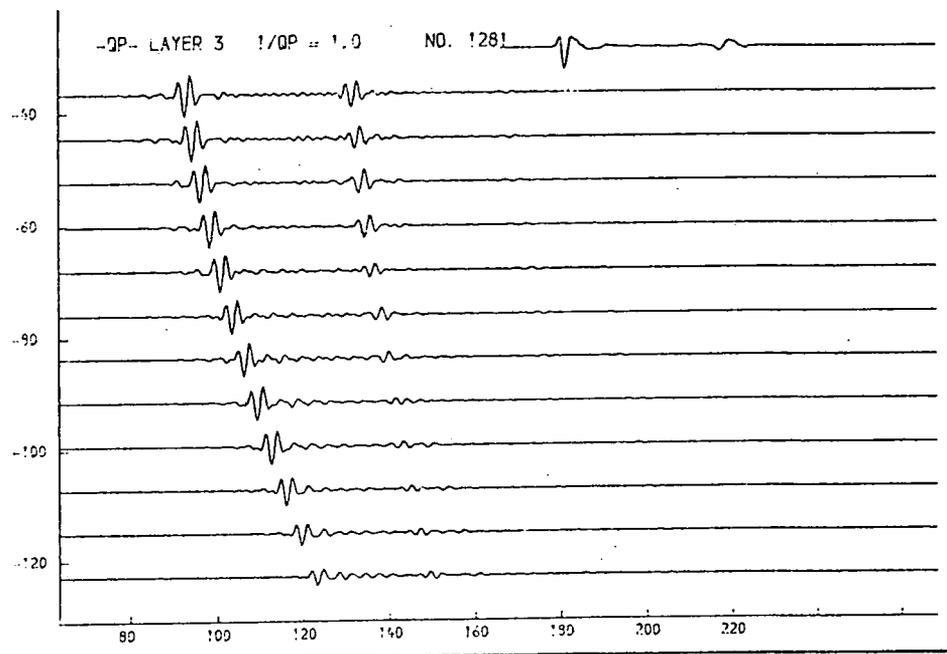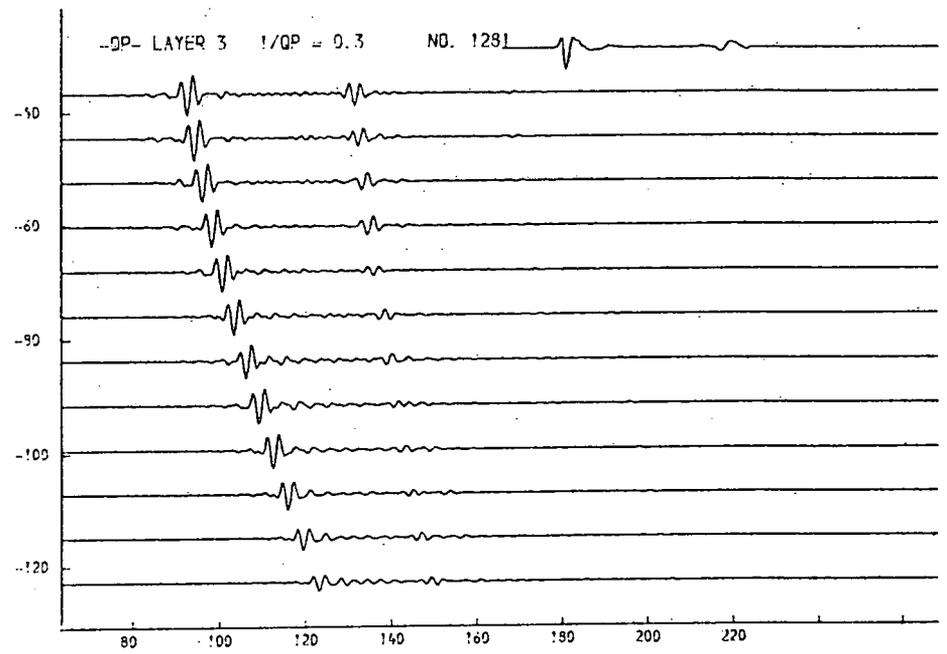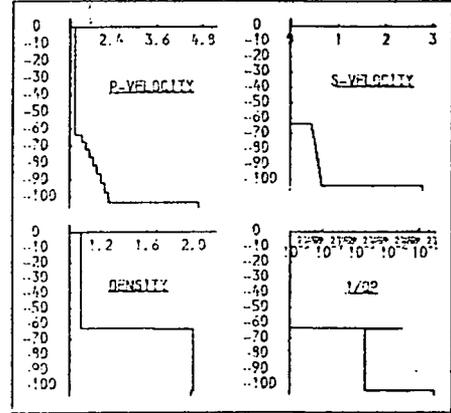
Fig. 9.72c. Layer 3, p-attenuation.

Over a wide range of values for this parameter, the amplitude of r2 at high offset is seen to be greater in the presence of the p-velocity gradient (c.f. figs. 9.61a,b,c,d).

THICKNESS (M.)	P-VELOCITY (M/S.)	S-VELOCITY (M/S.)	DENSITY (G/ML)	1/Q P	1/Q S
63.0	1.460	0.0	1.03	0.00001	0.00001
0.5	1.490	0.010	1.65	0.03000	0.06000
4.1	1.650	0.454	2.00	0.00200	0.02000
4.3	1.750	0.481	2.00	0.00200	0.02000
4.6	1.950	0.509	2.00	0.00200	0.02000
4.9	1.950	0.536	2.00	0.00200	0.02000
5.1	2.050	0.564	2.00	0.00200	0.02000
5.4	2.150	0.591	2.00	0.00200	0.02000
5.6	2.250	0.619	2.00	0.00200	0.02000
5.9	2.350	0.646	2.00	0.00200	0.02000
	4.700	2.800	1.98	3.00000	0.20000

-QP- LAYER 3   1/QP = 3.0   NO. 1281

-QP- LAYER 3   1/QP = 10.0   NO. 1281

Fig. 9.72d. Layer 3, p-attenuation.

The effect noted in figs. 9.72a,b and c is seen here at very high attenuation (c.f. fig. 9.61d), but the physical significance of this is in question at these very high values of 1/Qp.

THICKNESS (M.)	P-VELOCITY (M/S.)	S-VELOCITY (M/S.)	DENSITY (G/ML)	1/Q P	1/Q S
63.0	1.460	0.0	1.03	0.00001	0.00001
0.5	1.400	0.010	1.05	0.03000	0.06000
4.1	1.650	0.454	2.00	0.00200	0.02000
4.4	1.750	0.491	2.00	0.00200	0.02000
4.6	1.950	0.509	2.00	0.00200	0.02000
4.9	1.950	0.536	2.00	0.00200	0.02000
5.1	2.050	0.564	2.00	0.00200	0.02000
5.4	2.150	0.591	2.00	0.00200	0.02000
5.6	2.250	0.619	2.00	0.00200	0.02000
5.9	2.750	0.646	2.00	0.00200	0.02000
	4.700	2.900	1.99	0.10000	0.00100
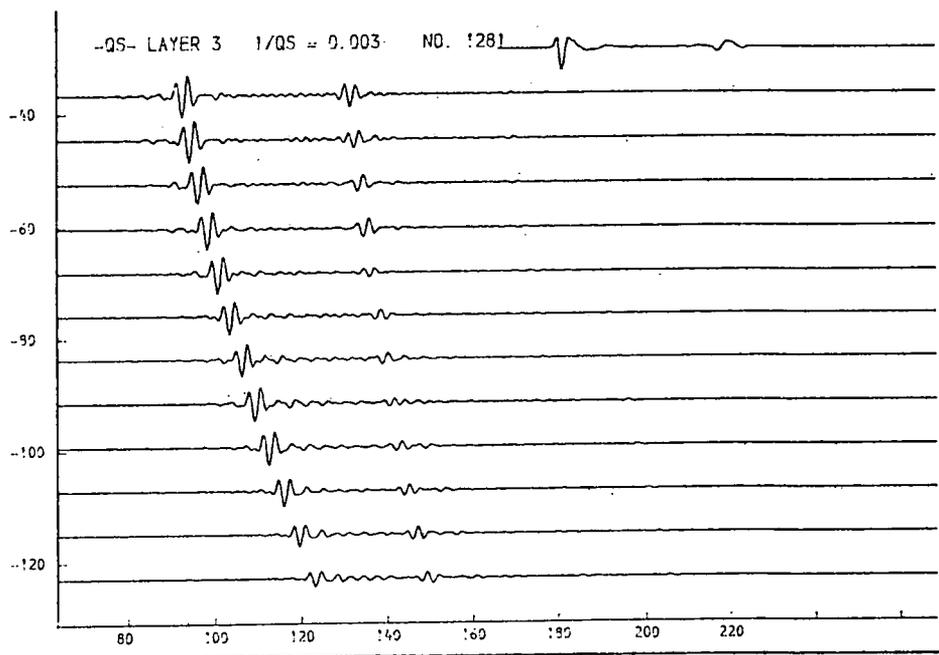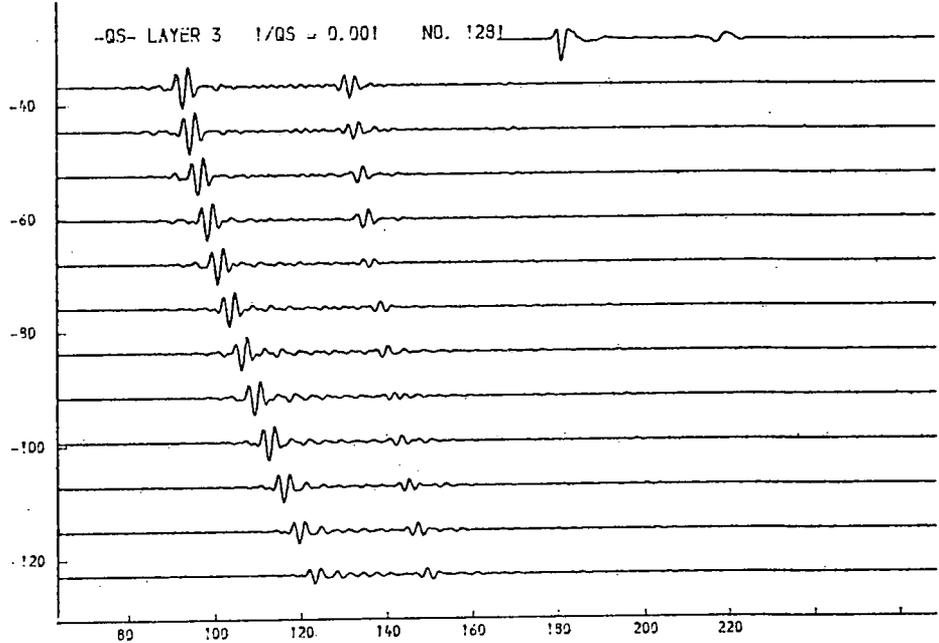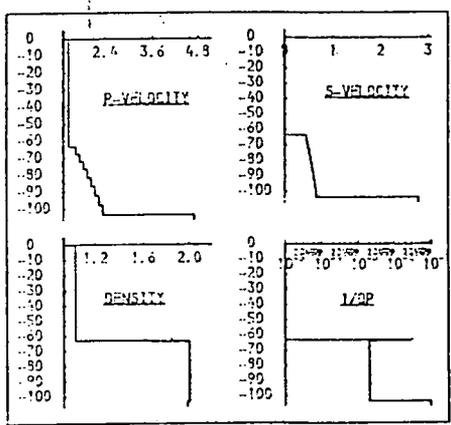
Fig. 9.73a.   Layer 3, s-attenuation.

The relative increase in the reflexion r2 at high offset can be seen (c.f. figs. 9.62a,b).

THICKNESS (M.)	P-VELOCITY (M/S.)	S-VELOCITY (M/S.)	DENSITY (G/HL)	1/Q P	1/Q S
63.0	1.460	0.0	1.03	0.00001	0.00001
0.5	1.490	0.940	1.65	0.07030	0.06960
4.1	1.650	0.454	2.00	0.00200	0.02000
4.4	1.750	0.481	2.00	0.00200	0.02000
4.6	1.850	0.509	2.00	0.00200	0.02000
4.9	1.950	0.536	2.00	0.00200	0.02000
5.1	2.050	0.564	2.00	0.00200	0.02000
5.4	2.150	0.591	2.00	0.00200	0.02000
5.6	2.250	0.619	2.00	0.00200	0.02000
5.9	2.350	0.646	2.00	0.00200	0.02000
	4.700	2.800	1.98	0.10000	0.01000

Fig. 9.73b.   Layer 3, s-attenuation.

The relative increase in the reflexion r2 at high offset can be seen (c.f. figs. 9.62a,b).

THICKNESS (M.)	P-VELOCITY (M/S.)	S-VELOCITY (M/S.)	DENSITY (G/HL)	1/Q P	1/Q S
63.0	1.460	0.0	1.03	0.00001	0.00001
0.5	1.480	0.010	1.05	0.03000	0.04000
4.1	1.650	0.454	2.00	0.00200	0.02000
4.4	1.750	0.481	2.00	0.00200	0.02000
4.6	1.850	0.509	2.00	0.00200	0.02000
4.9	1.950	0.536	2.00	0.00200	0.02000
5.1	2.050	0.564	2.00	0.00200	0.02000
5.4	2.150	0.591	2.00	0.00200	0.02000
5.6	2.250	0.619	2.00	0.00200	0.02000
5.9	2.350	0.646	2.00	0.00200	0.02000
	4.700	2.900	1.98	0.10000	0.30000

Fig. 9.73c.   Layer 3, s-attenuation.

Effects seen at 1/Qs>1.0 are considered to be artifacts of the modelling process rather than physically meaningful results.

THICKNESS (M.)	P-VELOCITY (M/S.)	S-VELOCITY (M/S.)	DENSITY (G/ML)	1/Q P	1/Q S
63.0	1.460	0.0	1.03	0.00001	0.00001
0.5	1.480	0.010	1.05	0.02000	0.06000
4.1	1.650	0.454	2.00	0.00200	0.02000
4.4	1.750	0.481	2.00	0.00200	0.02000
4.6	1.850	0.509	2.00	0.00200	0.02000
4.9	1.950	0.536	2.00	0.00200	0.02000
5.1	2.050	0.564	2.00	0.00200	0.02000
5.4	2.150	0.591	2.00	0.00200	0.02000
5.6	2.250	0.619	2.00	0.00200	0.02000
5.9	2.350	0.646	2.00	0.00200	0.02000
	4.700	2.900	1.98	0.10000	3.00000

Fig. 9.73d. Layer 3, s-attenuation.

Effects seen at 1/Qs>1.0 are considered to be artifacts of the modelling process rather than physically meaningful results.

Synthetic seismogramme models

for No. 496

(figs. 9.76 to 9.123)

FIELD RECORD NO. 496
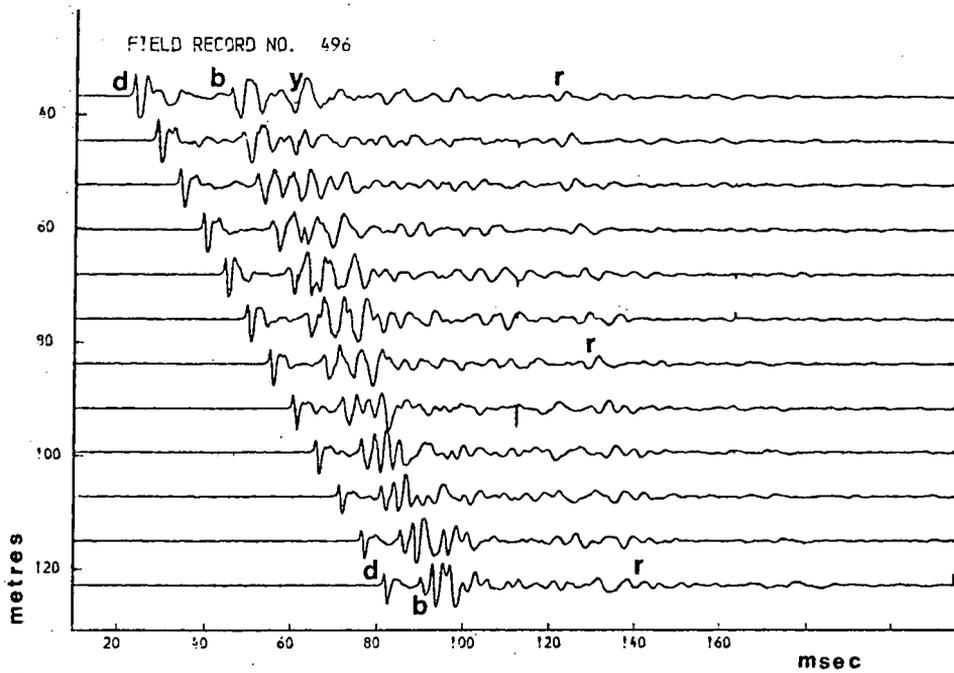
Fig. 9.76

The 12-channel seismogramme at the fix point no. 496 (see fig. 9.2).

    d - direct arrival   y - subbottom reflexion
    b - bottom reflexion   r - subbottom reflexion

THICKNESS (M.)	P-VELOCITY (M/S.)	S-VELOCITY (M/S.)	DENSITY (G/ML)	1/Q P	1/Q S
26.6	1.460	0.000	1.03	0.00000	0.00000
67.0	1.700	0.250	2.00	0.00100	0.03000
	3.500	2.000	1.98	0.00100	0.03000

TRAVEL-TIME MODEL - P = 1.70   NO. 496

TRAVEL-TIME MODEL FOR RECORD   NO. 496
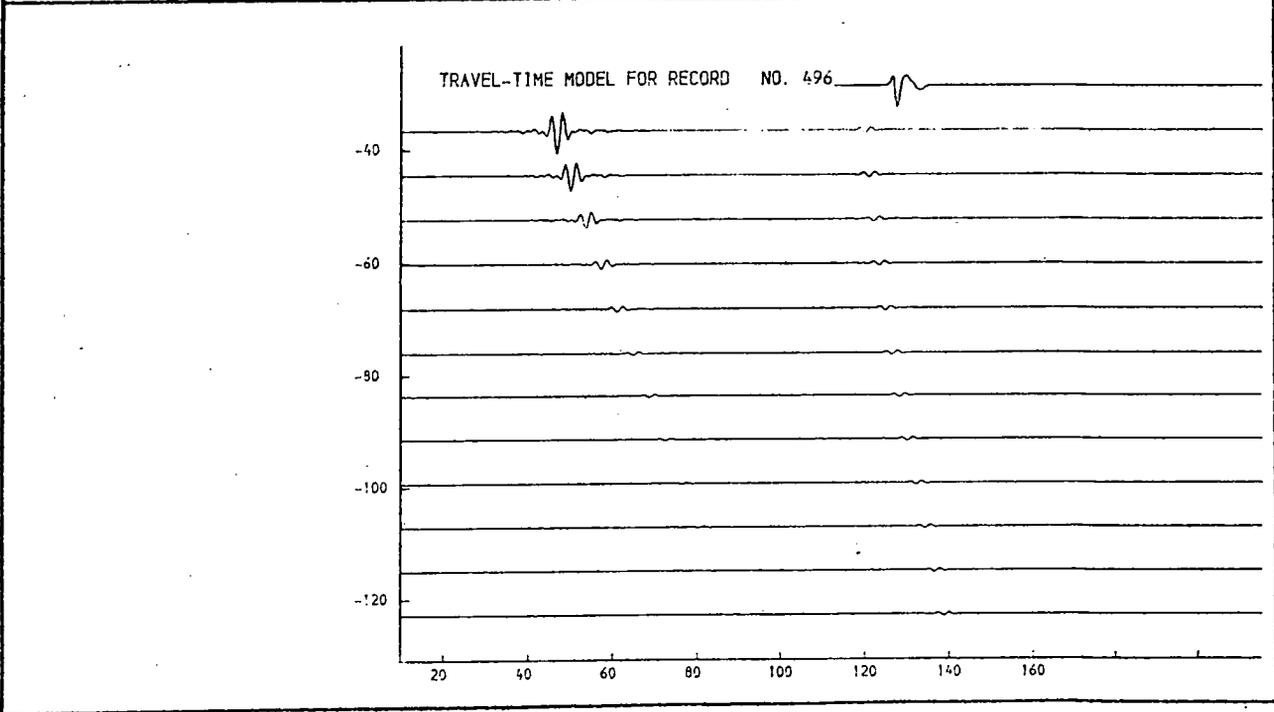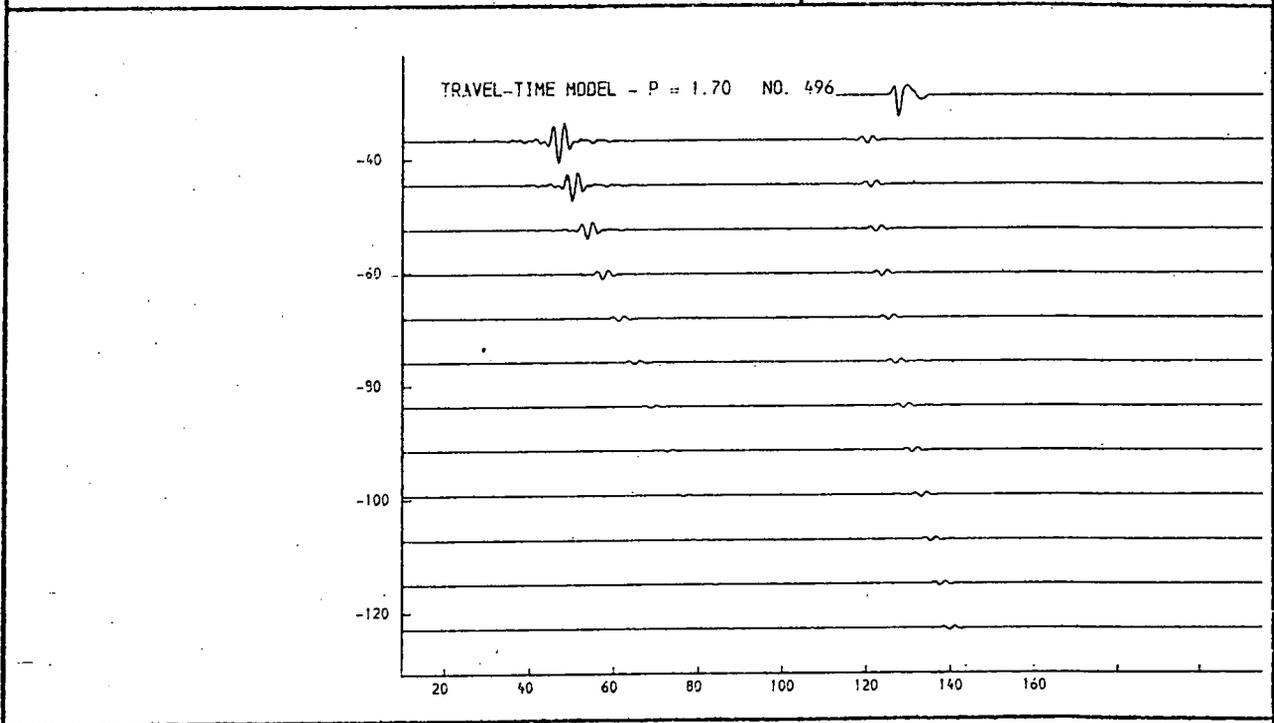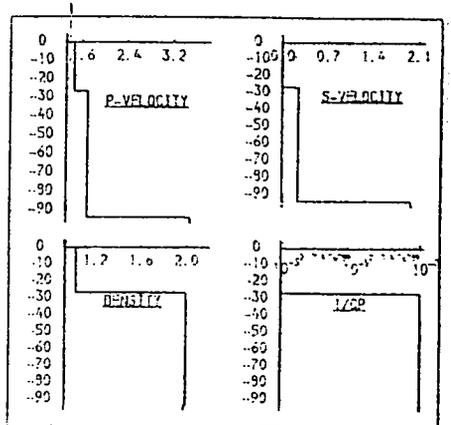
Fig. 9.77a. One layer, simple models.

These models, based on the travel-time analysis do not yield seismogrammes like the field records.   (Upper, velocity=1.70; lower, velocity=1.77).

THICKNESS (M.)	P-VELOCITY (M/S.)	S-VELOCITY (M/S.)	DENSITY (G/ML)	1/Q P	1/Q S
26.6	1.460	0.000	1.03	0.00000	0.00000
71.0	1.900	0.250	2.00	0.00100	0.03000
	3.500	2.000	1.98	0.00100	0.03000

TRAVEL-TIME MODEL - P = 1.90   NO. 496

TRAVEL-TIME MODEL   P = 1.95   NO. 496
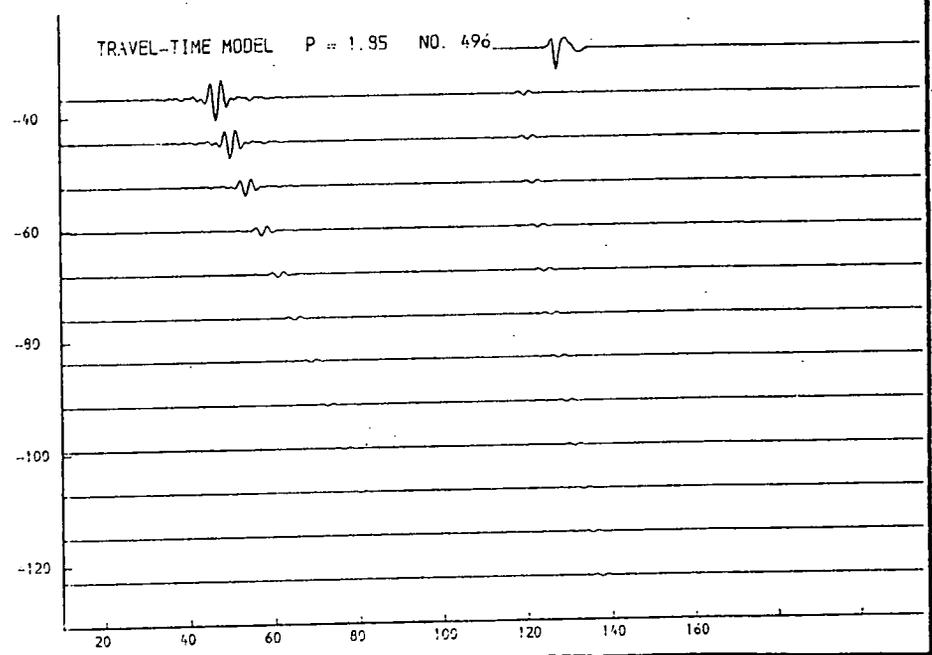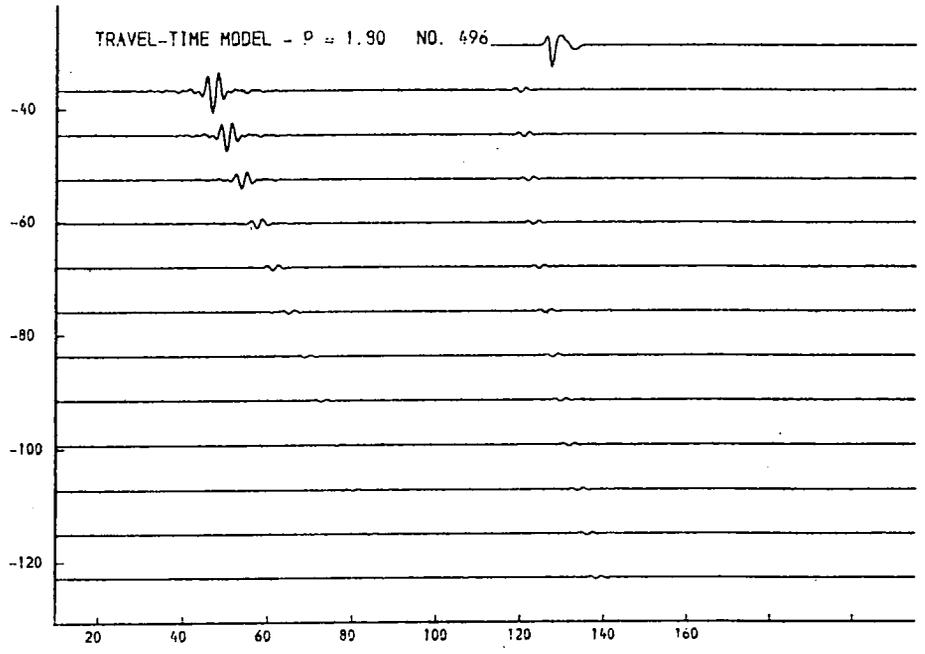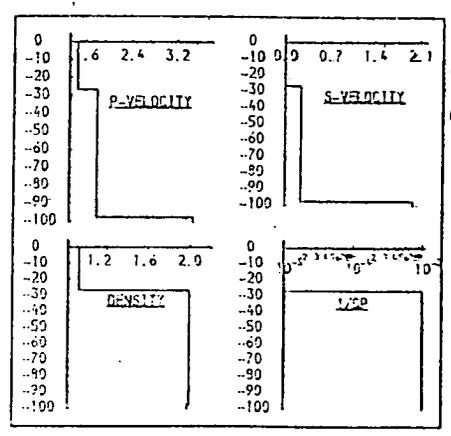
Fig. 9.77b. One layer, simple models.

Variation of the interval velocity (1.80, upper; 1.85, lower) does nothing to improve the overall appearance of the synthetic seismogramme.

THICKNESS (M.)	P-VELOCITY (M/S.)	S-VELOCITY (M/S.)	DENSITY (G/ML)	1/Q P	1/Q S
26.6	1.460	0.000	1.03	0.00000	0.00000
10.0	1.400	0.010	1.65	0.00100	0.01000
58.8	1.770	0.250	2.00	0.00100	0.03000
	3.500	2.000	1.98	0.00100	0.03000

P-VELOCITY .6 2.4 3.2

S-VELOCITY 0 0.7 1.4 2.1

DENSITY 1.2 1.6 2.0

1/QP 10^{-3} 10^{-2} 10^{-1}

P LAYER 1   P = 1.40   NO. 496

P LAYER 1   P = 1.50   NO. 496
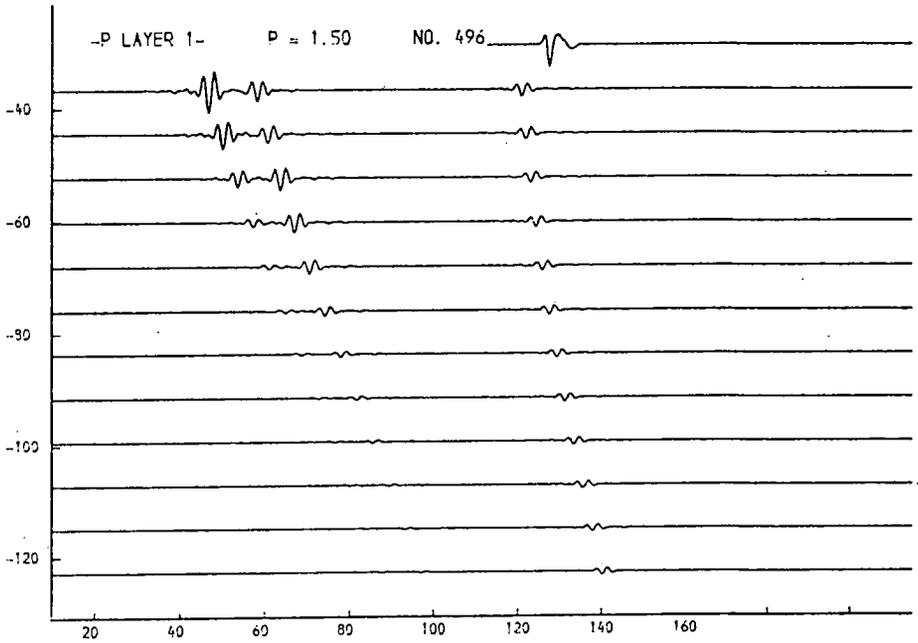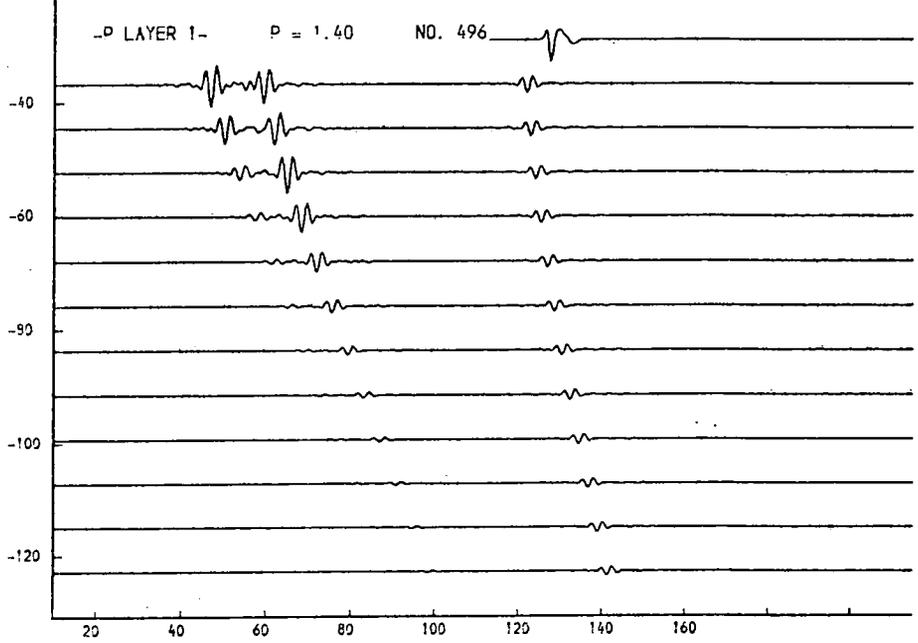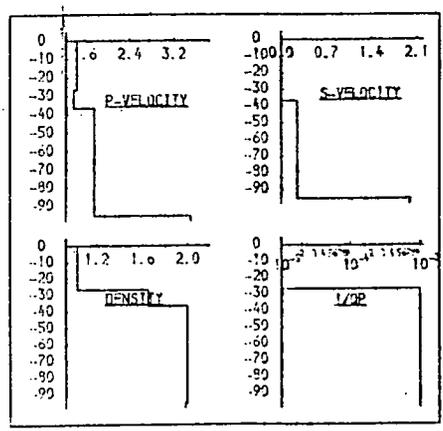
Fig. 9.78a. Simple 2-layered structure.

Variation of the p-velocity in the upper layer of a 2-layer structure does not produce models resembling the field record.

THICKNESS (M.)	P-VELOCITY (M/S.)	S-VELOCITY (M/S.)	DENSITY (C/ML)	1/Q P	1/Q S
26.6	1.460	0.000	1.03	0.00000	0.00000
10.0	1.600	0.010	1.65	0.00100	0.01000
59.9	1.770	0.250	2.00	0.00100	0.03000
	3.500	2.000	1.98	0.00100	0.03000

-P LAYER 1-   P = 1.60   NO. 496

-P LAYER 1-   P = 1.70   NO. 496

Fig. 9.78b. Simple 2-layered structure.

Variation of the p-velocity in the upper layer of a 2-layer structure does not produce models resembling the field record.

THICKNESS (M.)	P-VELOCITY (M/S.)	S-VELOCITY (M/S.)	DENSITY (G/ML)	1/Q P	1/Q S
26.6	1.460	0.000	1.03	0.00000	0.00000
10.0	1.900	0.010	1.65	0.00100	0.01000
58.9	1.770	0.250	2.00	0.00100	0.03000
	3.500	2.000	1.98	0.00100	0.03000

Fig. 9.78c. Simple 2-layered structure.

Variation of the p-velocity in the upper layer of a 2-layer structure does not produce models resembling the field record.

THICKNESS (M.)	P-VELOCITY (M/S.)	S-VELOCITY (M/S.)	DENSITY (G/ML)	1/Q P	1/Q S
26.6	1.460	0.000	1.03	0.00000	0.00000
10.9	2.300	0.010	1.65	0.00100	0.01000
58.9	1.770	0.250	2.00	0.00100	0.03000
	3.500	2.000	1.98	0.00100	0.03000

-P LAYER 1-   P = 2.3   NO. 496

-P LAYER 1-   P = 2.5   NO. 496

Fig. 9.78d.   Simple 2-layered structure.

Variation of the p-velocity in the upper layer of a 2-layer structure does not produce models resembling the field record.

Fig. 9.79a.   Simple 2-layered structure.

Low p-velocity in the topmost layer does not lead to any improvement.

THICKNESS (M.)	P-VELOCITY (M/S.)	S-VELOCITY (M/S.)	DENSITY (G/ML)	1/Q P	1/Q S
26.6	1.460	0.000	1.03	0.00000	0.00000
10.0	1.000	0.910	1.65	0.00100	0.01000
59.9	1.770	0.250	2.00	0.00100	0.03000
	3.500	2.000	1.98	0.00100	0.03000

—VERY LOW VELOS. IN LY 1 P=1.0 NO.496

—VERY LOW VELOS. IN LY 1 P=1.2 NO.496
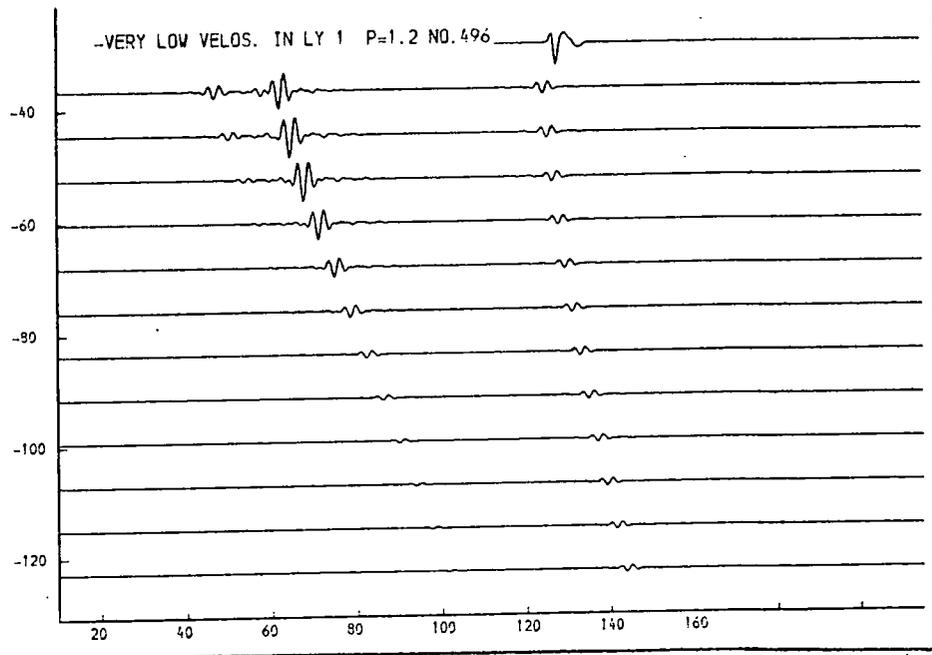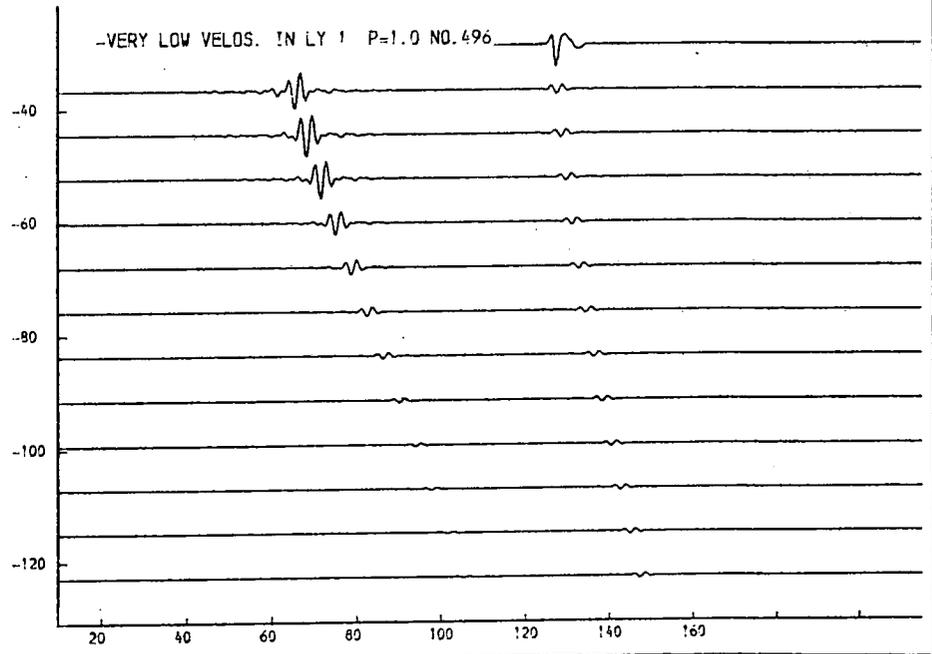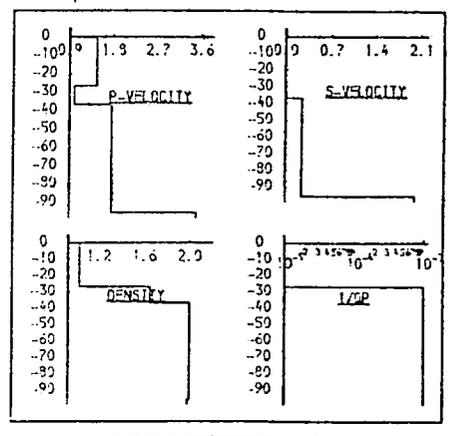
Fig. 9.79b. Simple 2-layered structure.

Low p-velocity in the topmost layer does not lead to any improvement.

THICKNESS (M.)	P-VELOCITY (M/S.)	S-VELOCITY (M/S.)	DENSITY (G/ML)	1/Q P	1/Q S
26.6	1.460	0.000	1.03	0.00000	0.00000
10.0	1.490	0.010	1.30	0.00300	0.01000
53.9	1.770	0.250	2.00	0.00300	0.03000
	3.500	2.000	1.98	0.03000	0.06000

-DENSITY LAYER 1- RHO=1.3 NO. 496

-DENSITY LAYER 1- RHO=1.45 NO. 496

Fig. 9.80a.   Simple 2-layered structure.

Density variation in the upper layer of a two-layer structure does not produce a better result.

THICKNESS (M.)	P-VELOCITY (M/S.)	S-VELOCITY (M/S.)	DENSITY (G/ML)	1/Q P	1/Q S
26.6	1.460	0.000	1.03	0.00000	0.00000
10.0	1.480	0.010	1.60	0.00300	0.01000
59.3	1.770	0.250	2.00	0.00300	0.03000
	3.500	2.000	1.98	0.03000	0.06000

-DENSITY LAYER 1- RHO=1.6 NO. 496

-DENSITY LAYER 1- RHO=1.7 NO. 496
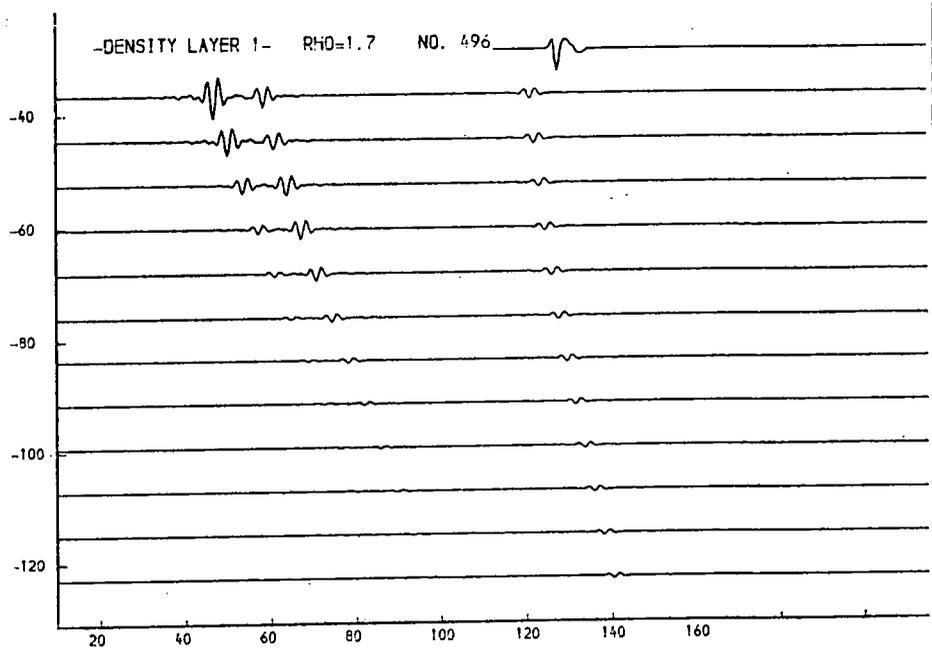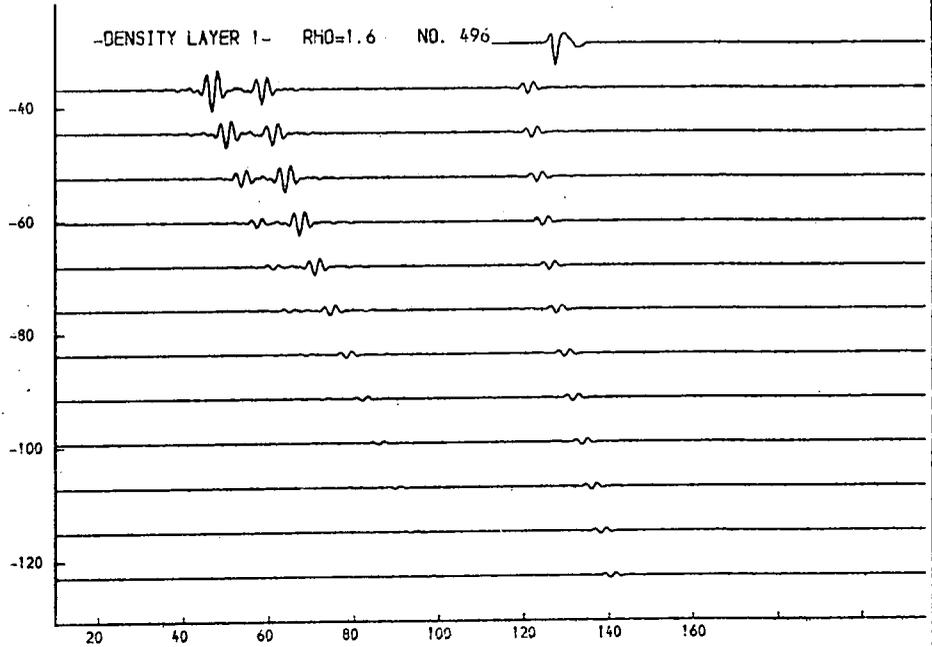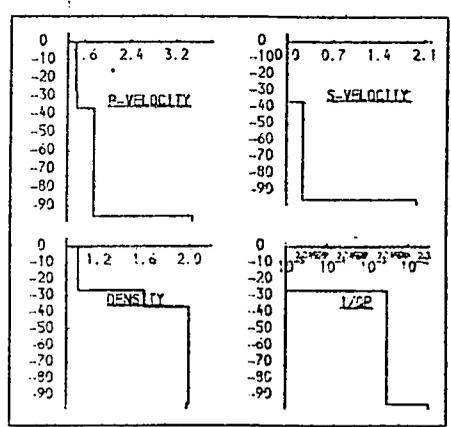
Fig. 9.80b. Simple 2-layered structure.

Density variation in the upper layer of a two-layer structure does not produce a better result.

THICKNESS (M.)	P-VELOCITY (M/S.)	S-VELOCITY (M/S.)	DENSITY (G/ML)	1/Q P	1/Q S
26.6	1.460	0.000	1.03	0.00000	0.00000
10.0	1.490	0.010	1.65	0.00100	0.01000
43.2	1.300	0.250	2.00	0.00100	0.03000
	3.500	2.000	1.98	0.00100	0.03000

P-VELOCITY .6 2.4 3.2

S-VELOCITY 0 0.7 1.4 2.1

DENSITY 1.2 1.6 2.0

1/Q

-P LAYER 2-   P = 1.30   NO. 496

-P LAYER 2-   P = 1.50   NO. 496

P-VELOCITY .6 2.4 3.2

S-VELOCITY 0 0.7 1.4 2.1

DENSITY 1.2 1.6 2.0

1/QP
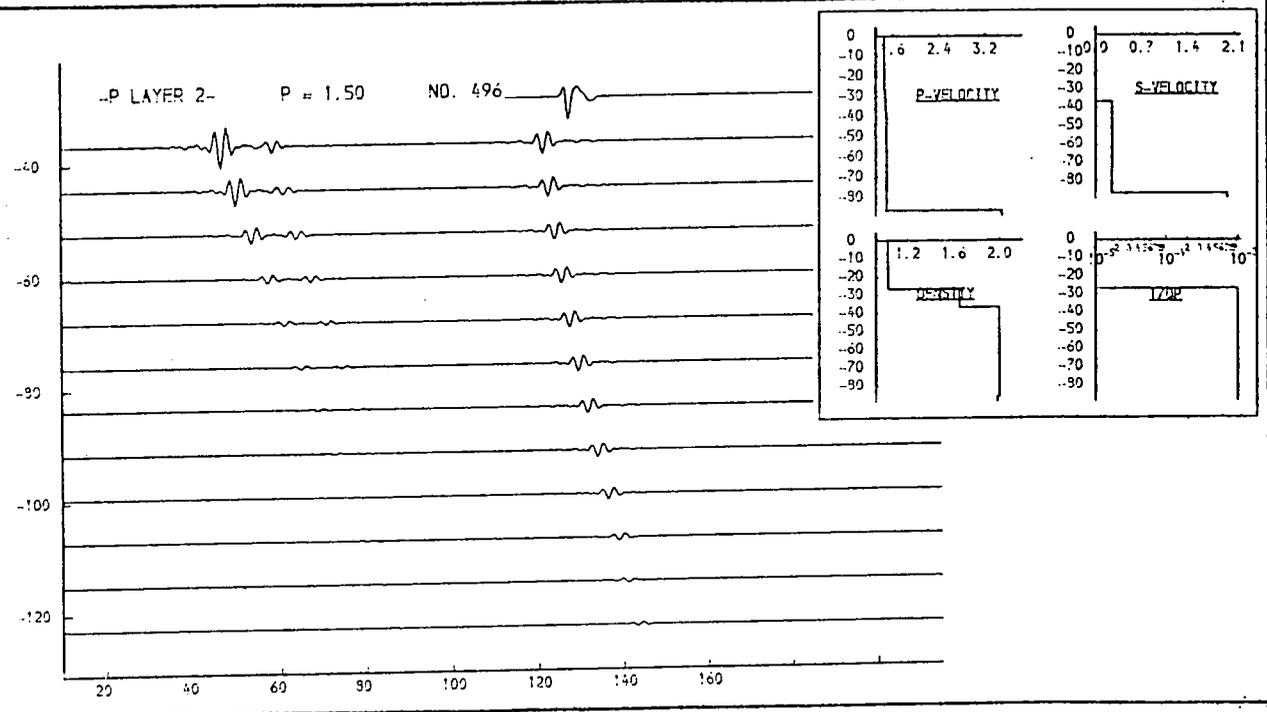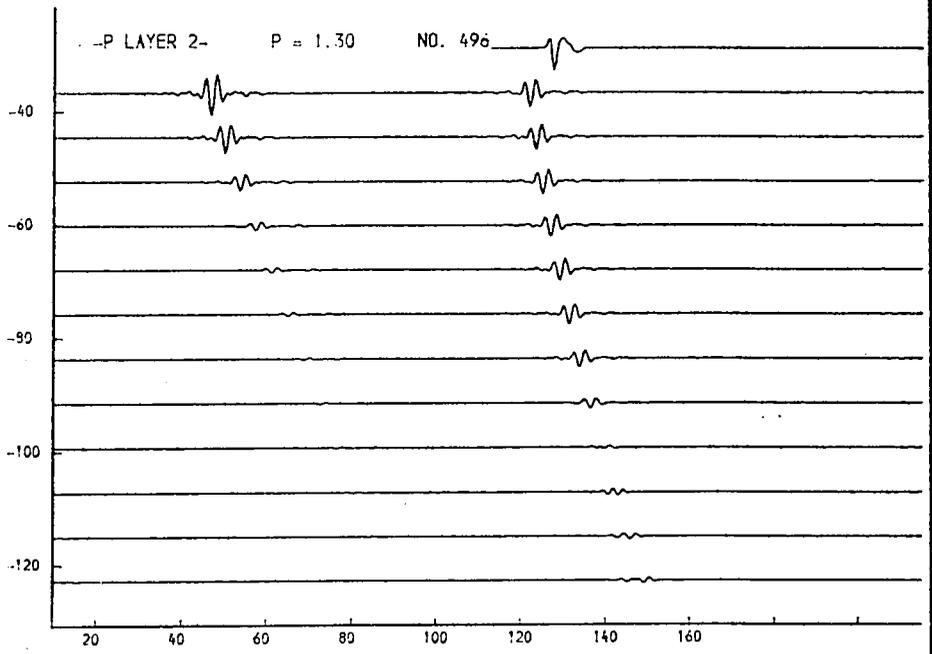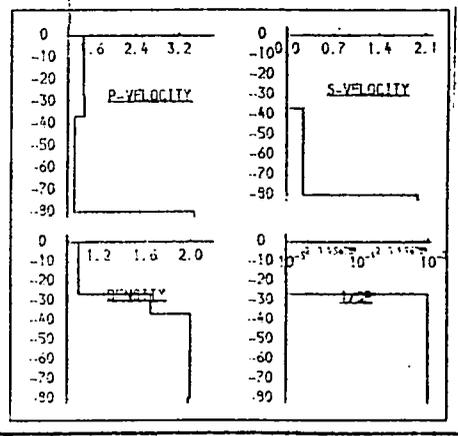
Fig. 9.81a.   Simple 2-layered structure.

Low values for the p-velocity in layer 2 do not bring about an improvement.

-P LAYER 2-   P = 1.90   NO. 496

-P LAYER 2-   P = 2.1   NO. 496
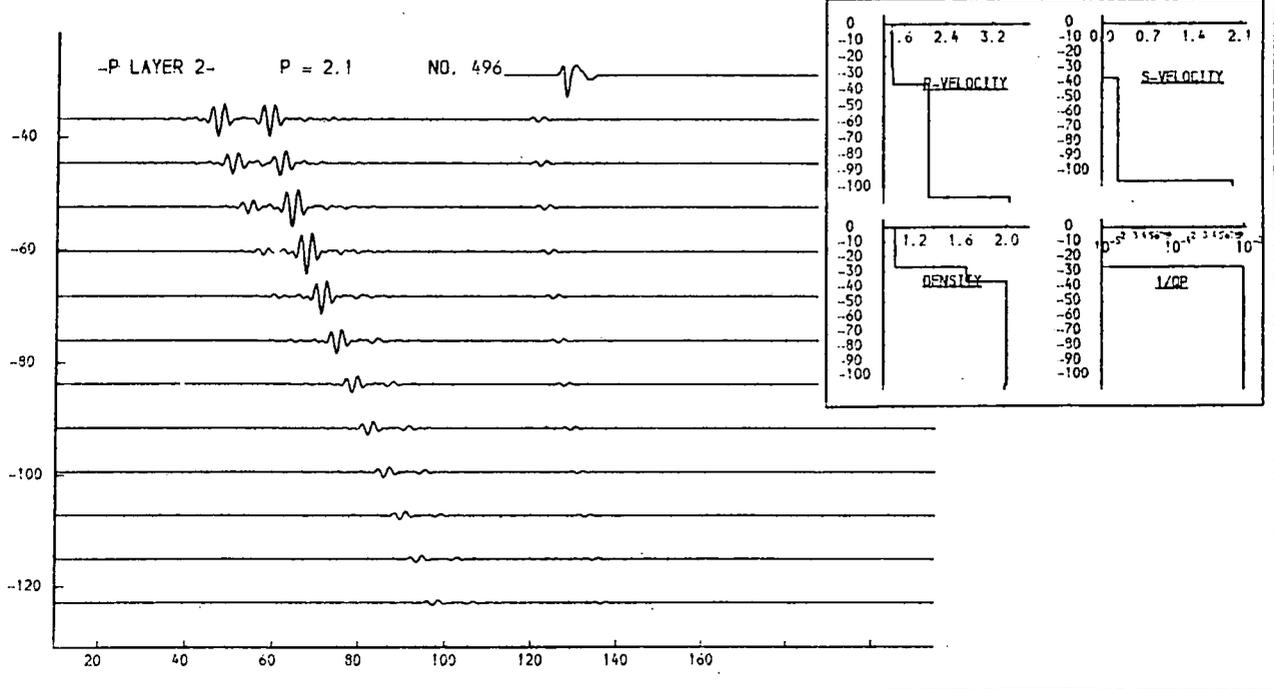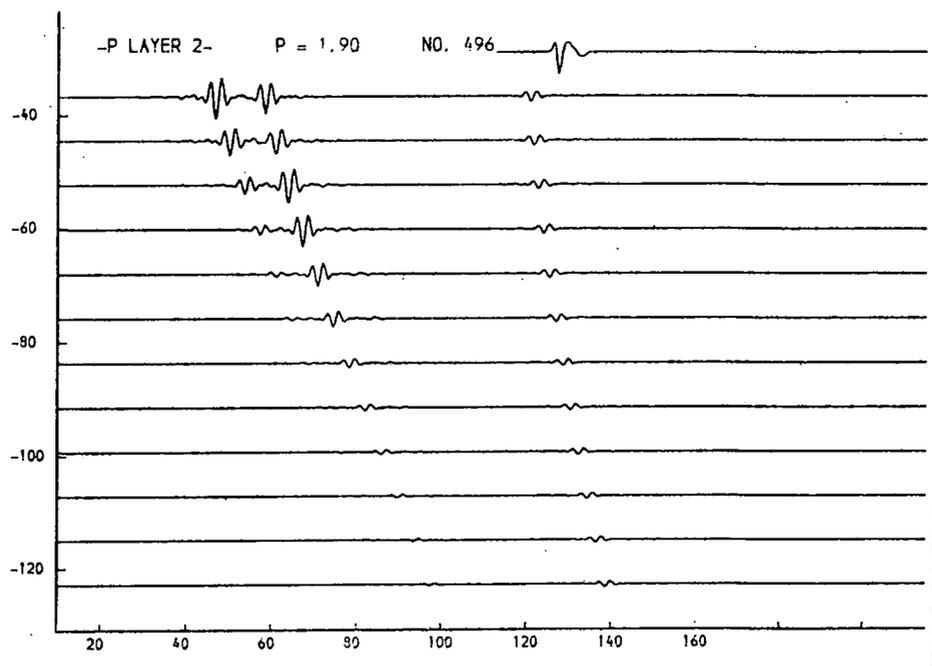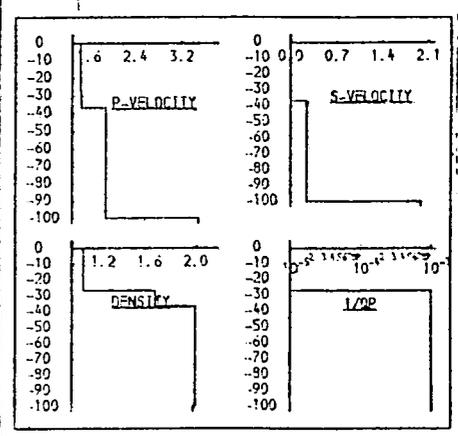
Fig. 9.81b.   Simple 2-layered structure.

Higher values for the p-velocity in layer 2 still give a poor fit, but do show that some acoustic energy can be re-directed towards the receivers at higher offset.

THICKNESS (M.)	P-VELOCITY (M/S.)	S-VELOCITY (M/S.)	DENSITY (G/ML)	1/Q P	1/Q S
26.6	1.460	0.000	1.03	0.00000	0.00000
10.0	1.480	0.010	1.65	0.00100	0.01000
58.9	1.500	0.010	2.00	0.00100	0.03000
	3.500	2.000	1.98	0.00100	0.03000

-S & P LAYER 2 P=1.5 S=0.01 NO. 496

-S & P LAYER 2 P=1.65 S=.15 NO. 496
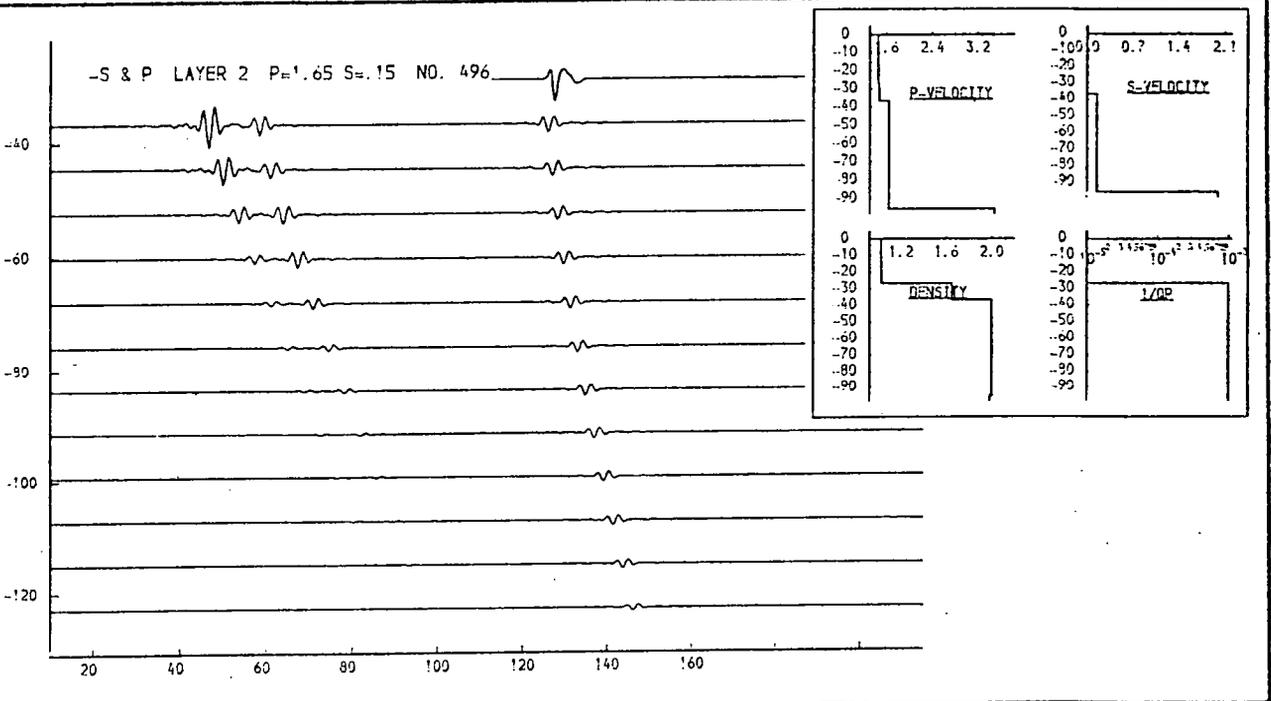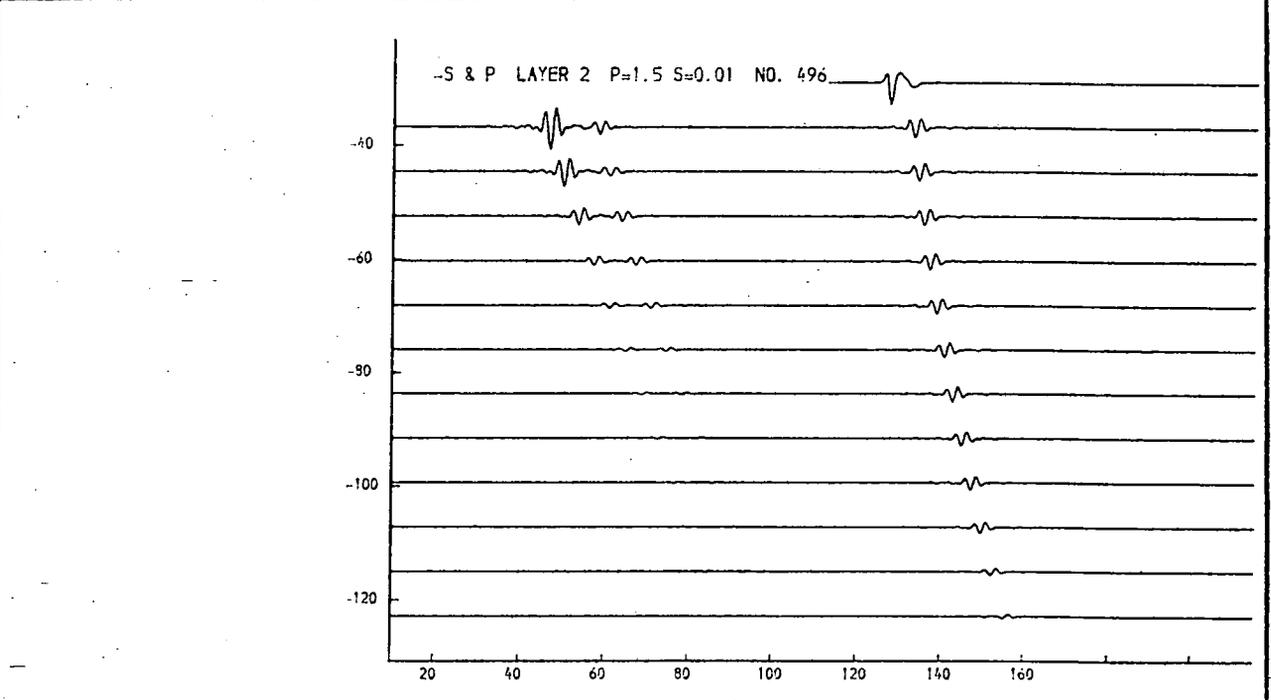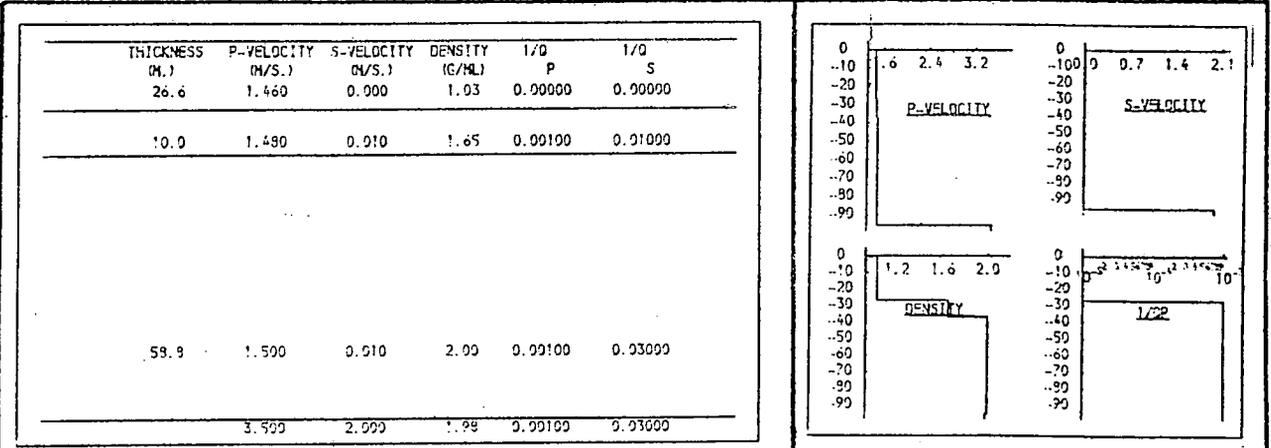
Fig. 9.82a. Simple 2-layered structure.

Variation of *p* and s-velocity together in layer 2 again produces poor models.

THICKNESS (M.)	P-VELOCITY (M/S.)	S-VELOCITY (M/S.)	DENSITY (G/ML)	1/Q P	1/Q S
26.6	1.460	0.000	1.03	0.00000	0.00000
10.0	1.480	0.010	1.65	0.00100	0.01000
59.9	1.950	0.300	2.00	0.00100	0.03000
	3.500	2.000	1.99	0.00100	0.03000

−S & P LAYER 2 P=1.95 S=0.3 NO. 496

−S & P LAYER 2 P=2.0 S=0.7 NO. 496

Fig. 9.82b. Simple 2-layered structure.

Variation of p and s-velocity together in layer 2 again produces poor models.

THICKNESS (M.)	P-VELOCITY (M/S.)	S-VELOCITY (M/S.)	DENSITY (G/ML)	1/Q P	1/Q S		THICKNESS (M.)	P-VELOCITY (M/S.)	S-VELOCITY (M/S.)	DENSITY (G/ML)	1/Q P	1/Q S
26.6	1.460	0.000	1.03	0.00000	0.00000		26.6	1.460	0.000	1.03	0.00000	0.00000
10.0	1.480	0.010	1.65	0.00100	0.01000		10.0	1.480	0.010	1.65	0.00100	0.01000
7.2	1.726	0.244	2.00	0.00100	0.03000		7.1	1.704	0.241	2.00	0.00100	0.03000
7.2	1.739	0.246	2.00	0.00100	0.03000		7.2	1.723	0.243	2.00	0.00100	0.03000
7.3	1.751	0.247	2.00	0.00100	0.03000		7.2	1.742	0.246	2.00	0.00100	0.03000
7.3	1.764	0.249	2.00	0.00100	0.03000		7.3	1.761	0.249	2.00	0.00100	0.03000
7.4	1.776	0.251	2.00	0.00100	0.03000		7.4	1.779	0.251	2.00	0.00100	0.03000
7.4	1.789	0.253	2.00	0.00100	0.03000		7.4	1.798	0.254	2.00	0.00100	0.03000
7.5	1.801	0.254	2.00	0.00100	0.03000		7.5	1.817	0.257	2.00	0.00100	0.03000
7.5	1.814	0.256	2.00	0.00100	0.03000		7.6	1.836	0.259	2.00	0.00100	0.03000
	3.500	2.000	1.98	0.00100	0.03000			3.500	2.000	1.98	0.00100	0.03000
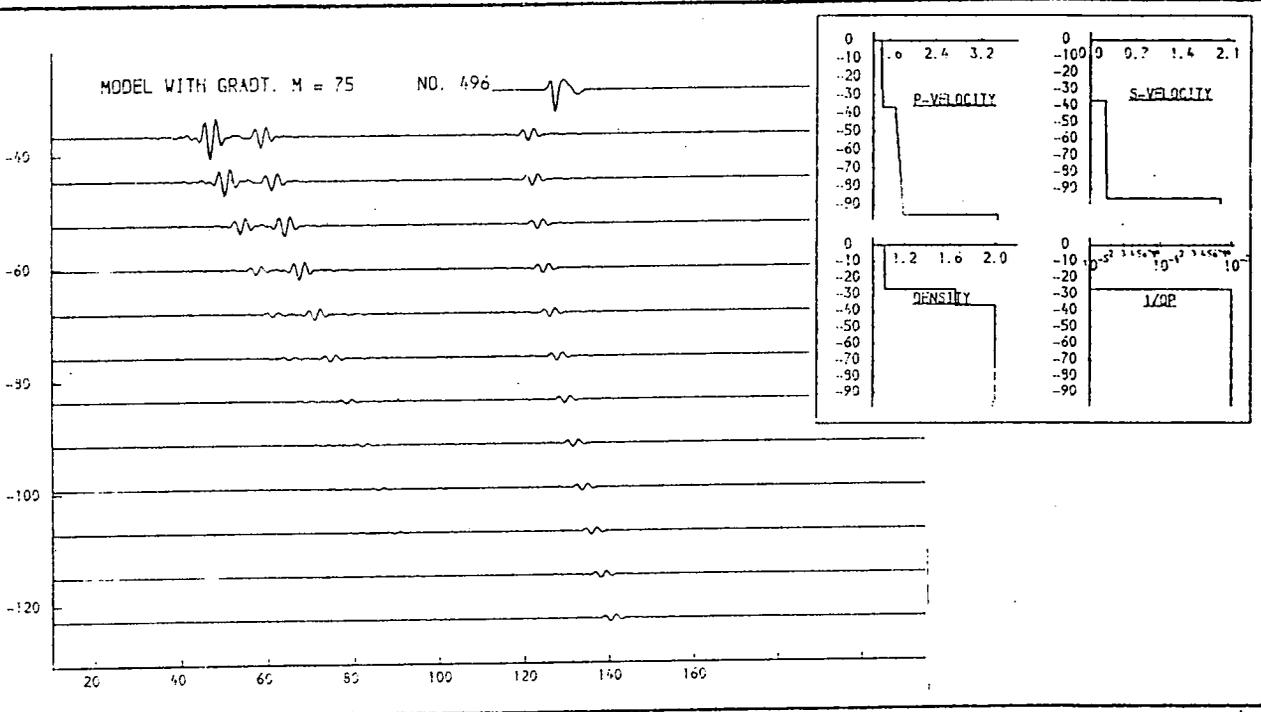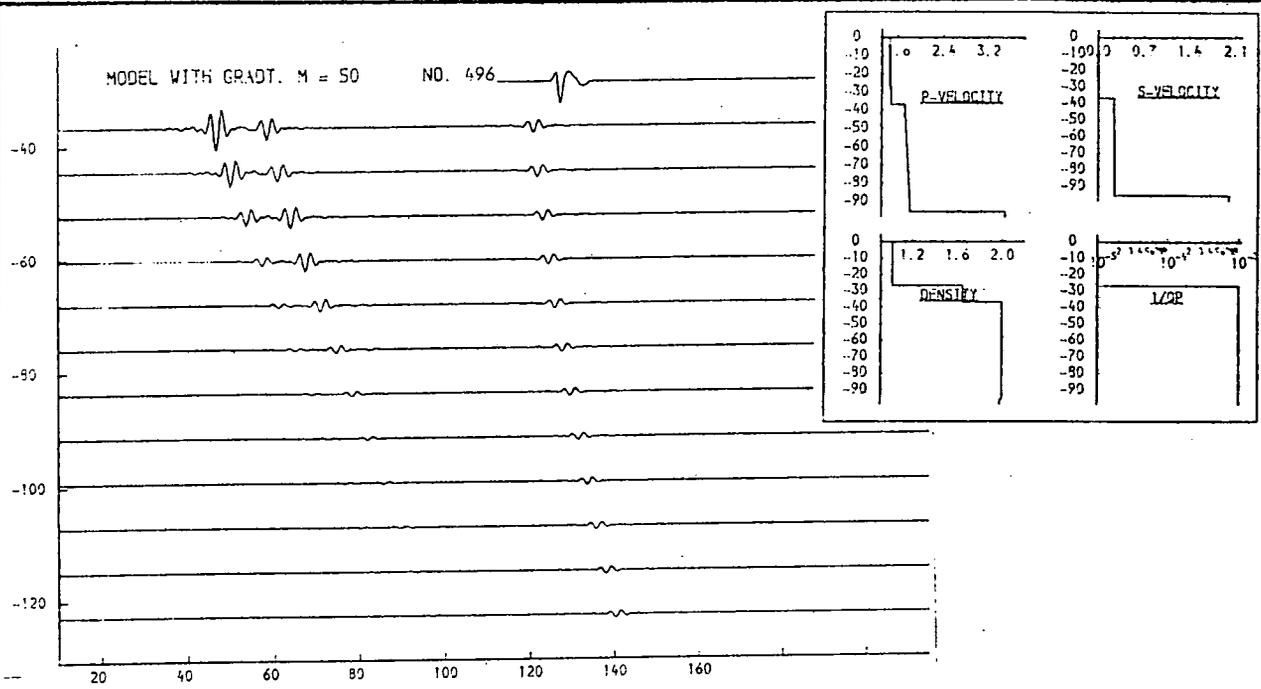
Fig. 9.83a. Layered model with gradients.

Variation of the p-velocity gradient. Gradient is upper figure ca. 1.5m/s/m.; in lower figure ca. 2.0m/s/m.

THICKNESS (M.)	P-VELOCITY (M/S.)	S-VELOCITY (M/S.)	DENSITY (G/ML)	1/Q P	1/Q S	THICKNESS (M.)	P-VELOCITY (M/S.)	S-VELOCITY (M/S.)	DENSITY (G/ML)	1/Q P	1/Q S
26.6	1.460	0.000	1.03	0.00000	0.00000	26.6	1.460	0.000	1.03	0.00000	0.00000
10.0	1.480	0.010	1.65	0.00100	0.01000	10.0	1.480	0.010	1.65	0.00100	0.01000
7.0	1.682	0.238	2.00	0.00100	0.03000	6.6	1.595	0.225	2.00	0.00100	0.03000
7.1	1.708	0.241	2.00	0.00100	0.03000	6.8	1.645	0.232	2.00	0.00100	0.03000
7.2	1.733	0.245	2.00	0.00100	0.03000	7.0	1.695	0.239	2.00	0.00100	0.03000
7.3	1.757	0.249	2.00	0.00100	0.03000	7.2	1.745	0.246	2.00	0.00100	0.03000
7.4	1.783	0.252	2.00	0.00100	0.03000	7.4	1.795	0.254	2.00	0.00100	0.03000
7.5	1.807	0.255	2.00	0.00100	0.03000	7.7	1.845	0.261	2.00	0.00100	0.03000
7.6	1.833	0.259	2.00	0.00100	0.03000	7.9	1.895	0.268	2.00	0.00100	0.03000
7.7	1.858	0.262	2.00	0.00100	0.03000	8.1	1.945	0.275	2.00	0.00100	0.03000
	3.500	2.000	1.98	0.00100	0.03000		3.500	2.000	1.98	0.00100	0.03000
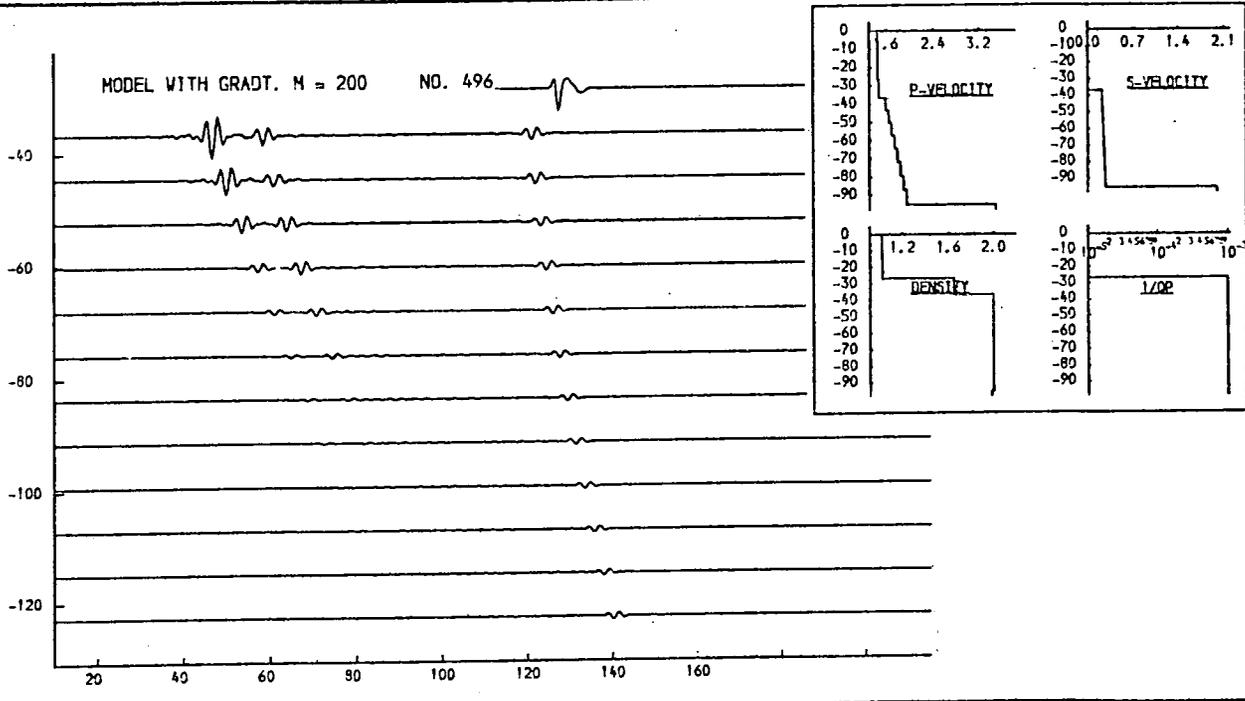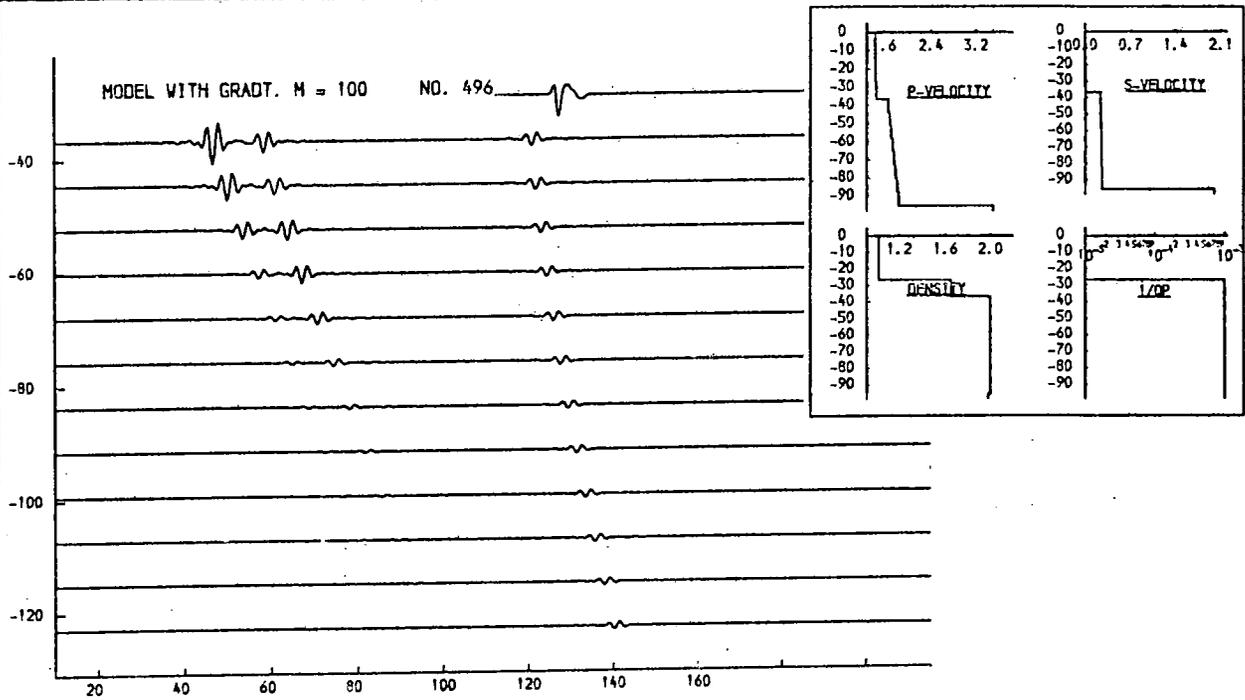
Fig. 9.83b. Layered model with gradients.

Variation of the p-velocity gradient. Gradient is upper figure ca. 2.5m/s/m.; in lower figure ca. 5.0m/s/m.

THICKNESS (M.)	P-VELOCITY (M/S.)	S-VELOCITY (M/S.)	DENSITY (G/ML)	1/Q P	1/Q S
26.6	1.460	0.000	1.03	0.00000	0.00000
1.0	0.000	0.019	1.65	0.02000	0.04050
7.6	1.551	0.219	2.00	0.00300	0.03000
7.9	1.614	0.228	2.00	0.00300	0.03000
8.2	1.676	0.237	2.00	0.00300	0.03000
8.5	1.739	0.246	2.00	0.00300	0.03000
8.9	1.801	0.254	2.00	0.00300	0.03000
9.2	1.864	0.263	2.00	0.00300	0.03000
9.5	1.926	0.272	2.00	0.00300	0.03000
9.8	1.989	0.281	2.00	0.00300	0.03000
	3.500	2.000	1.98	0.03000	0.06000

-P- LAYER 1   P = 0.80   NO. 496

-P- LAYER 1   P = 1.10   NO. 496
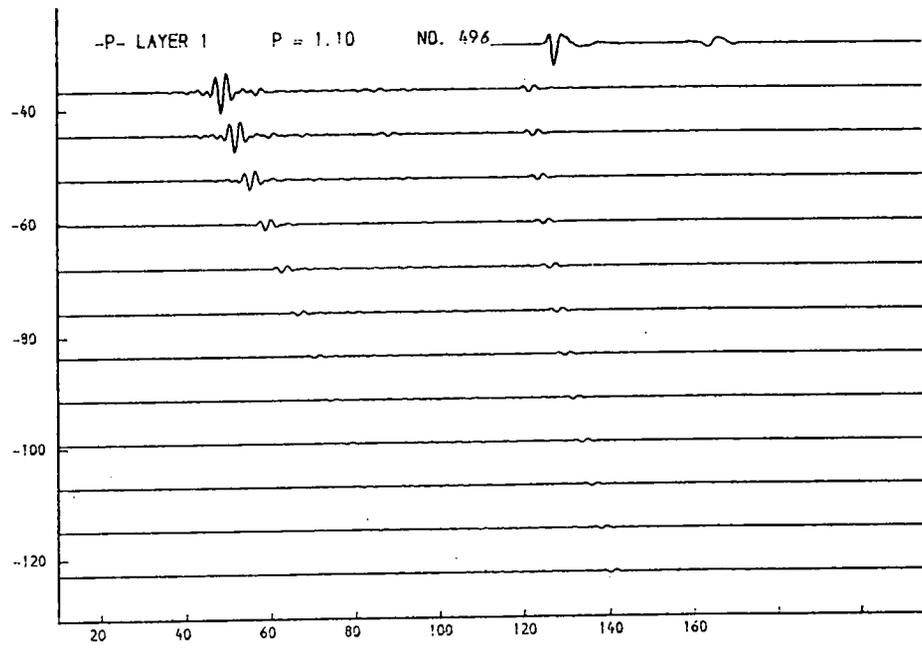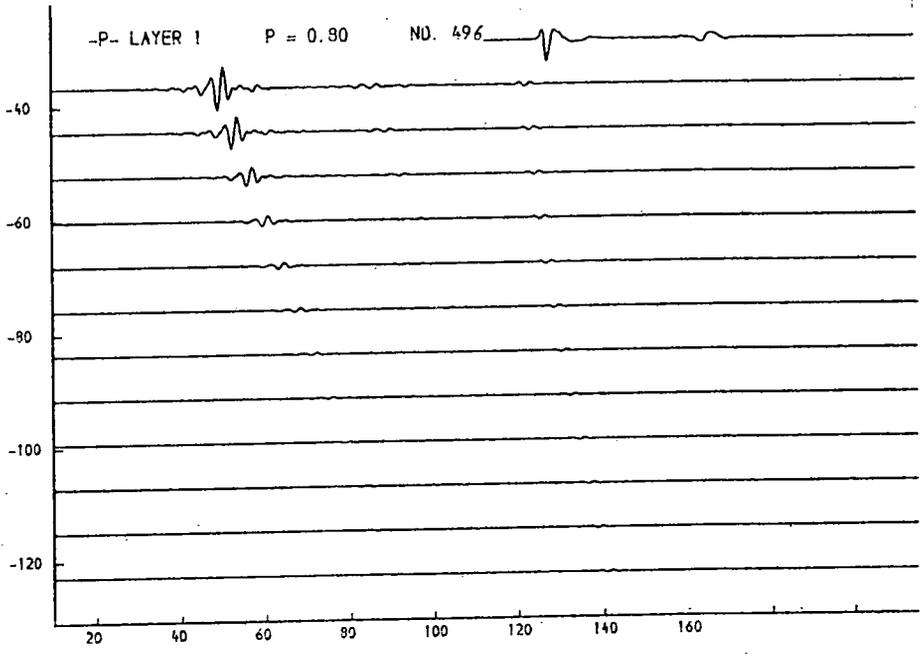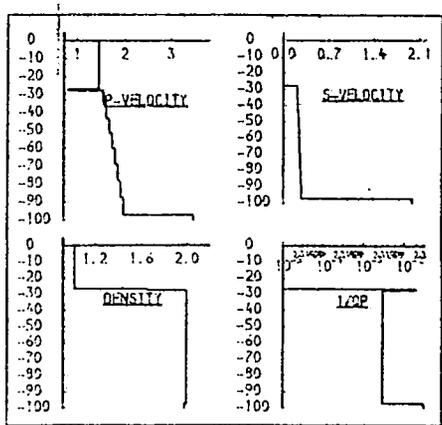
Fig. 9.84a. P-velocity, surficial layer above gradient.

Variation of the p-velocity in a surficial layer overlying a simple gradient of ca. 6m/sec/m.

THICKNESS (M.)	P-VELOCITY (M/S.)	S-VELOCITY (M/S.)	DENSITY (G/ML)	1/Q P	1/Q S
26.6	1.460	0.000	1.03	0.00000	0.00000
1.0	1.700	0.010	1.05	0.00300	0.01000
7.6	1.551	0.219	2.00	0.00300	0.03000
7.9	1.614	0.228	2.00	0.00300	0.03000
8.2	1.676	0.237	2.00	0.00300	0.03000
8.5	1.739	0.246	2.00	0.00300	0.03000
8.9	1.801	0.254	2.00	0.00300	0.03000
9.2	1.864	0.263	2.00	0.00300	0.03000
9.5	1.926	0.272	2.00	0.00300	0.03000
9.9	1.989	0.281	2.00	0.00300	0.03000
	3.500	2.000	1.99	0.03000	0.06000

Fig. 9.84b. P-velocity, surficial layer above gradient.

Variation of the p-velocity in a surficial layer overlying a simple gradient of ca. 6m/sec/m.

THICKNESS (M.)	P-VELOCITY (M/S.)	S-VELOCITY (M/S.)	DENSITY (G/ML)	1/Q P	1/Q S
26.6	1.460	0.000	1.03	0.00000	0.00000
	1.430	0.010		0.03000	0.04000
7.6	1.551	0.219	2.00	0.00300	0.03000
7.9	1.614	0.228	2.00	0.00300	0.03000
8.2	1.676	0.237	2.00	0.00300	0.03000
8.5	1.732	0.246	2.00	0.00300	0.03000
8.9	1.901	0.254	2.00	0.00300	0.03000
9.2	1.964	0.263	2.00	0.00300	0.03000
9.5	1.926	0.272	2.00	0.00300	0.03000
9.9	1.989	0.281	2.00	0.00300	0.03000
	3.500	2.000	1.99	0.03000	0.06000
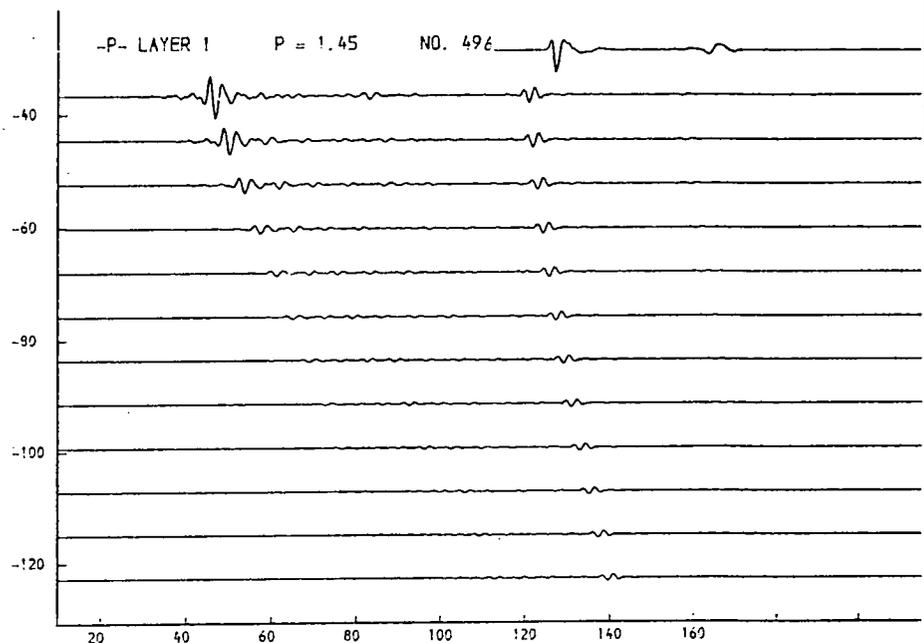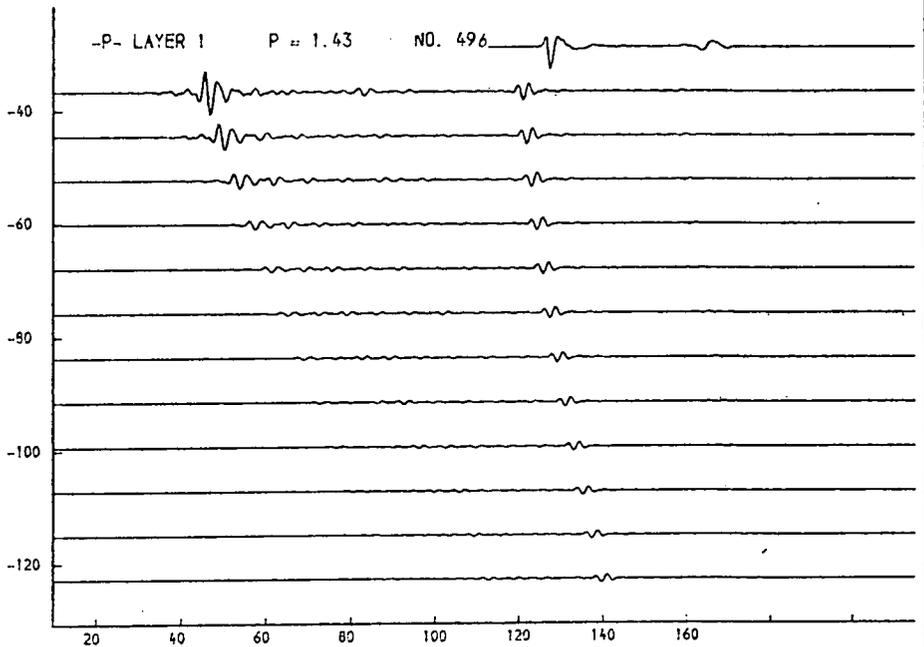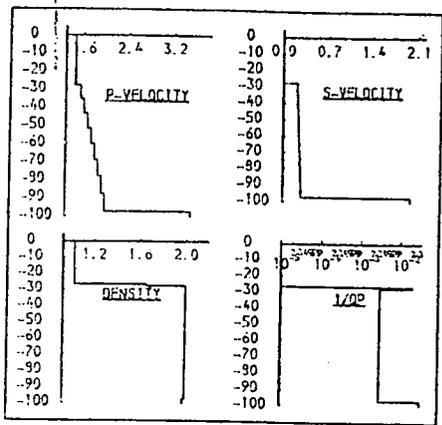
Fig. 9.84c.   P-velocity, surficial layer above gradient.

Variation of the p-velocity in a surficial layer overlying a simple gradient of ca. 6m/sec/m.

THICKNESS (M.)	P-VELOCITY (M/S.)	S-VELOCITY (M/S.)	DENSITY (G/ML)	1/Q P	1/Q S
26.6	1.460	0.000	1.03	0.00000	0.00000
1.0	1.480	0.010	1.05	0.03000	0.01000
7.6	1.551	0.219	2.00	0.00300	0.03000
7.9	1.614	0.228	2.00	0.00300	0.03000
8.2	1.676	0.237	2.00	0.00300	0.03000
8.5	1.739	0.246	2.00	0.00300	0.03000
8.9	1.801	0.254	2.00	0.00300	0.03000
9.2	1.864	0.263	2.00	0.00300	0.03000
9.5	1.926	0.272	2.00	0.00300	0.03000
9.9	1.989	0.291	2.00	0.00300	0.03000
	3.500	2.000	1.98	0.03000	0.06000

Fig. 9.84d. P-velocity, surficial layer above gradient.

Variation of the p-velocity in a surficial layer overlying a simple gradient of ca. 6m/sec/m.

THICKNESS (M.)	P-VELOCITY (M/S.)	S-VELOCITY (M/S.)	DENSITY (G/ML)	1/Q P	1/Q S
26.6	1.460	0.000	1.03	0.00000	0.00000
0.2	1.480	0.010	1.60	0.03000	0.01000
7.6	1.551	0.219	1.90	0.00300	0.03000
7.9	1.614	0.228	1.90	0.00300	0.03000
8.2	1.676	0.237	1.90	0.00300	0.03000
8.5	1.739	0.246	1.90	0.00300	0.03000
9.0	1.901	0.254	1.90	0.00300	0.03000
9.2	1.964	0.263	1.90	0.00300	0.03000
9.5	1.926	0.272	1.90	0.00300	0.03000
9.9	1.989	0.281	1.90	0.00300	0.03000
3.500	2.000	1.09	0.03000	0.06000	

-THICKNESS LAYER 1- H = 0.25 NO. 496

-THICKNESS LAYER 1- H = 0.5 NO. 496

Fig. 9.85a.   Thickness of surficial layer above gradient.

The thickness of a possible surficial layer of sediment having a velocity about the same as the bottom water is varied from 0.25 to 3.0 metres as indicated by the values for "H" given in the seismogramme header.

THICKNESS (M.)	P-VELOCITY (M/S.)	S-VELOCITY (M/S.)	DENSITY (G/ML)	1/Q P	1/Q S
26.6	1.460	0.000	1.03	0.00000	0.00000
0.7	1.480	0.010	1.60	0.03000	0.04000
7.6	1.551	0.219	1.90	0.00300	0.03000
7.9	1.614	0.229	1.90	0.00300	0.03000
8.2	1.676	0.237	1.90	0.00300	0.03000
8.5	1.739	0.246	1.90	0.00300	0.03000
8.9	1.901	0.254	1.90	0.00300	0.03000
9.2	1.964	0.263	1.90	0.00300	0.03000
9.5	1.926	0.272	1.90	0.00300	0.03000
9.9	1.989	0.281	1.90	0.00300	0.03000
	3.500	2.000	1.98	0.03000	0.06000

Fig. 9.85b. Thickness of surficial layer above gradient.

The thickness of a possible surficial layer of sediment having a velocity about the same as the bottom water is varied from 0.25 to 3.0 metres as indicated by the values for "H" given in the seismogramme header.

Fig. 9.85c. Thickness of surficial layer above gradient.

The thickness of a possible surficial layer of sediment having a velocity about the same as the bottom water is varied from 0.25 to 3.0 metres as indicated by the values for "H" given in the seismogramme header.

THICKNESS (M.)	P-VELOCITY (M/S.)	S-VELOCITY (M/S.)	DENSITY (G/ML)	1/Q P	1/Q S
26.6	1.460	0.000	1.03	0.00000	0.00000
	1.496	0.010	1.60	0.00000	0.00000
7.6	1.551	0.219	1.90	0.00300	0.03000
7.9	1.614	0.229	1.90	0.00300	0.03000
8.2	1.676	0.237	1.90	0.00300	0.03000
8.5	1.739	0.246	1.90	0.00300	0.03000
8.9	1.901	0.254	1.90	0.00300	0.03000
9.2	1.964	0.263	1.90	0.00300	0.03000
9.5	1.926	0.272	1.90	0.00300	0.03000
9.9	1.989	0.281	1.90	0.00300	0.03000
	3.500	2.000	1.98	0.03000	0.06000

Fig. 9.85d.   Thickness of surficial layer above gradient.

The thickness of a possible surficial layer of sediment having a
velocity about the same as the bottom water is varied from 0.25
to 3.0 metres as indicated by the values for "H" given in the
seismogramme header.

THICKNESS (M.)	P-VELOCITY (M/S.)	S-VELOCITY (M/S.)	DENSITY (G/ML)	1/Q P	1/Q S
26.6	1.460	0.000	1.03	0.00000	0.00000
7.7	1.494	0.210	1.85	0.02000	0.06000
7.6	1.501	0.219	1.80	0.00300	0.03000
7.9	1.584	0.228	1.94	0.00300	0.03000
8.2	1.676	0.237	1.98	0.00300	0.03000
8.5	1.739	0.246	1.91	0.00300	0.03000
8.9	1.901	0.254	1.94	0.00300	0.03000
9.2	1.964	0.263	1.96	0.00300	0.03000
9.5	1.926	0.272	1.98	0.00300	0.03000
9.9	1.989	0.281	2.00	0.00300	0.03000
	3.500	2.000	1.98	0.03000	0.06000

Fig. 9.85e.   Thickness of surficial layer above gradient.

The thickness of a possible surficial layer of sediment having a velocity about the same as the bottom water is varied from 0.25 to 3.0 metres as indicated by the values for "H" given in the seismogramme header.

THICKNESS (M.)	P-VELOCITY (M/S.)	S-VELOCITY (M/S.)	DENSITY (G/ML)	1/Q P	1/Q S
26.6	1.460	0.000	1.03	0.00000	0.00000
0.5	1.700	0.010	1.40	0.03000	0.01000
7.6	1.551	0.219	1.90	0.00300	0.03000
7.9	1.614	0.228	1.90	0.00300	0.03000
8.2	1.676	0.237	1.90	0.00300	0.03000
8.5	1.739	0.246	1.90	0.00300	0.03000
8.9	1.901	0.254	1.90	0.00300	0.03000
9.2	1.964	0.263	1.90	0.00300	0.03000
9.5	1.926	0.272	1.90	0.00300	0.03000
9.9	1.989	0.281	1.90	0.00300	0.03000
	3.500	2.000	1.99	0.03000	0.06000

Fig. 9.86a.   Thickness of surficial layer above gradient.

The possibility of a surficial layer having a low velocity is investigated.   Thickness is varied from 0.25 to 2.0 metres.

THICKNESS (M.)	P-VELOCITY (M/S.)	S-VELOCITY (M/S.)	DENSITY (G/ML)	1/Q P	1/Q S
26.6	1.460	0.000	1.03	0.00000	0.00000
0.2	1.500	0.010	1.60	0.03000	0.06000
7.6	1.551	0.219	1.90	0.00300	0.03000
7.9	1.614	0.228	1.90	0.00300	0.03000
8.2	1.676	0.237	1.90	0.00300	0.03000
8.5	1.739	0.246	1.90	0.00300	0.03000
8.9	1.801	0.254	1.90	0.00300	0.03000
9.2	1.864	0.263	1.90	0.00300	0.03000
9.5	1.926	0.272	1.90	0.00300	0.03000
9.9	1.989	0.281	1.90	0.00300	0.03000
	3.500	2.000	1.99	0.03000	0.06000

-THICKNESS LAYER 1- H = 0.75 NO. 496

-THICKNESS LAYER 1- H = 1.0 NO. 496
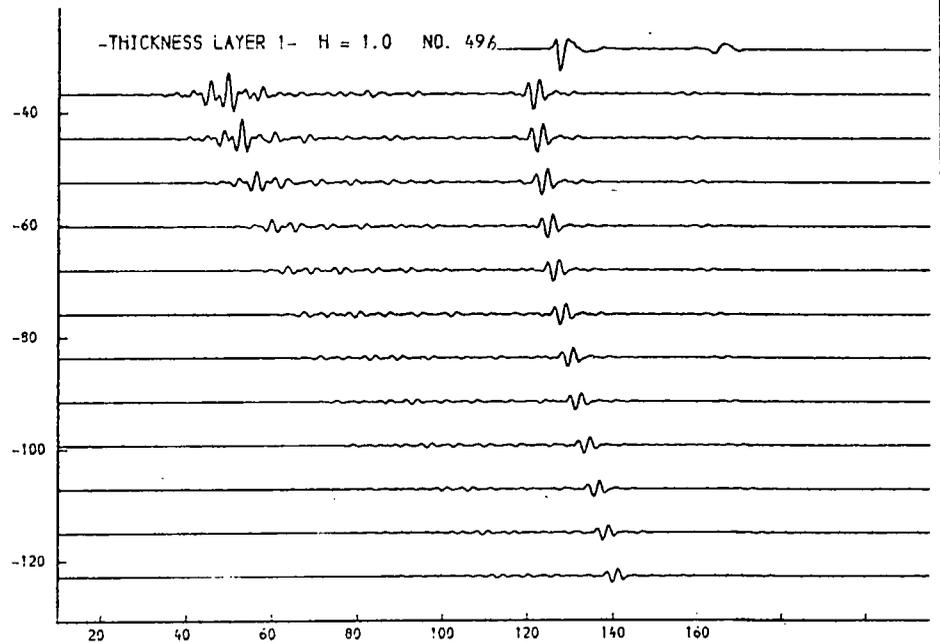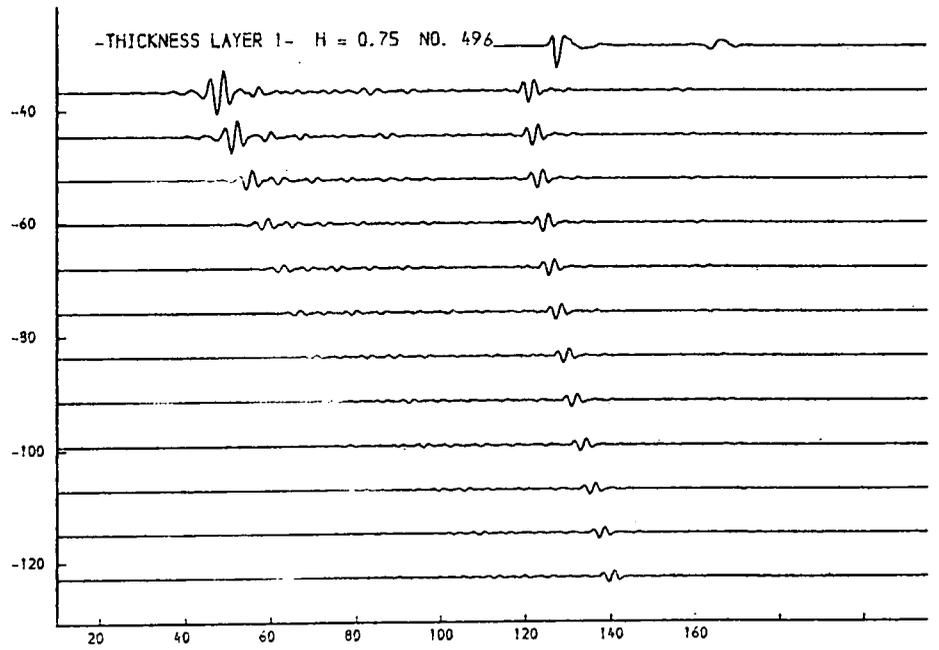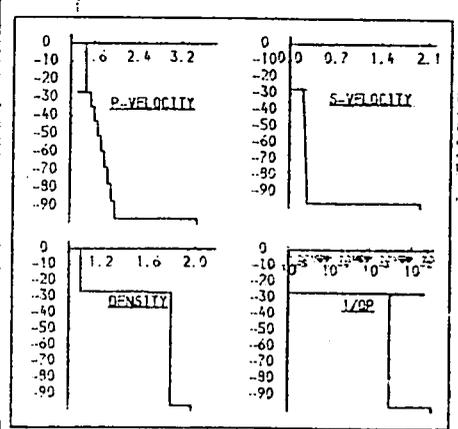
Fig. 9.86b.   Thickness of surficial layer above gradient.

The possibility of a surficial layer having a low velocity is investigated. Thickness is varied from 0.25 to 2.0 metres.

THICKNESS (H.)	P-VELOCITY (M/S.)	S-VELOCITY (M/S.)	DENSITY (G/ML)	1/Q P	1/Q S
26.6	1.460	0.000	1.03	0.00000	0.00000
7.6	1.551	0.219	1.90	0.00300	0.03000
7.9	1.614	0.229	1.94	0.00300	0.03000
8.2	1.676	0.237	1.99	0.00300	0.03000
8.5	1.739	0.246	1.91	0.00300	0.03000
8.9	1.801	0.254	1.94	0.00300	0.03000
9.2	1.864	0.263	1.96	0.00300	0.03000
9.5	1.926	0.272	1.93	0.00300	0.03000
9.9	1.989	0.291	2.00	0.00300	0.03000
	3.500	2.000	1.93	0.03000	0.06000

-THICKNESS LAYER 1- H = 1.25 NO. 496

P-VELOCITY   S-VELOCITY   DENSITY   1/QP

-THICKNESS LAYER 1- H = 1.50 NO. 496

P-VELOCITY   S-VELOCITY   DENSITY   1/QP
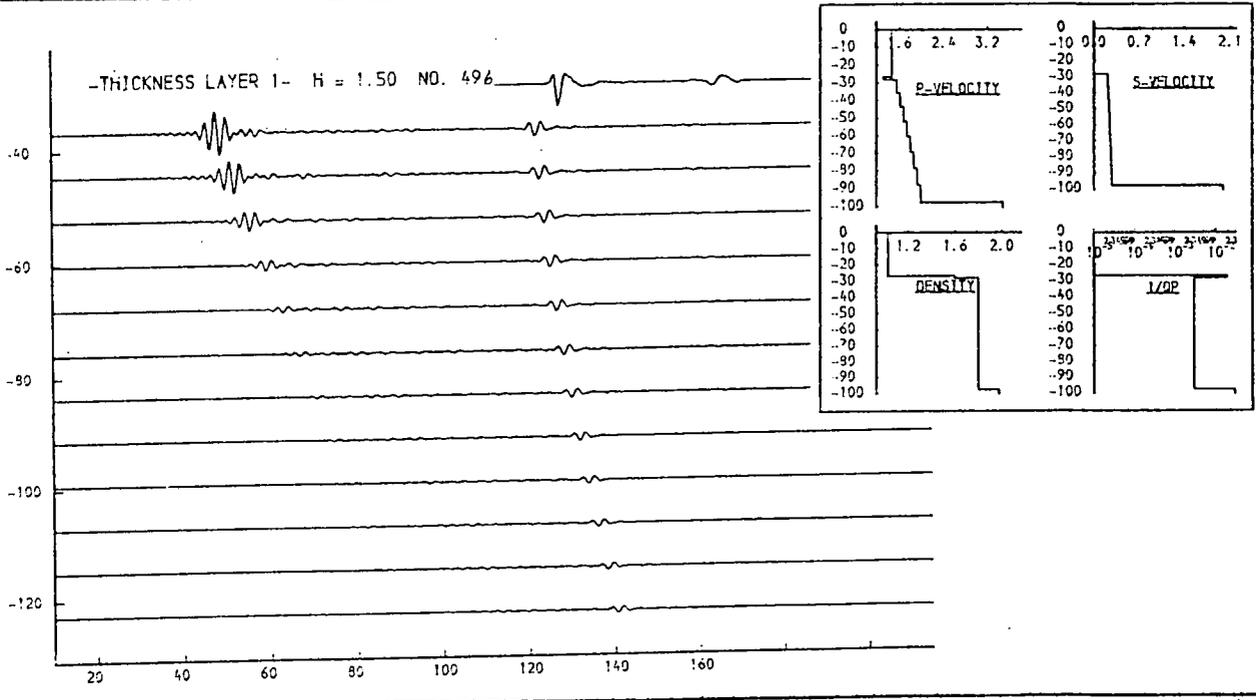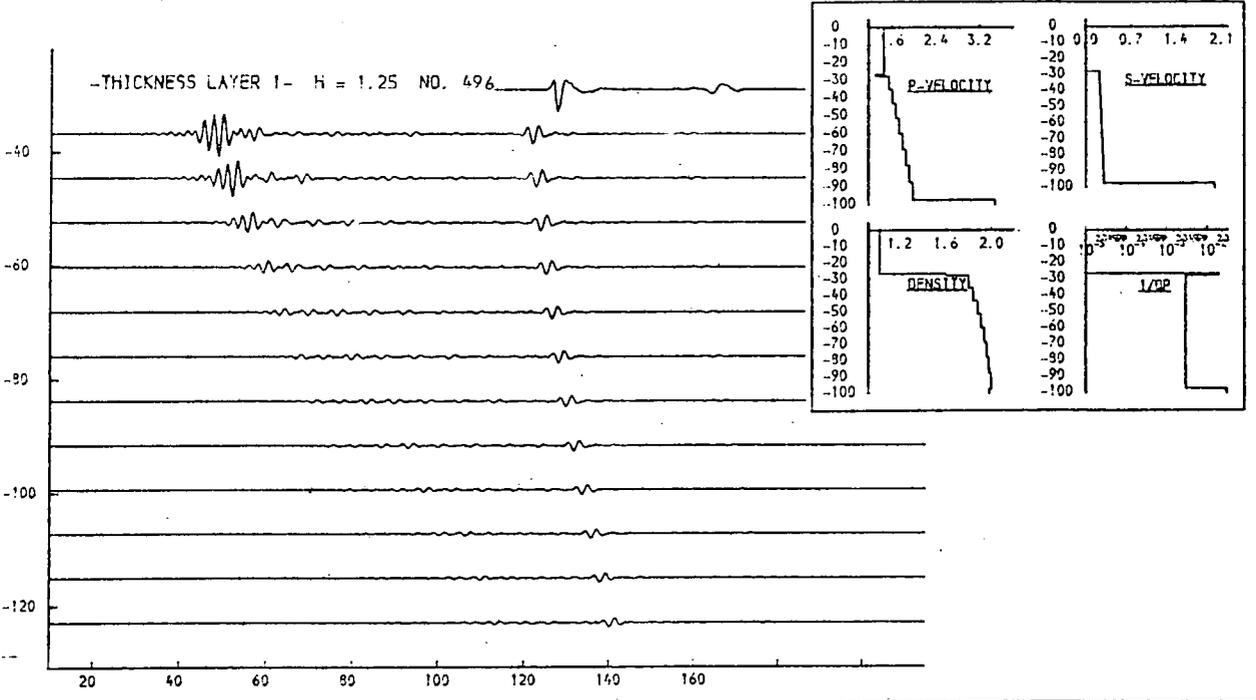
Fig. 9.86c. Thickness of surficial layer above gradient.

The possibility of a surficial layer having a low velocity is investigated. Thickness is varied from 0.25 to 2.0 metres.

THICKNESS (M.)	P-VELOCITY (M/S.)	S-VELOCITY (M/S.)	DENSITY (G/ML)	1/Q P	1/Q S
26.6	1.460	0.000	1.03	0.00000	0.00000
7.6	1.551	0.219	1.90	0.00300	0.03000
7.9	1.614	0.228	1.90	0.00300	0.03000
9.2	1.676	0.237	1.90	0.00300	0.03000
8.5	1.739	0.246	1.90	0.00300	0.03000
8.9	1.901	0.254	1.90	0.00300	0.03000
9.2	1.964	0.263	1.90	0.00300	0.03000
9.5	1.926	0.272	1.90	0.00300	0.03000
9.9	1.989	0.281	1.90	0.00300	0.03000
	3.500	2.000	1.98	0.03000	0.06000

-THICKNESS LAYER 1- H = 1.75   NO. 496

-THICKNESS LAYER 1- H = 2.0   NO. 496

Fig. 9.86d. Thickness of surficial layer above gradient.

The possibility of a surficial layer having a low velocity is investigated. Thickness is varied from 0.25 to 2.0 metres.

THICKNESS (M.)	P-VELOCITY (M/S.)	S-VELOCITY (M/S.)	DENSITY (G/ML)	1/Q P	1/Q S
26.6	1.460	0.000	1.03	0.00000	0.00000
3.0	1.490	0.210	1.15	0.03000	0.06000
7.2	1.507	0.213	2.00	0.00300	0.03000
7.5	1.583	0.224	2.00	0.00300	0.03000
7.9	1.658	0.234	2.00	0.00300	0.03000
8.2	1.733	0.245	2.00	0.00300	0.03000
8.6	1.907	0.255	2.00	0.00300	0.03000
8.9	1.992	0.266	2.00	0.00300	0.03000
9.3	1.958	0.276	2.00	0.00300	0.03000
9.6	2.033	0.287	2.00	0.00300	0.03000
	3.500	2.000	1.98	0.03000	0.06000

Fig. 9.87a. Density in surficial layer above gradient.

Variation in density of a 3m. thick surficial layer is investigated.

THICKNESS (M.)	P-VELOCITY (M/S.)	S-VELOCITY (M/S.)	DENSITY (G/ML)	1/Q P	1/Q S
26.6	1.460	0.000	1.03	0.00000	0.00000
3.0	1.490	0.210	1.45	0.02000	0.04000
7.2	1.507	0.213	2.00	0.00300	0.03000
7.5	1.593	0.224	2.00	0.00300	0.03000
7.9	1.658	0.234	2.00	0.00300	0.03000
8.2	1.733	0.245	2.00	0.00300	0.03000
8.6	1.907	0.255	2.00	0.00300	0.03000
8.9	1.992	0.266	2.00	0.00300	0.03000
9.3	1.958	0.276	2.00	0.00300	0.03000
9.6	2.033	0.297	2.00	0.00300	0.03000
	3.500	2.000	1.98	0.03000	0.06000

-DENSITY LAYER 1- RHO = 1.45 GRADT.300

-DENSITY LAYER 1- RHO = 1.6 GRADT.300

Fig. 9.87b. Density in surficial layer above gradient.

Variation in density of a 3m. thick surficial layer is investigated.

THICKNESS (M.)	P-VELOCITY (M/S.)	S-VELOCITY (M/S.)	DENSITY (G/ML)	1/Q P	1/Q S
26.6	1.460	0.000	1.03	0.00000	0.00000
3.0	1.480	0.010	1.15	0.03000	0.06000
7.2	1.507	0.213	1.60	0.00300	0.03000
7.5	1.583	0.224	1.70	0.00300	0.03000
7.9	1.659	0.234	1.90	0.00300	0.03000
8.2	1.733	0.245	1.90	0.00300	0.03000
8.6	1.907	0.255	2.00	0.00300	0.03000
8.9	1.982	0.266	2.00	0.00300	0.03000
9.3	1.958	0.276	2.00	0.00300	0.03000
9.6	2.033	0.287	2.00	0.00300	0.03000
3.500	2.000	1.98	0.03000	0.06000	

THICKNESS (M.)	P-VELOCITY (M/S.)	S-VELOCITY (M/S.)	DENSITY (G/ML)	1/Q P	1/Q S
26.6	1.460	0.000	1.93	0.00000	0.00000
3.0	1.480	0.010	1.30	0.03000	0.06000
7.2	1.507	0.213	1.60	0.00300	0.03000
7.5	1.583	0.224	1.70	0.00300	0.03000
7.9	1.659	0.234	1.90	0.00300	0.03000
8.2	1.733	0.245	1.90	0.00300	0.03000
8.6	1.907	0.255	2.00	0.00300	0.03000
8.9	1.982	0.266	2.00	0.00300	0.03000
9.3	1.958	0.276	2.00	0.00300	0.03000
9.6	2.033	0.287	2.00	0.00300	0.03000
3.500	2.000	1.98	0.03000	0.06000	

Fig. 9.88a.   Density in surficial layer above gradient.

A gradient in density accompanying the p-velocity gradient is considered, along with variation in density of a 3m. thick surficial layer.

THICKNESS (M.)	P-VELOCITY (M/S.)	S-VELOCITY (M/S.)	DENSITY (G/ML)	1/Q P	1/Q S
26.6	1.460	0.000	1.03	0.00000	0.00000
3.0	1.486	0.010	1.45	0.22000	0.04000
7.2	1.507	0.213	1.60	0.00300	0.03000
7.5	1.583	0.224	1.70	0.00300	0.03000
7.9	1.659	0.234	1.80	0.00300	0.03000
8.2	1.733	0.245	1.90	0.00300	0.03000
8.6	1.907	0.255	2.00	0.00300	0.03000
8.9	1.982	0.266	2.00	0.00300	0.03000
9.3	1.958	0.276	2.00	0.00300	0.03000
9.6	2.033	0.287	2.00	0.00300	0.03000
	3.500	2.000	1.98	0.03000	0.06000

THICKNESS (M.)	P-VELOCITY (M/S.)	S-VELOCITY (M/S.)	DENSITY (G/ML)	1/Q P	1/Q S
26.6	1.460	0.000	1.03	0.00000	0.00000
3.0	1.480	0.010	1.60	0.02000	0.04000
7.2	1.507	0.213	1.60	0.00300	0.03000
7.5	1.583	0.224	1.70	0.00300	0.03000
7.9	1.659	0.234	1.80	0.00300	0.03000
8.2	1.733	0.245	1.90	0.00300	0.03000
8.6	1.907	0.255	2.00	0.00300	0.03000
8.9	1.982	0.266	2.00	0.00300	0.03000
9.3	1.958	0.276	2.00	0.00300	0.03000
9.6	2.033	0.287	2.00	0.00300	0.03000
	3.500	2.000	1.98	0.03000	0.06000

Fig. 9.88b. Density in surficial layer above gradient.

A gradient in density accompanying the p-velocity gradient is considered, along with variation in density of a 3m. thick surficial layer.

THICKNESS (M.)	P-VELOCITY (M/S.)	S-VELOCITY (M/S.)	DENSITY (G/ML)	1/Q P	1/Q S		THICKNESS (M.)	P-VELOCITY (M/S.)	S-VELOCITY (M/S.)	DENSITY (G/ML)	1/Q P	1/Q S
26.6	1.460	0.000	1.03	0.00000	0.00000		26.6	1.460	0.000	1.03	0.00000	0.00000
8.3	1.682	0.238	1.86	0.00300	0.03000		8.3	1.692	0.238	1.82	0.00300	0.03000
8.4	1.708	0.241	1.87	0.00300	0.03000		8.4	1.708	0.241	1.84	0.00300	0.03000
8.5	1.733	0.245	1.88	0.00300	0.03000		8.5	1.733	0.245	1.86	0.00300	0.03000
8.6	1.757	0.248	1.89	0.00300	0.03000		8.6	1.757	0.248	1.88	0.00300	0.03000
8.8	1.783	0.252	1.90	0.00300	0.03000		8.8	1.783	0.252	1.90	0.00300	0.03000
8.9	1.807	0.255	1.91	0.00300	0.03000		8.9	1.807	0.255	1.92	0.00300	0.03000
9.0	1.933	0.259	1.92	0.00300	0.03000		9.0	1.933	0.259	1.94	0.00300	0.03000
9.1	1.958	0.262	1.93	0.00300	0.03000		9.1	1.958	0.262	1.96	0.00300	0.03000
	3.500	2.000	1.98	0.03000	0.06000			3.500	2.000	1.98	0.03000	0.06000

DENSITY GRADT. IN 1 & 2 .2-.5 NO. 496

P-VELOCITY S-VELOCITY DENSITY 1/QP

DENSITY GRADT. IN 1 & 2 .2-.5 NO. 496

P-VELOCITY S-VELOCITY DENSITY 1/QP
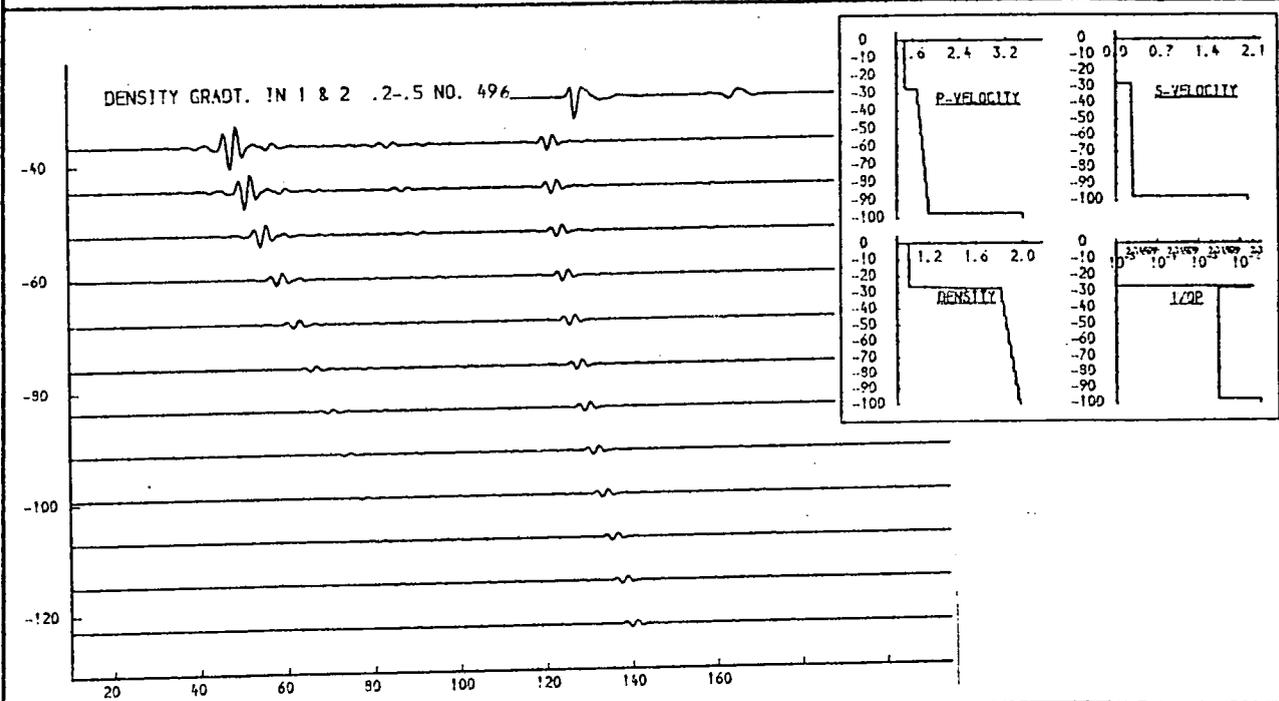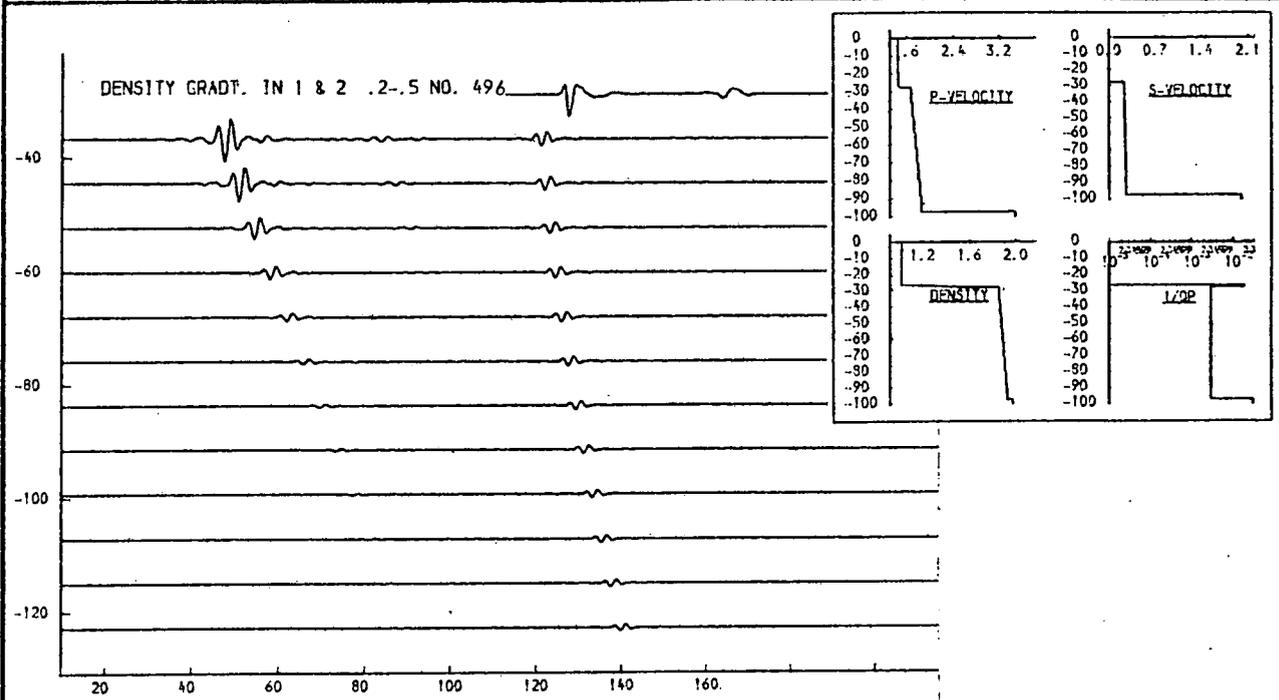
Fig. 9.89a.   Gradients in density and p-velocity.

Density gradients are inserted in both surficial and in the main layer.

THICKNESS (M.)	P-VELOCITY (M/S.)	S-VELOCITY (M/S.)	DENSITY (G/ML)	1/Q P	1/Q S
26.6	1.460	0.000	1.03	0.00000	0.00000
0.1	1.653	0.010	1.30	0.03000	0.04000
8.3	1.682	0.238	1.73	0.00300	0.03000
8.4	1.708	0.241	1.76	0.00300	0.03000
8.5	1.733	0.245	1.79	0.00300	0.03000
8.6	1.757	0.248	1.83	0.00300	0.03000
8.9	1.793	0.252	1.86	0.00300	0.03000
8.9	1.907	0.255	1.99	0.00300	0.03000
9.0	1.933	0.259	1.93	0.00300	0.03000
9.1	1.959	0.262	1.96	0.00300	0.03000
	3.500	2.000	1.98	0.03000	0.06000

THICKNESS (M.)	P-VELOCITY (M/S.)	S-VELOCITY (M/S.)	DENSITY (G/ML)	1/Q P	1/Q S
26.6	1.460	0.000	1.03	0.00000	0.00000
0.1	1.653	0.010	1.30	0.03000	0.04000
8.3	1.682	0.238	1.60	0.00300	0.03000
8.4	1.708	0.241	1.65	0.00300	0.03000
8.5	1.733	0.245	1.70	0.00300	0.03000
8.6	1.757	0.248	1.75	0.00300	0.03000
8.9	1.793	0.252	1.90	0.00300	0.03000
8.9	1.907	0.255	1.95	0.00300	0.03000
9.0	1.933	0.259	1.90	0.00300	0.03000
9.1	1.959	0.262	1.95	0.00300	0.03000
	3.500	2.000	1.98	0.03000	0.06000
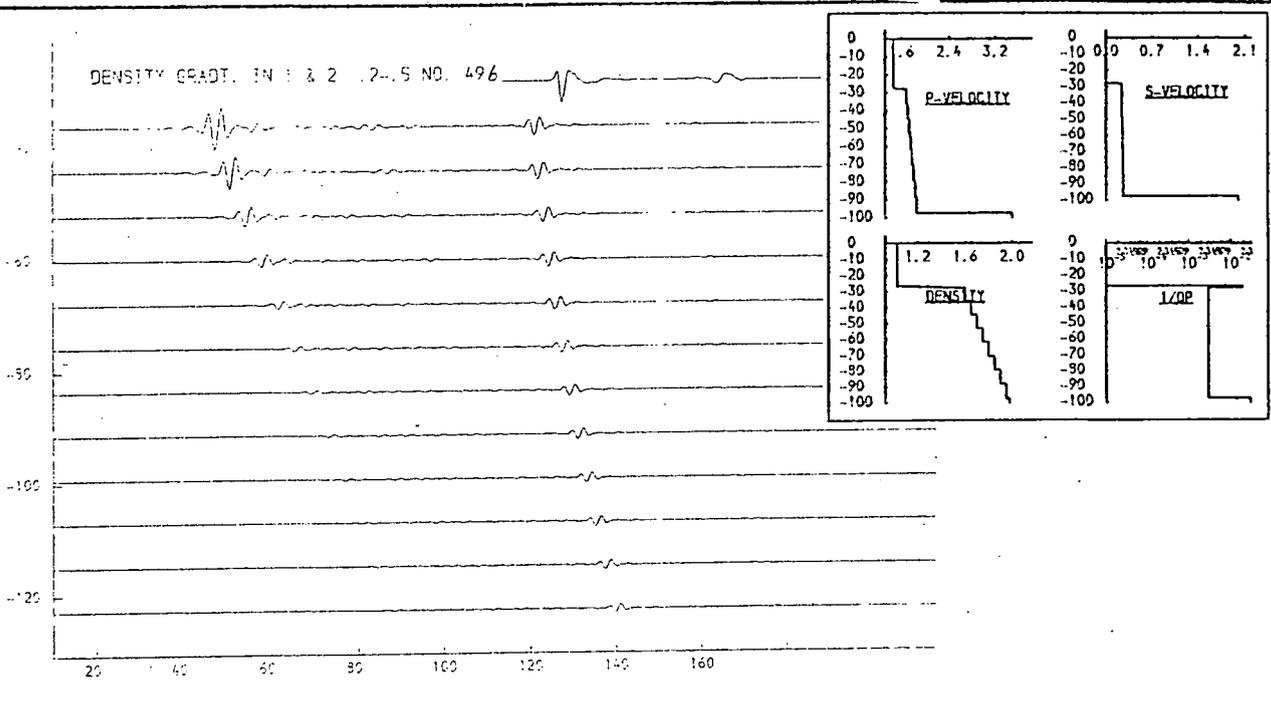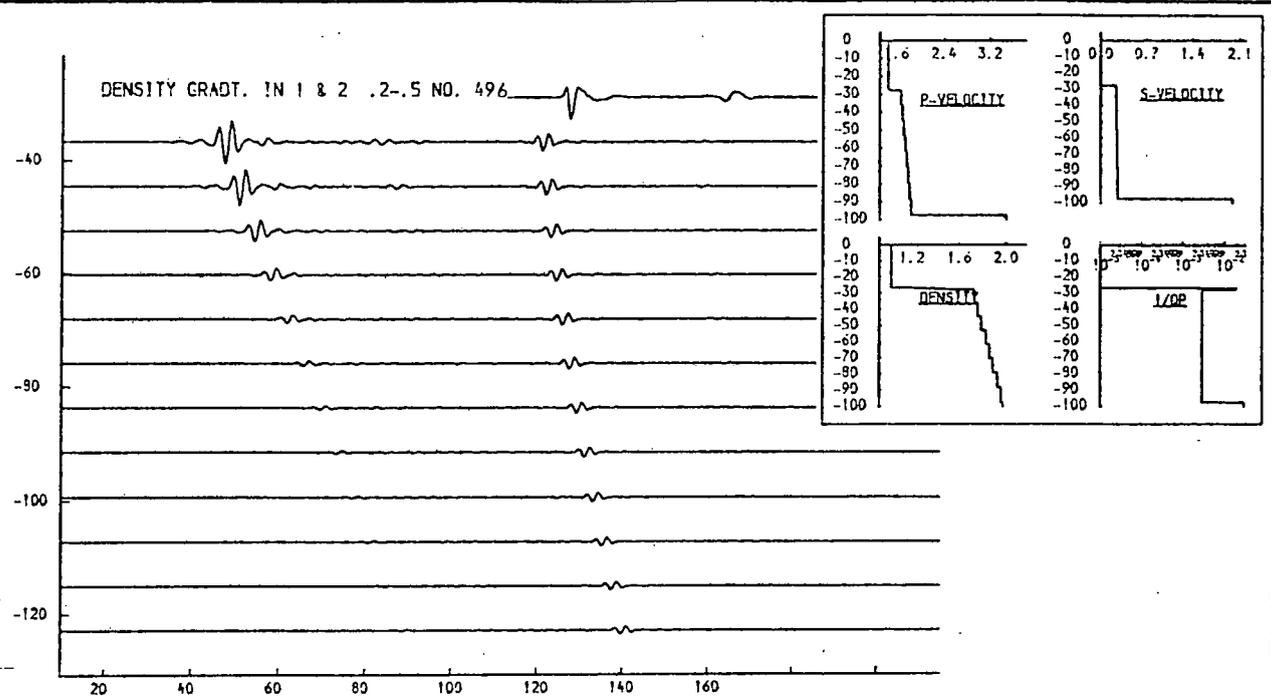
Fig. 9.89b. Gradients in density and p-velocity.

Density gradients are inserted in both surficial and in the main layer.

THICKNESS (M.)	P-VELOCITY (M/S.)	S-VELOCITY (M/S.)	DENSITY (G/ML)	1/Q P	1/Q S
26.6	1.460	0.000	1.03	0.00000	0.00000
3.0	1.490	0.010	1.35	0.02000	0.04000
7.6	1.595	0.225	1.71	0.00090	0.03000
7.9	1.645	0.232	1.77	0.00093	0.03000
8.0	1.695	0.239	1.82	0.00096	0.03000
8.3	1.745	0.246	1.87	0.00099	0.03000
8.5	1.795	0.254	1.93	0.00101	0.03000
8.8	1.845	0.261	1.98	0.00104	0.03000
9.0	1.895	0.268	2.03	0.00107	0.03000
9.2	1.945	0.275	2.09	0.00110	0.03000
	3.500	2.000	1.98	0.03000	0.06000

THICKNESS (M.)	P-VELOCITY (M/S.)	S-VELOCITY (M/S.)	DENSITY (G/ML)	1/Q P	1/Q S
26.6	1.460	0.000	1.03	0.00000	0.00000
3.0	1.490	0.010	1.35	0.02000	0.04000
6.9	1.464	0.207	1.57	0.00083	0.03000
7.4	1.551	0.219	1.67	0.00088	0.03000
7.8	1.639	0.231	1.76	0.00093	0.03000
8.2	1.726	0.244	1.85	0.00097	0.03000
8.6	1.814	0.256	1.95	0.00102	0.03000
9.0	1.901	0.269	2.04	0.00107	0.03000
9.4	1.989	0.281	2.13	0.00112	0.03000
9.8	2.076	0.293	2.23	0.00117	0.03000
	3.500	2.000	1.98	0.03000	0.06000
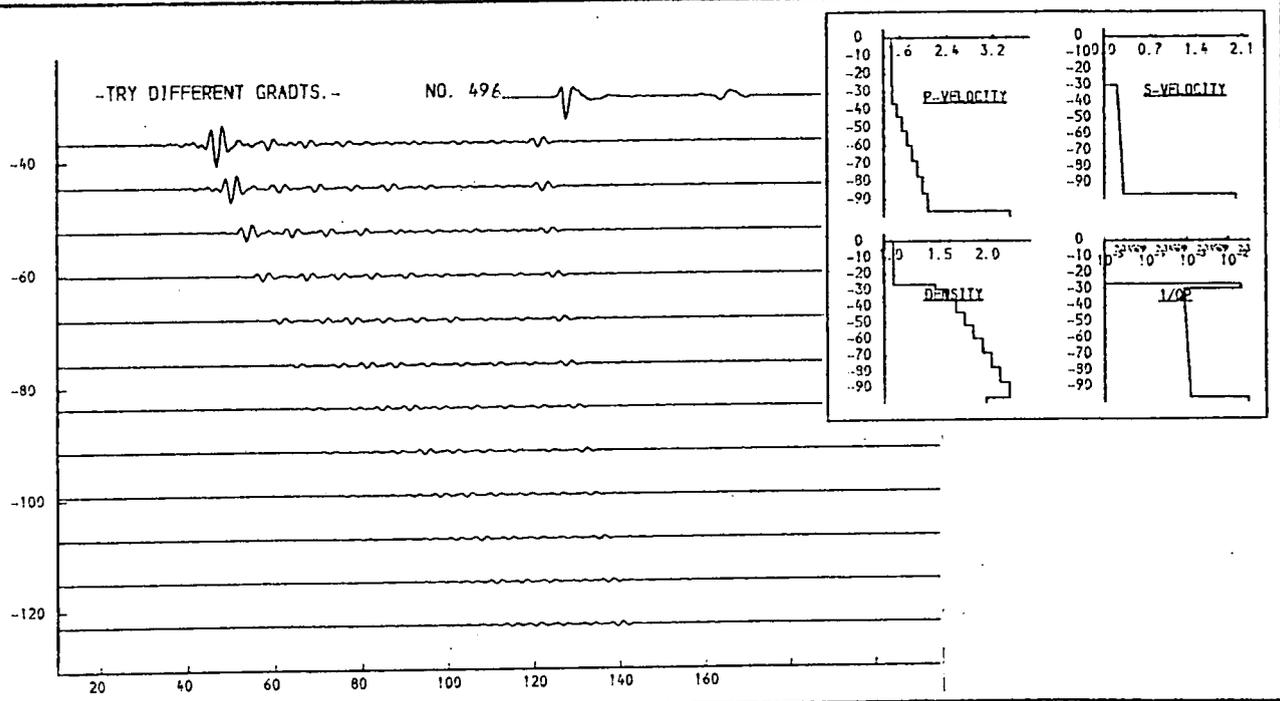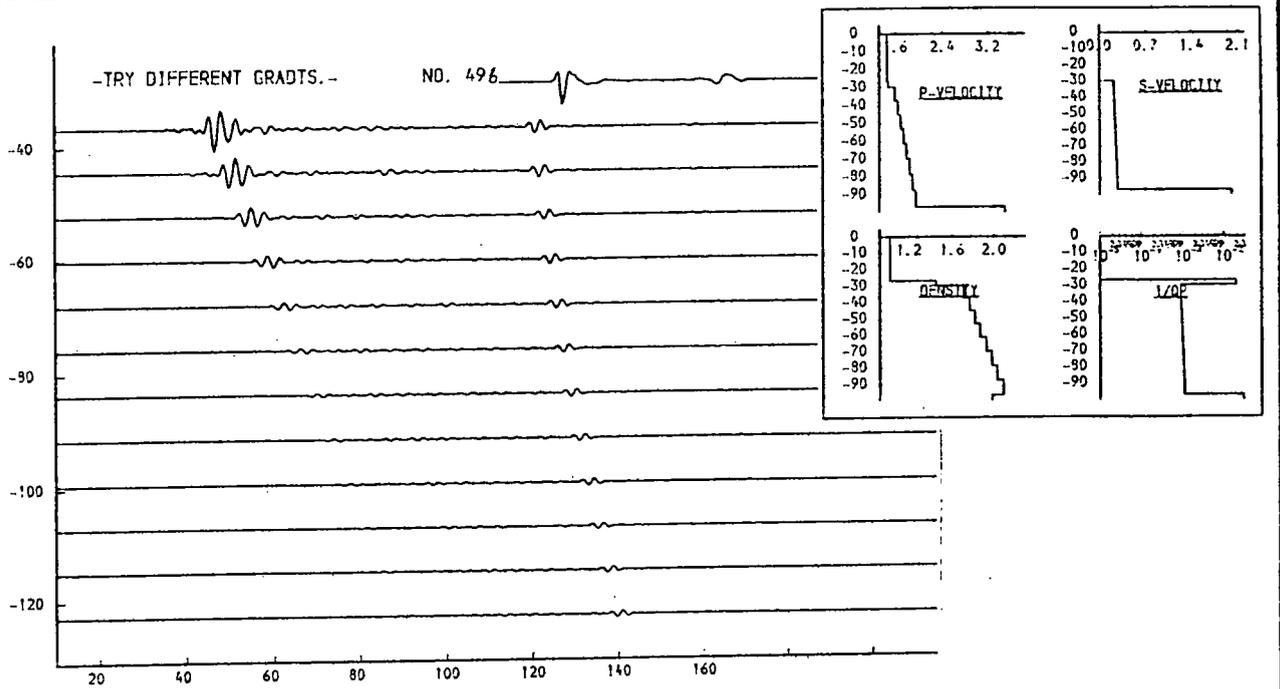
Fig. 9.90a. Gradient in p and s-velocity, density and attenuation.

Further gradient types are tried.

THICKNESS (M.)	P-VELOCITY (M/S.)	S-VELOCITY (M/S.)	DENSITY (G/ML)	1/Q P	1/Q S
26.6	1.460	0.000	1.03	0.00000	0.00000
1.0	1.490	0.010	1.45	0.00000	0.00000
8.0	1.692	0.239	1.91	0.00095	0.03000
8.1	1.709	0.241	1.93	0.00096	0.03000
8.2	1.733	0.245	1.96	0.00099	0.03000
8.3	1.757	0.248	1.99	0.00099	0.03000
8.5	1.783	0.252	1.91	0.00101	0.03000
8.6	1.807	0.255	1.94	0.00102	0.03000
8.7	1.933	0.259	1.97	0.00103	0.03000
8.9	1.959	0.262	1.99	0.00105	0.03000
3.500	2.000	1.98	0.03000	0.06000

THICKNESS (M.)	P-VELOCITY (M/S.)	S-VELOCITY (M/S.)	DENSITY (G/ML)	1/Q P	1/Q S
26.6	1.460	0.000	1.03	0.00000	0.00000
1.0	1.490	0.010	1.45	0.00000	0.00000
7.2	1.507	0.213	1.62	0.00085	0.03000
8.0	1.692	0.239	1.91	0.00095	0.03000
8.8	1.959	0.262	1.99	0.00105	0.03000
9.6	2.033	0.287	2.00	0.00115	0.03000
10.5	2.207	0.312	2.01	0.00125	0.03000
11.3	2.382	0.337	2.01	0.00135	0.03000
11.3	2.382	0.337	2.01	0.00135	0.03000
11.3	2.382	0.337	2.01	0.00135	0.03000
3.500	2.000	1.98	0.03000	0.06000
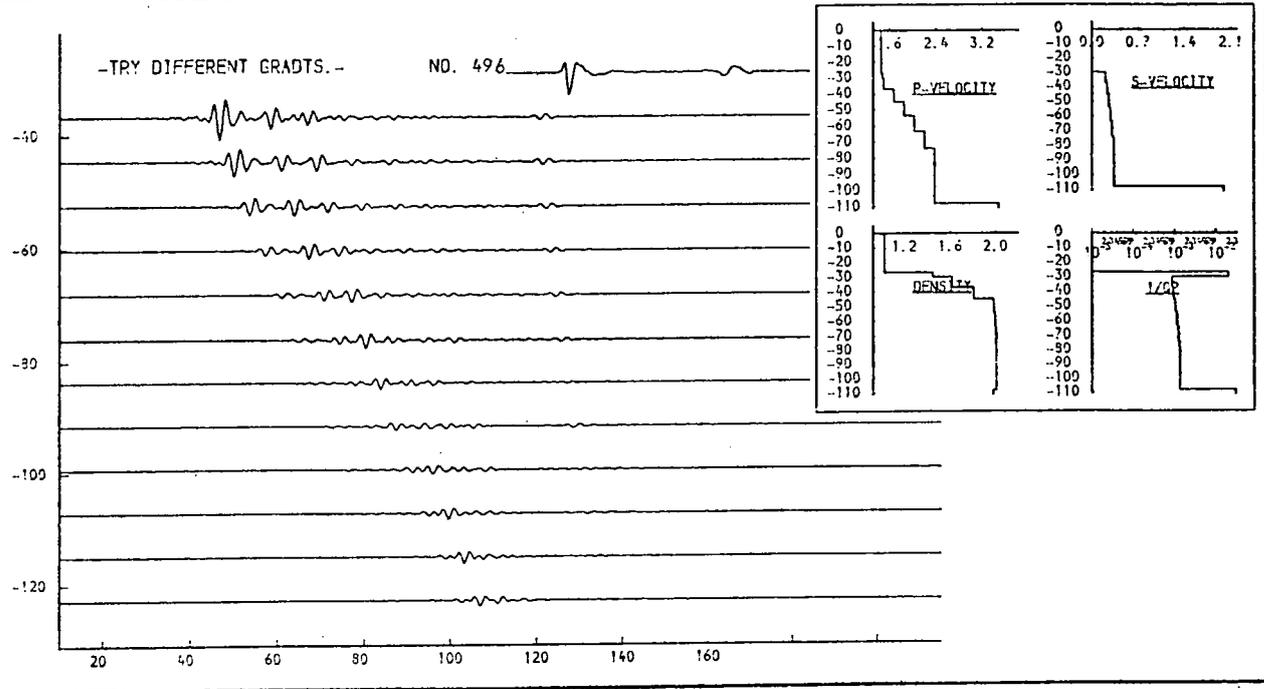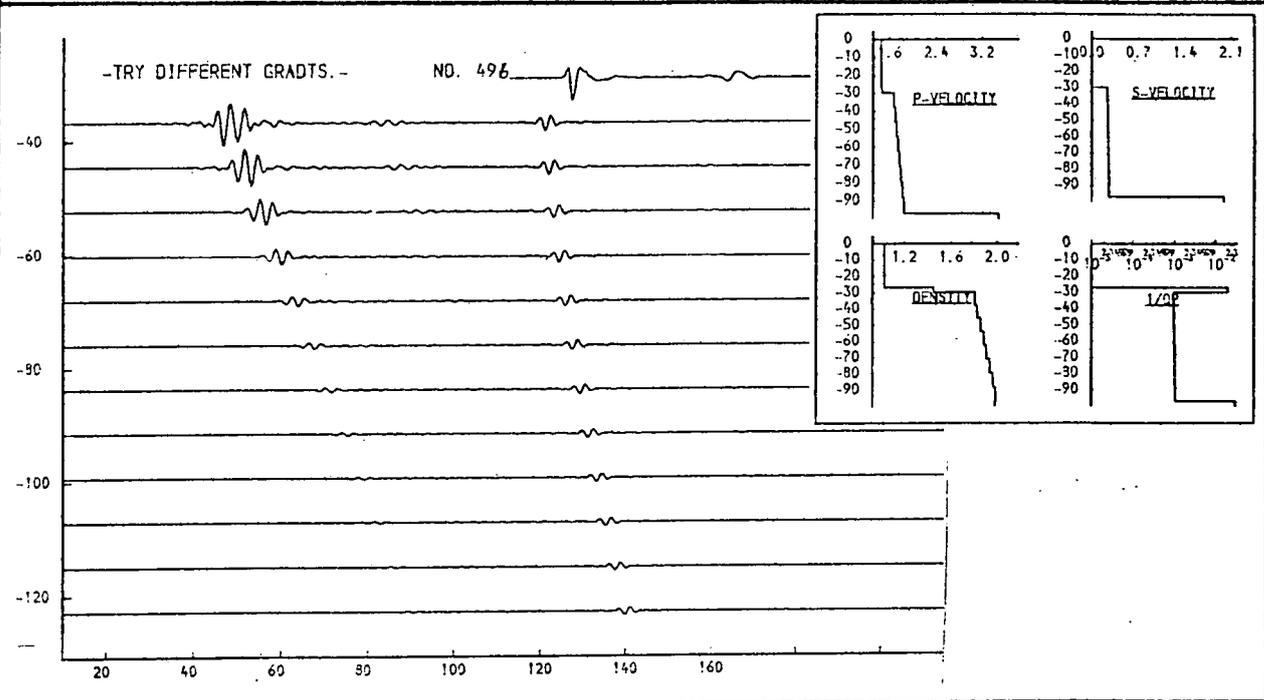
Fig. 9.90b. Gradient in p and s-velocity, density and attenuation.

Further gradient types are tried.

THICKNESS (M.)	P-VELOCITY (M/S.)	S-VELOCITY (M/S.)	DENSITY (G/ML)	1/Q P	1/Q S
26.6	1.460	0.000	1.03	0.00000	0.00000
7.6	1.705	0.227	1.90	0.00100	0.03000
16.2	1.755	0.241	1.90	0.00100	0.03000
36.3	1.900	0.270	1.90	0.00100	0.03000
	3.500	2.000	1.98	0.03000	0.06000

THICKNESS (M.)	P-VELOCITY (M/S.)	S-VELOCITY (M/S.)	DENSITY (G/ML)	1/Q P	1/Q S
26.6	1.460	0.000	1.03	0.00000	0.00000
7.1	1.505	0.213	1.90	0.00100	0.03000
7.6	1.605	0.227	1.90	0.00100	0.03000
16.2	1.705	0.241	1.90	0.00100	0.03000
36.3	1.910	0.270	1.90	0.00100	0.03000
	3.500	2.000	1.98	0.03000	0.06000

ALTER SURF GRADT. TIMES MAY BE WRONG.

P-VELOCITY
S-VELOCITY
DENSITY
1/Q

TEST STRONG SURFACE GRADT.   NO. 496

P-VELOCITY
S-VELOCITY
DENSITY
1/Q
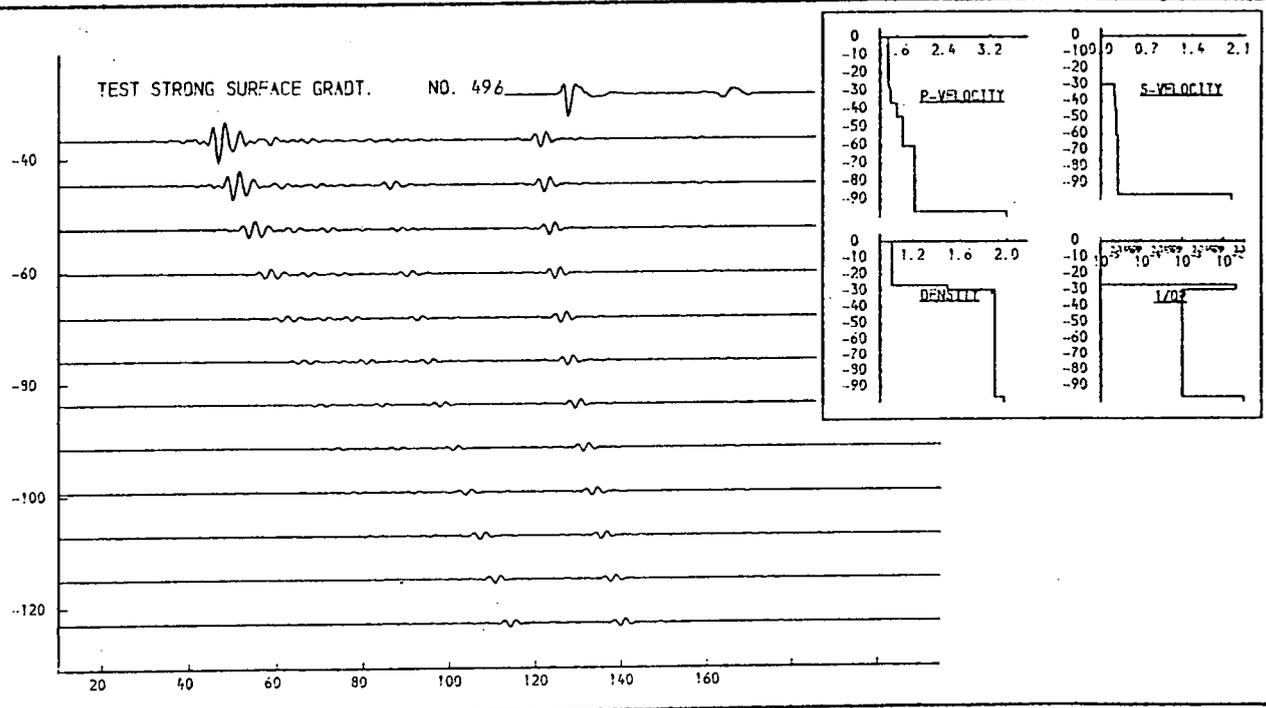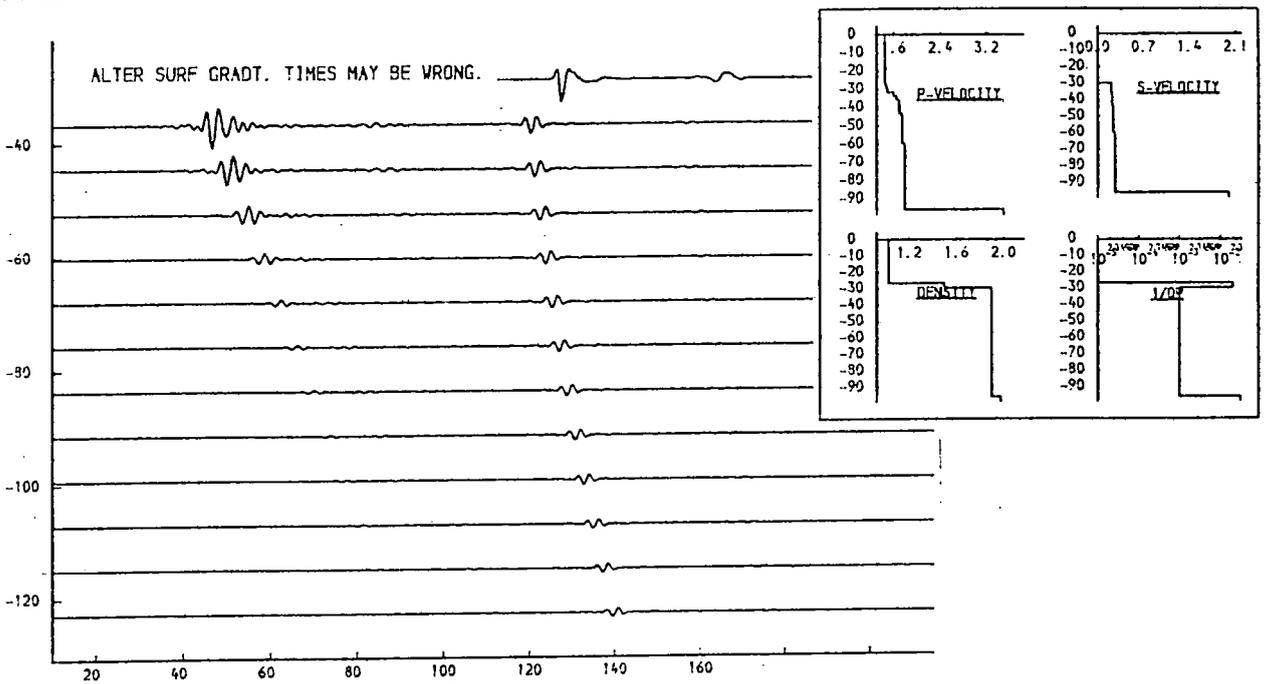
Fig. 9.91a.   Gradients in p and s-velocity.

Further gradient types are tested.

THICKNESS (M.)	P-VELOCITY (M/S.)	S-VELOCITY (M/S.)	DENSITY (G/ML)	1/Q P	1/Q S
26.6	1.460	0.000	1.03	0.00000	0.00000
7.6	1.705	0.227	1.90	0.00100	0.03000
16.2	1.755	0.241	1.90	0.00100	0.03000
36.3	1.900	0.270	1.90	0.00100	0.03000
	3.500	2.000	1.98	0.03000	0.06000

THICKNESS (M.)	P-VELOCITY (M/S.)	S-VELOCITY (M/S.)	DENSITY (G/ML)	1/Q P	1/Q S
26.6	1.460	0.000	1.03	0.00000	0.00000
7.6	1.705	0.227	1.90	0.00100	0.03000
16.2	1.755	0.241	1.90	0.00100	0.03000
36.3	1.900	0.270	1.90	0.00100	0.03000
	3.500	2.000	1.98	0.03000	0.06000

ALTER SURF GRADT., CHANGE DENSITIES.

ALTER SURF GRADT., CHANGE DENSITIES.

Fig. 9.91b.   Gradients in p and s-velocity.

Further gradient types are tested.

THICKNESS (M.)	P-VELOCITY (M/S.)	S-VELOCITY (M/S.)	DENSITY (G/ML)	1/Q P	1/Q S
26.6	1.460	0.000	1.03	0.00000	0.00000
3.4	1.659	0.500	2.00	0.00300	0.03000
3.6	1.233	0.500	1.99	0.00300	0.03000
3.7	1.902	0.500	1.98	0.00300	0.03000
3.9	1.932	0.500	1.97	0.00300	0.03000
4.1	1.959	0.500	1.96	0.00300	0.03000
4.2	2.033	0.500	1.95	0.00300	0.03000
4.4	2.108	0.500	1.94	0.00300	0.03000
4.5	2.182	0.500	1.93	0.00300	0.03000
4.7	2.257	0.500	1.92	0.00300	0.03000
4.9	2.333	0.500	1.91	0.00300	0.03000
	3.500	2.000	1.98	0.00300	0.03000

THICKNESS (M.)	P-VELOCITY (M/S.)	S-VELOCITY (M/S.)	DENSITY (G/ML)	1/Q P	1/Q S
26.6	1.460	0.000	1.03	0.00000	0.00000
3.4	1.659	0.234	2.00	0.00300	0.03000
3.6	1.233	0.245	1.99	0.00300	0.03000
3.7	1.902	0.255	1.98	0.00300	0.03000
3.9	1.932	0.266	1.97	0.00300	0.03000
4.1	1.959	0.276	1.96	0.00300	0.03000
4.2	2.033	0.232	1.95	0.00300	0.03000
4.4	2.108	0.299	1.94	0.00300	0.03000
4.5	2.182	0.308	1.93	0.00300	0.03000
4.7	2.257	0.312	1.92	0.00300	0.03000
4.9	2.333	0.329	1.91	0.00300	0.03000
	3.500	2.000	1.98	0.00300	0.03000

-9DEC 8 TRY GRADTS. 1&2   NO. 496

-9DEC 5 TRY GRADTS. 1&2   NO. 496

Fig. 9.92a.   Gradients with turning point in p-velocity.

THICKNESS (M.)	P-VELOCITY (M/S.)	S-VELOCITY (M/S.)	DENSITY (G/ML)	1/Q P	1/Q S
26.6	1.460	0.000	1.03	0.00000	0.00000
3.4	1.659	0.234	2.00	0.00300	0.03000
3.6	1.733	0.245	2.00	0.00300	0.03000
3.7	1.902	0.255	2.00	0.00300	0.03000
3.9	1.892	0.266	2.00	0.00300	0.03000
4.1	1.959	0.276	2.00	0.00300	0.03000
4.2	2.033	0.297	2.00	0.00300	0.03000
4.4	2.108	0.299	2.00	0.00300	0.03000
4.5	2.182	0.308	2.00	0.00300	0.03000
4.7	2.252	0.319	2.00	0.00300	0.03000
4.9	2.333	0.329	2.00	0.00300	0.03000
	3.500	2.000	1.98	0.00300	0.03000

-9DEC 1 TRY GRADTS. 1&2   NO. 496

-9DEC 1 TRY GRADTS. 1&2   NO. 496

Fig. 9.92b.   Gradients with turning point in p-velocity.

THICKNESS (M.)	P-VELOCITY (M/S.)	S-VELOCITY (M/S.)	DENSITY (G/ML)	1/Q P	1/Q S
26.6	1.460	0.000	1.03	0.00000	0.00000
3.0	1.480	0.010	1.25	0.02000	0.04000
9.4	1.989	0.281	2.00	0.00300	0.03000
9.1	1.926	0.272	2.00	0.00300	0.03000
8.9	1.964	0.263	2.00	0.00300	0.03000
8.5	1.801	0.254	2.00	0.00300	0.03000
8.3	1.739	0.246	2.00	0.00300	0.03000
8.0	1.676	0.237	2.00	0.00300	0.03000
7.7	1.614	0.228	2.00	0.00300	0.03000
7.4	1.551	0.219	2.00	0.00300	0.03000
	3.500	2.000	1.98	0.03000	0.06000

Fig. 9.93a.   Inverse gradient in p and s-velocity.

An inverse velocity gradient is shown, with variation in density of a surficial layer. Density in upper model is 1.25; in lower model is 1.40.

THICKNESS (M.)	P-VELOCITY (M/S.)	S-VELOCITY (M/S.)	DENSITY (G/ML)	1/Q P	1/Q S
26.6	1.460	0.000	1.03	0.00000	0.00000
9.6	1.490	0.040	1.50	0.03000	0.06000
9.4	1.989	0.281	2.00	0.00300	0.03000
9.1	1.926	0.272	2.00	0.00300	0.03000
8.9	1.864	0.263	2.00	0.00300	0.03000
8.5	1.801	0.254	2.00	0.00300	0.03000
8.3	1.739	0.246	2.00	0.00300	0.03000
8.0	1.676	0.237	2.00	0.00300	0.03000
7.7	1.614	0.228	2.00	0.00300	0.03000
7.4	1.551	0.219	2.00	0.00300	0.03000
	3.500	2.000	1.98	0.03000	0.06000

Fig. 9.93b. Inverse gradient in p and s-velocity.

An inverse velocity gradient is shown, with variation in density
of a surficial layer. Density in upper model is 1.50; in lower
model is 1.65.

THICKNESS (M.)	P-VELOCITY (M/S.)	S-VELOCITY (M/S.)	DENSITY (G/ML)	1/Q P	1/Q S
26.6	1.460	0.000	1.03	0.00000	0.00000
59.9	1.770	0.250	2.00	0.00100	0.03000
	3.500	2.000	1.98	0.00100	0.03000

-NEG GRADT. LAYER 1- P2 =1.77 NO. 496

-NEG GRADT. LAYER 1- P2 =1.9 NO. 496
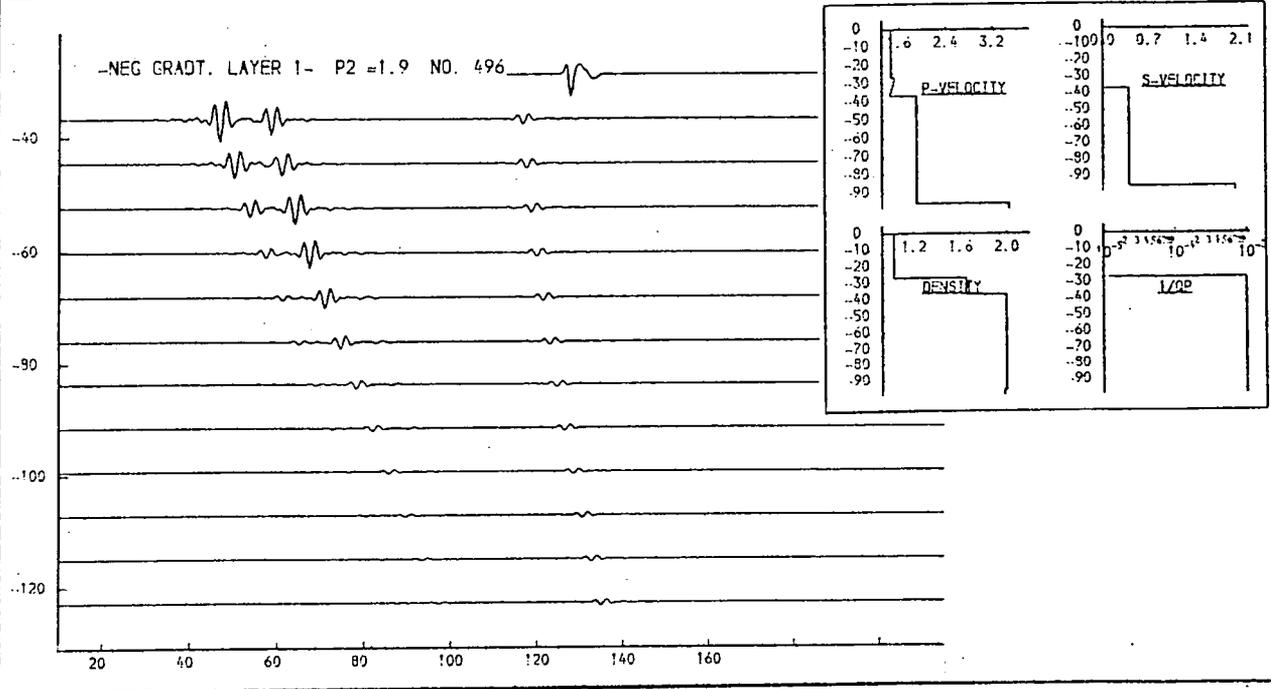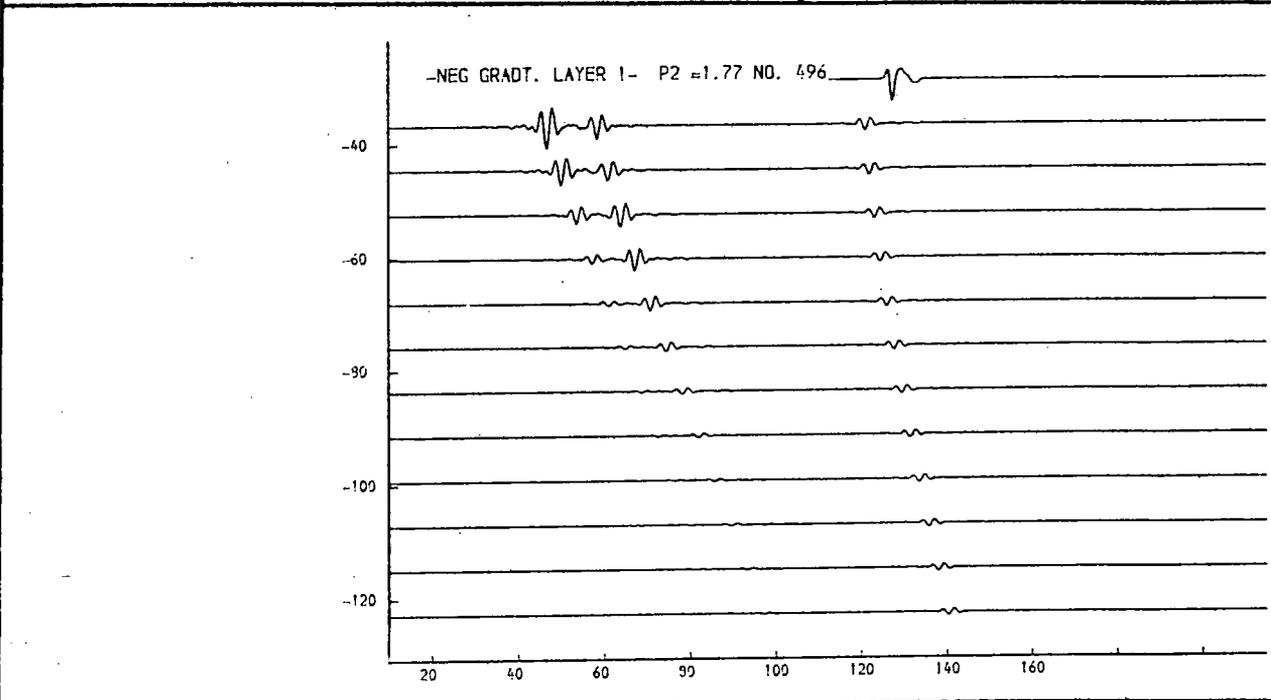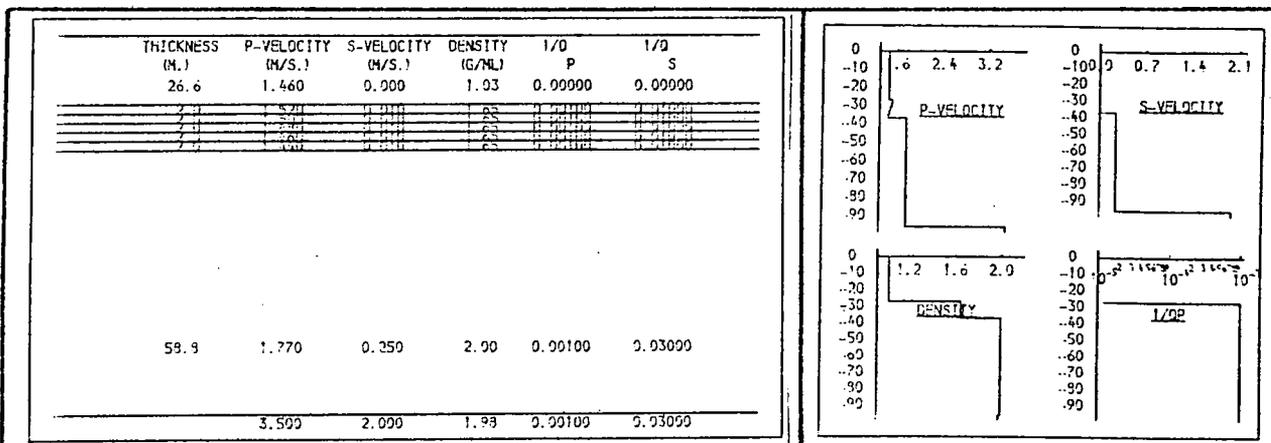
Fig. 9.94a.   Inverse gradient in p-velocity (upper layer).

An inverse p-velocity gradient is shown, in conjunction with variations in the p-velocity of a (uniform) underlying layer.

THICKNESS (M.)	P-VELOCITY (M/S.)	S-VELOCITY (M/S.)	DENSITY (G/ML)	1/Q P	1/Q S
26.6	1.460	0.000	1.03	0.00000	0.00000
59.9	2.100	0.700	2.00	0.00100	0.03000
	3.500	2.000	1.98	0.00100	0.03000

-NEG GRADT. LAYER 1- P2 =2.1 NO. 496

-NEG GRADT. LAYER 1- P2 =2.3 NO. 496

Fig. 9.94b.   Inverse gradient in p-velocity (upper layer).

An inverse p-velocity gradient is shown, in conjunction with variations in the p-velocity of a (uniform) underlying layer.
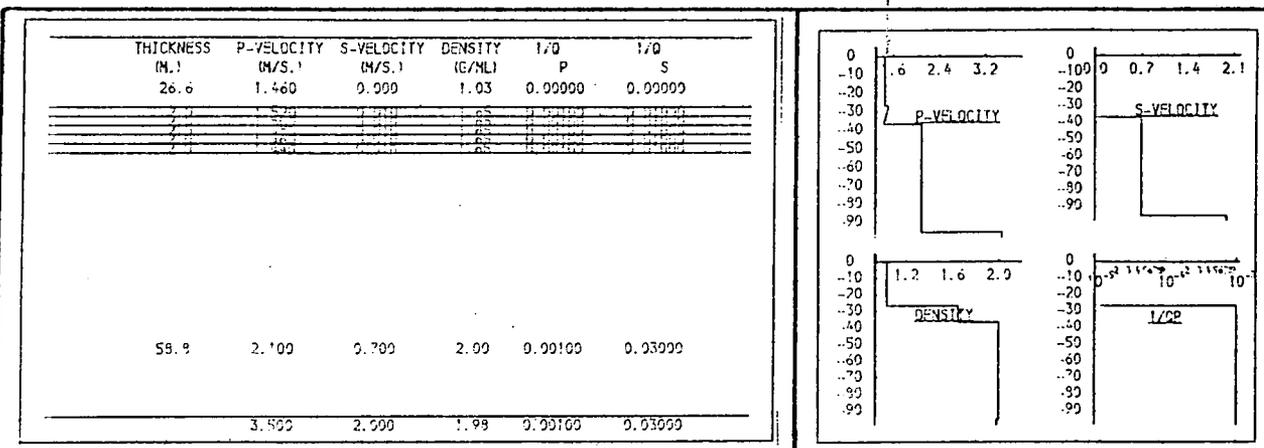
THICKNESS (M.)	P-VELOCITY (M/S.)	S-VELOCITY (M/S.)	DENSITY (G/ML)	1/Q P	1/Q S
28.6	1.460	0.000	1.03	0.00000	0.00000
0.5	1.480	0.010	1.65	0.03000	0.04000
8.3	1.642	0.550	2.00	0.00100	0.03000
8.4	1.667	0.550	2.00	0.00100	0.03000
8.5	1.693	0.550	2.00	0.00100	0.03000
8.6	1.717	0.550	2.00	0.00100	0.03000
8.7	1.743	0.550	2.00	0.00100	0.03000
8.9	1.767	0.550	2.00	0.00100	0.03000
9.0	1.792	0.550	2.00	0.00100	0.03000
9.1	1.818	0.550	2.00	0.00100	0.03000
	3.500	2.000	1.98	0.03000	0.06000

THICKNESS (M.)	P-VELOCITY (M/S.)	S-VELOCITY (M/S.)	DENSITY (G/ML)	1/Q P	1/Q S
28.6	1.460	0.000	1.03	0.00000	0.00000
0.5	1.493	0.010	1.65	0.03000	0.04000
8.3	1.642	0.496	2.00	0.00100	0.03000
8.4	1.667	0.511	2.00	0.00100	0.03000
8.5	1.693	0.526	2.00	0.00100	0.03000
8.6	1.717	0.542	2.00	0.00100	0.03000
8.7	1.743	0.558	2.00	0.00100	0.03000
8.9	1.767	0.574	2.00	0.00100	0.03000
9.0	1.792	0.590	2.00	0.00100	0.03000
9.1	1.818	0.607	2.00	0.00100	0.03000
	3.500	2.000	1.98	0.03000	0.06000
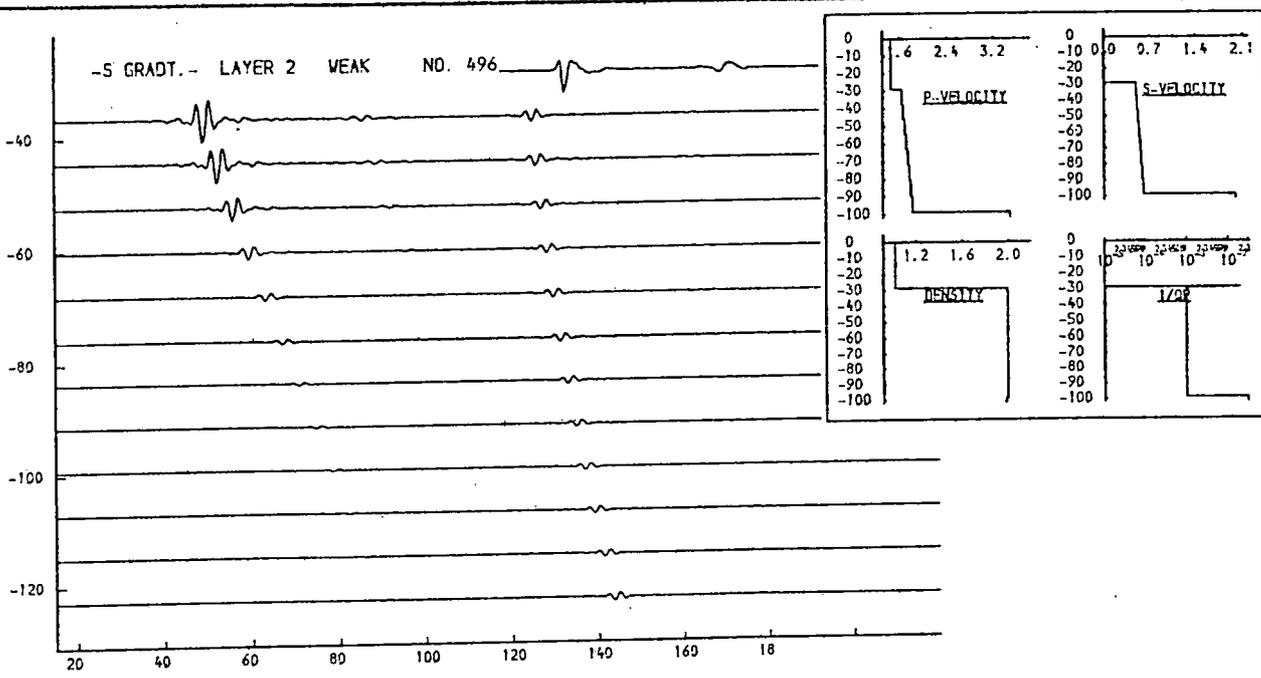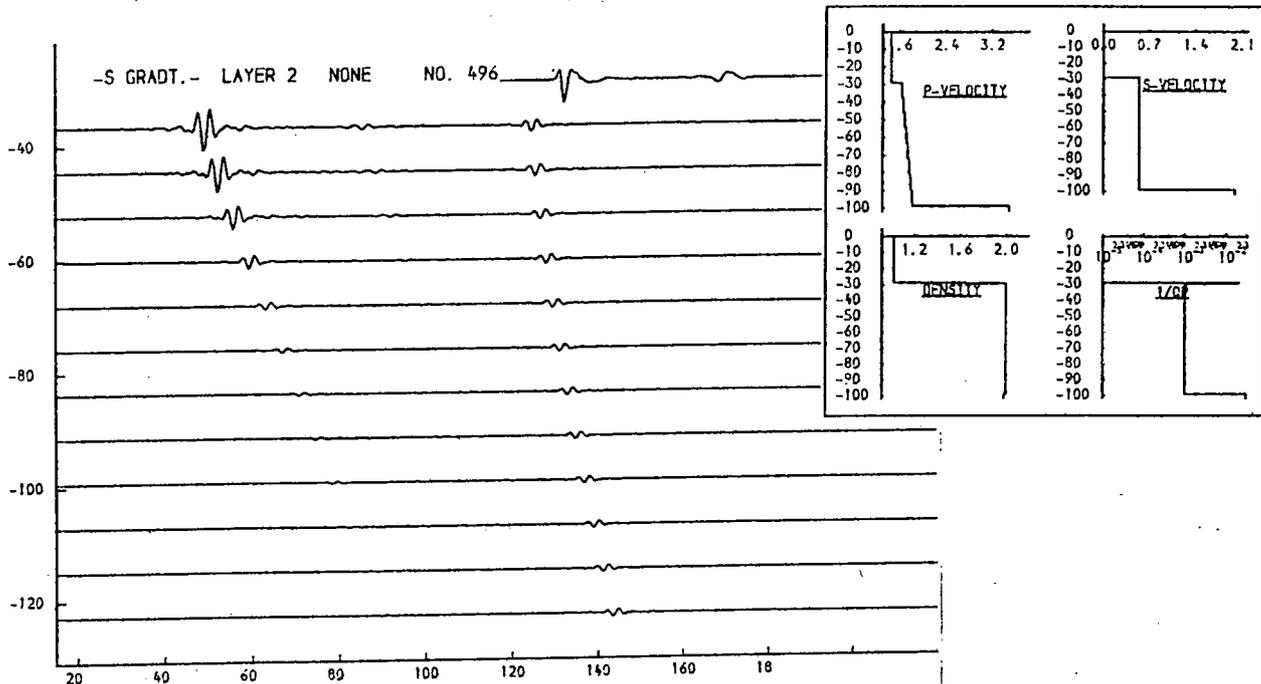
Fig. 9.95a.   Gradients in s-velocity.

Variations are shown in a s-velocity gradient for values of zero and 1.5m/sec/m.

THICKNESS (M.)	P-VELOCITY (M/S.)	S-VELOCITY (M/S.)	DENSITY (G/ML)	1/Q P	1/Q S
28.6	1.460	0.000	1.03	0.00000	0.00000
8.3	1.642	0.400	2.00	0.00100	0.03000
8.4	1.667	0.450	2.00	0.00100	0.03000
8.5	1.693	0.500	2.00	0.00100	0.03000
8.6	1.717	0.550	2.00	0.00100	0.03000
8.7	1.743	0.600	2.00	0.00100	0.03000
8.9	1.767	0.650	2.00	0.00100	0.03000
9.0	1.792	0.700	2.00	0.00100	0.03000
9.1	1.818	0.750	2.00	0.00100	0.03000
	3.500	2.000	1.98	0.03000	0.06000

THICKNESS (M.)	P-VELOCITY (M/S.)	S-VELOCITY (M/S.)	DENSITY (G/ML)	1/Q P	1/Q S
28.6	1.460	0.000	1.03	0.00000	0.00000
8.3	1.642	0.200	2.00	0.00100	0.03000
8.4	1.667	0.300	2.00	0.00100	0.03000
8.5	1.693	0.400	2.00	0.00100	0.03000
8.6	1.717	0.500	2.00	0.00100	0.03000
8.7	1.743	0.600	2.00	0.00100	0.03000
8.9	1.767	0.700	2.00	0.00100	0.03000
9.0	1.792	0.800	2.00	0.00100	0.03000
9.1	1.818	0.900	2.00	0.00100	0.03000
	3.500	2.000	1.98	0.03000	0.06000
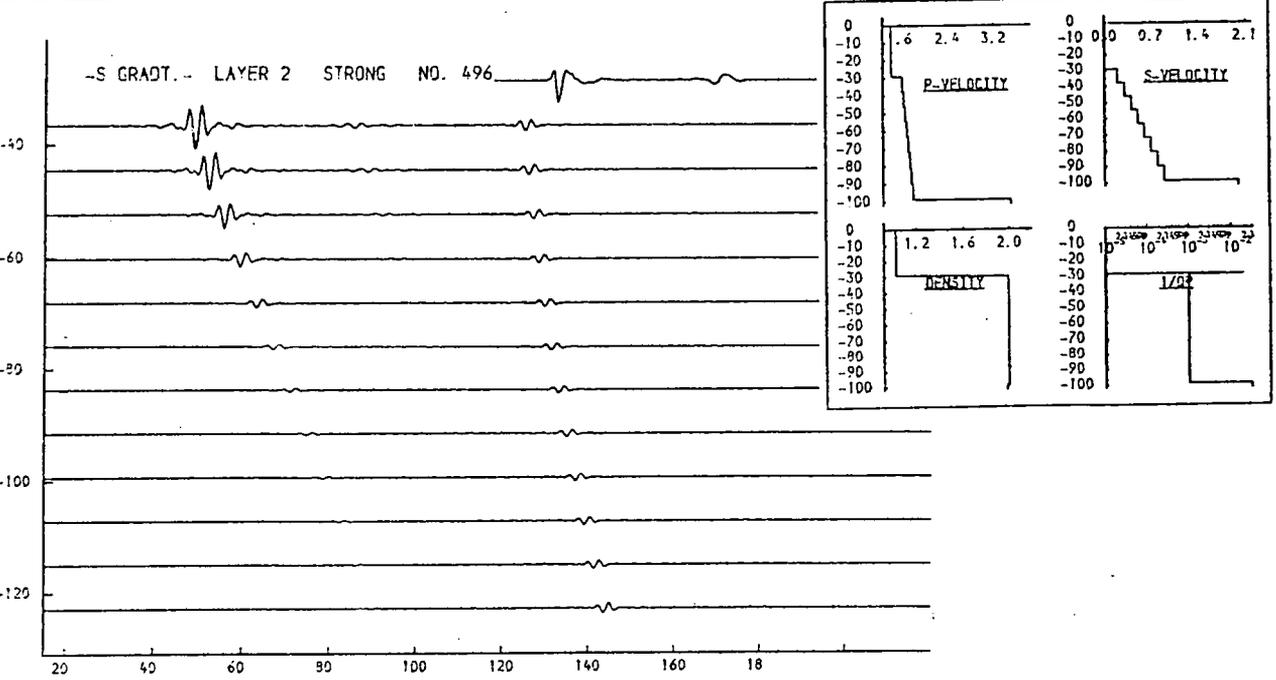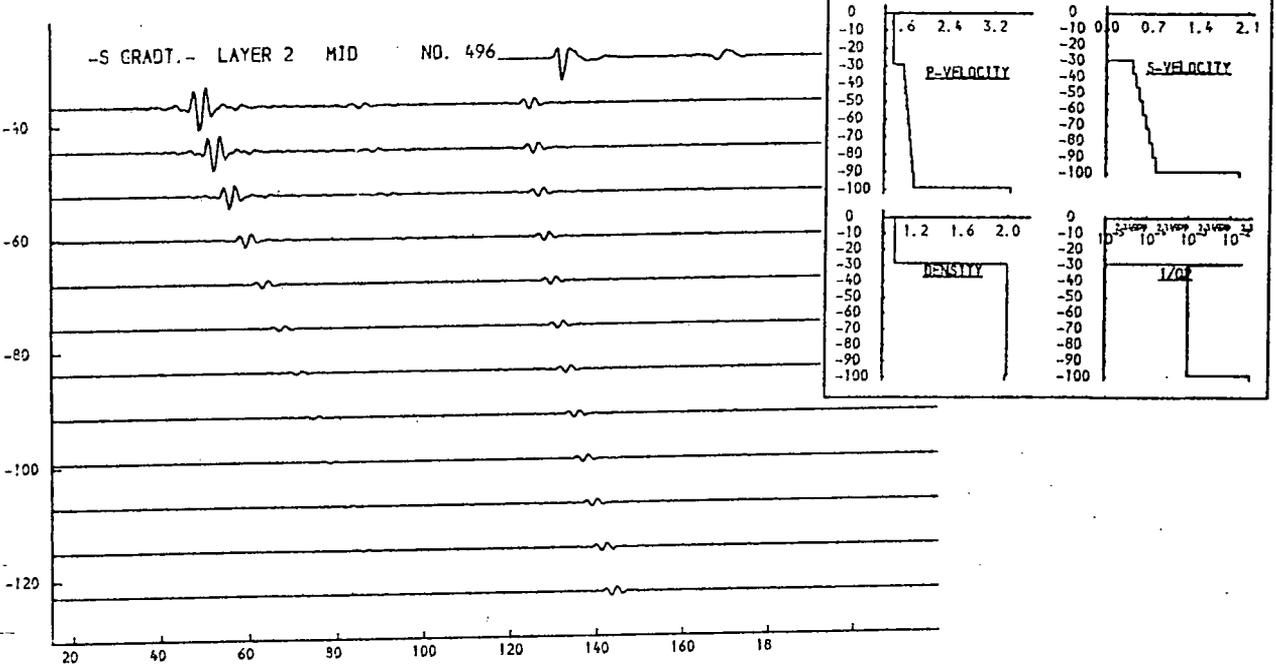
Fig. 9.95b.   Gradients in s-velocity.

Variations are shown in a uniform s-velocity gradient for values
of 5 and 13m/sec/m.

THICKNESS	P-VELOCITY	S-VELOCITY	DENSITY	1/Q	1/Q
(M.)	(M/S.)	(M/S.)	(G/ML)	P	S
16.8	1.471	0.849	1.03	0.00000	0.00000
10.0	1.480	0.010	1.65	0.00100	0.01000
59.9	1.770	0.250	2.00	0.00100	0.03000
	3.500	2.000	1.98	0.00100	0.03000

THICKNESS	P-VELOCITY	S-VELOCITY	DENSITY	1/Q	1/Q
(M.)	(M/S.)	(M/S.)	(G/ML)	P	S
21.8	1.471	0.849	1.03	0.00000	0.00000
10.0	1.480	0.010	1.65	0.00100	0.01000
59.9	1.770	0.250	2.00	0.00100	0.03000
	3.500	2.000	1.98	0.00100	0.03000

Fig. 9.96.   Gradient in bottom-water velocity.
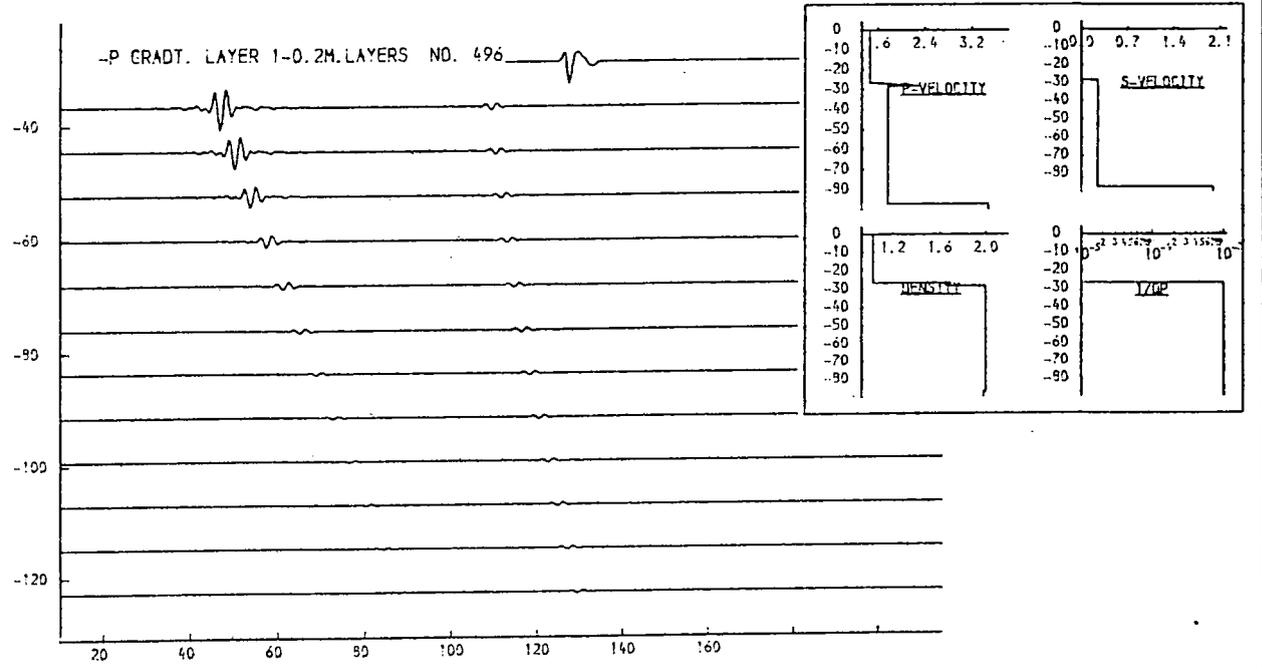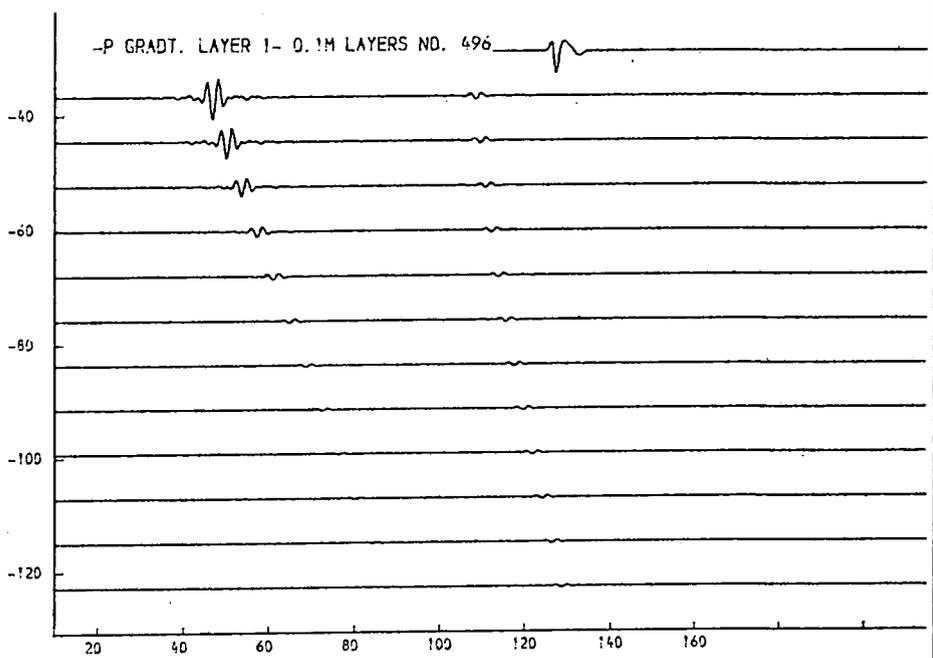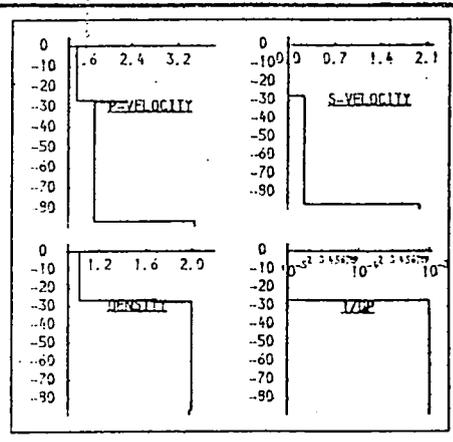
Fig. 9.97a. High p-velocity gradient.

Gradients of 1000m/sec/m. (upper) and 500m/sec/m. (lower) are shown, for variations in the immediate subbottom.

THICKNESS (M.)	P-VELOCITY (M/S.)	S-VELOCITY (M/S.)	DENSITY (G/ML)	1/Q P	1/Q S
26.6	1.460	0.000	1.03	0.00000	0.00000
59.9	1.770	0.250	2.00	0.00100	0.03000
	3.500	2.000	1.99	0.00100	0.03000

-P GRADT. LAYER 1- 0.5M. LAYERS NO. 496

-P GRADT. LAYER 1- 1.25M LAYERS NO. 496
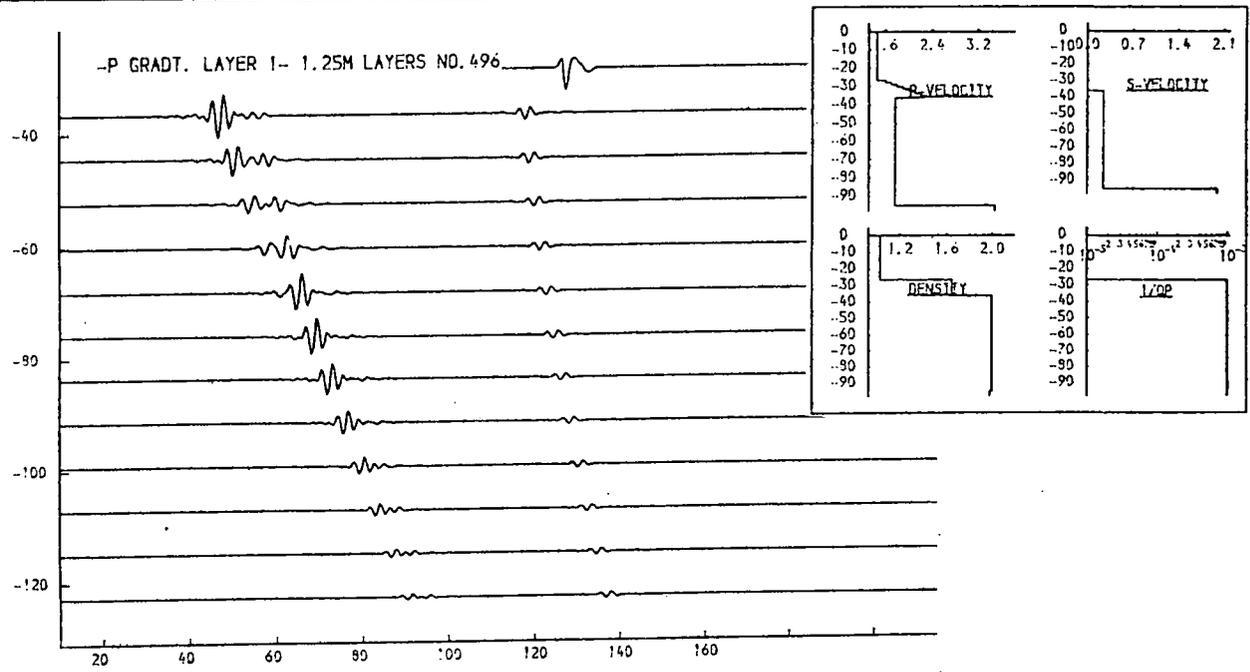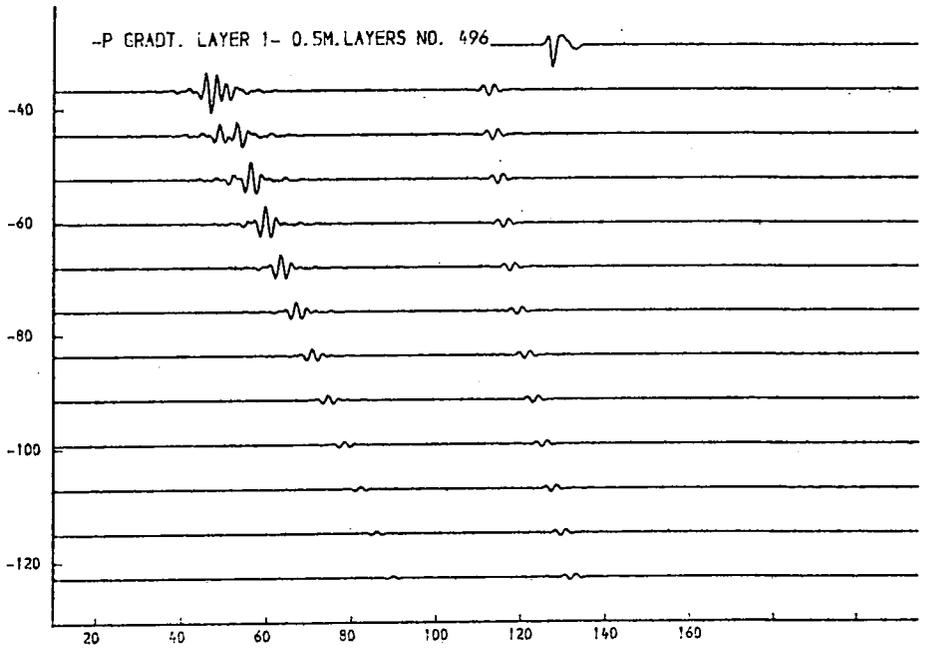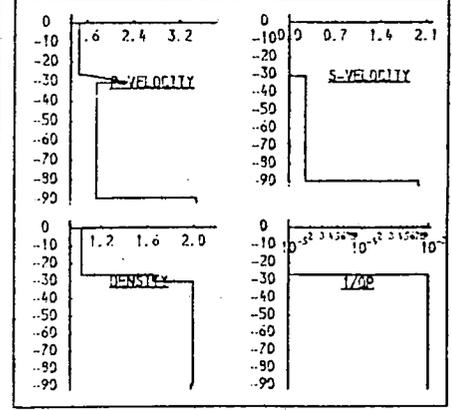
Fig. 9.97b. High p-velocity gradient.

Gradients of 200m/sec/m. (upper) and 80m/sec/m. (lower) are shown, for variations in the immediate subbottom.

THICKNESS (M.)	P-VELOCITY (M/S.)	S-VELOCITY (M/S.)	DENSITY (G/ML)	1/Q P	1/Q S
26.6	1.460	0.000	1.03	0.00000	0.00000
3.6	1.507	0.213	2.00	0.00100	0.00300
3.9	1.583	0.224	2.00	0.00100	0.00300
4.0	1.658	0.234	2.00	0.00100	0.00300
4.2	1.733	0.245	2.00	0.00100	0.00300
4.6	1.882	0.266	2.00	0.00100	0.00300
4.9	2.033	0.287	2.00	0.00100	0.00300
4.7	1.959	0.276	2.00	0.00100	0.00300
4.4	1.882	0.255	2.00	0.00100	0.00300
4.2	1.733	0.245	2.00	0.00100	0.00300
4.2	1.733	0.245	2.00	0.00100	0.00300
20.0	1.658	0.234	2.00	0.00100	0.00300
	2.000	0.600	1.99	0.00100	0.00300

THICKNESS (M.)	P-VELOCITY (M/S.)	S-VELOCITY (M/S.)	DENSITY (G/ML)	1/Q P	1/Q S
26.6	1.460	0.000	1.03	0.00000	0.00000
0.5	1.480	0.210	1.65	0.00100	0.00300
3.6	1.507	0.213	2.00	0.00100	0.00300
3.9	1.583	0.224	2.00	0.00100	0.00300
4.0	1.658	0.234	2.00	0.00100	0.00300
4.2	1.733	0.245	2.00	0.00100	0.00300
4.6	1.882	0.266	2.00	0.00100	0.00300
4.9	2.033	0.297	2.00	0.00100	0.00300
4.7	1.959	0.276	2.00	0.00100	0.00300
4.4	1.882	0.255	2.00	0.00100	0.00300
4.2	1.733	0.245	2.00	0.00100	0.00300
4.2	1.733	0.245	2.00	0.00100	0.00300
20.0	1.658	0.234	2.00	0.00100	0.00300
	2.000	0.600	1.99	0.00100	0.00300

Fig. 9.98a.   Velocity gradients.

Further velocity profiles are seen here.   The lower model differs from the upper in having the addition of a 1m. thick layer of surficial sediment of velocity 1.48km/s. and density 1.65gm/ml.

THICKNESS (M.)	P-VELOCITY (M/S.)	S-VELOCITY (M/S.)	DENSITY (G/ML)	1/Q P	1/Q S
26.6	1.460	0.000	1.03	0.00000	0.00000
2.8	1.551	0.210	2.01	0.00300	0.03000
2.8	1.651	0.210	2.01	0.00300	0.03000
3.7	1.902	0.255	2.00	0.00300	0.03000
4.1	1.959	0.276	2.00	0.00300	0.03000
4.4	2.108	0.298	2.00	0.00300	0.03000
4.7	2.257	0.319	2.00	0.00300	0.03000
4.9	2.333	0.322	2.00	0.00300	0.03000
4.5	2.192	0.309	2.00	0.00300	0.03000
4.2	2.033	0.287	2.00	0.00300	0.03000
3.0	1.882	0.266	2.00	0.00300	0.03000
3.6	1.733	0.255	2.00	0.00300	0.03000
3.3	1.593	0.224	2.00	0.00300	0.03000
3.3	1.593	0.224	2.00	0.00300	0.03000
3.3	1.593	0.224	2.00	0.00300	0.03000
4.4	1.593	0.313	2.00	0.00300	0.03000
4.4	1.593	0.313	2.00	0.00300	0.03000
4.4	1.593	0.313	2.00	0.00300	0.03000
	3.500	2.000	1.98	0.00300	0.03000

-9DEC 6 TRY GRADTS. 1&2   NO. 496

-9DEC 2 TRY GRADTS. 1&2   NO. 496

Fig. 9.98b. Velocity gradients.

These models differ from one another in the character of the velocity gradient near the seabed. The gradients do not exceed 5m/sec/m.

THICKNESS (M.)	P-VELOCITY (M/S.)	S-VELOCITY (M/S.)	DENSITY (G/ML)	1/Q P	1/Q S
26.6	1.460	0.000	1.03	0.00000	0.00000
1.0	1.460	0.013	1.45	0.00100	0.00600
3.5	1.456	0.210	2.00	0.00100	0.00600
4.1	1.739	0.246	1.98	0.00100	0.00600
4.7	1.999	0.281	1.96	0.00100	0.00600
5.2	2.176	0.307	1.94	0.00100	0.00600
5.3	2.239	0.316	1.93	0.00100	0.00600
5.0	2.114	0.299	1.94	0.00100	0.00600
4.9	2.051	0.290	1.95	0.00100	0.00600
4.6	1.926	0.272	1.96	0.00100	0.00600
4.5	1.863	0.263	1.97	0.00100	0.00600
4.3	1.901	0.254	1.98	0.00100	0.00600
4.0	1.676	0.237	1.99	0.00100	0.00600
3.9	1.614	0.229	1.99	0.00100	0.00600
14.9	1.551	0.219	2.00	0.00100	0.00600
	3.500	2.000	1.98	0.00100	0.00600

THICKNESS (M.)	P-VELOCITY (M/S.)	S-VELOCITY (M/S.)	DENSITY (G/ML)	1/Q P	1/Q S
26.6	1.460	0.000	1.03	0.00000	0.00000
1.0	1.460	0.013	1.45	0.00100	0.00600
3.5	1.456	0.210	2.00	0.00100	0.00600
4.1	1.739	0.246	2.00	0.00100	0.00600
4.7	1.999	0.281	2.00	0.00100	0.00600
5.2	2.176	0.307	2.00	0.00100	0.00600
5.3	2.239	0.316	2.00	0.00100	0.00600
5.0	2.114	0.299	2.00	0.00100	0.00600
4.9	2.051	0.290	2.00	0.00100	0.00600
4.6	1.926	0.272	2.00	0.00100	0.00600
4.5	1.863	0.263	2.00	0.00100	0.00600
4.3	1.901	0.254	2.00	0.00100	0.00600
4.0	1.676	0.237	2.00	0.00100	0.00600
3.9	1.614	0.229	2.00	0.00100	0.00600
14.9	1.551	0.219	2.00	0.00100	0.00600
	2.500	1.200	1.98	0.00100	0.00600

VELOGRADT. IN 2 DENSITY VARIES NO. 497

_P&S LAYER 3 P=2.5 S=1.2   NO. 497
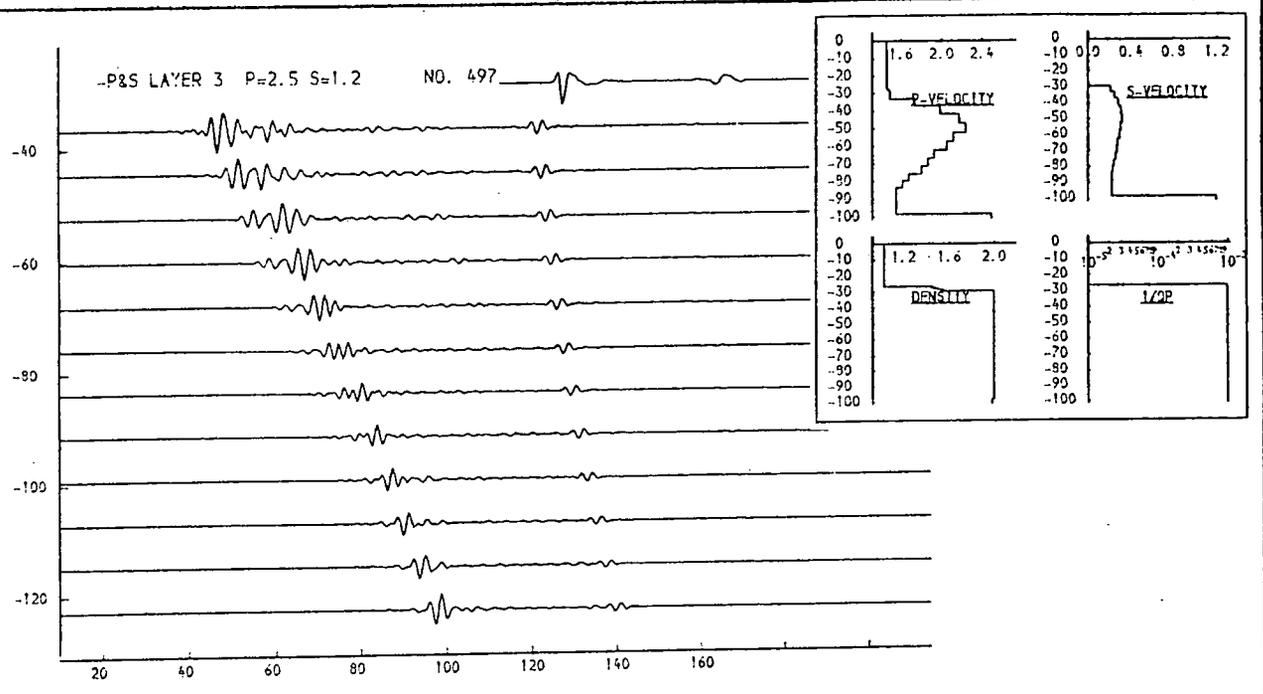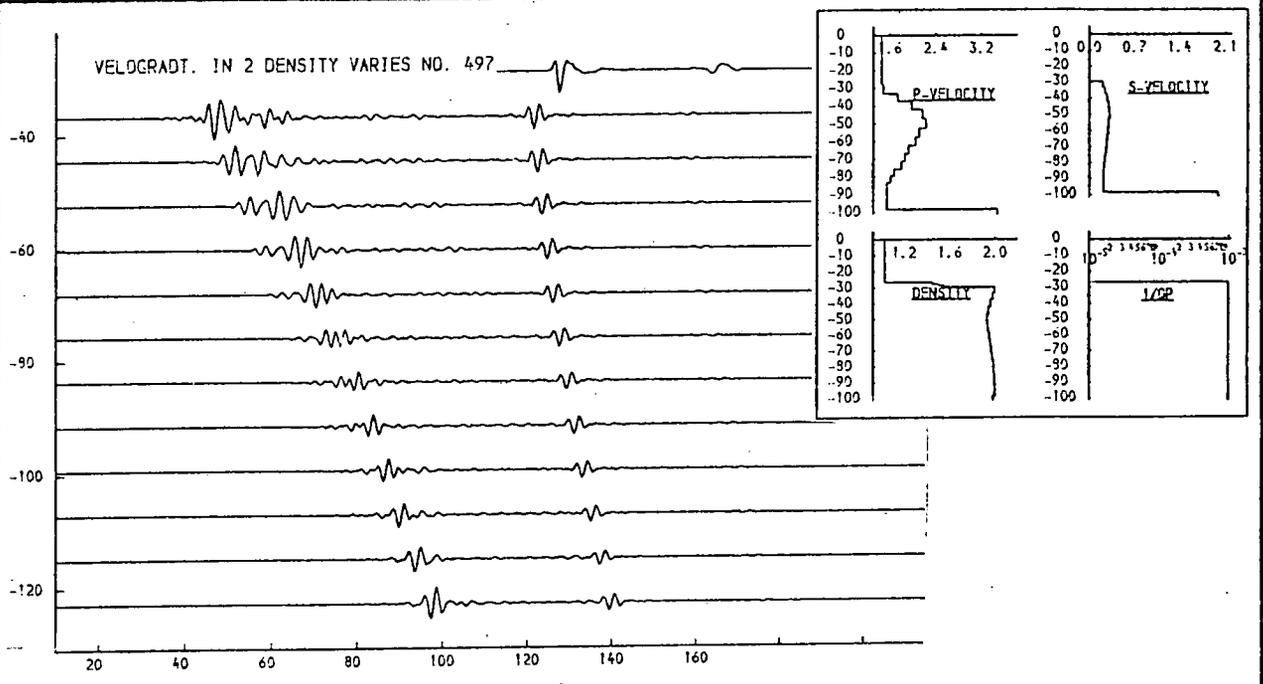
Fig. 9.99a.   Velocity gradients.

These models differ from one another in having a different velocity contrast at the deeper reflector "r", whose amplitude is affected.   This   is   irrelevant   to near-seabed characteristics, which are affected slightly by the different density profiles.

THICKNESS (M.)	P-VELOCITY (M/S.)	S-VELOCITY (M/S.)	DENSITY (G/ML)	1/Q P	1/Q S
26.6	1.460	0.000	1.03	0.00000	0.00000
0.5	1.588	0.818	1.65	0.03000	0.05000
3.4	1.653	0.299	2.00	0.03000	0.03000
2.9	2.133	0.299	2.00	0.03000	0.03000
2.9	2.233	0.328	2.00	0.03000	0.03000
3.0	2.432	0.328	2.00	0.03000	0.03000
5.6	2.257	0.319	2.00	0.03000	0.03000
5.4	2.192	0.308	2.00	0.03000	0.03000
5.2	2.108	0.298	2.00	0.03000	0.03000
4.8	1.959	0.276	2.00	0.03000	0.03000
4.6	1.882	0.266	2.00	0.03000	0.03000
4.4	1.807	0.255	2.00	0.03000	0.03000
4.3	1.733	0.245	2.00	0.03000	0.03000
3.0	1.583	0.224	2.00	0.03000	0.03000
3.0	1.583	0.224	2.00	0.03000	0.03000
3.0	1.583	0.224	2.00	0.03000	0.03000
3.0	1.583	0.224	2.00	0.03000	0.03000
3.7	1.507	0.213	2.00	0.03000	0.03000
3.0	1.583	0.224	2.00	0.03000	0.03000
	3.500	2.000	1.99	0.03000	0.06000

GRADT. 0.5M TOP   NO. 496

GRADT.   2.0M TOP NO. 496

Fig. 9.99b.   Velocity gradients.

The offset distance at which the high amplitudes presumably associated with near-critical reflexions from the higher velocity zone are observed is increased by the introduction of an additional 1.5m. thickness of a surficial layer.

THICKNESS (M.)	P-VELOCITY (M/S.)	S-VELOCITY (M/S.)	DENSITY (G/ML)	1/Q P	1/Q S
26.6	1.460	0.000	1.03	0.00000	0.99000
	1.676	0.919	2.00	0.00300	0.03000
2.4	2.233	0.422	2.00	0.00300	0.03000
2.9	2.152	0.337	2.00	0.00300	0.03000
4.0	2.632	0.329	2.00	0.00300	0.03000
5.6	2.257	0.319	2.00	0.00300	0.03000
5.4	2.182	0.308	2.00	0.00300	0.03000
5.2	2.109	0.299	2.00	0.00300	0.03000
4.9	1.958	0.276	2.00	0.00300	0.03000
4.6	1.882	0.266	2.00	0.00300	0.03000
4.4	1.907	0.255	2.00	0.00300	0.03000
4.3	1.733	0.245	2.00	0.00300	0.03000
3.9	1.583	0.224	2.00	0.00300	0.03000
3.9	1.583	0.224	2.00	0.00300	0.03000
3.9	1.583	0.224	2.00	0.00300	0.03000
3.9	1.583	0.224	2.00	0.00300	0.03000
3.7	1.502	0.213	2.00	0.00300	0.03000
3.9	1.583	0.224	2.00	0.00300	0.03000
	3.500	2.000	1.98	0.03000	0.06000

TRY STRONGER GRADT. 1.0M TOP   NO. 496

TRY VERY STR.GRADT. 1.0M TOP   NO. 496

Fig. 9.99c.   Velocity gradients.

ariations in the gradient in the immediate subbottom produce mall changes in the position of near-critical reflexions.

THICKNESS (M.)	P-VELOCITY (M/S.)	S-VELOCITY (M/S.)	DENSITY (G/ML)	1/Q P	1/Q S
26.6	1.460	0.000	1.03	0.00000	0.00000
0.1	1.460	0.010	1.50	0.00100	0.01000
5.2	2.176	0.230	2.00	0.00100	0.01000
5.3	2.239	0.250	2.00	0.00100	0.01000
5.0	2.114	0.220	2.00	0.00100	0.01000
4.9	2.015	0.200	2.00	0.00100	0.01000
4.6	1.926	0.180	2.00	0.00100	0.01000
4.5	1.964	0.150	2.00	0.00100	0.01000
4.3	1.901	0.150	2.00	0.00100	0.01000
4.3	1.676	0.090	2.00	0.00100	0.01000
4.3	1.614	0.080	2.00	0.00100	0.01000
14.9	1.551	0.030	2.00	0.00100	0.01000
	3.500	2.000	1.98	0.00100	0.03000

-AS ARC101 LOWER -S-   ARC102 NO.496

-AS ARC102 THICKER LAYERS ARC103 NO.496
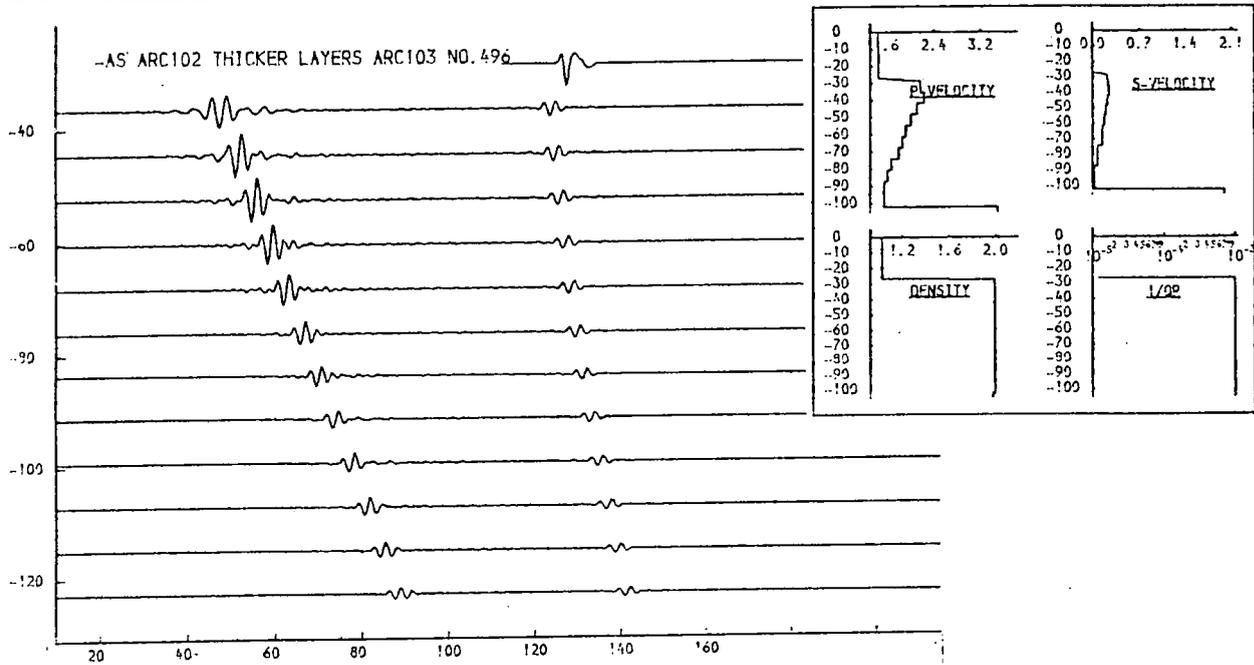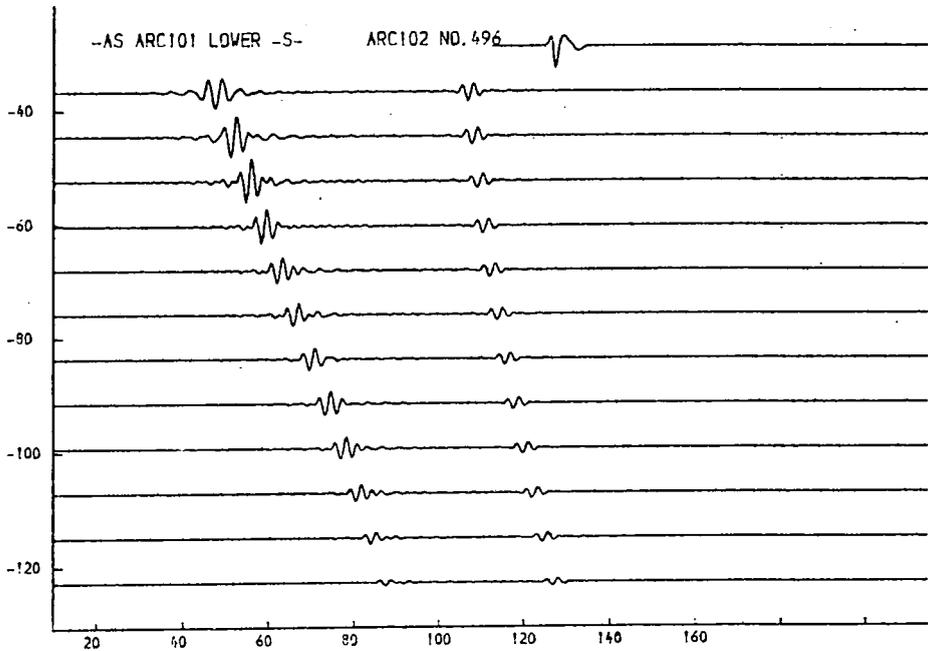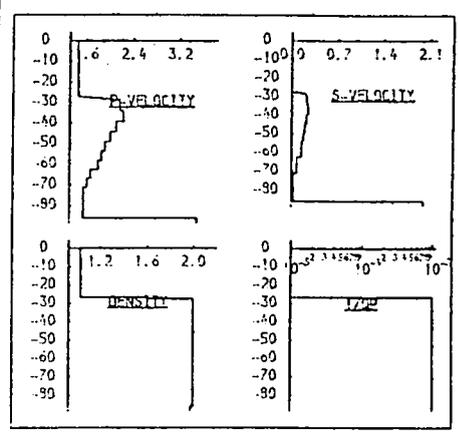
Fig. 9.99d.   Velocity gradients.

A very high gradient of ca. 450m/sec/m. within the top 2m. of sediment improves the model of the bottom reflexion. Differences in the layer thickness of deeper structure produce a small variation at high offset between the upper and lower models.

THICKNESS (M.)	P-VELOCITY (M/S.)	S-VELOCITY (M/S.)	DENSITY (G/ML)	1/Q P	1/Q S
26.6	1.460	0.000	1.03	0.00000	0.00000
	1.550	0.002			
11.9	3.557	1.576	2.00	0.00100	0.03000
8.9	1.933	0.259	2.00	0.00100	0.03000
8.3	1.709	0.241	2.00	0.00100	0.03000
7.7	1.593	0.224	2.00	0.00100	0.03000
7.7	1.593	0.224	2.00	0.00100	0.03000
7.7	1.593	0.224	2.00	0.00100	0.03000
	3.500	2.000	1.99	0.00100	0.03000

-H GRT. NR. SBD. BROADER LYS. NO. 496

-H GRT. NR. SBD. BROADER LYS. NO. 496
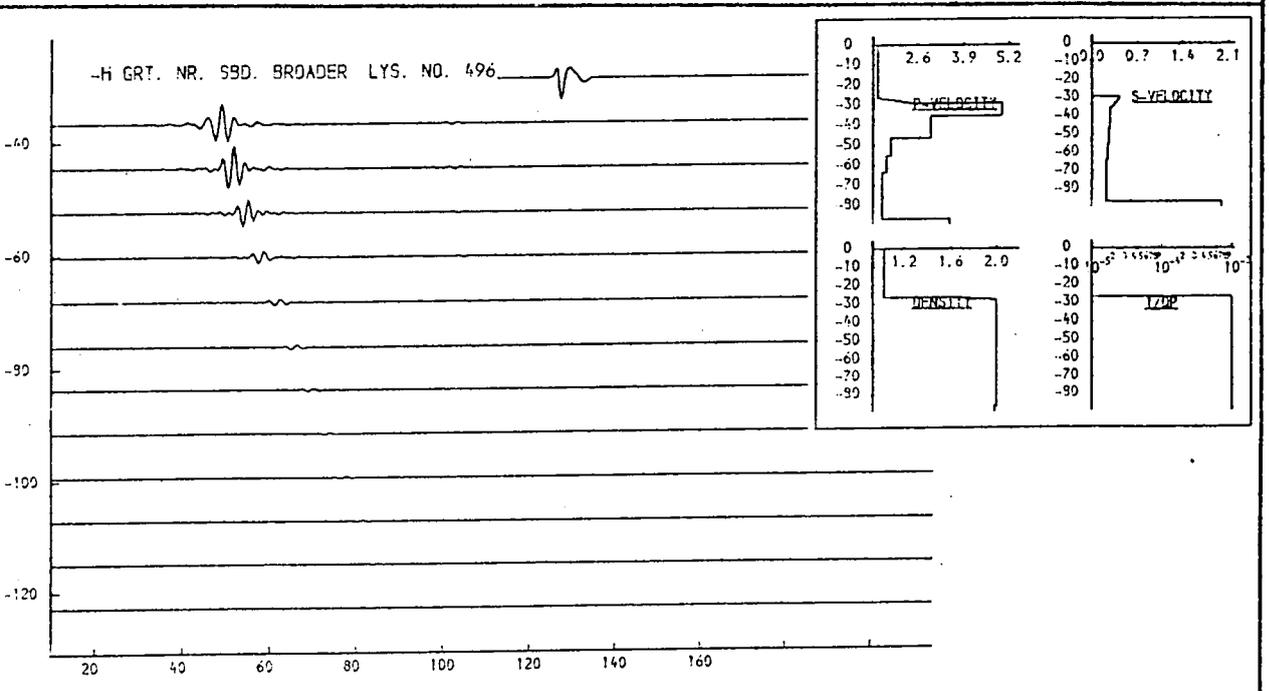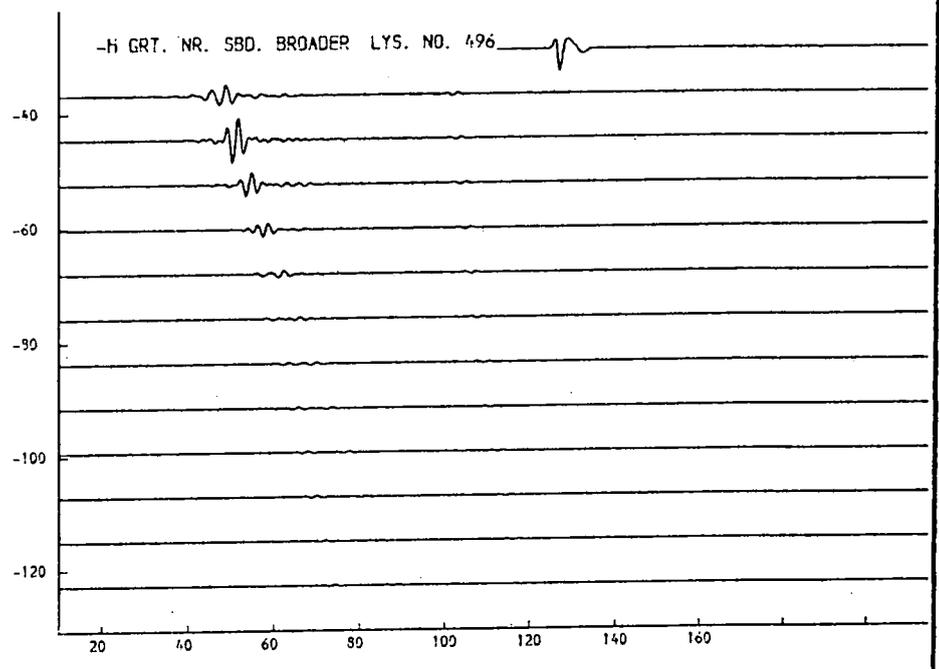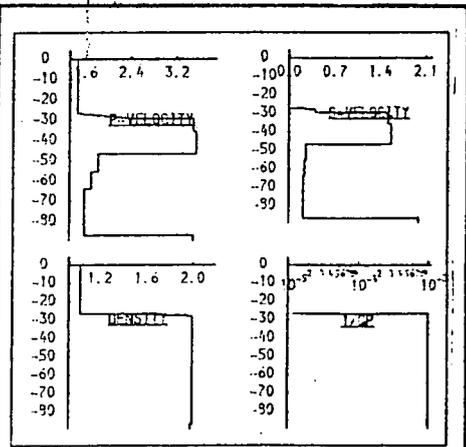
Fig. 9.100. Velocity gradients.

very rapid rise to high velocity at shallow depth appears to concentrate the reflected energy at small offset.

THICKNESS (M.)	P-VELOCITY (M/S.)	S-VELOCITY (M/S.)	DENSITY (G/ML)	1/Q P	1/Q S
26.6	1.460	0.000	1.03	0.00000	0.00000
5.2	2.145	0.500	2.00	0.00100	0.03000
4.5	1.945	0.300	2.00	0.00100	0.03000
31.2	1.600	0.100	2.00	0.00100	0.03000
	3.500	2.000	1.99	0.00100	0.03000

THICKNESS (M.)	P-VELOCITY (M/S.)	S-VELOCITY (M/S.)	DENSITY (G/ML)	1/Q P	1/Q S
26.6	1.460	0.000	1.03	0.00000	0.00000
5.9	2.145	0.500	2.00	0.00100	0.03000
4.5	1.945	0.300	2.00	0.00100	0.03000
31.2	1.600	0.100	2.00	0.00100	0.03000
	3.500	2.000	1.98	0.00100	0.03000

AS ARC107 2-M STEPSIZE   ARC-108 NO.496

AS ARC107 1-M STEPSIZE   ARC-109 NO.496

Fig. 9.101a. Velocity gradients.

ncreasing the depth below seabed of a velocity peak displaces
ear-critical reflexions to higher offset.

THICKNESS (M.)	P-VELOCITY (M/S.)	S-VELOCITY (M/S.)	DENSITY (G/ML)	1/Q P	1/Q S
26.6	1.460	0.000	1.03	0.00000	0.00000
0.3	1.500	0.310	1.70	0.00100	0.01000
3.0	2.600	0.500	2.00	0.00100	0.01000
4.0	2.800	0.500	2.00	0.00100	0.01000
5.0	3.000	0.500	2.00	0.00100	0.01000
5.0	2.800	0.500	2.00	0.00100	0.01000
3.0	2.600	0.500	2.00	0.00100	0.01000
5.0	2.145	0.500	2.00	0.00100	0.03000
4.5	1.845	0.300	2.00	0.00100	0.03000
31.2	1.600	0.700	2.00	0.00100	0.03000
	3.500	2.000	1.99	0.00100	0.03000

AS ARC109 WITH DENS GRAD. ARC-111 NO.496

AS ARC111 WITH VELO STEP. ARC-112 NO.496

Fig. 9.101b. Velocity gradients.

he broadening of the velocity peak (c.f. fig. 9.101a) broadens
he offset zone where reflexions are received.

THICKNESS (M.)	P-VELOCITY (M/S.)	S-VELOCITY (M/S.)	DENSITY (G/ML)	1/Q P	1/Q S
26.6	1.460	0.000	1.03	0.00000	0.00000
9.5	1.699	0.210	2.05	0.00300	0.06000
2.2	1.933	0.245	2.00	0.00300	0.03000
2.4	1.932	0.287	2.00	0.00300	0.03000
4.9	1.958	0.276	2.00	0.00300	0.03000
4.6	1.992	0.266	2.00	0.00300	0.03000
4.4	1.907	0.255	2.00	0.00300	0.03000
4.3	1.733	0.245	2.00	0.00300	0.03000
3.9	1.593	0.224	2.00	0.00300	0.03000
3.9	1.593	0.224	2.00	0.00300	0.03000
3.9	1.593	0.224	2.00	0.00300	0.03000
3.9	1.593	0.224	2.00	0.00300	0.03000
3.7	1.507	0.213	2.00	0.00300	0.03000
3.9	1.593	0.224	2.00	0.00300	0.03000
3.500	2.000	1.98	0.03000	0.06000

Fig. 9.102a. Velocity gradients-maximum velocity=1.95km/s.

Upper: The velocity profile shown is topped by a 0.5m. thick surficial layer.
Lower: The surficial layer has been increased to 2m.

THICKNESS (M.)	P-VELOCITY (M/S.)	S-VELOCITY (M/S.)	DENSITY (G/HL)	1/Q P	1/Q S
26.6	1.460	0.000	1.03	0.00000	0.00000
2.0	1.812	0.245	2.00	0.00300	0.03000
2.2	1.811	0.245	2.00	0.00300	0.03000
2.4	1.932	0.287	2.00	0.00300	0.03000
4.9	1.958	0.276	2.00	0.00300	0.03000
4.6	1.982	0.266	2.00	0.00300	0.03000
4.4	1.907	0.255	2.00	0.00300	0.03000
4.3	1.733	0.245	2.00	0.00300	0.03000
3.9	1.583	0.224	2.00	0.00300	0.03000
3.9	1.583	0.224	2.00	0.00300	0.03000
3.9	1.583	0.224	2.00	0.00300	0.03000
3.9	1.583	0.224	2.00	0.00300	0.03000
3.7	1.597	0.213	2.00	0.00300	0.03000
3.9	1.583	0.224	2.00	0.00300	0.03000
	3.500	2.000	1.98	0.03000	0.06000

MAX 1.95   NO. 496

MAX 1.95   NO. 496

Fig. 9.102b. Velocity gradients-maximum velocity=1.95km/s.

Similar models to those shown in fig. 9.102a, with the thickness of the surficial layer increased to 4m. In the upper model the density in that layer is constant, in the lower, it varies.

THICKNESS (M.)	P-VELOCITY (M/S.)	S-VELOCITY (M/S.)	DENSITY (G/ML)	1/Q P	1/Q S
26.6	1.460	0.000	1.03	0.00000	0.00000
3.9	1.833	0.213	2.55	0.03333	0.01333
3.4	1.933	0.585	2.00	0.00300	0.03000
2.6	2.132	0.287	2.00	0.00300	0.03000
5.2	2.108	0.299	2.00	0.00300	0.03000
4.9	1.959	0.276	2.00	0.00300	0.03000
4.6	1.892	0.266	2.00	0.00300	0.03000
4.4	1.807	0.255	2.00	0.00300	0.03000
4.3	1.733	0.245	2.00	0.00300	0.03000
3.9	1.583	0.224	2.00	0.00300	0.03000
3.9	1.583	0.224	2.00	0.00300	0.03000
3.9	1.583	0.224	2.00	0.00300	0.03000
3.9	1.583	0.224	2.00	0.00300	0.03000
3.7	1.507	0.213	2.00	0.00300	0.03000
3.9	1.583	0.224	2.00	0.00300	0.03000
	3.500	2.000	1.98	0.03000	0.06000

TRY VSTR.GR.LOWERPK.1.0M TOP   NO. 496

TRY VSTR.GR.LOWERPK.2.0M TOP   NO. 496

Fig. 9.103a. Rapid velocity increase near seabed.

A gradient of 100m/sec/m. near the seabed enhances arrivals at high offset. In the upper model, a surficial layer is 1m. thick, in the lower model, it is 2m. thick.

THICKNESS (M.)	P-VELOCITY (M/S.)	S-VELOCITY (M/S.)	DENSITY (G/ML)	1/Q P	1/Q S
26.6	1.460	0.000	1.03	0.00000	0.00000
4.0	1.490	0.010	1.65	0.03000	0.04000
8.4	1.633	0.243	2.13	0.33333	0.04000
2.4	1.632	0.287	2.00	0.00300	0.03000
2.6	2.132	0.287	2.00	0.00300	0.03000
5.2	2.109	0.298	2.00	0.00300	0.03000
4.9	1.958	0.276	2.00	0.00300	0.03000
4.6	1.982	0.266	2.00	0.00300	0.03000
4.4	1.907	0.255	2.00	0.00300	0.03000
4.3	1.733	0.245	2.00	0.00300	0.03000
3.9	1.593	0.224	2.00	0.00300	0.03000
3.9	1.593	0.224	2.00	0.00300	0.03000
3.9	1.593	0.224	2.00	0.00300	0.03000
3.7	1.597	0.213	2.00	0.00300	0.03000
3.9	1.593	0.224	2.00	0.00300	0.03000
	3.500	2.000	1.98	0.03000	0.06000

TRY VSTR. GR. LOWERPK. 4.0M TOP   NO. 496

TRY VSTR. GR. LOWERPK. 6.0M TOP   NO. 496

Fig. 9.103b. Rapid velocity increase near seabed.

With increasing thickness of a surficial layer beyond the value of 2m. (fig. 9.103a), an expected increasing displacement between bottom and subbottom events is seen, but other changes are very slight.

THICKNESS (M.)	P-VELOCITY (M/S.)	S-VELOCITY (M/S.)	DENSITY (G/ML)	1/Q P	1/Q S
26.6	1.460	0.000	1.03	0.00000	0.00000
5.3	2.239	0.316	2.00	0.00100	0.00600
5.0	2.114	0.299	2.00	0.00100	0.00600
4.0	2.251	0.299	2.00	0.00100	0.00600
4.6	1.926	0.272	2.00	0.00100	0.00600
4.5	1.864	0.263	2.00	0.00100	0.00600
4.3	1.801	0.254	2.00	0.00100	0.00600
4.0	1.676	0.237	2.00	0.00100	0.00600
3.0	1.614	0.228	2.00	0.00100	0.00600
14.9	1.551	0.219	2.00	0.00100	0.00600
	3.500	2.000	1.98	0.00100	0.00600

GRADT 2. 0 OF 1M. LAYERS ON TOP NO. 497

GRADT 2. 2 OF 1M. LAYERS ON TOP NO. 497
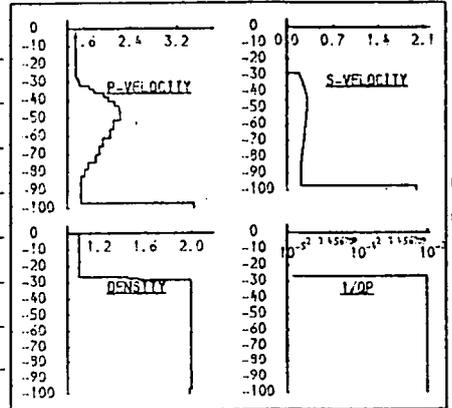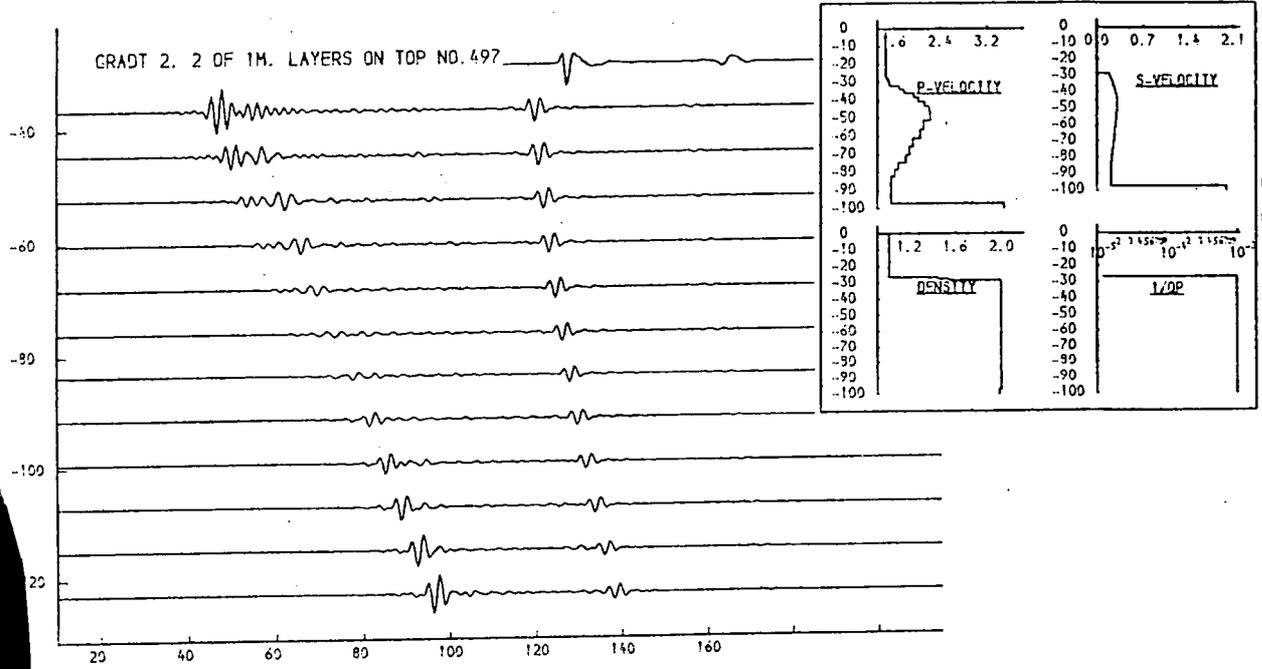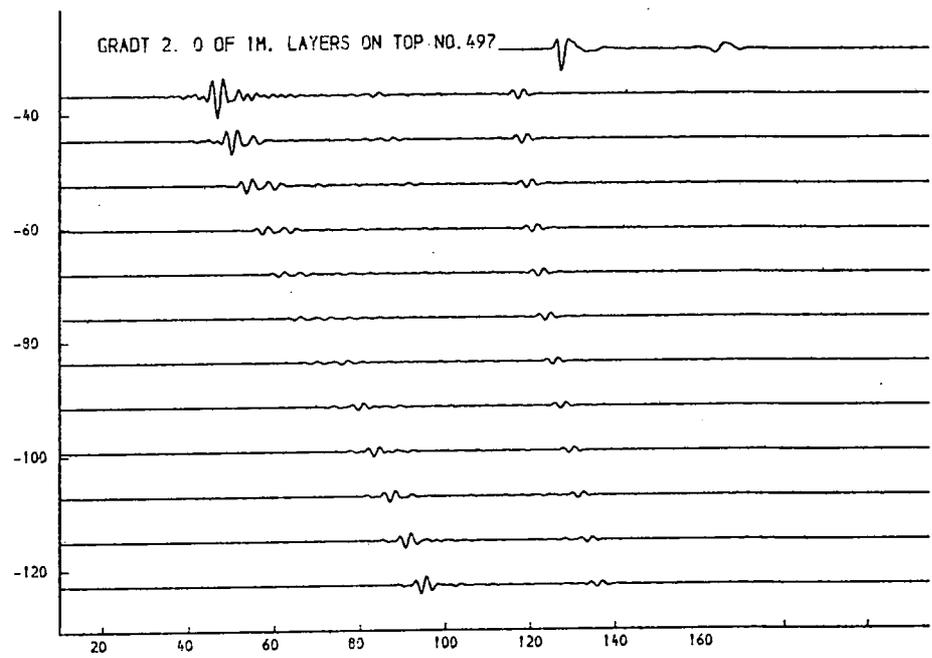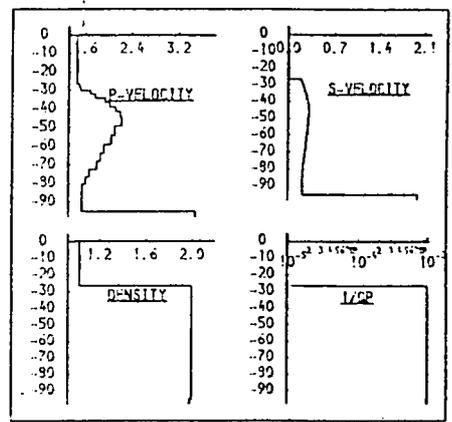
Fig. 9.104. Velocity gradients.

A lower subbottom gradient (ca. 35m/sec/m.) in conjunction with a higher peak velocity (2.24km/s., c.f. 1.96km/s. in fig. 9.102a,b) results in arrivals at high offset, these arrivals being stronger when a 2m. thick surficial layer is present (lower model).

THICKNESS (M.)	P-VELOCITY (M/S.)	S-VELOCITY (M/S.)	DENSITY (G/ML)	1/Q P	1/Q S
26.6	1.460	0.000	1.03	0.00000	0.00000
0.7	1.518	0.010	1.45	0.00100	0.01000
13.0	2.212	1.277	2.90	0.00100	0.01000
27.5	3.002	1.734	1.96	0.00100	0.01000
6.6	2.395	1.393	1.98	0.00100	0.03000
5.9	2.145	1.253	2.00	0.00100	0.03000
4.5	1.945	1.065	2.00	0.00100	0.03000
20.2	1.600	0.924	2.00	0.00100	0.03000
	3.500	2.000	1.98	0.00100	0.03000

THICKNESS (M.)	P-VELOCITY (M/S.)	S-VELOCITY (M/S.)	DENSITY (G/ML)	1/Q P	1/Q S
26.6	1.460	0.000	1.03	0.00000	0.00000
0.7	1.517	0.010	1.45	0.00100	0.01000
13.0	2.212	1.277	2.90	0.00100	0.01000
27.5	2.892	1.618	1.97	0.00100	0.01000
6.6	2.395	1.383	1.98	0.00100	0.03000
5.9	2.145	1.238	2.00	0.00100	0.03000
4.5	1.945	1.065	2.00	0.00100	0.03000
20.2	1.600	0.924	2.00	0.00100	0.03000
	3.500	2.000	1.98	0.00100	0.03000
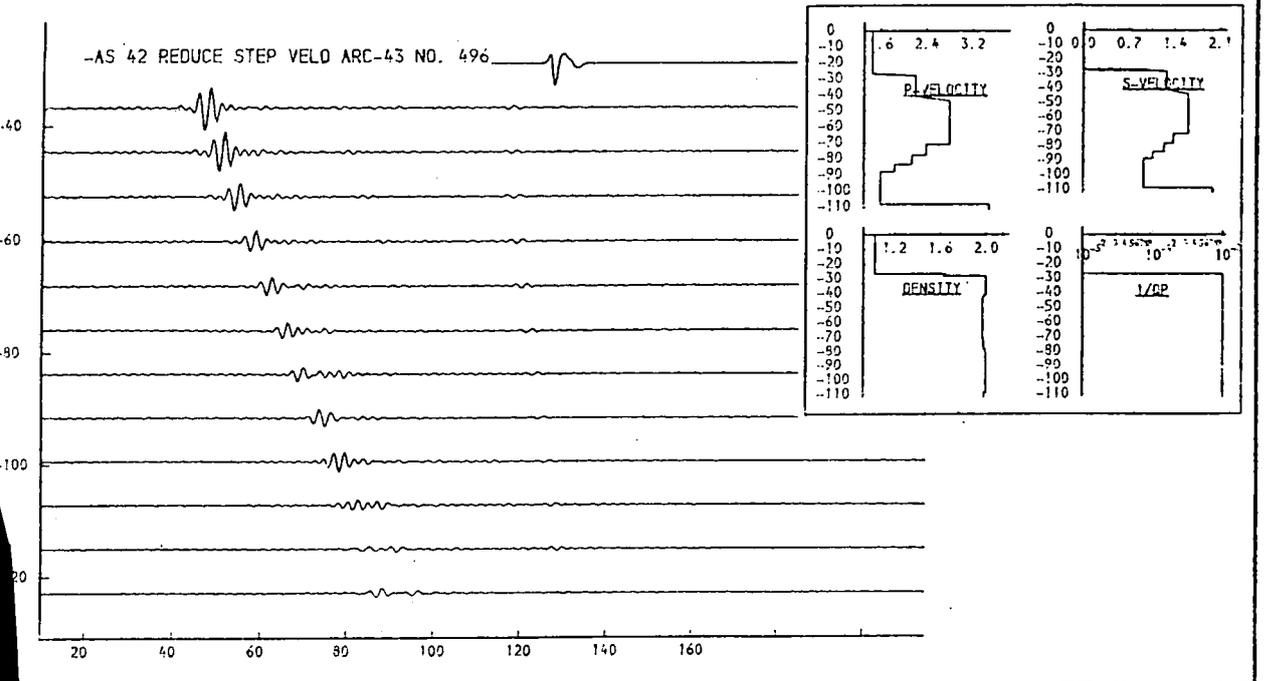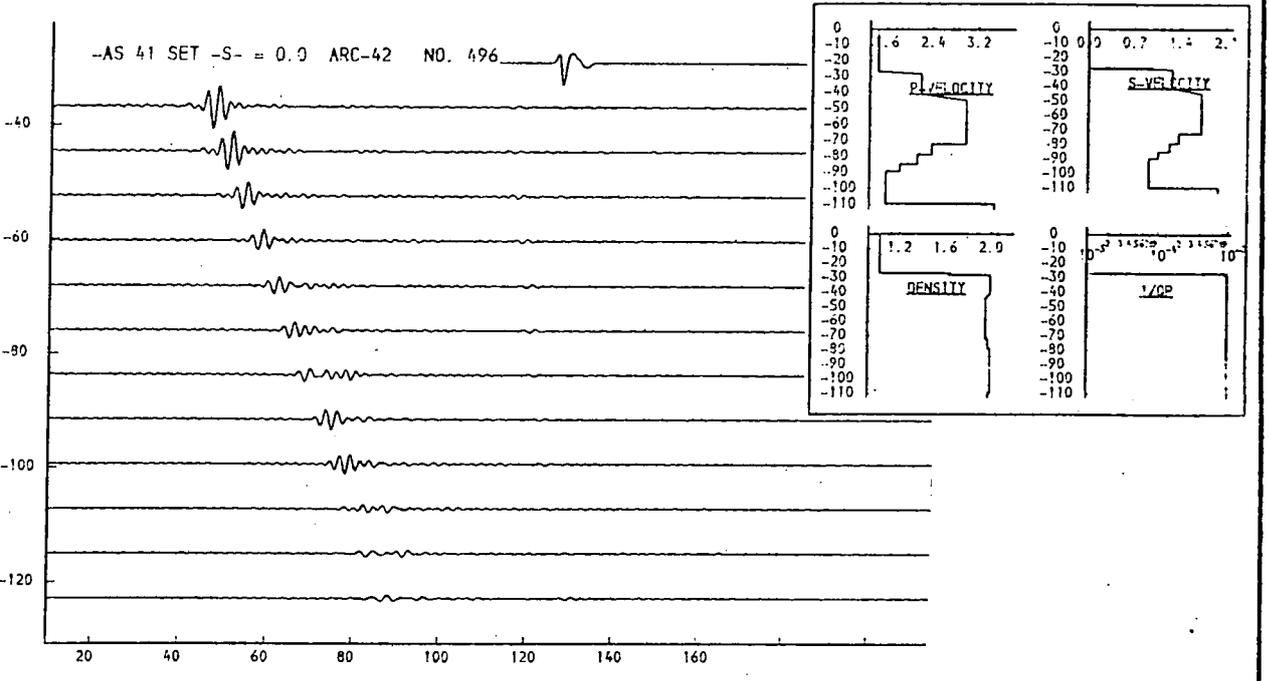
Fig. 9.105.   Stepped velocity increases.

A high gradient (ca. 350m/sec/m.) just below the seabed
produces a bottom reflexion having the general character
of that found in the field record. The deeper structure
in these models does not reproduce the other
characteristics of the field record.

THICKNESS (M.)	P-VELOCITY (M/S.)	S-VELOCITY (M/S.)	DENSITY (G/ML)	1/Q P	1/Q S
26.6	1.460	0.000	1.03	0.00000	0.00000
0.3	1.480	0.000	1.60	0.00100	0.01000
9.3	1.900	0.500	2.00	0.00100	0.01000
8.3	2.500	0.500	2.00	0.00100	0.01000
25.7	3.000	1.200	2.00	0.00100	0.03000
6.6	2.395	0.700	2.00	0.00100	0.03000
5.9	2.145	0.500	2.00	0.00100	0.03000
4.5	1.945	0.300	2.00	0.00100	0.03000
31.2	1.600	0.100	2.00	0.00100	0.03000
	3.500	2.000	1.98	0.00100	0.03000

THICKNESS (M.)	P-VELOCITY (M/S.)	S-VELOCITY (M/S.)	DENSITY (G/ML)	1/Q P	1/Q S
26.6	1.460	0.000	1.03	0.00000	0.00000
0.3	1.480	0.000	1.60	0.00100	0.01000
4.1	1.902	0.500	2.00	0.00100	0.01000
4.1	2.512	0.500	2.00	0.00100	0.01000
4.1	2.742	0.500	2.00	0.00100	0.01000
4.1	2.912	0.500	2.00	0.00100	0.01000
25.7	3.000	1.200	2.00	0.00100	0.03000
6.6	2.395	0.700	2.00	0.00100	0.03000
5.9	2.145	0.500	2.00	0.00100	0.03000
4.5	1.945	0.300	2.00	0.00100	0.03000
31.2	1.600	0.100	2.00	0.00100	0.03000
	3.500	2.000	1.98	0.00100	0.03000

Fig. 9.106a. Stepped velocity increases.

Variations in a stepped structure of velocity increases below an immediate subbottom gradient like that of fig. 9.105 produce peaks in the subbottom reflexion or headwave development in inappropriate places.

THICKNESS (M.)	P-VELOCITY (M/S.)	S-VELOCITY (M/S.)	DENSITY (G/ML)	1/Q P	1/Q S
26.6	1.460	0.000	1.03	0.00000	0.00000
0.7	1.680	0.440	2.60	0.00100	0.01000
8.3	2.040	0.500	2.00	0.00100	0.01000
8.3	2.500	0.500	2.00	0.00100	0.01000
25.7	3.000	1.200	2.00	0.00100	0.03000
6.6	2.395	0.700	2.00	0.00100	0.03000
5.9	2.145	0.500	2.00	0.00100	0.03000
4.5	1.945	0.300	2.00	0.00100	0.03000
31.2	1.600	0.100	2.00	0.00100	0.03000
	3.500	2.000	1.93	0.00100	0.03000

THICKNESS (M.)	P-VELOCITY (M/S.)	S-VELOCITY (M/S.)	DENSITY (G/ML)	1/Q P	1/Q S
26.6	1.460	0.000	1.03	0.00000	0.00000
0.7	1.680	0.440	2.60	0.00100	0.01000
4.1	2.513	0.500	2.00	0.00100	0.01000
4.1	2.742	0.500	2.00	0.00100	0.01000
4.1	2.912	0.500	2.00	0.00100	0.01000
25.7	3.000	1.200	2.00	0.00100	0.03000
6.6	2.395	0.700	2.00	0.00100	0.03000
5.9	2.145	0.500	2.00	0.00100	0.03000
4.5	1.945	0.300	2.00	0.00100	0.03000
31.2	1.600	0.100	2.00	0.00100	0.03000
	3.500	2.000	1.93	0.00100	0.03000

Fig. 9.106b. Stepped velocity increases.

Variations in a stepped structure of velocity increases below an immediate subbottom gradient like that of fig. 9.105 produce peaks in the subbottom reflexion or headwave development in inappropriate places.

THICKNESS (M.)	P-VELOCITY (M/S.)	S-VELOCITY (M/S.)	DENSITY (G/ML)	1/Q P	1/Q S
26.6	1.460	0.000	1.93	0.00000	0.00000
0.3	1.600	0.440	2.00	0.00100	0.01000
8.3	2.212	0.500	2.00	0.00100	0.01000
8.3	2.612	0.500	2.00	0.00100	0.01000
25.7	3.000	1.200	2.00	0.00100	0.03000
6.6	2.395	0.700	2.00	0.00100	0.03000
5.9	2.145	0.500	2.00	0.00100	0.03000
4.5	1.945	0.300	2.00	0.00100	0.03000
31.2	1.600	0.100	2.00	0.00100	0.03000
	3.500	2.000	1.93	0.00100	0.03000

THICKNESS (M.)	P-VELOCITY (M/S.)	S-VELOCITY (M/S.)	DENSITY (G/ML)	1/Q P	1/Q S
26.6	1.460	0.000	1.93	0.00000	0.00000
0.3	1.600	0.440	2.00	0.00100	0.01000
4.1	2.212	0.500	2.00	0.00100	0.01000
4.1	2.412	0.500	2.00	0.00100	0.01000
4.1	2.612	0.500	2.00	0.00100	0.01000
4.1	2.812	0.500	2.00	0.00100	0.01000
25.7	3.000	1.200	2.00	0.00100	0.03000
6.6	2.395	0.700	2.00	0.00100	0.03000
5.9	2.145	0.500	2.00	0.00100	0.03000
4.5	1.945	0.300	2.00	0.00100	0.03000
31.2	1.600	0.100	2.00	0.00100	0.03000
	3.500	2.000	1.93	0.00100	0.03000
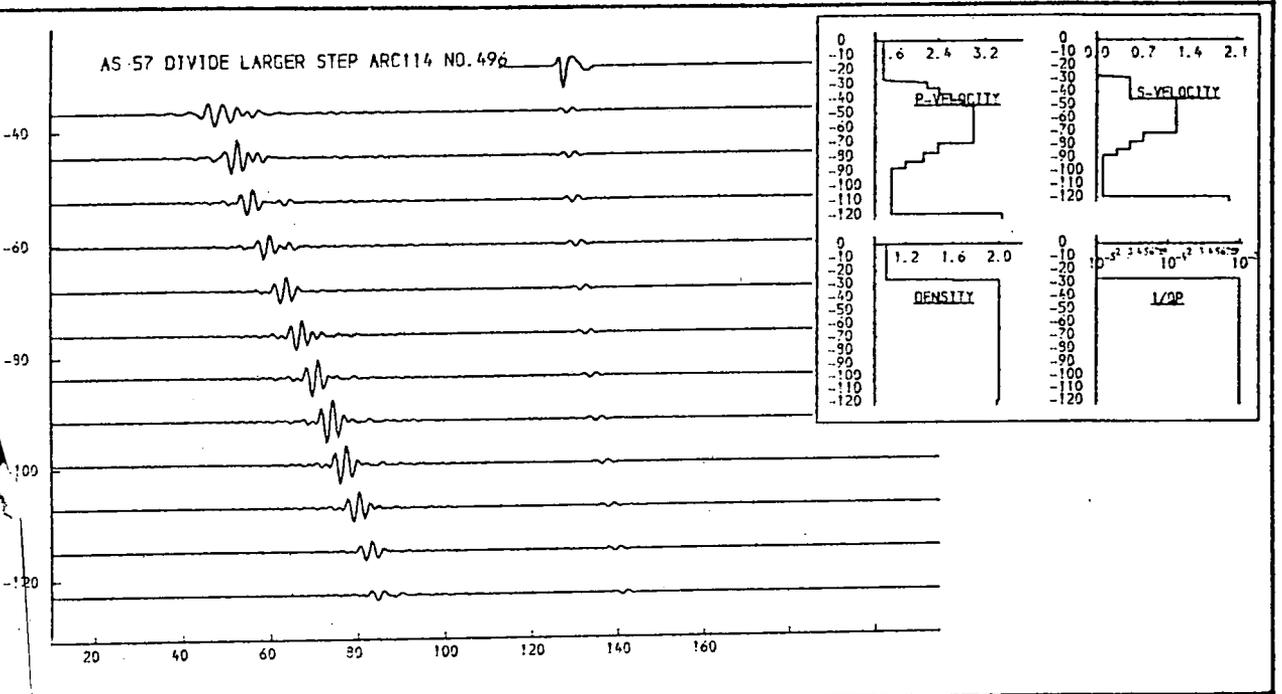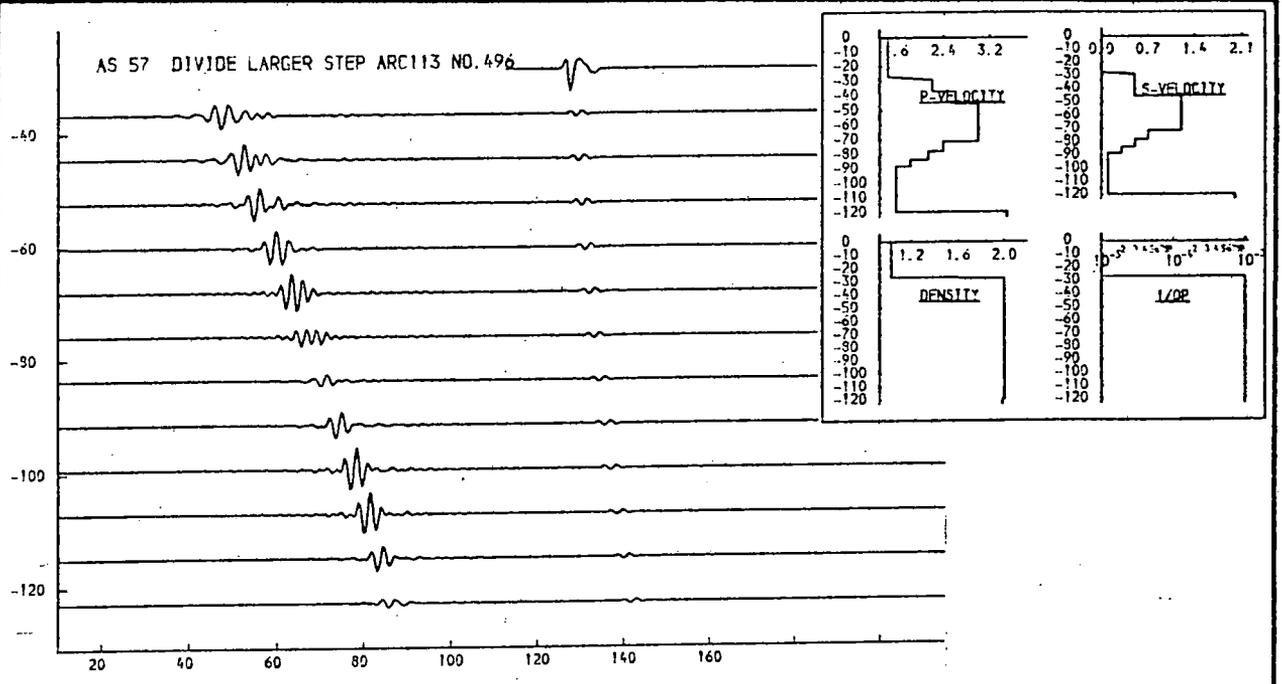
Fig. 9.106c. Stepped velocity increases.

Variations in a stepped structure of velocity increases below an immediate subbottom gradient like that of fig. 9.105 produce peaks in the subbottom reflexion or headwave development in inappropriate places.

THICKNESS (M.)	P-VELOCITY (M/S.)	S-VELOCITY (M/S.)	DENSITY (G/ML)	1/Q P	1/Q S
26.6	1.460	0.000	1.03	0.00000	0.00000
0.2	1.600	0.040	3.69	0.00100	0.01000
8.2	2.212	0.500	2.00	0.00100	0.01000
8.3	2.453	0.500	2.00	0.00100	0.01000
25.7	3.000	1.200	2.00	0.00100	0.03000
6.6	2.395	0.700	2.00	0.00100	0.03000
5.9	2.145	0.500	2.00	0.00100	0.03000
4.5	1.945	0.300	2.00	0.00100	0.03000
31.2	1.600	0.100	2.00	0.00100	0.03000
	3.500	2.000	1.93	0.00100	0.03000

THICKNESS (M.)	P-VELOCITY (M/S.)	S-VELOCITY (M/S.)	DENSITY (G/ML)	1/Q P	1/Q S
26.6	1.460	0.000	1.03	0.00000	0.00000
0.2	1.600	0.040	3.69	0.00100	0.01000
4.1	2.212	0.500	2.00	0.00100	0.01000
4.1	2.412	0.500	2.00	0.00100	0.01000
4.1	3.512	0.500	3.69	0.00163	0.01000
25.7	3.000	1.200	2.00	0.00100	0.03000
6.6	2.395	0.700	2.00	0.00100	0.03000
5.9	2.145	0.500	2.00	0.00100	0.03000
4.5	1.945	0.300	2.00	0.00100	0.03000
31.2	1.600	0.100	2.00	0.00100	0.03000
	3.500	2.000	1.98	0.00100	0.03000

AS 57 DIVIDE STEP IN 2   ARC111 NO.496

AS 57 DIVIDE STEP IN 4   ARC112 NO.496

Fig. 9.106d. Stepped velocity increases.

Variations in a stepped structure of velocity increases below an immediate subbottom gradient like that of fig. 9.105 produce peaks in the subbottom reflexion or headwave development in inappropriate places.

THICKNESS (M.)	P-VELOCITY (M/S.)	S-VELOCITY (M/S.)	DENSITY (G/ML)	1/Q P	1/Q S		THICKNESS (M.)	P-VELOCITY (M/S.)	S-VELOCITY (M/S.)	DENSITY (G/ML)	1/Q P	1/Q S
26.6	1.460	0.000	1.03	0.00000	0.00000		26.6	1.460	0.000	1.03	0.00000	0.00000
0.?	1.480	0.960	2.00	0.00100	0.01000		0.?	1.480	0.960	2.00	0.00100	0.01000
12.2	1.900	0.500	2.00	0.00100	0.01000		9.1	1.902	0.500	2.00	0.00100	0.01000
4.3	2.500	0.500	2.00	0.00100	0.01000		3.1	2.513	0.500	2.00	0.00100	0.01000
25.7	3.000	1.200	2.00	0.00100	0.03000		25.7	3.000	1.200	2.00	0.00100	0.03000
6.6	2.395	0.700	2.00	0.00100	0.03000		6.6	2.395	0.700	2.00	0.00100	0.03000
5.9	2.145	0.500	2.00	0.00100	0.03000		5.9	2.145	0.500	2.00	0.00100	0.03000
4.5	1.945	0.300	2.00	0.00100	0.03000		4.5	1.945	0.300	2.00	0.00100	0.03000
31.2	1.600	0.100	2.00	0.00100	0.03000		31.2	1.600	0.100	2.00	0.00100	0.03000
	3.500	2.000	1.98	0.00100	0.03000			3.500	2.000	1.93	0.00100	0.03000

Fig. 9.107a. Stepped velocity increases.

A greater step size below an initial subbottom gradient like that of fig. 9.105 begins to produce in the low-offset channels events more akin to those seen in the field record, but result is otherwise unsatisfactory.

THICKNESS (M.)	P-VELOCITY (M/S.)	S-VELOCITY (M/S.)	DENSITY (G/ML)	1/Q P	1/Q S
26.6	1.460	0.000	1.03	0.00000	0.00000
0.3	1.460	0.040	3.60	0.00100	0.01000
12.4	1.752	0.250	2.00	0.00100	0.01000
4.3	2.500	0.500	2.00	0.00100	0.01000
25.7	3.000	1.200	2.00	0.00100	0.03000
6.6	2.395	0.700	2.00	0.00100	0.03000
5.9	2.145	0.500	2.00	0.00100	0.03000
4.5	1.845	0.300	2.00	0.00100	0.03000
31.2	1.600	0.100	2.00	0.00100	0.03000
	3.500	2.000	1.98	0.00100	0.03000

THICKNESS (M.)	P-VELOCITY (M/S.)	S-VELOCITY (M/S.)	DENSITY (G/ML)	1/Q P	1/Q S
26.6	1.460	0.000	1.03	0.00000	0.00000
0.3	1.460	0.040	3.60	0.00100	0.01000
9.1	1.752	0.250	2.00	0.00100	0.01000
4.1	2.512	0.500	2.00	0.00100	0.01000
	3.613	0.500	3.00	0.03100	0.01000
25.7	3.000	1.200	2.00	0.00100	0.03000
6.6	2.395	0.700	2.00	0.00100	0.03000
5.9	2.145	0.500	2.00	0.00100	0.03000
4.5	1.845	0.300	2.00	0.00100	0.03000
31.2	1.600	0.100	2.00	0.00100	0.03000
	3.500	2.000	1.98	0.00100	0.03000

Fig. 9.107b. Stepped velocity increases.

A greater step size below an initial subbottom gradient like that of fig. 9.105 begins to produce in the low-offset channels events more akin to those seen in the field record, but result is otherwise unsatisfactory.

Fig. 9.108a. Gradients and step combined.

A stepped increase with high gradients (ca. 400m/sec/m.) both above and below the step begins to show some of the character of the field record at intermediate offset distance but does not give good agreement at low and high offset distances.

THICKNESS (M.)	P-VELOCITY (M/S.)	S-VELOCITY (M/S.)	DENSITY (G/ML)	1/Q P	1/Q S		THICKNESS (M.)	P-VELOCITY (M/S.)	S-VELOCITY (M/S.)	DENSITY (G/ML)	1/Q P	1/Q S
26.0	1.460	0.000	1.03	0.00000	0.00000		26.6	1.460	0.000	1.03	0.00000	0.00000
0.3	1.460	0.300	1.57	0.00100	0.01000		0.3	1.440	0.300	1.57	0.00100	0.01000
16.4	2.212	0.500	2.00	0.00100	0.01000		16.4	2.212	0.500	2.00	0.00100	0.01000
0.3	2.853	1.000	2.00	0.00100	0.01000		0.3	2.853	1.000	2.00	0.00100	0.01000
25.7	3.000	1.200	2.00	0.00100	0.03000		25.7	3.500	1.200	2.00	0.00100	0.03000
6.6	2.395	0.700	2.00	0.00100	0.03000		6.6	2.395	0.700	2.00	0.00100	0.03000
5.9	2.145	0.500	2.00	0.00100	0.03000		5.9	2.145	0.500	2.00	0.00100	0.03000
4.5	1.845	0.300	2.00	0.00100	0.03000		4.5	1.845	0.300	2.00	0.00100	0.03000
31.2	1.600	0.100	2.00	0.00100	0.03000		31.2	1.600	0.100	2.00	0.00100	0.03000
	3.500	2.000	1.98	0.00100	0.03000			3.500	2.000	1.98	0.00100	0.03000
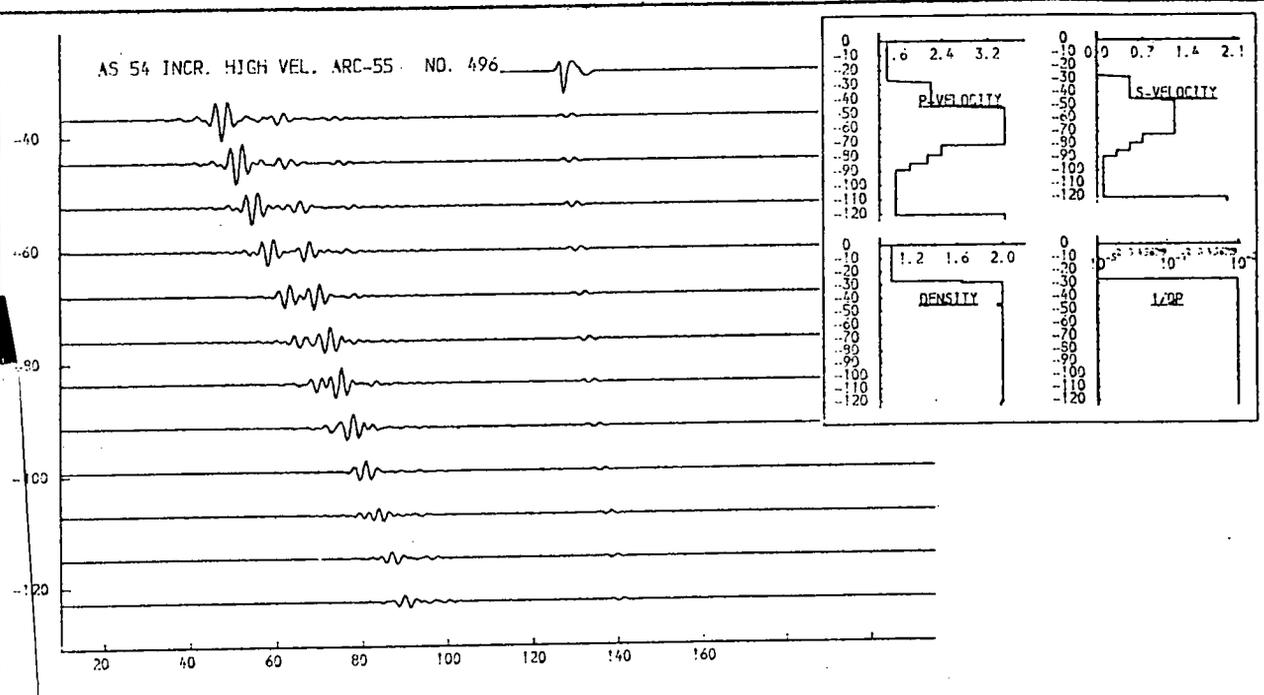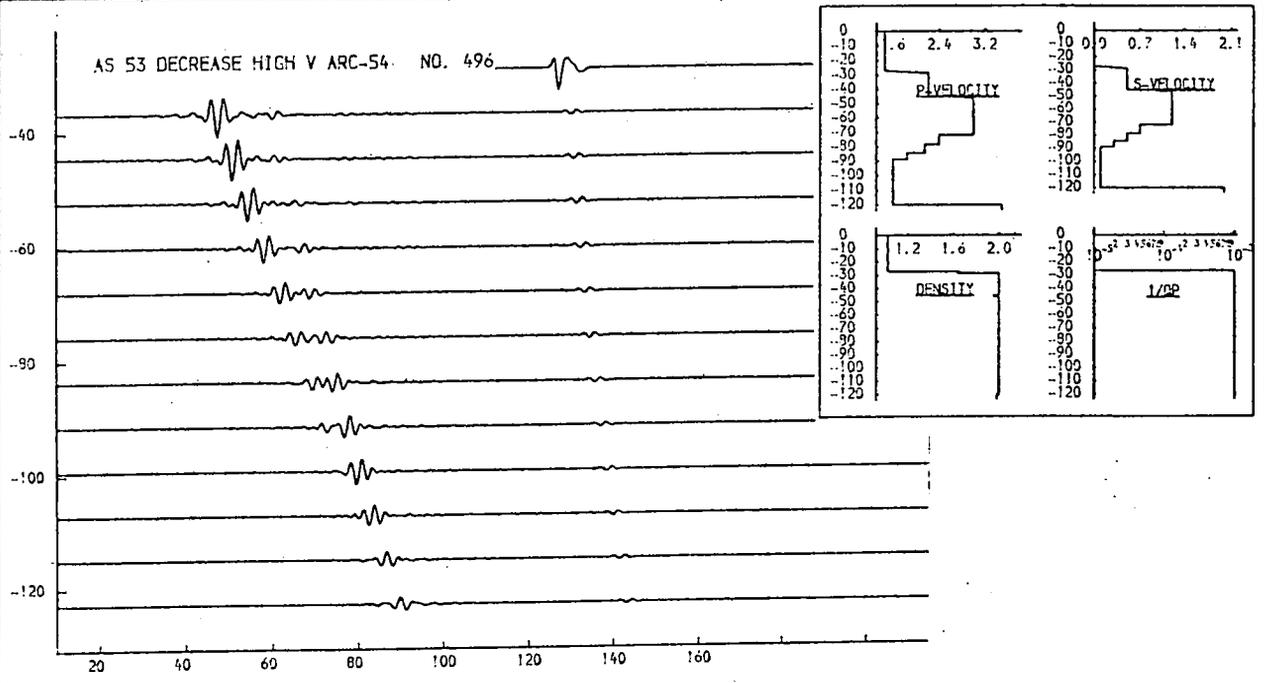
Fig. 9.108b. Gradients and step combined.

Changes in the maximum value of p-velocity alter the position of the peak reflexion amplitude.

THICKNESS (M.)	P-VELOCITY (M/S.)	S-VELOCITY (M/S.)	DENSITY (G/ML)	1/Q P	1/Q S
26.6	1,460	0.000	1.03	0.00000	0.00000
	1,490	0.110	2.02	0.00100	0.01000
6.5	2,212	0.500	2.00	0.00100	0.01000
7.4	1,912	0.100	2.00	0.00100	0.01000
7.0	2,100	1.200	2.00	0.00100	0.03000
31.2	1,550	0.100	2.00	0.00100	0.03000
	3,500	2.000	1.98	0.00100	0.03000
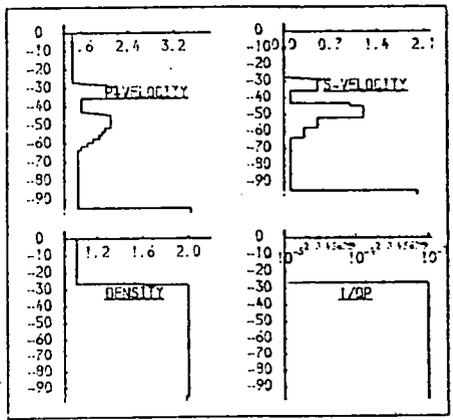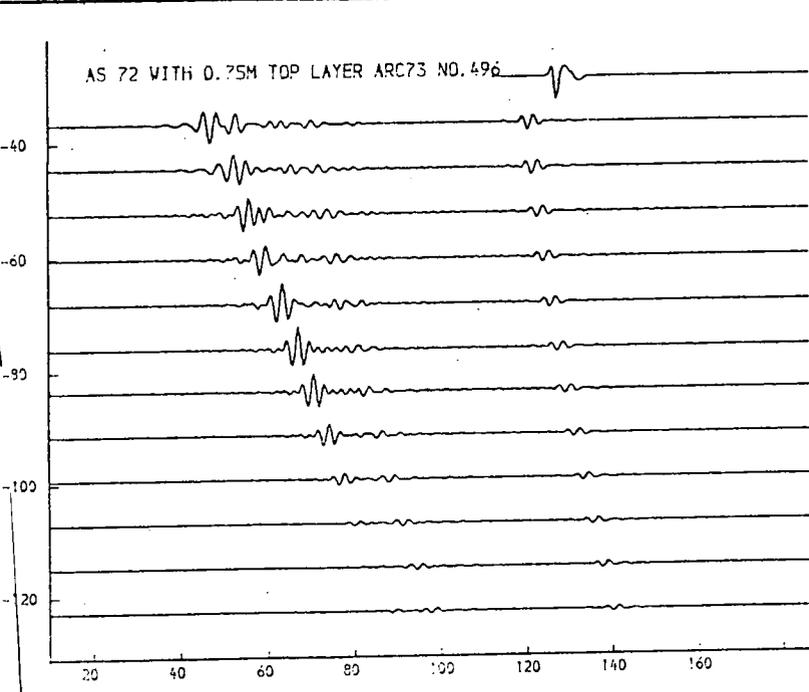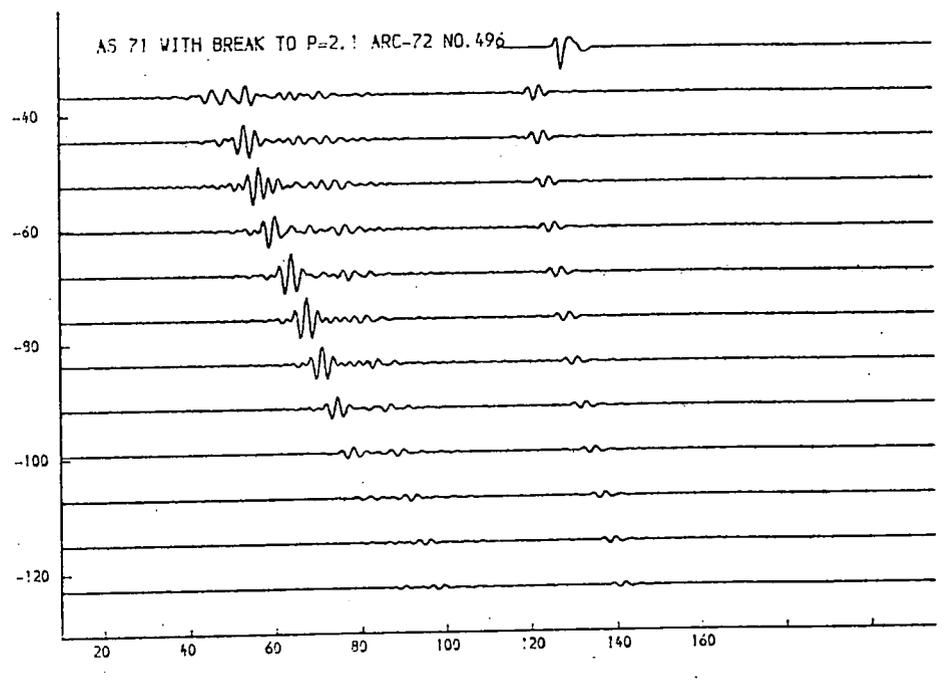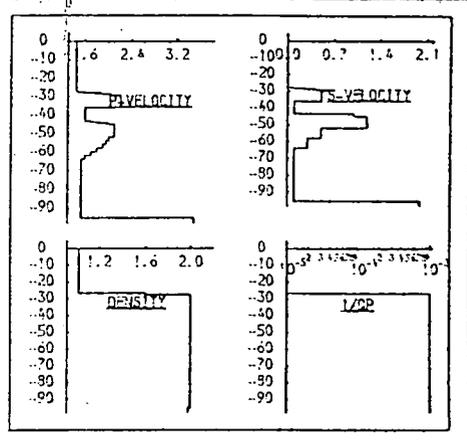
Fig. 9.109. Profiles with low-velocity layer.

The first subbottom event is too weak in this model.   The lower model differs from the upper in having a 0.75m thick surficial layer.

THICKNESS (M.)	P-VELOCITY (M/S.)	S-VELOCITY (M/S.)	DENSITY (G/ML)	1/Q P	1/Q S		THICKNESS (M.)	P-VELOCITY (M/S.)	S-VELOCITY (M/S.)	DENSITY (G/ML)	1/Q P	1/Q S
26.6	1.460	0.000	1.03	0.00000	0.00000		26.6	1.460	0.000	1.03	0.00000	0.00000
0.7	1.100	0.010	2.40	0.00100	0.01000		4.4	1.400	0.010	2.40	0.00100	0.01000
6.5	2.243	0.528	2.80	0.00100	0.01000		6.5	2.243	0.528	2.80	0.00100	0.01000
5.9	1.913	0.100	2.80	0.00100	0.01000		5.9	1.913	0.100	2.80	0.00100	0.01000
25.7	3.000	1.200	2.00	0.00100	0.03000		25.7	3.000	1.200	2.00	0.00100	0.03000
6.6	2.395	0.700	2.00	0.00100	0.03000		6.6	2.395	0.700	2.00	0.00100	0.03000
5.9	2.145	0.500	2.00	0.00100	0.03000		5.9	2.145	0.500	2.00	0.00100	0.03000
4.5	1.945	0.300	2.00	0.00100	0.03000		4.5	1.945	0.300	2.00	0.00100	0.03000
31.2	1.600	0.100	2.00	0.00100	0.03000		31.2	1.600	0.100	2.00	0.00100	0.03000
	3.500	2.000	1.98	0.00100	0.03000			3.500	2.000	1.98	0.00100	0.03000

AS 59 TAPER LOW V LAYER ARC-59 NO. 496

AS 59 1.0M ON TOP   ARC-60 NO. 496

Fig. 9.110a. Profiles with low-velocity layer.

A larger p-velocity step at shallower depth than in fig. 9.109 gives a better model for near-offset channels.

THICKNESS (M.)	P-VELOCITY (M/S.)	S-VELOCITY (M/S.)	DENSITY (G/ML)	1/Q P	1/Q S
26.6	1.460	0.000	1.03	0.00000	0.00000
				0.00100	0.01000
6.5	2.213	0.500	2.00	0.00100	0.01000
5.2	1.913	0.100	2.00	0.00100	0.01000
5.0	3.700	2.700	2.00	0.00100	0.03000
6.6	2.395	0.700	2.00	0.00100	0.03000
5.2	2.145	0.500	2.00	0.00100	0.03000
4.5	1.945	0.300	2.00	0.00100	0.03000
30.0	1.600	0.100	2.00	0.00100	0.03000
	3.500	2.000	1.98	0.00100	0.03000

THICKNESS (M.)	P-VELOCITY (M/S.)	S-VELOCITY (M/S.)	DENSITY (G/ML)	1/Q P	1/Q S
26.6	1.460	0.000	1.03	0.00000	0.00000
				0.00100	0.01000
6.5	2.213	0.700	2.00	0.00100	0.01000
5.2	1.913	0.100	2.00	0.00100	0.01000
5.0	4.000	2.000	2.00	0.00100	0.03000
6.6	2.395	0.700	2.00	0.00100	0.03000
5.9	2.145	0.500	2.00	0.00100	0.03000
4.5	1.945	0.300	2.00	0.00100	0.03000
30.0	1.600	0.100	2.00	0.00100	0.03000
	3.500	2.000	1.98	0.00100	0.03000

AS 9! VARY -P- P = 3.7   ARC82 NO.496

AS 9! VARY TOP GRADT.   ARC-90 NO.496

Fig. 9.110b. Profiles with low-velocity layer.

Steps to higher p-velocity values than in fig. 9.110a give a peak in the value of subbottom reflexions at offset distance which is too small.

THICKNESS	P-VELOCITY	S-VELOCITY	DENSITY	1/Q	1/Q
(M.)	(M/S.)	(M/S.)	(G/ML)	P	S
26.6	1.460	0.000	1.03	0.00000	0.00000
27.2	2.752	0.590	2.00	0.00100	0.01000
6.6	2.395	0.700	2.00	0.00100	0.03000
5.9	2.145	0.500	2.00	0.00100	0.03000
4.5	1.845	0.500	2.00	0.00100	0.03000
31.2	1.600	0.100	2.00	0.00100	0.03000
	3.500	2.000	1.98	0.00100	0.03000

AS 133 VARY P P=1.2 ARC133 NO.496

AS 133 VARY P P=1.3 ARC135 NO.496
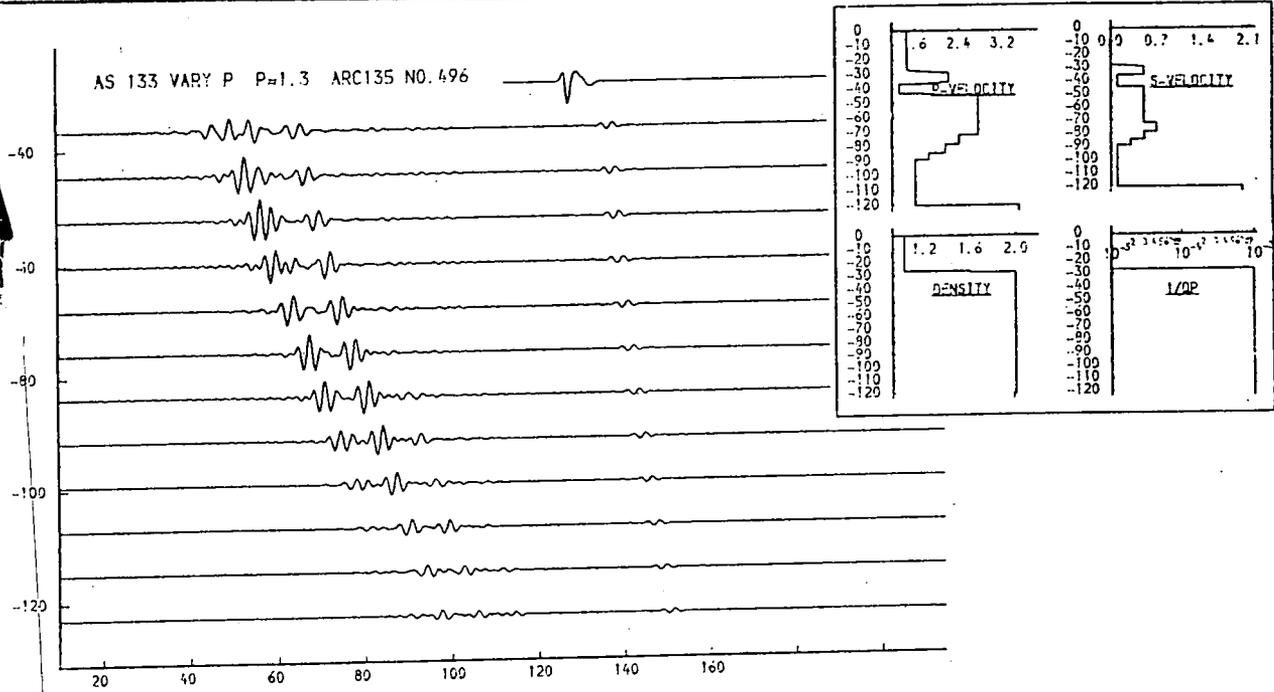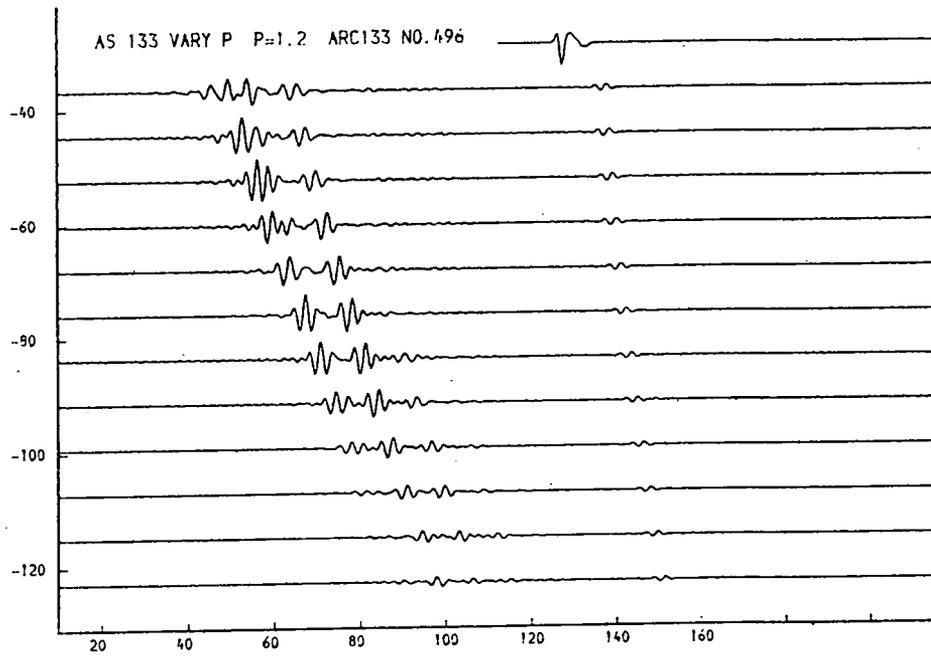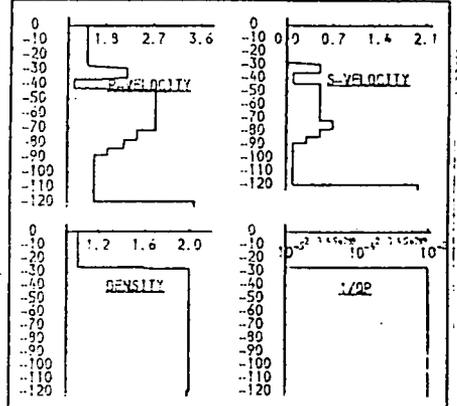
Fig. 9.110c. Profiles with low-velocity layer.

If the p-velocity in the re-entrant low-velocity layer is set too low, then the time-variation with offset of the subbottom arrival is incorrect.

THICKNESS (M.)	P-VELOCITY (M/S.)	S-VELOCITY (M/S.)	DENSITY (G/ML)	1/Q P	1/Q S
26.6	1.460	0.000	1.03	0.00000	0.00000
6.5	3.313	2.599	3.68	0.03100	0.01000
8.8	1.843	0.130	3.68	0.60100	0.01000
27.2	2.752	1.000	2.00	0.00100	0.01000
6.6	2.395	0.700	2.00	0.00100	0.03000
5.9	2.145	0.500	2.00	0.00100	0.03000
4.5	1.945	0.300	2.00	0.00100	0.03000
31.2	1.600	0.100	2.00	0.00100	0.03000
	3.500	2.000	1.99	0.00100	0.03000

AS 60 DECREASE HI VEL ARC-61 NO.496

AS 61 SET -S- HIGH   ARC-62 NO.496

Fig. 9.110d. Profiles with low-velocity layer.

Significant change in the value of s-velocity in the deeper high velocity layer does not produce a marked effect, but the peak amplitude of the subbottom reflexion is reduced a little for high s-velocity (lower model).

THICKNESS (M.)	P-VELOCITY (M/S.)	S-VELOCITY (M/S.)	DENSITY (G/ML)	1/Q P	1/Q S
26.6	1.460	0.000	1.03	0.00000	0.00000
0.1	1.480	0.240	2.00	0.00100	0.01000
6.5	2.212	0.500	2.00	0.00100	0.01000
5.2	1.543	0.100	2.00	0.00100	0.01000
10.0	2.602	1.000	2.00	0.00100	0.01000
2.1	2.450	0.600	2.00	0.00100	0.01000
31.2	1.600	0.100	2.00	0.00100	0.03000
	3.500	2.000	1.98	0.00100	0.03000

Fig. 9.111a. Profiles with low-velocity layer.

As the peak value of p-velocity is reduced from 2.75 to 2.60 (upper model), the peak amplitude of the first subbottom reflexion is displaced to higher offset and reduced in amplitude. Note frequency range for these models is 150-600Hz.

THICKNESS (M.)	P-VELOCITY (M/S.)	S-VELOCITY (M/S.)	DENSITY (G/ML)	1/Q P	1/Q S
26.6	1.460	0.000	1.03	0.00000	0.00000
	1.490	0.010	1.60	0.00100	0.01000
6.5	2.313	0.500	2.00	0.00100	0.01000
5.0	1.613	0.300	2.00	0.00100	0.01000
10.0	2.502	1.900	2.00	0.00100	0.01000
	2.800	1.500	2.00	0.00100	0.03000
		1.200	2.00		
31.2	1.600	0.100	2.00	0.00100	0.03000
	3.500	2.000	1.98	0.00100	0.03000

Fig. 9.111b. Profiles with low-velocity layer.

Further reduction in the peak value of p-velocity to 2.50 (lower model) displaces the peak amplitude (c.f. fig. 9.111a) of the subbottom reflexion to still higher offset until, for p=2.35, the peak is no longer seen. Note frequency range for these models is 150-600Hz.

THICKNESS (M.)	P-VELOCITY (M/S.)	S-VELOCITY (M/S.)	DENSITY (G/ML)	1/Q P	1/Q S
26.6	1.460	0.000	1.03	0.00000	0.00000
0.5	1.603	0.310	1.40	0.00130	0.01000
6.5	3.343	0.500	1.68	0.00100	0.01000
5.9	1.613	0.400	1.68	0.00100	0.01000
27.2	2.500	1.600	2.00	0.00100	0.01000
6.6	2.395	1.400	2.00	0.00100	0.03000
5.9	2.145	0.900	2.00	0.00100	0.03000
4.5	1.945	0.600	2.00	0.00100	0.03000
39.5	1.600	0.100	2.00	0.00100	0.03000
	3.500	2.000	1.99	0.00100	0.03000

THICKNESS (M.)	P-VELOCITY (M/S.)	S-VELOCITY (M/S.)	DENSITY (G/ML)	1/Q P	1/Q S
26.6	1.460	0.000	1.03	0.00000	0.00000
0.5	1.603	0.310	1.40	0.00130	0.01000
6.5	3.343	0.500	1.68	0.00100	0.01000
5.9	1.613	0.400	1.68	0.00100	0.01000
27.2	2.500	1.600	2.00	0.00100	0.01000
6.6	2.395	1.400	2.00	0.00100	0.03000
5.9	2.145	0.900	2.00	0.00100	0.03000
4.5	1.945	0.600	2.00	0.00100	0.03000
39.5	1.600	0.100	2.00	0.00100	0.03000
	3.500	2.000	1.99	0.00100	0.03000

Fig. 9.112. Profiles with low-velocity layer.

Variation in the thickness of a surficial layer.
Upper: 2m. thickness; Lower: 0.5m. thickness.

THICKNESS (M.)	P-VELOCITY (M/S.)	S-VELOCITY (M/S.)	DENSITY (G/ML)	1/Q P	1/Q S
26.6	1.460	0.000	1.03	0.00000	0.00000
4.0	1.480	0.040	1.40	0.00100	0.01000
4.5	2.213	0.500	1.58	0.00100	0.01000
5.0	1.613	0.400	1.03	0.00100	0.01000
27.2	2.500	1.600	2.00	0.00100	0.01000
6.6	2.395	1.400	2.00	0.00100	0.03000
5.9	2.165	0.900	2.00	0.00100	0.03000
4.5	1.945	0.600	2.00	0.00100	0.03000
39.5	1.600	0.100	2.00	0.00100	0.03000
	3.500	2.000	1.98	0.00100	0.03000

AS 165 B. GRDT. 0.20M. ARC167 NO.496

AS 165 B. GRDT. 0.40M. ARC168 NO.496

Fig. 9.113. Profiles with low-velocity layer.

Variation in the velocity gradient just below surface.
Upper: 800m/sec/m.; Lower: 400m/sec/m.

THICKNESS (M.)	P-VELOCITY (M/S.)	S-VELOCITY (M/S.)	DENSITY (G/ML)	1/Q P	1/Q S
26.6	1.460	0.000	1.03	0.00000	0.00000
12.2	2.752	0.500	2.00	0.00100	0.01000
6.6	2.395	0.450	2.00	0.00100	0.03000
5.9	2.145	0.400	2.00	0.00100	0.03000
4.5	1.845	0.300	2.00	0.00100	0.03000
31.9	1.550	0.100	2.00	0.00100	0.03000
	3.500	2.000	1.98	0.00100	0.03000

AS 141 VARY HV. THK = 1.0 ARC163 NO. 496

AS 141 VARY HV. THK = 2.0 ARC163 NO. 496

Fig. 9.114a. Profiles with low-velocity layer.

Variation in the thickness of the upper high-velocity layer. Upper: 1.0m.; Lower: 2.0m.

THICKNESS (M.)	P-VELOCITY (M/S.)	S-VELOCITY (M/S.)	DENSITY (G/HL)	1/Q P	1/Q S
26.6	1.460	0.000	1.03	0.00000	0.00000
4.2	1.488	0.250	2.60	0.00100	0.01000
3.5	2.242	0.500	2.60	0.00100	0.01000
6.9	1.382	0.234	2.60	0.00100	0.01000
12.2	2.752	0.500	2.00	0.00100	0.01000
6.6	2.395	0.450	2.00	0.00100	0.03000
5.9	2.145	0.400	2.00	0.00100	0.03000
4.5	1.845	0.300	2.00	0.00100	0.03000
31.0	1.550	0.100	2.00	0.00100	0.03000
	3.500	2.000	1.98	0.00100	0.03000

AS 141 VARY HV.THK = 3.5 ARC162 NO.496

AS 141 VARY HV.THK = 5.00 ARC161 NO.496
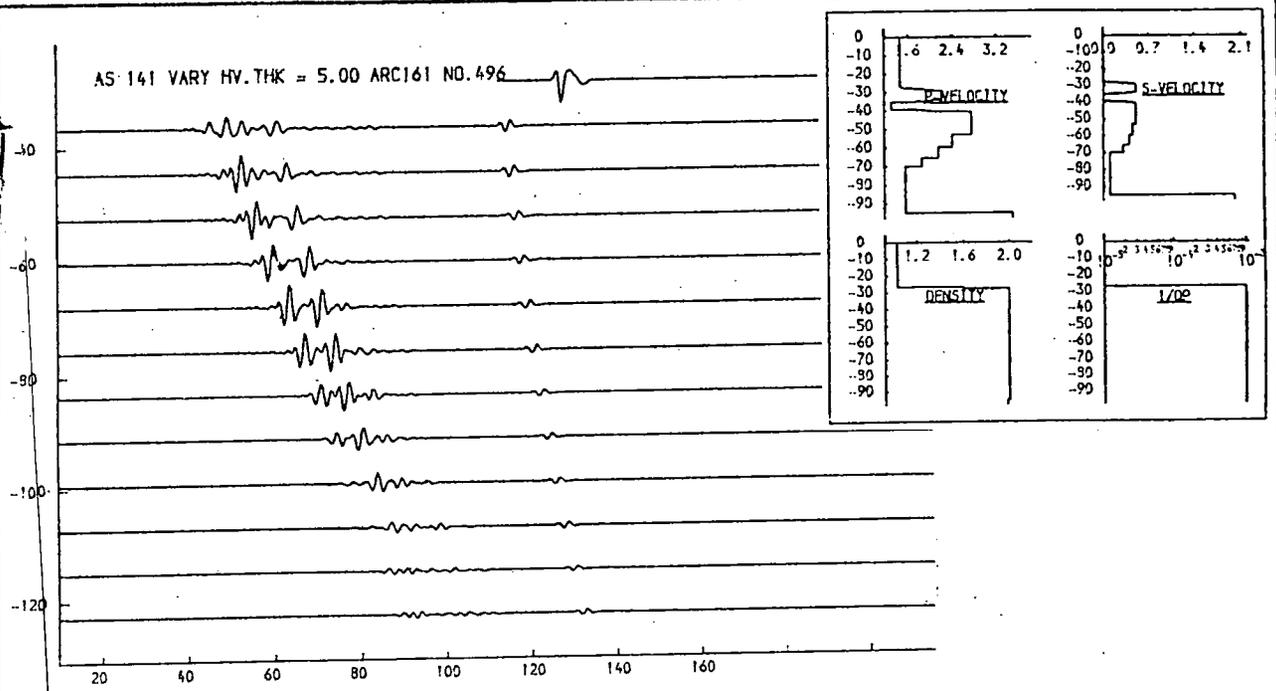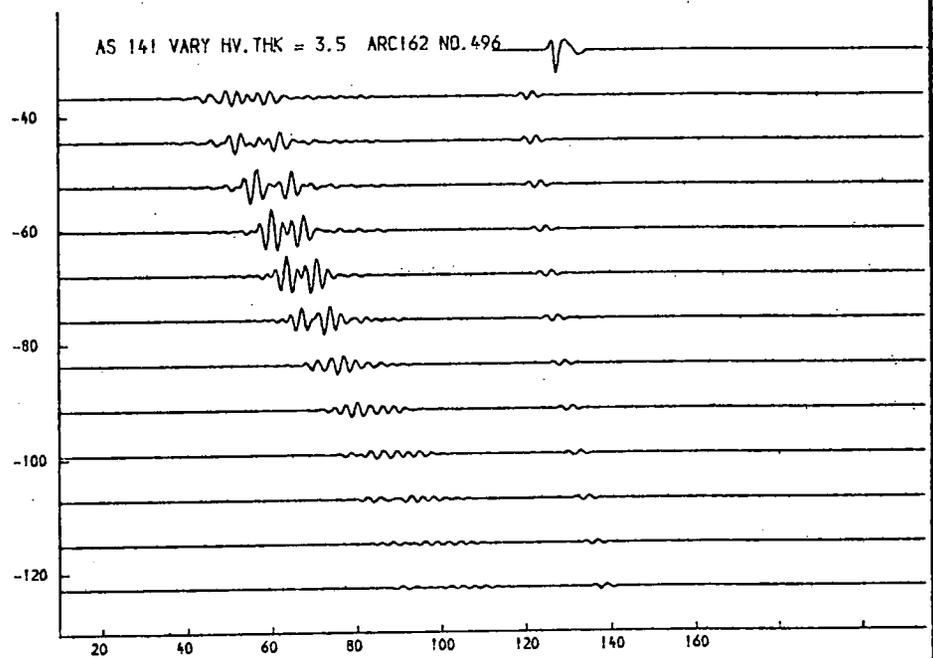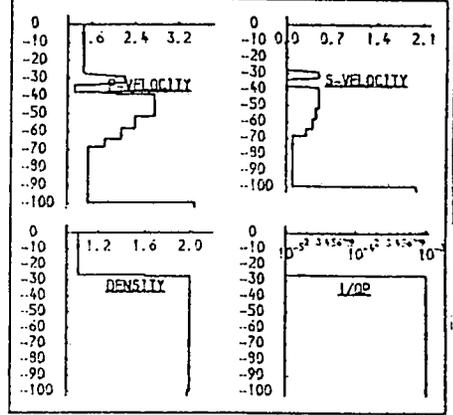
Fig. 9.114b. Profiles with low-velocity layer.

Variation in the thickness of the upper high-velocity layer. Upper: 3.5m.; Lower: 5.0m.

THICKNESS (M.)	P-VELOCITY (M/S.)	S-VELOCITY (M/S.)	DENSITY (G/ML)	1/Q P	1/Q S
26.6	1.460	0.000	1.03	0.00000	0.00000
4.2	1.480	0.350	1.60	0.00100	0.01000
7.5	2.233	0.500	2.00	0.00100	0.01000
6.9	1.340	0.350	1.60	0.00100	0.01000
27.2	2.752	0.500	2.00	0.00100	0.01000
6.6	2.325	0.450	2.00	0.00100	0.03000
5.3	2.145	0.400	2.00	0.00100	0.03000
4.5	1.945	0.300	2.00	0.00100	0.03000
31.2	1.600	0.100	2.00	0.00100	0.03000
	3.500	2.000	1.98	0.00100	0.03000

AS 141 VARY TH T=7.5M ARC182 NO.496

AS 141 VARY TH T=9.0M ARC182 NO.496
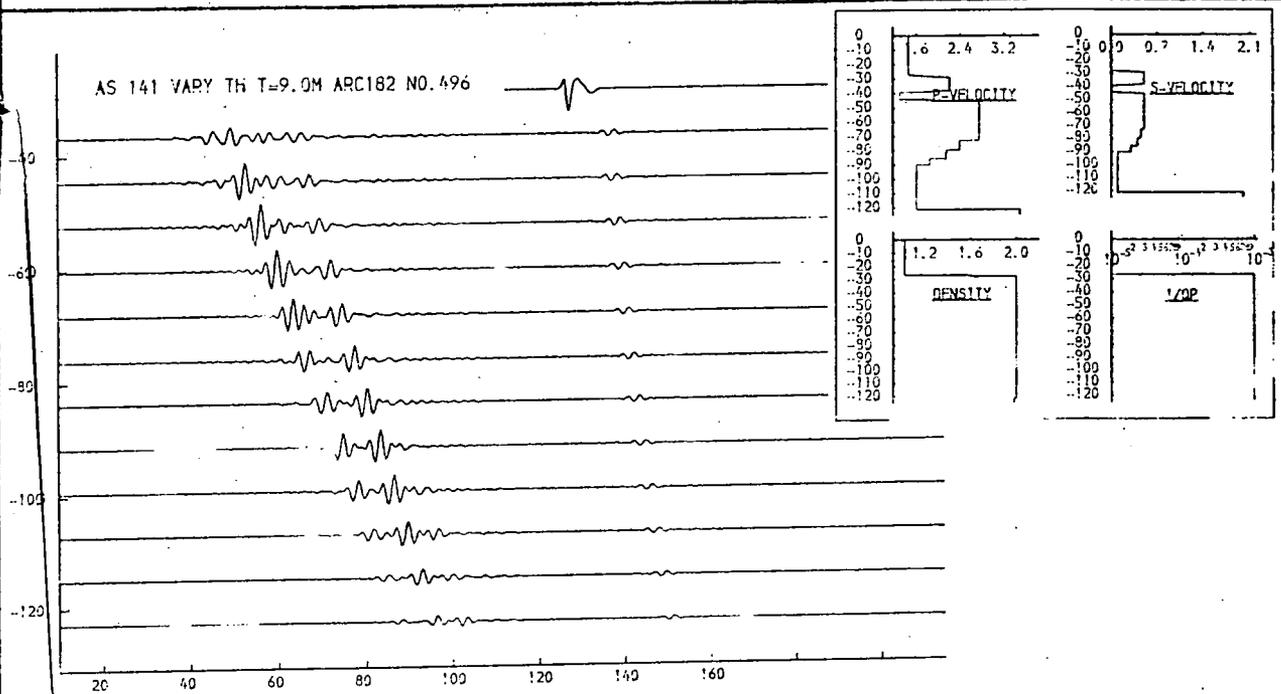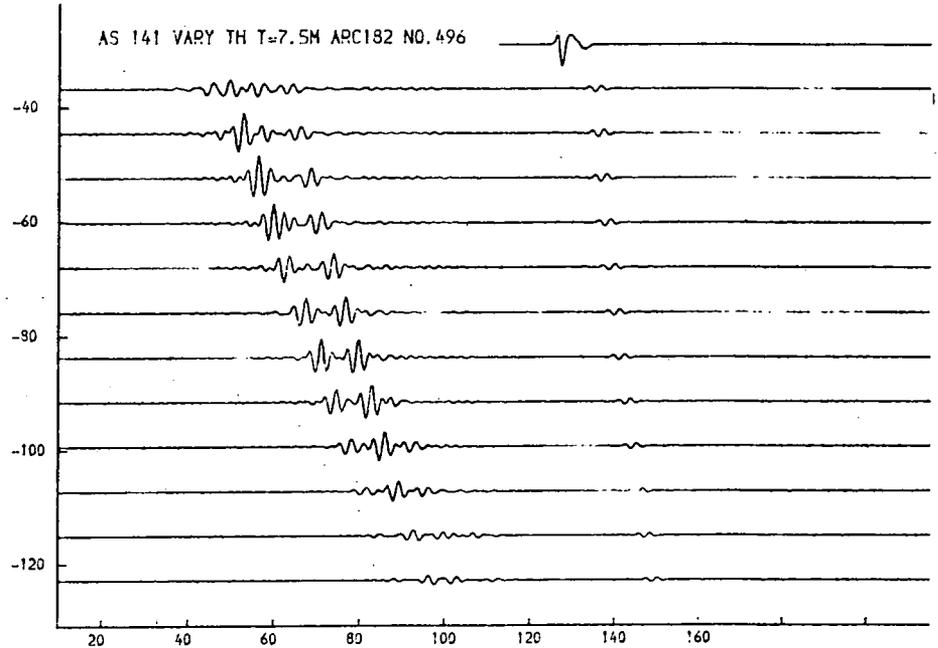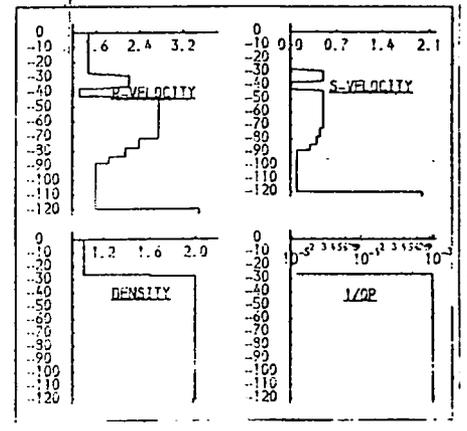
Fig. 9.114c. Profiles with low-velocity layer.

Variation in the thickness of the upper high-velocity layer. Upper: 7.5m.; Lower: 9.0m.

THICKNESS (M.)	P-VELOCITY (M/S.)	S-VELOCITY (M/S.)	DENSITY (G/ML)	1/Q P	1/Q S
26.6	1.460	0.000	1.03	0.00000	0.00000
0.3	1.480	0.510	1.60	0.00100	0.01000
10.2	2.212	0.500	2.00	0.00100	0.01000
8.2	1.590	0.380	2.00	0.00100	0.01000
27.2	2.752	0.500	2.00	0.00100	0.01000
6.6	2.395	0.450	2.00	0.00100	0.03000
5.9	2.145	0.420	2.00	0.00100	0.03000
4.5	1.945	0.700	2.00	0.00100	0.03000
31.2	1.600	0.100	2.00	0.00100	0.03000
	3.500	2.000	1.98	0.00100	0.03000

Fig. 9.114d. Profiles with low-velocity layer.

Variation in the thickness of the upper high-velocity layer. Upper: 10.0m.; Lower: 12.0m.

THICKNESS (M.)	P-VELOCITY (M/S.)	S-VELOCITY (M/S.)	DENSITY (G/ML)	1/Q P	1/Q S		THICKNESS (M.)	P-VELOCITY (M/S.)	S-VELOCITY (M/S.)	DENSITY (G/ML)	1/Q P	1/Q S
26.6	1.460	0.000	1.03	0.00000	0.00000		26.6	1.460	0.000	1.03	0.00000	0.00000
6.3	1.483	0.340	1.60	0.00100	0.01000		6.3	1.483	0.310	1.60	0.00100	0.01000
6.5	2.213	0.563	2.00	0.00100	0.01000		6.5	2.213	0.560	2.00	0.00100	0.01000
6.2	1.504	0.351	2.00	0.00100	0.01000		6.2	1.504	0.351	2.00	0.00100	0.01000
27.2	2.502	0.500	2.00	0.00100	0.01000		27.2	2.402	0.500	2.00	0.00100	0.01000
6.6	2.395	0.450	2.00	0.00100	0.03000		6.6	2.395	0.450	2.00	0.00100	0.03000
5.9	2.145	0.400	2.00	0.00100	0.03000		5.9	2.145	0.400	2.00	0.00100	0.03000
4.5	1.945	0.300	2.00	0.00100	0.03000		4.5	1.945	0.300	2.00	0.00100	0.03000
31.2	1.600	0.100	2.00	0.00100	0.03000		31.2	1.600	0.100	2.00	0.00100	0.03000
	3.500	2.000	1.98	0.00100	0.03000			3.500	2.000	1.98	0.00100	0.03000

AS 135 VARY STEP VELO ARC151 NO.496

AS 135 VARY STEP VELO ARC152 NO.496

Fig. 9.115a. Profiles with low-velocity layer.

Variation of the peak velocity in the lower high-velocity
layer. Upper: 2.5km/sec.; Lower: 2.4km/sec.

THICKNESS (M.)	P-VELOCITY (M/S.)	S-VELOCITY (M/S.)	DENSITY (G/ML)	1/Q P	1/Q S
26.6	1.460	0.000	1.93	0.00000	0.00000
6.3	1.680	0.360	1.99	0.00100	0.01000
6.5	3.223	0.583	2.99	0.00100	0.01000
8.4	1.500	0.535	2.00	0.00100	0.01000
27.2	2.202	0.500	2.00	0.00100	0.01000
6.6	2.105	0.450	2.00	0.00100	0.03000
5.9	2.000	0.400	2.00	0.00100	0.03000
4.5	1.945	0.300	2.00	0.00100	0.03000
31.2	1.600	0.100	2.00	0.00100	0.03000
	3.500	2.000	1.98	0.00100	0.03000

THICKNESS (M.)	P-VELOCITY (M/S.)	S-VELOCITY (M/S.)	DENSITY (G/ML)	1/Q P	1/Q S
26.6	1.460	0.000	1.03	0.00000	0.00000
6.3	1.680	0.360	1.99	0.00100	0.01000
6.5	3.213	0.570	2.99	0.00100	0.01000
8.4	1.500	0.535	2.00	0.00100	0.01000
27.2	2.102	0.500	2.00	0.00100	0.01000
6.6	2.055	0.450	2.00	0.00100	0.03000
5.9	2.000	0.400	2.00	0.00100	0.03000
4.5	1.945	0.300	2.00	0.00100	0.03000
31.2	1.600	0.100	2.00	0.00100	0.03000
	3.500	2.000	1.98	0.00100	0.03000
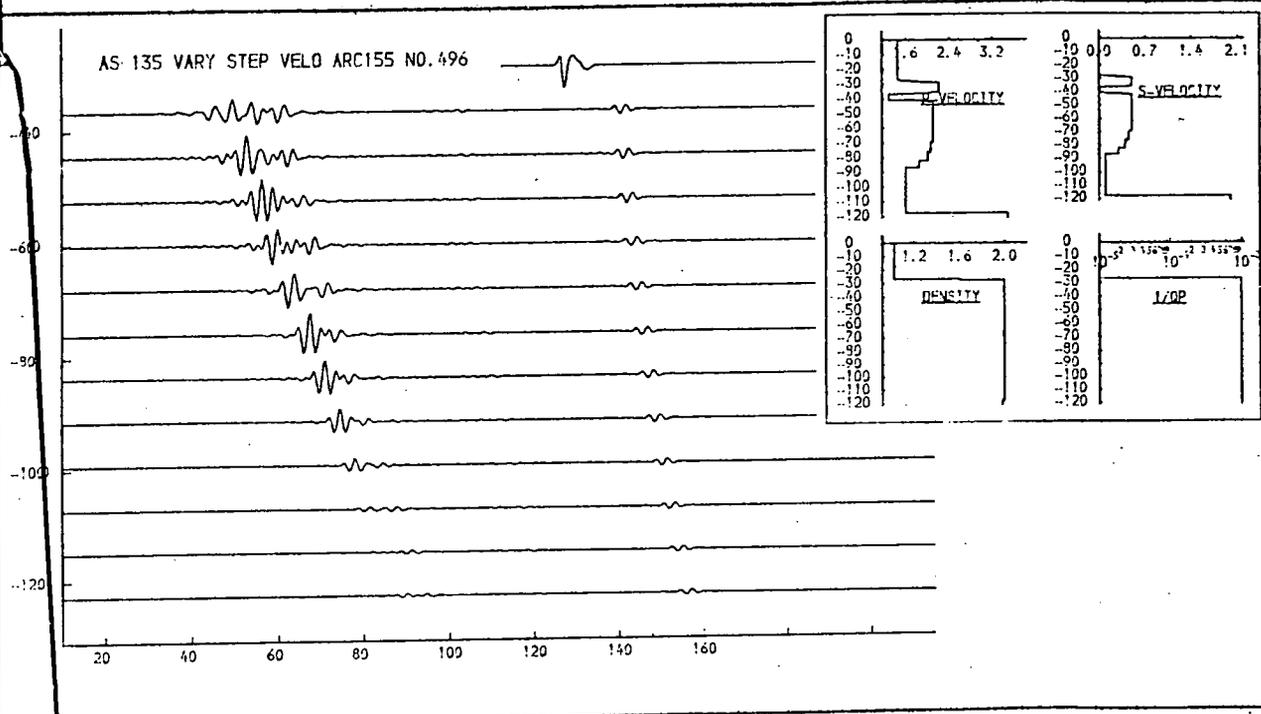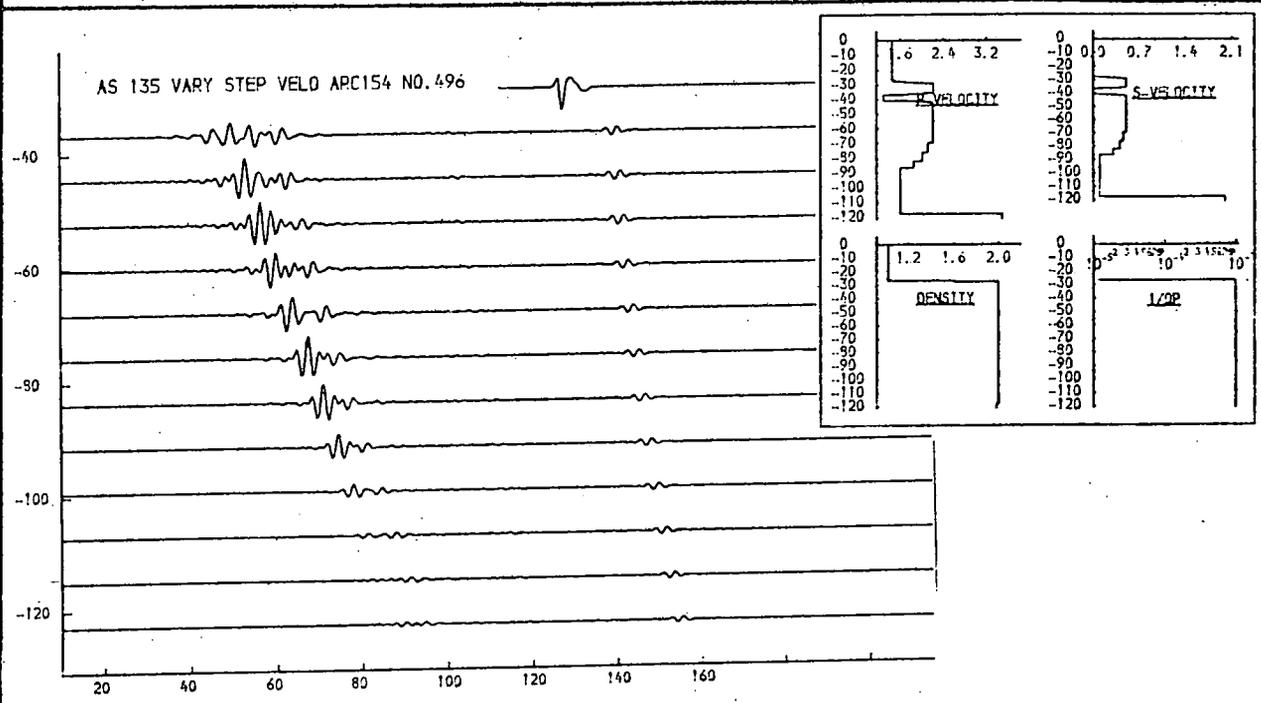
Fig. 9.115b. Profiles with low-velocity layer.

Variation of the peak velocity in the lower high-velocity layer. Upper: 2.2km/sec.; Lower: 2.1km/sec.

THICKNESS (M.)	P-VELOCITY (M/S.)	S-VELOCITY (M/S.)	DENSITY (G/ML)	1/Q P	1/Q S
26.6	1.460	0.000	1.03	0.00000	0.00000
4.2	1.455	0.010	1.00	0.00100	0.01000
6.5	3.213	2.520	2.00	0.00100	0.01000
6.3	1.500	0.500	3.00	0.00100	0.01000
27.2	2.002	0.500	2.00	0.00100	0.01000
5.9	2.000	0.400	2.00	0.00100	0.03000
4.5	1.945	0.300	2.00	0.00100	0.03000
31.2	1.600	0.100	2.00	0.00100	0.03000
	3.500	2.000	1.98	0.00100	0.03000

THICKNESS (M.)	P-VELOCITY (M/S.)	S-VELOCITY (M/S.)	DENSITY (G/ML)	1/Q P	1/Q S
26.6	1.460	0.000	1.03	0.00000	0.00000
4.2	1.455	0.010	1.00	0.00100	0.01000
6.5	3.213	2.520	2.00	0.00100	0.01000
6.3	1.500	0.500	3.00	0.00100	0.01000
27.2	1.902	0.500	2.00	0.00100	0.01000
5.9	1.970	0.400	2.00	0.00100	0.03000
4.5	1.945	0.300	2.00	0.00100	0.03000
31.2	1.600	0.100	2.00	0.00100	0.03000
	3.500	2.000	1.98	0.00100	0.03000

AS 135 VARY STEP VELO ARC156 NO.496

AS 135 VARY STEP VELO ARC157 NO.496
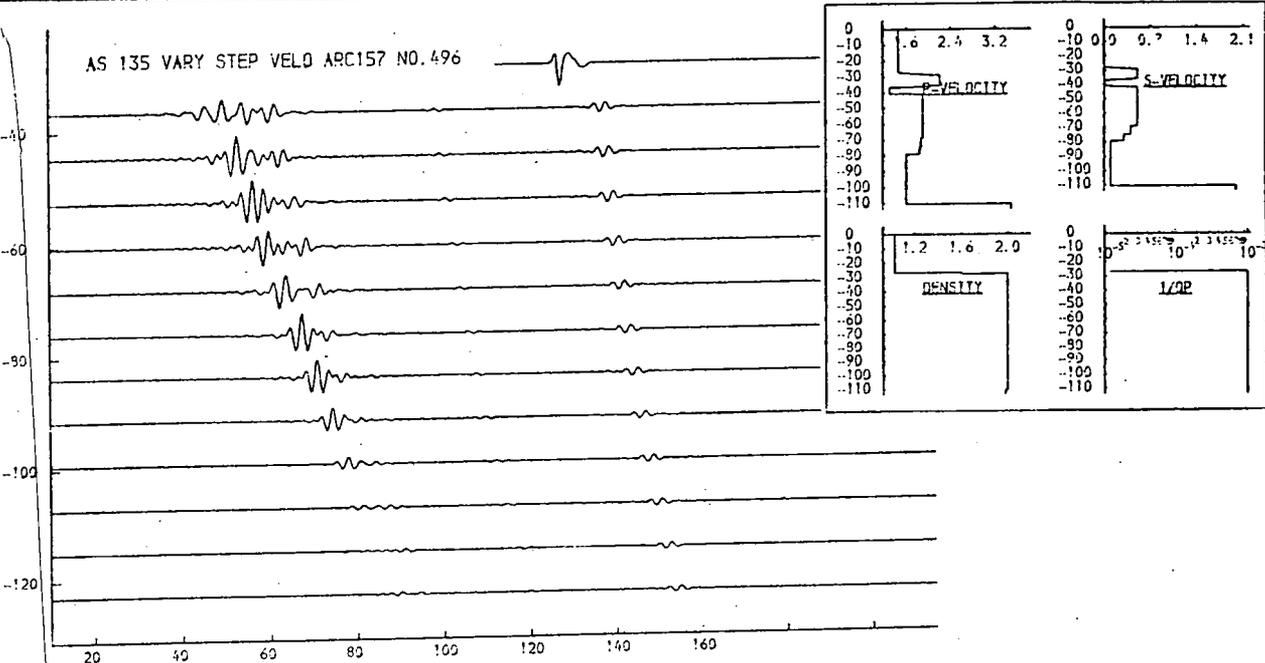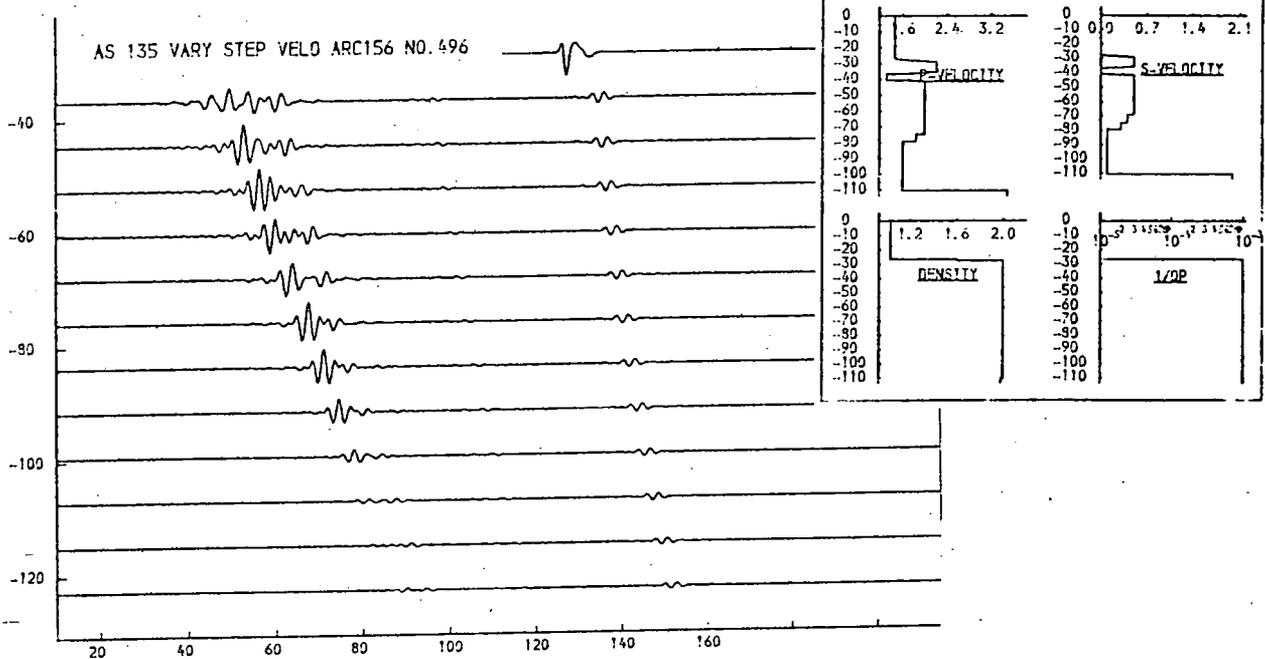
Fig. 9.115c. Profiles with low-velocity layer.

Variation of the peak velocity in the lower high-velocity layer. Upper: 2.0km/sec.; Lower: 1.9km/sec.

THICKNESS (M.)	P-VELOCITY (M/S.)	S-VELOCITY (M/S.)	DENSITY (G/ML)	1/Q P	1/Q S
26.6	1.460	0.000	1.03	0.00000	0.00000
6.3	1.402	0.340	2.00	0.00100	0.01000
6.5	2.243	0.500	2.02	0.00100	0.01000
6.1	2.39	0.35	2.04	0.00100	0.01000
27.2	2.752	0.500	2.00	0.00100	0.01000
6.6	2.395	0.450	2.00	0.00100	0.03000
5.9	2.145	0.400	2.00	0.00100	0.03000
4.5	1.945	0.300	2.00	0.00100	0.03000
31.2	1.600	0.100	2.00	0.00100	0.03000
	3.500	2.000	1.98	0.00100	0.03000

AS 135 VARY TH T=2.0M ARC144 NO.496

AS 135 VARY TH T=2.5M ARC144 NO.496

Fig. 9.116a. Profiles with low-velocity layer.

Vary thickness of the low-velocity layer. Upper: 2m.; Lower: 2.5m.

THICKNESS (M.)	P-VELOCITY (M/S.)	S-VELOCITY (M/S.)	DENSITY (G/ML)	1/Q P	1/Q S
26.6	1.460	0.000	1.03	0.00000	0.00000
6.1	1.493	0.340	1.03	0.00100	0.01000
6.5	2.243	0.562	2.03	0.00100	0.01000
6.8	1.379	0.303	2.00	0.00100	0.01000
27.2	2.752	0.500	2.00	0.00100	0.01000
6.6	2.395	0.450	2.00	0.00100	0.03000
5.9	2.145	0.400	2.22	0.00100	0.03000
4.5	1.945	0.300	2.00	0.00100	0.03000
31.2	1.600	0.100	2.00	0.00100	0.03000
	3.500	2.000	1.93	0.00100	0.03000

Fig. 9.116b. Profiles with low-velocity layer.

Vary   thickness   of   the   low-velocity   layer.
Upper: 4m.; Lower: 5.0m.

THICKNESS (M.)	P-VELOCITY (M/S.)	S-VELOCITY (M/S.)	DENSITY (G/ML)	1/Q P	1/Q S
26.6	1.460	0.000	1.03	0.00000	0.00000
16.4	2.212	0.500	1.60	0.00100	0.01000
10.0	2.900	1.200	2.00	0.00100	0.03000
6.6	2.395	0.700	2.00	0.00100	0.03000
5.0	2.145	0.500	2.00	0.00100	0.03000
4.5	1.945	0.300	2.00	0.00100	0.03000
30.0	1.550	0.050	2.00	0.00100	0.03000
	3.500	2.000	1.99	0.00100	0.03000

AS 187 2.0M LV.LAYER@1.55 ARC194 NO.496

AS 187 1.5M LV.LAYER@1.55 ARC193 NO.496

Fig. 9.117a. Profiles with low-velocity layer.

Vary thickness of low-velocity layer (p-velocity=1.55km/sec.) below a thicker overlying layer. Upper: 2.0m.; Lower: 1.5m.

THICKNESS (M.)	P-VELOCITY (M/S.)	S-VELOCITY (M/S.)	DENSITY (G/ML)	1/Q P	1/Q S
26.6	1.460	0.000	1.03	0.00000	0.00000
0.7	1.630	0.100	1.40	0.00100	0.01000
16.4	2.212	0.500	1.60	0.00100	0.01000
0.7	1.758	0.310	1.53	0.00100	0.01000
10.0	2.300	1.200	2.00	0.00100	0.03000
6.6	2.395	0.700	2.00	0.00100	0.03000
5.9	2.145	0.500	2.00	0.00100	0.03000
4.5	1.945	0.300	2.00	0.00100	0.03000
30.0	1.550	0.050	2.00	0.00100	0.03000
	3.500	2.000	1.98	0.00100	0.03000

AS 187 1.0M LV.LAYER@1.55 ARC192 NO.496

AS 187 0.5M LV.LAYER@1.55 ARC191 NO.496
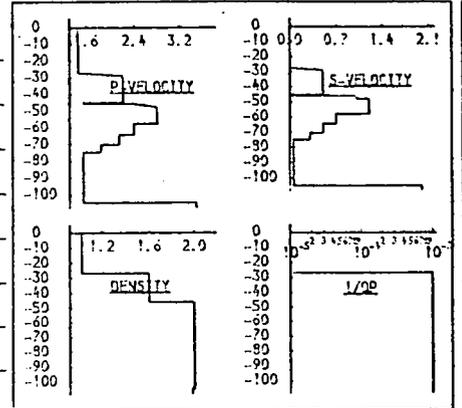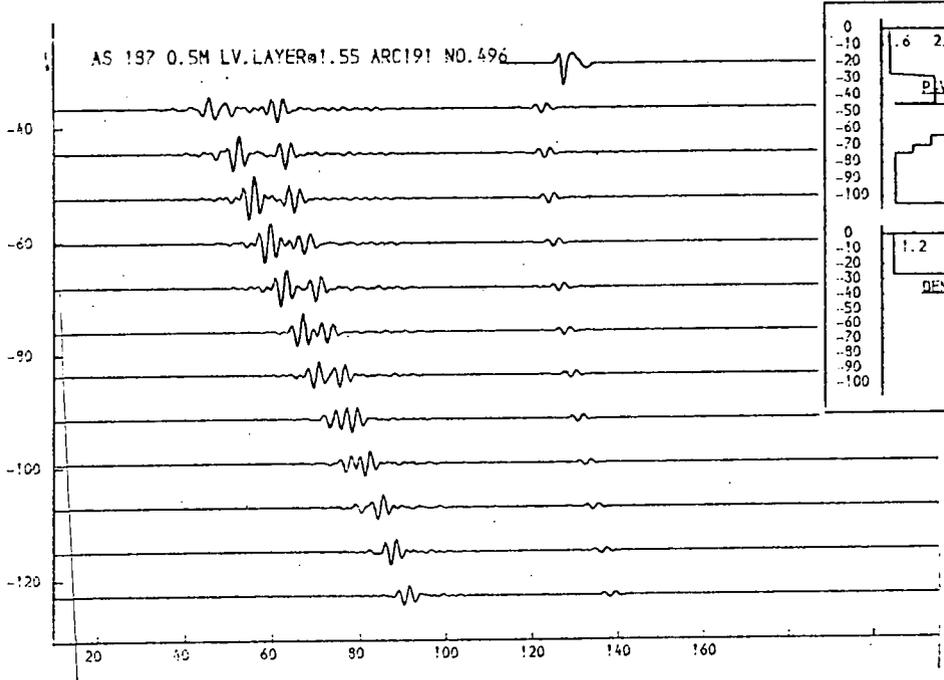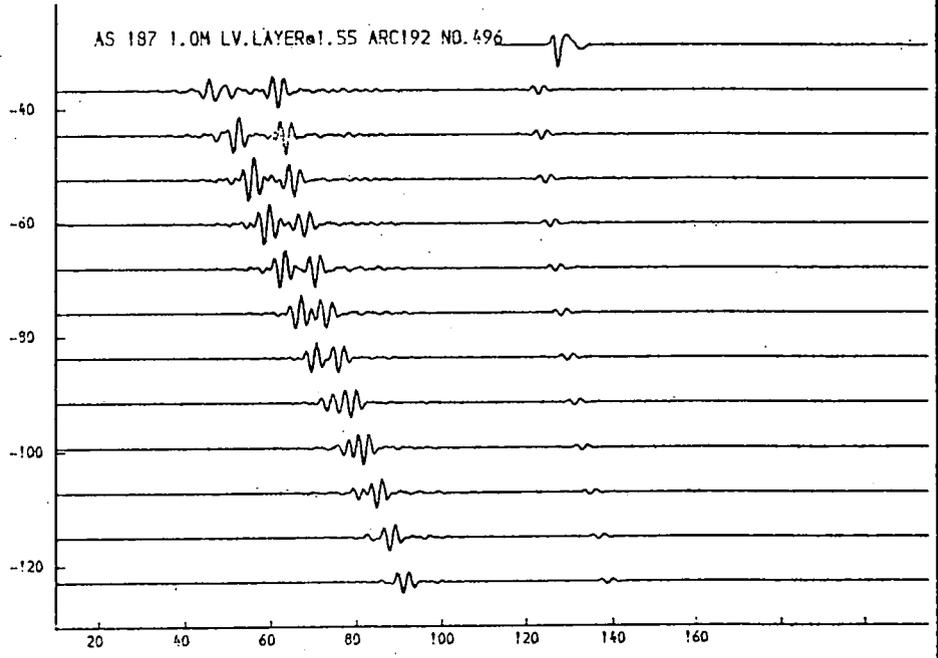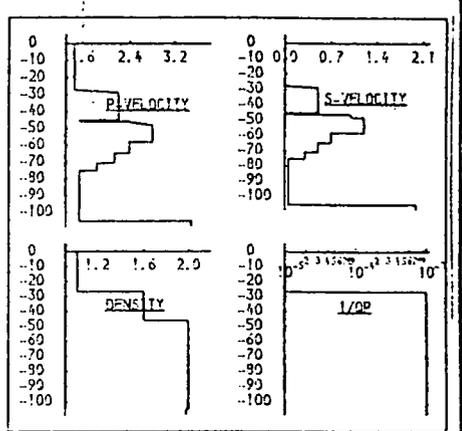
Fig. 9.117b. Profiles with low-velocity layer.

Vary   thickness   of   low-velocity   layer
(p-velocity=1.55km/sec.)   below a thicker overlying layer.
Upper: 1.0m.; Lower: 0.5m.

THICKNESS (M.)	P-VELOCITY (M/S.)	S-VELOCITY (M/S.)	DENSITY (G/ML)	1/Q P	1/Q S
26.0	1.460	0.000	1.03	0.00000	0.00000
16.4	2.212	0.500	1.70	0.00100	0.01000
10.0	2.800	1.200	2.00	0.00100	0.03000
6.6	2.395	0.700	2.00	0.00100	0.03000
5.9	2.145	0.500	2.00	0.00100	0.03000
4.5	1.845	0.300	2.00	0.00100	0.03000
16.5	0.900	0.001	2.00	0.00100	0.03000
	3.500	2.000	1.98	0.00100	0.03000

AS 216 VARY LV LAYER P =1.1 AR216 N.496

AS 215 ADJ.TOP GRDT.LVP=1.3 AR216 N.496

Fig. 9.117c. Profiles with low-velocity layer.

Lower velocity in the thin low-velocity layer: Upper, 1.1km/sec.; lower, 1.3km/sec. A deeper low velocity layer is included in this model (see also figs. 9.121 to 9.123).

THICKNESS (M.)	P-VELOCITY (M/S.)	S-VELOCITY (M/S.)	DENSITY (G/ML)	1/Q P	1/Q S
26.5	1.460	0.000	1.03	0.00000	0.00000
5.6	2.271	0.513	1.70	0.00100	0.01000
10.0	2.800	1.200	2.00	0.00100	0.03000
6.6	2.395	0.700	2.00	0.00100	0.03000
5.9	2.145	0.500	2.00	0.00100	0.03000
4.5	1.945	0.300	2.00	0.00100	0.03000
16.5	0.900	0.001	2.00	0.00100	0.03000
	3.500	2.000	1.98	0.00100	0.03000

THICKNESS (M.)	P-VELOCITY (M/S.)	S-VELOCITY (M/S.)	DENSITY (G/ML)	1/Q P	1/Q S
26.0	1.460	0.000	1.03	0.00000	0.00000
5.6	2.271	0.513	1.70	0.00100	0.01000
10.0	2.800	1.200	2.00	0.00100	0.03000
6.6	2.395	0.850	2.00	0.00100	0.03000
16.5	0.900	0.001	2.00	0.00100	0.03000
	3.500	2.000	1.98	0.00100	0.03000

SMOOTHER TO LV LAYER   ARC 217 N.496

CHG. GRADT. RISE TO LWR   ARC 218 N.496

Fig. 9.117d.   Profiles with low-velocity layer.

Upper: A more gradual transition to the upper low velocity zone
Lower: Similar to the upper figure with small modifications
to the gradients bounding the lower high-velocity zone.
A deeper low-velocity layer is included in this model (see
also figs. 9.121 to 9.123).

THICKNESS (M.)	P-VELOCITY (M/S.)	S-VELOCITY (M/S.)	DENSITY (G/ML)	1/Q P	1/Q S
26.0	1.460	0.000	1.03	0.00000	0.00000
0.7	1.480	0.010	1.10	0.00100	0.01000
5.6	2.221	0.513	1.70	0.00100	0.01000
10.0	2.800	1.200	2.00	0.00100	0.03000
6.6	2.395	0.850	2.00	0.00100	0.03000
2.5	1.900	0.500	2.00	0.00100	0.03000
2.5	1.700	0.150	2.00	0.00100	0.03000
16.5	0.900	0.001	2.00	0.00100	0.03000
	3.500	2.000	1.98	0.00100	0.03000

THICKNESS (M.)	P-VELOCITY (M/S.)	S-VELOCITY (M/S.)	DENSITY (G/ML)	1/Q P	1/Q S
26.0	1.460	0.000	1.03	0.00000	0.00000
4.2	2.037	0.100	1.70	0.00100	0.01000
10.0	2.800	1.200	2.00	0.00100	0.03000
6.6	2.395	0.850	2.00	0.00100	0.03000
2.5	1.900	0.500	2.00	0.00100	0.03000
2.5	1.700	0.150	2.00	0.00100	0.03000
16.5	0.900	0.001	2.00	0.00100	0.03000
	3.500	2.000	1.98	0.00100	0.03000

AS 218 CH DEEP GR. NSUR LY AEC219 N.496

SET S LOW AND LWR P AT TOP ARC220 N.496

Fig. 9.117e. Profiles with low-velocity layer.

Upper: A similar model to those of fig. 9.117d, with the addition of a thin layer of lower velocity in the upper low-velocity zone.
Lower: Similar to the upper figure, with reduction in the p and s velocities in the upper high velocity layer.

THICKNESS (M.)	P-VELOCITY (M/S.)	S-VELOCITY (M/S.)	DENSITY (G/ML)	1/Q P	1/Q S
26.6	1.460	0.000	1.03	0.00000	0.00000
0.3	1.100	0.640	1.40	0.00100	0.01000
16.4	2.212	0.500	1.60	0.00100	0.01000
2.0	2.300	1.000	2.00	0.00100	0.01000
15.7	2.600	1.200	2.00	0.00100	0.03000
6.6	2.325	0.700	2.00	0.00100	0.03000
5.9	2.145	0.500	2.00	0.00100	0.03000
4.5	1.935	0.700	2.00	0.00100	0.03000
31.2	1.600	0.100	2.00	0.00100	0.03000
	3.500	2.000	1.98	0.00100	0.03000

AS 185 LWR. P VEL. =2.6 ARC189 NO.496

AS 185 LWR. P VEL. =2.7 ARC188 NO.496
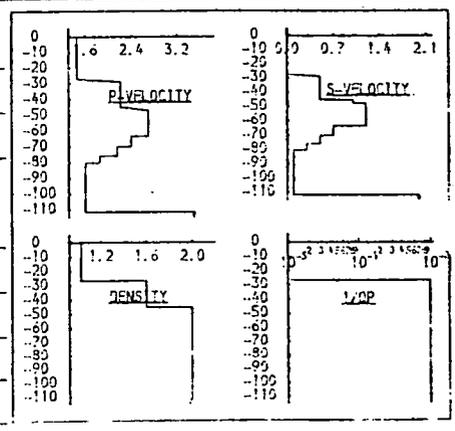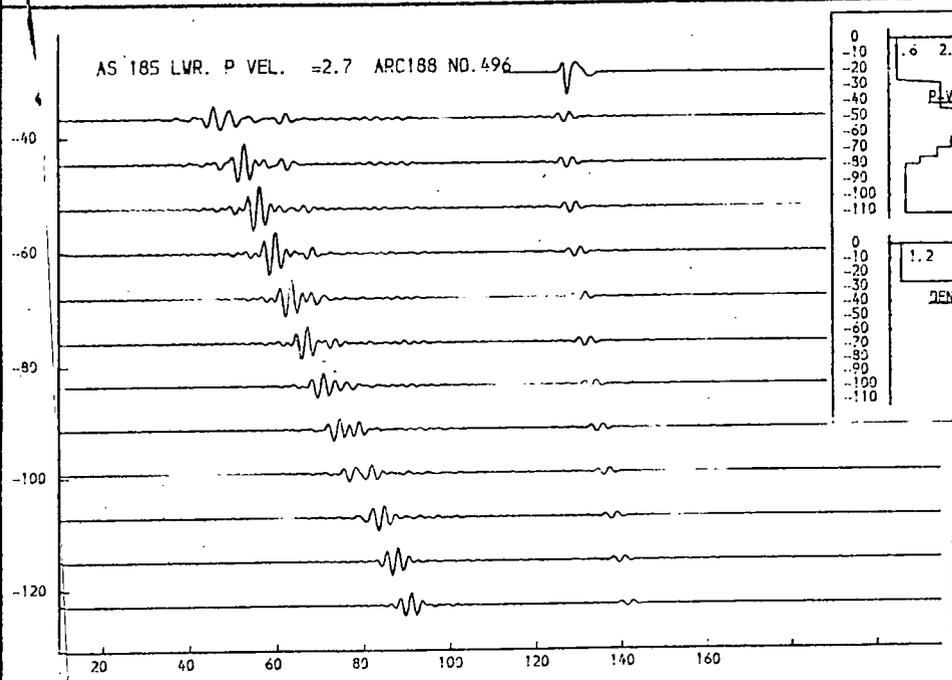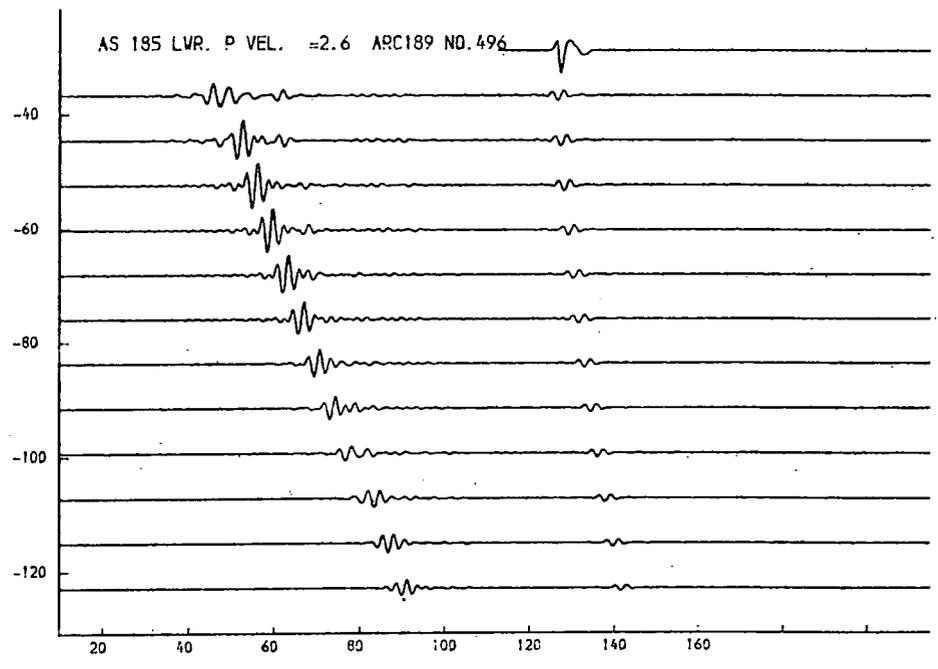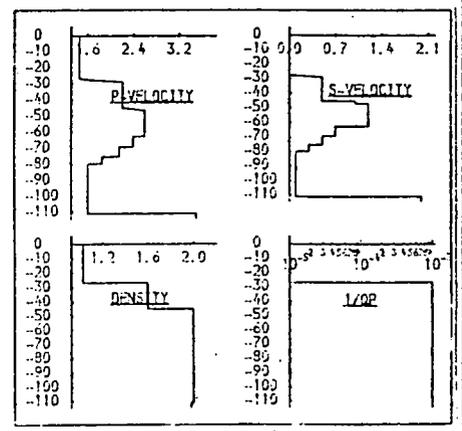
Fig. 9.118a. Stepped velocity profile.

The thin low velocity layer is removed and the maximum p-velocity of the lower step is varied. Upper: 2.6; Lower: 2.7.

THICKNESS (M.)	P-VELOCITY (M/S.)	S-VELOCITY (M/S.)	DENSITY (G/ML)	1/Q P	1/Q S
26.6	1.460	0.000	1.93	0.00000	0.00000
0.7	1.400	0.010	1.60	0.00100	0.01000
16.4	2.212	0.500	1.60	0.00100	0.01000
0.8	2.600	1.600	2.00	0.00100	0.01000
15.7	2.800	1.200	2.00	0.00100	0.03000
6.6	2.395	0.700	2.00	0.00100	0.03000
5.9	3.145	0.500	2.00	0.00100	0.03000
4.5	1.845	0.300	2.00	0.00100	0.03000
31.2	1.600	0.100	2.00	0.00100	0.03000
	3.500	2.000	1.98	0.00100	0.03000

Fig. 9.118b. Stepped velocity profile.

The thin low velocity layer is removed and the maximum p-velocity of the lower step is varied. Upper: 2.8; Lower: 2.9.

THICKNESS (M.)	P-VELOCITY (M/S.)	S-VELOCITY (M/S.)	DENSITY (G/ML)	1/Q P	1/Q S
26.6	1.460	0.000	1.03	0.00000	0.00000
0.7	1.460	0.000	1.40	0.00100	0.01000
16.4	2.212	0.450	1.60	0.00100	0.01000
0.4	2.200	0.450	2.00	0.00100	0.01000
15.7	2.600	0.600	2.00	0.00100	0.03000
6.6	2.395	0.600	2.00	0.00100	0.03000
5.9	2.145	0.500	2.00	0.00100	0.03000
4.5	1.845	0.300	2.00	0.00100	0.03000
31.2	1.600	0.100	2.00	0.00100	0.03000
	3.500	2.000	1.98	0.00100	0.03000

AS 189 CHG. S VEL. =0.6 ARC192 NO.496

AS 189 CHG. S VEL. =1.0 ARC190 NO.496
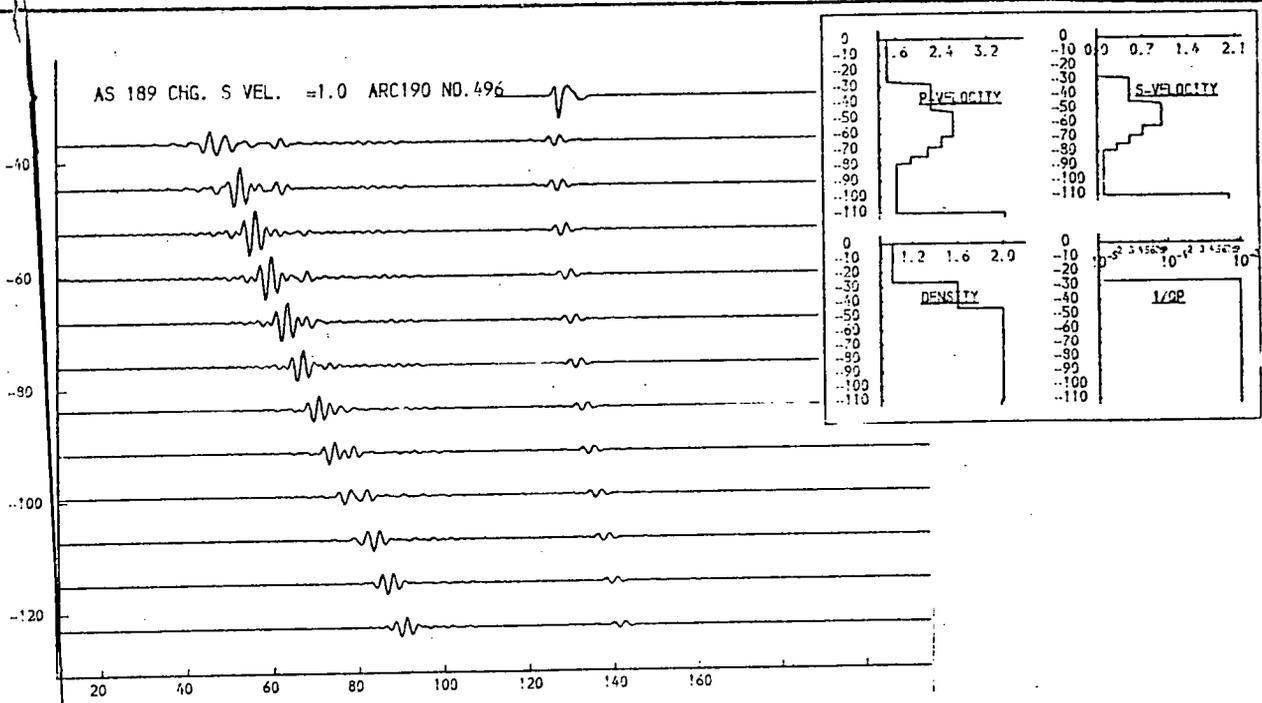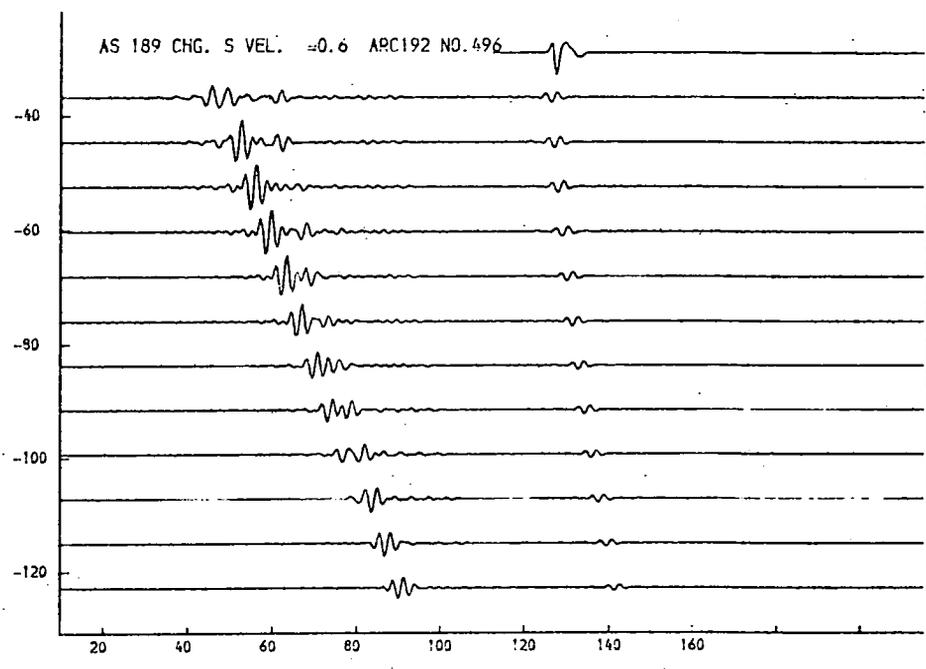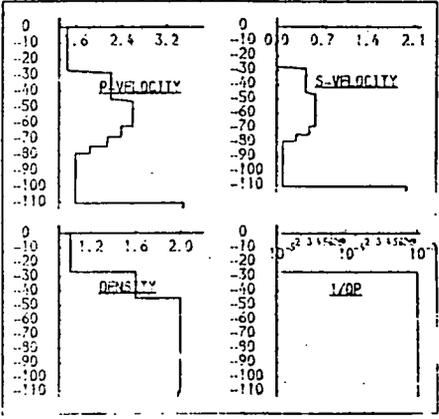
Fig. 9.119. Stepped velocity profile. ,

Variations in s-velocity in the lower high-velocity layer.
Upper: 0.6km/sec.; Lower: 1.0km/sec.

THICKNESS (M.)	P-VELOCITY (M/S.)	S-VELOCITY (M/S.)	DENSITY (G/ML)	1/Q P	1/Q S
26.6	1.460	0.000	1.03	0.00000	0.00000
~0.3~	~1.688~	~0.200~	~.60~	~0.00100~	~0.01000~
8.2	2.212	0.500	1.60	0.00100	0.01000
8.2	2.500	1.000	2.00	0.00100	0.01000
10.0	2.900	1.200	2.00	0.00100	0.03000
6.6	2.395	0.700	2.00	0.00100	0.03000
5.9	2.145	0.500	2.00	0.00100	0.03000
4.5	1.945	0.300	2.00	0.00100	0.03000
30.0	1.550	0.050	2.00	0.00100	0.03000
	3.500	2.000	1.93	0.00100	0.03000

THICKNESS (M.)	P-VELOCITY (M/S.)	S-VELOCITY (M/S.)	DENSITY (G/ML)	1/Q P	1/Q S
26.6	1.460	0.000	1.03	0.00000	0.00000
~0.3~	~1.688~	~0.200~	~.60~	~0.00100~	~0.01000~
4.1	2.212	0.500	2.00	0.00100	0.01000
4.1	2.350	0.700	2.00	0.00100	0.01000
4.1	2.500	0.850	2.00	0.00100	0.01000
4.1	2.650	1.000	2.00	0.00100	0.01000
10.0	2.900	1.200	2.00	0.00100	0.03000
6.6	2.395	0.700	2.00	0.00100	0.03000
5.9	2.145	0.500	2.00	0.00100	0.03000
4.5	1.945	0.300	2.00	0.00100	0.03000
30.0	1.550	0.050	2.00	0.00100	0.03000
	3.500	2.000	1.93	0.00100	0.03000

AS 187 SMOOTH STEP /2   ARC197 NO.496

AS 187 SMOOTH STEP /4   ARC197 NO.496
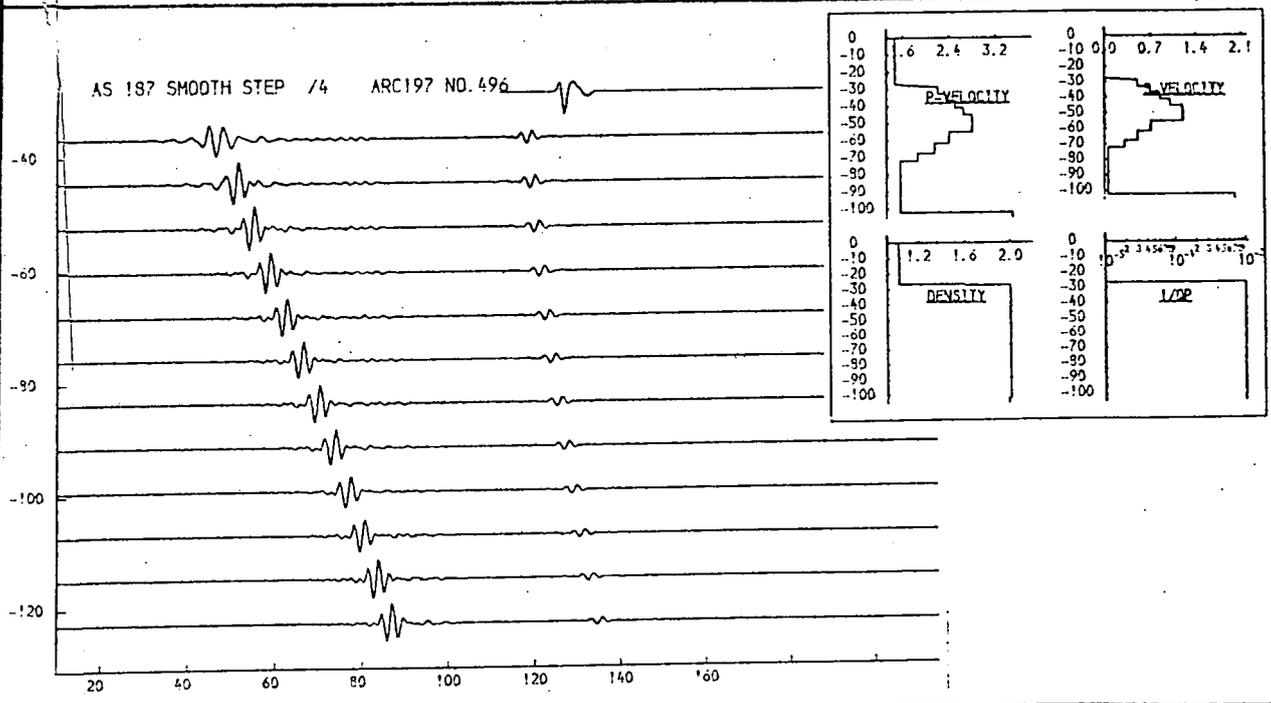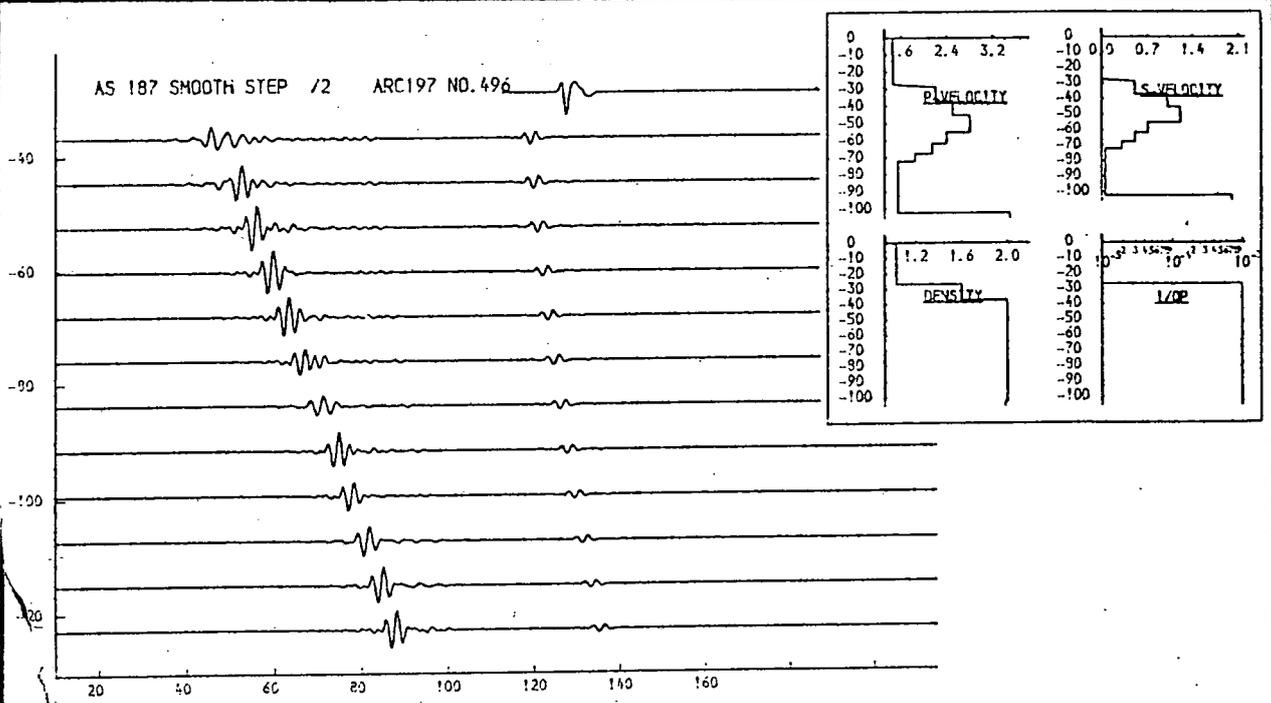
Fig. 9.120. Stepped velocity profile.

The upper step is subdivided: by 2 (upper) and by 4 (lower).

THICKNESS (M.)	P-VELOCITY (M/S.)	S-VELOCITY (M/S.)	DENSITY (G/ML)	1/Q P	1/Q S		THICKNESS (M.)	P-VELOCITY (M/S.)	S-VELOCITY (M/S.)	DENSITY (G/ML)	1/Q P	1/Q S
26.6	1.460	0.000	1.03	0.00000	0.00000		26.6	1.460	0.000	1.03	0.00000	0.00000
0.7	1.488	0.240	1.60	0.00100	0.01000		0.7	1.488	0.240	1.60	0.00100	0.01000
16.4	2.212	0.500	1.60	0.00100	0.01000		16.4	2.212	0.500	1.60	0.00100	0.01000
	2.500			0.00100	0.01000			2.500			0.00100	0.01000
10.9	2.800	1.200	2.00	0.00100	0.03000		10.9	2.800	1.200	2.00	0.00100	0.03000
6.6	2.395	0.700	2.00	0.00100	0.03000		6.6	2.395	0.700	2.00	0.00100	0.03000
5.9	2.145	0.500	2.00	0.00100	0.03000		5.9	2.145	0.500	2.00	0.00100	0.03000
4.5	1.945	0.300	2.00	0.00100	0.03000		4.5	1.945	0.300	2.00	0.00100	0.03000
28.5	1.500	0.050	2.00	0.00100	0.03000		26.6	1.400	0.001	2.00	0.00100	0.03000
	3.500	2.000	1.93	0.00100	0.03000			3.500	2.000	1.93	0.00100	0.03000

AS 194 ADJ. LOWEST LY.   ARC211 NO.496

AS 194 ADJ. LOWEST LY.   ARC212 NO.496

P-VELOCITY   S-VELOCITY   DENSITY   1/QP
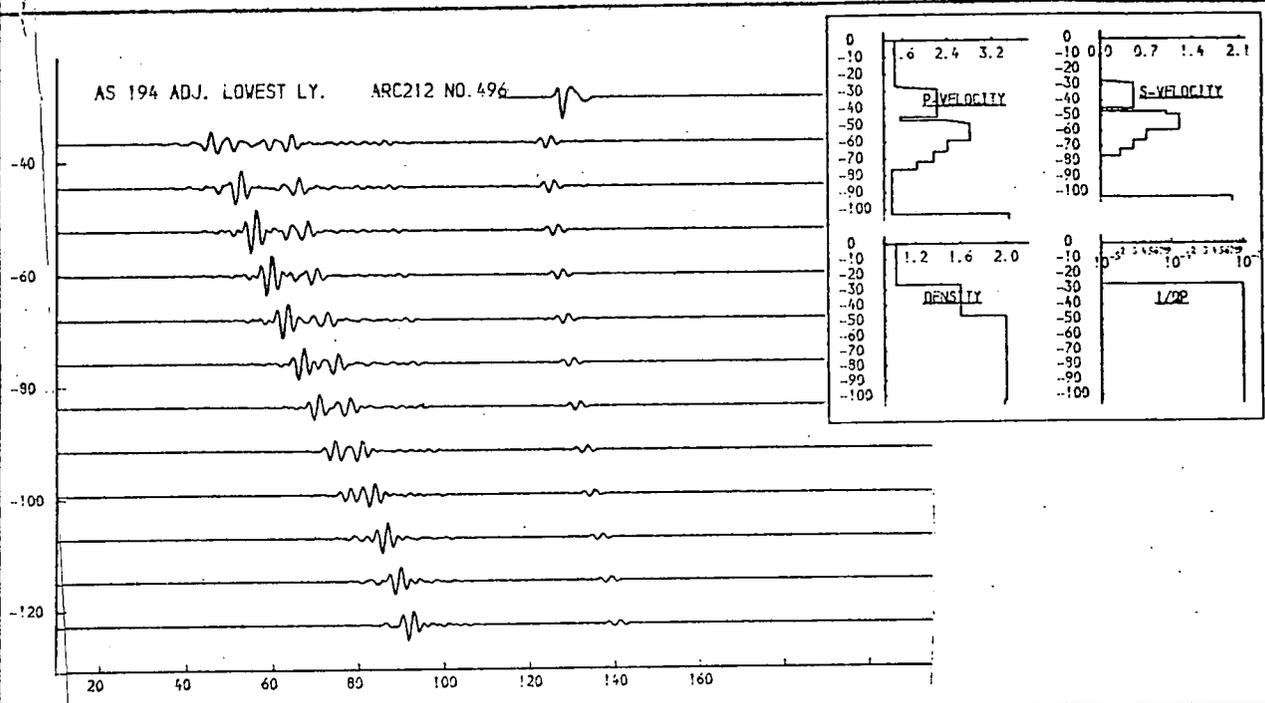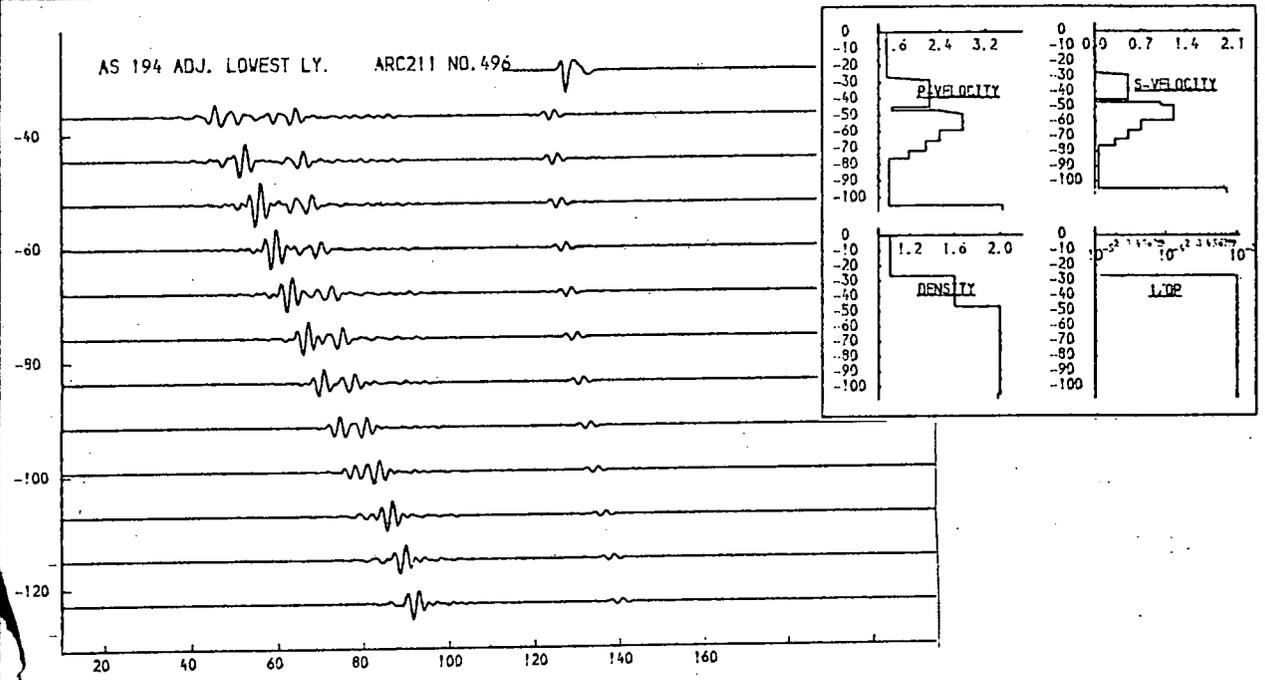
Fig. 9.121a. Modelling of deeper reflector.

The p-velocity in the deepest layer is varied. Upper: 1.5km/sec.; Lower: 1.4km/sec.

THICKNESS (M.)	P-VELOCITY (M/S.)	S-VELOCITY (M/S.)	DENSITY (G/ML)	1/Q P	1/Q S
26.6	1.460	0.000	1.03	0.00000	0.00000
0.7	1.480	0.010	1.60	0.00100	0.01000
16.4	2.212	0.500	1.60	0.00100	0.01000
4.8	2.500	0.101	1.60	0.00100	0.01000
10.0	2.800	1.200	2.00	0.00100	0.03000
6.6	2.395	0.700	2.00	0.00100	0.03000
5.9	2.145	0.500	2.00	0.00100	0.03000
4.5	1.945	0.300	2.00	0.00100	0.03000
22.8	1.200	0.001	2.00	0.00100	0.03000
	3.500	2.000	1.98	0.00100	0.03000

THICKNESS (M.)	P-VELOCITY (M/S.)	S-VELOCITY (M/S.)	DENSITY (G/ML)	1/Q P	1/Q S
26.0	1.460	0.000	1.03	0.00000	0.00000
0.7	1.480	0.010	1.60	0.00100	0.01000
16.4	2.212	0.500	1.60	0.00100	0.01000
4.8	2.500	0.101	1.60	0.00100	0.01000
10.0	2.800	1.200	2.00	0.00100	0.03000
6.6	2.395	0.700	2.00	0.00100	0.03000
5.9	2.145	0.500	2.00	0.00100	0.03000
4.5	1.945	0.300	2.00	0.00100	0.03000
16.5	0.900	0.001	2.00	0.00100	0.03000
	3.500	2.000	1.98	0.00100	0.03000

AS 194 ADJ. LOWEST LY.   ARC214 NO.496

AS 194 ADJ. LOWEST LY.   ARC215 NO.496

Fig. 9.121b. Modelling of deeper reflector.

The p-velocity in the deepest layer is varied.
Upper: 1.2km/sec.; Lower: 0.9km/sec.

THICKNESS (M.)	P-VELOCITY (M/S.)	S-VELOCITY (M/S.)	DENSITY (G/ML)	1/Q P	1/Q S
26.6	1.460	0.000	1.03	0.00000	0.00000
16.4	2.212	0.500	2.00	0.00100	0.01000
5.0	2.900	1.200	2.00	0.00100	0.01000
3.3	2.400	0.900	2.00	0.00100	0.03000
37.2	1.500	0.100	2.00	0.00100	0.03000
	3.500	2.000	1.98	0.00100	0.03000

THICKNESS (M.)	P-VELOCITY (M/S.)	S-VELOCITY (M/S.)	DENSITY (G/ML)	1/Q P	1/Q S
26.6	1.460	0.000	1.03	0.00000	0.00000
16.4	2.212	0.500	2.00	0.00100	0.01000
5.0	2.900	1.200	2.00	0.00100	0.01000
3.3	2.400	0.900	2.00	0.00100	0.03000
32.2	1.300	0.100	2.00	0.00100	0.03000
	3.500	2.000	1.98	0.00100	0.03000

AS 214 ADJ UNDERSIDE P=1.5 ARC300 NO.496

AS 214 ADJ UNDERSIDE P=1.3 ARC300 NO.496

Fig. 9.122a. Modelling of deeper reflector.

The underside of the deeper of the two layers is adjusted, and p-velocity is again varied. Upper: 1.5; Lower: 1.3.

THICKNESS (M.)	P-VELOCITY (M/S.)	S-VELOCITY (M/S.)	DENSITY (G/ML)	1/Q P	1/Q S
26.6	1.460	0.000	1.03	0.00000	0.00000
16.4	2.212	0.500	2.00	0.00100	0.01000
5.0	2.900	1.200	2.00	0.00100	0.01000
3.3	2.400	2.000	2.00	0.00100	0.03000
27.2	1.100	0.100	2.00	0.00100	0.03000
	3.500	2.000	1.98	0.00100	0.03000

THICKNESS (M.)	P-VELOCITY (M/S.)	S-VELOCITY (M/S.)	DENSITY (G/ML)	1/Q P	1/Q S
26.6	1.460	0.000	1.03	0.00000	0.00000
16.4	2.212	0.500	2.00	0.00100	0.01000
5.0	2.900	1.200	2.00	0.00100	0.01000
3.3	2.400	2.000	2.00	0.00100	0.03000
22.3	0.900	0.001	2.00	0.00100	0.03000
	3.500	2.000	1.98	0.00100	0.03000

Fig. 9.122b. Modelling of deeper reflector.

The underside of the deeper of the two layers is adjusted, and p-velocity is again varied. Upper: 1.1; Lower: 0.9.

THICKNESS (M.)	P-VELOCITY (M/S.)	S-VELOCITY (M/S.)	DENSITY (G/ML)	1/Q P	1/Q S
26.6	1.460	0.000	1.03	0.00000	0.00000
				0.00100	0.01000
16.4	2.212	0.500	2.00	0.00100	0.01000
				0.00100	0.01000
41.7	1.500	0.001	2.00	0.00100	0.03000
	3.500	2.000	1.99	0.00100	0.03000

THICKNESS (M.)	P-VELOCITY (M/S.)	S-VELOCITY (M/S.)	DENSITY (G/ML)	1/Q P	1/Q S
26.6	1.460	0.000	1.03	0.00000	0.00000
16.4	2.212	0.500	2.00	0.00100	0.01000
33.9	1.250	0.001	2.00	0.00100	0.03000
	3.500	2.000	1.98	0.00100	0.03000
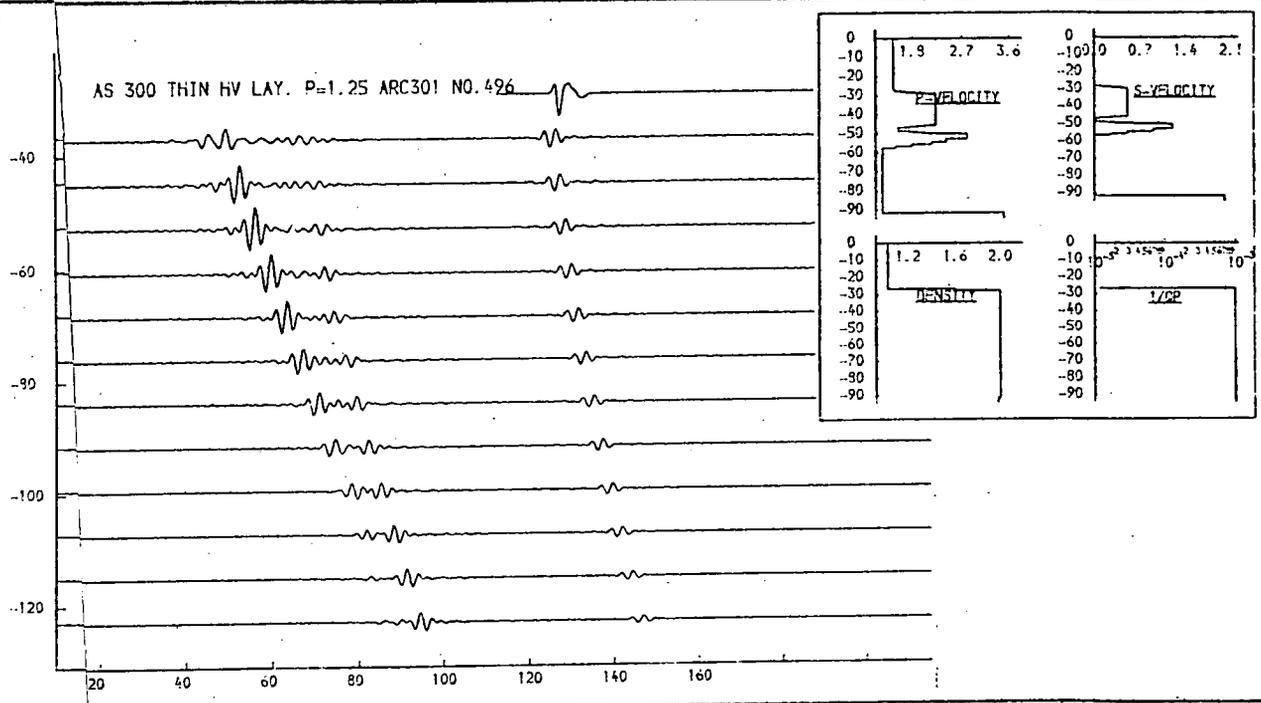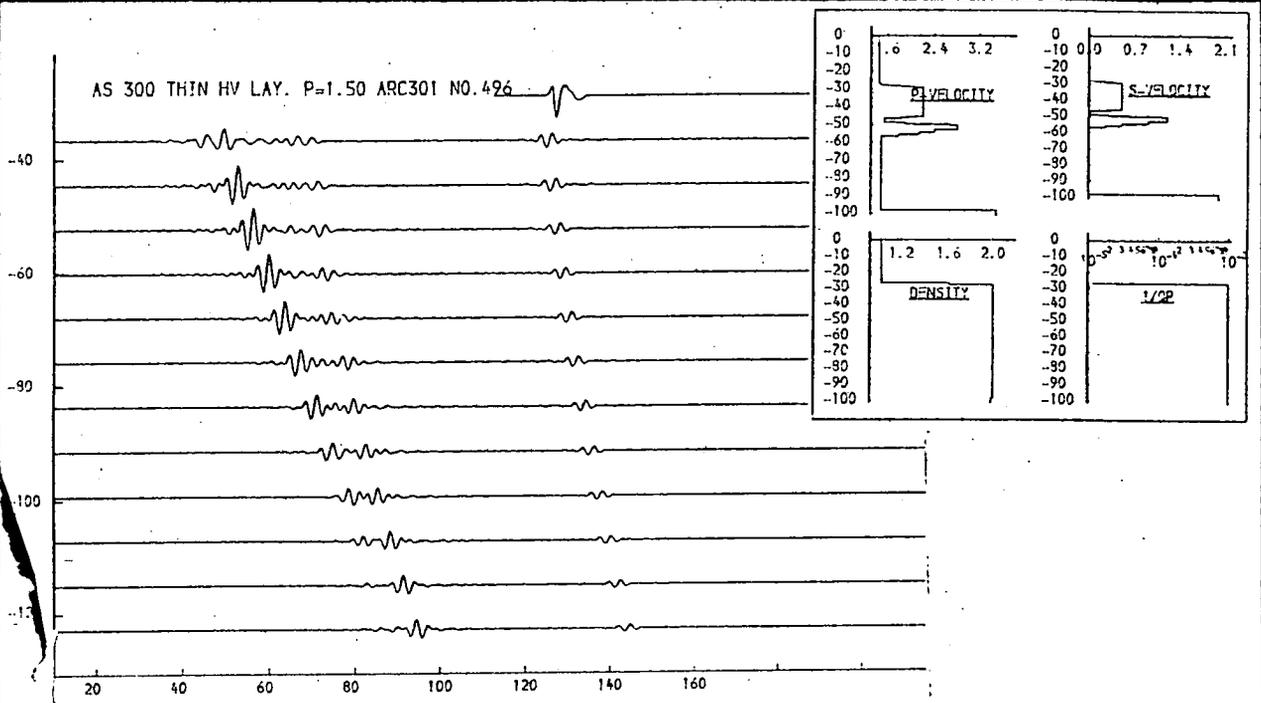
Fig. 9.123a. Modelling of deepest reflector.

The deeper of the two high-velocity layers is adjusted and
p-velocity is again varied. Upper: 1.5; Lower: 1.25.

THICKNESS (M.)	P-VELOCITY (M/S.)	S-VELOCITY (M/S.)	DENSITY (G/ML)	1/Q P	1/Q S
26.6	1.460	0.000	1.03	0.00000	0.00000
16.4	2.212	0.500	2.00	0.00100	0.01000
26.4	1.000	0.001	2.00	0.00100	0.03000
	3.500	2.000	1.98	0.00100	0.03000

THICKNESS (M.)	P-VELOCITY (M/S.)	S-VELOCITY (M/S.)	DENSITY (G/ML)	1/Q P	1/Q S
26.6	1.460	0.000	1.03	0.00000	0.00000
16.4	2.212	0.500	2.00	0.00100	0.01000
	2.900	1.200	2.00	0.00100	0.01000
13.4	0.700	0.001	2.00	0.00100	0.03000
	3.500	2.000	1.98	0.00100	0.03000

AS 300 THIN HV LAY. P=1.0 ARC301 NO.496

P-VELOCITY   S-VELOCITY   DENSITY   1/2P

AS 300 THIN HV LAY. P=0.7 ARC301 NO.496

P-VELOCITY   S-VELOCITY   DENSITY   1/2P
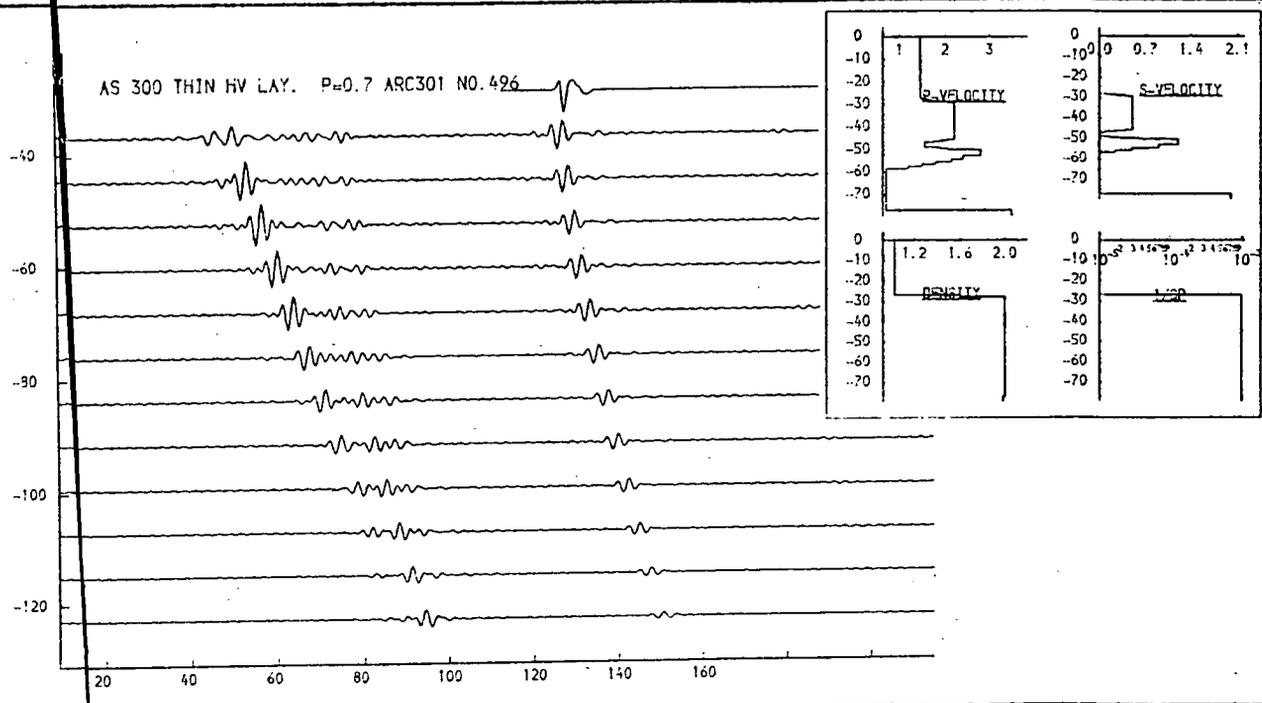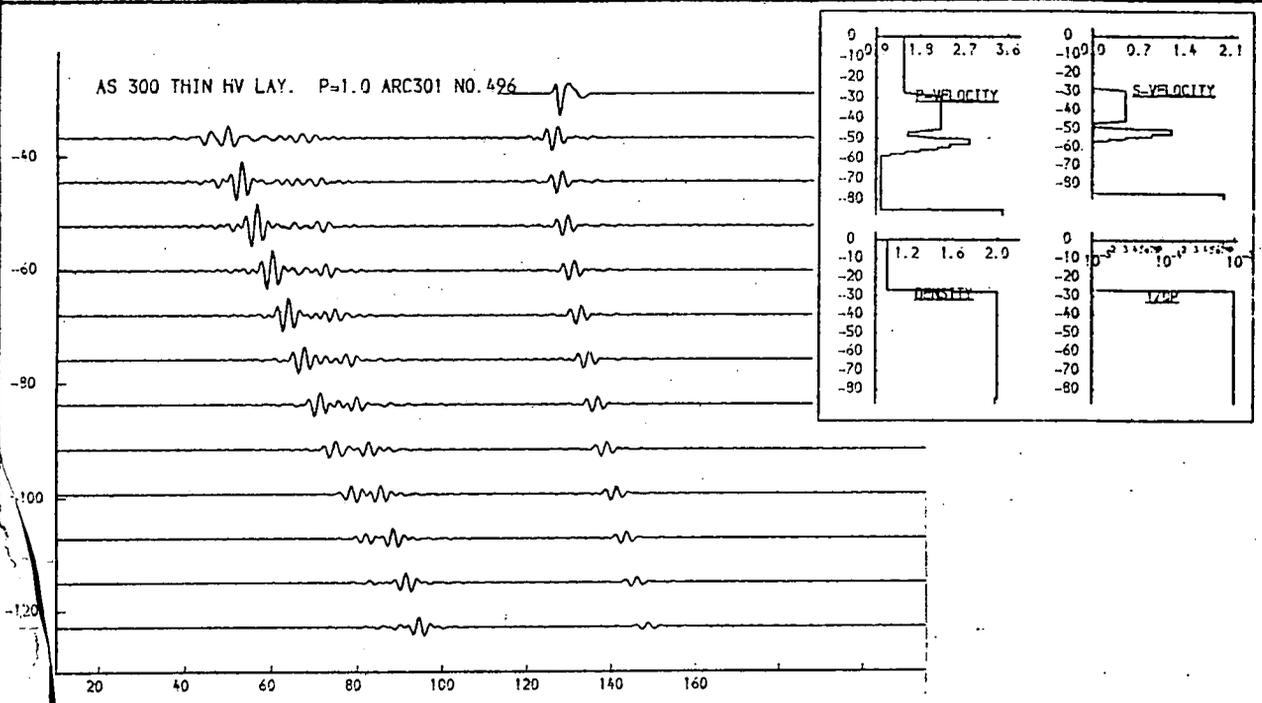
Fig. 9.123b. Modelling of deepest reflector.

The deeper of the two high-velocity layers is adjusted and p-velocity is again varied. Upper: 1.0; Lower: 0.7.

More synthetic seismogramme models

for nos. 1289 and 1281

(figs. 9.124 to 9.131)

THICKNESS (M.)	P-VELOCITY (M/S.)	S-VELOCITY (M/S.)	DENSITY (G/ML)	1/Q P	1/Q S
74.4	1.460	0.000	1.03	0.00000	0.00000
6.1	1.490	0.010	1.65	0.01000	0.04000
1.7	1.750	0.524	2.00	0.00100	0.03000
1.9	2.650	0.613	2.00	0.00100	0.03000
2.2	2.225	0.613	2.00	0.00100	0.03000
8.2	2.375	0.653	2.00	0.00100	0.03000
2.6	2.225	0.612	2.00	0.00100	0.03000
2.4	2.075	0.571	2.00	0.00100	0.03000
2.2	1.925	0.529	2.00	0.00100	0.03000
2.2	1.950	0.529	2.00	0.00100	0.03000
2.1	1.775	0.488	2.00	0.00100	0.03000
3.9	1.625	0.447	2.00	0.00100	0.03000
	2.700	1.900	1.98	0.01000	0.06000

'496' STYLE GR. VY. P = 2.7 NO. 1289

'496' STYLE GR. VY. P = 3.0 NO. 1289
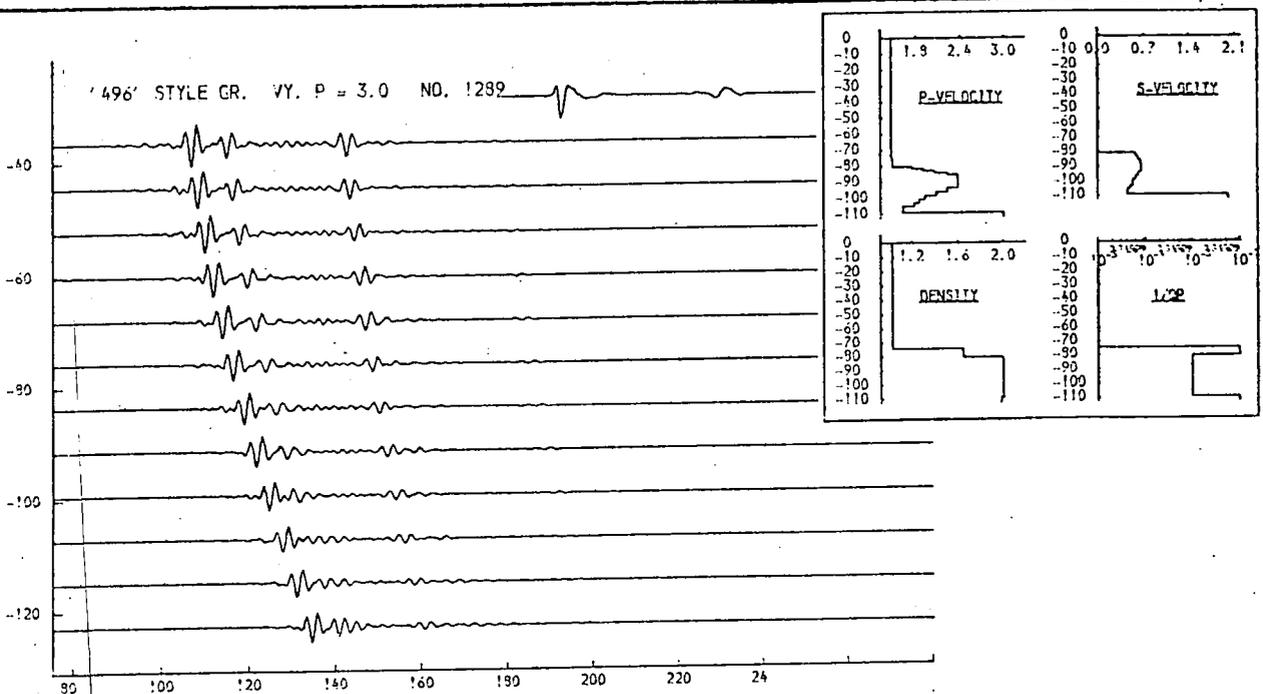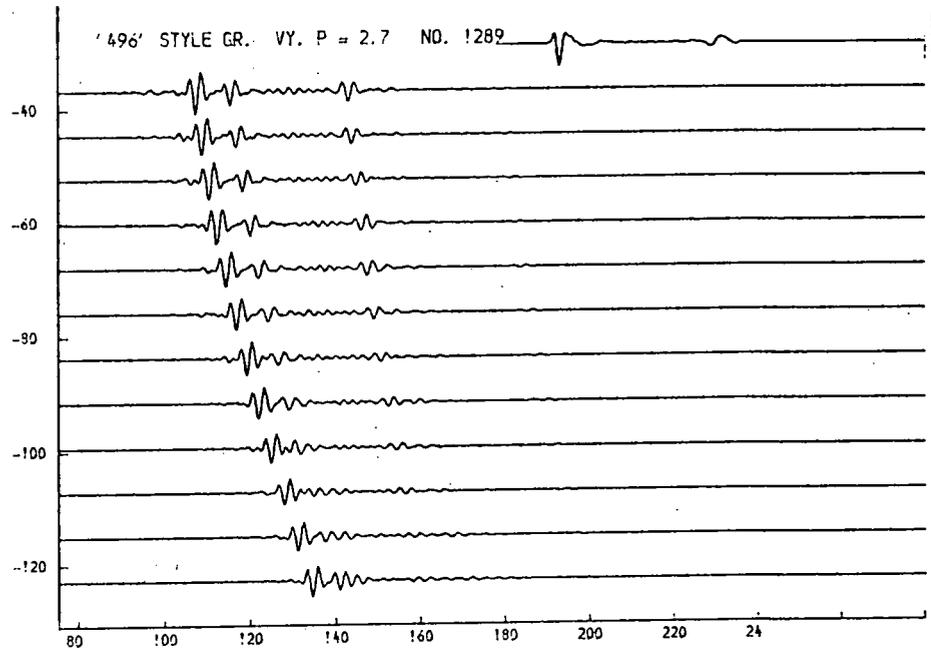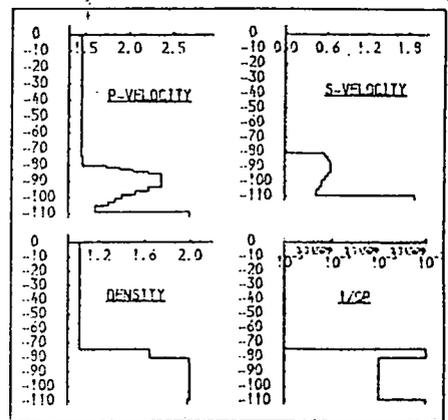
Fig. 9.124a. Alternative velocity structure for No. 1289.

The layer 2 of seismogramme no. 1289 is subdivided to form a velocity structure of the type found for no. 496. The p-velocity of the material below this layer is varied. Upper: 2.7km/s., lower 3.0km/s.

THICKNESS (M.)	P-VELOCITY (M/S.)	S-VELOCITY (M/S.)	DENSITY (G/HL)	1/Q P	1/Q S
74.4	1.460	0.000	1.03	0.00000	0.00000
6.1	1.490	0.010	1.65	0.01000	0.04000
1.3	2.050	0.571	2.00	0.00100	0.03000
1.3	2.050	0.612	2.00	0.00100	0.03000
8.2	2.375	0.653	2.00	0.00100	0.03000
2.6	2.225	0.612	2.00	0.00100	0.03000
2.4	2.075	0.571	2.00	0.00100	0.03000
2.2	1.925	0.529	2.00	0.00100	0.03000
2.2	1.850	0.529	2.00	0.00100	0.03000
2.1	1.775	0.499	2.00	0.00100	0.03000
3.9	1.625	0.447	2.00	0.00100	0.03000
	3.300	2.000	1.99	0.01000	0.06000

Fig. 9.124b.   Alternative velocity structure for No. 1289.

The layer 2 of seismogramme no. 1289 is subdivided to form
a velocity structure of the type found for no. 496.   The
p-velocity of the material below this layer is varied.
Upper: 3.3km/s., lower 3.6km/s.

THICKNESS (M.)	P-VELOCITY (M/S.)	S-VELOCITY (M/S.)	DENSITY (G/ML)	1/Q P	1/Q S
74.4	1.460	0.000	1.03	0.00000	0.00000
6.1	1.490	0.010	1.70	0.01000	0.04000
1.7	1.950	0.571	1.95	0.00100	0.03000
1.7	2.150	0.612	1.94	0.00100	0.03000
5.2	2.375	0.653	1.92	0.00100	0.03000
2.6	2.225	0.612	1.93	0.00100	0.03000
2.4	2.075	0.571	1.94	0.00100	0.03000
2.2	1.925	0.529	1.94	0.00100	0.03000
2.2	1.950	0.529	1.95	0.00100	0.03000
2.1	1.775	0.488	1.95	0.00100	0.03000
5.6	1.550	0.447	1.95	0.00100	0.03000
	3.200	1.600	1.91	0.01000	0.06000

'496' TYPE GR.   S = 1.6   NO. 1289

'496' TYPE GR.   S = 1.9   NO. 1289

Fig. 9.125a. Alternative velocity structure for No. 1289.

In these models, similar to those of figs. 9.124a and b,
the s-velocity is varied. Upper: 1.6km/s., lower 1.8km/s.

THICKNESS (M.)	P-VELOCITY (M/S.)	S-VELOCITY (M/S.)	DENSITY (G/ML)	1/Q P	1/Q S
74.4	1.460	0.000	1.03	0.00000	0.00000
6.1	1.490	0.010	1.70	0.01000	0.04000
1.9	2.250	0.521	1.95	0.00100	0.03000
1.9	2.254	0.613	1.93	0.00100	0.03000
1.9	2.375	0.612	1.91	0.00100	0.03000
5.2	2.375	0.653	1.92	0.00100	0.03000
2.2	2.225	0.612	1.93	0.00100	0.03000
2.4	2.075	0.571	1.94	0.00100	0.03000
2.2	1.925	0.529	1.94	0.00100	0.03000
2.2	1.950	0.529	1.95	0.00100	0.03000
2.1	1.775	0.488	1.95	0.00100	0.03000
5.6	1.550	0.447	1.95	0.00100	0.03000
	3.200	2.000	1.91	0.01000	0.06000

'496' TYPE GR.   S = 2.0   NO. 1289

'496' TYPE GR.   S = 2.2   NO. 1289

Fig. 9.125b.   Alternative velocity structure for No. 1289.

In these models, similar to those of figs. 9.124a and b,
the s-velocity is varied. Upper: 2.0km/s., lower 2.2km/s.

THICKNESS (M.)	P-VELOCITY (M/S.)	S-VELOCITY (M/S.)	DENSITY (G/ML)	1/Q P	1/Q S
63.0	1.460	0.000	1.03	0.0000!	0.0000!
3.0	1.513	0.417	1.96	0.00200	0.04000
3.0	1.606	0.442	2.00	0.00200	0.02000
2.1	1.719	0.473	2.00	0.00200	0.02000
2.4	1.944	0.535	2.00	0.00200	0.02000
2.8	2.281	0.627	2.00	0.00200	0.02000
9.0	2.394	0.659	2.00	0.00200	0.02000
2.8	2.281	0.627	2.00	0.00200	0.02000
2.7	2.169	0.596	2.00	0.00200	0.02000
2.6	2.056	0.565	2.00	0.00200	0.02000
2.4	1.944	0.535	2.00	0.00200	0.02000
2.3	1.831	0.504	2.00	0.00200	0.02000
2.1	1.719	0.473	2.00	0.00200	0.02000
6.0	1.606	0.442	2.00	0.00200	0.02000
	2.700	1.900	1.98	0.02000	0.04000

P-MAXIMUM IN L2 P3 = 2.7   NO. 1281

P-MAXIMUM IN L2 P3 = 3.0   NO. 1281

Fig. 9.126a. Alternative velocity structure for No. 1281.

The layer 2 of seismogramme no. 1281 is subdivided as was shown for no. 1289 in figs. 9.124a and b. The p-velocity in the material below this layer is varied. Upper: 2.7km/s., lower: 3.0km/s.

THICKNESS (M.)	P-VELOCITY (M/S.)	S-VELOCITY (M/S.)	DENSITY (G/ML)	1/Q P	1/Q S
63.0	1.460	0.000	1.03	0.00001	0.00001
2.2	1.606	0.442	1.65	0.00200	0.02000
2.0	1.606	0.442	2.00	0.00200	0.02000
2.1	1.719	0.473	2.00	0.00200	0.02000
2.4	1.944	0.535	2.00	0.00200	0.02000
2.9	2.281	0.627	2.00	0.00200	0.02000
9.0	2.324	0.659	2.00	0.00200	0.02000
2.9	2.281	0.627	2.00	0.00200	0.02000
2.7	2.169	0.596	2.00	0.00200	0.02000
2.6	2.056	0.565	2.00	0.00200	0.02000
2.4	1.944	0.535	2.00	0.00200	0.02000
2.3	1.831	0.504	2.00	0.00200	0.02000
2.1	1.719	0.473	2.00	0.00200	0.02000
6.0	1.606	0.442	2.00	0.00200	0.02000
	3.300	2.100	1.99	0.02000	0.04000

P-MAXIMUM IN L2 P3 = 3.3   NO. 1281

P-MAXIMUM IN L2 P3 = 3.6   NO. 1281
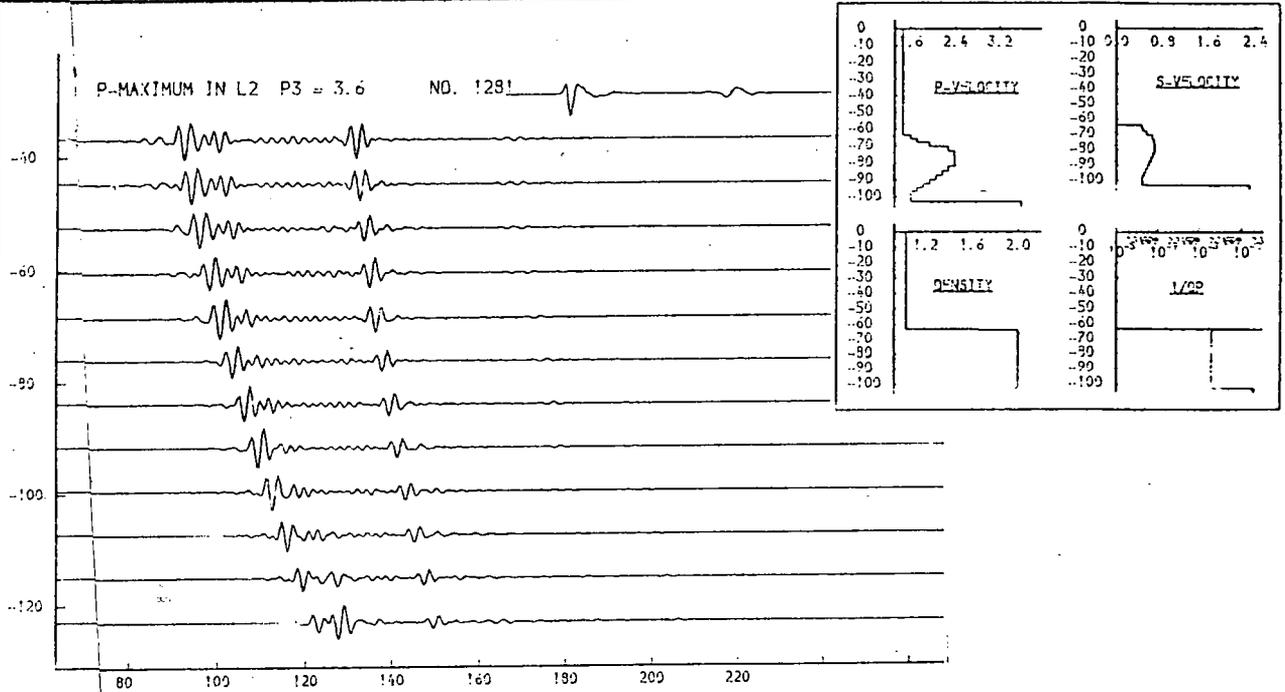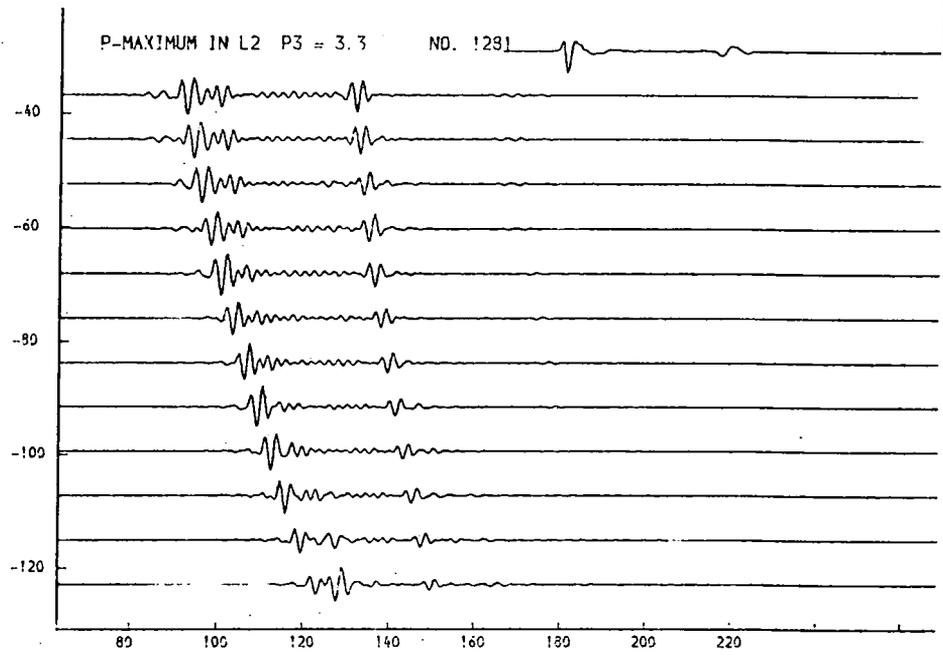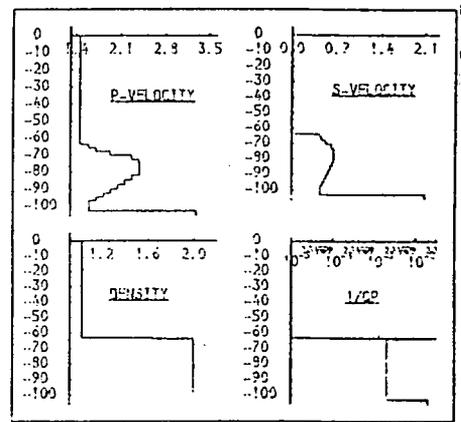
Fig. 9.126b. Alternative velocity structure for No. 1281.

The layer 2 of seismogramme no. 1281 is subdivided as was shown for no. 1289 in figs. 9.124a and b. The p-velocity in the material below this layer is varied. Upper: 3.3km/s., lower: 3.6km/s.

THICKNESS (M.)	P-VELOCITY (M/S.)	S-VELOCITY (M/S.)	DENSITY (G/HL)	1/Q P	1/Q S
63.0	1.460	0.000	1.03	0.00001	0.00001
2.2	1.622	0.412	2.00	0.00200	0.02000
2.0	1.606	0.442	2.00	0.00200	0.02000
2.1	1.719	0.473	2.00	0.00200	0.02000
2.4	1.944	0.535	2.00	0.00200	0.02000
2.8	2.231	0.627	2.00	0.00200	0.02000
9.0	2.394	0.659	2.00	0.00200	0.02000
2.8	2.231	0.627	2.00	0.00200	0.02000
2.7	2.169	0.596	2.00	0.00200	0.02000
2.6	2.056	0.565	2.00	0.00200	0.02000
2.4	1.944	0.535	2.00	0.00200	0.02000
2.3	1.871	0.504	2.00	0.00200	0.02000
2.1	1.719	0.473	2.00	0.00200	0.02000
6.0	1.606	0.442	2.00	0.00200	0.02000
	3.000	1.400	1.98	0.02000	0.04000

Fig. 9.127a. Alternative velocity structure for No. 1281.

In these models, similar to those of figs. 9.126a and b, the s-velocity of the underlying material is varied. Upper: 1.4km/s., lower: 1.6km/s.

THICKNESS (M.)	P-VELOCITY (M/S.)	S-VELOCITY (M/S.)	DENSITY (G/ML)	1/Q P	1/Q S
63.0	1.460	0.000	1.03	0.00001	0.00001
0.2	1.489	0.313	2.05	0.00214	0.00210
2.0	1.606	0.442	2.00	0.00200	0.02000
2.1	1.712	0.473	2.00	0.00200	0.02000
2.4	1.944	0.535	2.00	0.00200	0.02000
2.3	2.281	0.627	2.00	0.00200	0.02000
9.0	2.394	0.659	2.00	0.00200	0.02000
2.3	2.281	0.627	2.00	0.00200	0.02000
2.7	2.162	0.596	2.00	0.00200	0.02000
2.6	2.054	0.565	2.00	0.00200	0.02000
2.4	1.944	0.535	2.00	0.00200	0.02000
2.3	1.831	0.504	2.00	0.00200	0.02000
2.1	1.712	0.473	2.00	0.00200	0.02000
6.0	1.606	0.442	2.00	0.00200	0.02000
	3.000	1.800	1.98	0.02000	0.04000

P-MAXIMUM IN L2 P3=3.0 S3=1.8 NO. 1291

P-MAXIMUM IN L2 P3=3.0 S3=2.2 NO. 1291

Fig. 9.127b. Alternative velocity structure for No. 1281.

In these models, similar to those of figs. 9.126a and b, the s-velocity of the underlying material is varied. Upper: 1.8km/s., lower: 2.2km/s.

THICKNESS (M.)	P-VELOCITY (M/S.)	S-VELOCITY (M/S.)	DENSITY (G/ML)	1/Q P	1/Q S
74.4	1.460	0.000	1.03	0.00000	0.00000
6.1	1.480	0.010	1.65	0.01000	0.04000
3.0	1.934	0.532	2.00	0.00100	0.03000
3.0	1.953	0.537	2.00	0.00100	0.03000
3.1	1.972	0.542	2.00	0.00100	0.03000
3.1	1.991	0.547	2.00	0.00100	0.03000
3.1	2.009	0.553	2.00	0.00100	0.03000
3.2	2.029	0.558	2.00	0.00100	0.03000
3.2	2.047	0.563	2.00	0.00100	0.03000
3.2	2.066	0.569	2.00	0.00100	0.03000
2.0	1.480	0.010	1.65	0.01000	0.04000
	2.800	1.900	1.98	0.01000	0.06000

THICKNESS (M.)	P-VELOCITY (M/S.)	S-VELOCITY (M/S.)	DENSITY (G/ML)	1/Q P	1/Q S
74.4	1.460	0.000	1.03	0.00000	0.00000
6.1	1.480	0.010	1.65	0.01000	0.04000
3.0	1.934	0.532	2.00	0.00100	0.03000
3.0	1.953	0.537	2.00	0.00100	0.03000
3.1	1.972	0.542	2.00	0.00100	0.03000
3.1	1.991	0.547	2.00	0.00100	0.03000
3.1	2.009	0.553	2.00	0.00100	0.03000
3.2	2.029	0.559	2.00	0.00100	0.03000
3.2	2.047	0.563	2.00	0.00100	0.03000
3.2	2.066	0.569	2.00	0.00100	0.03000
2.0	1.480	0.010	1.65	0.01000	0.04000
	3.000	2.200	1.98	0.01000	0.06000
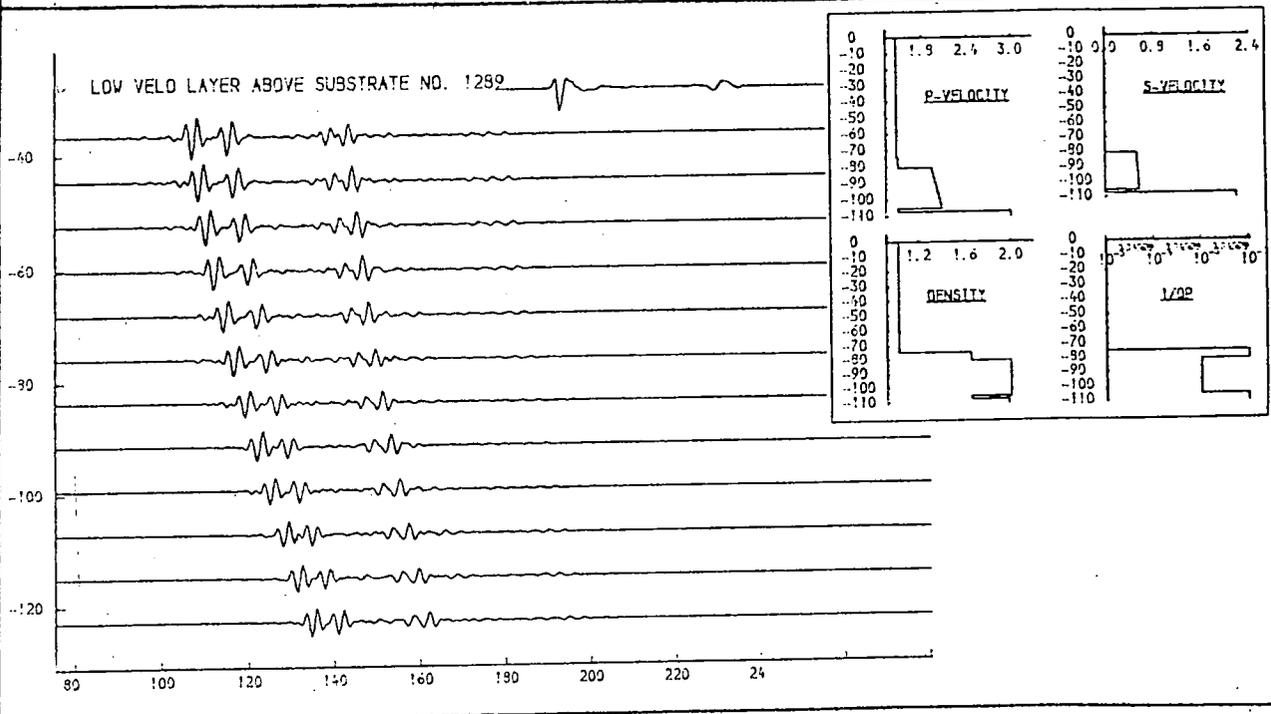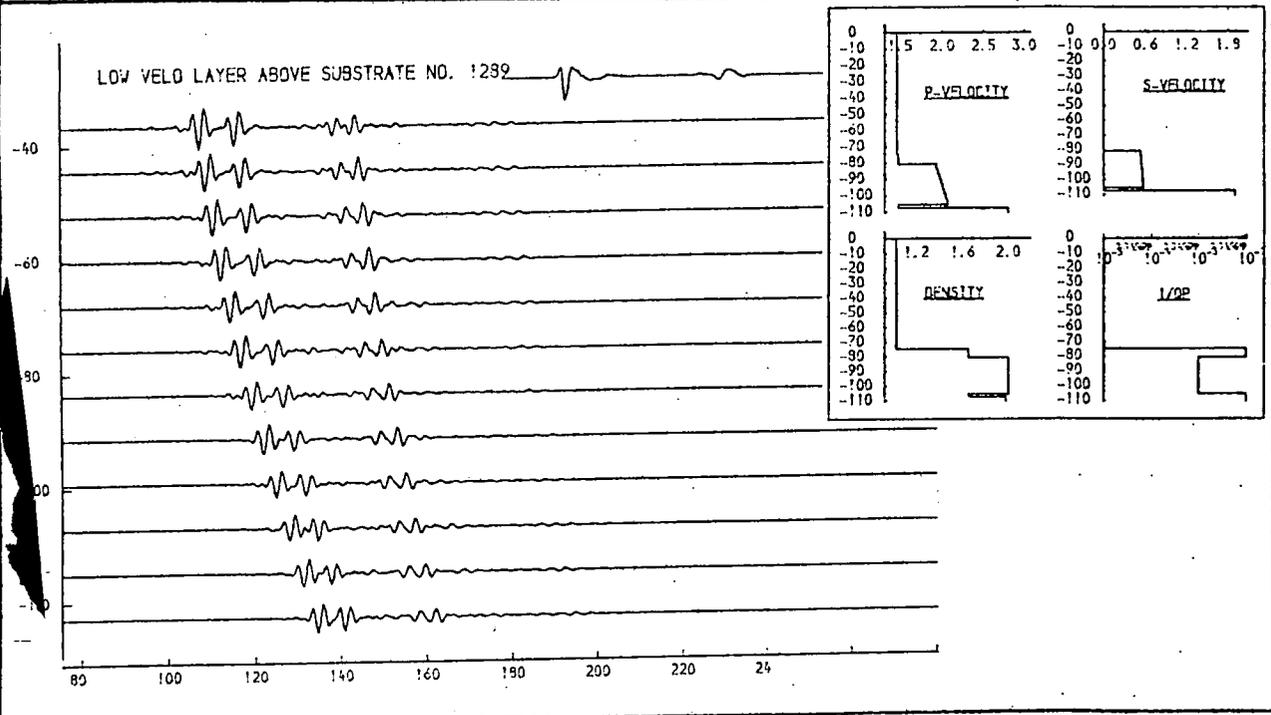
Fig. 9.128a. Low velocity layer below layer 2 (No. 1289).

Variation in p and s-velocity in layer 3 material in the presence of a thin low-velocity layer at the base of layer 2. Upper: p=2.8, s=1.9; lower: p=3.0, s=2.2.

THICKNESS (M.)	P-VELOCITY (M/S.)	S-VELOCITY (M/S.)	DENSITY (G/ML)	1/Q P	1/Q S		THICKNESS (M.)	P-VELOCITY (M/S.)	S-VELOCITY (M/S.)	DENSITY (G/ML)	1/Q P	1/Q S
74.4	1.460	0.000	1.03	0.00000	0.00000		74.4	1.460	0.000	1.03	0.00000	0.00000
6.1	1.480	0.010	1.65	0.01000	0.04000		6.1	1.480	0.010	1.65	0.01000	0.04000
3.0	1.934	0.532	2.00	0.00100	0.03000		3.0	1.934	0.532	2.00	0.00100	0.03000
3.0	1.953	0.537	2.00	0.00100	0.03000		3.0	1.953	0.537	2.00	0.00100	0.03000
3.1	1.972	0.542	2.00	0.00100	0.03000		3.1	1.972	0.542	2.00	0.00100	0.03000
3.1	1.991	0.547	2.00	0.00100	0.03000		3.1	1.991	0.547	2.00	0.00100	0.03000
3.1	2.009	0.553	2.00	0.00100	0.03000		3.1	2.009	0.553	2.00	0.00100	0.03000
3.2	2.028	0.558	2.00	0.00100	0.03000		3.2	2.028	0.559	2.00	0.00100	0.03000
3.2	2.047	0.563	2.00	0.00100	0.03000		3.2	2.047	0.563	2.00	0.00100	0.03000
3.2	2.066	0.569	2.00	0.00100	0.03000		3.2	2.066	0.563	2.00	0.00100	0.03000
2.0	1.480	0.010	1.65	0.01000	0.04000		2.0	1.480	0.010	1.65	0.01000	0.04000
	3.500	2.350	1.98	0.01000	0.06000			4.300	2.550	1.99	0.01000	0.06000

LOW VELO LAYER ABOVE SUBSTRATE NO. 1289

LOW VELO LAYER ABOVE SUBSTRATE NO. 1289

Fig. 9.128b. Low velocity layer below layer 2 (No. 1289).

Variation in p and s-velocity in layer 3 material in the presence of a thin low-velocity layer at the base of layer 2. Upper: p=3.5, s=2.35; lower: p=4.3, s=2.55.

THICKNESS (M.)	P-VELOCITY (M/S.)	S-VELOCITY (M/S.)	DENSITY (G/ML)	1/Q P	1/Q S
74.4	1.460	0.000	1.03	0.00000	0.00000
6.1	1.490	0.010	1.65	0.02000	0.01000
30.9	2.000	0.550	2.00	0.00100	0.03000
2.0	0.500	0.020	2.00	0.00100	0.03000
	4.700	2.550	1.99	0.03000	0.06000

THICKNESS (M.)	P-VELOCITY (M/S.)	S-VELOCITY (M/S.)	DENSITY (G/ML)	1/Q P	1/Q S
74.4	1.460	0.000	1.03	0.00000	0.00000
6.1	1.490	0.010	1.65	0.02000	0.01000
2.5	2.225	0.550	2.00	0.00100	0.03000
10.0	2.450	0.653	2.00	0.00100	0.03000
2.0	2.225	0.550	2.00	0.00100	0.03000
2.5	1.463	0.430	2.00	0.00100	0.03000
4.8	1.625	0.100	2.00	0.00100	0.03000
10.0	3.500	2.400	1.98	0.01000	0.06000
2.1	1.500	0.250	1.75	0.01000	0.06000
3.3	1.500	0.550	1.75	0.01000	0.06000
3.7	2.700	1.000	1.98	0.01000	0.06000
3.4	2.600	1.500	1.98	0.01000	0.06000
3.9	2.900	2.000	1.98	0.01000	0.06000
3.9	3.200	2.000	1.98	0.01000	0.06000
	3.500	2.400	1.98	0.01000	0.06000

Fig. 9.129.   Modelling of doublet character of r2.

Upper: A low-velocity layer is interposed between layers 2 and 3.
Lower: A series of velocity steps and gradients is used.

THICKNESS (M.)	P-VELOCITY (M/S.)	S-VELOCITY (M/S.)	DENSITY (G/ML)	1/Q P	1/Q S
50.0	1.460	0.000	1.03	0.00001	0.00001
9.0	2.394	0.658	2.00	0.00200	0.02000
2.9	2.306	0.634	2.00	0.00200	0.02000
2.8	2.219	0.610	2.00	0.00200	0.02000
2.7	2.131	0.586	2.00	0.00200	0.02000
2.5	2.044	0.562	2.00	0.00200	0.02000
2.5	1.956	0.459	2.00	0.00200	0.02000
2.3	1.369	0.350	2.00	0.00200	0.02000
2.2	1.781	0.200	2.00	0.00200	0.02000
5.1	1.694	0.100	2.00	0.00200	0.02000
2.0	1.606	0.050	2.00	0.00200	0.02000
5.7	1.519	0.020	2.00	0.00200	0.02000
	3.000	2.100	1.98	0.02000	0.04000

THICKNESS (M.)	P-VELOCITY (M/S.)	S-VELOCITY (M/S.)	DENSITY (G/ML)	1/Q P	1/Q S
50.0	1.460	0.000	1.03	0.00001	0.00001
4.9	1.934	0.532	2.00	0.00200	0.02000
4.9	1.953	0.537	2.00	0.00200	0.02000
4.9	1.972	0.542	2.00	0.00200	0.02000
5.0	1.991	0.547	2.00	0.00200	0.02000
5.0	2.009	0.553	2.00	0.00200	0.02000
5.1	2.028	0.558	2.00	0.00200	0.02000
5.1	2.047	0.563	2.00	0.00200	0.02000
5.2	2.066	0.568	2.00	0.00200	0.02000
	4.700	2.900	1.98	0.02000	0.04000

MODEL FOR 1281 AS IN SHOALER WATER 50M

P-VELOCITY   S-VELOCITY   DENSITY   1/QP

MODEL OF 1281 AS IF IN SHOALER WATER 50M

P-VELOCITY   S-VELOCITY   DENSITY   1/QP

Fig. 9.130a.   Models generated as if in shallower water.

Seismogrammes for No. 1281 expected if acoustic source and receivers were towed 50m. above the seabed.

THICKNESS (M.)	P-VELOCITY (M/S.)	S-VELOCITY (M/S.)	DENSITY (G/ML)	1/Q P	1/Q S
25.0	1.460	0.000	1.03	0.00001	0.00001
9.0	2.324	0.658	2.00	0.00200	0.02000
2.9	2.306	0.634	2.00	0.00200	0.02000
2.9	2.219	0.610	2.00	0.00200	0.02000
2.7	2.131	0.586	2.00	0.00200	0.02000
2.5	2.011	0.562	2.00	0.00200	0.02000
2.4	1.956	0.450	2.00	0.00200	0.02000
2.7	1.868	0.750	2.00	0.00200	0.02000
2.3	1.791	0.200	2.00	0.00200	0.02000
5.1	1.623	0.100	2.00	0.00200	0.02000
5.0	1.600	0.050	2.00	0.00200	0.02000
5.7	1.519	0.020	2.00	0.00200	0.02000
	3.000	2.100	1.98	0.02000	0.04000

THICKNESS (M.)	P-VELOCITY (M/S.)	S-VELOCITY (M/S.)	DENSITY (G/ML)	1/Q P	1/Q S
25.0	1.460	0.000	1.03	0.00001	0.00001
4.8	1.934	0.532	2.00	0.00200	0.02000
4.9	1.953	0.537	2.00	0.00200	0.02000
4.9	1.972	0.542	2.00	0.00200	0.02000
5.0	1.991	0.547	2.00	0.00200	0.02000
5.0	2.009	0.553	2.00	0.00200	0.02000
5.1	2.028	0.558	2.00	0.00200	0.02000
5.1	2.017	0.563	2.00	0.00200	0.02000
5.2	2.066	0.568	2.00	0.00200	0.02000
	4.700	2.300	1.98	0.02000	0.01000

MODEL FOR 1281 AS IN SHOALER WATER 25M

P-VELOCITY S-VELOCITY DENSITY 1/QP

MODEL OF 1281 AS IF IN SHOALER WATER 25M

P-VELOCITY S-VELOCITY DENSITY 1/QP

Fig. 9.130b. Models generated as if in shallower water.

Seismogrammes for No. 1281 expected if acoustic source and receivers were towed 25m. above the seabed.

THICKNESS (M.)	P-VELOCITY (M/S.)	S-VELOCITY (M/S.)	DENSITY (G/ML)	1/Q P	1/Q S
50.0	1.460	0.000	1.03	0.00000	0.00000
6.1	1.480	0.010	1.65	0.01000	0.04000
3.4	1.934	0.532	2.00	0.00100	0.03000
3.4	1.953	0.537	2.00	0.00100	0.03000
3.4	1.972	0.542	2.00	0.00100	0.03000
3.5	1.991	0.547	2.00	0.00100	0.03000
3.5	2.009	0.553	2.00	0.00100	0.03000
3.5	2.028	0.558	2.00	0.00100	0.03000
3.6	2.047	0.563	2.00	0.00100	0.03000
3.6	2.066	0.569	2.00	0.00100	0.03000
	4.700	2.550	1.98	0.01000	0.06000

THICKNESS (M.)	P-VELOCITY (M/S.)	S-VELOCITY (M/S.)	DENSITY (G/ML)	1/Q P	1/Q S
50.0	1.460	0.000	1.03	0.00000	0.00000
6.1	1.480	0.010	1.70	0.01000	0.04000
5.2	2.375	0.653	1.92	0.00100	0.03000
2.6	2.225	0.612	1.93	0.00100	0.03000
2.1	2.375	0.571	1.94	0.00100	0.03000
2.2	1.925	0.529	1.94	0.00100	0.03000
2.2	1.950	0.522	1.95	0.00100	0.03000
2.1	1.775	0.488	1.95	0.00100	0.03000
5.6	1.550	0.447	1.95	0.00100	0.03000
	3.200	2.000	1.91	0.01000	0.06000

MODEL OF 1289 AS IF IN SHOALER WATER 50M

P-VELOCITY   S-VELOCITY   DENSITY   1/QP

MODEL OF 1289 AS IF IN SHOALER WATER 50M

P-VELOCITY   S-VELOCITY   DENSITY   1/QP
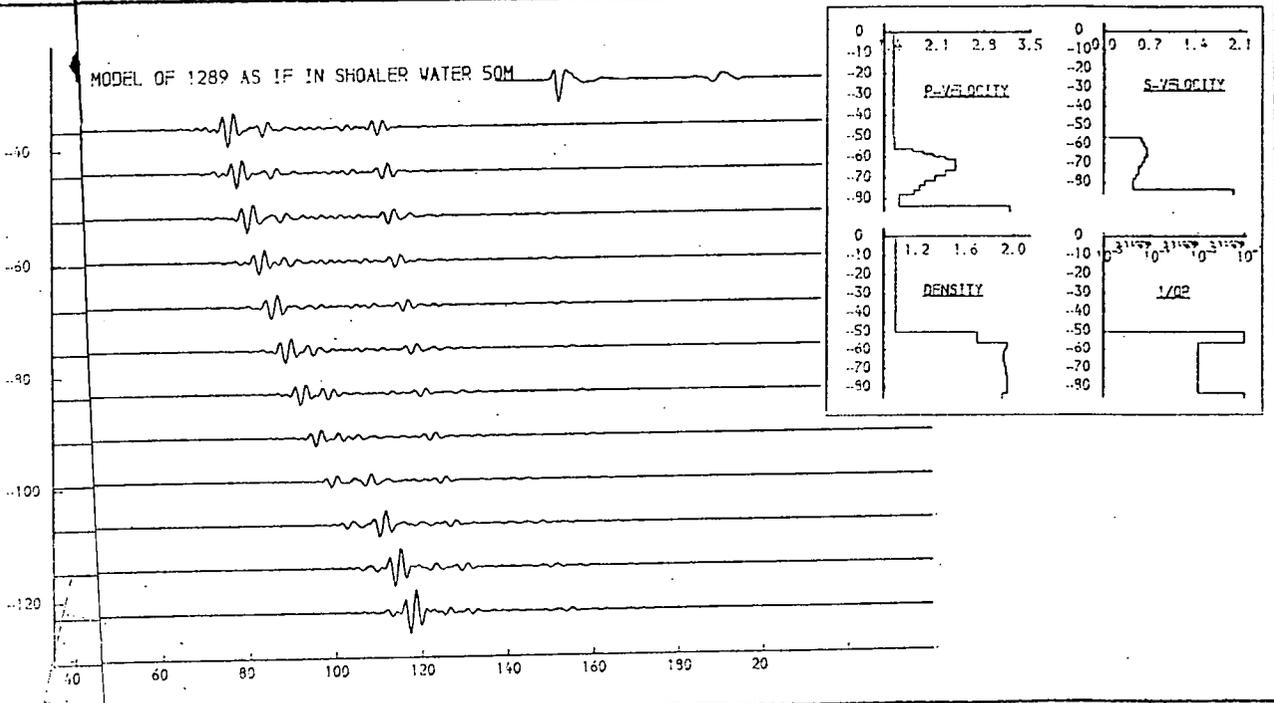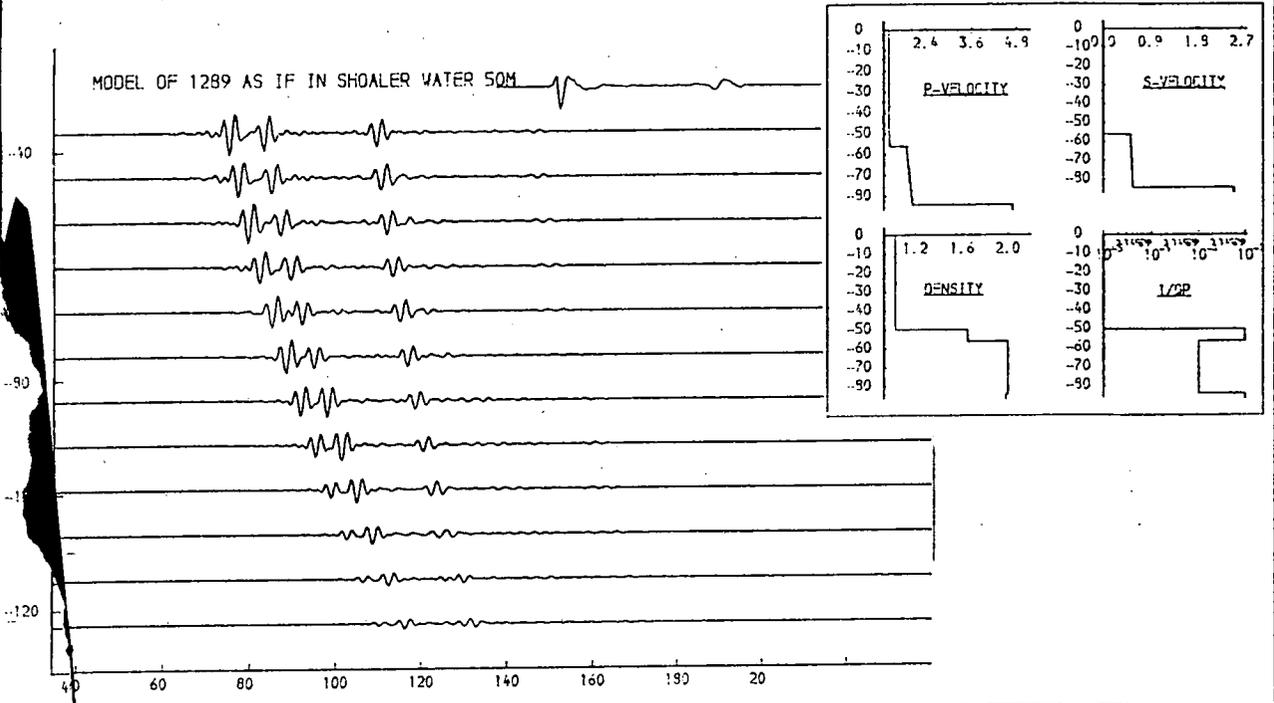
Fig. 9.130c.   Models generated as if in shallower water.

Seismogrammes for No. 1289 expected if acoustic source and receivers were towed 50m. above the seabed.

THICKNESS (M.)	P-VELOCITY (M/S.)	S-VELOCITY (M/S.)	DENSITY (G/ML)	1/Q P	1/Q S
25.0	1.460	0.000	1.03	0.00000	0.00000
6.1	1.480	0.010	1.65	0.01000	0.04000
29.0	2.000	0.550	2.00	0.00100	0.03000
	4.700	2.550	1.99	0.01000	0.06000

THICKNESS (M.)	P-VELOCITY (M/S.)	S-VELOCITY (M/S.)	DENSITY (G/ML)	1/Q P	1/Q S
25.0	1.460	0.000	1.03	0.00000	0.00000
6.1	1.480	0.010	1.65	0.01000	0.04000
9.5	1.855	0.470	2.00	0.00100	0.03000
1.4	2.585	0.650	2.00	0.00100	0.03000
2.3	2.225	0.550	2.00	0.00100	0.03000
10.0	2.450	0.653	2.00	0.00100	0.03000
2.6	2.225	0.550	2.00	0.00100	0.03000
2.4	2.975	0.650	2.00	0.00100	0.03000
1.7	2.450	0.550	2.00	0.00100	0.03000
2.1	1.700	0.150	2.00	0.00100	0.03000
4.9	1.625	0.100	2.00	0.00100	0.03000
	3.300	2.200	1.99	0.01000	0.06000

MODEL OF 1289 AS IF IN SHOALER WATER 25M

P-VELOCITY   S-VELOCITY   DENSITY   1/QP

MODEL OF 1289 AS IF IN SHOALER WATER

P-VELOCITY   S-VELOCITY   DENSITY   1/QP
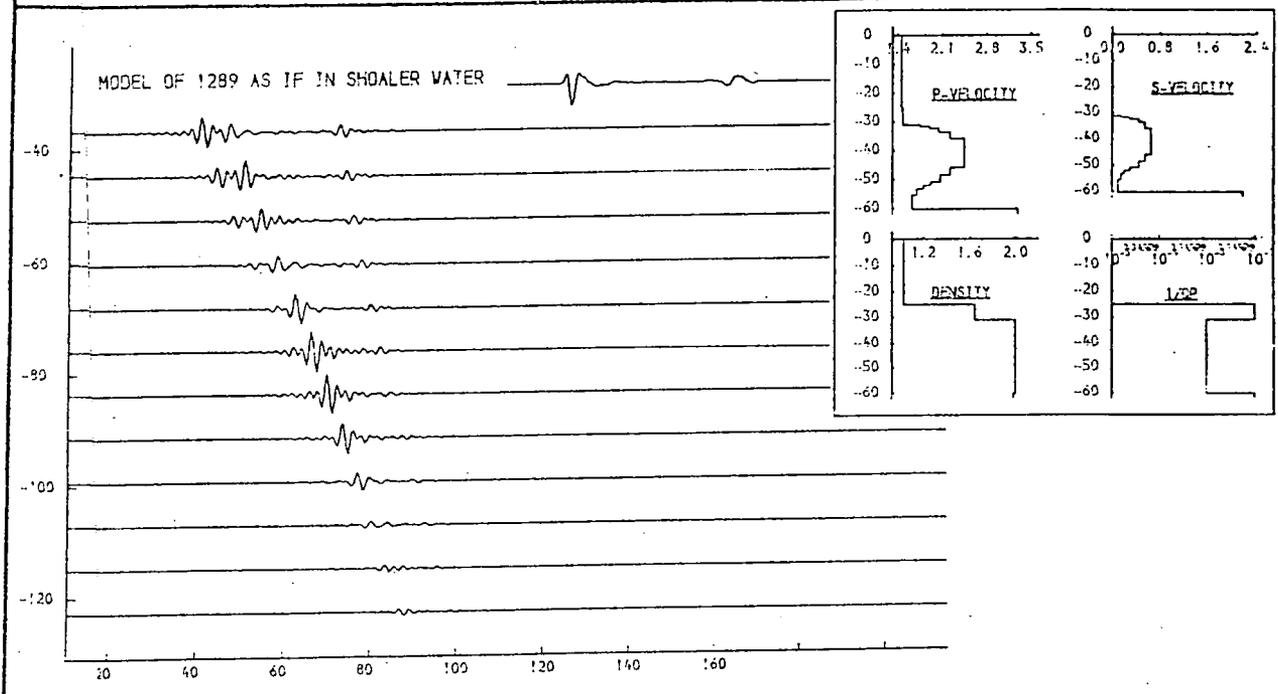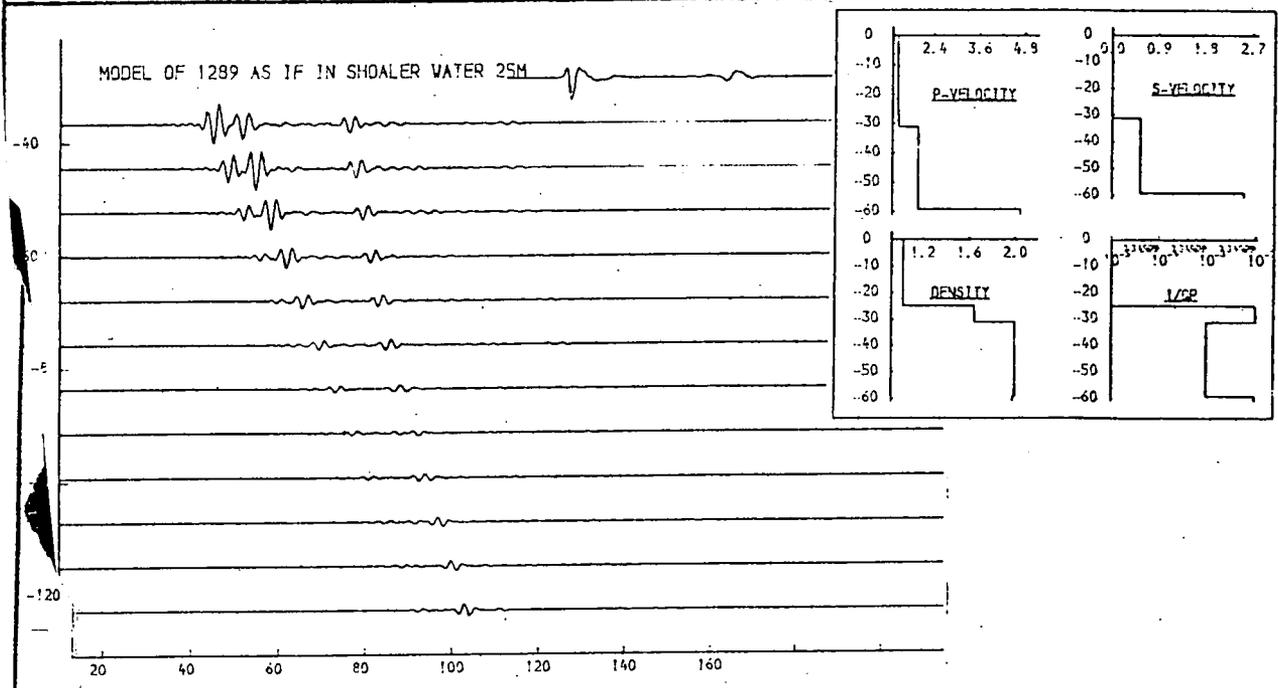
Fig. 9.130d.   Models generated as if in shallower water.

Seismogrammes for No. 1289 expected if acoustic source and receivers were towed 25m. above the seabed.

THICKNESS (M.)	P-VELOCITY (M/S.)	S-VELOCITY (M/S.)	DENSITY (G/ML)	1/Q P	1/Q S
63.0	1.460	0.000	1.03	0.00001	0.00001
2.7	1.404	0.418	1.55	0.00300	0.02000
3.0	1.606	0.442	2.00	0.00300	0.02000
5.1	1.719	0.473	2.00	0.00300	0.02000
2.4	1.944	0.535	2.00	0.00300	0.02000
2.9	2.291	0.627	2.00	0.00300	0.02000
9.0	2.394	0.658	2.00	0.00300	0.02000
2.9	2.291	0.627	2.00	0.00300	0.02000
2.7	2.169	0.596	2.00	0.00300	0.02000
2.6	2.056	0.565	2.00	0.00300	0.02000
2.4	1.944	0.535	2.00	0.00300	0.02000
2.7	1.831	0.504	2.00	0.00300	0.02000
2.1	1.719	0.473	2.00	0.00300	0.02000
6.0	1.606	0.442	2.00	0.00300	0.02000
	3.000	2.200	1.98	0.02000	0.04000

P-VELOCITY   S-VELOCITY

DENSITY   1/Q2

P-MAXIMUM IN L2 1/Q2=0.003   NO. 1231

P-MAXIMUM IN L2 1/Q2=0.004   NO. 1231

P-VELOCITY   S-VELOCITY

DENSITY   1/QP
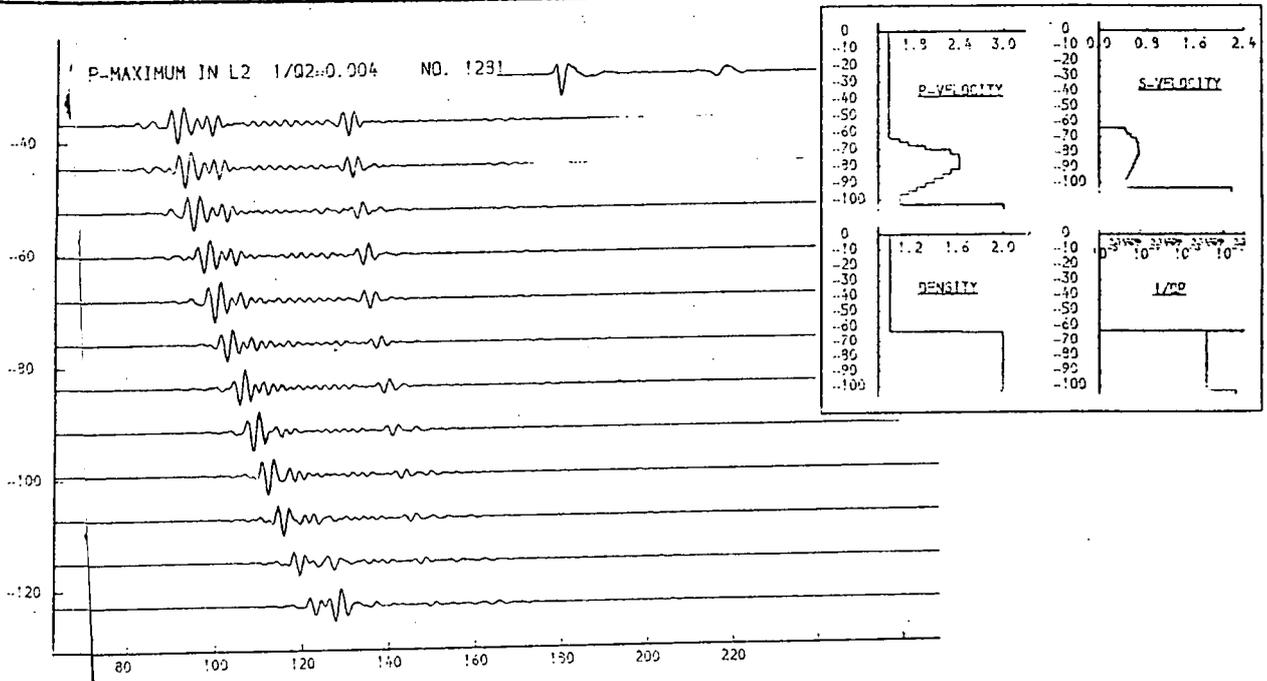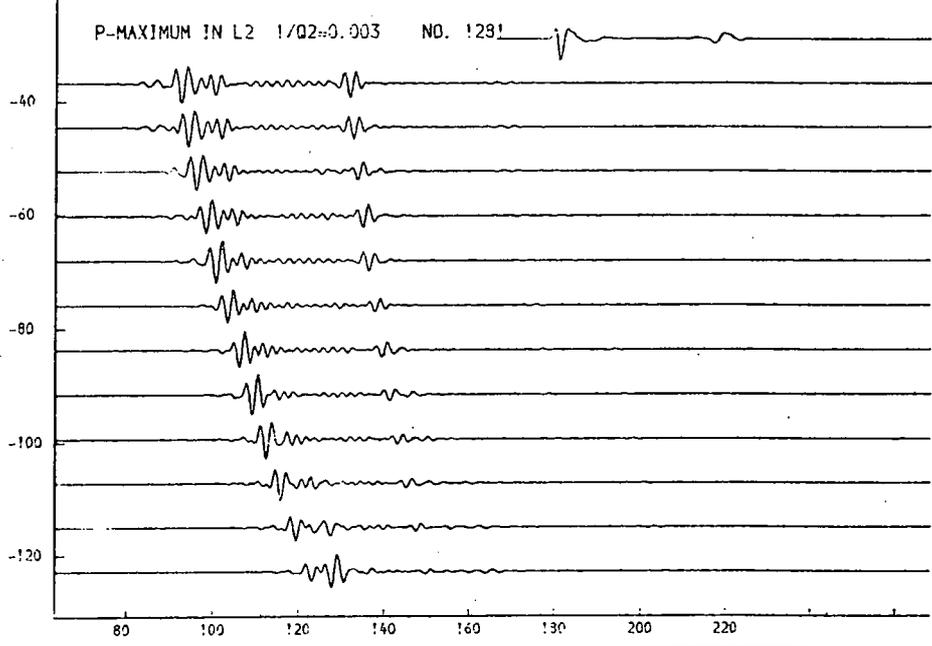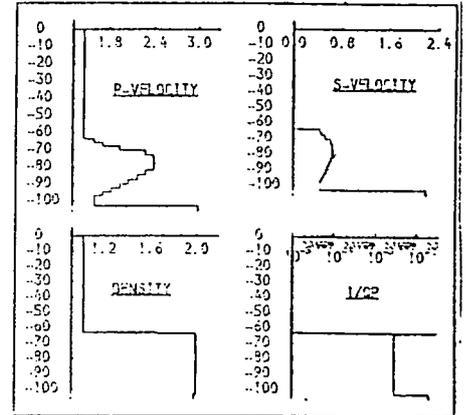
Fig. 9.131a. Effect of velocity profile on attenuation.

The value of 1/Qp in layer 2 is varied. Upper: 0.003, Lower: 0.004.

THICKNESS (M.)	P-VELOCITY (M/S.)	S-VELOCITY (M/S.)	DENSITY (G/ML)	1/Q P	1/Q S
63.0	1.460	0.000	1.03	0.00001	0.00001
3.0	1.606	0.442	2.00	0.00500	0.02000
2.1	1.219	0.473	2.00	0.00500	0.02000
2.4	1.344	0.535	2.00	0.00500	0.02000
2.9	2.291	0.627	2.00	0.00500	0.02000
9.0	2.794	0.659	2.00	0.00500	0.02000
2.9	2.291	0.627	2.00	0.00500	0.02000
2.7	2.169	0.596	2.00	0.00500	0.02000
2.6	2.056	0.565	2.00	0.00500	0.02000
2.4	1.344	0.535	2.00	0.00500	0.02000
2.3	1.831	0.504	2.00	0.00500	0.02000
2.1	1.219	0.473	2.00	0.00500	0.02000
6.0	1.606	0.442	2.00	0.00500	0.02000
	3.000	2.200	1.98	0.02000	0.04000

P-MAXIMUM IN L2   1/Q2=0.005   NO. 1281

P-MAXIMUM IN L2   1/Q2=0.008   NO. 1281
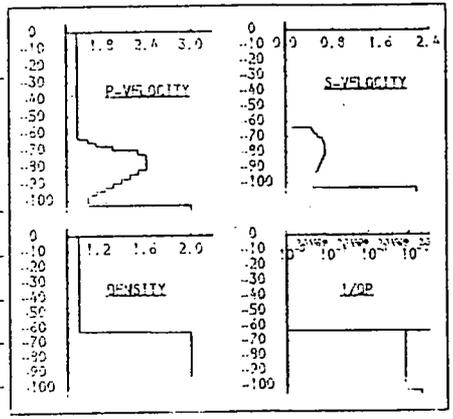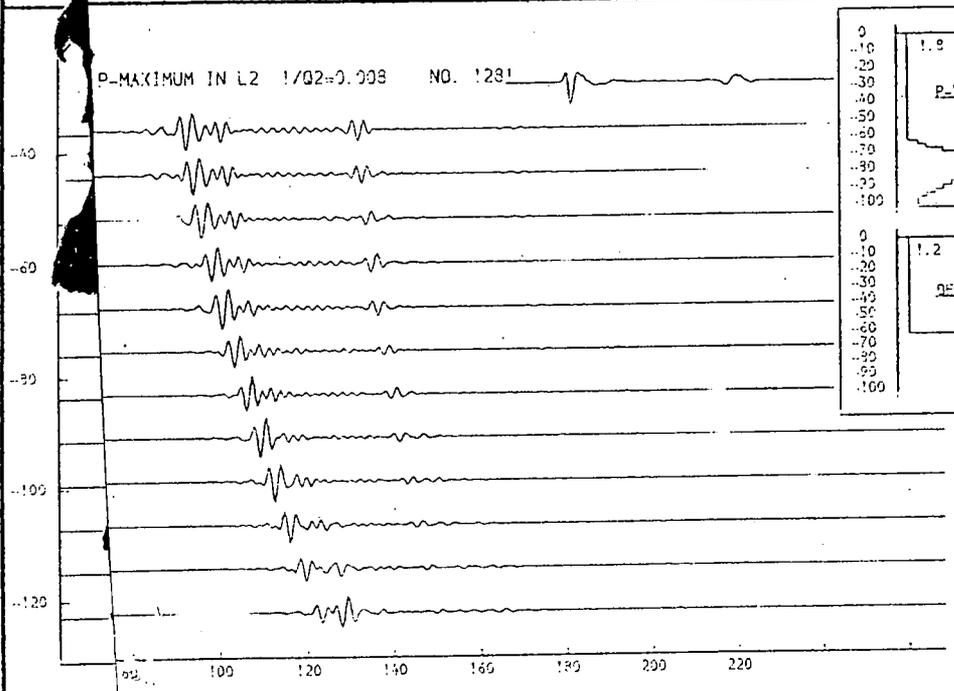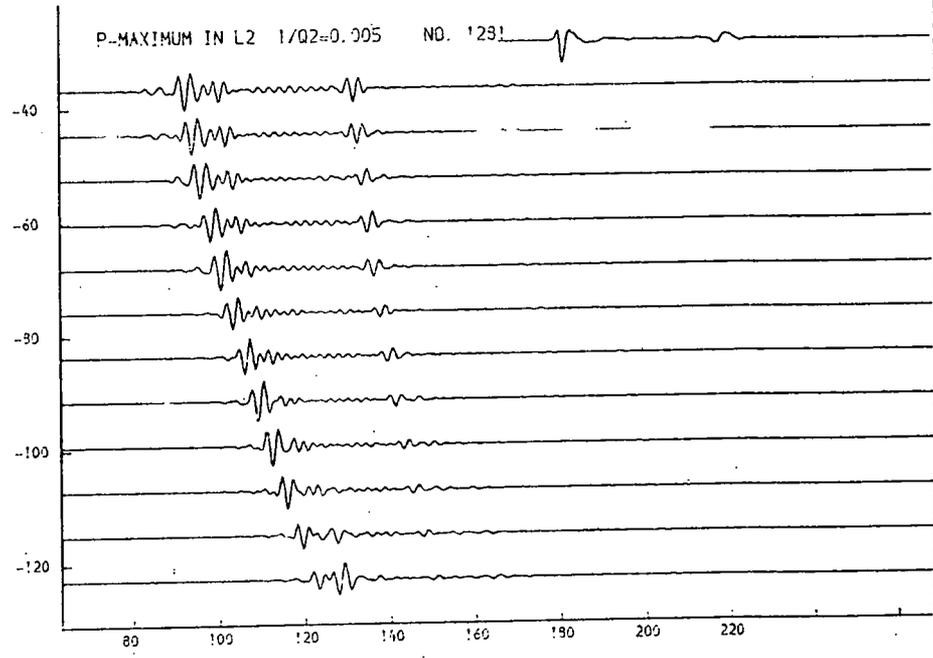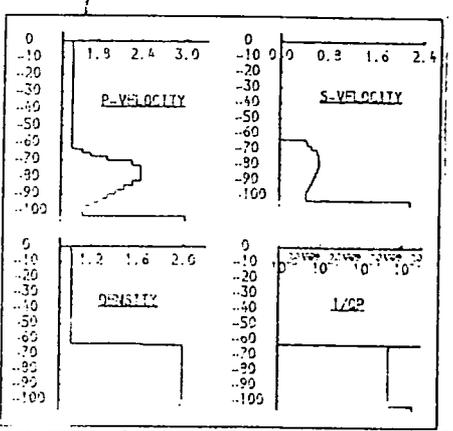
Fig. 9.131b. Effect of velocity profile on attenuation.

The value of 1/Qp in layer 2 is varied.   Upper: 0.005,
Lower: 0.008.

Canadian Journal of Earth Sciences

Journal canadien des sciences de la terre

Seismic profiling in Miramichi Bay, New Brunswick

K. HOWELLS AND A. G. MCKAY

Seismic profiling in Miramichi Bay, New Brunswick

K. HOWELLS AND A. G. MCKAY

Geophysics Division, Nova Scotia Research Foundation Corporation, 100 Fenwick St.,
Box 790, Dartmouth, N.S., Canada B2Y 3Z7

A combined echo sounder and seismic profiling survey in Miramichi Bay has detected two prominent seismic reflectors. The upper reflector probably represents a marine terrace, above which are recent sediments. The sea bed consists mainly of sands in the barrier island and Outer Bay area, whereas the Inner Bay consists mainly of sandy muds and muds. A discontinuous 'gas' reflector in the muds of the Inner Bay masks all deeper seismic reflectors where it is present. The lower seismic reflector is probably the Pennsylvanian bedrock surface. Between the upper and lower reflectors, proglacial sediments and glacial till are probably present. The bedrock surface has been eroded into deep, linear channels by a pre-Pleistocene drainage system which may have been subsequently overdeepened by glacial scouring. These channels may have been eroded along lines of weakness in the Carboniferous sediments representing structures, such as joints, fractures, or faults in the bedrock. These structures may be related to the extension of the Catamaran Fault Zone in the pre-Carboniferous basement rocks beneath Miramichi Bay.

———

Deux importants réflecteurs sismiques ont été révélés par un arpentage de la Baie de Miramichi fait avec un sondeur acoustique et un équipement de profil sismique. Le réflecteur supérieur représente probablement une terrasse marine au-dessus de laquelle se trouvent des sédiments récents. Le fond de la mer consiste principalement en sable dans la région des îles de barrière et de la baie extérieure, tandis que dans la baie intérieure il y a surtout de la boue et de la boue sableuse. Un réflecteur 'gazeux' discontinu dans les boues de la baie intérieure cache tous les réflecteurs plus profonds aux endroits où on le trouve. Le réflecteur sismique inférieur indique probablement la surface des roches du Pennsylvanien. Entre le réflecteur inférieur et le supérieur, il y a probablement des moraines et des dépôts proglaciaires. Dans la surface de la roche, de profonds canaux linéaires ont été creusés par l'érosion d'un système de rivières pré-Pléistocènes qui plus tard peut avoir été approfondi par l'action des glaces. Ces canaux peuvent avoir été érodés le long des lignes de discontinuité dans les sédiments Carbonifères, représentant des structures telles que des joints, fractures ou failles dans la roche. Ces structures peuvent être mises en relation avec la continuation de la zone de faille Catamaran dans les roches pré-Carbonifères au-dessous de la Baie de Miramichi.

[Traduit par le journal]

Introduction

A marine seismic profiling survey was carried out in Miramichi Bay, New Brunswick (Fig. 1), as part of the Miramichi Channel Study. Its purpose was to determine surficial sediment thicknesses to plan dredging operations for the deepening of a shipping channel. The survey was carried out for the Governments of Canada and New Brunswick and the field work was completed in July 1975. Figure 2 is a track plot of the seismic profiling survey, which covered a large part of Inner Miramichi Bay and some of the Outer Bay. Approximately 190 line miles (306 km) of seismic profiling have been used in the interpretation. Echo sounder records were also obtained for most of the survey.

Survey Equipment and Methods

The profiling equipment was installed on the 'Tudlik', a 35-ft (10.7 m) long hydrographic launch equipped with a Kelvin Hughes MS26B echo sounder. The acoustic source for the sub-bottom profiling was a Huntec ED10 'boomer' mounted in a catamaran. It was driven by a Teledyne 254 high voltage generator. A 20-element hydrophone array, or streamer, was used to receive the reflected energy from the bottom and subbottom. The interface unit, which controlled signal processing (amplification and filtering) and triggering for the boomer and streamer, was a Nova Scotia Research Foundation Corporation (N.S.R.F.C.) surface profiling system. All the profiling results were displayed on an E.P.C. dry paper recorder. The boomer and streamer were towed 15 m behind the launch.

The energy output from the Teledyne unit during the survey was 200 J, and the firing rate twice per second. The recorder sweep speed was 125 ms.
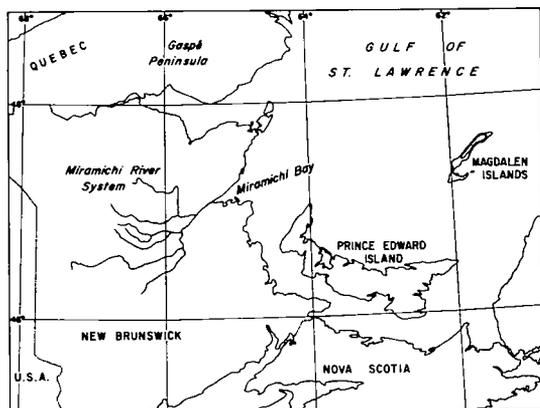
Fig 1. Location of Miramichi Bay and the Miramichi River System.

Position fixing for the survey was accomplished by a Del Norte Instrument two range microwave system. The slave stations were located on points set up by the Canadian Hydrographic Service, Department of the Environment. Three pairs of trisponder locations were used during the survey (Fig. 2). Most of Inner Miramichi Bay was covered by Oak Point and Burnt Church trisponder locations, with a small area, north of Portage Island, covered by Hay Point and Burnt Church Point locations. In the Outer Bay, on the seaward side of Portage and Fox Islands, trisponders located at Fox Point and Escuminac Point were utilized. Escuminac Point is approximately 6.6 km (4.1 mi) east of the Lower Escuminac jetty shown in the southeast corner of Fig. 2 and is outside the map-area.

The trisponder locations gave good intersections of range arcs over most of the area of interest, resulting in position-fixing repeatability of about 10 m, sufficiently precise as to require a correction for the distance between the position-fixing antenna and the acoustic equipment. In two places on the fringes of the area, survey lines came near the trisponder baseline, with resultant degradation in the accuracy of positioning. The areas affected are: (1) an approximately 2 km wide strip along the north shore of the estuary between Oak Point and Burnt Church; and (2) an approximately 3.5 km wide strip north of the Escuminac coastline, east of Fox Point.

Geographical Setting of Miramichi Bay

Miramichi Bay is one of the larger of a number of bays on the east coast of New Brunswick situated on the west side of the Gulf of St. Lawrence. It is triangular in shape, about

28 mi (45 km) along its north and south coasts and about 20 mi (32 km) wide at its seaward end. A group of about eight rivers form the Miramichi River system, which drain the central highlands of New Brunswick in an east to northeasterly direction into Miramichi Bay (Fig. 1), and thence into the Gulf of St. Lawrence. Loring and Nota (1973) state that the length of the 'Miramichi River' is 130 mi (209 km). According to Ambler (1976) its drainage area is 5200 mi^2 (13 468 km^2), and a conservative estimate of its annual suspended sediment load is about 100 000 t (100 000 Mg)[1] per year.

Miramichi Bay lies on the Maritime Plain, an area of low relief extending from Chaleur Bay to Cape George (Bostock 1970). It is underlain and bounded by flat lying or gently dipping, undifferentiated, red and grey arkosic sandstones, siltstones, conglomerates, mudstones, and minor shales of the Pictou Group of the Pennsylvanian Series (Kelley 1970; Potter et al. 1968). Alcock (1948) describes this area of New Brunswick as being heavily glaciated with abundant moraines, outwash sand, and gravel deposits. Chalmers (1888) shows gravel, peat, freshwater and marine alluvium, and marine deposits of Saxicava sand and Leda clay on land adjacent to the Miramichi estuary. Glacial striae parallel the course of the Southwest Miramichi River (Chalmers 1894).

A group of long, narrow barrier islands of low relief (Fig. 2) trend in an approximately north–south direction across Miramichi Bay, dividing it into the Inner and Outer Bay areas. The coastline in Fig. 2 and subsequent figures are taken from the Canadian Hydrographic Service (1975). The shoreline on this chart was taken from a survey by the Department of Public Works (1922).

Bathymetry

Figure 3 is a contoured version of the bathymetry of Miramichi Bay (contour interval 2.5 m). The bathymetric map was constructed using depth data from 1 : 10 000 field sheets provided by the Canadian Hydrographic Service, Atlantic Region (sheets 4558–4565). The depths are corrected to the 1927 North American datum using local sounding datum points near Burnt Church.

The bottom topography shows that most of the Inner Bay is relatively shallow with water depths of less than 7 m. Exceptions are the

---

[1] 1 t = 1 Mg in SI units.
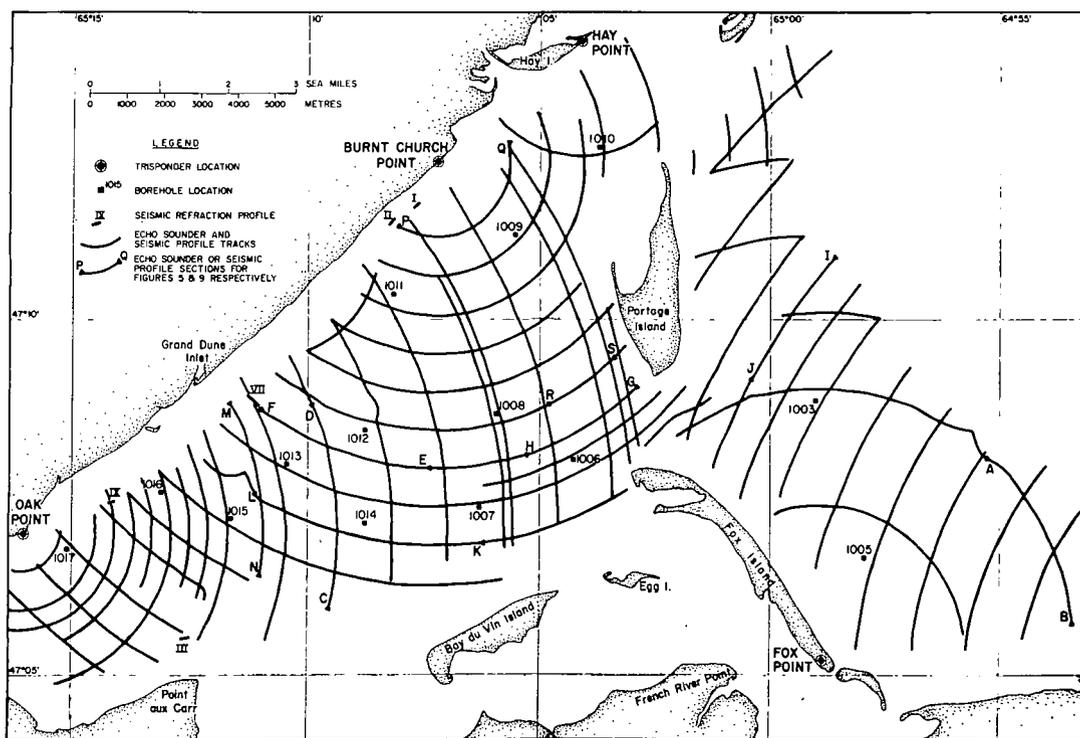
FIG. 2. Track plot of the seismic profiling and echo sounder survey. The Escuminac Point trisponder location is off the map, east of Fox Point (see text and Fig. 12).
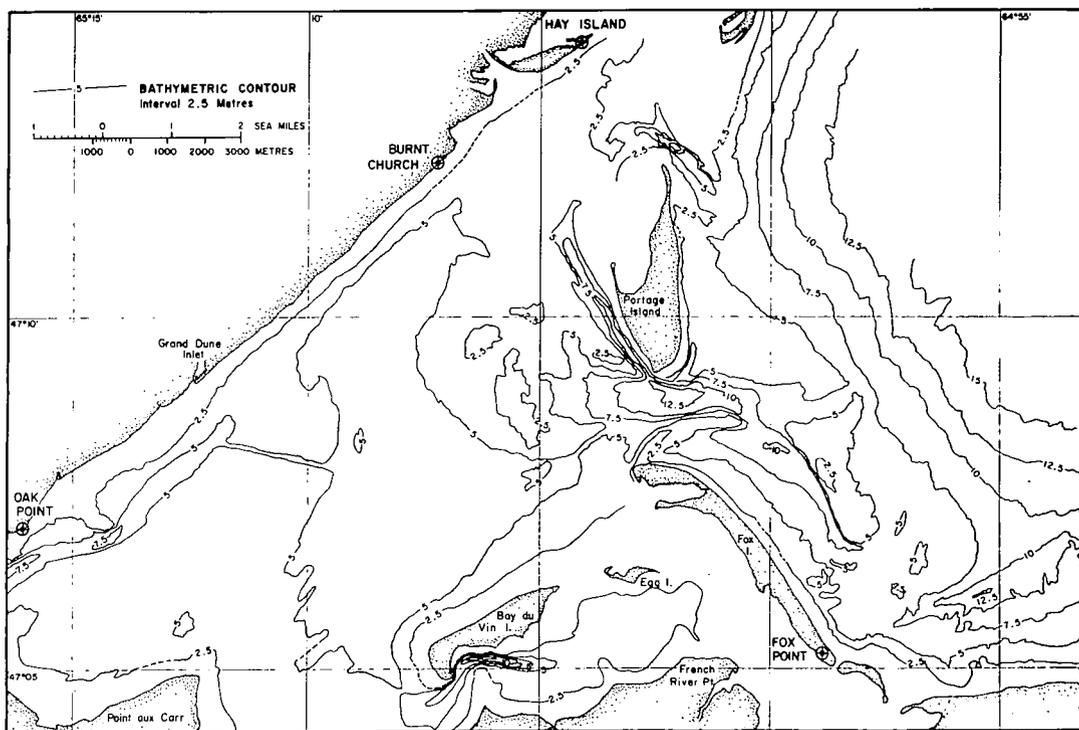
FIG. 3. Bathymetry of Miramichi Bay, contour interval 2.5 m. Contours drawn using Canadian Hydrographic Service field sheets (datum is mean low water).

narrow channels to the south of Bay du Vin Island (up to 15 m deep), to the west of Portage Island (up to 11 m deep), and to the north of Portage Island (the Portage gully – Neguac beach channel, up to 11 m deep). Reinson (1976a) has identified the channel to the west of Portage Island as ebb-dominated. The main Miramichi River channel (up to 9 m deep) also continues as a narrow, linear channel to about 600 m east of Oak Point. It extends as a weaker feature to the south of Grand Dune Inlet, where it swings away from the coast across the centre of the Inner Bay in an east-southeast direction. This section is artificial and was formed by dredging between 1910 and 1940 (echogram MN, Fig. 5), to allow access to Lower Newcastle–Chatham by larger vessels.

A broader channel up to about 14 m deep connects the Inner and Outer Bay areas between Portage and Fox Islands. The main water flow between the two areas takes place through this channel.

In the outer part of Miramichi Bay, the main channel divides in two, with one section swinging to the southeast parallel to the coast of Fox Islands, and the second section continuing seawards to the 7.5 m contour. Reinson (1976a) considers the main channel to be ebb-dominated outside and flood-dominated inside the barrier islands. In the outer part of Miramichi Bay, a gradual deepening of the water takes place outside the flat, shallow areas of Portage and Fox Islands. This deepening continues to the edge of the surveyed areas (15 m contour). An additional channel extends in a direction perpendicular to the coast of Fox Island at its southernmost end, north of Escuminac.

Extremely shallow areas (less than 2.5 m deep) are present between Bay du Vin, Egg and Fox Islands, and to the north and northwest of Portage Island. Also, to the west of Portage Island and its adjacent channel is a large, shallow area, covering about a quarter of the Inner Bay. Minimum water depths are less than 2 m and it appears to be a major depositional feature, described as a flood-tidal delta by Reinson (1976b).

Surficial Sediments

A preliminary analysis of the areal distribution of the bottom sediments has been made mainly using the echograms and shallow borehole data. The boreholes were drilled by Sub Surface

Surveys Ltd. of Fredericton, N.B. in a test boring program forming part of the Miramichi Channel Study. Fourteen boreholes are located in the survey area (Fig. 2). Most were drilled to depths of 3.7 m (12 ft) below the sea bed. However, three boreholes (1008, 1010, and 1015) reached 5.5 m (18 ft), whereas boreholes 1009 and 1013 only achieved 2.4 m (8 ft) and 1.8 m (6 ft) respectively (Figs. 6, 7).

Additional size analyses of 115 sediment samples in Miramichi Bay have also been measured by the Research and Productivity Council, New Brunswick for the Channel Study (Sutherland 1976). These results were received at the time of writing and have been incorporated in this paper only to confirm the generalized surficial sediment distribution in Fig. 4.

No penetration was achieved by the echo sounder over a large part of the Outer Bay (echogram AB, Fig. 5), whereas good penetration was obtained in the softer material covering approximately half of the Inner Bay (echograms KL, MN, and PQ in Fig. 5). The thickness variation of soft material is contoured at 1 m intervals using the echograms in Fig. 4. Penetrations of 1–3 m were obtained over most of the soft sediments. About 3500 m north of Bay du Vin Island, maximum penetrations of 5–6 m were observed on the echograms (Fig. 4). This area, where apparent maximum thicknesses of softer sediment are found, lies close to the boundary between the softer and harder material in the eastern part of the Inner Bay. However, gas in the sediments has obscured the true thicknesses of acoustically soft sediments in large areas of the Inner Bay, as described later.

Boreholes drilled in the softer material mapped by the echograms, encountered mainly very soft, grey to greyish brown or brownish black 'silt' (holes 1013–1017, Fig. 7) in the upper 4 m. Boreholes 1011 and 1012 passed through 1.8 and 3.1 m, respectively, of a very soft, grey, fine sandy 'silt'. Boreholes 1007, 1009, and 1010 sampled up to 3.5 m of soft to less soft, fine to very fine, sandy 'silt' (Fig. 6).

The particle size analyses of borehole and grab sample material in the Inner Bay (Sutherland 1976) show that this softer material consists of silty very fine sands and sandy coarse silts, sometimes with a considerable clay fraction (up to 15%). The particle size names are defined on the Wentworth scale.

In Fig. 4, these softer sediments have been
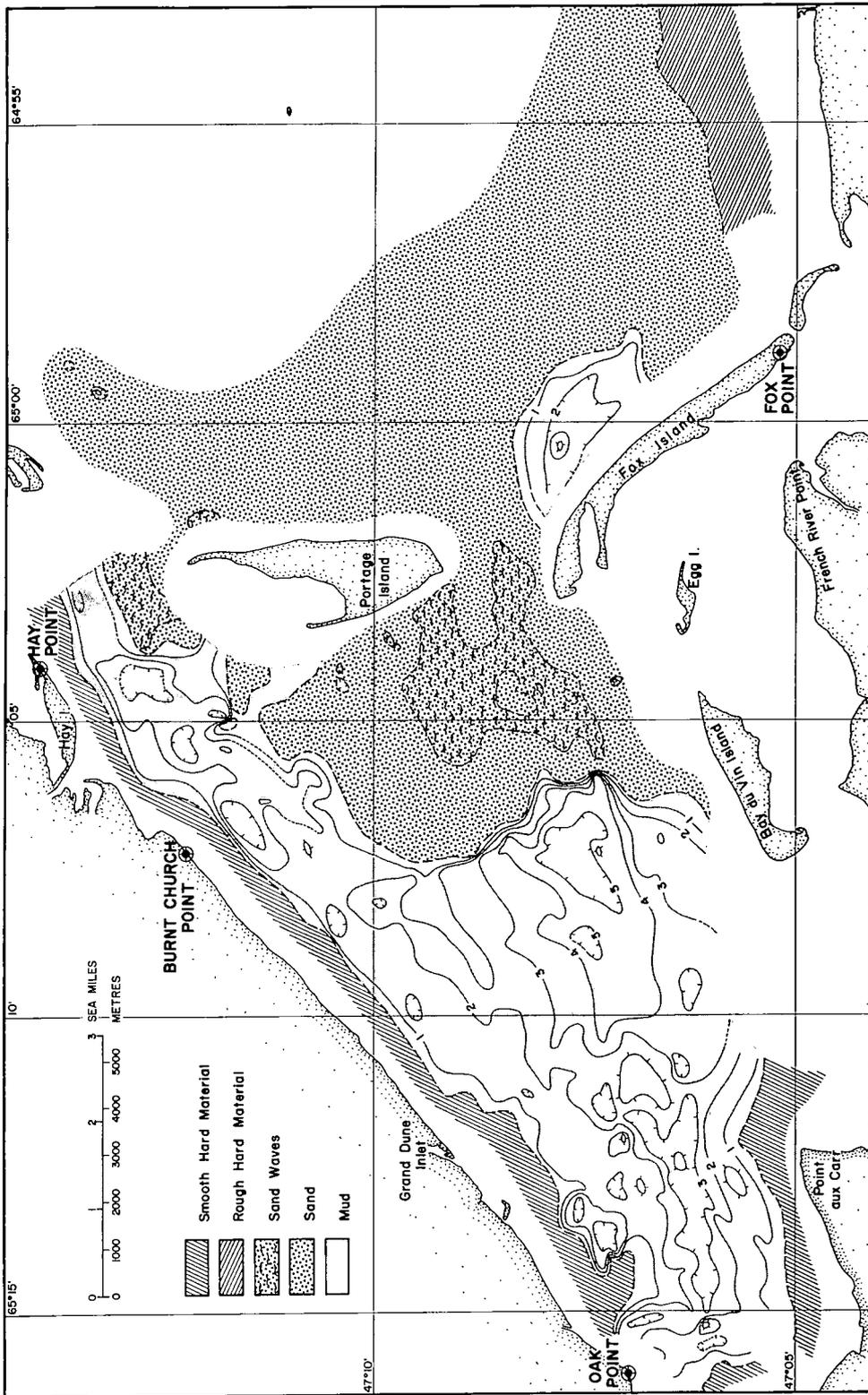
FIG. 4. Surficial sediment distribution obtained from echograms, seismic profiles, and borehole data. The thickness of the acoustically soft muds, measured from the echograms, is contoured at 1 m intervals.
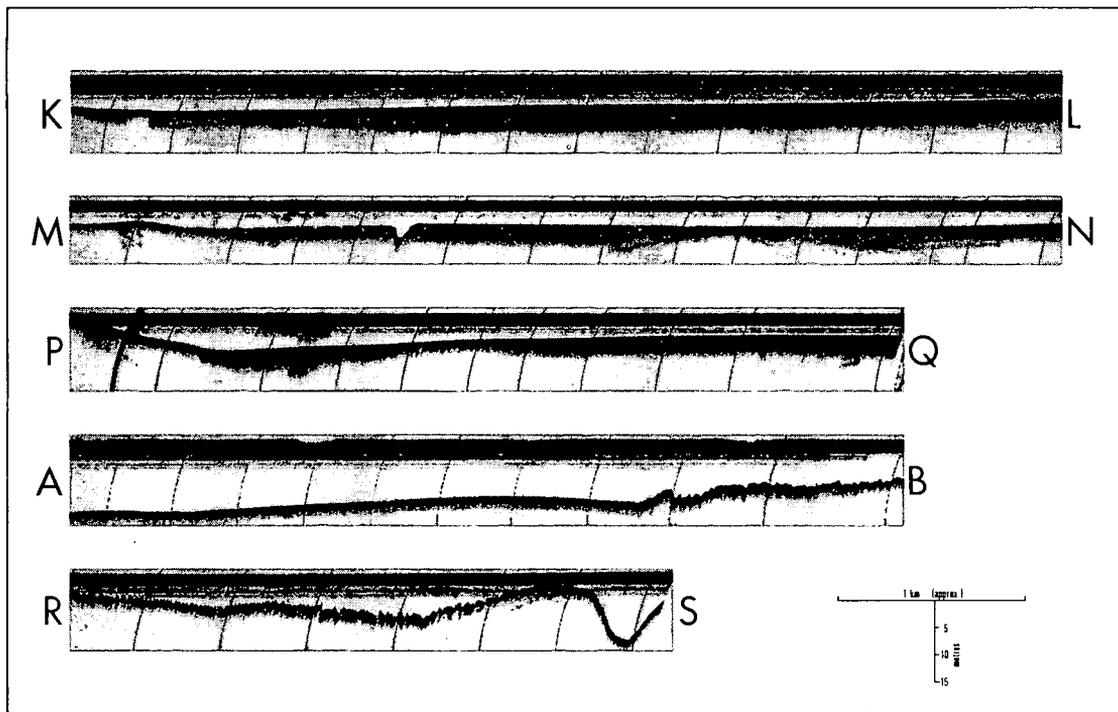
FIG. 5. Representative echograms. Locations on Fig. 2. KL: Inner Bay, smooth bottom with soft muds, about 3–5 m thick. MN: Inner Bay near Grand Dune Inlet, smooth bottom with soft muds. Dredged channel towards M and thinning of soft muds near coast, passing into sandy sediments. Note hard subbottom beneath muds with 'domed' surface towards N. PQ: Inner Bay near Burnt Church Point, soft muds with prominent gas reflector towards P. Muds thin and pass into sands near coast. Note thickness variations of muds. AB: Outer Bay, smooth hard bottom is sand passing abruptly into rough, hard bottom near Escuminac coast. The latter represents discontinuous sandy deposits on Pennsylvanian bedrock, possibly with some till. RS: Inner Bay, west of Portage Island, sand waves on hard sandy bottom showing variable wavelength and amplitude. Note Portage Island ebb channel towards S.

termed 'muds', an all-embracing name for the materials in which good echo sounder penetration was achieved. Some echograms show penetration below an upper reflecting horizon down to a lower reflector (profiles MN and PQ, Fig. 5). Also, the base of the soft 'muds' is not always flat lying, but shows topography in some areas (profiles MN and PQ, Fig. 5 and the thickness contours in Fig. 4). A small patch of possibly, a softer, poorly compacted, finer sand also occurs in the Outer Bay on the seaward side of Fox Island, as interpreted from the echograms.

The harder material in the eastern part of the Inner Bay and most of the Outer Bay, defined by little or no penetration on the echograms, is identified as silty fine sand to fine sand in boreholes 1003, 1005, 1006, and 1008 (Figs. 2, 6). This is confirmed by the particle size analyses (Sutherland 1976) which identify a suite of sands, from very fine to coarse, from the bore-

hole and grab samples. In the Outer Bay, the sands appear to coarsen in particle size towards the deeper water.

A measure of the hardness of the sediments encountered in the boreholes is shown by the variable N in Figs. 6 and 7. The variable N is the number of blows per foot on the casing using a 140 lb hammer. On sections of holes where N is zero (hole 1007, Fig. 6) the sediments were sufficiently soft that the casing was pushed downwards. This variable also shows the relative hardness of the sands compared with the 'muds'.

In the Outer Bay, echogram AB (Figs. 2, 5) shows the smooth, hard sands changing abruptly to a rougher, hard bottom type at the southeastern end of the profile. Figure 4 and the bathymetry on Fig. 3 show this bottom type to continue eastwards off the Escuminac coast, in a strip at least 2000 m wide. This rough, hard
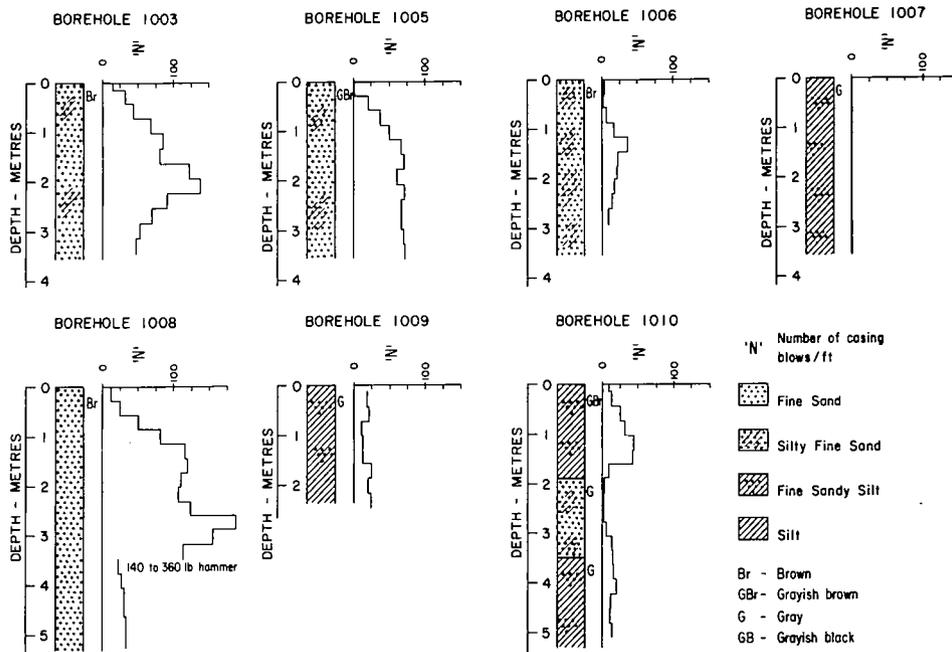
FIG. 6. Borehole results obtained by Sub Surface Surveys, Fredericton. Locations of Fig. 2.
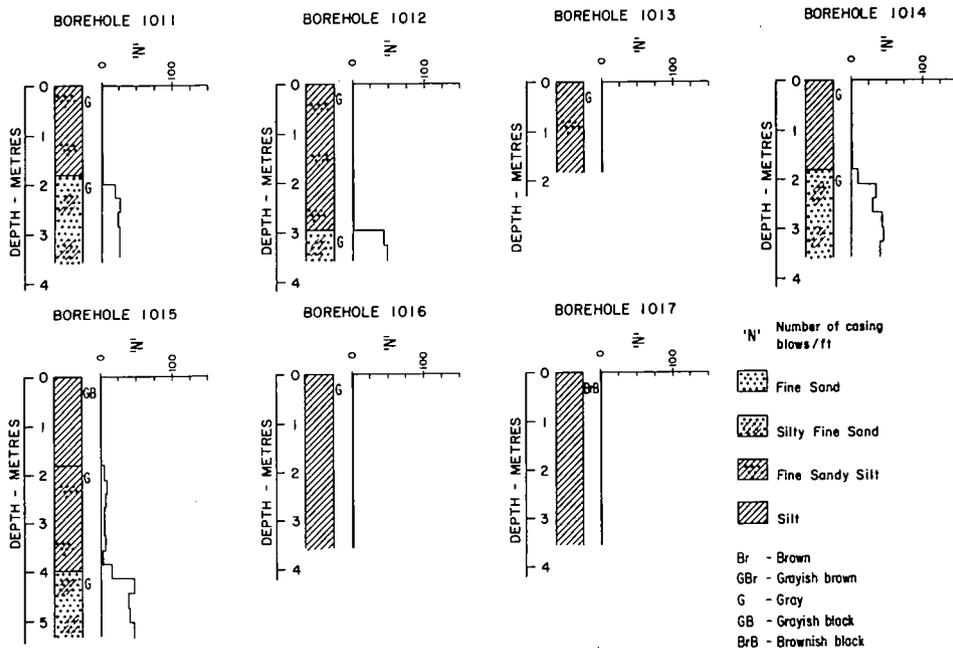
FIG. 7. Borehole results obtained by Sub Surface Surveys, Fredericton. Locations on Fig. 2.

bottom type may be Pennsylvanian bedrock or glacial moraine, partly coated with thin, discontinuous sand deposits. Reinson (1976b) has shown this area to be covered by a continuous sand layer, but the seismic profiles indicate that the sand is discontinuous. Definite identification of the underlying hard material requires borehole evidence, though Bousfield (1955) has also identified this area as rock.

Sand waves (Nova Scotia Research Foundation Corp. 1975) are conspicuous on both seismic profiling records and echograms in the Inner

Bay directly west of the channel between Portage and Fox Islands (Fig. 4). They were first reported from the examination of the results of a Canadian Hydrographic Survey by E. Owens in 1972 (personal communication). Reinson (1976a) has also confirmed the presence of sand waves to the west of Portage Island. A second sand wave area occurs directly north of Portage Island, with a small patch near the northeast tip of the same island. The sand waves show varying amplitude and wavelength, though most have amplitudes of about 0.75–1.5 m and wavelengths of about 20–90 m (echogram RS, Fig. 5). Sand ripples may also be present. The sand wave areas are located close to the Inner Bay entrance between gaps in the barrier islands, presumably where water current velocities are relatively large. The sand wave area to the west of Portage Island approximately coincides with an area of gravelly sand and sandy gravel mapped by Reinson (1976b). The coarse sand-wave material is indicative of relatively high current velocities.

A further bottom type is mapped as a coastal strip about 1000–1500 m wide between Oak Point and Hay Point (Fig. 4). On echograms (MN, Figs. 2, 5) this appears as a smooth, hard bottom with little or no penetration. It probably represents a sandy layer overlying Pennsylvanian bedrock and (or) moraine. Reinson (1976b) has mapped it as mainly muddy sand, sand, and gravelly sand. The seismic evidence suggests that these surficial deposits are relatively thin.

Discussion of the Surficial Sediments in Miramichi Bay

The deposition of large quantities of relatively, soft muddy silts in the Miramichi estuary probably reflects a low energy regime. The flat bottom in this part of the Inner Bay (water depths 3–6 m) may represent the effective wave base for these sediment types.

The offshore barrier islands at the mouth of Miramichi Bay (e.g. Portage and Fox Islands) have been shown to undergo rapid changes in morphology by Hunter and Tress (1976). They state that the changes are in response to storm waves, sea ice, tidal and non-tidal currents, with the main movement of sand into the area from the north and a weaker movement of sand from the east. The sands are said to be largely residual in character, derived from the sandstones and glaciofluvial surficial deposits around the outer limits of Miramichi Bay. For instance, there is a strong littoral drift of sand to the south in the Neguac area (Hunter and Tress 1976); the southern end of Portage Island has migrated south by almost a mile between 1837 and 1974. Kranck (1967) has measured similar southeast long shore migration of a sand spit in Kouchibouguac Bay (Fig. 12), which is about 20 km south of Miramichi Bay. Kranck also concludes that the Kouchibouguac Bay gravels are derived from reworked glacial till, probably deposited by Pleistocene glaciers. The sands in Kouchibouguac Bay also appear to be relict material. A similar origin for the Miramichi Bay sands and gravels may also be postulated. The flat, shallow areas of sand with depths of 2–5 m may also represent a shallower effective wave base than for the softer, muddy silts. The sands in the Outer Bay represent the effects of a higher energy regime than in the Inner Bay. The shallow depths in Inner Miramichi Bay suggest that the sediment budget may be approaching equilibrium. Further detailed sedimentological and geochemical analysis is in progress on the sediments of Miramichi Bay by other workers.

Refraction Experiments

Seismic refraction surveys determine the propagation velocity of seismic energy through rocks and surficial sediments. Contrasting lithologies may be correlated with certain velocities, or velocity ranges, providing borehole control is available. Knowledge of the seismic velocities is also useful in identifying seismic reflectors on reflection profiles. Owing to the larger distances the seismic energy must travel through the ground, refraction surveys require lower frequency energy sources than reflection surveys. However, in shallow water, short refraction profiles may be measured using seismic sources designed for reflection profiling.

In Miramichi Bay, short refraction profiles were measured with an N.S.R.F.C. single tip sparker and a hydrophone on 500 ft of buoyant cable. The hydrophone was paid out astern of the boat at the end of the cable. The sparker was towed directly astern of the boat, so that the distance between source and receiver gradually increased. The boat was stopped when all the cable was out and the hydrophone was then pulled in. Figure 8 shows the resulting refraction profile.

It should be noted that a refraction profile such as this is neither 'reversed' nor 'unreversed'
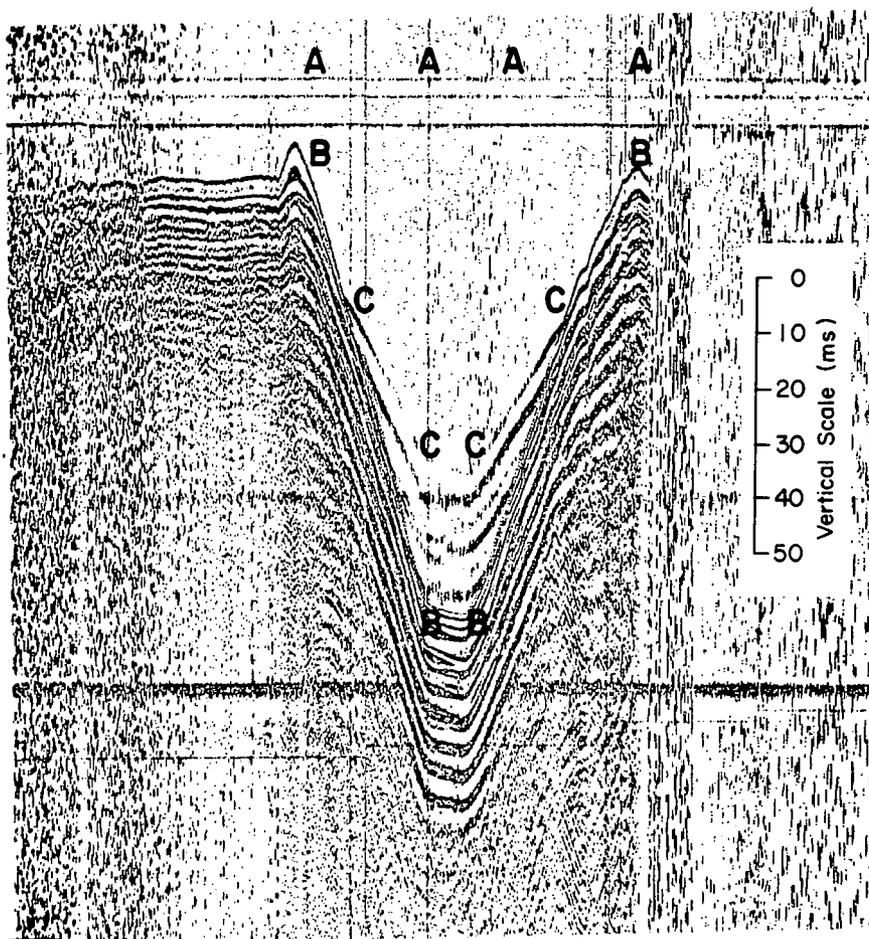
FIG. 8. Representative refraction profile. AA: sparker triggering event; BB: sound arrival at hydrophone after travelling directly through water; CC: refracted sound wave arrival at hydrophone after travelling through underlying rock.

in the classical sense. In an idealized situation, where the boat came to a sudden stop immediately the hydrophone cable was all paid out and then remained stationary until the whole cable was retrieved, the profile would be a true reversed line. In practice, the boat will drift during the recovery of the hydrophone so that the second part of the line is over a section of the seafloor displaced somewhat from the first part. However, it should be remembered that a normal reflection profile can be (and was) made simultaneously with the refraction profile by receiving the vertical incidence reflections at a hydrophone towed adjacent to the acoustic source. This serves as a check on any dips or other irregularities which may be present at the refraction site, and could be used to make corrections to velocity values obtained over dipping interfaces.

To simplify data reduction, however, it is best to choose sites offering the simplest geometry, and in the Miramichi estuary, such sites were not difficult to find.

Ten profiles were measured. Five of the profiles were interpretable (Table 1). The remaining five profiles, measured in water depths of 8 m or more, could not be interpreted as the seismic source was not powerful enough to allow the detection of the refracted energy from below that depth. Seismic velocity error is ± 0.1 km/s and depth error is ± 0.5 m. The seismic velocities measured from refraction profiles I, II, VII, and IX may be correlated with Pennsylvanian sandstones. The profile III velocity, which is lower, suggests the presence of glacial till.

In 1963, marine seismic refraction profiles (Miramichi River Study 1964) were measured to

determine overburden thickness on profiles along the proposed dredging area. A 12 kHz sonar reflection system was also employed. Profiles are not available from the reflection survey and seismic velocities are not reported for the refraction profiles. Hence, the interpreted bedrock depths along the few, isolated profiles in our survey area have not been incorporated in this paper.

The 'Gas Layer'

A number of seismic profiling records over part of the Inner Bay showed a prominent discontinuous reflecting horizon at depth of about 1–2 m (e.g. reflector g on profile EF, Fig. 9). The margins of the reflecting horizon curve, or dip, abruptly downwards. Reflecting horizons above this reflector are unaffected and may be continuous, whereas those at greater depths are masked due to the impenetrable 1–2 m deep reflector (e.g. reflectors b and c, profile EF, Fig. 9). This reflecting horizon was also detected on some of the echograms (e.g. the western part of echogram PQ in Fig. 5). The main areal extent of this shallow 'masking' reflector has been mapped using the seismic profiles and echograms. Other smaller occurrences of the masking reflector have been omitted owing to their size. This reflector is shown as the shaded areas on Fig. 10. It occurs entirely within the area of soft 'muds', as detected acoustically on the echograms (Fig. 4). On the echograms and seismic profiles, the masking reflector forms the lower penetration limit.

Schubel (1974) reports high resolution seismic profiling records, made with a boomer, which show confused areas characterized by bands of strong diffuse reflection which mask the underlying features in parts of Chesapeake Bay. Schubel (1974) names these zones of 'acoustically turbid' sediments and attributes them to the presence of gas bubbles entrapped in the interstices of a relatively thin (≤ 2 m) sediment layer with a resulting increase in the bulk compressibility. The increased bulk compressibility causes a decrease in the acoustic velocity in these sediments, and an increase in their acoustical reflectivity.

Similar seismic reflectors have been detected in the coastal areas of Nova Scotia. Examples occur in parts of northern Chedabucto Bay (Nova Scotia Research Foundation Corp. 1974), Bedford Basin, and Eastern Passage, Halifax Harbour (A. G. McKay, verbal communication,

TABLE 1. Results of short refraction profiles. For locations, see Fig. 2

Line number	Velocity in lower layer (km/s)	Depth to lower layer (m)
I	3.3	4.0
II	3.3	3.5
III	2.2	4.5
VII	3.1	6.5
IX	2.7	4.5

1976); St. Margaret's Bay (Keen and Piper 1976; Piper and Keen 1976); and Mahone Bay (D. E. T. Bidgood, verbal communication, 1976).

L. H. King suggested the reflector in St. Margaret's Bay was caused by gas which was confirmed from core evidence by Keen and Piper (1976). Gas in sediments has been detected in other marine areas of eastern Canada, such as the Gulf of St. Lawrence (Rashid et al. 1975) and the Labrador Shelf (Vilks et al. 1974). Keen and Piper (1976) concluded that their '2 m' reflector in St. Margaret's Bay is caused by gas, mainly methane, generated by the decay of organic material, such as kelp and phytoplankton, in the sediments. A similar origin is proposed for the gas and 'gas' reflector in the soft muds of the Miramichi estuary.

Keen and Piper (1976) suggest that their reflector is formed by a concentration gradient of the gaseous phase in the sediments, rise in gas being retarded at deeper levels, where viscosity is high, and increased at higher levels, where viscosity is low. Hence, the top of the gas-rich sediments forms an acoustic reflector due to a change in the reflection coefficient. However, recently, Kepkay (1976a, 1976b) has proposed, from preliminary analysis of seismic refraction and wide-angle reflection arrivals measured in sea bed seismic experiments in St. Margaret's Bay, that the gas reflector is the result of a less dense gas-rich sediment layer overlying a more dense gas-poor sediment layer. The gas-rich layer is bounded by the sea bed above and the 'gas' reflector below. Hence, Kepkay (1976a) proposes the 'gas' reflector represents the base of the gaseous layer. Obviously, this poses questions such as why is the gas partially trapped by the sea bed and why is gas seepage not detected on echograms or seismic profiles, why changes in sea bed reflecting characteristics over gas areas are not detected, and the cause of the gas-rich layer increasing in thickness at its
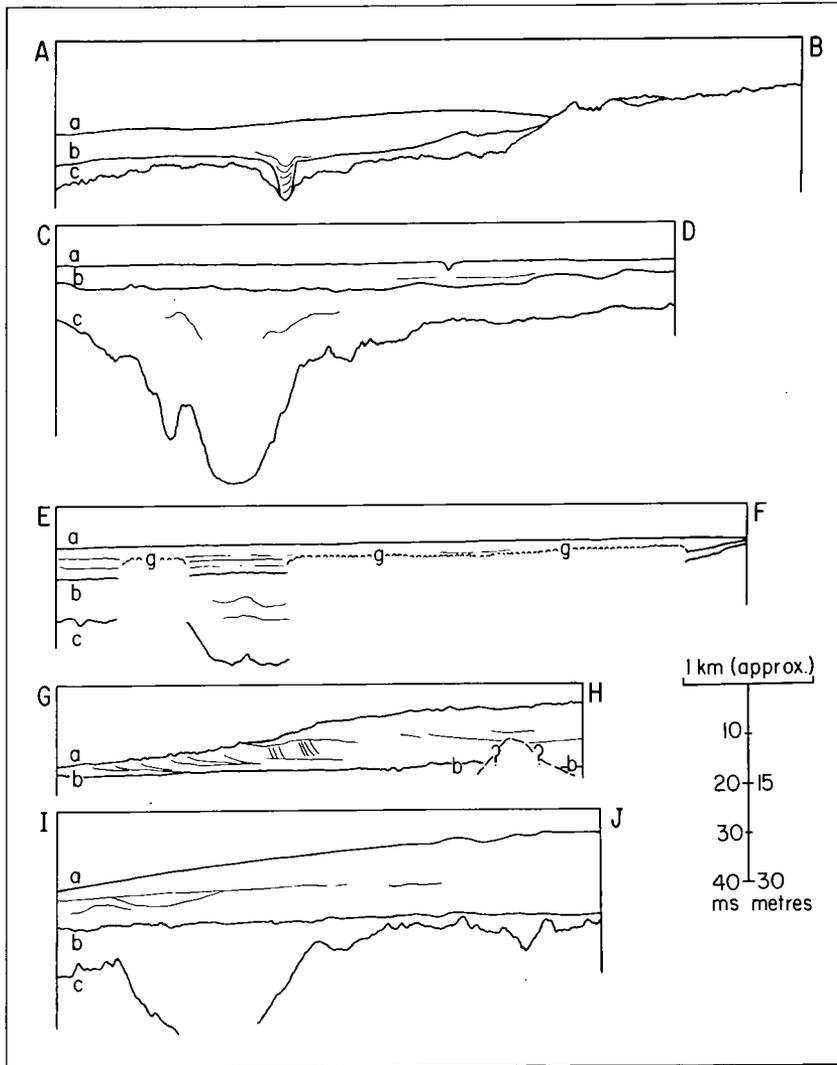
FIG. 9. Line drawings of representative seismic reflection profiles. Locations on Fig. 2, a: sea bed; b: main upper reflector; c: main lower reflector (bedrock); g: gas reflector. AB: Outer Bay, sands overlying probable bedrock thin towards shore near B and become discontinuous pockets. Channel formed by b is evidence that it is an erosional surface. Note distinct layering in channel. CD: Inner Bay, southern Miramichi bedrock channel. Dredged channel at seabed near D; b is near horizontal. Discontinuous layers above bedrock channel suggest considerable time lapse before channel was filled. EF: Inner Bay, soft muds, with gas reflector masking all deeper seismic reflectors, overlying harder material and bedrock. Layering is present above and below b. GH: Inner Bay, west of Portage Island, crossbedding in sands and gravelly sands with sand waves at surface. Erosional surface above b appears to truncate foreset beds. IJ: Outer Bay, east of Portage Island; Portage Island bedrock channel. Channel bottom not detected on seismic profile. Additional channelling between a and b planed by seismically less prominent erosional surface.

margins, as represented by the downward dip of the seismic reflector. Also, disruption of sedimentary layers may possibly occur due to the upward movement of the gas, whereas distinct, continuous seismic reflectors are seen on the seismic records between the sea bed and gas reflector.

The downward dip of the gas reflector at basin margins, near subbottom high and in thin sedimentary sequences is due to less gas production
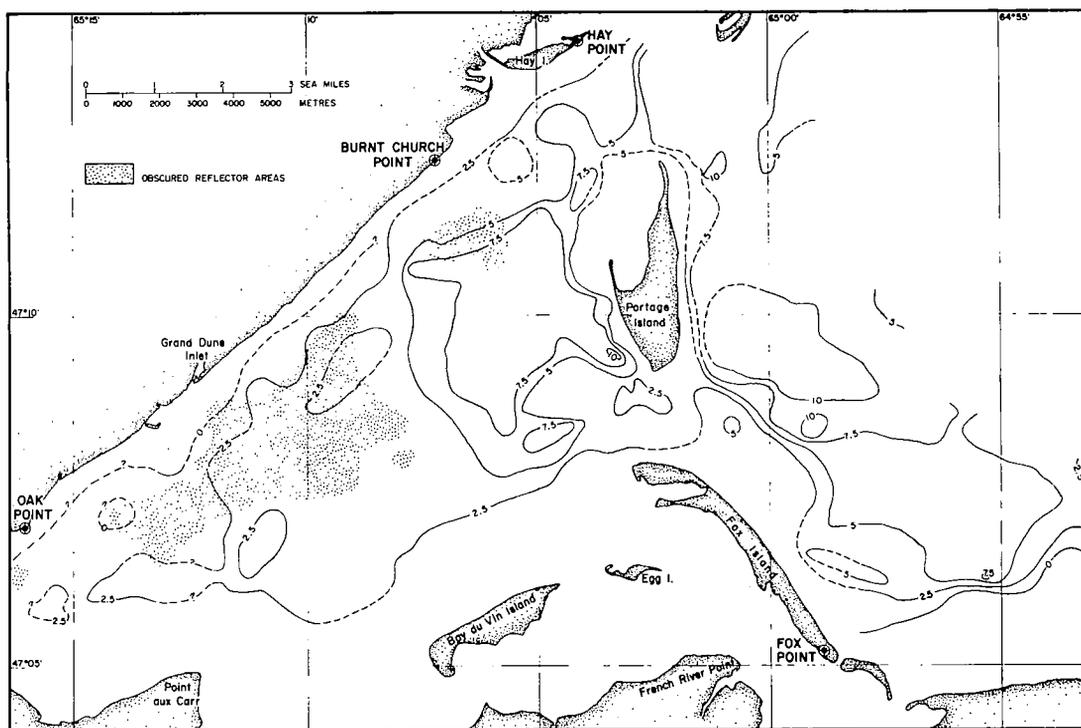
FIG. 10. Thickness of sediments between seabed and prominent upper reflector contoured at 2.5 m intervals. Dashed contours are tentative. Shaded areas locate presence of gas reflector in soft muds of the Inner Bay.

if some of the gas is generated at depths exceeding 8 m, according to Keen and Piper (1976). However, profile EF (Fig. 9) shows a discontinuous gas reflector with downward dipping margins away from basin margins, subbottom highs, and thin sedimentary sequences. We suggest that this is due to discrete areas of reduced amounts of decaying organic material within the sedimentary sequence, resulting in greatly diminished gas production. Variations in the depth of the gas reflector below the sea floor are seen in profile EF, decreasing from about 2.5 m, in the centre of the Inner Bay, to about 1.5 m near the coast at Grand Dune Inlet. Keen and Piper (1976) suggest that variations in water depth or overburden thickness, and changes in permeability may cause variations in the gas reflector depth. For Inner Miramichi Bay (profile EF, Fig. 9), water depths increase from about 7 m at F to about 8.5 m at E. Also, from the surficial sediment distribution (Fig. 4) the permeability probably does increase towards the shoreline due to a larger sand content in the sediments.

The Main Upper Reflector

A prominent upper seismic reflector (distinct from the gas reflector) was delineated by the seismic profiling survey in Inner and Outer Miramichi Bay. It is present on all the profiles in Fig. 9 (labelled 'b'), and is mostly continuous over the whole area, except where it is truncated by a prominent lower reflector close to shore (Fig. 9: southern part of profile AB and Fig. 10) and possibly, in a few, small isolated areas (Fig. 9: profile GH). This prominent reflector is horizontal or gently dipping. Figure 10 is a plot of the thickness of sediments between the sea floor and the upper reflector contoured at a 2.5 m interval. All reflector depths have been measured assuming a sediment velocity of 1500 m/s to comply with dredging requirements which necessitated that reflector depths not be overestimated. Though a reasonable value for the softer sediments, it is probably too low for the more compacted surficial deposits. Bedrock depths should therefore be regarded as minimum values.

The reflector is at relatively shallow (2.5–7.5

m) depths below the sea floor in the Inner Bay. It forms a shallow 'bowl-like' surface in the Outer Bay. Evidence that this reflector is partly an erosional surface is found in profile AB, (Fig. 9, reflector b), where it delineates a narrow, deep channel infilled with more recent sediment, directly underlain by a small bedrock channel. This suggests that the channel was a relatively stable feature possibly around the edge of an older spit or between older barrier islands, (K. Philpott, personal communications, 1976).

Above this seismic reflector horizon occur numerous weaker, discontinuous reflectors (all profiles on Fig. 9). Other erosional surfaces undoubtedly occur as can be seen on profile IJ, Fig. 9, where there is evidence of channelling in these overlying sediments and the channel itself has been eroded. The maximum depth of the channel below the erosion plane is about 2 m and its width about 850 m on this profile.

Other sedimentary structures were also detected on some profiles. For instance, profile GH, Fig. 9 shows cross-bedding in sands close to the southern tip of Portage Island (Fig. 2). The cross-bedding appears to show 0.5–1.5 m thick bottomset and foreset beds, with the depositional front advancing in a southwesterly to west-southwesterly direction. Further detailed seismic profiles are required to confirm this direction. The foreset beds are truncated at or close to the sea floor indicating that these deposits have undergone erosion or are being eroded presently. There is an indication of an erosional surface within the sedimentary sequence, close to the sea floor, near H on profile GH. This erosional surface appears to have truncated smaller scale foreset beds (possibly about 0.2 m thick).

Hence, both vertically and laterally there are variations in the surficial sediment type above the prominent upper reflector, as shown by their areal distribution (Fig. 4) and borehole evidence (Figs. 6, 7). A number of seismic profiles show sandy deposits near the barrier islands passing laterally into softer, muddy deposits with areas of gas. Some correlations may be made between some of the weaker reflectors and changes in lithology and hardness as represented by N on Figs. 6 and 7. For instance, a change in hardness and sediment type (silt to silty fine sand) at a depth of about 1.8 m in borehole 1014 correlates with a weak reflector, at about the same depth,

on adjacent seismic profiles. However, on other seismic profiles, weak reflections do not appear to correlate with lithology or hardness changes from the borehole records.

It would appear that none of the boreholes located on Fig. 2 penetrates the prominent upper reflector, with the possible exception of borehole 1015. Though the adjacent seismic record is partly masked by the gas reflector, a very tentative correlation is possible with the interface between fine sandy silt and silty fine sand, with an accompanying increase in N, at a depth of 4 m in the borehole. However, for a definite correlation additional boreholes are required at known positions on the seismic lines where the main upper reflector is prominent.

Kranck (1972) has identified four marine terraces in Northumberland Strait formed during the post-Pleistocene marine transgression. The erosional surface represented by the main upper reflector probably represents a similar marine terrace. Its average depth below a datum of about 10 m and 15 m in the Inner and Outer Bays respectively may be correlated with a date of about 3000–4500 BP as shown in the time-depth plots by Kranck (1972) and Grant (1970). However, this correlation must remain tentative until more data are available owing to regional differences in submergence rates.

Scott et al. (1977) have described relatively high recent sedimentation rates in some parts of Miramichi Bay. Their preliminary ^{210}Pb analysis from a single core gave rates of 0.36–1.2 cm/year; paleontological evidence from four short cores suggested accumulation of at least 20 cm of sediment between 1967 and 1975. These rates would certainly account for the 2 – >10 m of sediment accumulated above the upper seismic reflector if it is correlated with the 3000–4500 BP marine terrace. It seems likely that sedimentation and erosion rates have varied and that radiometric and paleontological evidence are required to determine the age of the reflector. Also, evidence from dating is required to determine whether this reflector is of the same age both inside and outside of the barrier islands.

The Prominent Lower Reflector

A prominent seismic reflector was observed on some profiles below the upper reflector (e.g. reflector C on profiles AB, CD, EF, and IJ, Fig. 9). No seismic penetration was detected
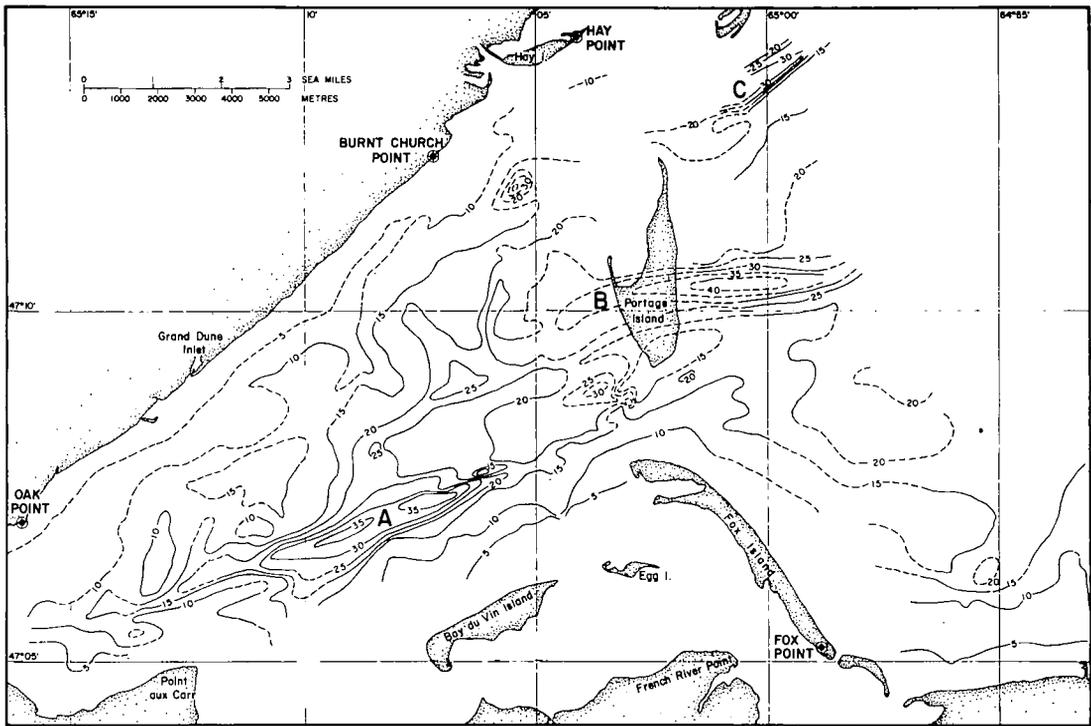
FIG. 11. Depth of prominent lower reflector (bedrock) below datum (mean low water) contoured at 5 m intervals. Dashed contours are tentative. Southern Miramichi (A), Portage Island (B), and Neguac Island (C) bedrock channels are labelled.

below this reflector, which is correlated with the Permo-Carboniferous bedrock surface. Traces of layering are present in the sediments between the bedrock and the prominent upper seismic reflector where the bedrock is deepest. It is suggested that the sediments overlying the bedrock and underlying the prominent upper reflector represent glacial till and proglacial deposits, though no confirmatory borehole evidence is available at present. The proglacial deposits may include equivalents to the Leda clay and Saxicava sand.

Bedrock depths below datum vary between 5 and >40 m in the Miramichi estuary. Directly north of the Escuminac coast (east of Fox Point), bedrock is at, or close to, the sea bed. The deepest bedrock depths are located in parts of the estuary where the bedrock surface has been eroded into narrow, linear channels (e.g. profiles CD and IJ in Fig. 9) with distinct trends (Fig. 11). Three main channels were detected: the southern Miramichi Channel, which runs from about 2 km north of Point aux Carr to the area between Portage and Fox Islands. It runs approximately

east-northeast (068°), has a maximum depth of 35–40 m and a maximum width of about 1.2 km; the Portage Island channel probably continues beneath Portage Island and is an excellent example of an eroded bedrock channel infilled and concealed by later sediment transport and deposition. Directly adjacent to Portage Island, this channel runs almost due east (085°), but there is a suggestion that in the Inner Bay and its seaward extension it may swing around to parallel the southern channel. This channel continues seaward beyond the limits of the survey area. In the Inner Bay, its continuation is difficult to trace due mainly to the masking effect of the gas reflector. This is the deepest channel in the survey area, with depths exceeding 40 m below datum, beyond the penetration of the seismic source used. It has a maximum width of about 1.4 km; the third channel, detected on only a few profiles, is the Neguac Island Channel, about 5.5 km east of Hay Point. The sparse coverage in this area indicates a channel with maximum depths of 30–35 m below datum, trending about 055° with a maximum width of

about 1 km. This is approximately parallel to the coastline between Oak Point and Burnt Church Point (Fig. 11).

Chalmers (1894) noted that borings for railway bridges on the Southwest Miramichi River penetrated bedrock at depths of 115 ft (35 m) after passing through gravels, sands, and clays.

Kranck (1971, 1972) has recognized a pre-Pleistocene drainage system eroded into the bedrock underlying Northumberland Strait. The deeper parts of the bedrock channels in the Miramichi estuary may also indicate overdeepening by glacial scouring (e.g. directly east of Portage Island). Alternatively, they may be subglacially excavated channels, or Rinnentaler, an origin proposed for channels in Mahone Bay by N. E. Barnes and D. J. W. Piper (personal communication, 1976). However, the linear nature of the channels suggests that the pre-Pleistocene drainage system or subglacial excavation may have been controlled by structures in the underlying relatively soft Carboniferous sediments. Differential erosion of variable bedrock lithologies is discounted as Carboniferous facies trends are approximately 030°–040° in the Miramichi estuary area (New Brunswick Department of Natural Resources 1969).

H. W. van de Poll (personal communication, 1976) has measured joint directions in Pennsylvanian rocks of eastern New Brunswick. To the north of the Miramichi estuary, on the south coast of Chaleur Bay, east-northeasterly (67.5°) and north-northeasterly (22.5°) joint directions were measured. A small amount of movement was observed by van de Poll on north-northeasterly joints.

To the south of Miramichi Bay, in the Kouchibouguac Park area, north-northwesterly (340°) and east-northeasterly (70°) joints were measured. From these observations, the southern Miramichi bedrock channel has the same direction as east–northeasterly joints measured to the north and south of Miramichi Bay. This pre-Pleistocene drainage channel may have been controlled by jointing in the Carboniferous sediments. However, jointing does not appear to have been involved in the erosion of the Portage Island and Neguac Island channels.

Anderson (1972) has described the Catamaran Fault as a right-lateral strike-slip fault, post-Middle Devonian and pre-Carboniferous in age. It cuts pre-Carboniferous rocks of the Mira-

michi Geanticline in north-central New Brunswick, striking easterly in the intrusive and metamorphic core of the geanticline and northeasterly in the Siluro–Devonian flank rocks (Fig. 12). Anderson (1972) also proposed a possible southwesterly extension of the Catamaran Fault for about 144 km on the basis of known faults, and a northeasterly extension of 160 km to join with a graben in the pre-Carboniferous basement under Miramichi Bay as postulated by Howie and Cumming (1967). With these additions, Anderson suggested that the Catamaran Fault may have a possible length of about 400 km. Howie and Barss (1974) have plotted a fault extending about 80 km in a northeasterly direction from Outer Miramichi Bay in their Fig. 2 displaying tectonic elements and pre-Carboniferous basement contours (Fig. 12). This would extend the Catamaran Fault to almost 500 km in overall length. Rast and Stringer (1974) have shown the Catamaran Fault extending seaward through Miramichi Bay on an east-northeasterly trend for about 25 km. To the southwest, they show an abrupt swing to a south-southwesterly direction at the juncture of the Catamaran Fault and a buried thrust (Fig. 12).

A plot of the bedrock channel directions in Miramichi Bay (Fig. 12) suggests that the Portage Island and southern Miramichi channels may also represent structures in the Carboniferous related to the underlying Catamaran Fault in the Siluro-Devonian basement rocks. The Neguac Island channel follows a direction similar to the fault proposed by Howie and Barss (1974) and the Caraquet Dike (Burke et al. 1973) of possible Triassic age (Fig. 12). This channel is also on strike with the southern flank of a narrow band of positive magnetic anomalies (the Tabusintac Lagoon magnetic unit) striking northeast, beginning about 10 km northeast of the southern end of Neguac Island (Fig. 12). The Tabusintac Lagoon magnetic unit is part of a composite 'Z' shape magnetic anomaly which Howie and Cumming (1967) assume to be caused by a folded belt of volcanics mapped by Smith (1957). If the steep gradients of the southern flank of the Tabusintac Lagoon magnetic unit represents a faulted margin, then the Neguac Island channel may be due to erosion of a related structure in the overlying Carboniferous sediments.

Haworth and MacIntyre (1975) show that the
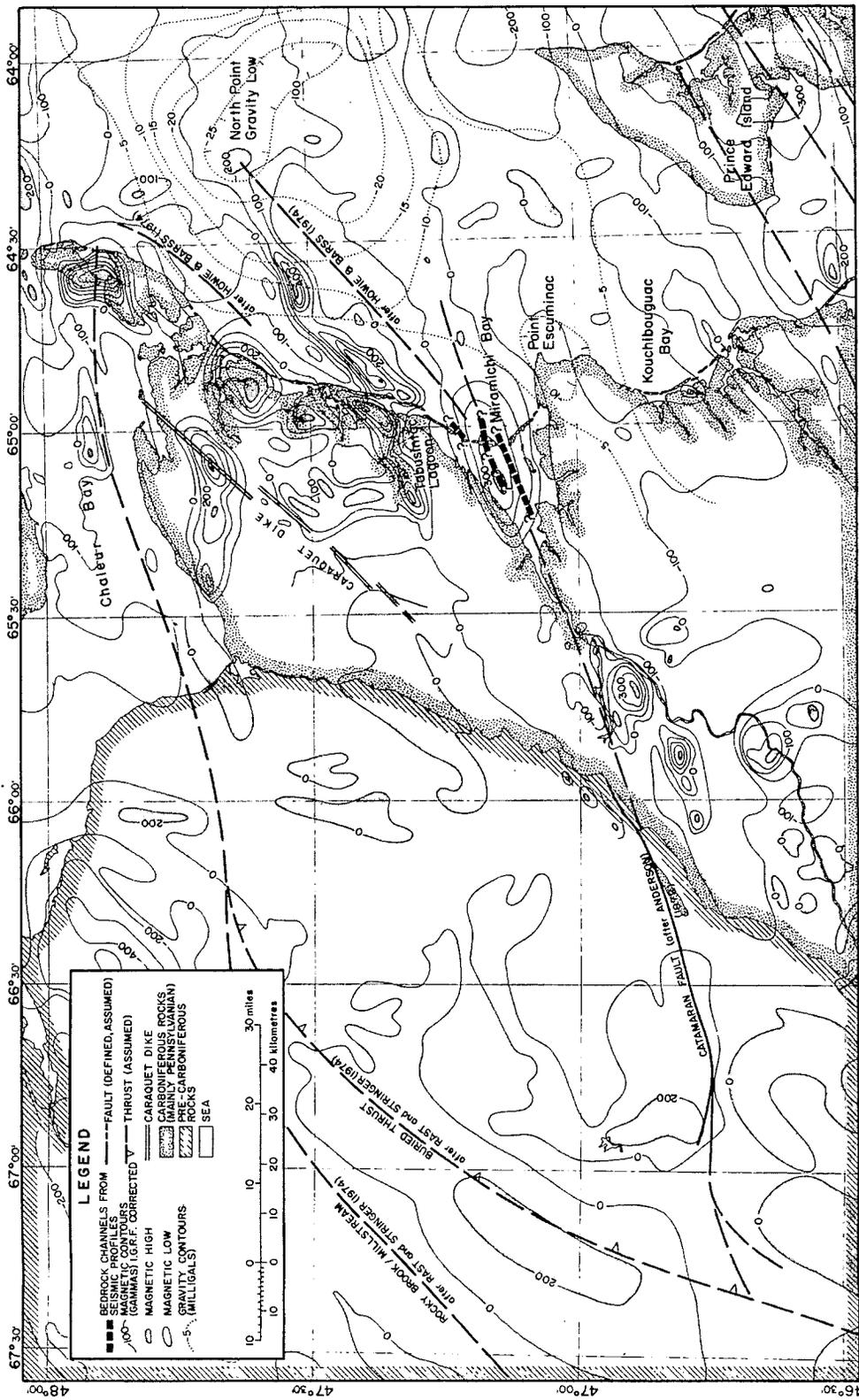
Fig. 12. Compilation showing simplified geology, main faults and thrusts, Caraquet dike, magnetic anomalies, North Point gravity low and Miramichi Bay bedrock channels.

magnetic and gravity fields in this part of New Brunswick are lineated in a general northeast direction following the pre-Carboniferous structural trends. Magnetic anomalies with respect to I.G.R.F. (International Geomagnetic Reference Field) have been traced from their magnetic map 801-E and superimposed on Fig. 12 (with the permission of the Geological Survey of Canada whose original 1 : 1000,000 I.G.R.F. compilation and 1 : 5000,000 Magnetic Anomaly Map of Canada were the basis for this part of map 801-E in Haworth and MacIntyre (1975)). It can be seen that an east-northeasterly band of positive magnetic anomalies passes through Miramichi Bay and out to sea where it coalesces with the Tabusintac Lagoon magnetic unit to the north to form a broad magnetic high about 55 km offshore. Howie and Cumming (1967) give a depth estimate of 10 000 ft (3.05 km) for the 400 γ positive magnetic anomaly overlying Miramichi Bay. They considered the magnetic source rocks to be at the surface of the pre-Carboniferous basement and that the resulting, thick Carboniferous section may be explained by a concealed graben. Bhattacharyya and Ray-chandhuri (1967), using filtered aeromagnetic maps, interpret the Miramichi Bay magnetic high (part of their magnetic sub-unit IIB) as a ridge in the pre-Carboniferous basement surface, and the Neguac – Beaver Brook magnetic low (their magnetic sub-unit IIA), directly north of the Miramichi magnetic high, as a trough in the basement surface. They then correlate this trough with the graben interpreted by Howie and Cumming (1967) from the depth estimate obtained using the positive magnetic anomaly over Miramichi Bay. However, McGrath et al. (1973), 'feel that the Miramichi Bay magnetic anomaly is probably caused by an intrabasement feature since there are no sloping-step anomalies as might be expected at the northern and southern contacts of a graben.' We agree with McGrath et al. (1973) for the following reasons: as previously described, the Tabusintac Lagoon and Miramichi Bay positive magnetic units continue offshore in a northeasterly to east-northeasterly direction for about 50–60 km where they coalesce to form a broad magnetic high (Fig. 12). This broad magnetic high coincides with a gravity low, named the 'North Point Low' by Howie and Cumming (1967). They interpret this gravity low as being caused by about 8000 ft (2.44 km) of Carboniferous and younger sediments and

evaporites underlain by a pre-Carboniferous basement, part of which may be low-density granites. If the North Point gravity low is mainly due to low density Carboniferous sediments and evaporites in a sedimentary basin then the coincident magnetic high probably represents intra-basement magnetization contrasts and is unlikely to be due to a shallowing of the pre-Carboniferous basement surface. Hence, the related Miramichi Bay magnetic high is probably due to intrabasement magnetization contrasts. It may represent a basic intrusive and may be related to the folded volcanics to the north. Rast and Stringer (1974) show Llandovery ocean crust beneath a considerable thickness of Siluro-Devonian sediments in their structural cross section through this area.

Also, the North Point gravity low extends as a weaker, narrow gravity low to the southwest, crossing the coast to the south of Miramichi Bay in the vicinity of Point Escuminac (traced on Fig. 12 from Gravity Map Series No. 149, Department of Energy, Mines and Resources, 1972). Hence, we consider the Carboniferous section under Miramichi Bay to be relatively thin (300–600 m) as suggested by borehole evidence in Howie and Cumming (1967). As a result, stresses affecting Carboniferous rocks in this area are likely to have produced structures closely related to those in the underlying basement rocks possibly as a result of reactivation of basement structures. Thus, the preglacial drainage system may have eroded bedrock channels along joints, faults, or fractures in the Carboniferous rocks in Miramichi Bay, but we prefer the explanation that they represent Carboniferous faults or fractures directly related to the underlying northeast extension of the polygenetic Catamaran Fault zone. Possibly, the southern Miramichi bedrock channel may be the eroded main fault or fracture zone and the Portage Island and Neguac Island channels eroded secondary or splay-fault zones. Alternatively, as previously described, the southern Miramichi channel may be eroded along joints and the other bedrock channels are eroded fault or fracture zones.

Summary and Conclusions

The seismic profiling survey in Miramichi Bay has detected two prominent reflecting horizons. The lower reflector is probably the Pennsylvanian bedrock surface, which has been eroded into at

least three, 35–40 m deep, bedrock channels or Rinnentaler. The direction and linearity of the bedrock channels suggest the pre-Pleistocene drainage system and subsequent glacial over-deepening or the subglacial excavation were controlled by lines of weakness in the bedrock caused by joints, fractures, or faults. Gravity and magnetic maps of the area suggest that the Carboniferous rocks are relatively thin under Miramichi Bay. Structures in the underlying pre-Carboniferous basement rocks are, therefore, likely to strongly affect structures produced in the Carboniferous rocks by post-Carboniferous stresses. Though the southern Miramichi bedrock channel may have been eroded along joints, it is suggested that the channels are eroded along fault or fracture zones in the Carboniferous which are the surface expression of the extension of the Catamaran Fault zone in the underlying basement rocks.

Glacial tills and proglacial sediments overlie the bedrock surface and infill the channels, with some suggestion of layering in places. The upper reflector is an erosional surface which is thought to be a marine terrace with a possible age of about 3000–4500 years BP.

Overlying the upper reflector are mainly acoustically soft muds (the Miramichi muds) in the shallow Miramichi Inner Bay with more sandy deposits near shore, as revealed both on echograms and on seismic profiles. These deposits show that current velocities are relatively low in this part of the Inner Bay. Bedrock is at relatively shallow depths in the near shore area between Oak Point and Burnt Church. Acoustically hard sandy deposits overlie the upper reflector in the barrier islands area and Miramichi Outer Bay. These sandy deposits may be the local equivalent of Kranck's (1971) Buctouche sand and gravel, which is a time transgressive lag deposit formed during the postglacial transgression of the sea. The surface layers of these sandy deposits, deposited or transported at the present time, may be the equivalent of the Egmont sand (Kranck 1971). The barrier islands and the Outer Bay are areas of strong currents. Movement of the sand into the Inner Bay near the southern part of Portage Island is indicated by cross-bedding and sand waves.

A shallow, discontinuous 'gas' reflector was detected in the soft muds of the Inner Bay. It masks all deeper seismic reflectors and is probably the result of the generation of methane by decaying organic material in the sediments. The gas layer, where present, prevents measurement of the true thickness of the soft muds.

Acknowledgements

ALCOCK, F. J. 1948. Problems of New Brunswick geology. Transactions of the Royal Society of Canada, Section 4, Vol. XLII, pp. 1–16.
AMBLER, D. C. 1976. Miramichi River navigation channel study. Surface water and sediment investigation. Water Survey of Canada, Department of Fisheries and Environment, Halifax, N.S.
ANDERSON, F. D. 1972. The Catamaran Fault, North-Central New Brunswick. Canadian Journal of Earth Sciences, 9, pp. 1278–1286.
BHATTACHARYYA, B. K., RAYCHANDHURI, B. 1967. Aeromagnetic and geological interpretation of a section of the Appalachian Belt in Canada. Canadian Journal of Earth Sciences, 4, pp. 1015–1037.
BOSTOCK, H. S. 1970. Physiographic subdivisions of Canada. In Geology and economic minerals of Canada. Chapt. 2. Edited by R. J. W. Douglas. Geological Survey of Canada, Economic Report No. 1, pp. 9–30.
BOUSFIELD, E. L. 1955. Some physical features of the Miramichi Estuary. Journal of the Fisheries Research Board of Canada, 12(3), pp. 342–361.
BURKE, K. B. S., HAMILTON, J. B., and GUPTA, V. K. 1973. The Caraquet Dike: Its tectonic significance. Canadian Journal of Earth Sciences, 10, pp. 1760–1768.
CANADIAN HYDROGRAPHIC SERVICE. 1975. Canadian Hydrographic Chart No. 4423. Department of Environment, Ottawa, Ont.
CHALMERS, R. 1888. Report of the surface geology of northeast New Brunswick. Geological Survey of Canada Annual Report, 1887/1888, Vol. 3, Part N, Map 288.
———— 1894. Report on the surface geology of eastern New Brunswick, northwest Nova Scotia and a portion of Prince Edward Island. Geological Survey of Canada Annual Report. New Series. Vol. 7. Drift Map.
DEPARTMENT OF ENERGY, MINES AND RESOURCES. 1972. Yarmouth-Burgeo, 1 : 1000,000. Earth Physics Branch, Ottawa, Ont.
DEPARTMENT OF PUBLIC WORKS. 1922. In Canadian Hydrographic Service Chart 4423, Miramichi Bay, 1975.
GRANT, D. R. 1970. Recent coastal submergence of the Maritime Provinces, Canada. Canadian Journal of Earth Sciences, 7, pp. 676–689.
HAWORTH, R. T., and MacINTYRE, J. B. 1975. The gravity

and magnetic fields of Atlantic offshore Canada. Geological Survey of Canada, Paper 75-9, Marine Sciences Paper 16.

HOWIE, R. D., and BARSS, M. S. 1974. Upper Palaeozoic rocks of the Atlantic Provinces, Gulf of St. Lawrence, and adjacent continental shelf. *In* Offshore geology of Eastern Canada. Geological Survey of Canada, Paper 74-30, Vol. 2, pp. 35–50.

HOWIE, R. D., and CUMMING, L. M. 1967. Possible basement graben beneath Miramichi Bay, New Brunswick. *In* Geology of the Atlantic Region. *Edited by* E. R. W. Neale and H. Williams. Geological Association of Canada, Special Paper No. 4, pp. 283–292.

HUNTER, G. T., and TRESS, R. G. 1976. Miramichi Channel study comparative shoreline analysis, 1837–1974. Airphoto Analysis Associates Consultants Ltd., Toronto, Ont., Report 75-115.

KEEN, M. J., and PIPER, D. J. W. 1976. Kelp, methane, and an impenetrable reflector in a temperate bay. Canadian Journal of Earth Sciences, 13, pp. 312–318.

KELLEY, D. G. 1970. *In* Geology and economic minerals of Canada. *Edited by* R. J. W. Douglas. Economic Report No. 1, Geological Survey of Canada, pp. 228–304.

KEPKAY, P. E. 1976a. The gas reflector in St. Margaret's Bay. *In* Geology of eastern bays workshop. Bedford Institute of Oceanography, Dartmouth, Nova Scotia.

—— 1976b. Preliminary investigations of the physical controls of gas, as a sub-bottom acoustic reflector, and its distribution in St. Margaret's Bay. *In* Studies of coastal bays in Nova Scotia. *Edited by* D. J. W. Piper and M. J. Keen. Progress report to the Department of Energy, Mines and Resources on research agreement #1135-D13-4-14/76, November, 1976.

KRANCK, K. 1967. Bedrock and sediments of Kouchibouguac Bay, New Brunswick. Journal of the Fisheries Research Board of Canada, 24(11), pp. 2241–2265.

—— 1971. Surficial geology of Northumberland Strait. Geological Survey of Canada Paper 71-53, Marine Science Paper 5.

—— 1972. Geomorphological development and post-Pleistocene sea level changes, Northumberland Strait, Maritime Provinces. Canadian Journal of Earth Sciences, 9, pp. 835–844.

LORING, D. H., and NOTA, D. J. G. 1973. Morphology and sediments of the Gulf of St. Lawrence. Fisheries Research Board of Canada, Bulletin 182.

McGRATH, P. H., HOOD, P. J., and CAMERON, G. W. 1973. Magnetic surveys of the Gulf of St. Lawrence and the Scotian shelf. *In* Earth science symposium on offshore Eastern Canada. *Edited by* P. J. Hood. Geological Survey of Canada, Paper 71-23, pp. 305–324.

MIRAMICHI RIVER STUDY FOR HARBOURS AND RIVERS ENGINEERING BRANCH. 1964. Development Engineering Branch, Department of Public Works, Ottawa, Ont.

NEW BRUNSWICK DEPARTMENT OF NATURAL RESOURCES. 1969. Mineral Resources Branch, Fredericton, N.B. New Brunswick (Geology). Plates 71-1, 71-2, Map 1 : 50 000.

NOVA SCOTIA RESEARCH FOUNDATION CORPORATION. 1974. Report on a subbottom seismic profiling survey over part of the shipping channel in Chedabucto Bay. Report 74-9, 5 p.

—— 1975. Miramichi Estuary, New Brunswick Subbottom profiling of areas proposed for shipping channel realignment, Report 8-75, 10p.

PIPER, D. J. W., and KEEN, M. J. 1976. Geological studies in St. Margaret's Bay, Nova Scotia. Geological Survey of Canada, Paper 76-18

POTTER, R. R., JACKSON, E. V., and DAVIES, J. L. 1968. Geological map of New Brunswick. New Brunswick Department of Natural Resources, Map Number N.R.-1.

RASHID, M. A., VILKS, G., and LEONARD, D. J. 1975. Geological environment of a methane-rich Recent sedimentary basin in the Gulf of St. Lawrence. Chemical Geology, 15, pp. 83–96.

RAST, N., and STRINGER, P. 1974. Recent advances and the interpretation of geological structure of New Brunswick. Geoscience Canada, 1(4), pp. 15–25.

REINSON, G. E. 1976a. Channel and shoal morphology in the entrance to the Miramichi Estuary, New Brunswick. *In* Report of activities, Part C. Geological Survey of Canada, Paper 76-1C, Report 9.

—— 1976b. Surficial sediment distribution in the Miramichi Estuary, New Brunswick. *In* Report of activities, Part C, Geological Survey of Canada, Paper 76-1C, Report 9.

SCHUBEL, J. R. 1974. Gas bubbles and the acoustically impenetrable, or turbid, character of some estuarine sediments. *In* Natural gases in marine sediments. *Edited by* I. R. Kaplan. Plenum Publishing Corp., New York, N.Y. pp. 275–298.

SCOTT, D. B., MEDIOLI, F. S., and SCHAFER, C. T. 1977. Temporal changes in foraminiferal distributions in Miramichi River estuary, New Brunswick. Canadian Journal of Earth Sciences, 14, pp. 1566–1587.

SMITH, C. H. 1957. Bathurst-Newcastle area; Northumberland, Restigouche and Gloucester Counties, New Brunswick. Geological Survey of Canada, Map 1-1957.

SUTHERLAND, J. K. 1976. Size analyses of Miramichi channel sediment samples. Report M/76/254, Research and Productivity Council, Fredericton, New Brunswick.

VILKS, G., RASHID, M. A., and VAN DER LINDER, W. J. M. 1974. Methane in Recent sediments of the Labrador shelf. Canadian Journal of Earth Sciences, 11, pp. 1427–1434.

Acoustic Velocity Measurements in Surficial Sediments of the Beaufort Sea

A. G. McKay
(Durham University, UK)

Abstract

A geotechnical site investigation of a continental shelf area now customarily includes the acquisition of high resolution subbottom profiling information by means of a ship-decoupled or "deep-tow" profiler. Such devices normally comprise an acoustic source of mid-audio frequency together with an appropriate hydrophone or short receiving array mounted on the end of a long tow cable by means of which they can be deployed close to the seabed. In this way, vertical-incidence travel time sections are obtained with enhanced resolution and decreased noise as compared with surface-tow devices. The author has previously reported improvements to such tools, which can be made by extending their acoustic receiving capability from single to multiple channel over an appropriate horizontal spread in order to observe reflexions at various angles and so derive interval velocities in sediment layers.

Experience during the summer of 1982 in the Beaufort Sea (Canadian Arctic) indicates that it is possible, without disrupting their basic profiling function, to extend further the use of such deep-tow profilers for the observation of headwaves in appropriate sediment conditions, namely when sediment acoustic velocity increases to ca. 1.10 times that of the bottom water within a few metres of the seabed. This method allows acoustic velocity to be determined in areas where the lower boundary of a sediment layer cannot be discerned sufficiently precisely to allow the use of the wide angle reflexion method. In Arctic regions the possibility of ice-bonding in seabed sediments is a potential engineering hazard. The identification of ice-bonding with anomalously high compressional wave velocities makes the measurement of that parameter important in these areas. Sixty measurements of acoustic velocity were made in a region of 45m. water depth. No unequivocal measurement of a velocity indicative of ice-bonding was found there.

The Beaufort Sea

The Beaufort Sea forms a section of the Northwest Passage to the north of the Yukon and Northwest Territories of Canada. As a navigable sea it is bounded by the permanent polar pack ice, whose summertime front is usually roughly coincident with the edge of the continental shelf. As a geological province, the Beaufort is normally taken to extend farther north and west to include the continental slope from the shallow shelf break at 100m. to the abyssal plain of the western Arctic Ocean (fig. 1).

As a potentially viable source of hydrocarbons, the Beaufort Sea has attracted considerable attention over the last decade. In the 1982 open-water season from late June to early November, four drillships were on station. Artificial islands have been built as drilling platforms in nearshore areas to depths of ca. 15m., and more elaborate platforms comprising a berm raised to within 10m. of the sea surface capped by a sand-filled caisson are being built
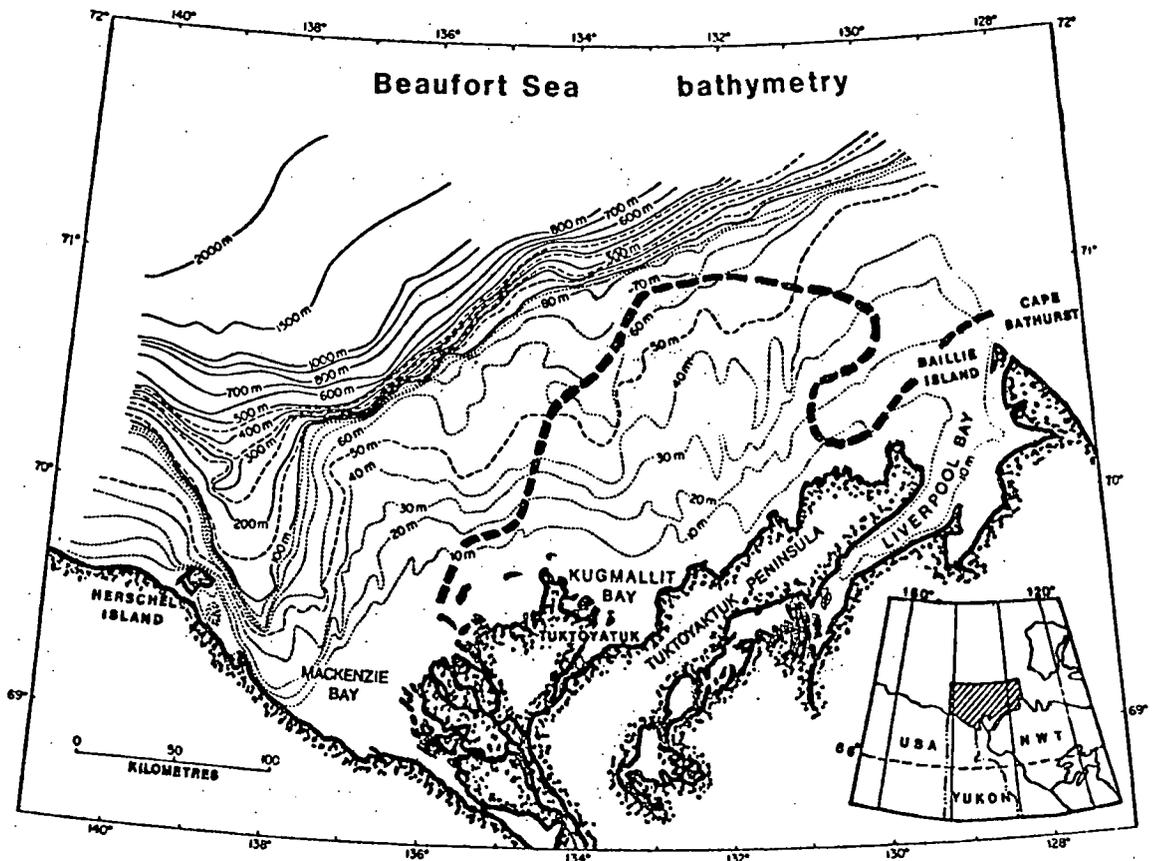
Fig. 1.   The Beaufort Sea. Bathymetry   Pelletier (1975).   The heavy
dashed line (the MacAulay Line) indicates the seaward limit of
deep acoustic permafrost as determined from high velocities found
by Neave et al. in a re-interpretation of oil industry seismics.

in 40m. of water (McCreath et al., 1982). These very large engineering works
require geotechnical information for the safe and efficient mining of aggregate
and its resiting on new foundations. This information is obtained by convention-
al bottom sampling techniques and drilling supplemented by the traditional
geophysical methods of subbottom profiling and sidescan sonar, to give indication
of sediment distribution.

Post-glacial change in sea level is a dominant factor in controlling the
pattern of surficial sedimentation.   The Beaufort lay on the periphery of the
Laurentide ice sheet centred over Hudson Bay (Andrews, 1973) and has experienced
subsidence following the release of pressure from that central area. The gradual
marine transgression and the relatively long open-water season have allowed the
reworking of coastal fluvio-glacial deposits and resulted in the general pattern
where fines, reworked and carried seawards from a later shoreline, overlie the
lag sands reworked from an earlier one (C.P. Lewis and D.L. Forbes, 1974).   This
pattern is modified by the encroaching sedimentation from the discharge of the
MacKenzie River (Pelletier, 1975).

Permafrost

MacKay et al. (1972) have described land permafrost conditions around the Tuktoyaktuk Peninsula, and on the basis of sediment structures, suggest that the mean annual ground temperature has not risen above 0°C for at least 40 000 years. As the marine transgression is more recent that this, relict sub-sea permafrost was to be expected on the Beaufort Sea shelf and its presence was confirmed in 1974 by drilling in Kugmallit Bay. Hunter and Hobson (1975) measured high acoustic velocities in the seabed sediments and showed that this indicated ice-bonding. A subsequent re-interpretation of oil-industry deep-seismic reflexion records with pre-emphasis of those headwave arrivals in the early part of the seismogramme which are suppressed in more conventional data analysis allowed Neave et al. (1978) to produce a map of ice-bonding and found that sediments affected in this way occur in a region seaward of the Tuktoyaktuk Peninsula as shown in fig. 1. The upper surface of this continuous zone of ice-bonding generally is at least 50m. below the seabed, and this deep-seated ice forms a large reservoir of potential fresh water which can be released by local change in the thermal regime to migrate upwards through the overlying unbonded sediments and refreeze on approaching closer to the seabed, where the bottom water is always below 0°C. That processes of this nature do occur is confirmed by the observation of such spectacular manifestations as the sub-sea pingos which have been described by Shearer et al. (1971). These are volcano-shaped ice-cored moated mounds, which can rise abruptly over 10m. above the general level of the seabed. Less obvious features such as small lenses of bonded or partially bonded sediment may occur at shallow depth below the seabed and Hunter, in the light of experience with seabottom arrays for use in small scale seismic refraction experiments (Hunter et al., 1979), has suggested that it may be possible to make the necessary observations with towed rather than seabed equipment and so realise the ability of doing areal surveys for near-seabed velocities, with the aim of detecting ice bonding.
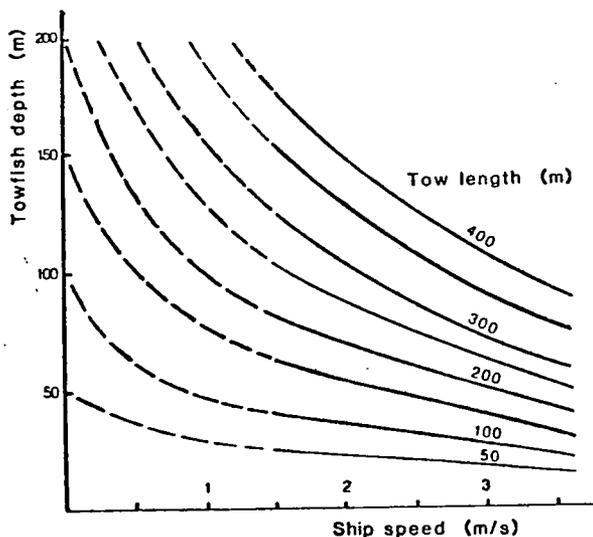
Fig. 2. Curves to show towing depth for different cable lengths and tow speeds (after Bidgood, 1973).

Methods of acoustic velocity measurement

Maries and Beckman (1961) reported the use of high resolution sparker equip-
ment to measure compressional wave velocity by the observation of headwave arrival
time while the separation between source and receiver was varied. The technique
is often useful in shallow sheltered water, but the author has found it
ineffective in water deeper than about 25m. (Howells and McKay, 1977) even when
the velocity contrast at the seabed is great, because the acoustic signal from a
spark discharge source of a few hundred joules is too weak for easy detection at
the required offset distance. To observe headwaves as first arrivals at shorter
offset distances, it becomes necessary to keep the acoustic source and receiver
closer to the seabed. Technology which can approach what is required was
developed over a decade ago in the form of deep-tow subbottom profilers (Speiss
and Tyce, 1973; Bidgood, 1973), but was slow in taking the rather small
evolutionary step required to convert these profilers into proper seismic systems
capable of observing a reflected sound field at many points with different source
to receiver offset. The explanation for the stunting of this natural develop-
ment is a little hard to discover. It appears probable that the greatly
clarified sections which these profiling machines offerred, when compared with
their ancestral surface-tow devices[1] , were so eagerly accepted by sediment-
ologists for preparing detailed surficial geology maps that the profiler makers
and operators, finding themselves in profitable demand, saw little reason for
change even in light of Mayer's (1980) observation of interference reflectors or
the requirements of sediment characterisation schemes (Hamilton, 1980) which need
measurements of velocity and attenuation. Progress towards attenuation measure-
ment from towed survey equipment has been accomplished by Dodds (1980) and
Tyce (1981), but the methods of velocity determination used by Porter et al.
(1974) or Bennell (1978) with surface equipment, although shown adaptable by
McKay during field trials in 1978, have yet to be implemented in commercial deep-
tow equipment. A device which does incorporate a hydrophone array for velocity
determination is that of the U.S. Naval Ocean Research and Development Activity.
(Fagot et al., 1982). The preliminary design of this equipment (Fagot, 1979)
omits the hydrophone which should be placed immediately adjacent to the acoustic
source to facilitate the location of that source relative to the other receivers
by the observation of acoustic arrivals. Field trials of this equipment are to
be reported elsewhere in this volume and this criticism may be answered there.

McKay and McKay (1982) have described additions to an existing commercial
deep-tow subbottom profiler which permitted the making of rudimentary wide-angle
reflexion profiles in water depths to 240m. with the equipment towed 30m. above
the seabed. It will be apparent from figure 2 that, although this towing height
is sufficient to allow for minor fluctuations in ship speed, it would not be
possible to approach significantly closer to the seabed without risk unless the
water depth were appreciably less, or the acoustic equipment were towed by a
vehicle capable of flying at constant altitude above the seabed, such as the
'Bottom-Referencing Underwater Towed Instrument Vehicle' developed at the
St. Andrews Biological Station in New Brunswick.

[1] It is not the purpose of this paper to discuss fully the
merits and drawbacks of the deep-tow method in making vertical-
incidence profiles, but it should be pointed out that in water
depths of less than 100m., and in good weather conditions, the
strong water-surface reflexion of a deep-tow acoustic source
may obscure more subbottom information than will the multiple
reflexion from a weakly reflecting seabed of the signal from a
surface-towed source.

Modified headwave arrival method as applied in the Beaufort Sea

The shelf area of the Beaufort Sea is relatively shallow water and advantage may be taken of this to fly acoustic equipment within a few metres of the seabed, given prior knowledge of the bathymetry, a ship with good speed control and continuous vigilance at the remote controls of the winch which winds the main tow cable. This approach puts the seismic equipment where it is needed for velocity determination (figures 3 and 4). The horizontal offset for the trailing receiver was 40m., chosen in the light of previous experience with different equipment in coastal waters off Cape Breton Island (McKay, 1979). Figure 5 shows super-imposed on one another in their proper time relationship the signals received at the two hydrophones. In the zone between **b** – the seabed, and **d** – the direct water wave , can be seen an ordinary vertical incidence section showing two main sediment units separated by the prominent reflector **S** . The arrival **SW** is the wide-angle reflexion at the trailing hydrophone from the reflector .**S**. The travel times to these reflectors together with the water-surface reflexions **Sv** and **Sw** can be used to find the average velocity in the composite layer com-prising that part of the water column below the trigger event **T** and the upper sediment unit, between **b** and **S** . From this, a value for the velocity in the upper sediment unit is found, by a modified form of Green's (1938) method. The result at the location of this figure shows the upper layer to have the same velocity as the bottom seawater to within an experimental error of ca. 3%.

At a location some 20km. away, the upper sediment layer is much thinner. A closer approach to the seabed with the acoustic equipment brought about the appearance of a headwave (figure 6). The arrival time of this mode of acoustic propagation can be used to find the p-wave velocity by a method given by the author (1982). The position of the remote receiver is first calculated from the surface reflexions **Sv, Sw** by the expression (see fig. 4) :

$$h = \frac{(b + c)^2 - d^2}{4a}$$

The travel time of the headwave propagating along ABCD (fig. 4) is :

$$T = \frac{(h_1 + h_2)}{v_1 \cos \theta_1} + \frac{x}{v_2}$$

where v_1 and v_2 are the velocities in upper and lower media, and θ_1 is the angle between AB^2 or CD and the vertical. Expressing x in terms of h_1 , h_2 and d and writing v_2 as $v_1 / \sin \theta_1$ leads to :

$$0 = (h_2 + h_1) \cos \theta_1 + (d^2 - (h_2 - h_1)^2)^{\frac{1}{2}} \sin \theta_1 - v_1 T$$

to give θ_1 and thence v_2 .
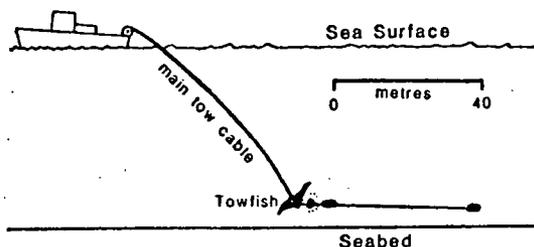
Fig. 3 Towing configuration.
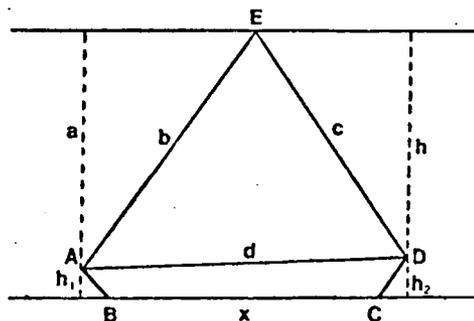
Fig. 4 Geometrical raypaths.
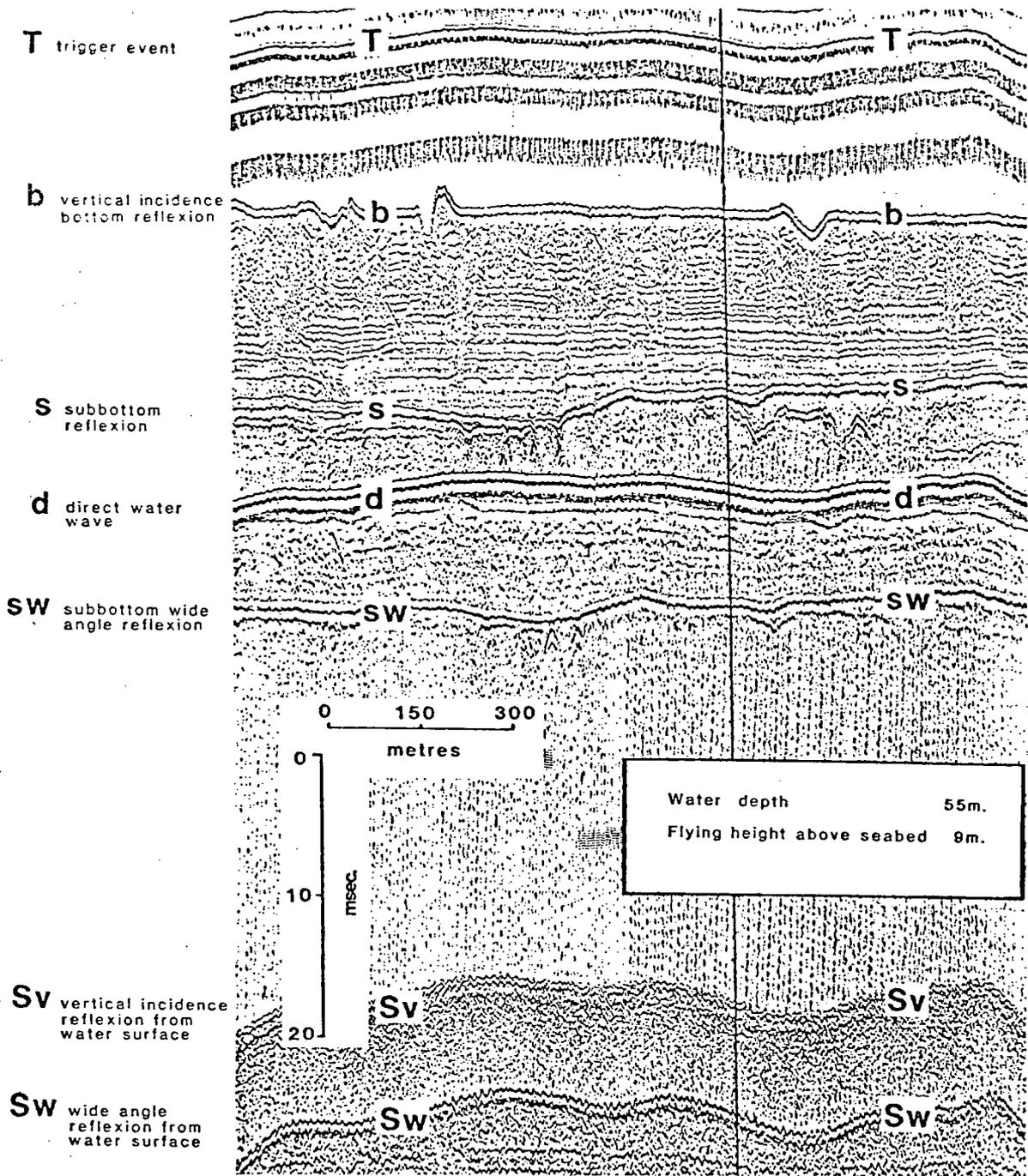
Fig. 5. This figure shows acoustic arrivals in variable density format. Signals received by the hydrophone close to the acoustic source and by the hydrophone remote from it are superimposed. The phase of arrivals **b**, **s** and **Sv** is inverted by the recording instrumentation. The phase of **Sv** and **Sw** is inverted by reflexion at the water surface.

T trigger event

b vertical incidence bottom reflexion

s subbottom reflexion

h headwave arrival

d direct water wave

| Water depth | 45m. |
| Flying height above seabed | 4m. |

Sv vertical incidence reflexion from water surface

Sw wide angle reflexion from water surface
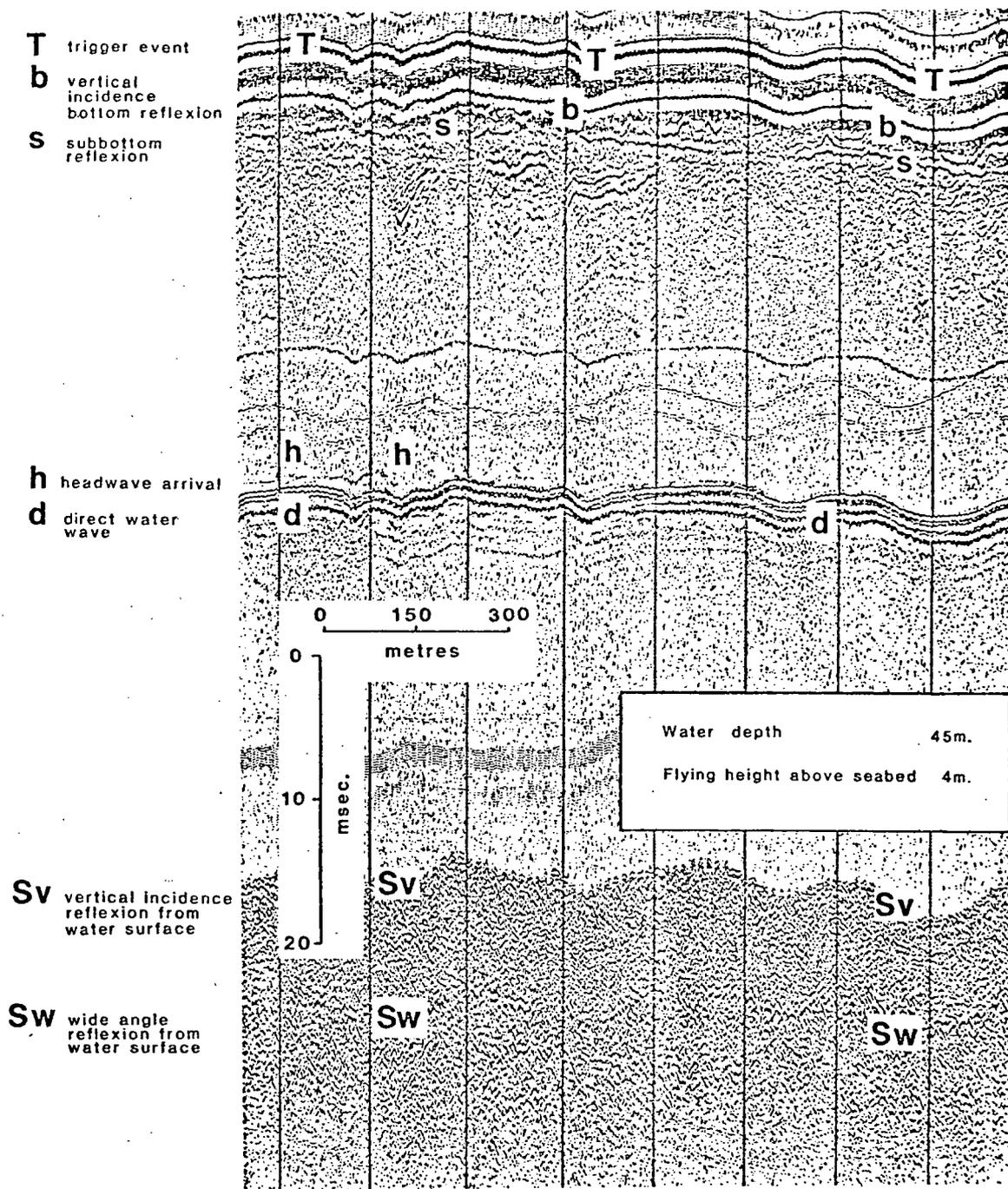
Fig. 6.   Arrivals are displayed and labelled as in fig. 5, but here can be seen a headwave arrival **h – h** coming in a little ahead of the direct arrival through the water **d – d**.   Because of the low flying height, about 4m. off bottom, the arrival of both bottom and subbottom reflexions follows too closely behind the direct arrival to be distinguishable from it.   Rougher sea conditions than for fig. 5 result in less clear surface reflexions **Sv**, **Sw**.

The ability of the acoustic equipment to accommodate only two hydrophone channels means that some assumption must be made as to which interface is associated with the observed headwave. In most instances the smoothe horizontal reflector **S** is the only reasonable possibility, but in some cases underlying layers are seen (e.g. near the centre of fig. 6) which may give rise to ambiguity. A total of 60 measurements have been made and the velocity for the lower layer is 1.13 times that of the seabottom water, with an experimental error of 3%. There is no definite indication of any velocity in the range above 1800 m/s. which would suggest partial ice bonding. In some cases, the choice of a deeper surface as the refracting interface leads to velocities above 2000 m/s., but there is no striking evidence for preferring the deeper surface to the shallower. Clearly, the ambiguity would be removed from these cases if a multichannel receiving array were available. It will be equally clear that such an array should be of cheap and robust construction in order to give the operator confidence in pursuing the investigation in the greatest possible depth.

Conclusions

It is possible to tow a spark-discharge acoustic source and hydrophone receivers very close to the seabed for the measurement of sediment velocities by a modified seismic refraction method, at the same time as a conventional vertical-incidence profile is being made. The method is applicable when the compressional wave velocity is greater than 1.10 times that of the bottom water in sediments within a few metres of the seabed. The values obtained in the small survey area are consistent but do not indicate ice bonding there at shallow depth. The method is applicable to velocity determination for other purposes, but requires refining to eliminate ambiguities and reduce measurement error. Such improvements could be achieved by the use of a multichannel receiving array. Extension of the method to deeper water would require a bottom-skimming tow vehicle and, beyond about 300m., a different type of acoustic source.

Acknowledgements

References

Bennell, J.D.   (1978). Seismic velocity gradients in sea floor sediments. Geol. Rep. 78-1, Marine Science Laboratories, Menai Bridge.

Bidgood, D.E.T.   (1973). A deep-towed sea bottom profiling system. Proc. Oceans 74 IEEE conf. 2. 96-107.

Dodds, D.J.   (1980). Attenuation estimates from high resolution subbottom profiler echoes. In : NATO Saclant Conference on Bottom-interacting Ocean Acoustics. Plenum Press.

Fagot, M.G. and Eckstein, B.E.   (1979). Deep-towed geophysical array development program. Progress report. Naval Ocean Research and Development Activity. Report No. NORDA-TN-41 ; NTIS No. AD-A073-903.

Fagot, M.G., Spychalski, S.E. and Gholson, N.H.   (1982). Deep Towed Seismic System : a hardware description. In: proc. S.E.G. 52nd. Annual Meeting. 130-133.

Green, C.H. (1938). Velocity determination by means of reflection profiles. Geophysics, 3, 295-305.

Hamilton, E.L. (1980). Geoacoustic modeling of the sea floor. J. Acoust. Soc. Am., 68, 1313-1340.

Howells, K. and McKay, A.G. (1977). Seismic profiling in Miramichi Bay, New Brunswick. Canadian J. Earth Sci., 14, 2909-2927.

Hunter, J.A. and Hobson, G.D. (1975). A seismic refraction method to detect sub-seabottom permafrost. In: Proceedings of the Symposium on Beaufort Sea Coastal and Shelf research. Arctic Inst. of N. America, San Francisco, California. 401-416.

Lewis, C.P. and Forbes, D.L. (1974). Sediments and sedimentary processes, Yukon Beaufort Sea coast. Terrain Sciences Division, Geological Survey of Canada report no. R57-38/1975.

Maries, A.C. and Beckman, W.C. (1961). A new geophysical method for the exploration of undersea coalfields. Mining Engineer, Jan 1961 262-275.

Mayer, L.A. (1980). Deep-Sea Carbonates : Physical property relationships and the origin of high-frequency acoustic reflectors. Marine Geology, 38, 165-183.

McCreath, D.R., Hodge, W.E. and Harrington, A.G. (1982). Geotechnical design considerations for the Gulf Oil mobile Arctic caisson, Beaufort Sea. In : proceedings of the second Canadian conference on Marine Geotechnical Engineering. Natl. Res. Council.

MacKay, J.R., Rampton, V.N. and Fyles, J.G. (1972). Relic Pleistocene Permafrost, Western Arctic, Canada. Science, 176, 1321-1323.

McKay, A.G. (1978). Observation of wide-angle reflections and refractions from a high resolution engineering seismic source. Geophys. Prospect. 16, 673 (abstract)

McKay, A.G. (1979). Acoustic velocity determinations from humpback refractions. Maritime Sediments, 15, (abstract).

McKay, A.G. and McKay, P.M. (1982). Compressional wave velocity measurement in seabed materials by use of equipment deployed near but above the bottom. J. Acoust. Soc. Am., 71, 871-878.

Neave, K.G., Judge, A.S., Hunter, J.A. and MacAulay, H.A. (1978). Offshore permafrost distribution in the Beaufort Sea as determined from temperature and seismic observations. In : Current Research, Part C, Geological Survey of Canada, Paper 78-1C, 13-18.

Pelletier, B.R. (1975). Sediment dispersal in the southern Beaufort Sea. Tech. Rep. 25a, Beaufort Sea Project, Geological Survey of Canada, Victoria B.C.

Porter, W.J., Bell, D.L. and Britton, L.C. (1974). Multichannel towed arrays for remote measurement of marine sediment acoustical properties. Offshore Technol. Conf., Dallas. Paper no. OTC 2015. American Institute of Mining, Metalurgical and Petroleum Engineers.

Shearer, J.M., MacNab, R.F., Pelletier, B.R. and Smith, T.B. (1971). Submarine Pingos in the Beaufort Sea. Science, 174, 816-818.

Tyce, R.C. (1981). Estimating acoustic attenuation from a quantitative seismic profiler. Geophysics, 46, 1364-1378.

AN ANOMALOUS SEISMIC FEATURE

IN THE SEABED SEDIMENTS OF

CHEDABUCTO BAY, NOVA SCOTIA AND

ITS IMPLICATIONS FOR HIGH

RESOLUTION SEISMIC PROFILING

A. G. McKay
Geophysics Division
Nova Scotia Research Foundation Corporation
100 Fenwick Street, Dartmouth, Nova Scotia

Introduction

During October 1974 a bathymetric and seismic survey of a shoal

area in Chedabucto Bay was done by the Nova Scotia Research Foundation

for the engineering consultants FENCO and Whitman, Benn & Associates

who were preparing a joint report for the Nova Scotia Department of

Development on the future facilities likely to be required by shipping

in the Strait of Canso. The purpose of the seismic work in conjunction

with a sediment sampling survey was to assess the feasibility of

dredging the approaches to the Strait, so that planned harbour

facilities in the inner part of the Strait might be located in an

appropriate water depth. The conclusion reached from the

investigations was that dredging was perfectly feasible should it ever

be required to allow the passage of oil tankers even larger than the

350,000 tonners which can navigate the existing natural channel in

safety.

A feature of particular geological interest appeared on the

seismic reflection records. Although it was alluded to in the original

survey report, it lay at a depth below what was of immediate

engineering interest and was not fully described. The feature

is of some importance to the understanding both of the local geology in

Chedabucto Bay and the interpretation of high resolution vertical

incidence profiles in general.

Survey Area and Methods

The seismic and bathymetric survey, done with a 44 ft. "Cape Island" style fishing boat was carried out in the area shown in Fig. 1. A Del Norte Instruments microwave positioning system operated by Integrated Survey Systems was used for navigation. The survey lines (Fig. 2 were arcs centred on each of the two shore stations (A and B in (Fig. 1) Position fixes were taken at 150 m intervals along the lines. The seismic records were made with a 6 metre hydrophone array receiving signals from a 24-tip sparker of about the same length, fired at 400 J twice per second. The seismic method revealed two sediment layers overlying an irregular surface considered to be rock or glacial till (Fig. 3). A sediment sampling program was undertaken following the seismic survey. This was done with a Benthos piston corer operated by Integrated Survey Systems of Halifax. The core sites were chosen by the consulting engineers with a view to obtaining samples of the seabed material to the depths to which dredging might be undertaken. For this reason core barrels longer than 30 feet were not used. However, some consideration was given to penetrating the lower sediment layer by locating three of the coring sites at points where, going on the seismic evidence, the core barrel might reach it, even though it was not expected that dredging of the lower layer would ever be contemplated. Altogether, fourteen cores were obtained ranging in length from 5 to 9 metres. The three cores expected to penetrate the lower sediment layer failed to bring up significant samples of it, but

the fact that the nose cone of the corer was damaged in all of these three, but in no other locations, gives a good indication that it is a much harder material than the upper layer. A pebble recovered from the nose cone of core no. 11 (Fig. 2) is the sole object believed to have been retrieved from the lower sediment layer.

Sections of the cores of the upper layer were analysed by Geocon of Fredericton for grain size distribution, wet density, shear strength, porosity, organic content and Atterberg limits. (See, e.g., Hough[1](1957) for definitions of the various parameters used to describe the engineering properties of a sediment).

With the exception of core no. 11, all of the samples were classified as brown to grey sandy silt with black streaks and an organic odour. Shear strength, from a vane test measurement, varied from 490 to 1860 kg m^{-2}. Porosity ranged from 28 to 43% with an average of 38%. Wet density ranged from 1575 to 1907 kg/m^3 and averaged 1781 kg/m^3. All samples had low to medium plasticity and all had a natural water content greater than the liquid limit. Two samples were tested for organic content by baking at 800°C for three hours, a treatment which reduced the dry weight by 4% in both of them. A summary of the grain size distribution is given in Fig. 4 and Fig. 5 shows the mean grain size found at different depths and locations. There is no very obvious pattern in the data on grain size, but core no. 11 does show by far the coarsest material sampled from the upper layer.

insignificant contributors of sediment compared to the coastal erosion

of glacial till cliffs. Gradual marine transgression allowed the

reworking of this ill-sorted material, the coarser materials being left

in the beach zone, while the fines were carried off farther seawards.

The continuation of this process led in time to two layers of recent

sediment in many regions of the Scotian Shelf. These ideas appear

quite adequate to explain the sedimentation of the part of Chedabucto

Bay discussed in this paper. That is to say (referring to Fig. 3) the

stratified layer of sediment between reflectors 1 and 2 represents the

coarser fractions of the reworked till. The very flat upper surface of

this layer (Figs. 3, 6) would result from the gradual submergence

of a beach zone. Subsequent deposition of the upper sediment layer

formed a mound of finer sediment on top of the flat surface. (Compare

Figs. 6, 7, 9). This mound of fine sediment suggests that during

its deposition the shallow part of the survey area experienced no net

flow at the seabed either landwards or seawards during the stronger

tidal regime which prevailed before the closing of the Canso Causeway

(O'Halloran and Mills, 1975).

Origin of Sediments

The effects of the eustatic rise in sea level which has accompanied glacial retreat have been augmented in Nova Scotia by tectonic subsidence of a type attributed to the differential unloading of an elastic lithospheric plate supported by a viscous substrate. In this process, investigated by Clark et al.[2] (1978), regions subjected to heavy loading by great thicknesses of ice can, on the melting of ice, be expected to recoil more or less in accordance with the old isostatic principle, but lightly-burdened peripheral regions will behave in a more complex manner, usually emerging at first and sinking later, a finding which is at variance with older theories. Current experimental work on the faunas of salt marsh deposits around the Maritime Provinces by D. Scott,[3] F. Medioli[4] and others and theoretical work by C. Beaumont (personal communications) suggests that in the Chedabucto Bay area, subsidence would have been the predominant movement, although a small initial emergence is possible. Grant[5] (1970) has suggested that the rate of relative rise in sea level during the past 1000 to 2000 years has averaged about 16 cm per century. The average rate over the 15,000 years or so which have elapsed since the existence of a shoreline at a depth of 120 m (Milliman & Emery[6]), 1968; MacLean, Fader and King,[7] 1977) is appreciably greater, at about 80 cm per century. The controlling influence which these sea level changes have had on sedimentation on the Scotian Shelf has been discussed by King[8] (1967), and by MacLean et al.[7] (1977). They regard rivers as

Gasified Sediments

One of the most prominent characteristics of the subsurface which the survey revealed was a large area of acoustic turbidity. The appearance of this phenomenon on a seismic cross section is shown in Fig. 8 and its areal extent is shown by the stippled markings in Fig. 9. It has become common practice to interpret such a feature as evidence for the presence of gas in the sediments, the general idea being that the large density and acoustic velocity contrast between water-saturated sediment and gas can be expected to produce scattered reflections within the gasified layer and the attenuation or obscuring of reflections from deeper interfaces. The existence of bay and estuarine fine-grained sediments which are almost impenetrable to seismic signals of frequency above a few hundred Hz has been known for some time. Schubel[10](1974) gives a detailed account of such phenomena in Chesapeake Bay, but points out that most shallow water profiling is done on a consulting basis without publication of the results; and that in consequence, although generally believed to be widespread, the location and extent of such acoustically turbid sediments is "largely unknown". This observation may still be a valid one, although there have been more descriptions given of the locations of such sediments since the publication of Schubel's work. For example, from coastal localities around the Canadian Maritime Provinces there have been accounts given of extensive acoustically turbid sediments in St. Margaret's Bay, Nova Scotia (Keen and Piper,[11]1976; Piper and Keen,[12] 1976); in the Miramichi Estuary, New Brunswick (Howells and McKay,[13] 1977); in Chedabucto Bay (MacLean et al., 1977) and in Sydney Harbour, Cape Breton (McKay,[14] 1979). Rawson[15](1976) has described acoustic turbidity in parts of the

U.K. Continental Shelf. The author has also observed such sediments at other localities in the Maritimes, viz. Halifax Harbour, Bedford Basin, Mahone Bay, Morien Bay and at Gabarus. D. Taylor Smith (personal communication) has observed in the Irish Sea an acoustic masking reflector which proved to be due not to gasification, but to a very high density of bivalve shells which formed an impenetrable layer a few metres below the seabed. Thus it is important to exercise some caution in identifying acoustic turbidity with gasification.

The profiles obtained in Chedabucto Bay are a little different in appearance from what is found in most other localities in that although the characteristic acoustically turbid appearance is obvious, subbottom reflectors can still be seen. It seems to be more usual for all deeper reflectors to be completely obscured where acoustically turbid sediment is found. That they were not obscured in this case was indeed fortunate from the point of view of compiling the report on the feasibility of dredging (O'Halloran and Mills[9], 1975; McKay[16], 1974). It also helps to give some insight into a potential problem which is usually ignored in the interpretation of high resolution vertical incidence seismic reflection data. It has become more usual to assume than to measure the acoustic velocity in seabed sediments surveyed by high resolution seismic equipment. Often the velocity assumed is that of the seawater, which can be a good value to use, for it is likely that the real acoustic velocity is within 10 or 15% of that value. Even if such an accuracy is not good enough, the examination of a few bottom samples will allow the making of an estimate to within about 5% of the true value for at least the uppermost layer, by recourse to the extensive literature on the subject of relating acoustic properties of

sediments to their mechanical properties (e.g., Hamilton, 1975[17], 1978[18]).

Lateral variations in sediment type can usually be picked up on the seismic cross section, and bottom samples taken from suitable locations can be used as indicators of any lateral change in acoustic velocity. However, in areas where gas is present in the sediment, none of these considerations is applicable. Wood's[19] (1930) theoretical treatment of the transmission of sound in turbid media is applicable to the problem of gas in sediments, provided bubble size and acoustic frequency are such that resonance phenomena are not encountered. His treatment is simply to derive a mean compressional-wave velocity for the gasified sediment:

$$C = \sqrt{\frac{E}{\rho}} \tag{1}$$

on the basis of mean density ρ and elasticity E where

$$\rho = x\rho_1 + (1-x)\rho_2 \tag{2}$$

and

$$\frac{1}{E} = \frac{x}{E_1} + \frac{(1-x)}{E_2} \tag{3}$$

where x is the fraction of gas and the subscript "1" refers to the gas and "2" to the gas-free sediment.

Equation 3 arises by considering a reduction in volume ΔV of the gasified sediment as a result of increase in pressure Δp. Clearly:

$$\Delta V = \Delta V_1 + \Delta V_2$$

also $\quad \Delta V = \dfrac{V \Delta p}{E}; \quad \Delta V_1 = \dfrac{V_1 \Delta p}{E_1}; \quad \Delta V_2 = \dfrac{V_2 \Delta p}{E_2}$

from which equation 3 follows directly.

This leads to values of less than 100 m/sec. for most possible gas-sediment mixtures, the reason for the very low value being that in the mixture the gaseous phase dominates the value of the mean elasticity whereas the non-gaseous phases dominate the density. From the sedimentological point of view the most interesting part of the graph (Fig. 10) of acoustic velocity versus gas content is the part covering gas concentrations of less than 0.1%: as gas content increases from zero to 0.1%, the acoustic compressional wave velocity decreases by a factor of between 2 and 5 depending upon whether the sediment has a high or low shear modulus. Anderson and Hampton[20] (1980) show that the factor 2 would be typical for sands, the factor 5 for clays. (These figures apply at a pressure of 1 atmosphere. The compressibility of gas varies with the ambient pressure in accordance with the elementary gas laws, the effect being that at higher pressures, the curves of Fig. 10 would be displaced to the right.)

These considerations are of great importance in interpreting vertical incidence seismic profiles. As an example, two different

interpretations of the profile shown in Fig. 8 are given in Figs. 11 and 12. Figure 11 is the interpretation which we get by assuming sediment velocities constant across the profile. Figure 12 results from assuming that the upper sediment reflector is more or less level across the profile and that the apparent dip in it is a result of a velocity anomaly. (The deep trough in reflector 2 which occurs around fix mark 29 gives quite a striking example of just how independent of topography in that lower reflector is the behaviour of the upper reflector).

The lowering of the acoustic velocity in the overlying sediment needed to account for such an apparent dip would be about 40% at the deepest part of the depression (fix mark 26). At the ambient pressure of about 3 1/2 atmospheres exerted by the overlying water column, this effect could be brought about by the presence of about 0.05% by volume of gas in the sediment. There is not usually any way of deciding from such a vertical incidence profile which of the two (or indeed of any number of intermediate) interpretations is the more likely to be correct. One could argue that a real increased thickness of sediment is responsible for the increased production of gas (at a level too low to affect the acoustic velocity), and its appearance on the profile. However there is a feature on one profile which suggests to the author that a depressed velocity may be the more likely explanation in this instance. This feature is shown in Fig. 13 and comes from the part of the survey area near the site of core no. 11 (Fig. 2), where the upper sediment layer was of a coarser material than usual (Figs 4 and 5). Two possible interpretations of this feature are given in Figs. 14 and 15. If one accepts the sloping reflectors a-a, b-b, c-c as evidence

of foreset bedding, then the interpretation given in fig. 15, an interpretation which allows variation of acoustic velocity, seems to be the more plausible. If the dip in the main reflector were real, we might reasonably expect bedding in the upper layer to resemble a pattern such as that indicated in fig. 16 rather than that in fig. 14. Some indication of the way the feature develops can be gathered from parallel survey lines, and this is illustrated in figure 17. The general appearance of fig. 13 was not, however, duplicated on another survey line. Many other lines define the area where the reflector dips sharply, but none of these shows cross-bedding. This situation clearly shows how mis-interpretation of subbottom features can easily arise when the only seismic investigation which has been made is a vertical-incidence survey — the currently accepted standard. Even the existence of irregular talweg in an apparent buried channel would not necessarily rule out that interpretation of a subbottom seismic feature. Drainage channels in areas like the eastern Canadian seaboard can have complex topography either as a result of fluctuating sea-level after the retreat of the Wisconsin ice-sheet or else from their earlier use as rinnentäler (D.J.W. Piper et al.[21]). The feature in Chedabucto Bay which has just been described might as easily be taken for a geomorphological depression as for a zone of decreased seismic velocity were it not for the chance evidence from the foreset bedding indicating that the latter interpretation is the more likely. The elongate shape of the feature is easier to explain as a structurally controlled seepage of gas from underlying

rocks of the upper Carboniferous than as a zone of increased

biogenic activity in the recent sediments.

Conclusion.

This information from Chedabucto Bay clearly shows how

indeterminacy or error can arise from relying on conventional high

resolution vertical incidence reflection profiles for defining

seabed conditions. It is clear that appropriate methods for the

evaluation of the acoustic p-wave velocity are required as a first

step in improving this situation.

REFERENCES.

1. B.K. Hough   Basic Soils Engineering. Ronald Press Co.
                       (1957).

2. J.A. Clark, W.E. Farrell and W.R. Peltier.
                       "Global changes in postglacial sea level: A
                       numerical calculation" Quaterny Reasearch,
                       9 p 265-287. (1978).

3. D.B. Scott and F.S. Medioli.
                       "Vertical zonations of marsh foraminifera as
                       accurate indicators of former sea levels."
                       Nature 272 p 528-531 (1978).

4. D.B. Scott and F.S. Medioli.
                       "Post-glacial emergence curves in the
                       Maritimes determined from marine sediments
                       in raised basins". Proc. Canadian Coastal
                       Conference, Burlington. (1980).

5. D.R. Grant.   "Recent coastal submergence of the Maritime
                       Provinces, Canada." Canadian J. of Earth
                       Sciences, 7, p 676-689. (1970).

6. J.D. Milliman and K.O. Emery.
                       "Sea levels during the past 35,000 years."
                       Science, 162, p 1121-1123 (1968).

7. B. MacLean, G.B. Fader and L.H. King.
                       "Surficial geology of Canso Bank and adjacent
                       areas." Geological Survey of Canada
                       paper no. 76-15. (1977).

8. L.H. King.   "Use of a conventional echo-sounder and
                       textural analyses in delineating sedimentary
                       facies: Scotian Shelf". Canadian J. of Earth
                       Sciences, 4, p 691-708. (1967).

9. D.P. O'Halloran and R.G. Mills
                       "Strait of Canso entrance channel study."
                       Report to the Nova Scotia Department of
                       Development. (1975).

rocks of the upper Carboniferous than as a zone of increased

biogenic activity in the recent sediments.

Conclusion.

This information from Chedabucto Bay clearly shows how

indeterminacy or error can arise from relying on conventional high

resolution vertical incidence reflection profiles for defining

seabed conditions. It is clear that appropriate methods for the

evaluation of the acoustic p-wave velocity are required as a first

step in improving this situation.

<u>REFERENCES.</u>

1.   B.K. Hough   Basic Soils Engineering. Ronald Press Co.
                              (1957).

2.   J.A. Clark, W.E. Farrell and W.R. Peltier.
                      "Global changes in postglacial sea level: A
                      numerical calculation" Quaternary Reasearch,
                      9 p 265-287. (1978).

3.   D.B. Scott and F.S. Medioli.
                      "Vertical zonations of marsh foraminifera as
                      accurate indicators of former sea levels."
                      Nature 272 p 528-531 (1978).

4.   D.B. Scott and F.S. Medioli.
                      "Post-glacial emergence curves in the
                      Maritimes determined from marine sediments
                      in raised basins". Proc. Canadian Coastal
                      Conference, Burlington. (1980).

5.   D.R. Grant.   "Recent coastal submergence of the Maritime
                      Provinces, Canada." Canadian J. of Earth
                      Sciences, 7, p 676-689. (1970).

6.   J.D. Milliman and K.O. Emery.
                      "Sea levels during the past 35,000 years."
                      Science, 162, p 1121-1123 (1968).

7.   B. MacLean, G.B. Fader and L.H. King.
                      "Surficial geology of Canso Bank and adjacent
                      areas." Geological Survey of Canada
                      paper no. 76-15. (1977).

8.   L.H. King.   "Use of a conventional echo-sounder and
                      textural analyses in delineating sedimentary
                      facies: Scotian Shelf". Canadian J. of Earth
                      Sciences, 4, p 691-708. (1967).

9.   D.P. O'Halloran and R.G. Mills
                      "Strait of Canso entrance channel study."
                      Report to the Nova Scotia Department of
                      Development. (1975).

10. J.R. Schubel.   "Gas bubbles and the acoustically impenetrable, or turbid, character of some estuarine sediments." Contribution no. 188 of the Chesapeake Bay Institute of the John Hopkins University. (1974)

11. M.J. Keen and D.J.W. Piper.
                        "Kelp, methane and an impenetrable reflector in a temperate bay." Canadian J. of Earth Sciences, 13, pp.312-318. (1976).

12. D.J.W. Piper and M.J. Keen.
                        "Geological studies in St. Margaret's Bay, Nova Scotia." Geological Survey of Canada, paper 76-18 (1976).

13. K. Howells and A.G. McKay.
                        "Seismic profiling in Miramichi Bay, New Brunswick." Canadian J. of Earth Sciences, 14, pp.2909-2927. (1977).

14. A.G. McKay.   "Depth sounding and seismic profiling survey, Sydney Harbour." Report no 79-1, Geophysics Division, Nova Scotia Research Foundation. (1979).

15. S. Rawson.   "An investigation into the occurrence of acoustic turbidity in marine sediments of the U.K. continental shelf." Tech. report 65, L.G.S.,Marine Geophysics Unit, Edinburgh, U.K. (1976).

16. A.G. McKay.   "Report on a sub-bottom seismic profiling survey over part of the shipping channel in Chedabucto Bay." Report no. 74-9, Geophysics Division, Nova Scotia Research Foundation. (1974).

17. E.L. Hamilton.   "Acoustic and related properties of the sea floor: density and porosity profiles and gradients." U.S. National Technical Information Service no. AD-A016-243. (1975).

18. E.L. Hamilton.   "Sound velocity-density relations in sea-floor sediments and rocks." Journal of the Acoustical Society of America, 63 (2), pp 366-377. (1978).

19. A.B. Wood.   A Textbook of Sound. G. Bell and Sons Ltd., London. (1930).

20. A.L. Anderson and L.D. Hampton.
    "Acoustics of gas-bearing sediments. (II) Measurements and models." Journal of the Acoustical Society of America 67(6), pp1890-1903. (1980).

21. D.J.W. Piper et al.
    Geological Survey of Canada paper.
    (in preparation).

22. A.L. Anderson.   "Acoustics of gas-bearing sediments." Tech. Rep. 74-19Q (ARL-TR-74-19) Appl. Res. Lab., The University of Texas at Austin.
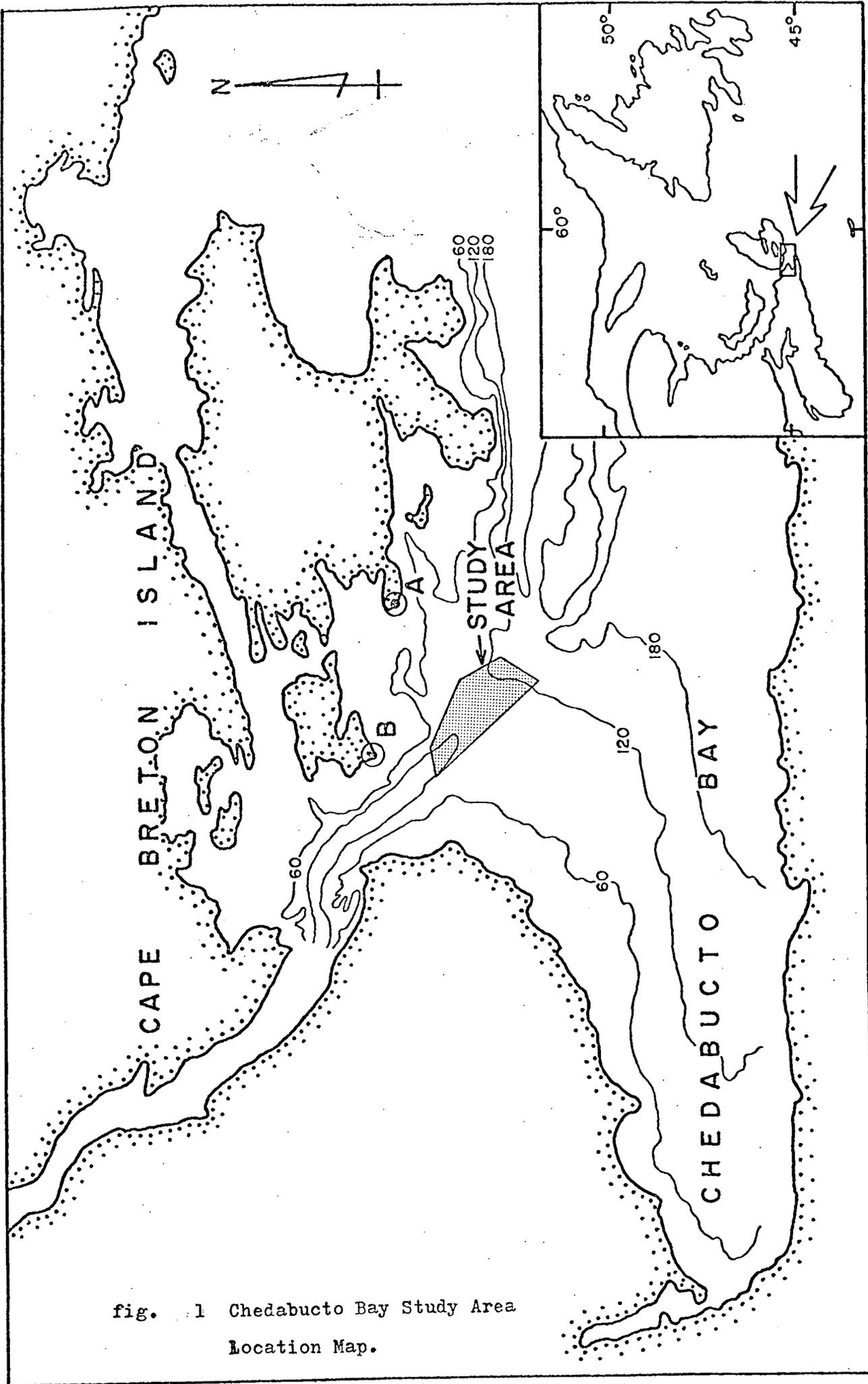
fig. 1 Chedabucto Bay Study Area
Location Map.
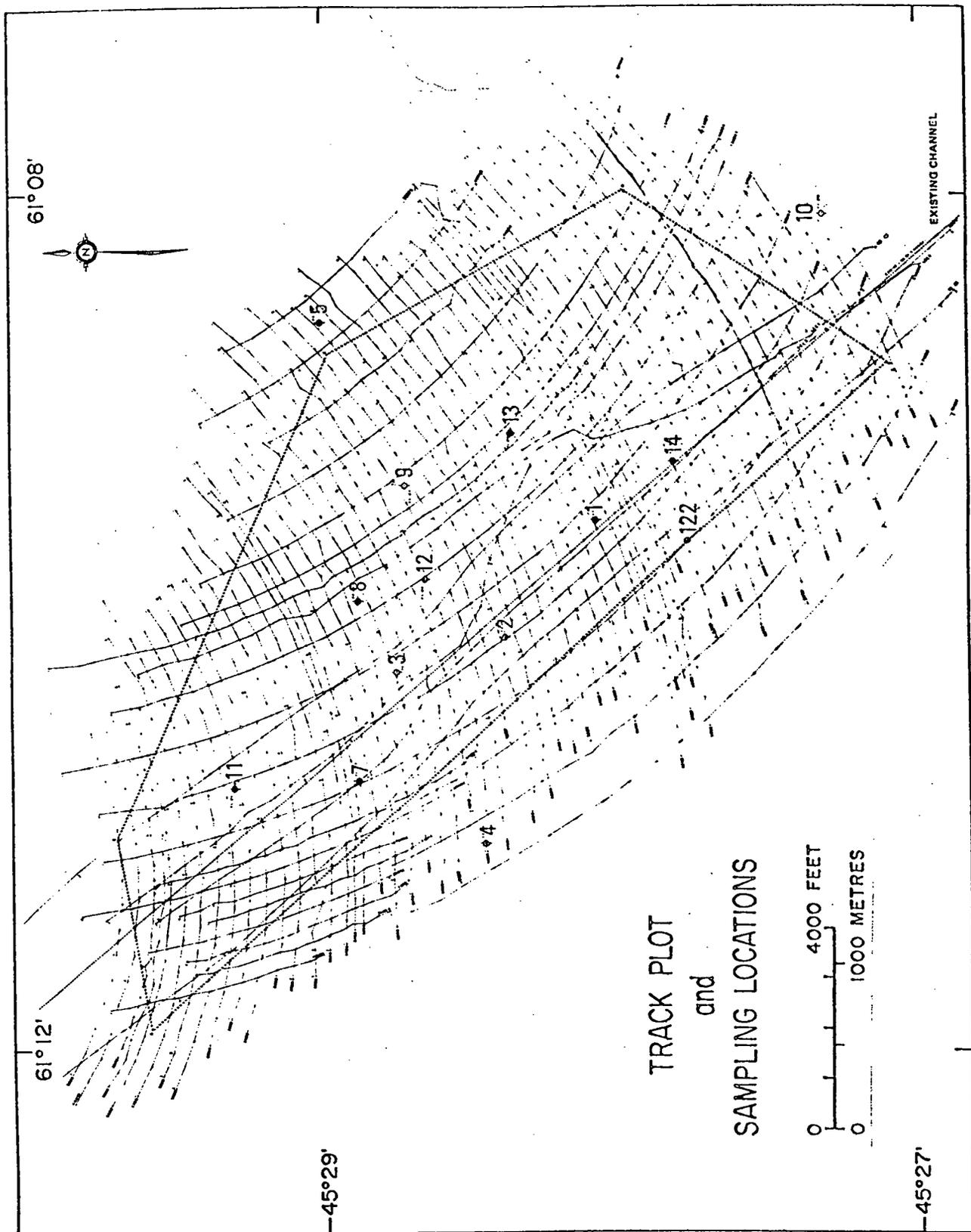
fig .2　Chedabucto Bay。Track plot and sample locations。

Approx. horizontal scale (feet)

0   1000   2000

| 7 | 8 | 9 | 10 | 11 |

0

10

20

30

Vertical scale (msec.)

Seabed

Reflector 1

40

Reflector 2

50

60

Multiple
reflections
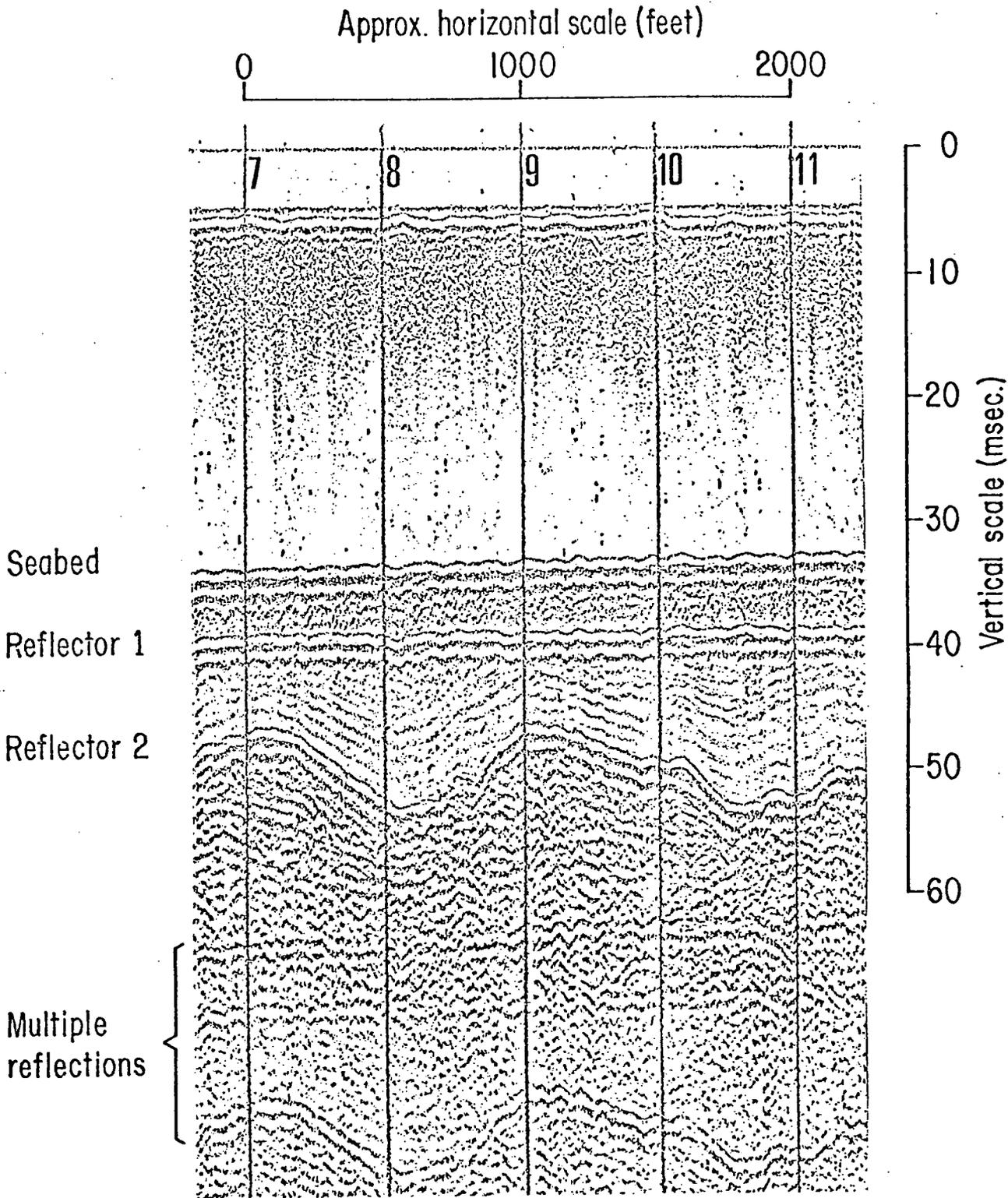
fig. 3   Typical vertical incidence profile
           from the seismic survey.
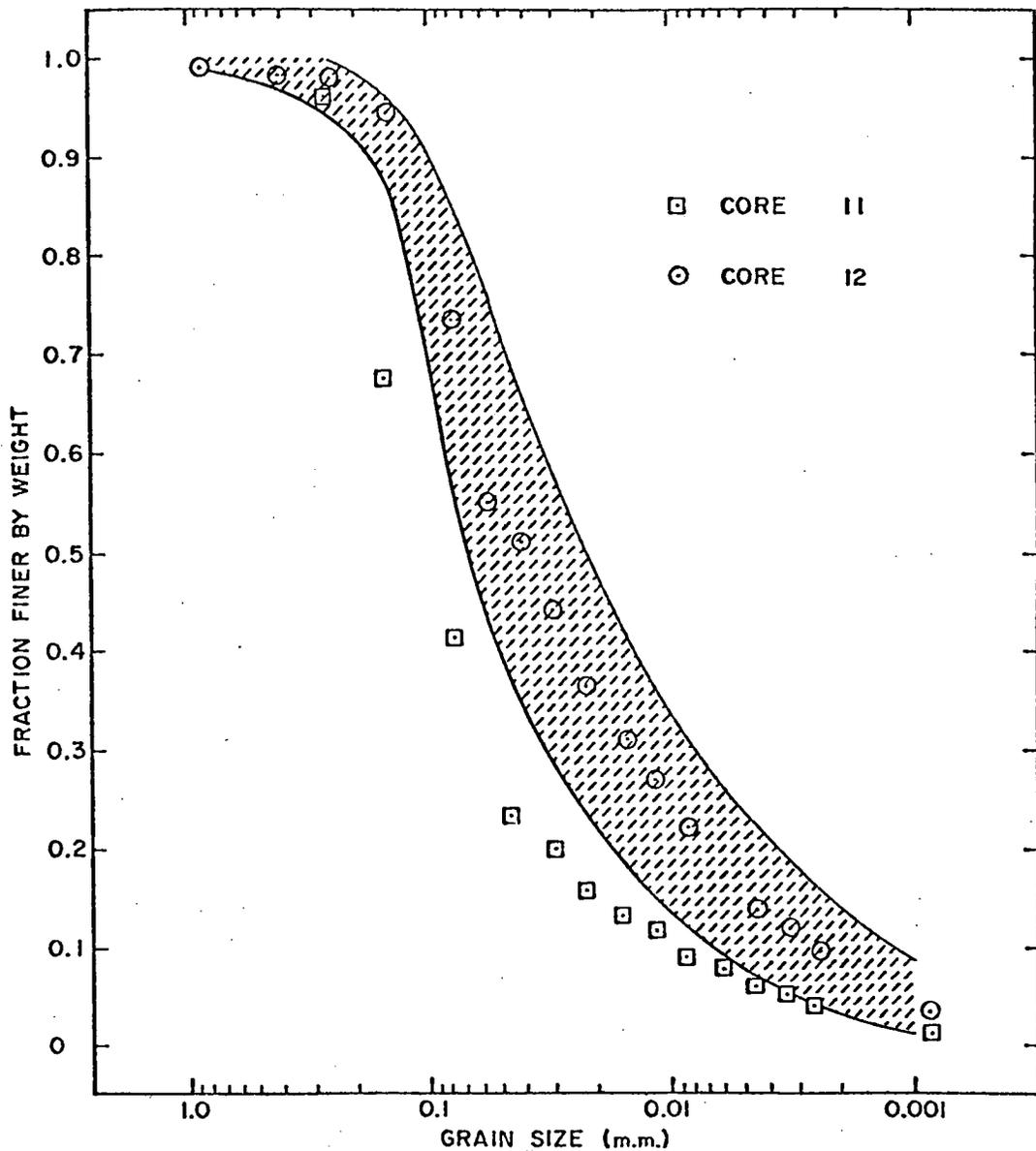
fig   4

Cumulative curves to show the grain size distribution from
piston core samples. Most of the samples lie within the shaded
area and core 12 is shown as a typical example.   The exception
was core 11 which had an appreciably coarser grain size.
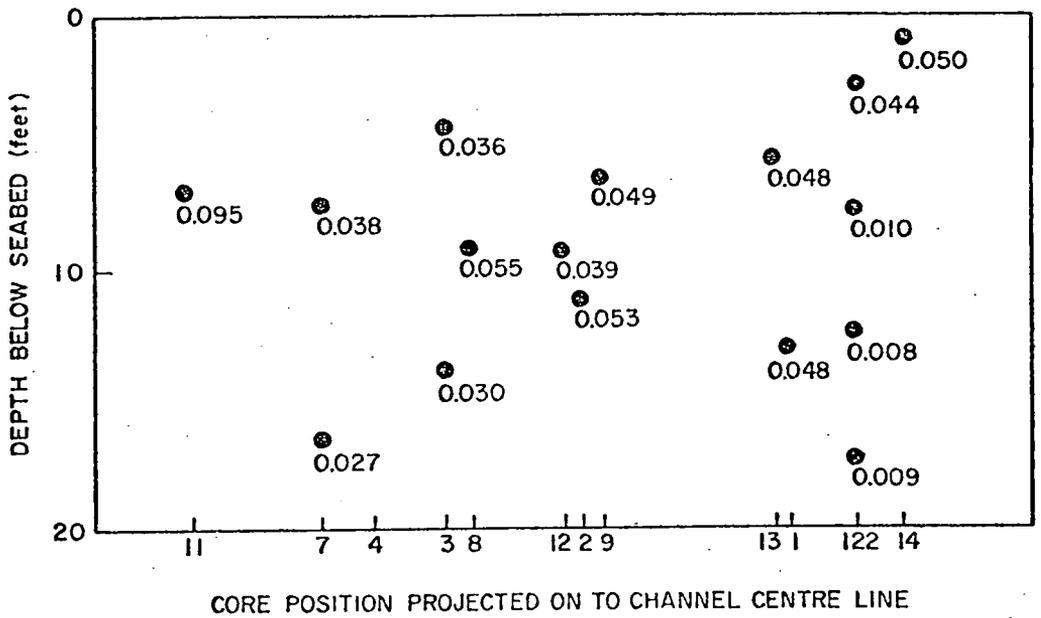
fig 5   Mean grain size at different depths and sample
         locations. The horizontal location of each
         core is projected on to the centre line of the
         channel. Grain size in mm.
         (see fig. 3.2 for actual sample locations)

TOP OF LOWER
SEDIMENT LAYER

(CONTOURS IN FEET)

AREAS WHERE LOWER SEDIMENT
LAYER DOES NOT OCCUR

EXISTING CHANNEL

61° 08'

61° 12'

45° 29'

45° 27'

4000 FEET

1000 METRES

4000

1000

0

0

fig.   6   Map showing depth below datum of the top of the
lower sediment layer. Datum is L.W.O.S.T.
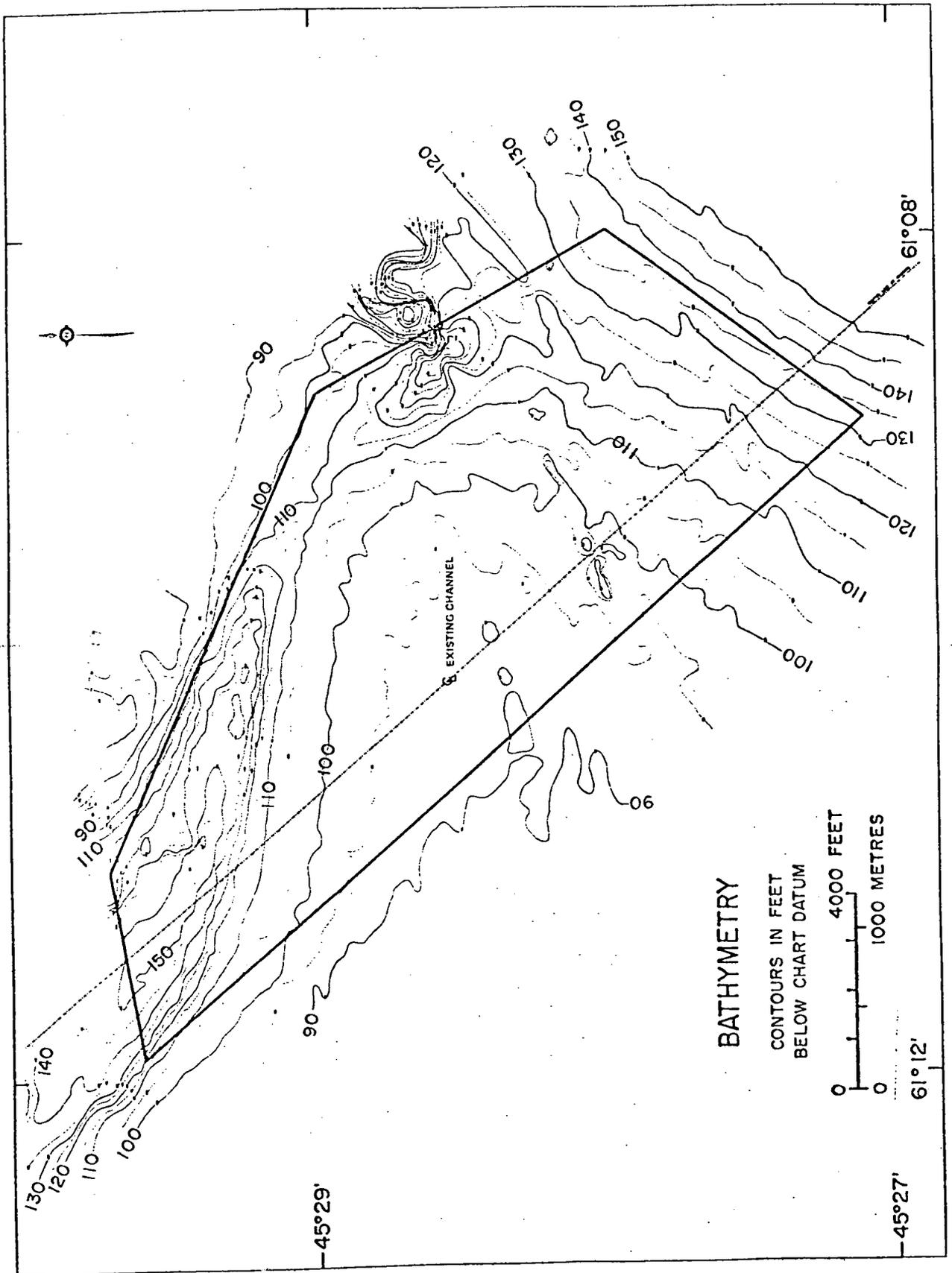
fig. 7 Bathymetry.
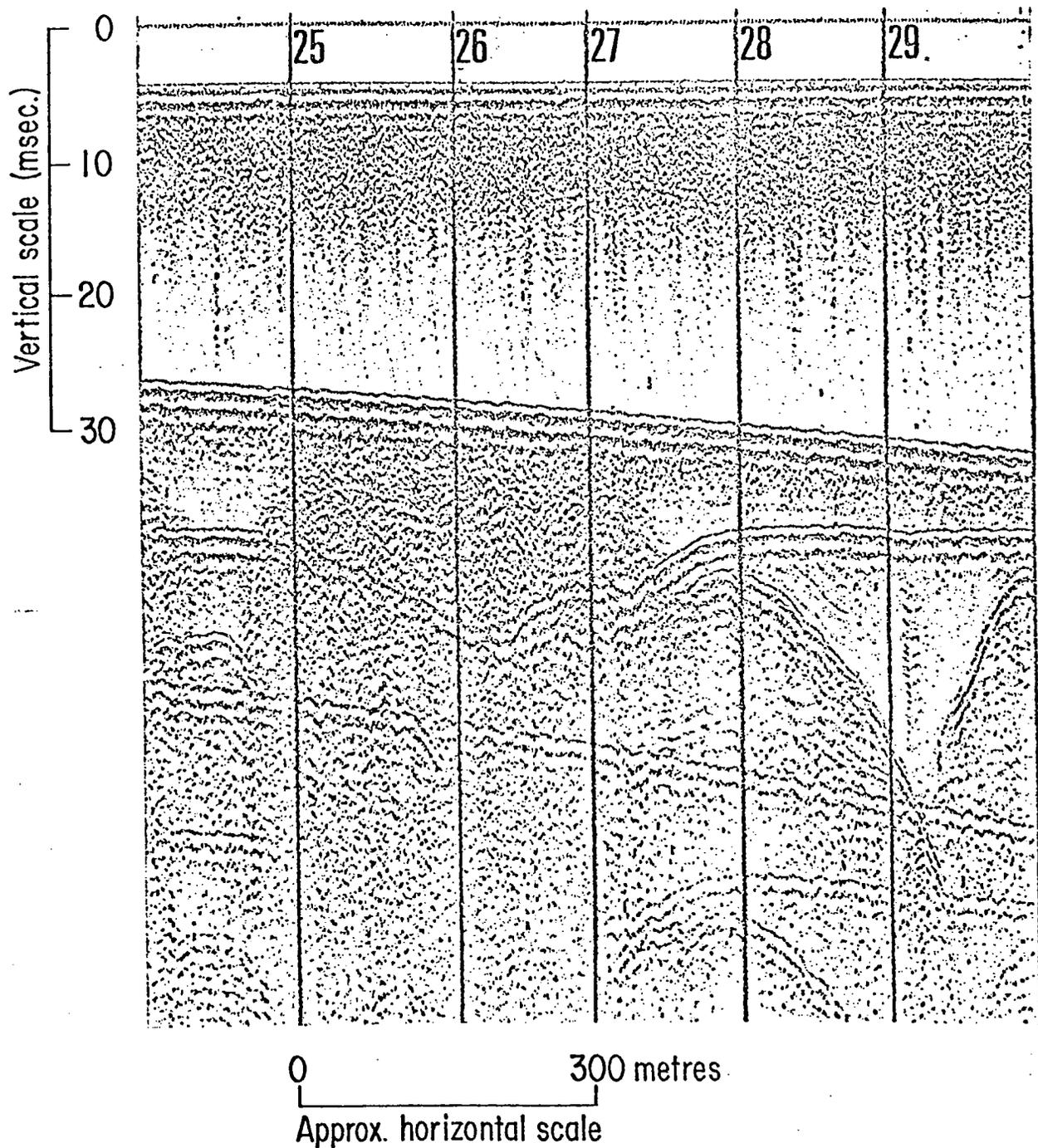
fig. 8 The appearance of gasified sediment as seen on
        a seismic cross section. Vertical scale is two-
        way travel time (msec.).

EXTENT of GASIFIED SEDIMENT

CONTOURS SHOW UPPER SEDIMENT LAYER THICKNESS (feet)

4000 FEET

1000 METRES
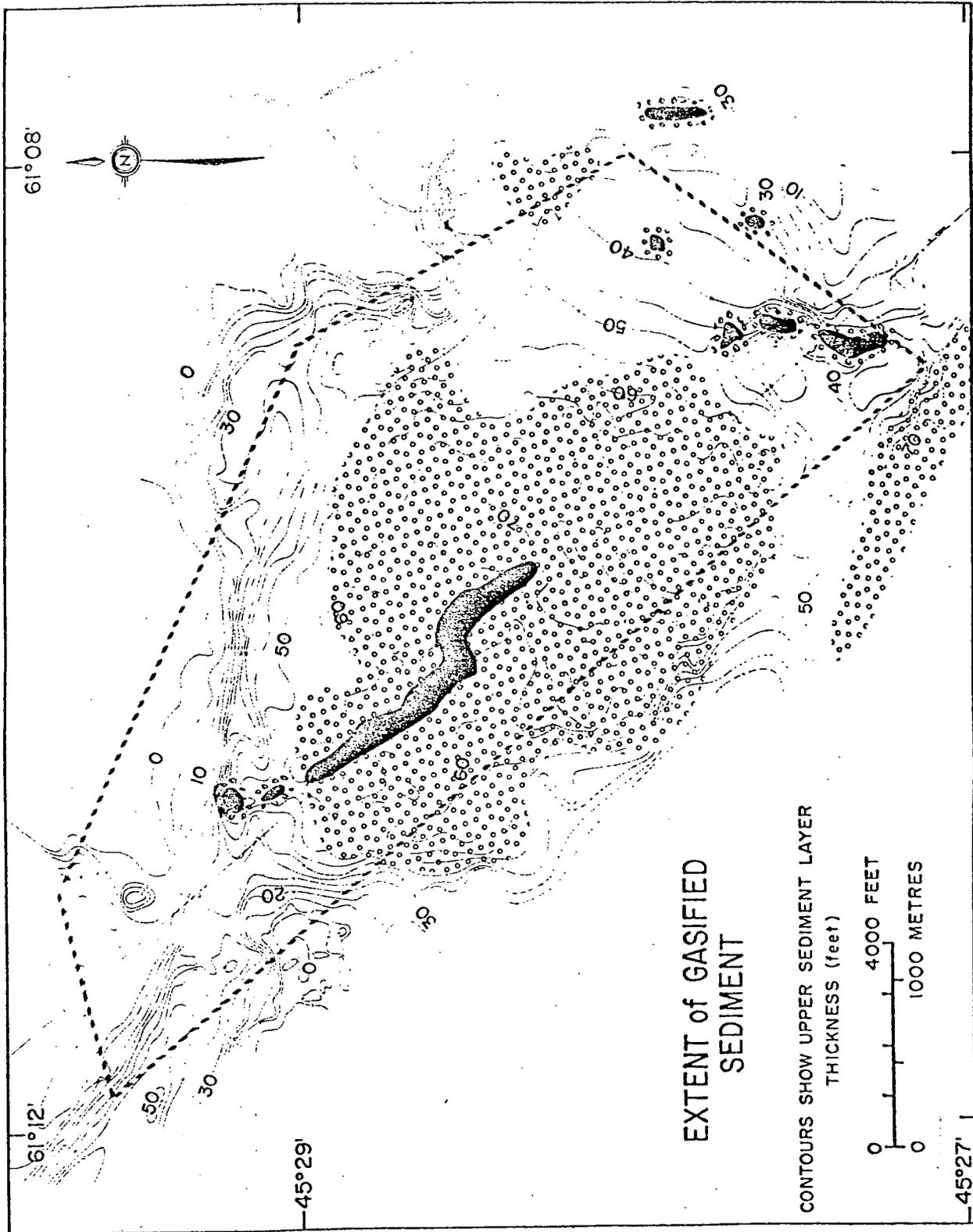
fig.   9 The extent of gasified sediment is shown by the stippling superimposed on this map of the thickness of the upper sediment layer. The areas shown in black are either depressions in the top surface of the lower sediment layer or else zones of increased gasification (sufficient to cause the depressing of the acoustic velocity by 15% or more).
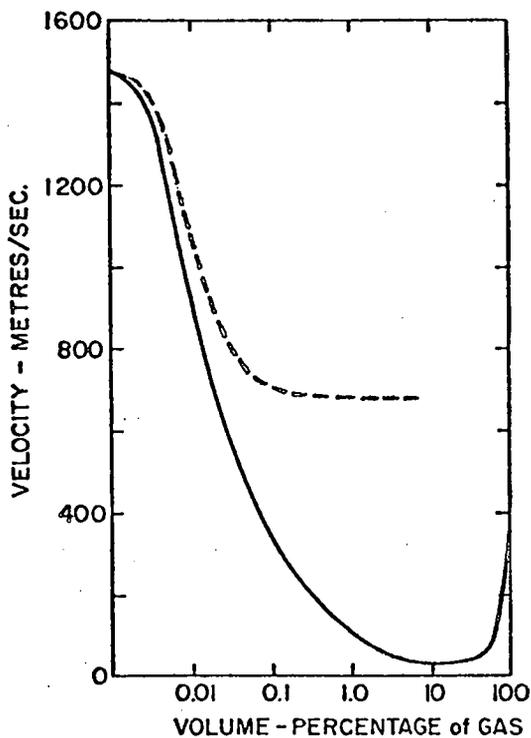
fig. 10.

The variation of compressional wave velocity with gas

content, following the treatment of Wood[19](1930) for a fluid

sediment (solid line). Anderson[22](1974) incorporated the

effect of a non-zero shear-modulus for the sediment. The

dashed line shows the variation in compressional wave

velocity which he predicts when the shear modulus is 0.4 x

10^{10} dyne/cm^2.
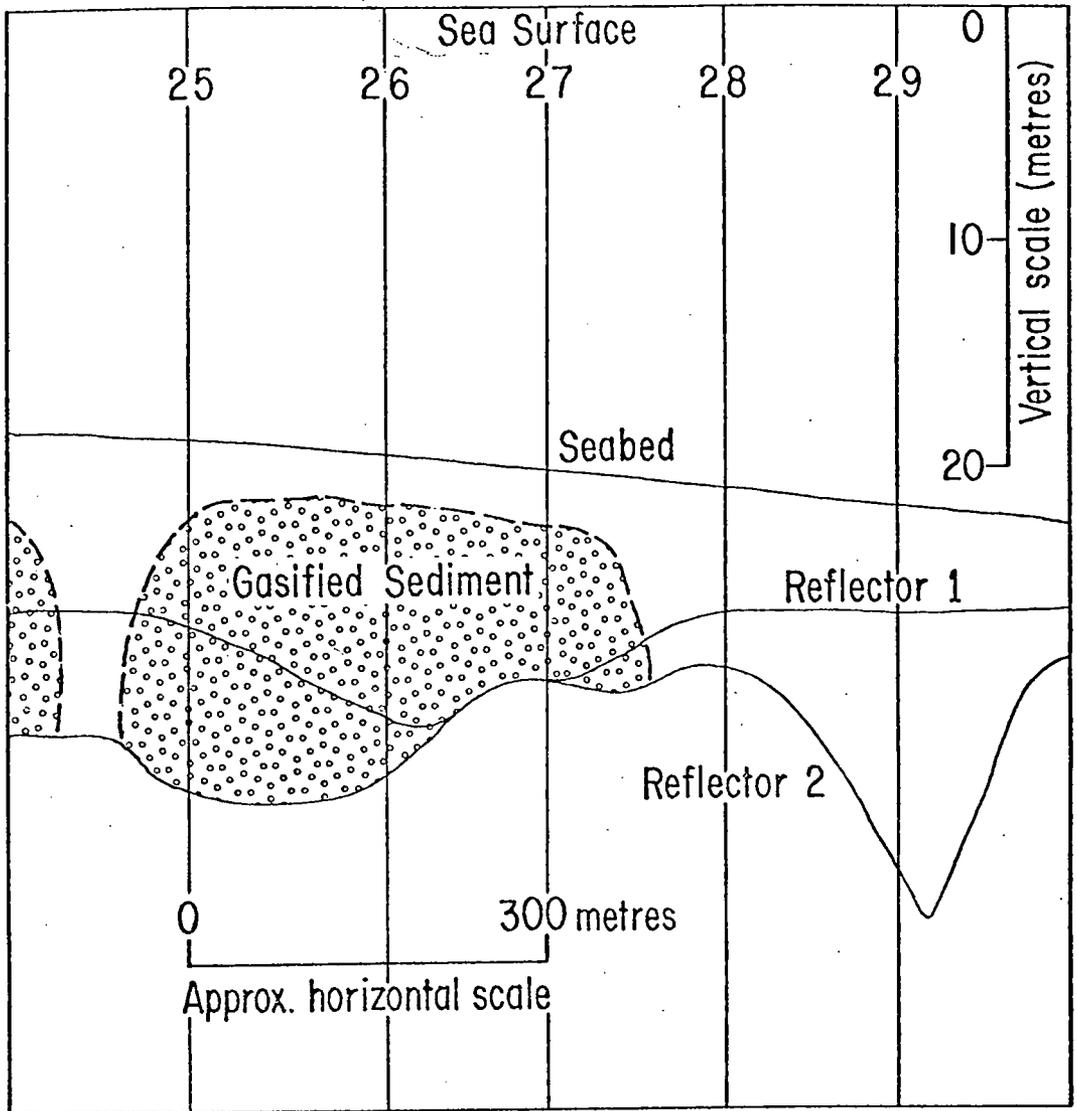
fig. 11 An interpretation of the profile in fig. 8 made
on the assumption that compressional wave velocities
are constant across the profile.
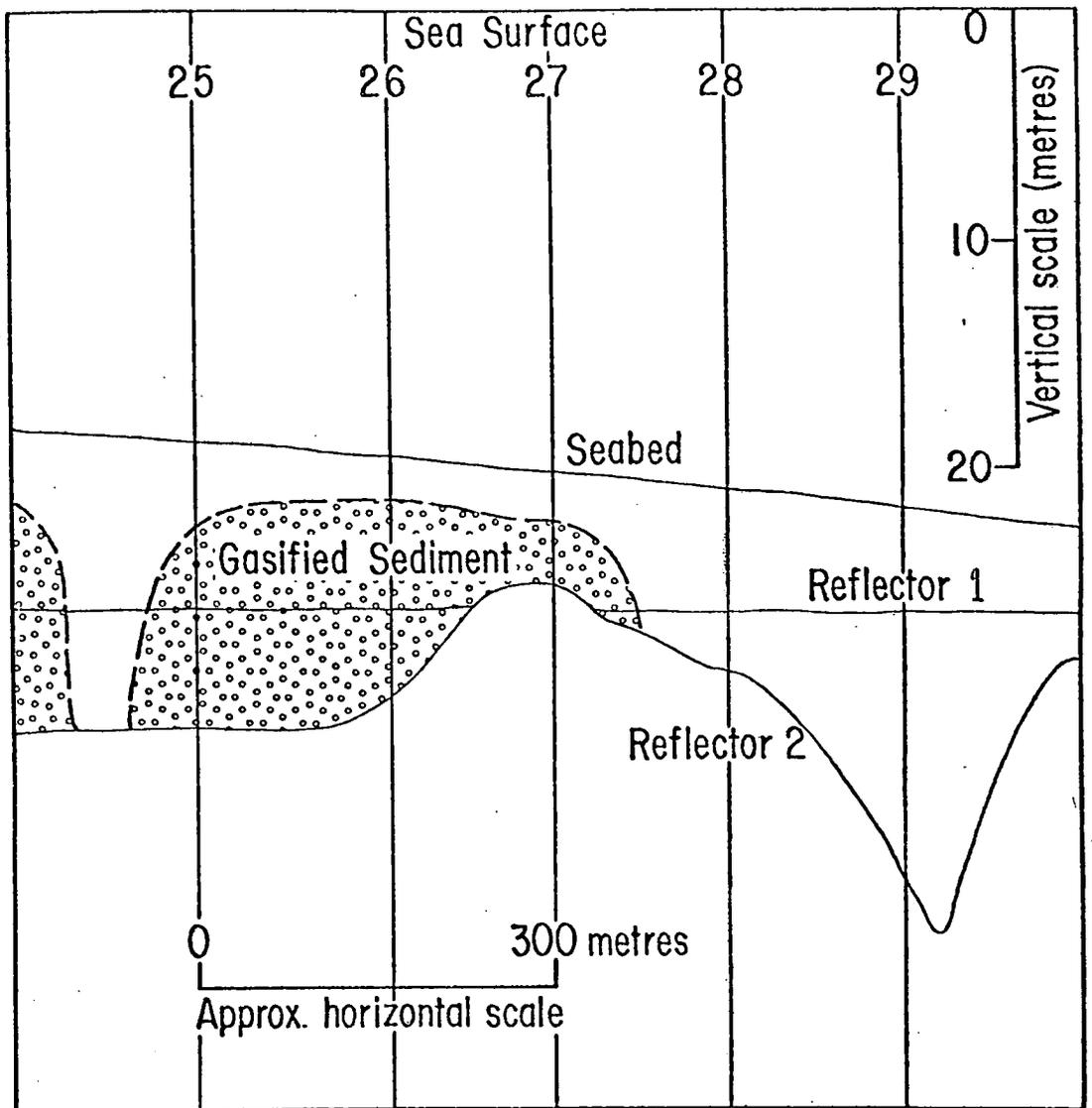
fig. 12. An alternative interpretation of the profile of
fig. 8 which allows variation in acoustic
velocity.

30

40

50

Vertical scale (msec.)

0 —————— 1000 feet

Approx. horizontal scale
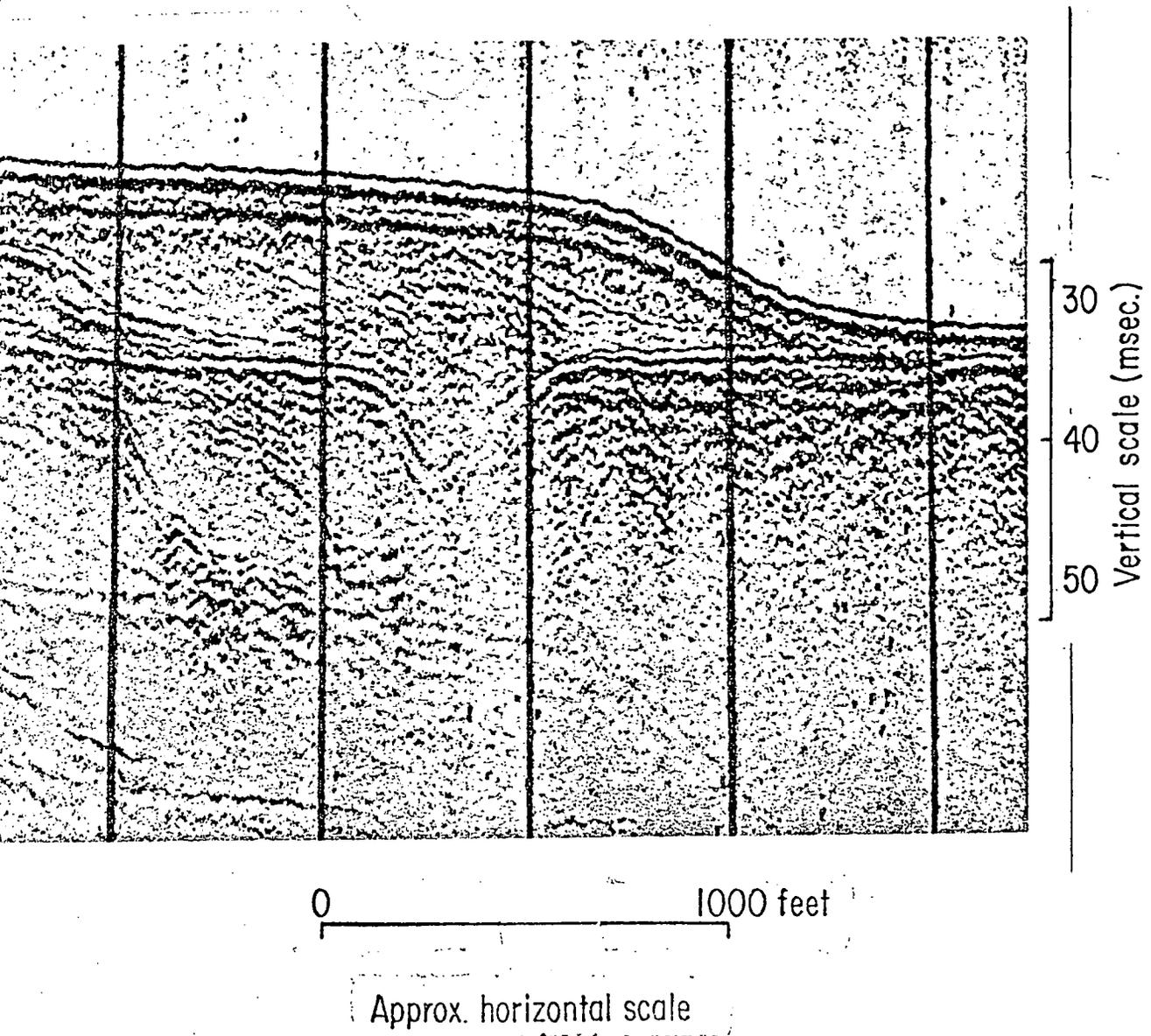
fig. 13 A dip or apparent dip in the upper reflector under-
          lying an area of foreset bedding in the upper
          sediment layer.
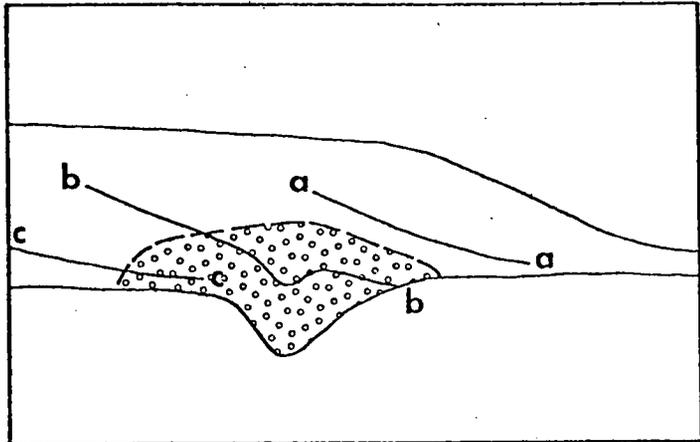
fig. 14 An interpretation of the profile in
         fig 13 made on the assumption of
         constant acoustic velocities.
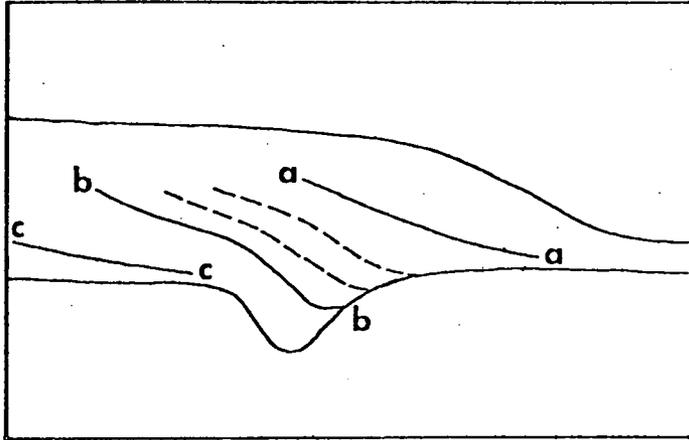
fig. 16   A conjectural pattern of bedding which
might be expected to occur over a real
dip in the underlying surface.
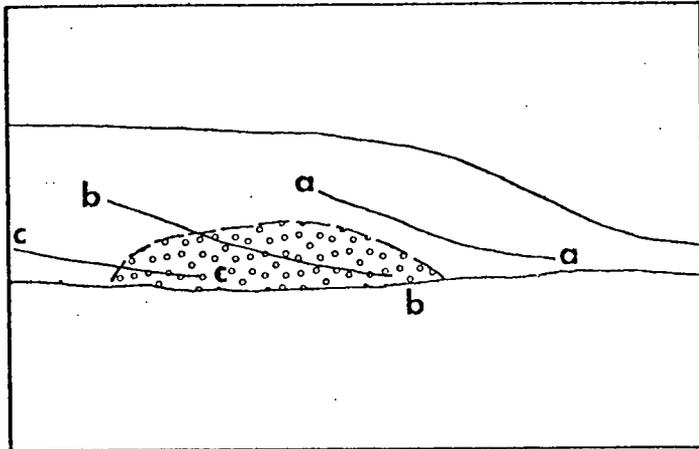
fig. 15 An alternative interpretation of the
profile of fig. 13.
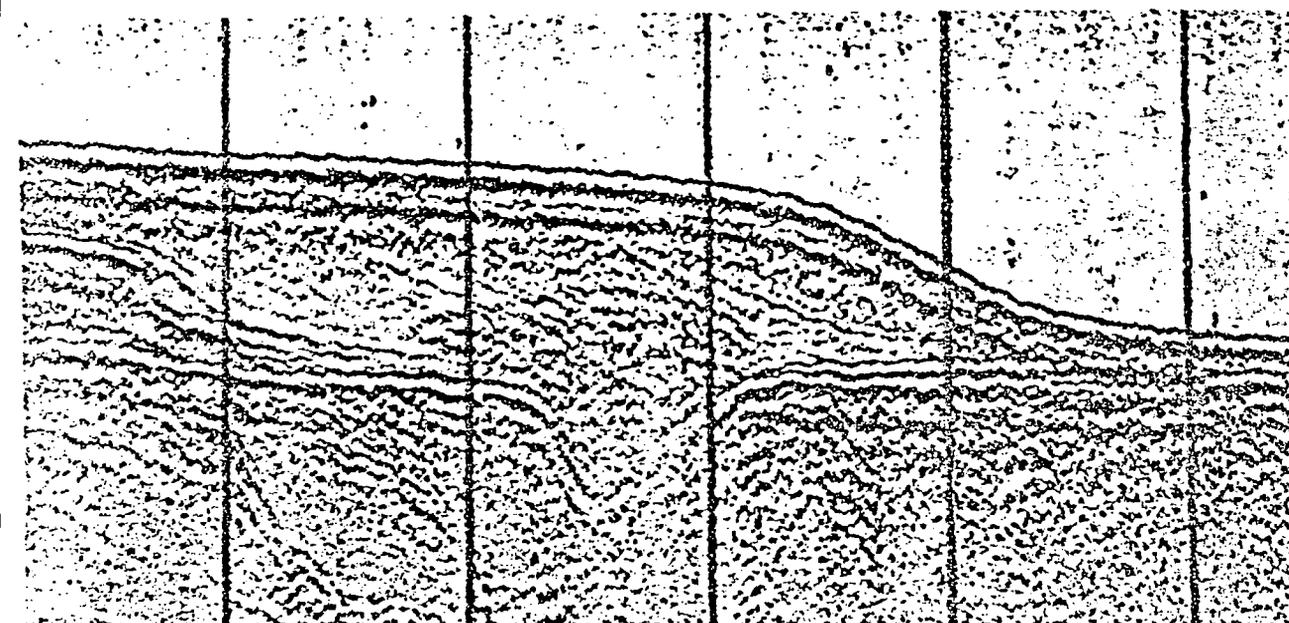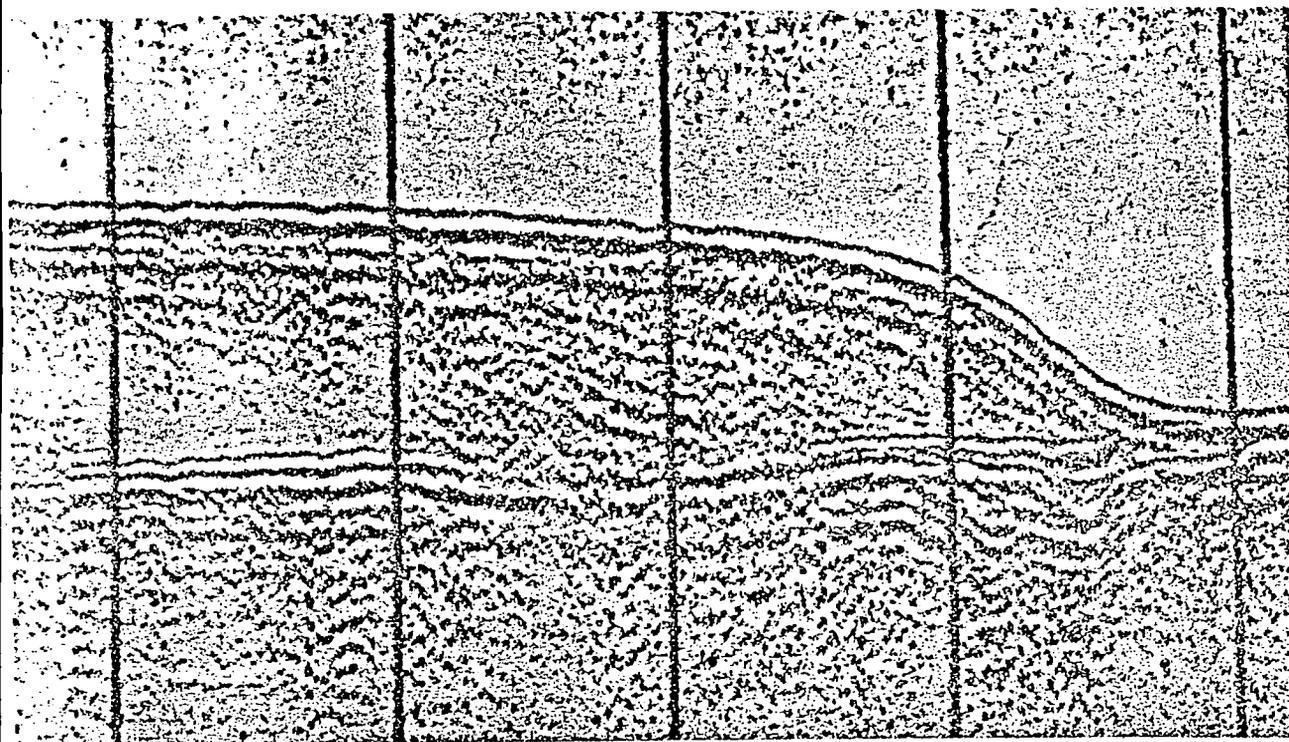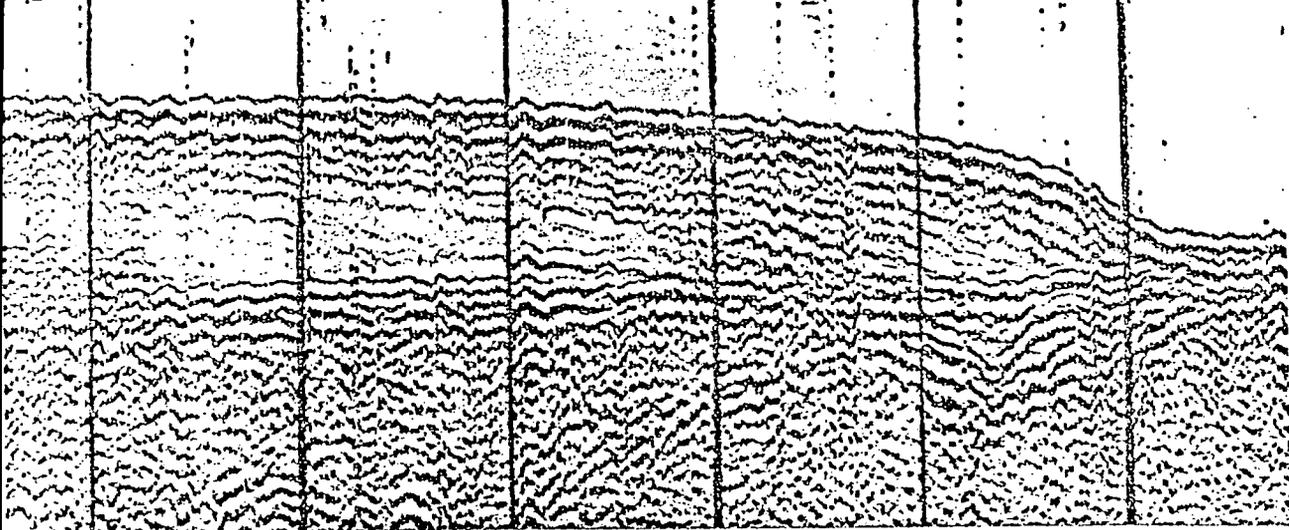
fig.   17   Area of foreset beds showing the development of the
dipping feature in the reflector at the upper surface
of the lower sediment layer. Scales are as shown in
fig   13.

centered on the measurement of reflectivity at vertical incidence, a parameter long used by fishermen in an intuitive way, and first put on a quantitative basis in the early 1960's. The compressional wave velocity is a more basic property of a sediment layer, but it cannot be measured with any accuracy unless the sensing devices are quite close to the layer (preferably less distant than ten times the layer thickness). Consequently, for all but the shallowest water, or the thickest sediment layers, the deep tow method is vital for remote velocity measurement.

The author has made some progress in adapting the N.S. Research Foundation equipment for this purpose, but it is regrettable that deep-tow systems have not been designed with anything other than vertical incidence profiling in mind.

The variation of reflectivity with angle of incidence depends on both compressional and shear wave velocities as well as density and attenuation contrast at the reflecting interface. Consequently, equipment designed for good compressional wave velocity measurement, by the method of wide angle reflection, might be expected to yield values for these other variables as well.
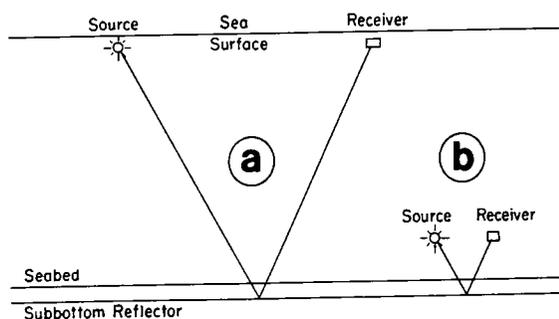
The wide-angle reflection method essentially measures an average velocity in the sediment layer and the overlying water column. Consequently, if the water velocity is not to dominate this average, the ratio of water depth below the sensors to sediment layer thickness must not be large. A deployment such as that shown in "a" above is poor; a deployment like "b" is much better.
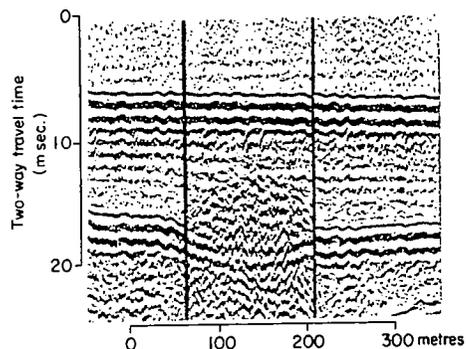
Flexure in subbottom reflector thought by the author to be more probably caused by p-wave velocity variation than by topography.
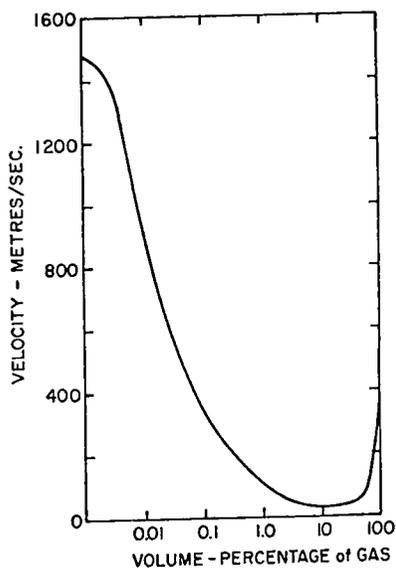
The graph (for ambient pressure of 1 atmosphere) of Wood's (1930) emulsion equation.

References

Green, C.H. (1938) Geophysics, 3, pp 295-305.

Keen, M.J. and D.J.W. Piper (1976) Canadian Journal of Earth Sciences, 13, pp 312-318.

McKay, A.G. (1978) Geophysical Prospecting, V. 16, (3), 673.

McKay, A.G. (1980) Canadian Journal of Earth Sciences (submitted February, 1980).

LePichon, X., J. Ewing and R.E. Houtz (1967) Journal of Geophysical Research 73, 2597-2614.

ON THE IMPORTANCE OF ACOUSTIC VELOCITY MEASUREMENT IN MARINE SEDIMENTS

SUR L'IMPORTANCE DES MESURES DE LA VITESSE DE PROPAGATION DU SON DANS LES SEDIMENTS MARINS

A.G. McKAY[1]

1) Nova Scotia Research Foundation Corporation, P.O. Box 790, Dartmouth, Nova Scotia. B2Y 3Z7

KEYWORDS/MOTS-CLES: Acoustic Measurement, Sedimentation, Underwater Mapping.

SOMMAIRE: Les avantages relatifs et les limites des techniques de réflexion acoustique pour la cartographie sous-marine des matériaux et des caractéristiques des fonds océaniques sont discutés.

The remote sensing technique of vertical incidence seismic reflection profiling to determine underwater geological features has been used for many years. The economic importance of offshore oil industry has given a great impetus to its development for revealing rock structures to depths of many kilometres. Shallow penetration seismic reflection work, which is done with much higher acoustic frequencies to find out detailed information about much smaller features in the sediments of the immediate subbottom, has not been refined to the same extent. Its main application at present is in assisting engineers to plan seabed installations such as harbour facilities, pipelines and cables.

High resolution seismic reflection profiles are usually interpreted without making field measurements of the acoustic velocity in the seabed sediments. This velocity usually lies between 1.5 and 1.7 km/sec. and can be expected to be almost constant within any one sedimentary unit.

However, in the presence of entrapped gas which may be derived from the decay of organic matter, the acoustic velocity can be much reduced because of the dominant influence of the gas on the compressibility of the sediment. In such an environment, the acoustic velocity can alter by up to 30% within horizontal distances of less than 100 metres, producing considerable distortion on the seismic cross sections and giving rise to features which may be interpreted as topography by the unwary.

The recognition of velocity anomalies on vertical incidence profiles is sometimes possible, especially when zones of "acoustic turbidity" appear on the seismic section and where a more plausible geological interpretation results from the assumption of velocity variation, but such a procedure at best leaves the interpreted results open to debate.

The method of "wide angle reflection" is a well-understood way of measuring acoustic velocities in layered materials. Its principle is simple in that it relies on the measurement of the travel time for an acoustic pulse over two or more distinct paths through the layered sediment thereby removing the mathematical indeterminacy inherent in any attempt at finding the two unknowns, velocity and depth, from a single equation (as is the case for a conventional vertical incidence profile). The distinct paths through the sediments are obtained by setting the sound source and receiver at different horizontal separations.

Measurement which is precise and computation which is far from trivial are required to obtain acoustic velocities in this way, but neither consideration can excuse the design of profiling equipment suited only to the gathering of vertical incidence information.

The last decade has seen the pioneering in Canada of deep-tow sediment-profiling seismic equipment. Such sensing devices, by virtue of being close to the bottom, remote from the noise produced by the towing ship and by surface turbulence, have led to a much more detailed picture of the seabed of continental shelves.

They have also opened up the possibility of the remote sensing of such acoustic properties of seabed materials as are of interest in attempts to predict the engineering properties of sediments. Surprisingly, interest has

A sub-bottom profiling survey of the St. Magnus Bay deep, Shetland

A. G. McKay

Nova Scotia Research Foundation, Dartmouth, Nova Scotia, Canada

Synopsis

This survey of St. Magnus Bay, Shetland revealed an infilled elongate basin beneath the deep inner part of the bay. Speculations as to the origin of the bay by meteorite impact remain unconfirmed.

A meteorite impact origin for the deep in St. Magnus Bay on the west coast of Shetland has been proposed by Flinn (1970) and discussed by Sharp (1970). In August 1972, with a view to investigating the sub-bottom features of the bay, a survey was made by a Durham University party on board M.V. Miranda towards the end of a charter by the Natural Environment Research Council.

The equipment used was an O.R.E. model 1036 with a Gifft recorder and an E.G. and G. sparker with a Flexotir array as the receiver and a 254 recorder. As the bathymetry of the bay was already well known from surveys by the Admiralty and by the University of Liverpool (Flinn 1970), the Miranda survey was aimed at sub-bottom profiling. The O.R.E. transducer was tuned to a 3 KHz signal capable of defining, with high resolution, reflectors up to 25 m beneath the sea bed. The sparker was fired at 3 K Joule to define any deeper layers. The survey lines shown in Figure 1 were completed in good weather conditions. Navigation was primarily by compass sights on landmarks and by radar, but Decca Navigator readings were also noted. The size of the vessel (1500 tons) limited the closeness of approach to land, especially in view of the tidal currents encountered.

The profiles obtained are presented in Figure 2. Over the outer lip of the bay no sub-bottom penetration was obtained. From this observation it seems reasonable to conclude that the volcanic sequence of tuff, andesite, rhyolite and basalt found on Papa Stour and Esha Ness postulated by Flinn *et al.* (1968) to be continuous between them does outcrop at the sea floor there. Under the deep inner part of the bay, there is what appears to be a partially infilled elongate basin whose bed reaches 60 m below the present sea floor. The sediments in it show some degree of layering as can be seen in Figure 2. Its shape is outlined in Figure 3 where the depths indicated assume an acoustic velocity in the sediments the same as that in water. The depression has the appearance of a glacial scour, but its direction does not fit in well with that of the ice sheet flow lines deduced by Peach and Horne (1879) from a study on land of erratics left by the last glaciation. (Flinn 1967 disagrees with Peach and Horne on the mode of glaciation of Shetland, but his resulting ice flow lines in the vicinity of St. Magnus Bay are much the
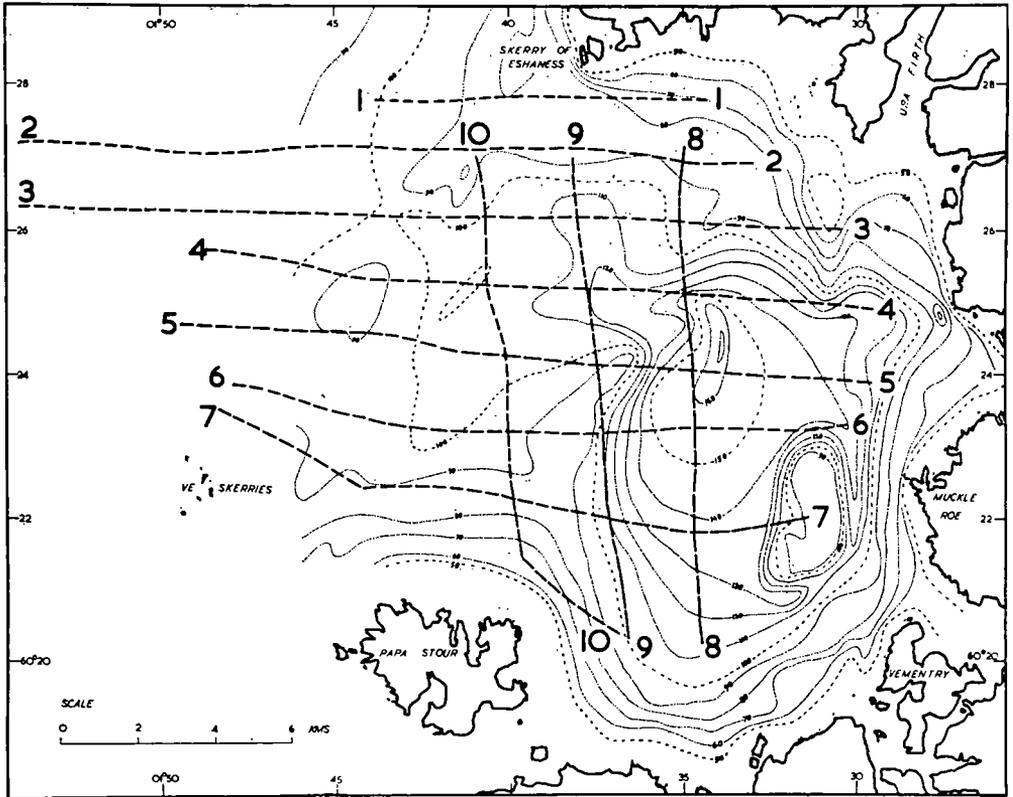
FIG. 1. St. Magnus Bay. Survey Track Chart. Bathymetry in metres, based on a map by Flinn (1970).

same.) Flinn (1967) investigated an arcuate belt of deeps off the north-east of Scotland and postulated their formation as syphons under a stationary ice front by which melt-water escaped under the ice to the sea. The St. Magnus Bay scour may be evidence for a similar syphon escape from under the Shetland ice cap during a stationary phase in its evolution. Alternatively, it may owe its shape to earlier phases of the Pleistocene glaciation. Whatever the exact time of its erosion, the central part of St. Magnus Bay has clearly been eroded to a depth of about 230 m below the present surface level of the sea. This lends weight to the argument by Flinn (1970) that the central part of St. Magnus Bay must be underlain by a soft type of rock. As there is no evidence in the erratics carried to the headlands that there is in the bay any rock markedly different from the durable volcanics, granite, sandstone and schists known on land around the bay, Flinn (1970) considers it possible that the soft rock is a meteorite explosion breccia. In the hope of getting some clue as to its type, an attempt was made to find the acoustic velocity in the rock underlying the sediments by the use of a radio transmitting sono-buoy in conjunction with the sparker as sound source. This source is too high in frequency and low in power for refraction work, but no other working source was available on
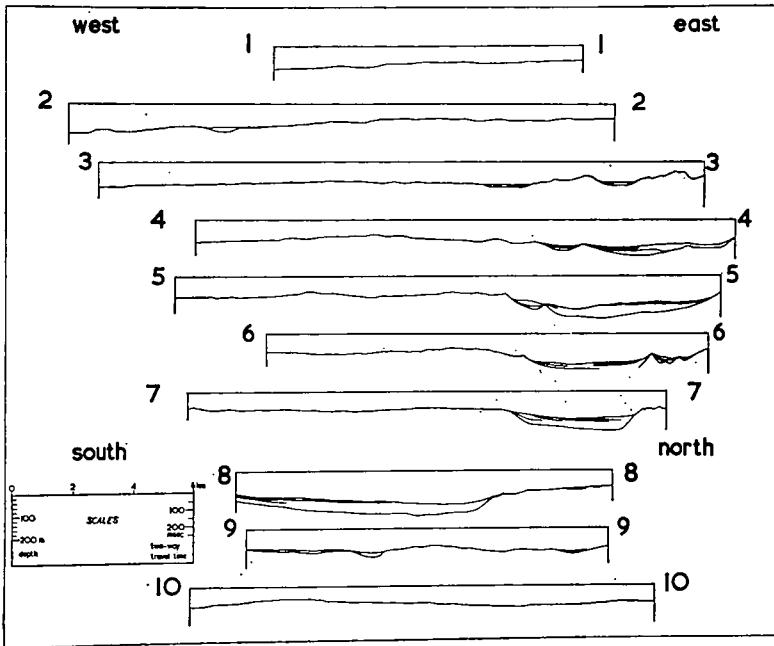
FIG. 2. Sub-bottom profile sections. Numbering corresponds to line numbers on track chart. Depth scale assumes a sediment acoustic velocity equal to that of the seawater.
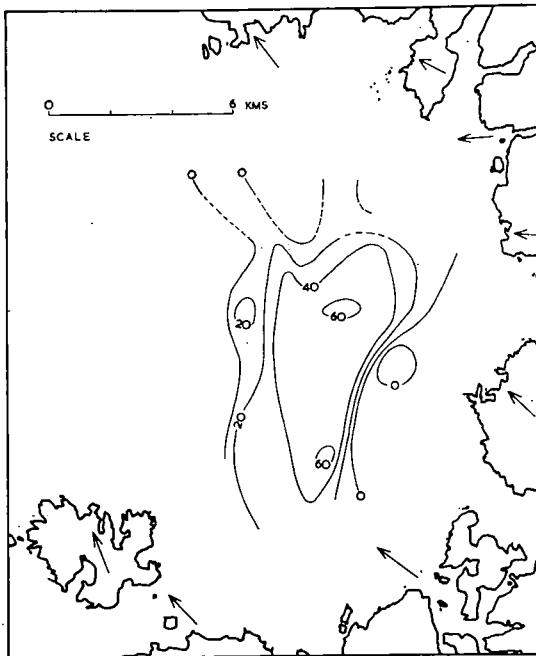
FIG. 3. Shape of the St. Magnus Bay scour. Depth of sediment in metres. The arrows show the direction of ice movement as deduced by Peach and Horne (1879). (The area shown is the eastern part of that in Fig. 1).

board. Nothing other than multiple reflections from the sea floor was discernible in the resulting records.

From sub-bottom profiling records, it is sometimes possible to distinguish a change in the type of rock forming the acoustic basement from an alteration in the intensity or the fine detail of the reflector on the record. The records were examined to see whether any change occurred in the appearance of the deepest observable reflector near the edges of the scour channel, but none was apparent. While this argues against the presence of a breccia beneath the scour, the evidence is insufficient to completely rule out that possibility.

Sharp (1970) has advocated a gravity survey of the bay to help in interpreting the underlying structure. This would be difficult with a ship-borne meter in view of the frequent changes of course necessary. It could no doubt be accomplished with a sea-bed meter, but the depth of water would make this a lengthy task.

REFERENCES

FLINN, D. 1967. Ice front in the North Sea. *Nature Lond.* **215,** 1151–1154.
——, 1970. Two possible submarine meteorite craters in Shetland. *Proc. geol. Soc. Lond.,* **1663,** 131–135.
FLINN, D., MILLER, J. A., EVANS, A. L. and PRINGLE, I. R. 1968. On the age of the sediments and contemporaneous volcanic rocks of western Shetland. *Scott. J. Geol.* **4,** 10–19.
PEACH, B. N. and HORNE, J. 1879. Glaciation of the Shetland Islands. *Q. Jl geol. Soc. Lond.* **35,** 778–811.
SHARP, A. W. 1970. St. Magnus Bay, Shetland: a probable British meteorite crater of large size. *The Moon* **2,** 144–156.

Interval Velocity Measurements off N.W. Scotland Made with Disposable Sono-Buoys

A.G. McKay and J.H. Peacock

Abstract

During the course of normal-incidence airgun profiling, nine wide-angle profiles were obtained by the use of V.H.F. transmitting sonobuoys.

Introduction

On the Durham University Cruise on the R.V. 'John Murray', in June and July 1970, several successful velocity-depth profiles were obtained in the region to the W. and N. of Scotland with V.H.F. radio-transmitting sonobuoys used in conjunction with an airgun in a manner similar to that described by X. Le Pichon et al. (1968), and R. Houtz et al. (1970).

After amendments to the design of the buoy by its makers (Ultra Electronics Ltd.) the measured frequency response of the buoy/V.H.F. radio system was found to be flat within 6dB from 3Hz to 600 Hz. No alteration was made to the input sensitivity of the buoy's amplifier, with the result that sea-noise, being of higher amplitude in this new frequency range came near to saturating it in all but the calmest weather. Nevertheless, of the ten buoys used, seven gave good records, and two others (nos.6 and 9) have been interpreted, but for future work, modifications will be made to the sensitivity.

The airgun used has been developed in Durham by J.H. Peacock. It is of 10 cu.in. high pressure (c.3500 p.s.i.) capacity, and is fired electrically with an accuracy of $\pm$ 1 msec.

The buoys were used in regions where the sea-bed was flat, and where no dip in the subsurface layers appeared on the vertical-incidence profile. This eases the interpretation of the records.

A variable-area recorder was used on board ship to monitor the normal-incidence or sono-buoy profiles. Both were f.m. recorded on magnetic tape at 3.3/4 i.p.s. on an EMIDATA deck.

Reduction of Data

For interpretation, the records were replayed on the variable area recorder. Filters were set to pass the band of 16Hz to 60Hz to this display unit. Arrivals interpreted as wide-angle reflections were reduced by a program written by X. Le Pichon and adapted by R. Whitmarsh (N.I.O.,England). Refracted arrivals were reduced graphically. The results are displayed in tables 1 and 2.

Results

Table 1 shows the interval velocities and thicknesses obtained from arrivals interpreted as wide-angle reflections. On some of the records, refracted arrivals could also be picked and velocities calculated from these are shown in Table 2.

Station 2, near St. Kilda is the only shallow water station. Wide angle reflections were completely obscured by seabed multiples, but refracted arrivals stand out clearly, showing the usefulness of this technique for shallow refraction work.

Station 6 appears to exhibit a velocity reversal with depth, but the quoted standard errors show that this need not be so. This is one of the poorer stations, with much sea-noise on the record.

The record from station 1, to the S.W. of the Anton-Dohrn Kruppe is one of the clearest and allowed the determination of interval velocities to over 4 km. beneath the seabed. The velocities in layers 3 and 4 are typical of consolidated sediments.

Station 3 is 15 miles E of an unreversed refraction line of Ewing and Ewing (1969) where they observed a 2.48 km. thickness of semi-consolidated sediments with a velocity of 2.08 km/sec. At station 3 we observe a total of 2.0 km. of semi-consolidated sediments with about the same velocity.

Geology Department,
University of Durham,
England.

March 1971.

References

Ewing J. and Ewing M., 1959, Seismic refraction measurements in the Atlantic Ocean: Geol. Soc. America Bull., v.70, p.291-318.

Houtz R., Ewing J. and Buhl P., 1970, Seismic data from sonobuoy stations in the Northern and Equatorial Pacific: Journal of Geophysical Research, v.75, no.26.

Le Pichon X., Ewing J. and Houtz R., 1968, Velocity determination made while reflection profiling: Journal of Geophysical Research, v.73, no.8.

Table 1

Wide Angle Reflections

Station No.	Velocities (km/sec)			Water Depth	Thicknesses (metres)		
	V1	V2	V3		T1	T2	T3
1	1.935 ± 0.042	1.957 ± 0.072	3.882 ± 0.237	2008 ± 9	1090 ± 24	894 ± 33	2281 ± 140
2				146 ± 1			
3	2.120 ± 0.077	2.035 ± 0.641	2.045 ± 0.235	1970 ± 9	742 ± 27	466 ± 147	780 ± 90
4	1.809 ± 0.041	2.032 ± 0.056		1181 ± 6	480 ± 11	668 ± 20	
5	2.133 ± 0.037			1233 ± 5	1730 ± 31		
6	1.830 ± 0.211	1.648 ± 0.108		948 ± 4	434 ± 50	275 ± 18	
7	1.808 ± 0.020			1299 ± 6	732 ± 9		
8	1.761 ± 0.075			1875 ± 8	520 ± 22		
9	2.258 ± 0.590			1830 ± 8	550 ± 143		

Table 2

Station No.	Position of Buoy latitude	longitude	Direction of Steaming	Velocity from Refractions (km/sec) V1	V2	V3	V4
1	57°07'N	12°12'W	120°				4.3 ± 0.4
2	57°56'	08°48'	290°	4.52 ± 0.20	6.48 ± 0.65		
3	58°13'	10°08'	290°		2.14 ± 0.20		
4	59°56'	11°36'	050°				
5	59°19'	07°52'	140°		2.4 ± 0.2		
6	60°50'	03°45'	330°				
7	59°57'	08°57'	231°				
8	58°46'	10°27'	120°				
9	58°37'	09°56'	120°				

Compressional-wave velocity measurement in seabed materials by use of equipment deployed near, but above the bottom

Alasdair G. McKay and P. M. McKay

Atlantic Geoscience Society, 35 Edward Street, Dartmouth, Nova Scotia, Canada B2Y 2P6

For the measurement at midaudio frequencies of the acoustic compressional wave velocity, methods are described which make use of either the refraction or the wide-angle reflection techniques in ways which do not require station keeping by the survey vessel (as when equipment is deployed on the bottom) but still minimize the adverse effect of a long water column between the sensing equipment and the seabed. Some results from areas on the Nova Scotia shelf are presented, ranging from about 3.0 km/s in a nearshore sedimentary rock sequence through 1.6 km/s on a shelf-edge sandbank to 1.25 km/s in a deep intrashelf basin.

PACS numbers: 43.30.Cq, 43.30.Bp, 43.30.Sf

INTRODUCTION

The compressional wave velocity in the immediate subbottom is a parameter of importance in the solution of problems concerned with sound propagation in the water column. Its value can also be a guide to the geotechnical properties of the seabed.

Hamilton[1] has summarized an extensive set of information on seabed sediment acoustic velocities and derived regression equations which can be used to predict the velocity at a given depth in the ocean bed for three clases of sediment: siliceous, calcareous, and turbidite. Houtz[2] has compiled similar data for sediments covered by shallower water in the vicinity of rapidly outbuilding continental shelves. Although such work has led to a greatly increased understanding of the acoustic properties of the seabed over large areas, it must be remembered that the information on which it is based comes from data obtained with a low-frequency sound source such as an airgun, from which wide-angle reflection profiles are obtained in the manner of Le Pichon et al.[3] Despite notable improvements in the method by Bryan[4] and Wrolstad,[5] such data are not usually able to resolve detail in the first few tens of meters below the seabed, although it is this zone which is of the greatest interest to those who, for engineering purposes, try to derive mechanical from acoustic properties or who, in dealing with sound propagation in the water column, are concerned with any acoustic frequency other than the very lowest.

Good methods have been evolved for making *in situ* velocity measurements by means of equipment deployed on the bottom, e.g., by Roberts et al.,[6] Hunter et al.,[7] and Bryan,[8] but these have the disadvantage of requiring station work by the survey vessel. The methods we describe here overcome this problem by deploying a sound source and receivers close to but above the seabed.

I. THE WIDE-ANGLE REFLECTION METHOD

As summarized by Maynard et al.,[9] from the original work by Green[10] and Dix,[11] the wide-angle reflection method gives an average value for the acoustic velocity in the water and sediment column below the point of observation. In water up to about 50 m deep, a small-scale version of the technique of Le Pichon et al.,[3] is adequate for making measurements in layered sediments of the immediate subbottom. The results shown in Table I were derived from data gathered during the course of a high-resolution vertical-incidence seismic survey carried out for engineering purposes on Lake Erie. During the running of survey lines, a single hydrophone was floated just below the surface and let out on a 100 m long cable in places where the geometry of sediment layers was sufficiently simple to allow the application of the inversion methods of Green[10] or Le Pichon et al.[3] Bennell[12] has adopted a similar technique in water off N. Wales. The main problem with this technique lies in choosing areas where the sediment interfaces are plane throughout the period that the separation between the acoustic source and the hydrophone is increasing. It is usually necessary to make quite a large number of such profiles and choose a few which are suitable for interpretation.

When the depth of water increases relative to the thickness of the sediment layer, the water acoustic velocity tends to dominate the average and it becomes increasingly difficult to obtain a meaningful value for the velocity in the sediments. Houtz[2] considers that the thinnest layer for which a valid interval velocity can be found in this way is about 1/12th of the water depth.

TABLE I. Results of wide-angle reflection experiments with source and receiver at the water surface, in Lake Erie. Water velocity 1.450 km/s.

Number	Velocity (km/s)	Layer thickness (m)	Water depth (m)
1	1.560 ± 0.035	12	27
2	1.290 ± 0.031	19	44
3	1.310 ± 0.033	18	43
4	1.230 ± 0.045	16	39
5	1.473 ± 0.050	16	52

Although Bryan's[4] differential method, applicable when continuously varying time–distance records are available, suggests that it may be possible to improve on this ratio to the extent that the velocity can be found in layers as thin as 1/50th of the water depth, such a figure would apply only to the very highest quality data. However, the development during the last decade of deep-tow seismic profiling equipment has opened up the possibility, at least for the seabed of continental shelves, of improving the sediment to water column ratio by deploying the sensing equipment deep in the water rather than near the surface. A further advantage of a deep-tow deployment is that any effect of velocity variations within the water column is minimized by having the acoustic equipment below the surface region where fluctuations are usually greatest. For example, data on water velocities from the Emerald Basin on the Scotian Shelf show that these can vary by about 50 m/s within the top 100 m of water column, but at greater depths the velocity remains constant to within 5 m/s.

Deep-tow equipment has been in commercial use for a number of years and has been described by Bidgood,[13] Tyce,[14] and Parrott *et al.*[15] An instrument package can be towed as close to the seabed as ca. 30 m. Although considerable funding and expertise has gone into the development of such systems over the past decade, there has been little interest in making use of them for determining seabed sediment acoustic velocities and correspondingly little thought has been given to incorporating features in their design which would allow ready adaptation for this purpose, or for the investigation of reflectivity other than at vertical incidence. The obvious difference with an equipment package towed near the bottom from one towed near the surface is that it is not easy to alter the spacing between the acoustic source and receiver after deployment. One way around the problem is to use a number of receivers towed at constant depth in the way Porter *et al.*[16] have done for near-surface equipment while another is to use only one receiver flown up and down the water column in order to obtain changes in the angle of reflection at the horizons of interest. The authors have found both methods useful, but in different circumstances, and the technique of continuously varying tow depth is discussed in a later section.

It is important to note that the maintenance of a fixed geometrical relationship between acoustic source and receivers would be very difficult to realize when equipment is towed far below the surface (Fig. 1). We have made no attempt to do this other than within the very broad limits (ca. ± 5 m) which can be set by varying the ship's speed and the length of the main tow cable. Instead, the location of source and receivers is calculated continuously from observations of the travel times over the path lengths a, d, and $(b + c)$ in the water column (Fig. 2 and Appendix).

The equipment which we adapted to carry additional receivers was a Nova Scotia Research Foundation deep-tow profiler, whose underwater vehicle, towed on 600 m of cable, has an operational depth of up to 300 m. The standard acoustic source used in this system was
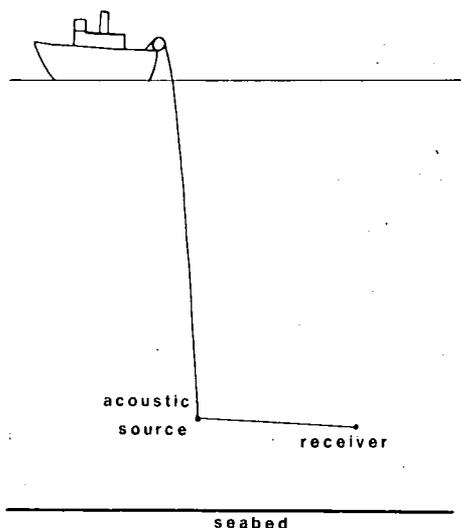
FIG. 1. The deployment of acoustic equipment for the measurement of acoustic velocity in the seabed.

a single-tip spark-discharge unit ("sparker"), whose acoustic output varies with depth of operation as shown in Fig. 3. We devised a multi-tip sparker which had its tips distributed along a 2-m line athwart the tow direction. This produces a total pulse length about half that of the single-tip sparker at double the frequency. Depending on tow depth and frequency output, the beam pattern produced by the multi-tip sparker has a theoretical width of between 15° and 40° in the mainlobe, which is centered on a vertical plane through the direction of towing.

The main tow cable could accommodate a total of four audio frequency signal channels after three channels for the depth compensation and power circuits necessary for the basic functioning of the system had been allocated. This small number of channels available is a rather serious restriction on the gathering of wide-angle information. One of the four was used for a hydrophone towed close to the acoustic source. In one configuration, the remaining three channels were given over to hydrophones towed at 37, 55, and 67 m behind the acoustic source. In another, a total of six hydro-
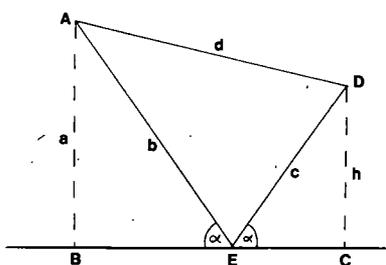
FIG. 2. Diagram to show the geometrical relationships from which Eq. (1) is derived. Upper-case letters denote points, lower case denote the length of straight lines. Physically, all lines shown are in the water column, with the exception of the horizontal lines through E which can represent either the sea surface or the seabed.
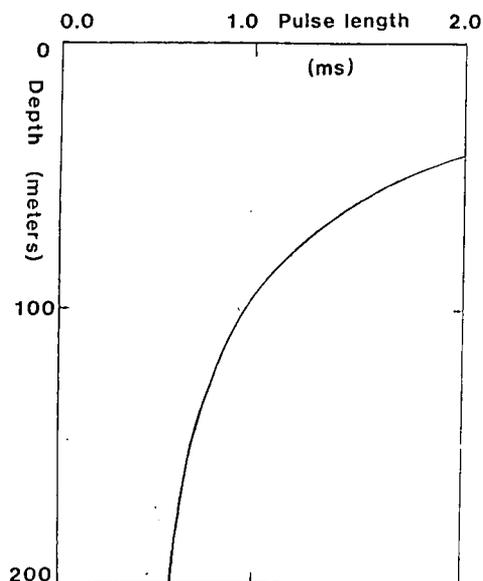
FIG. 3. Variation with depth of operation of a single-tip-sparker acoustic source. Electrical input 200 J.

phones were deployed over a similar spread, but their output was fed in turn to a single channel by means of a switching mechanism. At one time we attempted to elaborate this procedure by deploying eight sparker sources spread evenly in the space between the first and second hydrophones. The high voltage discharge was gated to each of the sources in turn by means of relays in a submersible oil-filled housing. This arrangement of eight sources and six receivers gave a total of 48 different offsets by which we had hoped to obtain near continuous profiles analogous with those made by using sonobuoys. Although the high voltage gate was thoroughly tested and worked well, we were unable to give a satisfactory guarantee of its safety and so reverted to the simple hydrophone switching alone.

The advantage of a switching method[17] is that it makes possible observations at more reflection angles. Its disadvantage lies in the difficulty of maintaining the desirable geometry required for the observation at the different hydrophones of reflections from a common depth point, unless very fine control can be exercised over the ship's speed and the cycling rate of the switch mechanism. We did not find it possible to synchronize these sufficiently well to provide common depth-point data, and the only velocities which have been calculated from information obtained by the switching method are from areas where sediment interfaces are planar.

In calculating velocities from such data, we have used the method of Green[10] with an appropriate correction which is needed because the offset receivers will not necessarily be at the same level as the acoustic source. The position of each receiver can be found from the relationship:

$$h = [(b+c)^2 - d^2]/4a \qquad (1)$$

derived in the Appendix. Once the travel times of the reflected arrivals have been reduced to a common datum

level, a plot of the (distance)^2 versus (reflected travel time)^2 leads to an evaluation of the average velocity by measurement of the gradient of a straight line fitted to the data. This simple method assumes a least-distance raypath between source and receiver and ignores the difference between this and the actual least-time path. For sediment velocities within 10% of that of the water, this difference is less than 0.2% for incidence angles up to 45°. This is smaller than the 0.1-ms accuracy of measurement of the reflected travel times, which typically had values around 50 ms or less. More precise methods of computation such as that of Le Pichon et al.[3] or Westbrook[18] proceed on the basis of least-time raypaths, but require more time-distance data points than we had available. From Fig. 2 it will be clear that a sufficiently accurate position for the point D can be obtained only if the difference between $(b+c)$ and d is not too small. In the case where d is 70 m and a is 30 m, we find an uncertainty in h of 0.5 m when the accuracy of picking travel times is 0.1 ms. This would lead to an uncertainty of ± 7 m/s in the average velocity in the water and sediment layers above the subbottom reflector of interest and a correspondingly greater error in the sediment velocity, when the effect of the water layer is removed. The extent to which it is greater will depend on the ratio of water column to sediment thickness: e.g., ± 28 m/s for a 3:1 ratio.

Another factor which could affect the interpretation of travel-time observations is the possibility of phase change on reflection. The theoretical expression of Brekhovskikh[19] giving the reflection coefficient of a sound wave incident from a liquid on the plane boundary of a solid is

$$R = \frac{Z_1 \cos^2 2\theta_s + Z_t \sin^2 2\theta_s - Z_0}{Z_1 \cos^2 2\theta_s + Z_t \sin^2 2\theta_s + Z_0}, \qquad (2)$$

where

$$Z_0 = \rho_0 v_0/\cos \theta_0, \quad Z_1 = \rho_1 v_1/\cos \theta_1, \quad Z_t = \rho_1 v_s/\cos \theta_s,$$

with "ρ" density and "v" velocity, the subscripts "0" referring to liquid, "1" to solid, and "s" to shear waves in the solid. The angles θ_1 and θ_s are derived from the angle of incidence θ_0 by Snell's Law, which may be extended to describe lossy media by the use of a complex wavenumber. Merkulova[20] has derived analytical expressions for complex impedances which arise in this treatment, but a numerical insight into the behavior of Brekhovskikh's reflection coefficient can be as easily obtained by entering appropriate complex values for the variables in Eq. (2). We have calculated this expression for the ranges of sediment parameters we expected to encounter on the seabed, namely: compressional wave velocity 1.0 to 1.7 km/s, shear wave velocity[21] from 0.0 to 0.2 km/s, density 1.4, and attenuation[22] logarithmic decrement 0.0 to 0.1.

On the basis of this viscoelastic model, the variation in phase of R is less than 30° except near the intromission angle (i.e., θ_0 such that $R=0$, or in the case of lossy sediments, such that R is at a minimum) and near and above the critical angle [i.e., $\theta_0 = \sin^{-1}(v_0/v_1)$]. With our experimental equipment (towed ca. 30 m off

bottom with maximum separation between source and receiver ca. 70 m) reflections at or above the critical angle would be unobservable for sediments having a velocity less than ca. 2 km/s.

Reflections near the intromission angle can occur at shorter spacings between source and receiver, but the arrival time of the very weak reflection which occurs in these circumstances is difficult to measure, so that such a problem is unlikely to be overlooked in data processing. Until now we have rejected, for the purpose of travel-time interpretation, any data with this appearance, instead of trying to make phase-change corrections.

To give an idea of the numerical value of the possible errors which might arise from phase changes on reflection, we can consider the case of a 180° phase shift, an acoustic source operating at 2 kHz and a reflected travel time of 50 ms. Here the error in neglecting the phase shift would be 0.25 ms, leading to an error of 0.5% in the average velocity in water and sediment. For a typical ratio of sediment to water layer thickness of 1:3 or 1:4, this would put the value of the sediment velocity in error by about 2%. For the phase changes of less than 30°, which we expect to encounter, this error would be ca. 0.25%. We do not consider this an important effect at the level of accuracy to which we are able to make observations, but it may prove to be one of the more serious obstacles to possible future attempts at refining the method by making more precise measurements of travel time, unless values for the shear wave velocity and attenuation can be determined. It could be possible to attempt this by observing the variation with angle of the amplitude of the reflection coefficient R and fitting the

observations with theoretical curves derived from Eq. (2) or else from the corresponding expressions which relate to the modeling of the seabed as a porous viscoelastic material.[23] Such observations would require at the very least a 12-channel array of amplitude-calibrated hydrophones, something which is far beyond the rudimentary equipment we had available.

Results have been obtained from three areas of the Scotian shelf: the Emerald Basin, the Sable Island Bank, and an unnamed basin near Canso Bank. A sedimentalogical description of these areas has been given by King.[24] The two basin areas have water depths of about 200 m. The sediments are layered clays overlying silts. The Sable Island Bank is a shallower region near the shelf edge and the area investigated there lay in 100 m of water, with sand as the seabed material. Results obtained are shown in Table II. The errors quoted are derived from the standard deviation of points from the best straight line fitted to (travel time)^2 versus (distance)^2. The low velocities which we have measured in the basins occur in the LaHave Clay,[24] from which piston cores retrieved for micropalaeontological purposes have been observed to expand after being brought on deck. The amount of this expansion has never been measured accurately, but from discussion with Scott et al.,[25] who have done the coring, we conclude that it can range from about 5% to 10%, after recovery from a depth of about 200 m. This range is in approximate agreement with the proportion of gas which Wood's[26] emulsion equation would predict on the basis of the observed acoustic velocities at the given hydrostatic load, and provides some indication of the validity of the values we have obtained, in the absence

TABLE II. Results of wide-angle reflection experiments with source and receiver towed deep in the water column. Localities are on the Scotian Shelf and are named following King.[24]

Number	Locality	Sediment velocity (km/s)	Sediment type	Approx. water depth (m)	Layer thickness (m)	Method of data gathering
1	Sable Island Bank	1.596 ± 0.030	sand	90	8	Switching
2	Sable Island Bank	1.600 ± 0.038	sand	90	8	Switching
3	Sable Island Bank	1.661 ± 0.025	sand	90	13	Switching
4	Sable Island Bank	1.572 ± 0.026	sand	90	11	Switching
5	Sable Island Bank	1.615 ± 0.020	sand	90	12	Switching
6	Emerald Basin	1.420 ± 0.019	clay	220	14	Switching
7	Emerald Basin	1.347 ± 0.025	clay	220	14	Switching
8	Emerald Basin	1.376 ± 0.028	clay	220	15	Switching
9	Emerald Basin	1.310 ± 0.060	clay	230	13	Three-hydrophone spread
10	Emerald Basin	1.385 ± 0.046	clay	240	16	Three-hydrophone spread
11	Emerald Basin	1.261 ± 0.085	clay	230	15	Three-hydrophone spread
12	Emerald Basin	1.234 ± 0.050	clay	220	15	Three-hydrophone spread
13	Canso Bank Basin	1.351 ± 0.071	clay	200	27	Three-hydrophone spread
14	Canso Bank Basin	1.415 ± 0.038	clay	200	9	Three-hydrophone spread
15	Canso Bank Basin	1.310 ± 0.063	clay	200	9	Three-hydrophone spread

of any independent velocity measurements. A further confirmation of the low velocities found in the basin areas comes from an examination of vertical incidence profiles in the neighborhood of pockmarks, large crater-like features described by King and MacLean.[27] Horizontal layering as seen on a vertical incidence seismic section is distorted beneath the pockmark. We have deduced velocities on the assumption that this distortion does result from a lower acoustic velocity in the sediment than in the water and find them in agreement with velocities calculated from wide-angle travel-time data. (The "pockmark method" of velocity determination does not lead to accuracies better than about ±5%.)

Hunter et al.,[7] have made direct measurements of acoustic velocities in the area of our experiments on Sable Island Bank, by deploying 12-channel arrays of hydrophones on the seabed and detonating small charges of explosive near one end of the array. They give velocity values for the seabed material (Sable Island Sand[24]) between 1595 and 1775 m/s, which appear to be in agreement with our results, but they subdivide the layer which we have taken as one unit, and assign higher velocities to the deeper parts of it, such that their minimum average value for our layer is about 1700 m/s. The discrepancy may result from the fact that Hunter's[7] refraction lines are unreversed, although it does seem that interfaces are near horizontal in this region. Al-
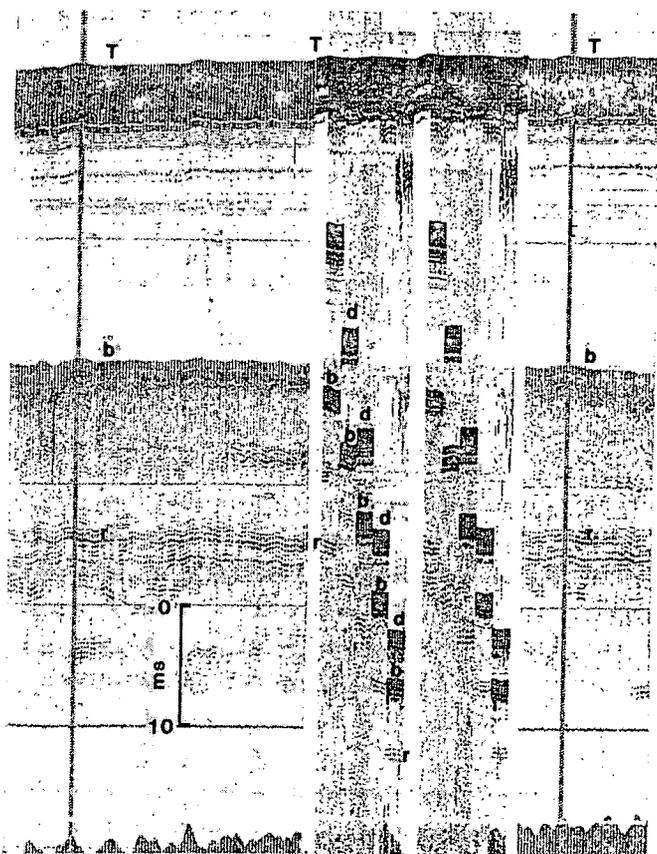

FIG. 4. Wide-angle reflection profiles made by the switching method on Sable Island Bank. The two sequences of switching are shown superimposed on a vertical incidence profile. (T–T), time = 0 event; (d–d), direct (water wave) arrival; (b–b), bottom-reflected arrival; (r–r), subbottom-reflected arrival. The two vertical lines are time marks and are 2 min apart (equivalent to about 200 m horizontal movement).
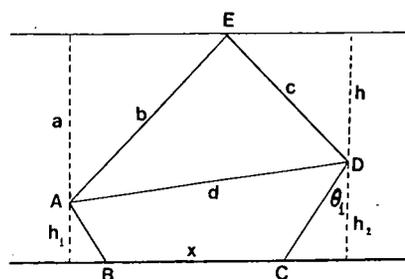

FIG. 5. Ray paths AED (surface reflected), AD (direct), and ABCD (refracted) between a source at A and a receiver at D. Lower-case letters denote distances. θ_1 is the angle of incidence for which $v_2 \sin \theta_1 = v_1$, where v_1, v_2 are the acoustic velocities in the upper and lower media (above and below BC).

ternatively, it may be due to lateral velocity variation and minor navigational inconsistency. It is difficult to reconcile the depths of interfaces given by Hunter et al.,[7] with reflectors on our vertical incidence record. This makes it seem likely that the two sets of results do not refer to exactly the same position on the seabed.

II. THE REFRACTION METHOD

Where rock rather than unconsolidated sediment lies at or near the seabed, the wide-angle reflection method is seldom applicable for velocity determination because reflections from deeper interfaces are not usually observed when the acoustic source in use is one designed for high resolution engineering purposes. However, the reduced attenuation found in a cemented material makes it more likely that a head wave[28] will be observable. The technique was employed by Maries and Beckmann[29] who used a hydrophone on a long cable which could be let out astern during the running of survey lines. We have found this technique useful in up to about 25 m of water,[30] but in deeper areas, at the offset distance required for the observation of a head wave as a first arrival, the signal from a spark discharge source of a few hundred joules is usually too weak for easy detection. An alternative method is to trail both source and receiver at constant separation some distance astern and arrange for them to rise and fall in the water column. A second hydrophone is placed immediately adjacent to the source so that its position can be located at any instant by observing the reflection from bottom or surface. The travel time of a wave traveling along the path ABCD of Fig. 4 is

$$T = (h_1 + h_2)/v_1 \cos \theta_1 + x/v_2 , \qquad (3)$$

where the distances and angle are defined in Fig. 5, v_1 is the velocity in the water column and v_2 the velocity of the headwave. The expressing of x in terms of h_1, h_2, d, and the application of Snell's Law lead to

$$0 = \cos \theta_1 \{ \cos \theta_1 (h_1 + h_2) + \sin \theta_1$$
$$\times [d^2 - (h_2 - h_1)^2]^{1/2} - v_1 T \} . \qquad (4)$$

The application of Eq. (1) to the direct and surface-reflected arrivals (with appropriate phase change correction for a pressure-release surface) leads to a value for h_2, and the equation can be solved for the angle θ_1
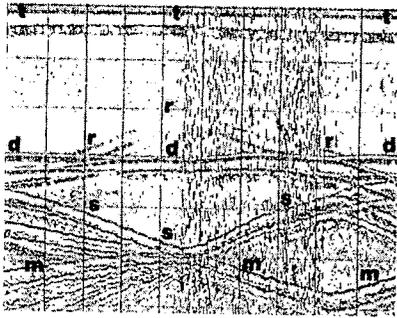
FIG. 6. Display on a variable-density recorder of a head-wave arrival (r–r). The time-0 event is at (t–t), the direct arrival (d–d) and the surface reflection (s–s). (m–m) is a multiple reflection. The horizontal lines are 10 ms apart.

(by the conventional substitution $t = \tan\theta_1/2$ leading to a quadratic in t) to give $v_2 = v_1/\sin\theta_1$.

Because of possible difficulties in identifying the first phase of the head wave, it is desirable to have a differential method of deriving v_2, by analogy with the conventional refraction method of exploration geophysics, or with Bryan's[4] method for thin layers on continuous wide-angle reflection profiles. Such a method can be obtained conveniently by looking at the rate of change of arrival time of the head wave at points where the source is momentarily at constant level in the water column. Partial differentiation of Eq. (4), for constant h_1 leads to

$$0 = \cos\theta_1 - \sin\theta_1(h_2 - h_1)/[d^2 - (h_2 - h_1)^2]^{1/2} - \frac{v_1\partial T}{\partial h_2}. \quad (5)$$

The partial derivative can be evaluated as

$$\frac{\partial T}{\partial h_2} = \frac{\partial T}{\partial s_1}\frac{\partial s_1}{\partial h_2},$$

where s_1 is the travel time of the surface reflection to the remote hydrophone $(v_1 s_1 = b + c)$, and the resulting equation solved for θ_1 and thence v_2 as before.

During the course of a high resolution vertical incidence reflection survey of the offshore coalfield of Cape Breton Island,[31] we made a few measurements in this way of the head-wave velocity in the seabed rocks in water depths up to 40 m. The separation between source and receiver was 30 m and these were flown from near the surface to within a few meters of the bottom by slowing down and speeding up the survey vessel (a 40-ft fishing boat). A record made in this way is shown in Fig. 6. The results, in Table III, show velocities falling into two groups, the higher values characterizing weathered sandstones, the lower weathered shales in the cyclothemic sequence of outcrops on the seabed.

With the method we describe, the velocity measurement is made over a path length of 30 m, whereas in conditions of 40 m depth of water and rock velocity of 2.1 km/s, a separation between source and receiver of about 200 m would be required for the observation of a head wave with conventional surface-towed equipment. Clearly this method gives considerably better resolution of abrupt lateral changes in velocity than could be achieved by the use of equipment near the sea surface. The advantage over sea-bottom methods such as those of Roberts et al.[6] or Hunter et al.,[7] is that our method does not require the survey vessel to make a station. In the water depths of 40 m and the good weather conditions which we encountered, the sea-surface reflection was appropriate for triangulation, by Eq. (1), to find the location of the remote receiver. In much deeper water, it would be necessary to use the bottom reflection, a second acoustic source or a pressure transducer to locate this receiver.

III. CONCLUSIONS

As ways of measuring at midaudio frequencies the velocity of the compressional acoustic wave in seabed materials, the methods described may be found more convenient then those which require station work, and more accurate than upward extrapolations from information on deeper strata. The wide-angle method in particular could be employed continuously whenever deep-tow vertical-incidence profiling surveys are being conducted. In view of this, it is unfortunate that profiling systems are being built with no provision made for their immediate use in seabed acoustic velocity determination, or even for their easy adaption to that end.

The velocity of the compressional wave is a good indicator of sediment bonding by ice[32] or gas hydrate, and a measurement of this same parameter is the only

TABLE III. Results of refraction experiments.

Number	Locality Lat. N.	Long. W	Rock velocity (km/s)	Water depth (m)	Method of derivation
1	46°23′	60°17′	2.20 ± 0.05	29	Travel time
1	46°23′	60°17′	2.17 ± 0.12	29	Gradient of travel time
2	46°14′	59°49′	2.00 ± 0.15	43	Travel time
3	46°14′	59°48′	2.13 ± 0.07	41	Travel time
4	46°14′	59°48′	3.00 ± 0.10	42	Travel time
5	46°14′	59°48′	2.86 ± 0.15	41	Travel time
5	46°14′	59°48′	2.60 ± 0.21	41	Gradient of travel time

reliable remote method for detecting sediment gasification. Both bonding and gasification[33] have implications for the design of structural foundations. This is one of the more pressing reasons for the need to change the present, inadequate, vertical-incidence, seismic profiling systems normally used in seabed surveys for engineering purposes.

ACKNOWLEDGMENTS

APPENDIX: DERIVATION OF EQ. (1)

In Fig. 1, the acoustic source is at A and the receiving hydrophone is at D. We know the distance a from the vertical incidence reflection time, the separation d of the source and hydrophone, and the total distance $(b + c)$ along the reflected wave path. We require the distance h in order to locate the receiving hydrophone. From $\triangle$ DAE

$$d^2 = b^2 + c^2 + 2bc \cos 2\alpha ,$$

$$d^2 = (b + c)^2 - 2bc(1 - \cos 2\alpha) .$$

But

$$1 - \cos 2\alpha = 2 \sin^2 \alpha ,$$

$$d^2 = (b + c)^2 - 4bc \sin^2 \alpha ,$$

$$\sin \alpha = a/b ,$$

$$d^2 = (b + c)^2 - 4a^2 c/b ,$$

since $\triangle$ ABE is similar to $\triangle$ ECD,

$$c/b = h/a ,$$

$$d^2 = (b + c)^2 - 4ah ,$$

hence

$$h = [(b + c)^2 - d^2]/4a .$$

[1] E. L. Hamilton, "Sound velocity gradients in marine sediments," J. Acoust. Soc. Am. 65, 909–922 (1979).

[2] R. E. Houtz, "Preliminary sonobuoy study of rapidly accumulating shelf sediments," J. Geophys. Res. 83, 5397–5404 (1978).

[3] X. LePichon, J. Ewing, and R. E. Houtz, "Deep-sea sediment velocity determination made while reflection profiling," J. Geophys. Res. 73, 2597–2614 (1968).

[4] G. M. Bryan, "Sonobuoy measurements in thin layers," in *Physics of Sound in Marine Sediments*, edited by Loyd Hampton (Plenum, New York, 1974), pp. 119–130.

[5] K. Wrolstad, "Interval velocity and attenuation measurements in sediments from marine seismic reflection data," J. Acoust. Soc. Am. 68, 1415–1435 (1980).

[6] E. W. Roberts, P. G. Simpkin, and D. Taylor-Smith, "An *in-situ* acoustic probe for sea-bed sediments," Mar. Technol. 72–77 (1972).

[7] J. A. Hunter, H. A. MacAulay, R. A. Burns, and R. L. Good, "Measurement of seabottom sediment velocities on the Scotian Shelf," Rep. Eng. Geophys. Sec., Geol. Survey of Canada, Ottawa (1980).

[8] G. M. Bryan, "The hydrophone-pinger experiment," J. Acoust. Soc. Am. 68, 1403–1408 (1980).

[9] G. L. Maynard, G. H. Sutton, D. M. Hussong, and L. W. Kroenke, "The seismic wide angle reflection method in the study of ocean sediment velocity structure," in *Physics of Sound in Marine Sediments*, edited by Loyd Hampton (Plenum, New York, 1974), pp. 89–115.

[10] C. H. Green, "Velocity determination by means of reflection profiles," Geophys. 3, 295–305 (1938).

[11] C. H. Dix, "Seismic velocities from surface measurements," Geophys. XX(1), 68–86 (1955).

[12] J. D. Bennell, "Seismic velocity gradients in sea floor sediments," Geol. Rep. 78-1, Marine Science Laboratories, Menai Bridge, North Wales (1978).

[13] D. E. T. Bidgood, "A deep-towed sea bottom profiling system," Proc. Oceans 74 IEEE Conf. 2, 96–107 (1974).

[14] R. C. Tyce, L. A. Mayer, and F. N. Spiess, "Near-bottom profiling: High lateral variability, anomalous amplitudes, and estimates of attenuation," J. Acoust. Soc. Am. 68, 1391–1402 (1980).

[15] D. R. Parrott, D. J. Dodds, L. H. King, and P. C. Simpkin, "Measurement and evaluation of the acoustic reflectivity of the sea floor," Can. J. Earth Sci. 17(6), 722–737 (1980).

[16] W. J Porter, D. L. Bell, and L. C. Britton, "Multichannel towed arrays for remote measurement of marine sediment acoustical properties," Offshore Technol. Conf., Dallas, paper No. OTC 2015, American Institute of Mining, Metallurgical, and Petroleum Engineers (1974).

[17] A. G. McKay, "Observation of wide-angle reflections and refractions from a high-resolution engineering seismic source," Geophys. Prospect. 16 (3), 673 (A) (1978).

[18] G. K. Westbrook, Ph. D. thesis, University of Durham, England (1974).

[19] L. M. Brekhovskikh, *Waves in Layered Media* (Academic, New York, 1960).

[20] V. M. Merkulova, "Reflection of sound waves from the boundary between a liquid and a solid absorbing medium," Sov. Phys.-Acoust. 15(3), 404–405 (1970).

[21] E. L. Hamilton, "Geoacoustic modelling of the sea floor," J. Acoust. Soc. Am. 68, 1313–1340 (1980).

[22] R. D. Stoll, "Acoustic waves in ocean sediments," Geophys. 42 (4), 715–725 (1977).

[23] R. D. Stoll and T. K. Kan, "Reflection of acoustic waves at a water–sediment interface," J. Acoust. Soc. Am. 70, 149–156 (1981).

[24] L. H. King, "Surficial geology of the Halifax–Sable Island map area," Canadian Department of Energy Mines and Resources Marine Sciences Papers No. 1, 16 pp. (1970).

[25] D. Scott, F. Medioli, and A. A. Miller, personal communication, Geology Dept., Dalhousie University, Halifax, Nova Scotia (1980).

[26] A. B. Wood, *A Textbook of Sound* (Bell), London, (1930).

[27] L. H. King and B. MacLean, "Pockmarks on the Scotian Shelf," Geol. Soc. Am. Bull. 81, 3141–3148 (1970).

[28] P. A. Heelan, "On the theory of head waves," Geophys. 18, 871–893 (1953).

[29] A. C. Maries and W. C. Beckmann, "A new geophysical method for the exploration of undersea coalfields," Min. Eng., 262–275 (Jan., 1961).

[30] K. Howells and A. G. McKay, "Seismic profiling in Miramichi Bay, New Brunswick," Can. J. Earth Sci. 14 (12), 2909–2927 (1977).

[31]D. D. Prentiss, A. G. McKay, K. Howells, and D. E. T. Bidgood, "Marine seismic reflection surveys over part of the underwater extension of the Sydney Coal Basin, Cape Breton Island," Geol. Assoc. Can. Halifax '80 Programme with Abstracts 5, 76 (1980).

[32]J. A. Hunter, A. S. Judge, H. A. Macaulay, R. L. Good,

R. M. Gagné, and R. A. Burns, "Permafrost and frozen sub-seabottom materials in the Southern Beaufort Sea," Beaufort Sea Project Tech. Rep. No. 22, Geol. Survey Can. (1976).

[33]G. C. Sills, "Seabed soils containing gas bubbles," personal communication, Dept. Eng. Sci., Univ. Oxford (1980).